



# ACTA RADIOLOGICA

FOUNDED IN 1921 BY GOSTA FORSSELL

OFFICIAL ORGAN OF THE RADIOLOGICAL SOCIETIES OF DENMARK FINLAND NORWAY AND SWEDEN

EDITOR  
ERIK LINDGREN

ASSOCIATE EDITORS  
ULF RUDHE      ULF BERGVALI

---

## ADVISORY BOARD

Diagnostic radiology OLLE OLSSON  
Therapeutic radiology LARS GUNNAR LARSSON  
Radiation physics HURT LIDÉN  
Radiation biology BORJE LARSSON

## EDITORIAL BOARD

Denmark G. THOMSEN S. KAAE  
Finland P. VIRTAMA L. R. HOLSTI  
Norway J. FRIMANN DAHL E. POPPE  
Sweden L. G. LARSSON O. BARTLEY

---

THERAPY PHYSICS BIOLOGY

INDICES to Vol. 11 (1972)

February April June August October December

## Contents of Volume 11 — THERAPY PHYSICS BIOLOGY

Quantitative effects of $^{131}\text{I}$ on different tissue components in foetal and goitrogen challenged mouse thyroids By C. WALINDER	1
Dose rate dependence in the goitrogen stimulated mouse thyroid — A comparative investigation of the effects of roentgen $^{131}\text{I}$ and $^{125}\text{I}$ irradiation By G. WALINDER, C. J. JONSSON and ANNE MARIE SJODÉN	24
Immunoglobulins in carcinoma of the uterine cervix By S. PLESNIČAR	37
Function of the reticuloendothelial system in whole body irradiated mice By B. E. SCHILDT and K. H. ERIKSSON	48
Mitotic index in human squamous cell carcinoma By R. SFALY, ANITA IMMERMANN and B. SIEPSTONF	59
Method of staging system construction By S. S. KUROHARA, F. W. GEORGE III, A. VONCTAMA and J. H. WEBSTER	65
Antibodies to a HeLa cell line in carcinoma of the cervix uteri — The effect of radiation therapy By ANA FINHORN and J. JONSSON	83
Automatic production of isodose curves By O. KALNAES and J. MUNK	90
Physical measurements including depth dose data and isodose curves for 8 MV roentgen rays By S. K. AGARWAL, R. A. SCHIEELE and J. WAKLEY	97
Concepts W and G used in radiation dosimetry — Comments on current definitions By C. A. CARLSSON	106
Correction of isodose-diagrams for $^{60}\text{Co}$ and 35 MeV electrons at penetration of lung tissue By ULLA BRITA NORDBERG	113
Immobilisation, compensation and field shaping in megavolt therapy By N. F. SORENFSEN and A. SELL	129
Digital stereoscinatigraphic experiments with a gamma-camera By I. I. LARSON	135
Determination of small mass differences in roentgenography — II — Experimental investigations with a roentgen diffraction apparatus By I. HOLLENDER and G. LYSELL	145
Computerized treatment planning and inhomogeneities By R. I. NELSON	161
Treatment of inoperable pulmonary tumours with high-energy electrons By T. LANDBERG, ULLA BRITA NORDBERG, H. OLIVÉCRONA, M. LINDBERG and H. HENRIKSON	172

# CONTENTS OF VOLUME 11 — THERAPY PHYSICS BIOLOGY

iii

European trial on therapy of nephroblastoma	192
Clinical and cytogenetic investigation in children of parents treated with radioiodine By J EINHORN MAJ HUITEN J LINDSTEN HARRIET WICKLUND and P ZETTERQVIST	193
Cervical plexus lesions following post-operative radiation therapy of mammary carcinoma By P WESTLING H SVENSSON and P HELE	209
Value of pelvic pneumography in gynecologic brachytherapy By I J WEIGENBERG	217
Haemopoietic aspects of the changes in the natural radiation resistance of mice after hypoxia By M BERAN and B TRIBUKAIT	225
Preparation methods of liver and lung radiopharmaceuticals with $^{86}\text{Sr}$ $^{99}\text{Tc}$ and $^{113}\text{In}$ By P E ÅSARD and INGEBORG BOIS-SVENSSON	240
Effect of irradiation on the release of lymphocytes from the thymus By U ERNSTROV	257
Reduction in strontium absorption in pregnant lactating and suckling rats By K KOSTIAL V GRUDEN A DRAKOVIC V JUVANIC and I SIMONOVIC	277
Books received	288
Determination of dose distribution in the pelvis by measurement and by computer in gynecologic radiation therapy By I JOELSSON B I RUDEN A COSTA ANDREE DUTREIT and J C ROSENWALD	289
General equation for the calculation of nominal standard dose By R L DIXON	305
Selenium labelled toluidine blue as an agent for parathyroid scanning—Theoretic considerations By T G BRIEN	312
Incidence of pulmonary carcinoma in Iceland between 1931 and 1964 By G FR PETERSEN	321
Current status of intrathecal radiogold in the treatment of medulloblastoma By L H V GOLD S V KIEFFER G J D'ANGIO V T FALLOV and D M LONG	329
Attempt to modify the ionizing radiation induced histopathologic effects on the central nervous system by reserpine administration By V I HARIRI V AKEL S FALAKALI and O I LUNGER	341
Effect of ionizing radiation on nuclear energy transduction in normal and neoplastic glia—A quantitative cytochemical investigation By W M KIRSCH D SCHULZ E FLUCHS and P NAKANE	349
Atrophy following radiation therapy for central nervous system neoplasms By G H WILSON J BYFIELD and W V HANAFEE	361
Intracavitary radium treatment of malignant tumours of the urinary bladder By M PEDERSEN and S E HERTING	369
Radiologic pulmonary changes following cobalt 60 treatment of mammary carcinoma By S HAGEN and A KOLBENSVEDT	386
Intraarterial distribution of colloidal bismuth compounds injected in man By G LUNDELL	395
Effect of subcutaneous fat on bone mineral content measurements with the single-energy photon absorptiometry technique By L ZETZ	401



Carcinoma of the thyroid in children and young adults — A review of 52 patients By BERTA JFRED and T. LOWHAGEN	411
Virus particles in relation to radiation induced changes in the thymus of C H mice By B. JARPLID	422
Late effects of irradiation on the thyroid gland in mice — I — Irradiation of adult mice By G. WALINDER	433
Effect of 180 MeV proton or $^{60}\text{Co}$ gamma radiation on the incorporation of $^{125}\text{I}$ iodo 2 deoxyuridine into intestinal and splenic deoxyribonucleic acid of mice By K. J. JOHANSON and B. LARSSON	452
Retention of $^{125}\text{I}$ given as $^{125}\text{I}$ 5 iodo 2 deoxyuridine to mice after 180 MeV proton or $^{60}\text{Co}$ gamma irradiation By K. J. JOHANSON	465
Effect of incorporated $^{226}\text{Ra}$ on colony forming units of bone marrow and spleen in mice By V. SVOBODA and V. KLENER	472
Involution and recovery of the thymus and spleen of the Mongolian gerbil following roentgen irradiation By J. L. MONTGOMERY and R. C. RILEY	481
Effects of fractionated doses of electrons on human skin By S. BELLETTI and G. TUNESI	490
Thyroid radionuclide uptake measurements — Report of a panel of experts of the International Atomic Energy Agency	501
Influence of ionizing radiation on ciliary cell activity in the respiratory tract By K. FUJIMURA, C. H. HÄKANSSON and N. G. TOREMÄLM	513
Radiation sensitivity of tissues irradiated during mantle treatment of Hodgkin's disease By T. LANDBERG, L. BALDETORP, L. G. LINDBERG and GUDRUN SVANIN TAPPER	521
Thymic shielding in irradiated mice By B. JARPLID	536
Closed stereotaxic hypophysectomy by means of $^{60}\text{Co}$ gamma radiation By E. O. BACKLUND, T. RAHN, B. SARBY, A. DE SCHRYVER and J. WENNERSTRAND	545
Effects of $^{60}\text{Co}$ gamma radiation on the distribution, catabolism and incorporation of $^{125}\text{I}$ 5-iodo-2 deoxyuridine into intestinal and splenic deoxyribonucleic acid in mice By K. J. JOHANSON	556
Comparison of tumor uptake and kinetics of different radiopharmaceuticals under experimental conditions By D. EMRICHT, A. VON ZUR MÜHLEN, F. WILLGEROTH and A. LAMMICH	566
Late effects of irradiation on the thyroid gland in mice — II — Irradiation of mouse foetuses By G. WALINDER and ANNE MARIE SJÖDÉN	577
Modification of isodose curves by means of compensating filters By N. F. SØRENSEN	590
Angular distribution of radiation scattered from a phantom exposed to 10 to 50 kVp roentgen rays By D. M. J. BRISTOCK and T. E. BURLIN	593
Procedures in radiation therapy dosimetry with 5 to 50 MeV electrons and roentgen and gamma rays with maximum photon energies between 1 and 50 MeV — Recommendations by the Nordic Association of Clinical Physicists	603

## Subject index to Volume 11 — Therapy Physics Biology

### Radiation therapy

Immunoglobulins in carcinoma of the uterine cervix	37
Method of staging system construction	63
Antibodies to a HeLa cell line in irradiated carcinoma of the cervix uteri	83
Computerized treatment planning and inhomogeneities	161
Treatment of inoperable pulmonary tumours with high energy electrons	172
European trial on therapy of nephroblastoma	192
Clinical and cytogenetic investigation in children of parents treated with radioiodine	193
Cervical plexus lesions following post-operative radiation therapy of mammary carcinoma	209
Pelvic pneumography in gynecologic brachytherapy	217
Determination of dose distribution in the pelvis by measurement and by computer in gynecologic radiation therapy	289
Incidence of pulmonary carcinoma in Iceland between 1931 and 1964	321
Intrathecal radioiodine in the treatment of medulloblastoma	329
Attempt to modify the ionizing radiation induced histopathologic effects on the central nervous system by reserpine	341
Atrophy following radiation therapy for central nervous system neoplasms	361
Intracavitary radium treatment of malignant tumours of the urinary bladder	369
Radiologic pulmonary changes following cobalt 60 treatment of mammary carcinoma	386
Carcinoma of the thyroid in children and young adults	411
Effects of fractionated doses of electrons on human skin	490
Radiation sensitivity of tissues irradiated during mantle treatment of Hodgkin's disease	521
Closed stereotaxic hypophysectomy by means of $^{60}\text{Co}$ gamma radiation	545

### Radioactive isotopes

Quantitative effects of $^{131}\text{I}$ on foetal and gonitrogen challenged mouse thyroids	1
Dose rate dependence in the gonitrogen stimulated mouse thyroid — Effects of roentgen $^{131}\text{I}$ and $^{132}\text{I}$ irradiation	24
Direkt stereoskintigraphic experiments with a gamma-camera	133
Clinical and cytogenetic investigation in children of parents treated with radioiodine	193
Preparation methods of liver and lung radiopharmaceuticals with $^8\text{Sr}$ , $^{99}\text{Tc}$ and $^{111}\text{In}$	240
Selenium labelled toluidine blue as an agent for parathyroid scanning	312

Intrathecal radiogold in the treatment of medulloblastoma	329
Intracavitary radium treatment of malignant tumours of the urinary bladder	369
Radiologic pulmonary changes following bismuth compounds	395
Effect of 180 MeV proton or $^{60}\text{Co}$ gamma radiation on the incorporation of $^{125}\text{I}$ iodo-2 deoxyuridine into intestinal and splenic deoxyribonucleic acid in mice	452
Retention of $^{125}\text{I}$ given as $^{125}\text{I}$ 5-iodo 2'-deoxyuridine to mice after 180 MeV proton or $^{60}\text{Co}$ gamma irradiation	465
Effect of incorporated $^{226}\text{Ra}$ on colony forming units of bone marrow and spleen in mice	472
Thyroid radionuclide uptake measurements	501
Closed stereotaxic hypophysectomy by means of $^{60}\text{Co}$ gamma radiation	545
Effects of $^{60}\text{Co}$ gamma radiation on the distribution catabolism and incorporation of $^{125}\text{I}$ 5-iodo-2'-deoxyuridine into intestinal and splenic deoxyribonucleic acid in mice	556
Tumor uptake and kinetics of different radiopharmaceuticals under experimental conditions	566

### Radiation physics

Automatic production of isodose curves	90
Depth dose data and isodose curves for 8 MeV roentgen rays	97
Concepts W and G used in radiation dosimetry	106
Correction of isodose-diagrams for $^{60}\text{Co}$ and 35 MeV electrons at penetration of lung tissue	113
Immobilisation compensation and field shaping in megavolt therapy	129
Digital stereoscutigraphic experiments with a gamma-camera	135
Determination of small mass differences in roentgenography	145
Determination of dose distribution in the pelvis by measurement and by computer in gynecologic radiation therapy	281
General equation for the calculation of nominal standard dose	305
Effect of subcutaneous fat on bone mineral content measurement with the single energy photon absorptiometry technique	401
Modification of isodose curves by means of compensating filters	590
Angular distribution of radiation scattered from a phantom exposed to 10 to 60 kVp roentgen rays	593
Procedures in radiation therapy dosimetry	603

### Technique

Method of staging system construction	65
Digital stereoscutigraphic experiments with a gamma-camera	135
Determination of small mass differences in roentgenography	145
Computerized treatment planning and inhomogeneities	161
Preparation methods of liver and lung radiopharmaceuticals with $^{85}\text{Sr}^m$ , $^{99}\text{Tc}^m$ and $^{113}\text{In}^m$	240
Selenium labelled toluidine blue as an agent for parathyroid scanning	312
Attempt to modify the ionizing radiation induced histopathologic effects on the central nervous system by reserpine	311
Effect of subcutaneous fat on bone mineral content measurements with the single energy photon absorptiometry technique	401

# Radiation biology

Quantitative effects of $^{131}\text{I}$ on foetal and goitrogen challenged mouse thyroids	1
Dose rate dependence in the goitrogen stimulated mouse thyroid — Effects of roentgen $^{131}\text{I}$ and $^{133}\text{I}$ irradiation	24
Immunoglobulins in carcinoma of the uterine cervix	37
Function of the reticuloendothelial system in whole body irradiated mice	48
Mitotic index in human squamous cell carcinoma	59
Clinical and cytogenetic investigation in children of parents treated with radioiodine	193
Effect of irradiation on the release of lymphocytes from the thymus	257
Strontium absorption in pregnant lactating and suckling rats	288
Effect of ionizing radiation on nuclear energy transduction in normal and neoplastic glia	349
Virus particles in relation to radiation induced changes in the thymus of C H mice	422
Late effects of irradiation on the thyroid gland in mice—I—Adults	433
Effect of 180 MeV proton or $^{60}\text{Co}$ gamma radiation on the incorporation of $^3\text{H}$ 5-iodo 2-deoxyuridine into intestinal and splenic deoxyribonucleic acid of mice	452
Retention of $^{125}\text{I}$ given as $^{125}\text{I}$ 5-iodo 2-deoxyuridine to mice after 180 MeV proton or $^{60}\text{Co}$ gamma irradiation	465
Effect of incorporated $^{226}\text{Ra}$ on colony forming units of bone marrow and spleen in mice	472
Involution and recovery of the thymus and spleen of the Mongolian gerbil following roentgen irradiation	481
Effects of fractionated doses of electrons on human skin	490
Influence of ionizing radiation on ciliary cell activity in the respiratory tract	513
Radiation sensitivity of tissues irradiated during mantle treatment of Hodgkin's disease	521
Thymic shielding in irradiated mice	536
Effects of $^{60}\text{Co}$ gamma radiation on the distribution catabolism and incorporation of $^3\text{H}$ 5-iodo 2-deoxyuridine into intestinal and splenic deoxyribonucleic acid in mice	556
Tumor uptake and kinetics of different radiopharmaceuticals under experimental conditions	566
Late effects of irradiation on the thyroid gland in mice—II—Foetuses	577

# Miscellaneous

Incidence of pulmonary carcinoma in Iceland between 1931 and 1964	321
Atrophy following radiation therapy for central nervous system neoplasms	361

## List of Authors

- Agnew S. K. 9  
 Alu Y. 341  
 Asard P. E. 240  
 Becklund E. O. 34  
 Baldet rp L. 1  
 Biletu S. 490  
 Ben t ck D. M. J. 23  
 Beran M. 23  
 Biss en s n Ing bore ? 0  
 Br t T. G. 31  
 Br l T. E. 13  
 E f l d J. 31  
 Carlson C. A. 10  
 Costa A. 264  
 D Ang G. J. 324  
 Dixon R. L. 30  
 Durak c A  
 Du eix Andree 24  
 E m J. 193  
 E n h r N na 83  
 En t D  
 Er k en k. H. 48  
 Er t r r L  
 Falakal S. 341  
 Falt A. T. 329  
 Fu t E. 344  
 Fu lwa a k. 13  
 Gere H. F. W. t  
 G d L. H. A. 324  
 Guder N  
 Haven S. 2  
 Hakan v. C. H. 13  
 H n n r W. N. 31  
 Har N. I. 341  
 H l P. 1  
 H r r k n H. 1  
 Herting S. E. 313  
 Hender L. 143  
 Hulten Maj. 193  
 Imirerman Anita. 9  
 Jarplid B. 422 33  
 Jereb Berta. 411  
 Joellson I. 281  
 J ban on K. J. 432 413 31  
 J n s r C. J. 24  
 J n s n J. 83  
 Ju r r c A. 2  
 Kalnaes O. 90  
 Koeffler S. A. 323  
 Kirsch W. M. 344  
 Klemer A. 2  
 K l b r s t v d t A. 301  
 K n t i a l K.  
 Kur h r a S. S. 1  
 Lammich A. 11  
 Landberg T. I. 2 1  
 Larsson L. 437  
 Lars on E. I. 133  
 Lindberg I. G. 1  
 Lindgren M. 1  
 Lind ten J. 113  
 Long D. M. 324  
 L w h a g e n F. 411  
 Lund H. C. 34  
 Lysell G. 14  
 M n t a u r J. I. 481  
 n z u s M. H. n A. 24  
 Munk J. 40  
 Nakane P. 344  
 N l o n R. F. 11  
 N w d b e r g U l a B. t a 113 1  
 O s e r r o a H. 1  
 Pedersen M. 319  
 Peter en G. Fr. 371  
 Ple n i c a r S. 31  
 Rahn T. 343  
 Rides R. C. 481  
 Rosenwald J. C. 289  
 Ruden B. I. 33  
 Sarby B. 343  
 S c h e e l e R. A. 9  
 Schildt B. E. 48  
 Schulz D. 341  
 de S h r o v e r A. 34  
 Seal R. 33  
 Self A. 111  
 Stepton B. 9  
 S n c l  
 S y d e n A n n e M a r i e 24 3  
 S r e n s e n N. I. 121 30  
 Svahn Tapper Cudru. 1  
 S e n s e n H. 09  
 S b o d a A. 4 1  
 T r e m a l m N. G. 13  
 Tribukait B. 7  
 Tuncer O. I. 341  
 Tures G. 440  
 Vongtama V. 1  
 Wakley J. 2  
 Walnd r G. I. 74 433  
 W b a t J. H. 1  
 W e n g e n b e r g I. J. 1  
 W e n s t a n d J. 4  
 W e i l l g f. 09  
 W k l u n d H a r r t. 13  
 W l l g e r t h I. 14  
 W l o n G. H. 31  
 Z e n z L. 401  
 Z e t t e r q u i t P. 113

# List of Supplements to Acta Radiologica

Nos 173—322

(Issued December 1979)

For Suppl. Nos 1—172 inclusive see list issued December 1960 in Vol. 34 fasc. 6

The supplements are published from time to time and are not included in the subscription rate. Prices and year of publication of numbers already issued are detailed below.

- 173 ERIK ODEBLAD, BJÖRN WESTER and SVEN ERIK ENGLUND. Disappearance measurements. Theoretical, technical, biological and medical aspects. 1959. Price Sw. Kr. 30.
- 174 LARS BULLING and ERIK SEVERIN. Slipping epiphysis of the hip. A roentgenological and clinical study based on a new roentgen technique. 1959. Price Sw. Kr. 30.
- 175 ÅKE HANSGREN. Studies on the distribution and fate of  $C^{14}$  and T labelled p-aminosalicylic acid (PAS) in the body. 1959. Price Sw. Kr. 25.
- 176 LARS BJÖRFF. Can radiographic studies on the Fallopian tubes in rabbits. 1959. Price Sw. Kr. 25.
- 177 PEKKA VLORINEN. The roentgenographic slit methods. A survey and analysis of procedures based on the use of a narrow bundle of roentgen rays (scanography). 1959. Price Sw. Kr. 25.
- 178 BENGT H. O. ROSENGREN. Determination of cell mass by direct X-ray absorption. 1959. Price Sw. Kr. 25.
- 179 S. HULTBERG, O. DAHL, R. THORAEUS, E. J. VIKTERLOF and R. WALSTAM. Halocurie cobalt 60 therapy at the Radiumhemmet. Equipment, technique and dose measurements. 1959. Price Sw. Kr. 30.
- 180 BENGT LILJA. Motor activity of the stomach. 1959. Price Sw. Kr. 25.
- 181 PER AMUNDSEN. The diagnostic value of conventional radiological examination of the heart in adults. (Appendix by R. G. CARPENTER. An account of the statistical analysis of the relative heart volumes of 755 patients in various disease groups.) 1959. Price Sw. Kr. 20.
- 182 H. M. TRUBY. Acoustico-cineradiographic analysis: considerations with especial reference to certain consonantal complexes. 1959. Price Sw. Kr. 35.
- 183 ERIK BJÖRST. Radiographic studies of the anatomy of single and multiple renal arteries. 1959. Price Sw. Kr. 30.
- 184 GUSTAF NOTTER. A technique for destruction of the hypophysis using  $Y^{90}$  spheres. A radiologic, endocrine and histologic study. 1959. Price Sw. Kr. 35.
- 185 BENGT LILJEGREN. The subarachnoid cisterns. An anatomic and roentgenologic study. 1959. (Out of print.)
- 186 BENGT LILJEGREN. Pontine angle tumour. Encephalographic appearances. 1959. Price Sw. Kr. 30.
- 187 HOLGER SKOLDBORN. On the design, physical properties and practical application of small condenser ionization chambers. 1959. Price Sw. Kr. 30.
- 188 JENS NIELSEN. Anno Aetatis Suae LX. Papers dedicated to Jens Nielsen, professor of radiotherapy at the University of Copenhagen, on his sixtieth anniversary, December 19. 1959. Price Sw. Kr. 40.

- 189 OLOF DAHL and KARL JOHAN VIKTERLOF Attainment and value of precision in deep radiotherapy. Some fundamentals with special reference to moving beam therapy with 200 to 250 kV roentgen rays and cobalt 60 gamma radiation 1960 *Price Su* 1 = 35
- 190 RUNE SOREMARK Distribution and kinetics of bromide ions in the mammalian body. Some experimental investigations using  $\text{Br}^{80m}$  and  $\text{Br}^{82}$  1960 *Price Su* Kr 30
- 191 ULF BORELL and INGMAR FERNSTROM Radiologic pelvimetry 1960 *Price Su* Kr 30
- 192 NILS LINDVALL Renal papillary necrosis. A roentgenographic study of 155 cases 1960 (Out of print)
- 193 PALL EDHOLM The tomogram. Its formation and content 1960 *Price Su* Kr 30
- 194 RAIMO KIVILLOTO Pleural calcification as a roentgenologic sign of non-occupational endemic anthophyllite asbestosis (Mineralogic appendix by OLAVI KUOVO) 1960 *Price Su* 1 r 25
- 195 SVEN SCHJELLER Roentgenographic studies on epiphyseal growth and ossification in the knee 1960 *Price Su* 1 r 35
- 196 Å. A. HULTBOM and BO TÖRNBERG Mammary carcinoma. The biologic character of mammary carcinoma studied in 517 cases by a new form of malignancy grading 1960 *Price Su* 1 r 35
- 197 LARS R. HOLST The mitotic and radioprotective effect of cysteine and lysine in rat 1960 *Price Su* 1 r 30
- 198 OSBORNE BARTLEY The isometric relaxation phase of the left ventricle. An electrocardiographic study 1960 *Price Su* 1 r 35
- 199 GUNNAR WILLER VESTBY Vaso- seminal vesiculography in hypertrophy and carcinoma of the prostate with special reference to the ejaculatory ducts 1960 *Price Su* 1 r 35
- 200 BJORN NORDENSTROM Contrast examination of the cardiovascular system during increased intrabronchial pressure 1960 *Price Su* Kr 30
- 201 GIOVANNI DI CHIRO RISA encephalography and conventional neuroradiologic methods. A comparative study 1961 *Price Su* 1 r 35
- 202 LARS BJÖRK Velopharyngeal function in connected speech. Studies using tomography and cineradiography synchronized with speech spectrography 1961 *Price Su* Kr 25
- 203 BENGT O. NYLÉN Cleft palate and speech. A surgical study including observations on velopharyngeal closure during connected speech using synchronized cineradiography and sound spectrography 1961 *Price Su* Kr 25
- 204 E. R. KJELLBERG, B. NORDENSTROM, U. RUDHE, V. O. BJÖRK and G. MALMSTRÖM Cardioangiographic studies of the mitral and aortic valves 1961 *Price Su* 1 = 30
- 205 GUNNAR CARLBERGER Kinetics and distribution of radioactive cobalt administered to the mammalian body 1961 *Price Su* Kr 30
- 206 HANS MOELL Kidney size and its deviation from normal in acute renal failure. A roentgenographic study 1961 *Price Su* Kr 25
- 207 LEIF KJELD HANSEN Micturition cystourethrography with automatic serial exposures. An opinion on the value of the method 1961 *Price Su* Kr 30
- 208 FINN LUNDWALL Cancer of the vulva. A clinical review 1961 *Price Su* 1 r 30
- 209 ISMARI LINDGREN Anatomical and roentgenologic studies of tuberculous infections in BCG-vaccinated and non vaccinated subjects with biophysical investigations of calcified foci 1961 *Price Su* Kr 25
- 210 PER ERIK F. BERGNER The significance of certain tracer kinetical methods especially with respect to the tracer dynamic definition of metabolic turnover 1961 *Price Su* 1 r 30
- 211 P. VUORINEN, I. ANTILA, U. WEGFLICH, A. KALPILA and T. KORHONEN Renal cortical index and other roentgenographic renal measurements 1961 *Price Su* 1 r 25

- 212 LARS ANDREN Pelvic instability in newborns with special reference to congenital dislocation of the hip and hormonal factors. A roentgenologic study. 1962 *Price Sw Kr 30*
- 213 NILS-MAGNUS OHLSSON Left heart and aortic blood flow in the dog. Precision motion analysis of high speed (270 frames/sec) cinefluorographic recordings. 1962 *Price Sw Kr 35*
- 214 BENGT TJERNBERG Lymphography. An animal study on the diagnosis of  $\vee \times 2$  carcinoma and inflammation. 1962 *Price Sw Fr 35*
- 215 PAAVO KJALMI Periarthrosis calcarea of the shoulder joint. Its differentiation from other stiff and painful shoulders. 1962 *Price Sw Kr 30*
- 216 P. EDHOLM, I. FERNSTROM, H. LINDBLOM and S. I. SELDINGER Roentgen television in practice with special regard to puncture examinations. 1962 *Price Sw Kr 35*
- 217 FOLKE EDSBYR Carcinoma of the vulva. An analysis of 560 patients with histologically verified squamous cell carcinoma. 1962 *Price Sw Kr 30*
- 218 P. SOILA, M. GRONROOS, O. KAUPPILA and L. PYYKOVEN Wasserlösliche viskosierte wasserlösliche und jodolige Kontrastmittel in der Hysterosalpingographie. Vergleichende Untersuchungen. 1962 *Price Sw Kr 25*
- 219 STIG SANDMARK Hiatal incompetence. Studies on mechanics and principles of examination for hiatus hernia and gastro-oesophageal reflux. 1963 *Price Sw Kr 25*
- 220 MAX LUNDBERG Free movements in the temporomandibular joint. A cineradiographic study. 1963 *Price Sw Kr 30*
- 221 ÅKE NORHAGEN Selective angiography of the hepatic veins. Experimental investigations of basal circulatory dynamics. 1963 *Price Sw Kr 35*
- 222 ERLING HANSEN JACOBSEN Genetically significant radiation doses in diagnostic radiology. 1963 *Price Sw Fr 35*
- 223 ÅSTRID BROHULT Alkoxylglycerols and their use in radiation treatment. An experimental and clinical study. 1963 *Price Sw Kr 30*
- 224 CARL OLOF ÖJENFORS Pulmonary interstitial emphysema — An experimental roentgen-diagnostic study. 1964 *Price Sw Kr 35*
- 225 GEORG THEANDER Variation in shape of gallbladder during cholecystography. 1964 *Price Sw Kr 30*
- 226 HILCO BOGREN The composition and structure of human gallstones. 1964 *Price Sw Kr 30*
- 227 LARS NORDQVIST The sagittal diameter of the spinal cord and subarachnoid space in different age groups — A roentgenographic post mortem study. 1964 *Price Sw Kr 25*
- 228 LENNART VICTORIN Bone resorption in cases with complete upper denture — A quantitative roentgenographic photogrammetric study. 1964 *Price Sw Kr 30*
- 229 ARNTNY ENGESET Irradiation of lymph nodes and vessels — Experiments in rats with reference to cancer therapy. 1964 *Price Sw Kr 30*
- 230 LARS HOLLENDER Determining the elements of the interior orientation in roentgenography. 1964 *Price Sw Kr 30*
- 231 HANS HENRIK HOLM The hydrodynamics of micturition — Examination by means of micro-manometer and uroflowmeter of the hydrodynamic conditions in normal subjects and in patients suffering from obstruction in the posterior part of the urethra. 1964 *Price Sw Kr 30*
- 232 ESSE CEDERQVIST Clinical application of whole body counting of  $^{85}\text{Sr}$  and  $^{45}\text{Ca}$  in patients with and without widespread malignant skeletal disease. 1964 *Price Sw Kr 30*
- 233 SIVZ PAULIN Coronary angiography — A technical, anatomic and clinical study. 1964 *Price Sw Fr 40*
- 234 TROELS MUNKNER The influence of para-aminosalicylic acid on the  $\text{I}^{131}$  metabolism. 1965 *Price Sw Fr 30*



- 235 ANDERS LUNDERQUIST Angiography in carcinoma of the pancreas 1965 *Price Su. Kr 35*
- 236 RENE WALSTAM Studies on therapeutic short-distance and intracavitary gamma beam techniques — Physical considerations with special reference to radiation protection 1965 (Out of print)
- 237 KAI SETALA Differences in pharmacodynamic response to colchicine between benign and malignant epidermal hyperplasias — An experimental study in skin tumor resistant mice 1965 *Price Su. Kr 30*
- 238 UNO ERIKSON Circulation in traumatic amputation stumps — An angiographical and physiological investigation 1965 *Price Su. Kr 35*
- 239 CARL GUSTAF STANDERTSKJÖLD NORDENSTAM The pulmonary circulation during pneumonia — A cineradiographic study 1965 *Price Su. Kr 35*
- 240 ANTTI CEDERBERG Granulocyte distribution in bone marrow blood and different organs in whole body irradiated rats 1965 *Price Su. Kr 35*
- 241 KAI SETALA Decorporation of radiostrontium Radioactive assay techniques — An experimental study on mice 1965 *Price Su. Kr 30*
- 242 SHINJI TANAHASHI Conformation radiotherapy — Rotation techniques as applied to radiography and radiotherapy of cancer 1965 *Price Su. Kr 40*
- 243 J. TH. VAN DER WERFF Radioactive bismuth <sup>212</sup>Bi — Experimental studies and clinical applications 1965 *Price Su. Kr 35*
- 244 SAMUEL S. KUROHARA Effects of ionizing radiation on creatine metabolism in patients treated for malignancy and in rats 1965 *Price Su. Kr 35*
- 245 IER WESTLING Studies of the prognosis in Hodgkin's disease 1965 *Price Su. Kr 35*
- 246 SVEN GOTTMAR ERICSSON Quantitative microradiography of cementum and abraded dentine — A methodological and biological study 1965 *Price Su. Kr 35*
- 247 MAURI WILJASALO Lymphographic differential diagnosis of neoplastic diseases 1965 *Price Su. Kr 35*
- 248 SVEN SCHELLER Roentgenographic studies on the ossification of the distal femoral epiphysis 1965 *Price Su. Kr 30*
- 249 ROAR NISSEN MEYER Castration as part of the primary treatment for operable female breast cancer — A statistical evaluation of clinical results 1965 *Price Su. Kr 35*
- 250 ELLIS BERVEN SVEN HULTBERG HANS LEDVIG-HOTTMER ROLF SIEVERT LARS SÄNTENSON and BENGT SYLÉN The first fifty years Radiumhemmet 1910—1937 and King Gustaf V Jubilee Clinic 1938—1960 1965 *Price Su. Kr 30*
- 251 MATS HANERLING Renal phlebography — An experimental study in the pig 1966 *Price Su. Kr 30*
- 252 GUNNAR WESTBERG Gas myelography and percutaneous puncture in the diagnosis of spinal cord cysts 1966 *Price Su. Kr 30*
- 253 SVEN IVAR SELDINGER Percutaneous transhepatic cholangiography 1966 *Price Su. Kr 35*
- 254 FIRST NORDIC RADIATION PROTECTION CONFERENCE Proceedings Stockholm 1966 Edited by K. Lidén and Erik Lindgren *Price Su. Kr 35*
- 255 LAWRENCE JOSEPH VAN CLARA Application of digital computers in radiation dosimetry 1966 *Price Su. Kr 35*
- 256 HANS LUDIN Aortography Fluid dynamics and technical problems 1966 *Price Su. Kr 35*
- 257 HJALMAR LÖLIN Contrast medium in kidney during angiography — A densitometric method for estimation of renal function 1966 *Price Su. Kr 30*

- 258 ELMABETH JOHANSSON PER HOLSTAD and GUNAR SODERBERG Cytologic vascular and histologic patterns of dysplasia carcinoma in situ and early invasive carcinoma of the cervix. 1966 *Price Ss Kr 40*
- 259 PAUL EDHOLM Anatomical angles determined from two radiographic projections — Instrument description and measurement techniques. 1966 *Price Ss Kr 40*
- 260 TORSTEN ALMEN A steering device for selective angiography and some vascular and enzymatic reactions observed in its clinical application 1966 *Price Ss Kr 40*
- 261 HAI SETALA, BJORN LINDROOS and OTTO WYSSOVEN Cancer chemotherapy studies cytoplasmic barrier in malignant epidermal cells against the effect of colchicine — An electron microscopic study in mice 1966 *Price Ss Kr 25*
- 262 KLAS ROSENGREN Hyaline membrane disease — A radiological investigation in rabbits 1967 *Price Ss Kr 35*
- 263 JAN NILSON Angiography in tumours of the urinary bladder 1967 *Price Ss Kr 35*
- 264 PER ERIK HEERL Postmortal changes of the lung — A roentgenographic microscopic and bacteriological follow up study on a pediatric series and on animals with experimental pneumonia. 1967 *Price Ss Kr 30*
- 265 HAI SETALA OTTO WYSSOVEN and BJORN LINDROOS Ultrastructural changes in benign and malignant epidermal states in mice after topical beta radiation. 1967 *Price Ss Kr 30*
- 266 GÖRAN NYLANDER Vascular response to vasopressin as reflected in angiography — An experimental study in the dog 1967 *Price Ss Kr 35*
- 267 JOHAN FOLIN Angiography in renal tumours — Its value in diagnosis and differential diagnosis as a complement to conventional methods 1967 *Price Ss Kr 35*
- 268 EERO TALA Carcinoma of the lung — A retrospective study with special reference to pre-diagnosis period and roentgenographic signs 1967 *Price Ss Kr 35*
- 269 CARL O. HENRIKSON Iodine 125 as a radiation source for odontological roentgenology 1967 *Price Ss Kr 35*
- 270 CATIONS IN INTRAVASCULAR CONTRAST MEDIA AND DEVELOPMENT OF SPECIFIC METRIZOATE FORMULAE — PHARMACOLOGIC AND CLINICAL STUDIES Proc Symposia at Copenhagen November 1964 and Sandefjord September 1966 1967 *Price Ss Kr 40*
- 271 ERNA TARKKAINEN Intracostal vein meningo-rachidography — A technical, anatomic and clinical study 1967 *Price Ss Kr 35*
- 272 ALLAN LINDERQVIST Arterial segmental supply of the liver — An angiographic study 1967 *Price Ss Kr 35*
- 273 HAI SETALA MAX SIURALA OTTO WYSSOVEN and ERNA TARKKAINEN Quantitative three-dimensional scintillography of the stomach with technetium ( $^{99m}\text{Tc}$ ) 1967 *Price Ss Kr 30*
- 274 PER BERGSSJO Radiation induced early changes in size and vascularity of cervical carcinoma — A colpophotographic and clinical study 1968 *Price Ss Kr 35*
- 275 SUNE ERICSON The parotid gland in subjects with and without rheumatoid arthritis 1963 *Price Ss Kr 40*
- 276 ROIS JENSEN Anterior teeth relationship and speech — Studies using cineradiography synchronized with speech recording 1968 *Price Ss Kr 35*
- 277 SVEN AHLBACK Osteoarthritis of the knee — A radiographic investigation. 1968 (Out of print)
- 278 IRENE SJÖGREN KJELL BERGSTRÖM and HERMAN LODIN Echo-encephalography in infants and children. Comparison with cerebral pneumography in measuring ventricular size 1963 *Price Ss Kr 35*

- 279 BERTIL JARPLID Radiation induced asymmetry and lymphoma of thymus in mice 1968 *Price Su Kr 35*
- 280 ERKKI M. LAASONEN Information transmission in roentgen diagnostic chains — Experimental and clinical studies 1968 *Price Su Kr 35*
- 281 RASMUS STENSTRÖM Arthrography of the knee joint in children — Roentgenologic anatomy, diagnosis and the use of multiple discriminant analysis 1968 *Price Su Kr 35*
- 282 KARL KARLSTEDT Carcinoma of the uterine corpus — Factors bearing on the curability 1968 *Price Su Kr 35*
- 283 LEO STJERNVALL Pharmacodynamic response of epidermal hyperplasias to topical vinblastine treatment 1968 *Price Su Kr 35*
- 284 HANS FLODIN Distribution and kinetics of labelled vitamin B<sub>12</sub> 1968 *Price Su Kr 35*
- 285 ERKKI KORVISTO Comparative study of roentgen diagnostic classifications — Computer analysis of 124 496 roentgen reports 1969 *Price Su Kr 35*
- 286 JØRGEN JENSEN Malformations of the inner ear in deaf children — A tomographic and clinical study 1969 *Price Su Kr 35*
- 287 PENTTI J. TASKINEN Radiotherapy and TNM classification of cancer of the larynx — A study based on 1 447 cases seen at the Radiotherapy Clinic of Helsinki during 1936—1961 1969 *Price Su Kr 35*
- 288 ROBERT T. NASH Decision processes employing radioisotope scanning 1969 *Price Su Kr 35*
- 289 SIRKKA WILJASALO Lymphographic polymorphism in Hodgkin's disease — Correlation of lymphography to histology and duration 1969 *Price Su Kr 35*
- 290 ULF WELANDER Multicolor combination images in subtraction angiography — A new photographic method and its applications 1969 *Price Su Kr 40*
- 291 ILONA SCHRECK PUROLA Failure of malignant epidermal cells to respond to vinblastine sulfate — A study in skin tumor resistant mice 1969 *Price Su Kr 35*
- 292 GIOVANNI RUGGIERO GIANFRANCO CRISTI and CLAUDIO TREVISAN Clinical aspects of encephalography 1969 *Price Su Kr 30*
- 293 PEKA VIRTANEN and TAPPO HELELA Radiographic measurements of cortical bone — Variations in a normal population between 1 and 90 years of age 1969 *Price Su Kr 20*
- 294 L. STJERNVALL E. E. NISLÄNEN and J. TARKKANEN Penetration of cytoplasmic barrier in malignant epidermal hyperplasia by colchicine in dimethyl sulfoxide — A polarization microscopic study in skin tumor resistant mice 1969 *Price Su Kr 20*
- 295 KAARINA TOURLI KASILA Heart size determination by photofluorography 1970 *Price Su Kr 35*
- 296 HANS ROVING Otosclerosis — A tomographic-clinical study 1970 *Price Su Kr 35*
- 297 IFR LANCELAND Population screening for female breast tumours. A clinical investigation 1970 *Price Su Kr 35*
- 298 JOHAN FORBEN Effect of cysteine on chromosome aberrations induced by radiation of human lymphocytes in vitro 1970 *Price Su Kr 30*
- 299 RUNE SUNDGREN Selective angiography of the left gastric artery 1970 *Price Su Kr 35*
- 300 NIELS KRISTIAN LARSEN The lower urinary tract in infancy and childhood — Micturition cinematography with simultaneous pressure flow measurement 1970 *Price Su Kr 35*
- 301 M. AUKERI Ultrasound examination of pleural plaques — Experimental, pathologic and clinical studies 1970 *Price Su Kr 35*
- 302 INGEMAR JOHANSSON Radiotherapy of carcinoma of the uterine cervix with special regard to external irradiation 1970 *Price Su Kr 35*

- 303 KAARINA AANTAA Location of the placenta — A comparison between radiography, ultrasound, thermography, isotopes. 1971 *Price Sc Kr 22*
- 304 LENNART DIENER Intraosseous phlebography of the lower limb — Toxic item investigation of thrombotic venous disease. 1971 *Price Sc Kr 40*
- 305 BERNDT STROMBERG The normal and diseased superficial flexor tendon in the human hand. A morphologic and physiologic investigation. 1971 *Price Sc Kr 33*
- 306 TRYGVE AAKHUS Angiography in acute mechanical obstruction of the small intestine. 1971 *Price Su Fr 40*
- 307 PERTTU METSALA Effect of dimethyl sulfoxide (DMSO) on cytoplasmic barriers of malignant epidermal cells — An investigation in skin tumor resistant mice. 1971 *Price Su Kr 35*
- 308 JORGEN RYGLÅRD Mechanism of blood clearance of colloidal gold in mice — An atoxic clinical investigation using activation analysis. 1971 *Price Su Kr 35*
- 309 LAURI PATOMAKI A mathematical model for radiation fields of telecobalt treatment units — With special reference to the isodoses of Rocus. 1971 *Price Su Fr 12*
- 310 RADIOBIOLOGIC INVESTIGATIONS. Edited by Erik Lindgren and Bernhard Lishchik. 1971 *Price Su Kr 45*
- 311 HALVOR VERMUND Enhancement of radiation effects by chemotherapy. 1971 *Price Su Kr 35*
- 312 PERTTU KASARI Osteomedullography of the tibia. 1971 *Price Su Kr 10*
- 313 PROCEEDINGS OF THE SIXTH CONFERENCE OF THE NORDIC ASSOCIATION OF CLINICAL PHYSICISTS held in Århus, Denmark, 1970. Edited by C. B. Madsen and K. Lulén. *Price Su Fr 15*
- 314 BIRGER HELIN Heart volume in human kidney transplantation. 1972 *Price Su Fr 22*
- 315 UGO WEGELINS Angiography of the hand. Clinical and postmortem investigations. 1972 *Price Su Fr 35*
- 316 P. E. S. PALMER Haemangiosarcoma of Kaposi. 1972 *Price Su Fr 12*
- 317 JULIANI RAUSTE Lymphographic findings in granulomatous inflammations and connective tissue diseases — Differential diagnosis between these diseases and lymphoma. 1972 *Price Su Fr 30*
- 318 OVE MATTSSON Formation of the tomographic image — With special reference to filtering. 1972 *Price Sc Fr 32*
- 319 PROGRESS IN VETERINARY RADIOLOGY. Proceedings of the 2nd International Conference of Veterinary Radiologists held in Stockholm, 1970. Edited by Sten Erik Olsson. 1972 *Price Sc Fr 42*
- 320 TJAKKO KUTTERS Carcinoma of the uterine cervix. Aspects of clinical and gynaecological referred for radiation therapy. 1972 *Price Su Fr 50*
- 321 BO LUNSTRÖM Angiographic abnormalities following percutaneous needle biopsy of the kidney. 1972 *Price Sc Fr 40*
- 322 LARS FJELLGREN Mode of accumulation of depleten lananines in the excretory system and certain organs. 1972 *Price Sc Fr 40*



## QUANTITATIVE EFFECTS OF $^{131}\text{I}$ ON DIFFERENT TISSUE COMPONENTS IN FOETAL AND GOITROGEN CHALLENGED MOUSE THYROIDS

by

G WALINDER

The effect of  $^{131}\text{I}$  and roentgen irradiation on the thyroid gland of the CBA mouse has been previously investigated (WALINDER & SJÖDEN). The quantitative effects of  $^{131}\text{I}$  irradiation on the epithelium, colloid, stroma and the blood of the thyroid gland in mouse foetuses as well as in juvenile and adult mice will be investigated in the present contribution and certain conclusions will be drawn regarding the mechanism primarily responsible for the arrest of thyroid growth previously reported.

### Material and Methods

The management and housing of the CBA mice were the same as in the earlier experiments (WALINDER, WALINDER & SJÖDEN). The foetuses were given  $^{131}\text{I}$  (carrier free  $\text{Na}^{131}\text{I}$ ) from the Radiochemical Centre, Amersham, England, by intravenous injections to the mothers on the 18th day of pregnancy. The mothers had been maintained on an iodine deficient diet ( $0.3 \mu\text{g I per g pellet}$ ) from the first day of pregnancy, in other words from the day when a vaginal

From the Division of Radiobiology, the Research Institute of National Defence, Sundbyberg, Sweden. Submitted for publication 15 October 1970.

plug was first observed. This diet was changed to a normal one on the 19th day of pregnancy (20 to 30  $\mu\text{g}$  I per g pellet). The foetuses and juvenile mice were killed with chloroform at varying times after the injection and their thyroid glands removed for examination. No sex discrimination was made of mice under 11 days of age but the juvenile animals over this age that were examined were all males. The adult mice of the material were males and had been maintained on an iodine deficient diet for 7 or 14 days before the intraperitoneal injection of  $^{131}\text{I}$ . One day after this injection, this was changed to a normal diet and at the same time the animals were given propylthiouracil (PTU, Pharmacia Uppsala Sweden) or 3-amino-1,2,4 triazole (3 ATA, Schuchardt, Munich) in the drinking water (1 g PTU or 1 g 3 ATA per l of water). The mice were killed with chloroform at varying times after the injection of radioiodine.

### *Morphometric methods*

*Sectioning and staining of the thyroid tissue.* For the quantitative determinations of the different components of the gland (epithelium, colloid, stroma, blood) the tissue was fixed in Stieve's solution, dehydrated with alcohol and xylene in the conventional way and embedded in paraplast. The thyroid glands were then cut into serial sections in accordance with the scheme below. This was repeated until sections had been taken right through the gland.

Section No	Thickness of section $\mu \pm \text{SD}$	Staining method
1-2	$5.0 \pm 0.1$	Haematoxylin-eosin
3-4	$10.20 \pm 0.16$	Haematoxylin-eosin
5-9	$10.20 \pm 0.16$	Unstained or specific staining

Sections 1 to 4 were stained with Ehrlich's haematoxylin-eosin. Where the gland tissue had been exposed to high doses of radiation the thickness of sections 5 to 9 was reduced and stained with van Gieson's technique, Heidenhain's azan, PAS according to Hotchkiss or silver stained by the Foot & Foot method. All the staining work followed the techniques described by Romeis (1948).

The thickness of the sections was determined by the following method. Fifty serial sections were cut from eight paraplast cylinders of different diameters (precision turned) and weighed. Six cylinders were sectioned with the nominal section thickness of the microtome set at 5  $\mu$  and six cylinders with the microtome at 10  $\mu$ . The mean thickness of the sections was calculated from the dimensions and density of the cylinders. The mean values thus obtained were presumed to equal the mean thickness of the sections from a serially sectioned gland. The

results of the measurements appear in the section scheme. The standard deviations were calculated from the mean values obtained from the six  $5\ \mu$  cylinders and the six  $10\ \mu$  cylinders.

The thyroid weight was determined by the method described in an earlier paper (WALINDER 1971).

*Determination of epithelial cell number* The number of epithelial cells in the thyroid glands was determined by summing the cell nuclei or more correctly speaking by counting the number of nuclear centres in the tissue sectioned as described. Many of the cell nuclei counted in this way had been cut through and consequently some of their nuclear centres lay outside the section. It was therefore necessary to correct the calculations to allow for this. The method is presented in Fig. 1.

With the lettering given in Fig. 1 and assuming that the nuclei are spherical all those counted will have their centres within a volume bounded by the sectional area and with a thickness of  $d + 2h$  where  $d$  is the thickness of the section and  $h$  the distance from the edge of the section to the centre in those nuclei that have been cut through and are barely visible in the microscope. The constant  $h$  thus depends on the intensity of the nuclear staining and the resolving power of the microscope.

The determination of  $h$  was made by counting the number of cell nuclei in sections No. 2 ( $N_2$ ) and No. 4 ( $N_{10}$ ) according to the section scheme and by measuring the areas of the corresponding sections ( $A_2$  and  $A_{10}$  respectively). The number of cell nuclei per unit volume as obtained from a  $5.0\ \mu$  section is assumed to be equal to that from the subsequent  $10.2\ \mu$  section. Thus

$$\frac{N_2}{A_2 (5.0 + 2h)} = \frac{N_{10}}{A_{10} (10.2 + 2h)}$$

By repeating this procedure until sections had been taken right through the gland a mean value of  $h$  could be determined.

This method of calculation of cell number is largely identical with a technique described earlier by FLODERUS (1944) for arriving at the numbers of different types of cells in the hypophysis. As was mentioned,  $h$  corresponds to the distance between the edge of the section and the centre in the cut spherical nuclei whose parts that fall within the section are barely visible in the microscope. For elongated nuclei  $h$  must be regarded rather as a mean distance between the section edge and the centre. The shape of the cell nuclei may vary quite considerably, especially in thyroid tissue damaged by radiation. The technique for determining the correction factor  $h$  now described, is not dependent on the nuclear shape however. The only condition is that nuclei of different appearances in the border zones of both the  $5.0\ \mu$  and  $10.2\ \mu$  sections should be randomly distributed.



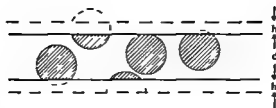


Fig. 1 Method of calculating the number of epithelial cell nuclei in sections from thyroid tissue. Some of the spherical cell nuclei were cut across and in some of these the nuclear centres lay outside the section. The centres belonging to the smallest nuclear calottes visible in the microscope were situated at a distance  $h$  from the surface of the section, i.e. the nuclei visible in the microscope had their centres within a section with the thickness  $d + 2h$  where  $d$  is the thickness of tissue sectioned.

ed or in other words that the  $h$  value is not dependent on the thickness of the section. The number of cells in the thyroid gland is finally obtained from the expression

$$N = \frac{V N_A S}{(d + 2h) A}$$

where  $N_A$  is the total number of cells in the  $d$  mm thick sections,  $A$  the total area of these sections and  $S$  the tissue shrinkage factor (see WALINDER). In all, 10 000 cells or more were counted in each gland. The ocular was equipped with a squared net to facilitate the counting. Any mitotic figures were also recorded simultaneously with the cell count.

*Determination of relative occurrence of different tissue types.* The method employed for determining the relative occurrence of different types of tissue in the thyroid gland is a generalization of a technique described earlier by UOTILA (UOTILA 1947; UOTILA & KANVAS 1952). If a lobe from a thyroid gland be placed in a rectangular coordinate system as in Fig. 2, the volume  $V_\varphi$  for a certain tissue component may be calculated from the expression

$$V_\varphi = \iint \varphi(x, y) (z_1 - z_2) dx dy, \quad (1)$$

where  $\varphi(x, y)$  is the fraction of the secant ( $z_1 - z_2$ ) that passes through the tissue component in question and  $A$  the area of the lobe projected in the  $xy$  plane (see Fig. 3).

The mean value theorem for double integrals then produces

$$V_\varphi = \varphi(\bar{x}, \bar{y}) \iint (z_1 - z_2) dx dy = \varphi(\bar{x}, \bar{y}) V, \quad (2)$$

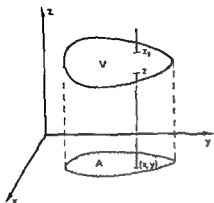


Fig. 7. A thyroid lobe placed in a system with rectangular coordinates. The secants at right angles to the  $xy$  plane cut the thyroid at the points  $z_1$  and  $z_2$ .  $V$  is the volume of the lobe and  $A$  the area of the lobe projected in the  $xy$  plane.

where  $V$  is the total volume of the lobe and  $(x, y)$  a point within  $A$ . The volume  $V$  of the glands from foetus and juvenile mice was determined in the manner described earlier (WALINDER) or by direct weighing (adult mice) under the assumption that the density of the gland tissue is  $1 \text{ g/cm}^3$ . The quantity  $\varphi(x, y)$  cannot be determined mathematically. It is evident from eq. (2) that the sufficient and necessary condition that would permit a result from measurements in a two-dimensional tissue section to be directly transferable to the three dimensional organ is that  $\varphi(x, y)$  would be a stochastic variable and hence independent of  $x$  and  $y$  or in other words that the component under examination is randomly distributed in the whole organ. All papers known to the writer that deal with quantitative determinations of organ components are based on the assumption that the components are randomly distributed. As the dose from  $^{131}\text{I}$  that has accumulated in the thyroid gland is much higher to the central parts of the lobes than to their peripheries or to the isthmus, radiation induced tissue changes in the gland can not a priori be expected to be randomly distributed even if this happen in the controls. In the present work, therefore, the dependency of the function  $\varphi(x, y)$  on the variables  $x$  and  $y$  for epithelium, colloid and stroma plus blood from animals given  $^{131}\text{I}$  was investigated by solving eq. (1) graphically. This was done by measuring the relative amount of epithelial tissue, colloid and stroma plus blood along equidistant secants (at a distance of  $96 \mu$  from one another) in every tenth section from serial sectioned thyroid glands i.e. in section No. 1 from each series of sections as in the previously described section scheme (Fig. 3).

The values obtained from the measurements were plotted on a normal probability paper with  $\varphi(x, y)$  as the abscissa and the cumulative number of secants with  $\varphi$  values smaller than and equal to the corresponding abscissa value as the ordinate (cf. Fig. 8). If straight lines are obtained when the values are

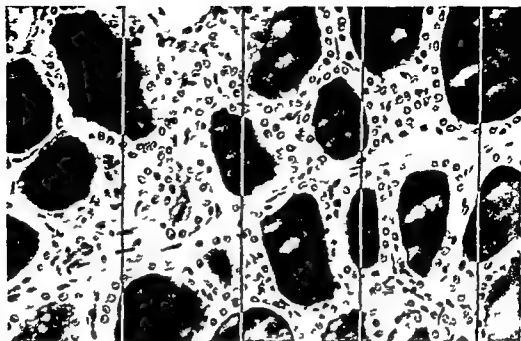


Fig. 3. A section from a thyroid gland divided into parallel equidistant secants. The white parts of the secants pass over the colloid and the black parts over the epithelium, stroma and blood. A division of the sum of all the white lengths of a secant by the length of the whole secant produces  $f(x)$ . The amount of a certain tissue component may be determined by adding the products of the  $f(x)$ 's and the corresponding  $(z_1 - z_2)$  values over all the secants in all sections from a serially sectioned lobe and multiplying the sum by the distance between the secants (96  $\mu$ ) and the thickness of the sections (PAS  $\times 310$ ).

plotted on a normal probability paper this does not necessarily mean that the component in question is randomly distributed in the whole thyroid gland; the volumes in which there is a deviating distribution of the component must however be negligible in relation to the total thyroid volume. Hence the linearity of the probability curve has been assumed to be the practical criterion that  $p$  can be considered a stochastic variable. Only the values from one mouse for each type of treatment are given in the results; these were however checked in two or three other animals identically treated. The distribution investigation served to facilitate this control. It was possible where straight lines were obtained to limit the control to measurements in a few sections from each animal and the total amount of the component in question could be obtained from eq. (2).

**Determination of cell survival.** The survival of the cells in the thyroid gland was studied by the administration of tritium labelled thymidine ( $^3\text{H}$  TdR) 24 hours or more before the  $^{131}\text{I}$  injection. The total tritium activity in the tissue

after the irradiation, and in appropriate cases after the goitrogen treatment, was considered to be a measure of the cell survival. The reliability of this method will be taken up in connection with the discussion of the methods. Thymidine  $6\text{ T(n)}$  was used in these experiments, it was supplied by the Radiochemical Centre, Amersham, in the form of sterilized solutions with a specific activity of  $2000\text{ mCi/mM}$ .

The administration of  $^3\text{H TdR}$  to the foetuses was carried out by intravenous injections to the mothers ( $10\text{ }\mu\text{Ci}$ ) on the 17th day of pregnancy, in other words 1 day before  $4\text{ }\mu\text{Ci }^{131}\text{I}$  was injected. The injection of  $^3\text{H TdR}$  ( $10\text{ }\mu\text{Ci}$ ) into the adult mice was preceded by treatment for 12 days with 3 ATA. After the injection of  $^3\text{H TdR}$ , the animals were put on an iodine deficient diet for 7 days after which time  $3\text{ }\mu\text{Ci }^{131}\text{I}$  were injected in 55 mice. One day after the  $^{131}\text{I}$  injection the 3 ATA treatment was restarted. Measurements of the retention were carried out in 40 of the  $^{131}\text{I}$  injected mice at different times during the first 14 days after the injection, and the other mice were killed 42 days after the injection. In addition to the groups injected with  $^3\text{H TdR}$ , a third group of mice received 3 ATA but was not treated with  $^3\text{H TdR}$  or  $^{131}\text{I}$ .

After the animals had been killed the thyroid glands were removed without delay and weighed and dehydrated in an alcohol bath. The tissue was then dissolved in NCS solubilizer (Nuclear Chicago Co). The strong chemoluminescence produced by some of the organic substances dissolved was quenched with HCl as suggested by HERBERG (1960). An amount of 4 g omniflour (NEC Chemicals GmbH) in 1 litre of toluene was used as the scintillator fluid, the samples were measured in a liquid scintillation computer (Beckman Liquid Scintillation System) and adapted to darkness and to the temperature in the computer for one day before the start of the measurements. Correction for quenching is facilitated by the extension ratio standard built into the Beckman computer. The measurement values obtained from a tritium standard as a function of the extension ratio standard value were investigated by dissolving 1, 2, 4 and 8 thyroid glands in NCS solubilizer to the same end volume and adding  $0.01\text{ }\mu\text{Ci }^3\text{H TdR}$  (the tritium standard) to each of the four solutions.

## Results

### *Foetuses and juvenile mice*

*Histologic radiation effects* The histologic appearances in the thyroid tissue of 3 day-old irradiated mice did not differ appreciably from those observed in the controls apart from the absence of mitotic figures. From the 5th day of life and onwards histologic differences could be observed between the thyroid tis-

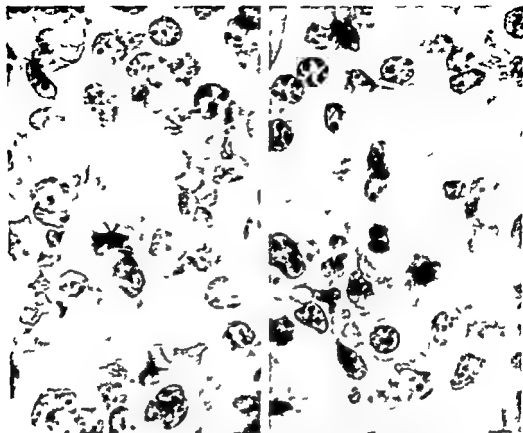


Fig. 4 Two atypical mitotic figures in 11-day mice that had received  $4 \mu\text{Ci } ^{131}\text{I}$  by intravenous injection of the mothers on the 18th day of pregnancy. The figure on the right indicates anaphase bridges and that on the left a pair of chromosomes departing from the metaphase plate (H&E  $\times 1250$  oil immersion).

sue of the controls and the tissue of the irradiated mice. The mitotic figures in the glandular tissue of the 5, 11 and 17-day old irradiated mice were often atypical (Fig. 4). The nuclei were polymorphic with numerous giants, necrotic changes of karyorrhexis and pyknosis type were common, and the cytoplasm was usually vacuolated and foamy (Fig. 5). Areas of follicles with high cuboidal or columnar cells, often with giant nuclei as well as areas of solid masses of low epithelial cells devoid of colloid filled lumina were evident. Table I indicates that the mean volume of the follicular cells did not deviate from a similar value in the thyroids of the controls.

The results of the quantitative examinations of the thyroid growth in newborn

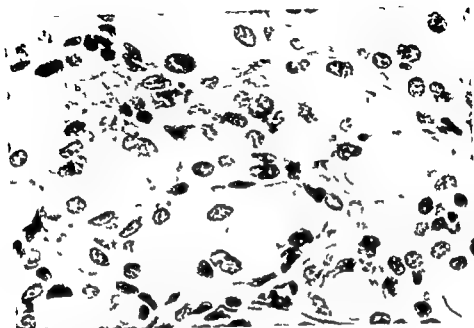


Fig 5 Thyroid tissue from a 17 day-old mouse that had received 4  $\mu\text{Ci}$   $^{131}\text{I}$  by intra venous injection of the mother on the 18th day of pregnancy. Polymorphic nuclei and foamy cytoplasm evident (H&E  $\times 500$ )

mice are given in Table 1 and Figs 6 and 7. The animals received  $^{131}\text{I}$  through the injection of 4  $\mu\text{Ci}$  to the mothers on the 18th day of gestation. The mean value for the total integrated dose was then 4 600 rad at the centre of the thyroids (WALINDER). The radioiodine was released rapidly (more quickly than with lower doses) and half the dose had been delivered within two days, in other words before the animals were born.

Table 1 and Figs 6 and 7 reveal that the growth of the thyroid glands was rapidly stopped with this dose, the reason being a hold up in epithelial cell division. It has been demonstrated (WALINDER & SJÖDEN 1971) that even a dose of 3 700 rad produces significantly lower thyroid weights two months after the injection of  $^{131}\text{I}$ , than those in the controls ( $p < 0.01$ ). During the seven days immediately following the injection there was a paucity of mitotic figures (Table 1). The cells were able to synthesize colloid more or less to the same extent as the unirradiated cells, an indication that the functional activity of the surviving epithelium had not been appreciably affected by the radiation. Cell division started again one week after the injection and soon presented approximately the same mitotic index as in the controls. The difference in the slope of the curves

Table 1

*Quantitative development of the foetal and juvenile thyroid gland. The animals in the group  $^{131}\text{I}$  irradiated mice were given  $4 \mu\text{Ci } ^{131}\text{I}$  the mean integrated dose to the central parts of the gland ( $\bar{D}_{az}$ ) was calculated to be 4 600 rad. The density of all thyroid components was assumed to be  $1 \text{ g/cm}^3$ .*

Age of animals (days)	Thyroid weight (mg)	Weight of epithelium ( of (mg) thyroid wt)	Weight of colloid ( of (mg) thyroid wt)	Weight of stroma and blood ( of (mg) thyroid wt)	Number of epithelial cells ( $\times 10^4$ )	Mean weight per epithelial cell $10^{-6}$ mg	Mitoses counted in 10 000 cells			
Controls										
18 day old fetus	0.20	84	0.17	3	0.006	13	0.03	15	11	50
1	0.25	77	0.19	13	0.03	10	0.03	17	11	30
5	0.36	74	0.27	16	0.06	10	0.04	24	11	20
11	0.60	69	0.41	20	0.12	11	0.07	39	11	30
38	1.76	49	0.86	38	0.67	13	0.23	63	14	
60	2.50	45	1.11	42	1.05	13	0.33	72	15	
Irradiated mice										
1	0.18	73	0.13	13	0.07	14	0.03	13	10	1
3	0.19	75	0.14	10	0.02	15	0.03	12	12	6
5	0.22	72	0.16	14	0.03	14	0.03	15	11	20
11	0.40	62	0.25	20	0.08	18	0.07	20	13	30
17	0.72	56	0.40	24	0.17	20	0.14	26	15	1
38	1.41	40	0.56	35	0.49	25	0.35	42	13	
60	1.89	32	0.60	41	0.77	27	0.51	48	13	

from control animals and from irradiated animals in Fig. 7 indicates that there was however continued cell death.

The percentage of stroma and blood was fairly constant in the control mice whereas the corresponding value for the irradiated animals increased with age apparently due to rising hyperaemia rather than to fibrotic changes. The relative occurrence of stroma cells was approximately the same in the irradiated mice as in the controls. Of the total number of cells counted in the 60 day old control mouse 20 per cent were stroma cells (18/10) the corresponding figure in the irradiated 60 day-old mouse being 21 per cent (13/10). Only about 10 per cent of the total number of cells in the thyroid gland in the 18 day foetuses were stroma cells.

Fig. 8 gives the cumulative number of secants with  $\varphi_c$  values smaller than and equal to the corresponding abscissa values as a function of  $\mu$  ( $\times$ ) for irradiated and unirradiated thyroid epithelium in the 60-day-old mice in Table 1. Despite the fact that the dose to the apices of the lobes and the isthmus was lower than in the more central parts of the gland, no skew symmetry of the

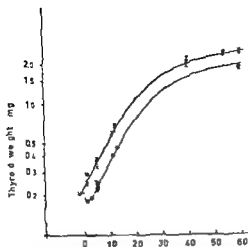


Fig 6 Thyroid weights of foetal and juvenile mice  $\times$  denotes unirradiated controls and  $\bullet$  irradiated mice The dashed line indicates the supposed course of the curve during the first week after the injection of  $^{131}\text{I}$  The vertical lines through some of the points denote  $\pm$  standard errors of the mean weights of several glands

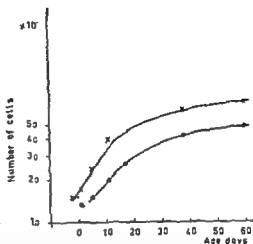


Fig 7 Number of epithelial cells in foetal and juvenile mice  $\times$  denotes unirradiated controls and  $\bullet$  irradiated mice The dashed line indicates the supposed course of the curve during the first week after the injection of  $^{131}\text{I}$

curves was noted. Measurements in the isthmus revealed that  $\varphi_e$  values in that region were more like those of the controls than was the case for central parts of the lobe. The reason why the distribution curve for the relative occurrence of irradiated epithelium was linear must be that the volumes in which the  $\varphi_e$  values deviating from the  $\epsilon$  in the central parts of the lobe were measured were too small to have any noticeable effect on the shape of the curve. The same linearity in the distribution curve was obtained for the juvenile mice and in the measurements of the relative occurrence of colloid and stroma and blood. Thus all control determinations of the weight of the different thyroid components in mice whose thyroid weights could be ascertained by weighing i.e. in mice of 11 days of age or over could be based on the previously deduced equation (2). It then emerged that the  $\varphi_e$ -values varied less than the thyroid weights; in other words the differences in the latter were not to any great extent due to variations in the relations between the different components in the thyroid tissue.

*Determination of cell survival with  $^3\text{H}$  TdR.* Ten pregnant females were each given  $10 \mu\text{Ci } ^3\text{H}$  TdR, injected intravenously on the 17th day of pregnancy.



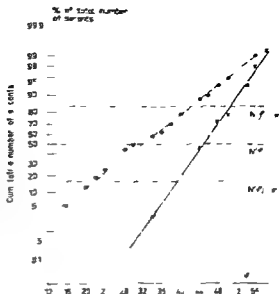


Fig. 11. The cumulative number of secants in irradiated and unirradiated mouse thyroids 60 days of age plotted in a normal distribution diagram as a function of the percentage of the secant lengths that have passed over epithelial nuclei. Each point denotes the number of secants in per cent of the total number of secants with values smaller than and equal to its abscissa value.

3. In 5 of the mothers, 4  $\mu\text{Ci}^{131}\text{I}$  were injected on the 18th day of pregnancy. For the determination of the  $^3\text{H}$  TdR level the measurements covered a time of 100 minutes. As the background for these measurements was 20 cpm, the standard deviation was  $0.1 \sqrt{N} = 30$  cpm, where  $N$  represented the values given in Table 2. The deviation was thus always less than 1 per cent of the measurement values mentioned. The tritium activity in the irradiated thyroid glands of mice that were killed at the age of 38 days was a factor 1.5 lower than in the unirradiated controls of the same age. Comparison with Table 1 discloses that this factor corresponds to the relation between the number of epithelial and the number of mesenchymal cells in irradiated and unirradiated mice at the age of 38 days. The results also indicate that the tritium activity in the thyroids did not decline between the 38th and 113th days of life in the controls nor did it fall between the 38th and 70th days of life in the irradiated mice. Thus, no further cell death occurred between the 38th and 70th days of life in the irradiated thyroid glands. An interpretation of this result follows in the discussion on the reliability of the method.

#### Adult mice

**Histologic radiation effects** The gonitrogen treatment brought about an increase in the number and size of the epithelial cells in the thyroid. The colloid became

Table 2

*Thyroid retention of  $^3\text{H}$  TdR injected on the 17th day of gestation*

Number of mice	Sex	Age at sacrifice (days)	Amount ( $\mu\text{C}$ ) of $^3\text{H}$ TdR injected	Total central dose thyroid rad	Thyroid weight (mg)	$^3\text{H}$ TdR CPM
15	8 ♂ + 7 ♀	38	4.0	4600	20.11	344
15	8 ♂ + 7 ♀	38	—	—	26.4	506
5	♂	70	4.0	4600	11.0	110
5	♂	70	—	—	17.8	169
5	♀	70	—	—	15.2	172
5	♀	113	—	—	21.7	179

vacuolated and often contained cellular residues (Fig 9). The cytoplasm of the hypertrophied epithelium was also vacuolated and was foamy. There was a marked variability in nuclear size and stainability, particularly in the irradiated tissue, where large nuclei with centrifugal distribution of chromatin as well as hyperchromatic and pyknotic nuclei were present (Fig 9b). Large hyperchromatic nuclei of the type depicted at the bottom of Fig 9b were not observed in the controls. The most important difference between the irradiated and unirradiated glands however was the absence of mitotic figures in the former.

The prolonged goitrogen treatment (42 days administration of 3 ATA) gave rise to widespread tissue degeneration in the thyroid glands. The differences between irradiated and unirradiated tissue were more accentuated than after 20 days of PTU administration. Most of the follicles had lost their colloid and literally become coalescent, the bizarre nuclei suggested widespread necrobiosis.

The results of the morphometric investigations in the thyroid glands of the adult mice are given in Table 3 and Fig 11. The mice included in Table 3 were 120 days old at the time of the radioiodine injection. At that time the relative amount of colloid and the number of epithelial cells in their thyroid glands differed from the corresponding figures in Table 1 for 60 day-old mice. In all probability, these differences are to be explained at least in part, by the age dependent and seasonal changes of the thyroid tissue in the CBA mouse described elsewhere (WALINDER, SJÖDEN & JONSSON 1971).

The mean value for the maximum dose to the central parts of the thyroids was calculated from previously deduced formulae (WALINDER) as well as from the thyroid weights in Table 3 and the retention values from a parallel group of mice investigated at the same time as the experimental animals (see Fig 12).

No significant effects on the glandular epithelium were noted during the first week. The growth that could be observed during this first period and that ob-

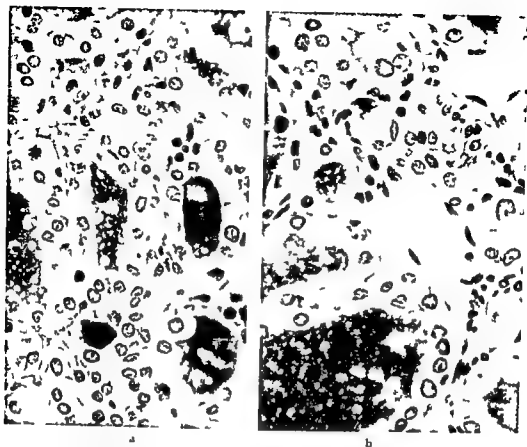
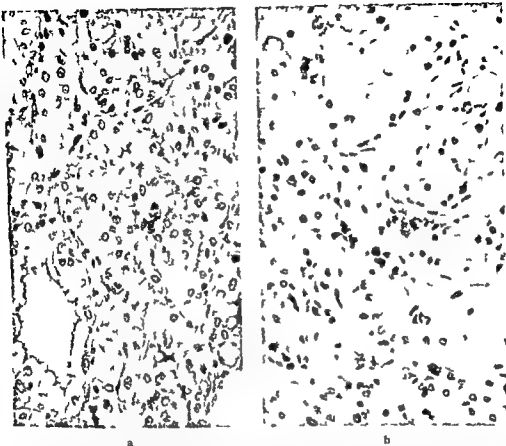


Fig 9 Thyroid tissue after 25 days treatment with PTU (cf normal thyroid tissue in fig 3). The tissue in (b) was also irradiated with  $\bar{D}_m = 8400$  rad from  $^{125}\text{I}$  injected 1 day before the administration of PTU. The mitotic frequency is relatively high in the unirradiated gland whereas no mitotic figures are evident in the irradiated tissue. Some of the large nuclei in the irradiated tissue are pale with chromatin margination while others are hyperchromatic. The colloid is vacuolated and contains cell fragments with pyknotic nuclei (PAS  $\times 500$ ).

erved in the nongonitrogen challenged controls was due mainly to the continuous colloid accumulation that takes place in the CBA mouse's thyroid, as described elsewhere (WALINDER, SJÖDEN & JONSSON). From the second week after the radioiodine injection and onwards, however, the thyroid glands of the gonitrogen challenged mice rose significantly in weight. This was due both to a gain in the number of epithelial cells and to their size. Whereas the size of the cells did not seem to have been affected by the radiation, the new formation of epithelial cells had been retarded in the mice given  $^{125}\text{I}$  as compared with the situation in the unirradiated PTU controls. This was also reflected in the fact that 14 days after



a

b

Fig 10 Thyroid tissue after 42 days treatment with 3 ATA. The tissue in (b) was also irradiated with  $\bar{D}_{\text{max}} = 8100$  rad from  $^{131}\text{I}$  injected 1 day before the 3 ATA treatment. The pale colloid is highly vacuolated with many of the follicles devoid of or containing only a few fragments of colloid. After combined treatment with 3 ATA and  $^{131}\text{I}$  (b) colloid filled follicles are rare and the greater part of the tissue consists of a massive clump of cells showing widespread necrobiosis (PAS  $\times 310$ ).

the  $^{131}\text{I}$  injection the mitotic index in the irradiated thyroid cells was lower than the value for the thyroidal epithelium in the unirradiated mice. No mitotic figures were evident after 26 days in the thyroids of the irradiated mice among over 15 000 cells counted. The relative occurrence of epithelium, colloid, stroma and blood was fairly constant not only between different sections from the same gland but also between glands of different weights from mice in one and the same group that were killed simultaneously. This was observed irrespective of

Table 3

*Quantitative effects of  $^{131}\text{I}$  on PTU (propylthiouracil) challenged thyroid glands in adult mice. The mean integrated dose to the central parts of the glands was calculated to be 8 400 rad (PTU group) and 10 000 rad (non PTU challenged group) respectively. The density of all components in the thyroid is assumed to be 1 g/cm<sup>3</sup>. The weights of the glands are given with  $\pm$ SE of the mean.*

Goi- trogen regi- men	Time after injec- tion days	Mean weight per thyroid (mg)	Epithelium		Colloid		Stroma and blood		Num- ber of epi- thelial cells ( $\times 10$ )	Mean weight per epi- thelial cell ( $10^{-6}$ mg)	Mitoses counted in 10 000 cells
			Total weight ( $\circ$ )	Weight (mg)	Total weight ( $\circ$ )	Weight (mg)	Total weight ( $\circ$ )	Weight (mg)			
Controls											
PTU											
	1	3.60 $\pm$ 0.09	31.5	1.13	56.6	2.06	13.2	0.46	6.3	1.8	
	7	4.16 $\pm$ 0.19	28.2	1.17	58.7	2.44	13.1	0.54	5.9	2.0	
	14	5.75 $\pm$ 0.27	43.5	2.50	44.0	2.53	12.5	0.72	7.8	3.2	48
	26	7.41 $\pm$ 0.32	51.6	3.82	35.0	2.59	13.4	0.99	9.6	4.0	18
Irradiated mice											
PTU											
	1	3.60 $\pm$ 0.09	31.5	1.13	56.6	2.06	13.2	0.46	6.3	1.8	
	7	4.10 $\pm$ 0.15	30.0	1.23	57.0	2.34	13.0	0.53	6.0	2.1	
	14	4.87 $\pm$ 0.18	44.2	2.15	43.7	2.13	12.1	0.59	6.5	3.3	10
	26	5.51 $\pm$ 0.22	46.7	2.57	38.9	2.14	14.4	0.68	6.6	3.9	<1
Irradiated mice											
N1											
	1	3.60 $\pm$ 0.09	31.5	1.13	56.6	2.06	13.2	0.46	6.3	1.8	
	7	3.85 $\pm$ 0.18	28.6	1.10	57.4	2.21	14.0	0.54			
	14	4.05 $\pm$ 0.12	25.4	1.03	61.6	2.49	13.0	0.53			
	26	3.99 $\pm$ 0.15	27.5	1.10	60.1	2.40	12.4	0.49	6.4	1.7	

whether the mice had been irradiated or not. The same feature applied with respect to the number of cells per unit of area. Similarly to the results in the investigation of the relative occurrence of different components in the thyroid tissue of the mouse foetus and juvenile mice, no skew symmetry in the cumulative number of secants as a function of  $\varphi(x)$  was obtained. Control investigations in mice that had undergone exactly the same treatment as those included in Table 3 disclosed standard errors for the  $\varphi$  values that were much lower than those obtained by weighing the thyroids. The weights for the different thyroid components in Table 3 were obtained from eq. (2), and consequently in practice their standard errors were the same, in percentage terms, as those that have been advanced for the thyroid weights. This also applies to the calculation of the number of cells.

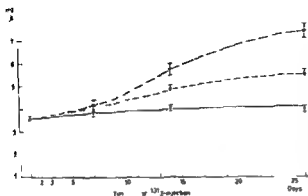


Fig 11 The increase in the thyroid weight as a function of the time after the injection of  $^{131}\text{I}$  in unchallenged animals (x---x) in animals given PTU alone (v---v) and in mice receiving  $^{131}\text{I}$  ( $\bar{D}_{\text{max}} = 8400$  rad) one day prior to the start of the PTU treatment (•---•). The vertical lines through the mean values denote  $\pm$  SE.

**Determination of cell survival with  $^3\text{H}$  TdR** The results from the experiments with  $^3\text{H}$  TdR are given in Table 4. The relation between the tritium activities in irradiated and unirradiated glands was approximately equal to that between the cell numbers in the respective glands. Table 4 indicates that mice that had received  $^3\text{H}$  TdR had the same thyroid weights as the control animals. This suggests that the tritium administration had no significant effect on the results.

### Discussion

**The goitrogen stimulation** The two goitrogenic substances that were used in the experiments, PTU and 3-ATA, differed slightly from one another in their action. The growth of the gland commenced at a slightly slower rate in the mice given 3-ATA than in those treated with PTU, due to a greater loss of colloid in the former group (cf. figs 9, 10). Furthermore, a high degree of hyperaemia was observed in the thyroids of the mice that had received 3-ATA. After 12 days treatment with this substance the gland was intensely red. However, 3-ATA possesses certain advantages over PTU and is less toxic (DOVIACH, personal communication). This is reflected, among other things, in the fact that the decrease in body weight that is often observed in CBA mice after PTU treatment does not occur with 3-ATA. In addition, it is easy with 3-ATA to obtain 1 per cent solutions without alkalization of the water, and this in its turn means that the mice consume larger quantities of water. The reason why PTU was chosen as the goitrogenic substance in the morphometric investigations was that this would allow direct comparisons to be made with the results of an earlier work (WALLINER & SJÖDÉN). On the other hand, 3-ATA was used for the prolonged goitrogen

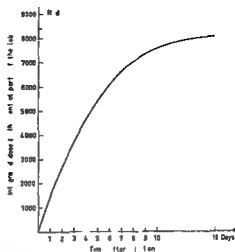


Fig 12 The dose of  $^{125}\text{I}$  accumulated in the centre of a thyroid lobe calculated from gland weights and retention values obtained from similar animals at the same time as the experimental group. The dashed line denotes the infinity dose ( $D_{\infty}$ ) calculated to be 8400 rad. The corresponding dose for non goitrogen challenged mice was 10 000 rad.

treatment because of the risk that the toxic action of the thiouracil might otherwise have had a deleterious effect on the results.

**Investigation of thyroidal cell death with  $^3\text{H}$  TdR** The thyroid cells were tritium labelled with  $^3\text{H}$  TdR before the injection of  $^{125}\text{I}$  into the mice. The following conditions must be fulfilled if total measurement of the tritium activity in the thyroid gland after exposure to  $^{125}\text{I}$  is to constitute a measure of the survival of the epithelial cells in the gland: (1) The incorporation of  $^3\text{H}$  TdR into the DNA of the cells must be complete before  $^{125}\text{I}$  is injected. (2) The only occurrence that could lead *in vivo* to a removal of the DNA bound tritium from the gland is that the cells die. (3) The re-utilization of  $^3\text{H}$  TdR from dead cells in surviving thyroidal epithelium must be negligible. (4) Radiation effects from  $^3\text{H}$  TdR must also be negligible. (5) It must be possible to make corrections for  $^3\text{H}$  TdR uptake and retention in stroma cells. (6) Before the measurement of the tritium activity in the scintillation counter all tritium labelled breakdown products must be removable without affecting the DNA activity.

(1) It has been demonstrated by several investigators that as early as a few hours after the administration of  $^3\text{H}$  TdR the tritium that is left in the cells has either been incorporated into the DNA or is present as acid soluble breakdown products, the latter being mainly in the form of tritiated water (LUNDIN 1963, CLEAVER 1967, AMANO *et al.* 1959). It is improbable that any further incorporation of tritium into the DNA takes place after 24 hours.

(2) Hydrogen losses must be considered unlikely, as labels in the 6 position of TdR are chemically very stable (EVANS & STANFORD 1963). An observation reported by PELC (1968), namely that DNA can be synthesized in cells that are not dividing, in other words also in cells that are not in the S period of the interphase,

Table 4

Thyroid retention of  $^3\text{H}$  TdR administered on the 12th day of 3-ATA treatment. After a further 7 days during which the mice had been maintained on an iodine deficient diet (without 3-ATA)  $^{131}\text{I}$  was injected and the animals again put on a 3-ATA regimen for 42 days beginning one day after the radioiodine injection. The determination of tritium activities was carried out in 5 (4) pooled thyroids.

Number of mice	Time after injection (days)	Injected amount of activity		$\bar{D}_m$ rad	Thyroid weight mg/mouse	Mean number of cells per thyroid gland		Mean tritium activity CPM/thyroid
		$^{131}\text{I}$	$^3\text{H}$ TdR			Epithelium	Stroma	
10	1	—	$10 \mu\text{Ci}$	—	$3.7 \pm 0.2$			1150
15	49	$3 \mu\text{Ci}$	$10 \mu\text{Ci}$	8100	$6.0 \pm 0.2$	$6.9 \times 10^4$	$2.6 \times 10^4$	654
14	42	—	$10 \mu\text{Ci}$	—	$11.2 \pm 0.7$	$1.2 \times 10^4$	$3.4 \times 10^4$	1046
20	42	—	—	—	$11.3 \pm 0.8$	$1.2 \times 10^4$	$3.2 \times 10^4$	

constitutes a serious objection to the uncritical use of  $^3\text{H}$  TdR labelling of DNA as a measure of cell survival in damaged tissue. This metabolic DNA as PELC calls it has a much shorter half life in the cells than their mitotic rate can explain (PELC 1968).

DEVIK & HALVORSEN (1963) demonstrated that the labelling index and the number of grains (in an autoradiograph) over the nuclei in the liver after hepatectomies were both higher than in normal livers after injection of  $20 \mu\text{Ci}$   $^3\text{H}$  TdR. The biologic half life for  $^3\text{H}$  TdR in the liver cells after hepatectomies was just over 400 days i.e. approximately the same as the expected half life calculated from the mitotic rates (PELC 1968). The initial excretion from normal livers, on the other hand was rapid (half life, 28 days). The constancy in the tritium activity in the thyroid gland that was observed in the present investigation after the administration of  $^3\text{H}$  TdR to mouse foetuses and goitrogen challenged mice (Tables 2 and 4), is not obtained in mice that have access without this stimulant to drinking water containing  $^3\text{H}$  TdR for one week. In the latter animals the activity in the thyroid declined by a factor 2 over a period of 48 days (WALLINDER, unpublished). It is thus improbable that DNA fractions of the type described by PELC were of any appreciable significance in the assessment of cell survival by  $^3\text{H}$  TdR labelling under the experimental conditions that prevailed in the present investigation.

(3) The results obtained (Tables 2 and 4) suggest that the re utilization of  $^3\text{H}$  TdR was negligible as the radiation induced decrease in the number of cells (compared with the controls) would otherwise not have been matched by a proportionally speaking correspondingly large decline in the activity (See also the discussion under item 5).



(4) The thyroid weights in the juvenile controls (according to Table 2) did not differ from those observed in untreated animals at 70 and 113 days of age (WALINDER). The goitrogen stimulated thyroid growth was not affected by  $^3\text{H}$  TdR (Table 4). Nor did comparisons between Tables 1 and 2 and between Tables 3 and 4 bring out anything to indicate that the tritium labelling had heightened the  $^{131}\text{I}$  effect.

(5) The observation made under item (2) that injected  $^3\text{H}$  TdR largely becomes incorporated in chromosomal DNA, both in mouse foetuses and in goitrogen stimulated adult mice, makes it reasonable to assume that cells which divide at the same rate also incorporate  $^3\text{H}$  TdR at the same rate, even if they are of different types. Thus, logically speaking, the initial tritium labelling of the epithelial cells ought to be percentually the same on an average as in the stroma cells, a line of reasoning that has previously been found to be correct in the goitrogen stimulated thyroid glands of rats (GREIG *et coll* 1969). The growth rate in epithelial and mesenchymal cells in the goitrogen challenged rat thyroid (GREIG *et coll* 1969) is similar to that observed in the goitrogen stimulated CBA mouse.

(6) It proved unnecessary in these investigations to extract DNA from the tissue before the activity was measured. The drying process with different alcohol baths effectively removed all acid soluble breakdown products. This could be demonstrated by homogenization of the tissue after alcohol drying in cold TCA, no tritium activity was obtained in the supernatant (WALINDER & WALINDER 1971).

### Conclusions

Both the experiments in mouse foetuses and juvenile mice and those in adult mice, suggested that the growth inhibiting effect of radiation on the thyroid tissue consisted mainly in a disturbance of cell division. Functionally and morphologically speaking, the non dividing epithelial cells of both adult and young mice are very resistant to radiation. During cell division, however, the risk that earlier undetectable damage will lead to death of the cell increases considerably, such death may occur either in the rapidly growing young thyroid, or on application of a goitrogenic challenge. The effect of irradiation on the goitrogen stimulated thyroids in the adult mice resembled that evident in the mouse foetuses given  $^{131}\text{I}$  on the 18th day after conception. It differed, however, from the latter through the fact that cell division in the irradiated glands did not begin again during the period covered by the investigation.

DOBBS *et coll* (1967, 1968) have demonstrated that the giant nuclei often observed in a growing and irradiated thyroid gland in man and in the rat contain

more than twice the diploid amount of DNA. This indicates that the DNA synthesis has also continued after the time the cell would normally have divided. Syntheses of DNA, colloid and, as has been demonstrated earlier (WALINDER & SJÖDEN) uptake of radioiodine are not such radiosensitive processes as inhibition of cell division. The bizarre nuclear deformities that appear when cell division is resumed in juvenile mice and in goitrogen challenged adult mice demonstrate however that serious damage occurs as a result of the radiation but does not manifest itself until after the cell has begun to divide.

The  $^3\text{H}$  TdR experiments indicated that a fairly high degree of cell death occurred in young and goitrogen challenged adult mice with the doses given in the present investigation. Thus the decrease in cell numbers was not caused by a temporary pause in mitosis in otherwise undamaged cells in the  $^{131}\text{I}$  irradiated thyroids; the relative cell decrease (as compared with the control values) that occurred was instead a consequence of lethal damage—an observation that received further confirmation in the non parallelism of the curves in Fig. 7 and the widespread and bizarre nuclear disturbances (Figs 4, 5, 9, 10). The relative increase in the number of stroma cells (from 22 to 27 per cent) in the goitrogenic stimulated and irradiated thyroids suggested that these cells were somewhat more resistant to irradiation than the epithelial cells; this confirms the observations reported by GREIG *et al.* (1969). A similar relative increase in the number of stroma cells was not observed in the growing and irradiated thyroid of the juvenile mice. The processes that were primarily responsible for the arrest of cell division and the subsequent death of the cells are not known. MOORE & COLVIN (1968) however have reported that the incidence of aberrant metaphase chromosomes in the thyroid cells is 40.3 per cent for the Chinese hamster sacrificed immediately after roentgen irradiation with 500 R; this is in other words half the lowest dose that produces significant deterioration of the goitrogen stimulated growth in the thyroid of the adult CBA mouse (WALINDER & SJÖDEN). They observed moreover, that there was a marked depression in growth in the thyroid cells cultured immediately after and 30 days following exposure to doses above 250 R. It is thus probable that it was largely chromosome damage that had caused the mitotic death in the thyroid of the CBA mouse after irradiation, and possibly this was also responsible, at least in part, for the arrested mitosis.

## SUMMARY

The effects of radiation on cell number and on the relative amount of tissue components in the thyroid gland were investigated morphometrically in immature mice and in adult goitrogen challenged CBA mice at different times after the injection of  $^{131}\text{I}$ . Cell survival was examined by measuring residual tritium activity in the glands of mice injected with tritium labelled thymidine before the administration of radioiodine. The

radiation induced growth arrest of the thyroid tissue appeared to be due mainly to mitotic death of the cells

## ZUSAMMENFASSUNG

Die Effekte von Strahlung auf verschiedene Gewebekomponenten der Thyreoidea von nichterwachsenen und erwachsenen kropferzeugend behandelten CBA Mäusen zu verschiedenen Zeitpunkten nach der Injektion von  $^{131}\text{I}$  wurden untersucht. Das Überleben der Zellen wurde durch Messen der verbleibenden Tritiumaktivität in der Thyreoidea von Mäusen, denen vor Gabe von Radiojod Tritium gezeichnetes Thymidin injiziert worden war, bestimmt. Die Strahleninduzierte Hinderung des Wachstums des Thyreoideagewebes scheint im wesentlichen durch den mitotischen Tod der Zellen hervorgerufen zu sein.

## RÉSUMÉ

Les effets quantitatifs de l'irradiation sur différents composants tissulaires de la glande thyroïde ont été étudiés sur des souris immatures et sur des souris CBA soumises à un goître génétique à différents intervalles de temps après l'injection de  $^{131}\text{I}$ . La survie des cellules a été étudiée par la mesure de l'activité résiduelle du tritium dans les glandes de souris ayant reçu une injection de thymidine marquée au tritium avant l'administration d'iode radioactif. L'arrêt de croissance du tissu thyroïdien dû à l'irradiation paraît résulter surtout de la mort mitotique des cellules.

## REFERENCES

- AMANO M, MESSIER B and LeBLOND C P. Specificity of labelled thymidine as a DNA precursor in autoradiography. *J Histochem Cytochem* 7 (1959) 153
- BELL E. I DNA. Its packaging into I somes and its relation in protein synthesis during differentiation. *Nature* 224 (1969) 326
- CLEAVER J E. Thymidine metabolism and cell kinetics. p. 56. North Holland Publ. Co. Amsterdam 1967
- DEVIK F and HALVORSEN K. Observations by biochemical analysis and autoradiography on labelled deoxyribonucleic acid in the normal and regenerating liver of mice. *Nature* 197 (1963) 148
- DOBYSN B M and ROBINSON L R. Desoxyribonucleic acid content associated with nuclear changes in  $^{131}\text{I}$  irradiated human thyroids. *J clin Endocr* 28 (1968) 875
- RUDD A E and SANDERS M A. Desoxyribonucleic acid synthesis in the irradiated and stimulated thyroid gland. *Endocrinology* 81 (1967) 1
- EVANS E A and STANFORD F G. Stability of thymidine labelled with tritium or carbon 14. *Nature* 199 (1963) 762
- FLÖDERL S. Untersuchungen über den Bau der menschlichen Hypophyse mit besonderer Berücksichtigung der quantitativen mikromorphologischen Verhältnisse. *Acta path microbiol scand* (1944) Suppl. No 53
- GREIG W R, SMITH J F B, DUGUID W P et coll. Assessment of rat thyroid as a radiobiological model. The effects of X irradiation on cell proliferation and DNA syntheses in vivo. *Int J radiat Biol* 16 (1969) 211

- HERBERG R J Determination of carbon 14 and tritium in blood and other whole tissues  
Analyst Chem 32 (1960) 42
- LUNDIN P M Tritiated thymidine Distribution and metabolism in the rat Acta isotop 3  
(1963) 181
- MOORE W and COLVIN M Chromosomal changes in the Chinese hamster thyroid following  
 $\gamma$  irradiation in vivo Int J radiat Biol 14 (1968) 161
- PELG S R Biological implications of DNA turnover in the higher organisms Acta histo-  
chem (1968) Suppl II p 41
- ROMEIS B Mikroskopische Technik Leibniz Verlag Munchen 1948
- UOTILA U Einfaches Verfahren zur Bestimmung des Volumens und Gewichtes des Schild-  
drüsenkolloids Acta Soc Med Duodecim 23 (1947) 77
- and HANNA O Quantitative histological method of determining the proportions of the  
principal components of thyroid tissue Acta endocr 11 (1952) 49
- WALINDER G Determination of the  $^{131}\text{I}$  dose to the mouse thyroid Acta radiol Ther Phys  
Biol 10 (1971) 558
- and SJÖDEN A M Effect of irradiation on thyroid growth in mouse foetuses and goitrogen  
challenged adult mice Acta radiol Ther Phys Biol 10 (1971) 579
- and JOHANSSON C J Ageing processes in the thyroid gland of the CB $\alpha$  mouse FOA  
Reports Vol 5 No 7 (1971)
- and WALINDER E Effects of  $^{131}\text{I}$  on the cellular survival in mouse thyroids Acta radiol  
(1971) Suppl No 310 p 235

## DOSE RATE DEPENDENCE IN THE GOITROGEN STIMULATED MOUSE THYROID

A comparative investigation of the effects of roentgen,  
 $^{131}\text{I}$  and  $^{125}\text{I}$  irradiation

by

G WALINDER, C-J JONSSON and ANNE MARIE SJÖDEN

Animal experiments have demonstrated that the radiation doses necessary to produce a certain damage to the thyroid gland are much lower after roentgen exposures than those needed to give the corresponding effects after administration of  $^{131}\text{I}$ . This is true both for radiation induced inhibition of epithelial proliferation (ABBATT et coll 1957, McCLELLAN et coll 1963, WALINDER & SJÖDEN 1971) and for neoplastic changes (DOMACH 1963, POTTER et coll 1960). Corresponding differences in the dose effect relationships have also been observed in man (SAENGER et coll 1963, SHELINE et coll 1962, DOLPHIN 1968).

The following three factors have been suggested as possible reasons why roentgen doses have such a markedly stronger effect than the corresponding  $^{131}\text{I}$  doses

1 *Inhomogeneous dose distribution*: The dose distribution in the thyroid from  $^{131}\text{I}$  which has been assimilated in the gland has been presumed to be inhomogeneous so that some parts of the tissue receive a much lower dose than

Submitted for publication 23 February 1971

that which is calculated on the assumption of a uniform distribution. By the term uniform dose distribution is meant in this connection only the absence of such local dose variations as are not dependent on the geometrical form of the source. It should be stressed that an inhomogeneity in the activity distribution does not necessarily mean that there is an equally considerable lack of uniformity in the dose distribution since contributions from the surrounding tissue often serve to compensate for small local variations in the activity.

2 *Dose rate dependence* The dose rate at roentgen exposures is usually much higher than that from  $^{131}\text{I}$  which has been incorporated in the thyroid.

3 *Perithyroidal damage* The injuries which are observed in the perithyroidal tissue after external irradiation might play some role as regards the extent of the terminal effects in the thyroid. This extra thyroïdal exposure has no counterpart when mouse thyroids are irradiated internally with  $^{131}\text{I}$ . The beta radiation accounts for more than 99 % of the  $^{131}\text{I}$  dose (cf WALINDER 1955, 1957) and half a millimeter outside the gland this has fallen to only 5 % of the surface dose (WALINDER 1971).

In an earlier investigation (WALINDER) it was demonstrated that the distribution of the dose in the thyroid gland of the CBA mouse after  $^{131}\text{I}$  administration is not so inhomogeneous that it could account for the great differences that have been observed in the glands between the effects produced by roentgen radiation and those occurring when  $^{131}\text{I}$  is used (WALINDER & SJÖDEN).

In order to investigate the significance of points 2 and 3 the effects of radiation by external roentgen rays and by internal  $^{131}\text{I}$  reported earlier by WALINDER & SJÖDEN, have been compared in the present investigation with the corresponding dose-effect relationship after injection with the short lived nuclide  $^{125}\text{I}$  ( $T_{1/2} = 2.26$  hours). In the final discussion a comparison is made by compilation between the necrotizing effects of external radiation and those produced after short term and long term internal irradiation with  $^{90}\text{Y}$  applicators in human pituitaries.

### Material and Methods

Male CBA mice were used for the experiments and the housing and management of the animals were the same as in earlier investigations (WALINDER). The  $^{131}\text{I}$  was given by intraperitoneal injection, and for the last 14 days before the injection the mice were maintained on an iodine deficient diet (roughly  $0.1 \mu\text{g I/g}$  food pellet). One day after the administration of the radioiodine propylthiouracil (PTU) was given in the drinking water, in the form of 0.1 % solutions. After 28 days on the PTU regimen the animals were killed with chloroform.

The radioiodine was delivered by the Radiochemical Centre Amersham, and the  $^{127}\text{I}$  was obtained in equilibrium with the mother nuclide,  $^{135}\text{Te}$ . The daughter nuclide,  $^{135}\text{I}$ , was separated from  $^{135}\text{Te}$  by the customary chemical methods and the yield was carefully measured and tested (at the Isotope Laboratory, Radiumhemmet Stockholm). All the mice in one and the same group were injected within a period of 10 minutes at times worked out on the basis of the measurements made during the testing of the yield.

*Determination of distribution of  $^{131}\text{I}$  dose in thyroid* For a comparison to be possible between the effects of the two nuclides  $^{131}\text{I}$  and  $^{135}\text{I}$ , the uptake of the iodine must take place rapidly and the distribution of the  $^{131}\text{I}$  dose in the tissue must be at least as uniform as that of the  $^{135}\text{I}$  dose during the greater part of the irradiation time. The dose distribution for the beta radiation from  $^{131}\text{I}$  was studied by the same method as was used for measurement of the dose distribution of  $^{131}\text{I}$  described earlier (WALINDER). As in the case of  $^{131}\text{I}$  radiations, the gamma dose from  $^{135}\text{I}$  is negligible in comparison with the beta dose, in the mouse thyroid.

The mice were killed with chloroform 0.5, 1 and 2 hours after 4.5  $\mu\text{Ci}$   $^{131}\text{I}$  had been injected. The thyroid glands were removed quickly, embedded in ice blocks and reduced by frozen sectioning to approximately half the lobe thickness. The film was pressed against the cut surfaces of the lobe halves and the exposure was carried out at  $-12^\circ\text{C}$ . The blackening of the film was measured with a microphotometer (Schnell photometer G II, C. Zeiss, Jena) connected to a recorder and the exposure times were adjusted so that the blackening would be within the region which, according to earlier investigations (WALINDER 1957, WALINDER), is linearly proportional to the dose.

*Uptake and retention measurements* The uptake and retention of  $^{131}\text{I}$  were measured both before the experiments were begun and in a parallel group of animals studied at the same time as the experimental mice. After the animals had been killed their thyroid glands were removed, weighed, and homogenized in saturated NaOH solutions. The activity in the homogenate was measured in a well type crystal connected to a two channel computer (Picker Autowell II System). By correcting for the differences in the decay rate for  $^{131}\text{I}$  and  $^{135}\text{I}$  the retention curve for the latter could be calculated.

*Dose calculations* On the assumption that the dose distribution was uniform the following calculations of the  $^{131}\text{I}$  dose in the mouse thyroid were carried out.

The calculations were based on the semi theoretical formulas deduced by LOEVINGER et coll (1956). The shape of the thyroid lobe in the CBA mouse deviates slightly from the drop model described by LOEVINGER, and may be represented by an ellipsoid of revolution with the radius of revolution equal to

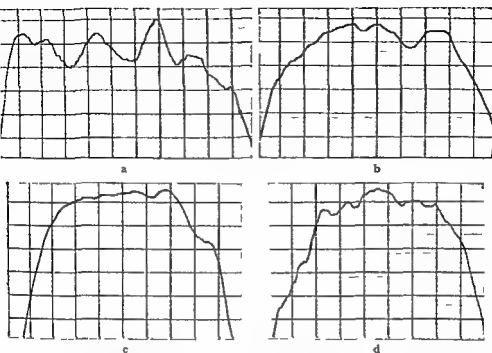


Fig. 1 Dose distribution in the thyroid 0.5 (a), 1 (b) and 2 (c) hours after intraperitoneal injections of  $^{131}\text{I}$  and 24 hours after  $^{131}\text{I}$  (d). As early as 1 hour after the injection of  $^{131}\text{I}$  the dose distribution is virtually as uniform as that obtained 24 hours after an injection of  $^{131}\text{I}$ .

half the length of the major axis. The lower part of the lobe narrows steeply, immediately before its transition into the isthmus (cf. Fig. 2).

As a first approximation in the calculations it was assumed that the thyroid lobe is spherical in shape. The beta dose to the centre of a sphere is obtained according to LOEVINGER *et coll.* from the formula given below, assuming that the dose distribution is uniform.

$$D_p(0, r) = D_p(0, \infty) \left\{ c^2 \left[ a \left( \frac{vr}{c} + \left( 1 + \frac{vr}{c} \right) e^{1-vr/c} - 3 \right) + 1 - a(1 + vr) e^{1-vr} \right] \right\}$$

where  $\left[ \right] \equiv 0$  for  $vr > c$ .

$D_p(0, r)$  is the dose at the centre of the sphere and  $D_p(0, \infty)$  the dose in an infinite radiation source with the same concentration of activity as in the sphere. The constant  $c$  is 1.5 for beta energies between 0.5 and 1.5 MeV and



Table 1

Physical constants for  $^{131}\text{I}$  and the calculated dose to the centre of a  $1.79 \text{ mm}^3$  large thyroid lobe at an activity concentration of  $1 \mu\text{Ci}$  per g tissue

$E_\beta$ (max)* MeV	Relative* occurrence	$\bar{E}_\beta$ ** MeV	$\nu^*$ cm/g	$\epsilon^*$	$\alpha$	$\frac{D_\beta(0 \text{ r})}{D_\beta(0 \infty)}$	$D_\beta(0 \text{ r}) \frac{\text{rad g}}{\text{h } \mu\text{Ci}}$
2.13	III	0.87	6.76	1.0	0.51	0.17	0.30
1.60	24*	0.60	10.1	1.0	0.76	0.25	0.32
1.16	23*	0.41	15.9	1.5	1.20	0.46	0.40
0.97	20	0.33	20.5	1.5	1.54	0.56	0.39
0.73	15*	0.24	30.9	1.5	2.33	0.74	0.38
Mean value							0.36

\* LOEVTINGER et coll (1956)

\*\* MARINELLI et coll (1947)

1 for beta energies between 1.5 and 3 MeV. The constant  $\alpha$ , III obtained from the following expression

$$\alpha = [3\epsilon^2 - (\epsilon^2 - 1)]^{-1}$$

in other words for the  $\epsilon$  values mentioned,  $\alpha$  will be equal to 1/3.35 and 1/3 respectively.

The apparent absorption coefficient,  $\mu$

$$\mu = \frac{18.6}{(E_{\text{max}} - 0.036)^{1.37}} \text{ cm}^2 \text{ per g tissue}$$

$D_\beta(0 \infty)$ , finally, is obtained from the expression

$$D_\beta(0 \infty) = 3.7 \cdot 10^4 \cdot \bar{E}_\beta \cdot 1.6 \cdot 10^{-8} \cdot 3600 = 2.13 \bar{E}_\beta \text{ rad/h}$$

with an activity concentration of  $1 \mu\text{Ci/g}$ .  $\bar{E}_\beta$  is the mean energy of the beta particles. As already pointed out the gamma doses in the small mouse thyroids are completely negligible in comparison with the beta doses from  $^{131}\text{I}$  and  $^{131}\text{I}$ .

The method of conversion of the centre dose in a sphere obtained in this way, into the corresponding dose in the ellipsoidal thyroid lobes will be discussed in the section dealing with the results of the dose calculations.

The total dose will finally be obtained by multiplying the calculated dose value for  $1 \mu\text{Ci } ^{131}\text{I}$  per g tissue by the thyroidal retention of the nuclide integrated during the radiation period.

## Results

**Dose distribution in the mouse thyroid.** Fig. 1 shows the relative doses measured in the cut surfaces of the thyroid lobes 0.5, 1 and 2 hours after the injection of  $^{131}\text{I}$ , and the distribution of the  $^{131}\text{I}$  dose 24 hours after the injection.

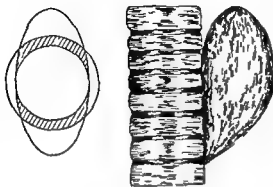


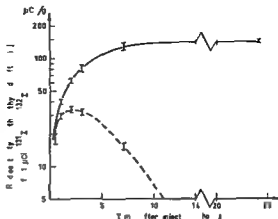
Fig 2 Sketch of a model (left) for calculating the dose to the centre of a thyroid lobe. The sketch (an ellipsoid of revolution) may be compared with the drawing (right) of a thyroid lobe seen through an operating microscope (magnification about 30X). The larger sphere in the sketch has the same volume as the ellipsoid of revolution. The calculations were based on the assumption that the centre-dose in the thyroid lobe was greater than that received from the part of the large sphere that is inscribed in the ellipsoid (i.e. the inscribed sphere + the shaded volume) but less than the centre-dose in a spherical radiation source of the same volume (and with the same activity) as the ellipsoid.

The relatively large variation in the  $^{131}\text{I}$  distribution observed in the thyroid tissue 0.5 hours after the injection evened up within the next half hour. Two hours after the injection of  $^{131}\text{I}$  the dose distribution in the thyroid showed greater uniformity than that obtained 24 hours after a  $^{131}\text{I}$  injection; this was probably to be explained by the higher beta energies of the  $^{131}\text{I}$  nuclide. Thus the assumption forming the basis for the calculations, namely that the dose distribution from  $^{131}\text{I}$  had during the greater part of the radiation period been at least as uniform as that obtained from  $^{131}\text{I}$  seems to have been correct.

**Dose calculations** The mean weight of the thyroids in the mice that were used for uptake measurements directly after the experiments, was  $3.58 \pm 0.09$  mg (mean weight  $\pm$  standard error). A sphere with a density of  $1 \text{ g/cm}^3$  and a weight of 1.79 mg (lobe weight = half the thyroid weight) has a radius of 0.753 mm. On the basis of this value and of the previously mentioned expression for  $D_p(0, \infty)$  and the physical constants for  $^{131}\text{I}$  given in Table 1 it was possible to calculate the dose at the centre of the thyroid lobe with a constant activity concentration of  $1 \mu\text{Ci/g}$ . The calculated dose values to the centre of the sphere will be seen in the last column in Table 1. The total dose at the centre was finally calculated by adding together the products obtained by multiplying the  $D_p(0, \infty)$  values for the different components by their relative occurrence in the decay scheme.

The centre-dose in the  $1.79 \text{ mm}^3$  large sphere was converted to the corresponding centre dose in the ellipsoid-shaped thyroid lobe of the same volume (the radius of revolution = half the major axis) using the following reasoning. The mean dose at the centre of the sphere was calculated to be 0.36 rad/h. The similarly calculated dose at the centre of a sphere of the same size as the sphere

Fig. 3 Retention curves for  $^{131}\text{I}$  (—) and  $^{123}\text{I}$  (---). The latter curve was calculated from the former curve which was received from direct activity measurements. Before the injection of  $^{131}\text{I}$  the mice had been kept on a low iodine diet for 14 days.



inscribed in the ellipsoid will be 0.30 rad/h, for an activity concentration of 1  $\mu\text{Ci/g}$  (Fig. 2). The dose contribution to the common centre from the spherical shell between the two spheres is thus 0.06 rad/h. The part of this shell lying within the ellipsoid constitutes 48 % of its total volume. As the relative proportion of the total shell volume that is located within the ellipsoid increases with decreasing radius of the outer sphere it is obvious that the dose contribution from the intracapsular shell between the 1.79 mm<sup>3</sup> large sphere and the inscribed sphere should be at least 0.03 rad/h or in other words that the dose rate at the centre of the thyroid lobe should lie between 0.33 rad/h and 0.36 rad/h counting with 1  $\mu\text{Ci}$  per g of tissue. In our calculations, we have used as a best estimation the figure 0.34 rad/h for the central dose in the ellipsoidal lobe. The integrated dose at the centre of the thyroid lobe will then be

$$0.34 \int_0^{\infty} f(t) dt$$

where  $f(t)$  is the activity per g of tissue as a function of time. The integral was solved graphically from the retention curve for  $^{131}\text{I}$  (Fig. 3).

When the retention curve for  $^{131}\text{I}$  was converted into the corresponding curve for  $^{123}\text{I}$  it was assumed that the half life was 8.05 days for the former nuclide and 2.26 hours for the latter (EMERY & VEAL 1954).

Three groups with 20 mice in each received injections of 14.8, 30.2 and 46.9  $\mu\text{Ci}$   $^{123}\text{I}$  respectively, and thus received an integrated mean dose of 1200 rad, 2400 rad and 3700 rad to the centre of the lobes. The corresponding doses at the periphery of the glands were 500 rad, 1000 rad and 1500 rad (LOE VINGER *et al.* 1956). One half of the total dose had been delivered after 4 hours and 90 % of it about 10 hours after the injection (Fig. 4).

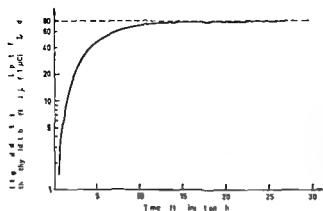


Fig. 4 The calculated integrated dose from  $^{131}\text{I}$ . Fifty per cent of the total dose had been delivered after about 4 hours and 90% of the dose after about 10 hours.

**Radiation effects** The radiation induced inhibition of the goitrogen stimulated thyroid growth was significant in all the experimental groups (Table 2)

Table 3 sums up the results described in the present paper and the corresponding results from the previously reported investigations on roentgen irradiation and the effects of  $^{131}\text{I}$  (WALINDER & SJÖDEN)

As seen from the table there was no difference between the dose response relationship after roentgen irradiations and after irradiation with  $^{131}\text{I}$ . These two types of exposure were definitely more effective than  $^{131}\text{I}$  radiation. This subject is taken up in the discussion of the results.

### Discussion

For direct comparisons to be possible between the growth inhibiting effects of different types of radiation on goitrogen stimulated thyroid tissue the reaction to the stimulation must obviously be the same in both cases. That this was not in the present investigation will be evident from the thyroid weights of the controls after the PTU administration (cf. Table 3). This may explain why as low an amount as  $14.8 \mu\text{Ci } ^{131}\text{I}$  which gave a dose of about 500 rad at the periphery and a maximum dose of 1200 rad at the centre of the lobe resulted in an effect which surpassed in significance even the effect of 1000 R of roentgen radiation (1 R = 0.95 rad ICRU 1964). This difference was probably only an apparent one however and would seem to have been due to differences in the response to the goitrogen challenge.

The differences noted between the effects in the goitrogen challenged thyroid gland of the CBA mouse after one and the same dose of  $^{131}\text{I}$  or of roentgen rays were accordingly in all essentials a consequence of the different lengths of the exposure times for the two types of radiation. Inhomogeneities in the distribution

Table 2

*Inhibition of goitrogen stimulated thyroidal growth with different doses of  $^{131}\text{I}$ . P denotes the significance of the growth inhibition*

No of animals	Injected amount of $^{131}\text{I}$ ( $\mu\text{Ci}$ )	$\bar{D}(\text{max})$ (rad)	Body weight (g)	Thyroid weight (mg) Means $\pm$ SE	p
20	—	—	30.7	9.12 $\pm$ 0.24	
20	14.8	1.200	29.7	7.10 $\pm$ 0.20	< 0.001
20	30.2	2.400	29.6	6.44 $\pm$ 0.23	< 0.001
20	46.9	3.700	29.7	6.24 $\pm$ 0.23	< 0.001

Table 3

*Compilation of the results obtained with different forms of radiation to the thyroid as reported in earlier investigations (WALINDER & SJÖDEN) and in the present paper (1 R = 0.95 rad ICRU 1964). Means  $\pm$  standard error. P denotes the significance of the growth inhibition*

Animal group	Dose (max)	Time between exposure (injection) and start of PTU	Thyroid weights (mg)*		p
			Irrad. mice	Controls	
1	1.500 R	14 days	7.0 $\pm$ 0.4	8.4 $\pm$ 0.3	< 0.01
2	1.500 R	1 day	6.4 $\pm$ 0.2	8.4 $\pm$ 0.3	< 0.001
3	1.500 R fractionated	500 R 14 days + 500 R 7 days + 500 R 1 day	7.3 $\pm$ 0.2	8.4 $\pm$ 0.3	< 0.01
4	1.000 R	14 days	7.7 $\pm$ 0.2	7.8 $\pm$ 0.2	—
5	1.000 R	1 day	6.6 $\pm$ 0.2	7.8 $\pm$ 0.2	< 0.01
6	4.700 rad I	14 days	7.0 $\pm$ 0.1	7.1 $\pm$ 0.2	—
7	6.600 rad $^{131}\text{I}$	14 days	5.9 $\pm$ 0.2	7.1 $\pm$ 0.2	< 0.01
8	3.600 rad $^{131}\text{I}$	1 day	7.8 $\pm$ 0.2	8.8 $\pm$ 0.3	= 0.01
9	5.000 rad I	1 day	5.8 $\pm$ 0.2	8.8 $\pm$ 0.3	< 0.001
10	1.200 rad I	1 day	7.1 $\pm$ 0.2	8.1 $\pm$ 0.2	< 0.001
11	2.400 rad I	1 day	6.4 $\pm$ 0.2	9.1 $\pm$ 0.2	< 0.001

\*  $\pm$  Standard error of the mean

PTU was given in the drinking water for 27–30 days (0.1 % PTU)

of the  $^{131}\text{I}$  dose in the thyroid tissue, or injuries in the perithyroidal tissue, seem to have played only a negligible part, if any, in this connection.

It seems unlikely that the corresponding differences which have been observed in human thyroid tissue after roentgen irradiation and exposure to  $^{131}\text{I}$  would

have a different cause from the dose rate dependence which has been demonstrated in the mouse. A similar dose rate dependence can in actual fact be deduced from the data in compilations on the irradiation of human hypophyseal tissue.

As has been shown by TOBIAS *et coll* (1955) and by LAWRENCE *et coll* (1958) the dose required to produce necrosis after irradiation of human hypophyseal tissue with 910 MeV  $\alpha$  particles, 340 MeV protons and 190 MeV deuterons is 26 000 to 30 000 rad. The exposures to the particles were given three times a week for 14 to 63 days. The particle beam was delivered in the form of microsecond pulses about 68 times per second and the dose rates were accordingly very high. Most of the patients received 200 to 300 rad per minute. Microscopic evidence of histologic damage was apparent in all patients who received over 20 000 rad regardless of the time interval between irradiation and death. Necrosis was present in those receiving 26 000 rad or more. Nevertheless in a case receiving 30 000 rad/14 days where the sella appeared to be empty upon macroscopic examination a thin layer of pituitary cells was observed microscopically (LAWRENCE *et coll* 1958). TOBIAS and his coworkers could find no RBE differences between 910 MeV  $\alpha$  particles, 340 MeV protons, 190 MeV deuterons and 200 kV roentgen rays, which is consistent with the fact that the LET values are of the same order of magnitude for these four kinds of radiation (cf. discussion by LAWRENCE *et coll* 1958). This has been confirmed in two more extensive investigations by LARSSON (1962) and STEVENSON (1969).

The corresponding effects of  $^{90}\text{Y}$  spheres implanted in the pituitary transnasally revealed that the dose necessary to produce hypophyseal necrosis was about 90 000 rad when the spheres were left in the gland (NOTTER 1959; NOTTER & WALINDER 1959). In the past few years, hypophysectomy with  $^{90}\text{Y}$  spheres has been replaced with  $^{90}\text{Sr}$   $^{90}\text{Y}$  applicators with the low-energetic  $^{90}\text{Sr}$  radiation screened off. The dose rate from these applicators has been so high that exposure times of less than one hour could be used (NOTTER *et coll* 1968). With a treatment time of 50 minutes the dose required to cause necrosis was around 30 000 rad.

The difference between the necrotizing doses on treatment with  $^{90}\text{Y}$  spheres and with  $^{90}\text{Y}$  applicators is a pure dose rate effect, as the irradiation qualities were identical and the radiation sources were so positioned as to avoid irradiation of extrahypophyseal tissue. The dose required to produce necrosis in human hypophyseal tissue is thus about 3 times greater when the dose is delivered during the course of a few days (the physical half life of  $^{90}\text{Y}$  is about 65 hours) than when it is delivered within 1 hour. When the dose necessary for producing necrosis in the pituitary from TOBIAS' external radiation sources is compared with that from  $^{90}\text{Y}$  spheres the dose ratio is found to be 3—4 i.e. a figure similar

to that found by us for roentgen and  $^{131}\text{I}$  irradiation of the growing thyroid tissue in mice

The radiation induced inhibition of the PTU stimulated thyroïdal growth is chiefly a result of mitotic death. It is of considerable interest to note that with an increase in the exposure time from some hours to several days the dose causing interphase death in human hypophyseal tissue is increased with the same factor as for the mitotic death in the mouse thyroid. It is hard to believe that the mechanisms underlying a mitotic death could be identical with those which cause an interphase death. The relation between the injuries and the recovery mechanism (or the requirement that there must be several radiation injuries close together in time to insure that the effects under study will arise) would, however, seem to be the same with both types of cell death. The dose necessary to destroy human thyroid tissue completely, by an administration of  $^{131}\text{I}$ , is of the same size (about 100 000 rad, Ministry of Health, England 1960) as the dose required on ablation of human hypophyseal tissue with  $^{90}\text{Y}$  spheres left in the gland (NOTTER & WALINDER 1959).

The severe injuries that were observed in the thyroid tissue of children on the Rongelap atoll after the 1954 bomb test at Bikini (CONARD *et coll.* 1966) cannot be attributed solely to incorporation of  $^{131}\text{I}$ , but were also a sequela of the short lived radioiodine nuclides which in all probability were of greater significance than their relative dose contributions gave cause to expect. The high external dose (175 rad) probably played a highly important role in determining the extent of the injuries. The increased frequency of thyroid carcinoma among the population of Hiroshima and Nagasaki gives further evidence of the significance in this respect, of short term external irradiation. Incorporation of radioiodine nuclides was inconsiderable in the Japanese population (WOOD *et coll.* 1968).

### Acknowledgement

The authors are indebted to Mr Lars Johansson at the Isotope Laboratory of Radiumhemmet for supplying us with radioiodine solutions for separating  $^{131}\text{I}$  from  $^{130}\text{Te}$  and for measurements of the  $^{131}\text{I}$  activities.

### SUMMARY

The doses of radiation necessary to inhibit gonadotropin stimulated thyroid growth in the CBA mouse are much lower after roentgen exposures than those needed to produce the same effects after  $^{131}\text{I}$  administrations. Similar differences in the effectiveness of the two types of radiation have been observed in several different animals as well as in man. A comparison of the dose-effect relationships after irradiation of the mouse thyroid with roentgen rays  $^{131}\text{I}$  and  $^{130}\text{Te}$  has shown that the difference in the effectiveness of the three

types of radiation largely consists of a dose rate effect. Inhomogeneities in the distribution of the  $^{131}\text{I}$ -dose and effects on the perithyroidal tissue produced by external irradiation are of little significance in this connection.

## ZUSAMMENFASSUNG

Die Strahlendosen die notwendig sind um den kropferzeugend stimulierten Zuwachs der Thyroidea der CBA Maus zu unterdrücken sind wesentlich niedriger nach Röntgenbestrahlungen als solche die notwendig sind um die gleichen Effekte nach  $^{131}\text{I}$  Gabe hervorzurufen. Ähnliche Unterschiede in der Effektivität dieser zwei Arten von Strahlung sind bei verschiedenen Säugetieren ebenso wie beim Menschen beobachtet worden. Ein Vergleich des Dosis Effekt Verhältnisses nach Bestrahlung der Thyroidea der Maus mit Röntgenstrahlen  $^{131}\text{I}$  und  $^{137}\text{Cs}$  hat gezeigt dass der Unterschied in der Effektivität der drei Typen von Strahlung im wesentlichen auf der Wirkung der Dosismenge beruht. Inhomogenitäten der Verteilung der  $^{131}\text{I}$  Dosis und Wirkungen auf das perithyreoidale Gewebe durch die externe Bestrahlung sind in diesem Zusammenhang von geringer Bedeutung.

## RÉSUMÉ

La dose de radiation nécessaire pour inhiber la croissance d'une thyroïde stimulée par un goitrogène chez des souris CBA est bien moindre pour les rayons de Roentgen que celle qui est nécessaire pour produire les mêmes effets après administration de  $^{131}\text{I}$ . Des différences semblables d'efficacité de ces deux types de radiation ont été observées sur plusieurs espèces animales différentes ainsi que chez l'homme. La comparaison des rapports entre la dose et l'effet sur la thyroïde des souris après irradiation par les rayons de Roentgen par  $^{131}\text{I}$  et par  $^{137}\text{Cs}$  a montré que la différence d'efficacité de ces trois types de radiation est principalement due à l'effet du débit de dose. Les hétérogénéités de la distribution de la radiation par  $^{131}\text{I}$  et les effets de l'irradiation externe sur le tissu perithyroïdien ont peu d'influence sur ces différences d'efficacité.

## REFERENCES

- ABBATT J D, DONIACH I, HOWARD FLANDERS P and LOGOTHETOPOLLOS J H. Comparison of the inhibition of goitrogenesis in the rat produced by X rays and radioactive iodine. *Brit. J. Radiol.* 88 (1957) 86.
- COWARD R A. Medical survey of the people of Rongelap and Utrik islands 13, 14 and 15 years after exposure to fallout radiation. Brookhaven National Laboratory, BNL-50220 (1970).
- , RALL J D and DUTROW W W. Thyroid nodules as a late sequela of radioactive fallout in a Marshall island population exposed in 1954. *New Engl. J. Med.* 274 (1966) 1392.
- DOLPHIN G W. The risk of thyroid cancers following irradiation. *Health Phys.* 15 (1968) 219.
- DONIACH I. Effects including carcinogenesis of  $^{131}\text{I}$  and X rays on the thyroid of experimental animals. A review. *Health Phys.* 9 (1963) 1357.
- EMERY E W and VEAL N. Radiation dosimetry of iodine 132. *Nature* 174 (1954) 839.
- ICRU Report No. 10a. Physical aspects of irradiation. NBS Handbook 85. National Bureau of Standards, Washington D.C. 1964.



- LARSSON H. On the application of a 185 MeV proton beam to experimental cancer therapy and neurosurgery. A biophysical study. Acta Univ. Upsalensis 11 (1962)
- LAWRENCE J. H., TOBIAS C. A. and BORN J. L. Hypophysectomy for advanced breast cancer using high energy particle beam, — proton and alpha particles. In: Radioactive Isotope in Klinik und Forschung. Strahlentherapie (1958) Sonderband 38 p. 245
- LOEVINGER R., JAPHA E. M. and BROWNELL G. L. Discrete radioisotope sources. In: Radiation dosimetry. Chap. 16. Edited by G. J. Hine and G. L. Brownell. Academic Press, New York 1956
- MARINELLI L. D., BRINCKERHOFF R. F. and HINE R. F. Average energy of  $\beta$  rays emitted by radioactive isotopes. Rev. mod. Phys. 19 (1947) 25
- MCCLELLAN R. O., CLARKE W. J., RAGAN H. A. et coll. Comparative effects of  $^{131}\text{I}$  and  $\gamma$  irradiation on sheep thyroids. Hlth Phys. 8 (1963) 1-63
- MINISTRY OF HEALTH, England. Radiological hazard to patients. Second Report of the Committee. HMSO London 1960
- POTTER G. A technique for destruction of the hypophysis using  $^{90}\text{Y}$  spheres. Acta radiol. (1959) Suppl. No. 184
- und WALINDER G. Dosismessungen an  $^{90}\text{Y}$  Kugeln zur Ausschaltung der Hypophyse. Strahlentherapie 110 (1959) 95
- MELANDER O. und DAHLGREN S. Klinische Ergebnisse nach interstitieller Bestrahlung der Hypophyse mit  $^{90}\text{Sr}$ . Strahlentherapie 136 (1963) 643
- POTTER G. D., LINDSAY S. and CHAIKOFF I. L. Induction of neoplasms in rat thyroid glands by low doses of radioiodine. Arch. Path. 69 (1960) 257
- SAENGER E. L., SELTZER R. A., STERLING T. P. and KEREKES J. G. Carcinogenic effects of  $^{131}\text{I}$  compared with  $\gamma$  irradiation—A review. Hlth Phys. 9 (1963) 1371
- SHELINE G. E., LINDSAY S., MCGORMACK K. R. and GALANTE M. Thyroid nodules occurring late after treatment of thyrotoxicosis with radioiodine. J. clin. Endocr. 22 (1962) 1
- STENSON S. Effects of high-energy protons on healthy organs and malignant tumours. Acta Univ. Upsalensis 73 (1969)
- TOBIAS C. A., ROBERTS J. L., LAWRENCE J. H. et coll. Irradiation hypophysectomy and related studies using 340-MeV protons and 190-MeV deuterons. Peaceful Uses of Atomic Energy. Proc. of the Internat. Conf. in Geneva, 10 (1955) 95
- WALINDER G. Colloidal  $^{75}\text{As}_2\text{S}_3$ . Its use and possible use in the treatment of papillomatosis of the urinary bladder. Acta radiol. 44 (1955) 521
- Measurements of the relative beta depth doses in tissue equivalent material. Acta radiol. 48 (1957) 68
- Determination of the  $^{131}\text{I}$  dose to the mouse thyroid. Acta radiol. Ther. Phys. Biol. 10 (1971) 558
- and SJÖDÉN A. M. The effect of irradiation on thyroid growth in mouse foetuses and gonadotropin challenged adult mice. Acta radiol. Ther. Phys. Biol. 10 (1971) 579
- WOOD J. W., TAMAGAKI H., VERHEIJN S. et coll. Thyroid carcinoma in atomic bomb survivors. ABCC Technical Report 4—68 (1966)

FROM RADIUMHEMMET (DIRECTOR PROF J EINHORN), KAROLINSKA SJUKHUSET,  
STOCKHOLM, SWEDEN AND THE ONCOLOGICAL INSTITUTE (DIRECTOR PROF ■  
RAVNIHAR), LJUBLJANA, YUGOSLAVIA

---

## IMMUNOGLOBULINS IN CARCINOMA OF THE UTERINE CERVIX

by

S PLESNIGAR

In recent years the problem of immunologic competence in patients with solid tumours has attracted much attention. Investigations using different microbial antigens permit the conclusion that in patients with solid tumours the delayed hypersensitivity is impaired (LAMB et coll 1962, SOLOWAY & RAPAPORT 1965, GROSS 1965, KRANT et coll 1968). Similar results have been obtained using cross-reacting chemicals like 2,4-dinitrochlorobenzene (LEVIN et coll 1964, KRANT et coll 1968).

In contrast to the frequent decrease in the cell mediated immunity, the ability of patients with malignant tumours to respond to antigenic stimuli leading to the formation of humoral antibodies seems to be relatively well preserved. A reduced response to primary immunization with tetanus toxoid has been reported (LYTTON et coll 1964) but other authors using different microbial antigens, have observed a relatively well preserved antibody formation capacity in patients with malignant disease (BALCH 1950, PARFENTIEV et coll 1951, LARSON & TOMLINSON 1953, SOUTHAM & MOORE 1954, LESKOWITZ et coll 1957, LEVIN

---

Submitted for publication 8 December 1970

et coll 1964) Additional information on the immunologic profile in patients with malignant diseases could be obtained by measuring serum immunoglobulin concentrations. Changes in IgG and IgM immunoglobulin levels have been observed in the serum of patients with hepatomas (McKELEY & FAHEY 1965), Burkitt's lymphoma (NGU et coll 1966) and lymphogranulomatosis maligna (GOLDMAN & HOBBS 1967). In a series of patients with bronchogenic carcinoma moderate increases in IgA levels have been observed only in cases with long survival (KRANT et coll 1968). Recently it has been found that antibodies cytotoxic to malignant melanoma cells are located largely in the IgM fraction of the patients' sera (LEWIS et coll 1969).

The present investigation is concerned with the serum IgG, IgA and IgM immunoglobulin levels in patients with carcinoma of the uterine cervix. The patients were divided into three groups according to the TNM classification. The immunoglobulin levels were simultaneously evaluated in a group of healthy controls. The determination of serum immunoglobulin levels was done by the radial immunodiffusion method.

*Material.* Seventy-seven consecutive cases of histologically verified squamous cell carcinoma of the uterine cervix were examined. Only previously untreated cases at first admission were included in the study. No patients presenting symptoms or signs of hepatic or renal involvement or with known distant metastases were included in this investigation. None of the cases had a monoclonal gammopathy.

The patients ranged in age from 30 to 75 years; the arithmetic mean for the group was 54 years (1 SD = 11.8 years).

The extent of the disease according to TNM classification is defined as follows (LEISSNER & NYSTROM 1968):

Stage I — Tumour infiltration confined to the cervix with subdivision to the microscopically observed lesion with no palpable mass of tumour.

Stage II — Tumour infiltration extending outside the cervix towards the vagina in the caudal direction or towards the parametrium in the lateral direction.

Stage III — Tumour extent exceeding the caudal third of the vagina or reaching to the pelvic wall.

In the stage I group 24 cases were included; the mean age for the group was 48 years, in the stage II group 31 cases; mean age 53 years, in the stage III group 22 cases; mean age 59 years. To the 36 to 70 year age group which corresponds to the age interval of the two groups of elderly healthy controls reported by JOHANSSON (1968), belonged 61 out of the 77 patients. Considering the 53 patients in stages II and III together, 8 patients did not belong to the age group mentioned above. The control group consisted of 38 female blood donors.

of ages ranging from 21 to 63 years. The arithmetic mean for the control group was 36 years (1 SD = 11.7 years). Out of the 38 women, 18 were in the 36 to 70 year age group.

**Methods.** Blood samples were collected when the extent of the disease was graded. The serum was separated from blood obtained without stasis from the antecubital vein. Aliquots were frozen at  $-20^{\circ}\text{C}$  until determination was performed at a later date.

Quantitative determination of IgG, IgA and IgM immunoglobulins was carried out by the radial immunodiffusion method (MANGINI et coll. 1965; McKEEL & FAHEY 1965), which had been slightly modified. All sera were investigated using this same method at the same laboratory. Equal amounts of 2% agar (Special Agar Noble, Difco) in phosphate buffer, pH 8.6 and of antiserums diluted to a concentration of 1:15 for IgG immunoglobulin and 1:30 for IgA and IgM immunoglobulin were mixed. The antiserum agar mixture was poured onto microscopic slides (25 mm  $\times$  75 mm for the determination of IgA and IgM immunoglobulins and 35 mm  $\times$  75 mm for the determination of IgG immunoglobulin) to form layers 1 mm thick. Using a gel puncher (LKB, Gel puncher No. 6807 A) two wells 2.3 mm in diameter were cut on each slide shortly before use and filled with 2  $\mu$ l undiluted serum. After incubation for 72 hours in a humidity chamber at room temperature the slides were removed and dried overnight. Amido-black was used for staining. The area of precipitation was determined by measuring four diameters at an angle of  $45^{\circ}$  whereupon the immunoglobulin concentrations were determined by comparing the surface area with the graphic curve plotted for the standard reference sera.

The reference sample was obtained by mixing the serum samples of 28 healthy controls and subsequently preparing aliquots in four dilutions. These dilutions were used for plotting the reference curves for each group of slides. The absolute concentrations of IgG, IgA and IgM immunoglobulins in the reference sample were separately determined using a stabilized standard human serum (Batch No. 369 A) from Behringwerke AG (Marburg/Lahn, Germany). For comparison a set of reference sera from Hyland Immunoplates at three different concentrations (Hyland Laboratories, Calif., USA), was used. The results with the different standards were fairly similar, and it was decided to accept as absolute values of the reference sample: 932 mg IgG/100 ml, 215 mg IgA/100 ml and 104 mg IgM/100 ml.

The statistical analysis was made by determining the arithmetic mean and standard error of the mean. Using the *t* test the significance of differences in the immunoglobulin levels was calculated by comparing first, immunoglobulin levels of each stage with the level of the control group and second, the value of the immunoglobulin level of one stage with that of each of the other two stages.

Table 1

*Comparison of immunoglobulin levels in different Swedish series of healthy women (mg/100 ml)*

	IgG	IgA	IgM
NORBERG (1967)	Mean value $\pm$ SD	Mean value $\pm$ SD	Mean value $\pm$ SD
Elderly women	1 055 $\pm$ 210	201 $\pm$ 78	76 $\pm$ 26
Blood donors			
women)	1 099 $\pm$ 217	184 $\pm$ 63	77 $\pm$ 30
JOHANSSON et coll	Arithmetic mean	Arithmetic mean	Arithmetic mean
(1968)	(range)	(range)	(range)
20—35 years	1 267	126	111
women	(756—1 688)	(82.5—185)	(54.3—159)
36—50 years	1 454	170	108
women	(961—2 037)	(101—264)	(37.0—272)
51—70 years	1 355	151	86.3
women	(910—1 961)	(87.1—212)	(31.1—160)
Present series	Arithmetic mean $\pm$ SE	Arithmetic mean $\pm$ SE	Arithmetic mean $\pm$ SE
	(range)	(range)	(range)
Blood donors	1 035 $\pm$ 26.6	175 $\pm$ 9.1	103 $\pm$ 4.8
women 21—63 years	(719—1 441)	(93—293)	(69—167)

## Results

In Table 1 the values of immunoglobulin levels in the control series are compared with data published for the Swedish population by other authors (NORBERG 1967 JOHANSSON et coll 1968). The mean concentration of IgG immunoglobulin in the sera investigated by the present author is close to that reported by NORBERG and somewhat lower than that presented by JOHANSSON. The IgA levels for the given group determined by the three authors do not show any large differences. In the present series of patients the values of IgM immunoglobulin are higher than those reported by NORBERG but close to the values of JOHANSSON. In the series presented by the latter author the immunoglobulin concentrations for the same sex vary in different age groups. NORBERG found no differences when values for IgG and IgM immunoglobulin concentrations of female blood donors were compared with the group of elderly women.

In Table 2 the mean concentrations for the three classes of immunoglobulins in patients with uterine cervix carcinoma are presented. The frequency distribution of serum immunoglobulin levels is illustrated in Figs 1 and 2. The stage I group value for IgG immunoglobulins was significantly higher than the control group value ( $p < 0.01$ ). In the stage II group the mean concentration of IgG immunoglobulin was lower, the stage III group levels were almost identical with those of the control group. The value of IgG immunoglobulin in stage I was

Table 2

*Immunoglobulin levels (mg/100 ml) in cases of uterine cervix carcinoma divided according to TNM classification*

TNM	No	Mean age (years)	IgG	IgA	IgM
			Arithmetic mean $\pm$ SE range	Arithmetic mean $\pm$ SE range	Arithmetic mean $\pm$ SE range
Stage I	24	48	1 456 $\pm$ 32.2 1 107—1 827	192 $\pm$ 8.6 67—280	111 $\pm$ 5.8 54—201
Stage II	31	55	1 256 $\pm$ 43.1 788—2 149	192 $\pm$ 9.2 90—315	97 $\pm$ 5.2 45—166
Stage III	22	59	1 030 $\pm$ 23.5 700—1 270	203 $\pm$ 6.8 120—295	73 $\pm$ 5.8 27—149
Controls	38	36	1 035 $\pm$ 26.5 719—1 441	175 $\pm$ 9.1 93—295	103 $\pm$ 4.8 69—167

also significantly higher than that in the stage III group ( $p < 0.01$ ). In all three stage groups the value of IgA tended to be higher than in the control group these differences were not significant however. No significant differences were observed when the mean values for all three stages were compared with the control value of IgA immunoglobulin. There was a significant difference between the mean concentration of IgM immunoglobulin for the stage I and II groups compared with the concentration of the control group. The value for the stage III group was significantly lower than that for the control group ( $p < 0.01$ ) and that for the stage I group ( $p < 0.01$ ).

### Discussion

A comparison of the age distribution of the patient group (30 to 75 years mean age 54 years) with that of the control group (21 to 63 years mean age 36 years) reveals a considerably greater proportion of younger women in the control group. The question arises whether the differences in immunoglobulin levels noted in the various groups analysed in this paper might simply represent an age dependent variation. As noted above the majority of stage II and III patients fall into the 36 to 70 year age group. This correlates well with the age distribution in two groups of elderly women presented by JOHANSSON (Table 1). In comparing IgG immunoglobulin levels there is agreement between our controls and those reported by NORBERG. On the other hand JOHANSSON's values are

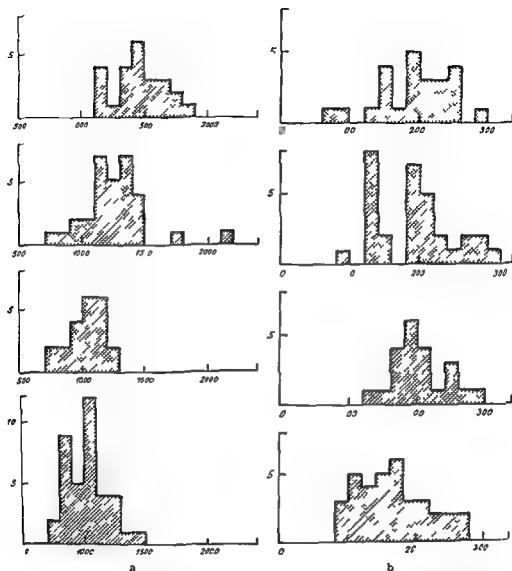


Fig 1 Frequency distribution of serum IgG (a) and IgA (b) immunoglobulin levels in 77 patients with carcinoma of the uterine cervix compared with 38 healthy controls. From top to bottom: Stage I (34 cases), Stage II (31 cases), Stage III (22 cases) and controls. Values expressed in mg per 100 ml.

higher than both the values in NORBERG's series and the series of controls in this report.

Nonetheless, no consistent age dependent differences could be found in either of the series of these authors. It seems reasonable to conclude that variations in

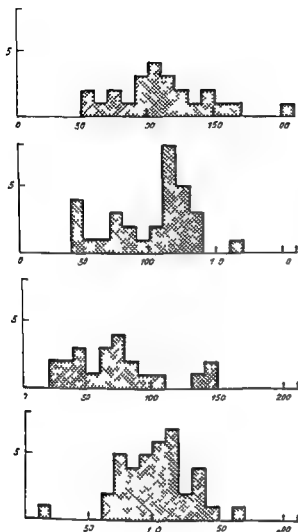


Fig 2 Frequency distribution of serum IgM immunoglobulin levels in 77 patients with carcinoma of the uterine cervix compared with 38 healthy controls. From top to bottom: Stage I (34 cases), Stage II (31 cases), Stage III (22 cases) and controls. Values expressed in mg per 100 ml.

IgG immunoglobulin concentrations could be related to the different stages in the progress of the cancer process. The IgM immunoglobulin levels, on the other hand, do appear to be age dependent as their tendency is to decrease with advancing age. Our series revealed the same trend, i.e. IgM immunoglobulin levels were lowest in stage III patients, which group comprised predominantly elderly females (mean age 59 years). The average IgM level in 18 females in the control series, in which the lowest values were noted, was 88 mg/100 ml. This figure is identical with the value observed in JOHANSSON's oldest group of



patients, and it closely approximates the value for elderly females described by NORBERG

When comparing the values for IgG, IgA and IgM immunoglobulin for the three healthy control groups (Table 1), differences were found in the immunoglobulin values of the various groups. A possible explanation of the observed differences might be the use of different standard sera used for determination of the absolute value of the reference sample. We observed that the IgG, IgA and IgM immunoglobulin values in the control group of the present investigation are close to the value for healthy adult females reported by STROOP *et coll*. The reported immunoglobulin levels in their series were as follows:  $\text{IgG} = 1.064 \pm 0.287 \text{ mg/100 ml}$ ,  $\text{IgA} = 174 \pm 74 \text{ mg/100 ml}$ ,  $\text{IgM} = 109 \pm 41 \text{ mg/100 ml}$ . Strop's method for the determination of immunoglobulin levels calls for standard sera similar to our own (STROOP *et coll* 1969).

A comparison of the serum immunoglobulin levels in the three different stages in patients with cervical carcinoma with those of healthy controls reveals higher immunoglobulin IgG levels in the earlier stages of the disease. The serum level of IgG immunoglobulin is dependent upon the intensity of antigenic stimulation and on the functional capacity of the antibody producing mechanism (ANDERSEN 1966). Consequently, the increase in IgG immunoglobulins in stage I cervical carcinoma might be the result of intensive antigenic stimulation. Inasmuch as the rate of degradation of IgG immunoglobulins appears to be directly proportional to its serum concentration, a decreased rate of degradation cannot be invoked to explain the elevated IgG immunoglobulin levels. It has been observed, however, that IgG immunoglobulins are catabolized at a faster rate in cancer patients than in healthy individuals (TEE & WATKINS 1967). Decreased IgM immunoglobulin concentrations have been reported in Burkitt's lymphoma (NGU *et coll* 1966), in Hodgkin's disease (GOLDMAN & HOBBS 1967) as well as in hepatomas (MCHELVY & FAHEY 1965) and in other solid tumours (DOSTALOVA *et coll* 1970). Decreased concentrations have also been observed in healthy elderly women (JOHANSSON *et coll* 1968). Since the majority of stage III patients are in the older age group, the mechanism responsible for decreased concentrations of IgM immunoglobulins is more likely related to immunologic deteriorations occurring with age, than it is to the disease *per se*. In contrast to the observed changes in IgG and IgM immunoglobulins, IgA immunoglobulin levels remain fairly constant regardless of the stage of the disease. Increased levels of IgM immunoglobulins have been observed in long term survivors of carcinoma of the lung, for example (KRANT *et coll* 1968). In the sera of patients investigated in the present report, increased levels of IgA immunoglobulins were observed as compared with those of healthy controls; the differences, however, were not significant.

The present investigation is confined to the determination of immunoglobulin levels by means of radial immunodiffusion in patients with cervical carcinoma. From these data it cannot be concluded whether the observed differences in IgG immunoglobulins, are due to alterations of the patient's immunologic status to antigens in some way associated with malignant disease, or to some other reason. The changes occurring in IgG and possibly IgM immunoglobulins, on the other hand, do seem to be related to the extent of the disease.

### Acknowledgements

The author wishes to thank Professor J. Einhorn and Associate Professor J. Zajicek for their help and cooperation in the work.

### SUMMARY

The levels of immunoglobulins IgG, IgA and IgM were measured in seventy seven untreated patients with carcinoma of the uterine cervix. The results were correlated with the clinical staging of the disease. Compared with control values immunoglobulins IgG were elevated in stage I of the disease ( $p < 0.01$ ). In the stage III group the mean concentration for the immunoglobulin IgM was below the value for the control series ( $p < 0.01$ ). These changes were statistically significant. In all three stages levels for IgA immunoglobulin were slightly elevated as compared with the healthy control; these differences were however not significant.

### ZUSAMMENFASSUNG

Die Konzentration der IgG, IgA und IgM Immunoglobuline wurde bei siebenundsiebzig unbehandelten Patienten mit Carcinoma Colli uteri gemessen. Die Ergebnisse wurden mit dem klinischen Stadium der Krankheit verglichen. Im Vergleich zu der Kontrollgruppe ist die Konzentration der IgG Immunoglobuline im Stadium I der Krankheit erhöht ( $p < 0.01$ ). Im Stadium III wurde festgestellt, dass die durchschnittliche Konzentration für IgM Immunoglobuline unter der Konzentration in der Kontrollserie war ( $p < 0.01$ ). Diese Unterschiede sind statistisch signifikant. In allen drei Stadien war die Konzentration der IgA Immunoglobuline etwas erhöht im Vergleich zu der Kontrollgruppe; diese Unterschiede sind jedoch nicht statistisch signifikant.

### RÉSUMÉ

Les taux d'immunoglobulines IgG, IgA et IgM ont été mesurés chez soixante-dix sept malades atteintes de cancer du col de l'utérus non traité. Les résultats ont été mis en corrélation avec le stade clinique de cette affection. Comparées aux taux des témoins les immunoglobulines IgG ont été élevées au stade I ( $p < 0.01$ ). Dans le groupe du stade III le taux moyen de l'immunoglobuline IgM est inférieur au taux de la série témoin ( $p < 0.01$ ). Ces différences sont statistiquement significatives. Aux trois stades les taux d'immunoglobuline IgA sont un peu élevés par rapport aux témoins sains mais ces différences ne sont cependant pas significatives.

## REFERENCES

- ANDERSEN S B The metabolism of human gammaglobulin *Dan med Bull* 13 (1966) 81
- BALCH H H Relation of nutritional deficiency in man to antibody production *J Immunol* 64 (1950) 397
- BARTH W F WOCHNER R D WALDMANN T A and FAHEY J L Metabolism of human gamma macroglobulins *J clin Invest* 43 (1964) 1036
- DOSTÁLOVÁ A SCHÖN E ALBELKA V and HOLÍK F Observation of immunoglobulins in the course of a tumour disease *Neoplasma* 17 (1970) 231
- FAHEY J L and MCKELVEY E M Quantitative determination of serum immunoglobulins in antibody agar plates *J Immunol* 94 (1964) 84
- GOLDMAN J M and HOBBS J R The immunoglobulins in Hodgkin's disease *Immunology* 13 (1967) 421
- GROSS L Immunological defect in aged population and its relationship to cancer *Cancer (Philad)* 18 (1965) 201
- HOBBS J R Secondary antibody deficiency *Proc roy Soc Med* 61 (1968) 883
- JENSEN K B Metabolism of human  $\gamma$  macroglobulin (IgM) in normal man *Scand J clin Lab Invest* 24 (1969) 205
- JOHANSSON S G O HOGMAN C F and KILLANDER J Quantitative immunoglobulin determination *Acta path microbiol scand* 74 (1968) 519
- KRANT M J MANSKOPF G BRANDRUP C S and MAPOFF M A Immunologic alterations in bronchogenic cancer *Cancer (Philad)* 21 (1968) 623
- LAMB D PILNEY F KELLY W D and GOOD R A A comparative study of the incidence of anergy in patients with carcinoma leukemia Hodgkin's disease and other lymphomas *J Immunol* 89 (1962) 555
- LARSON D L and TOMLINSON L J Quantitative antibody studies in man. III Antibody response in leukemia and other malignant lymphomata *J clin Invest* 32 (1953) 317
- LEISSNER H and NYSTROM C Cancer of the cervix uteri and aging *In* Cancer and aging p 189 Nordiska Bokhandels Forlag Stockholm 1968
- LESKOWITZ S PHILLIPINO L HENDRICK G and GRAHAM J B Immune response in patients with cancer *Cancer (Philad)* 10 (1957) 1103
- LEVY R H LANDY M and FREI E The effect of 6 mercaptopurine on immune response in man *New Engl J Med* 271 (1964) 16
- LEWIS M G IKONOPISOV R L NAIRN R C et coll Tumor specific antibodies in human malignant melanoma and their relationship to the extent of the disease *Brit med J* 1969 III p 547
- LYTTON B HUGHES L E and FULTHORPE A J Circulating antibody response in malignant disease *Lancet* 1964 I p 69
- MANCINI G CARONARA A O and HEREMANS J F Immunochemical quantitation of antigens by single radial immunodiffusion *Immunochimistry* 2 (1965) 235
- MCKELVEY E M and FAHEY J L Immunoglobulin changes in disease quantitation on the basis of heavy polypeptide chains IgG( $\gamma$ A) and IgM( $\gamma$ M) and of light polypeptide chains type K(I) and type L(II) *J clin Invest* 44 (1965) 1778
- NGU V A MCFARLANE H OSLEKOVA B O and UDZOZO I O K Immunoglobulins in Burkitt's lymphoma *Lancet* 1966 II p 414
- NORBERG R The immunoglobulin content of normal serum *Acta med scand* 181 (1967) 485
- PARFENTJEV I A CLIFTON E E and DURAN REYNALS F Alternation of immunological

- response in malignancy decline of proteus agglutinin *Science* 113 (1951) 523
- SCHWARTZ R S Immunoglobulin metabolism *Med Clin N Amer* 50 (1966) 1487
- SOLOWEY A C and RAPAPORT F T Immunologic responses in cancer patients *Surg Gynec Obstet* 121 (1965) 756
- SOUTHAM C M and MOORE A E Anti virus antibody studies following induced infections of man with West Nile Virus and other viruses *J Immunol* 72 (1954) 446
- STOOP J W ZEGERS B J M SANDER P C and BALLIEX R E Serum immunoglobulin levels in healthy children and adults *Clin exp Immunol* 4 (1969) 101
- TEZ D E H and WATKINS J Catabolism of serum G-globulins in a cancer patient and a normal volunteer *Brit med J* 1967 IV p 210

## FUNCTION OF THE RETICULOENDOTHELIAL SYSTEM IN WHOLE-BODY IRRADIATED MICE

by

B E SCHINDT and K H FRIKSSON

It is a generally accepted fact that whole body ionizing radiation increases the susceptibility of experimental animals to infection a number of different host defence mechanisms against infection have been considered responsible (KLEMPARSKAYA et coll 1961 LEONE 1962, SMITH et coll 1963 STONER 1967), the reticuloendothelial system in particular having recently aroused considerable attention Based on the assumption of a causal relationship between radiation resistance and the functional state of the reticuloendothelial system the phagocytic capacity of the latter has been the subject of intensive research and its other functional aspects have also been investigated (MICHEM & LOUITIT 1966, SELVARAJ & SEAFRA 1966, SCHAFER et coll 1965, STONER 1967 SBARRA 1970)

Reports on the effect of irradiation on the phagocytosis are, however, conflicting Irradiation has thus been reported both to depress (MARZANO et coll 1963, SABA & DI IUZIO 1969) and stimulate (FLEMMING et coll 1970 FRED et coll 1970 ANTONIJEVIC 1970 SIVIC 1970) reticuloendothelial system

---

Submitted for publication 10 January 1971

Table 1

*Phagocytic index for  $^{51}\text{Cr}$  RBC following injection into irradiated mice*

Exposure R <sup>1</sup>	n	Time post irrad days	Phagocytic index h value $\pm$ SE	p <sup>2</sup>	Corrected phagocytic index $\alpha \pm$ SE	p
Controls	16	—	0.381 $\pm$ 0.014	—	14.12 $\pm$ 0.39	—
R <sub>s</sub>	8	7	0.392 $\pm$ 0.039	> 0.05	14.95 $\pm$ 0.50	> 0.05
R	11	2	0.366 $\pm$ 0.017	> 0.05	14.63 $\pm$ 0.41	> 0.05
R	10	7	0.239 $\pm$ 0.020	< 0.001	11.12 $\pm$ 0.50	< 0.01
R	9	1	0.242 $\pm$ 0.030	< 0.01	12.42 $\pm$ 0.50	< 0.05
R	12	2	0.245 $\pm$ 0.014	< 0.001	11.64 $\pm$ 0.37	< 0.01
R	7	7	0.216 $\pm$ 0.025	< 0.001	11.07 $\pm$ 0.32	< 0.01

<sup>1</sup> R<sub>s</sub> = Sublethal R<sub>1</sub>  $\rightarrow$  LD and R = LD<sub>2</sub> irradiation<sup>2</sup> statistical significance compared to controls

$$\alpha = \frac{\text{body weight}}{\text{weight of liver + spleen}} \sqrt{h} \quad \text{where } h = \frac{0.693}{T/2}$$

phagocytosis as well as having no effect at all (GABRIELLI & AUSKAPS 1953, BENACERRAF et coll 1959 PAUMGARTNER et coll 1967). In view of the conflicting results most of which were obtained by determining the disappearance rate of indigestible test substances such as colloidal carbon, gold or chromic phosphate, an investigation of the effect of ionizing radiation on the system with a metabolizable test substance of marked biologic significance was undertaken. This investigation also formed part of a program examining the effect of combined injuries from nuclear explosions on the reticuloendothelial function. A computer program is now also presented for the calculation of the phagocytic index (h value) and certain statistical parameters.

**Materials and Methods** Inbred CBA male mice 70 to 100 days old and weighing 23.5 to 28.5 g were given food and water ad libitum and housed under strictly standardized conditions. Pentobarbital sodium (Mebumal) was administered intraperitoneally in a dose of 60 mg/kg before serial blood sampling.

Xenogen erythrocytes labelled with  $^{51}\text{Cr}$  (Na  $^{51}\text{CrO}_4$ , AB Atomenergi, Studsvik, Sweden) were used for the tests and will be called  $^{51}\text{Cr}$  RBC. The labelling procedure has previously been described in detail (SCHILDT 1970a). The specific activity of the test substance solution was approximately 2.2  $\mu\text{Ci}/100 \mu\text{l}/20 \text{ mg Hb}$ . SCHILDT employed human erythrocytes, since preliminary tests gave no evidence as to the existence of natural anti human RBC antibodies in the mouse serum. A low titre was however later present at careful serologic examinations so that the mouse serum was therefore examined for the

existence of antibodies against erythrocytes from ten rabbits. Rabbit RBC proved less incompatible than human RBC, a weak, non hemolytic antibody against the rabbit RBC, however, sometimes occurred in pooled mouse serum, its activity being strengthened when tested in active serum. It thus seems to be an antibody of the natural anti species type. Four rabbits against whose RBC the mouse serum presented the weakest reaction, were finally chosen as RBC donors for this and other investigations.

The validity of  $^{51}\text{Cr}$  RBC as a test substance for reticuloendothelial system phagocytosis was checked by the autoradiographic localization of the  $^{51}\text{Cr}$  RBC injected into the mouse (APPELGREN & SCHILDT 1970). Radioactivity was present in tissues containing the fixed reticuloendothelial system in whole body autoradiograms. Autoradiomicrograms of the liver disclosed a slight accumulation of  $^{51}\text{Cr}$  in the Kupffer cells.

The animals received whole body irradiation ten at a time in plastic wheels from a roentgen apparatus (MULLER MG 300) operating at 260 kV and 10 mA, a 0.5 mm Cu filter (inherent filtration 5 mm Al) was used at a dose rate of 74 R/min (universal dosimeter, Philips 37470) and a FTD of 45 cm. The animals were exposed to doses corresponding to LD<sub>0</sub> (approximately 660 R), LD<sub>10</sub>, and a sublethal dose (half the LD<sub>0</sub>), during an observation period of 30 days, based on the quarterly determinations of the roentgen resistance of CBA mice carried out at this institution.

The disappearance of the  $^{51}\text{Cr}$  RBC from the blood was determined in six groups of 15 animals each 1 to 8 days after exposure to varying doses from sublethal to LD<sub>0</sub>, according to Table 1. The method, described elsewhere (SCHILDT 1970a), includes the following essential features: 50  $\mu\text{l}$  of  $^{51}\text{Cr}$  RBC were injected intravenously and blood samples of 20  $\mu\text{l}$  each taken at 0.5, 1.0, 1.5, 2.0 and 4.0 min. Their radioactivity was measured in a well type scintillation detector (Picker Autowell II). As blood volume and hematocrit had previously been determined (SCHILDT 1971) the relative amount of the  $^{51}\text{Cr}$  RBC remaining in the blood could be calculated as a percentage of the total amount injected for each animal. Plotted against time on semilog paper, the initial observation points form a straight line, thus representing a mono-exponential function. The half time value ( $T/2$ ) and the phagocytic index

$$K = \frac{\ln C_1 - \ln C_2}{t_2 - t_1} \quad \text{according to BROZZI et coll. 1953)} \quad \text{was calculated by}$$

a computer as described below and  $K$  used as an index of the disappearance rate. A correction for the effect of possible weight changes of the principal organs of the reticuloendothelial system (liver and spleen) upon the disappearance rate, was made by calculating the corrected phagocytic index  $a = (\text{body weight/weight of liver and spleen})^{2/3} K$  (BENAGERRAF et coll. 1959),

this is thought to measure the phagocytic activity of the reticuloendothelial cells independently of variations in the size of these organs

The content of  $^{51}\text{Cr}$  in organs of the reticuloendothelial system was determined since changes in the content and distribution of the radioactivity earlier had proved to be a sensitive indicator of effects upon the function of the system undetected by the phagocytic index (SCHILDT 1970b). Two hours after injection of the  $^{51}\text{Cr}$  RBC the radioactivity in the liver, spleen, lungs and femoral bone marrow was measured. The organs were taken out, washed, weighed, placed in test tubes and their radioactivity measured in a well type scintillation detector (cf. Table 2).

A computer program was designed to calculate in each experimental animal  $T/2$  and  $K$  values for the intravenously injected  $^{51}\text{Cr}$  RBC and further to determine mean values and standard errors for the individual groups as well as evaluate the statistical significance of differences between them by means of Student's  $t$  test (Fig. 1).

Calculation of the experimental data according to this computer program offers two indisputable merits. First, it eliminates the subjective influence associated with the common graphic method when determining the disappearance rate. Secondly, it is far superior as regards speed and accuracy. The division of the program into two parts also permits checking of the credibility of the individual data and has proved to be of great practical importance.

The disappearance of  $^{51}\text{Cr}$  RBC in the blood represents initially a monoexponential function

$$C_t = C_0 e^{-Kt} \quad (1)$$

where

$t$  = time after injection in minutes,  $C_0$  = radioactivity at zero time ( $t_0$ ) and  $C_t$  = radioactivity remaining in blood at the time  $t$  as percentage of total activity injected.

Logarithmic transformation of (eq. 1) gives a linear relationship

$$\ln C_t = \ln C_0 - Kt \quad (2)$$

where

$K$  is approximated according to the method of least squares and the half time value ( $T/2$ ) is obtained as

$$T/2 = 0.693/K \quad (3)$$

when the natural logarithm is used.

The program described in detail elsewhere (ERIKSSON & HANSSON 1970), was written in Fortran IV for IBM 360/75 and consists of two parts (Fig. 1).



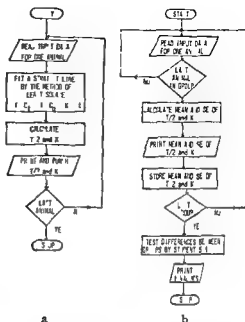


Fig. 1 Block diagram for computer program  
a) Part one b) Part two

The first part fits a straight line to the observation points and the slope is utilized to calculate  $T/2$ . The second part calculates  $\bar{X}$ , SE and  $t$  values. Input data to the computer were presented on punch cards. Results of the first part of the program were checked for credibility. The cards containing observations giving rise to unreasonable values, e.g. negative  $T/2$  were removed and the remainder were processed in the second part of the program.

## Results

The capacity of the irradiated animals to engulf the  $^{51}\text{Cr}$  RBC injected is significantly diminished (Table 1, Fig. 2). Sublethal irradiation does not influence the phagocytic capacity while exposure corresponding to  $\text{LD}_{10}$  significantly suppresses phagocytosis ( $p < 0.001$ ) although not until the seventh day post irradiation. Exposure to  $\text{LD}_0$  results in a significant ( $p < 0.01$ ) depression of the phagocytosis as early as 24 hours after irradiation. The capacity to clear the test substance from the circulating blood then stays at the same low level for at least one week. These results thus indicate that whole body irradiation gives rise to a dose dependent reduction of the phagocytosis of xenogen erythrocytes.

The corrected phagocytic index ( $\alpha$ ) was calculated to determine whether this influence might be caused by a weight reduction in the main organs of

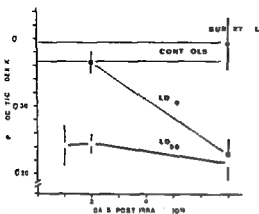


Fig 2 Phagocytic index for  $^{51}\text{Cr}$  RBC following injection into irradiated mice

the reticuloendothelial system Table 1 indicates that the  $\alpha$  index represents the same significant differences between irradiated and control animals as does the  $\lambda$  value. These results support the existence of a true depression of reticuloendothelial system phagocytosis following exposure to mid lethal and lower doses, the fact that sublethal exposure ( $0.5 \text{ LD}_{50}$ ) failed to affect the phagocytosis is related to the sharply sloping dose response curve.

The distribution of the material engulfed between the main organs of the reticuloendothelial system appears in Table 2. Two hours after the injection of the  $^{51}\text{Cr}$  RBC the radio content of the liver was significantly lower in mice exposed to  $\text{LD}_{10}$  and  $\text{LD}_{50}$ . Reduction of the radioactivity of the spleens became significant two days after exposure to  $\text{LD}_{50}$  of the animals. The radio-content of the lungs was likewise significantly reduced only in mice exposed to  $\text{LD}_{50}$  one or two days previously.

### Discussion

This investigation indicates that irradiation in the range  $\text{LD}_{10}$  to  $\text{LD}_{50}$  significantly reduces the capacity of the reticuloendothelial system of mice to identify and engulf foreign erythrocytes. Although the particular compound now being considered has not been used in any other similar investigation analogous results have been reported when test substances such as colloidal gold (MARZANO et coll 1963) or gelatinized  $^{125}\text{I}$  labelled tritolein (SABA & DiLUZIO 1969) have been used. With colloidal carbon, on the other hand irradiation was reported always to enhance phagocytosis (ANTONIJEVIC 1970, FRED et coll 1970, SLJIVIC 1970). This finding seems, however, to be dependent on the dose of the test substance administered (FLEMMING et coll

Table 2

*Organ-content of radio chromium three hours following injection of  $^{51}\text{Cr}$  RBC into irradiated mice*

Exposure R <sup>a</sup>	n	Time post irrad days	$^{51}\text{Cr}$ content/gram / of total amount inj			B W <sup>a</sup> WL+S
			Liver	Spleen	Lungs	
Controls	16	—	13.5 ± 0.8	12.5 ± 1.2	3.5 ± 0.3	20.7
R <sub>s</sub>	8	2	15.1 ± 0.9	11.2 ± 1.3 <sup>1</sup>	4.0 ± 0.3 <sup>1</sup>	20.6
R	10	2	8.6 ± 0.6 <sup>a</sup>	10.3 ± 0.9	3.1 ± 0.4	19.2
R <sub>s</sub>	9	1	7.4 ± 0.4 <sup>a</sup>	10.1 ± 1.1 <sup>1</sup>	2.2 ± 0.2	20.2
R	12	2	3.4 ± 0.2 <sup>a</sup>	4.5 ± 0.7 <sup>a</sup>	2.2 ± 0.5	18.8

*Statistical significance compared to controls*

p &gt; 0.05

■ &lt; 0.05

p &lt; 0.01

<sup>a</sup> p < 0.001<sup>b</sup> R<sub>s</sub> = sublethal R<sub>t</sub> = LD and R<sub>s</sub> = LD<sub>50</sub> irradiation  
ratio between body weight and weight of liver plus spleen

1970) Following identical exposures, the phagocytic activity was above the control level when determined by small carbon doses (8 to 16 mg) but below this level when measured by large carbon doses (50 mg). This observation is essential for the validity of conclusions to be drawn from investigations of reticuloendothelial system phagocytosis. Below a certain dose called a critical dose the disappearance rate ( $\bar{A}$ ) increases as the dose decreases until it has reached a maximum value (BIOZZI & STIFFEL 1965), the phagocytic capacity then exceeds the amount of test substance presented to the phagocyte. The blood perfusion of the organs of the reticuloendothelial system (because of its size mainly the liver with the spleen connected in series) under the circumstances is the limiting factor.

It is thus necessary in order to make it possible to draw conclusions with regard to the phagocytic capacity to challenge all reticuloendothelial cells by an injection exceeding this critical dose. The critical dose for  $^{51}\text{Cr}$  RBC has previously been determined as 7.8 mg hemoglobin with 10 mg as a standard (SCHILDT 1970a).

Too low a dose of the test substance has been employed in many previous investigations on the effect of irradiation on reticuloendothelial phagocytosis, as previously stated, small doses do not truly measure the phagocytic capacity. Another important factor is the blood perfusion of the reticuloendothelial

organs. Conclusions regarding the phagocytic capacity cannot be drawn for certainty unless the perfusion rate has been unchanged. Although information on the effect of whole body irradiation upon hepatic blood flow, has not been published, local irradiation (500 to 2000 R) seems to reduce the hepatic blood flow as calculated from the disappearance rate of radiogold (FRIDRICH & SCHAFER 1965). Preliminary data indicate a reduction in the nutrient liver blood flow in whole body irradiated mice as well as measured by the atraumatic densitometry of indocyanine green (DANIELSSON *et coll* 1971).

A depressive effect of irradiation on reticuloendothelial system function was demonstrated in the present investigation by a markedly reduced amount of radio-chromium in the principal organs of the reticuloendothelial system three hours after injection of the  $^{51}\text{Cr}$  RBC (Table 2). This was particularly marked as regards the liver. Even though the phagocytic index was unchanged two days after exposure to  $\text{LD}_{50}$  as compared to the control mice the hepatic content of  $^{51}\text{Cr}$  was significantly ( $p < 0.001$ ) reduced. The organ distribution and content of the test substance thus provide valuable information complementary to the phagocytic index. As pointed out also by others, generalizations as to the reticuloendothelial system function cannot be made by evaluating blood clearance activity only (MURSON *et coll* 1970, NUC & LEONHARDT 1970). Furthermore an altered tissue distribution has been observed despite the fact that no alternation in clearance rate was evident (GABRIELI & ALSAAPS 1953).

Radiation damage to the phagocytes is an unlikely explanation for the impaired phagocytic capacity after irradiation. It is well established that supralethal doses cause no visible morphologic signs of damage to reticuloendothelial cells (CLIMEDSON & NELSON 1960). Even after kilo-roentgen doses these cells in organ cultures of lymph nodes and thymus retained their phagocytic capacity (GILMAN & TROWELL 1965).

The role of cellular or humoral factors in the mechanism of the radiation induced impairment of phagocytosis was investigated by SABA & DILUZIO (1969). These authors stated that lethal irradiation selectively depresses hepatic and splenic phagocytosis. Opsonification of the test substance augmented its intravascular clearance in irradiated rats by enhancing bone marrow uptake while the liver and spleen uptake remained unaltered. The total bone marrow content of  $^{51}\text{Cr}$  from the radio-content of the femoral marrow proved to be  $18.5 \pm 2.4$  per cent of the total amount injected per gram marrow in controls as compared to  $13.7 \pm 1.1$  per cent in mice exposed 24 hours previously and  $10.4 \pm 2.1$  per cent 48 hours after exposure to  $\text{LD}_{50}$ . Exposed mice thus had a significantly lower bone marrow uptake in comparison with controls.

An increased capillary permeability might explain the apparent increase of the phagocytic activity previously reported after irradiation. This theory is supported by many observations. Excessive loss of albumin into the gastro intestinal tract following whole body irradiation is thus documented (BIRAE et coll 1962). Considerable amounts of colloidal carbon occurred in the intestinal mucosa of irradiated mice and were thought to explain the enhanced carbon clearance reported (FLEMMING & FLEMMING 1969). Increased capillary permeability has been established for albumin — Evans blue (LUNDBORG & SCHILDT 1971) and dextran molecules of varying sizes (ARTURSON & THOREN 1968). The leakage was correlated both to the exposure dose and the following time lapse. With the exposure in the LD<sub>0</sub> range, capillary leakage was evident as early as 1 to 2 days and reached a maximum during the second week after the exposure.

Irrespective of whether the phagocytic activity is increased or decreased, it must be stressed that no simple causal relationship exists between phagocytic function and radiation resistance (FLEMMING et coll 1967). As regards the susceptibility of irradiated animals to bacterial infection, the inflammatory response and the ability of the phagocytes to kill the ingested material are probably of even greater importance than the engulfment per se. There is no doubt that the inflammatory response is delayed and diminished (SMITH et coll 1963) and that the intracellular killing is markedly depressed (GORDON et coll 1955; SBARRA 1971) during the post irradiation period.

### Acknowledgements

The authors take this opportunity of thanking B. Gullbring who performed the serologic examinations.

### SUMMARY

The influence of whole body roentgen irradiation on the function of the reticuloendothelial system was investigated in mice by determining the phagocytic index for and tissue localization of <sup>51</sup>Cr labelled xenogen erythrocytes injected intravenously. Exposure to LD<sub>10</sub> reduced the phagocytic capacity significantly within 7 days while the same effect was evident as early as 1 day after LD<sub>50</sub>. Sublethal exposure (0.5 × LD<sub>0</sub>) failed to affect phagocytosis to any degree. Possible explanations for the impaired capacity after irradiation are discussed.

### ZUSAMMENFASSUNG

Der Einfluss einer Ganzkörper Röntgenbestrahlung auf die Funktion des retikuloendothelialen Systems der Maus wurde durch Bestimmung des phagozytären Index und die Gewebelokalisation <sup>51</sup>Cr gezeichneter fremder intravenös injizierter Erythrozyten untersucht. Bestrahlung mit einer LD<sub>10</sub> verringert die phagozytäre Kapazität signifikant innerhalb von 7 Tagen während derselbe Effekt bereits 1 Tag nach einer LD<sub>0</sub> zu sehen ist. Sublethal

bestrahlung ( $0.5 \times LD_{50}$ ) beeinflusst die Phagozytose in keiner Weise. Mögliche Erklärungen für die gestörte Kapazität nach Bestrahlung werden diskutiert.

## RÉSUMÉ

Les auteurs ont étudié l'influence de l'irradiation de tout le corps par les rayons de Roentgen sur la fonction du système réticulo-endothélial chez des souris en déterminant pour des érythrocytes xénogènes injectés par voie veineuse et marqués au  $^{51}\text{Cr}$  l'index phagocytaire et leur localisation tissulaire. L'exposition à une dose létale 10 pour cent réduit la capacité phagocytaire de façon importante avant le septième jour alors que le même effet est évident dès le premier jour après une dose létale 50 pour cent. Une exposition subléthale ( $0.5 \times LD_{50}$ ) n'affecte pas du tout la phagocytose. Les auteurs examinent les explications possibles de la diminution du pouvoir phagocytaire après irradiation.

## REFERENCES

- ANTONJEVIC M. A comparison of the effect of single and fractionated irradiation on the phagocytic function of the RES in normal and starved rats. *Strahlentherapie* 139 (1970) 228.
- APPELGREN L. E. and SCHILDT B. E. Autoradiographic localization of rabbit red cells injected into the mouse. *Acta path. microbiol. scand.* 78 (1970) 215.
- ARTURSON G. and THOREN L. Capillary permeability following ionizing radiation. In: *Combined injuries and shock*. Edited by B. Schiltdt and L. Thoren. Almqvist & Wiksell, Stockholm, 1968.
- BENACERRAF B., KIVY ROSENBERG E., SEBASTYEN M. M. and ZWEIFACH B. The effect of high doses of x irradiation on the phagocytic, proliferative and metabolic properties of the RES. *J. exp. Med.* 110 (1959) 49.
- BIOZZI G., BENACERRAF B. and HALPERN B. N. Quantitative study of the granulopoietic activity of the RES. *Brit. J. exp. Path.* 34 (1953) 441.
- and STIFFEL C. The physiopathology of the RE cells of the liver and spleen. In: *Progress in liver disease II*. Edited by H. Popper and F. Schaffner. Grune & Stratton, New York, 1965.
- BIRKE G., LILJEDAHN S. O., PLANTIN L. O. and WETTERFORS J. Acute radiation injury. Pathophysiological aspects of the massive leakage of albumin into the gastro intestinal tract. *Nature* 194 (1962) 1243.
- CLEVEDSON C. J. and NELSON A. The adult organism. In: *Mechanisms of radiobiology*. Vol. II. Edited by M. Frérea and A. Forsberg. Academic Press, New York, 1960.
- DANIELSON B., ERIKSSON K. H., KARLSMARK B. and SCHILDT B. Estimation of nutrient liver blood flow in mice by atraumatic densitometry. *Acta chir. scand.* 137 (1971) 621.
- ERIKSSON K. H. and HANSSON M. Fortran program for calculation of blood clearance rate in mice. (In Swedish.) Research Institute of National Defence. FOA 1 Report C 1355—45, 1970.
- FLEMING K. and FLEMING C. Korrelation zwischen Phagozytose Index K. und Überlebenszeit bei röntgenbestrahlten Mäusen. *Strahlentherapie* 138 (1969) 611.
- — und GRAACK B. Strahlenresistenz bei pharmakologisch veränderten Phagozytoseaktivität des RES. *Strahlentherapie* 133 (1967) 280.
- — und NOTHDLIFT W. The phagocytic activity of the RES of mice following whole body irradiation. *J. Reticuloendothel. Soc.* 7 (1970) 1.

An increased capillary permeability might explain the apparent increase of the phagocytic activity previously reported after irradiation. This theory is supported by many observations. Excessive loss of albumin into the gastro intestinal tract following whole body irradiation is thus documented (BIRKE et coll 1962). Considerable amounts of colloidal carbon occurred in the intestinal mucosa of irradiated mice and were thought to explain the enhanced carbon clearance reported (FLEMMING & FLEMMING 1969). Increased capillary permeability has been established for albumin — Evans blue (LUNDBORG & SCHILDT 1971) and dextran molecules of varying sizes (ARTURSON & THOREN 1968). The leakage was correlated both to the exposure dose and the following time lapse. With the exposure in the LD<sub>0</sub> range, capillary leakage was evident as early as 1 to 2 days and reached a maximum during the second week after the exposure.

Irrespective of whether the phagocytic activity is increased or decreased, it must be stressed that no simple causal relationship exists between phagocytic function and radiation resistance (FLEMMING et coll 1967). As regards the susceptibility of irradiated animals to bacterial infection, the inflammatory response and the ability of the phagocytes to kill the ingested material are probably of even greater importance than the engulfment per se. There is no doubt that the inflammatory response is delayed and diminished (SMITH et coll 1963) and that the intracellular killing is markedly depressed (GORDON et coll 1955, SBARRA 1971) during the post irradiation period.

### Acknowledgements

The authors take this opportunity of thanking B. Gullbring who performed the serologic examinations.

### SUMMARY

The influence of whole body roentgen irradiation on the function of the reticuloendothelial system was investigated in mice by determining the phagocytic index for and tissue localization of <sup>51</sup>Cr labelled venogen erythrocytes injected intravenously. Exposure to LD<sub>50</sub> reduced the phagocytic capacity significantly within 7 days while the same effect was evident as early as 1 day after LD<sub>0</sub>. Sublethal exposure (0.5 × LD<sub>0</sub>) failed to affect phagocytosis to any degree. Possible explanations for the impaired capacity after irradiation are discussed.

### ZUSAMMENFASSUNG

Der Einfluss einer Ganzkörper Röntgenbestrahlung auf die Funktion des retikuloendothelialen Systems der Maus wurde durch Bestimmung des phagozytären Index und die Gewebezirkulation <sup>51</sup>Cr-gezeichneter fremder intravenös injizierter Erythrozyten untersucht. Bestrahlung mit einer LD<sub>50</sub> verringert die phagozytäre Kapazität signifikant innerhalb von 7 Tagen während derselbe Effekt bereits 1 Tag nach einer LD<sub>50</sub> zu sehen ist. Sublethal

## MITOTIC INDEX IN HUMAN SQUAMOUS CELL CARCINOMA

by

R. SEAL, ANITA IMMERMAN and B. SHEPSTONE

The investigation of the cell kinetics (growth fraction and cycle time) of solid tumour systems both in human subjects and experimental animals necessitates serial biopsies and rests on the assumption that the mitotic index within each tumour both in regard to time and space is reasonably constant. This implies that in the absence of clinical variations in the appearance of tumours, the microscopic growth patterns in their clinically similar parts are the same. As it seemed that the knowledge available on these questions could be amplified it was decided that an investigation might be of value.

*Diurnal variation* The variation in the mitotic index at different times through the twenty-four hours of day and night in normal tissues is recognized but is absent in human large bowel carcinoma and squamous cell carcinoma in other regions (DUBLIN et coll 1940; DUBLIN 1944) as well as in squamous cell carcinoma in mice (BLUMENFELD 1943). However, only 14 human cases have been reported and to which a further 5 cases are now added. All the latter had histologically confirmed previously untreated extensive carcinomas involving

Submitted for publication 14 September 1970



Table 1

*Mitotic index (per thousand cells) in squamous cell carcinoma of the uterine cervix. Biopsies at six hour intervals. Ninety-five per cent confidence limits in brackets*

Case No.				
69 1387	23 (15-34)	25 (17-36)	19 (12-29)	21 (13-31)
69 1482	9 (5-17)	11 (6-19)	15 (9-24)	10 (5-18)
69 1488	9 (5-17)	10 (5-18)	7 (3-14)	
69 1504	12 (7-20)	12 (7-20)	7 (3-14)	6 (3-13)
69 1530	19 (12-29)	24 (16-35)	22 (14-33)	22 (14-33)

Table 2

*Mitotic index (per thousand cells) in squamous cell carcinoma of the mouth. Multiple biopsies at a single fixed time. Ninety-five per cent confidence limits in brackets*

Case No.				
69 369	16 (10-25)	19 (11-29)	16 (10-25)	14 (8-23)
69 353	7 (3-14)	4 (2-10)	5 (2-11)	
69 260	39 (28-52)	44 (32-58)	35 (25-48)	51 (38-66)
69 1432	9 (5-17)	10 (5-18)	12 (7-20)	
69 900	11 (5-19)	9 (5-17)	7 (3-14)	9 (5-17)
69 539	13 (7-22)	8 (4-15)	12 (7-20)	

the whole uterine cervix they were of the clinical exophytic type. No medication was given during the period the biopsies were made they were performed painlessly at four opposing points thus avoiding possible interference with the mitotic index by local anaesthetic and previous trauma due to biopsy. The procedures were carried out every six hours for a period of 24 hours (i.e. four per case). The specimens were fixed in Bouin's solution embedded in paraffin wax sectioned and stained with haematoxylin and eosin phloxine. One thousand cells from a representative section were counted, infected and necrotic areas being avoided. The results appear in Table 1 no diurnal variation was noted which accords with the findings of others. This finding is essential to investigations with DNA precursors in cell kinetics, as well as in those involving metaphase inducing agents for estimation of the potential tumour doubling time. Any tissue, such as normal tissue, that undergoes cyclic activity must be carefully assessed by these means since pulses of agents given at different regions of the diurnal pattern may be expected to produce widely differing results.

Table 3

*Mitotic index (per thousand cells) in multiple squamous cell carcinoma of the head and neck*

Case No		
69/475	Palate	16 ( 9—26)
	Tongue	21 (13—32)
69/660	Tongue	43 (31—57)
	Floor of mouth	26 (17—38)
68/1660	Tongue	4 ( 2—10)
	Antrum	9 ( 5—17)
69/554	Mouth	16 ( 9—26)
	Gland neck	26 (17—37)

*Topographic variation of mitotic index* It seemed possible that variation in the mitotic index within individual tumours at one fixed point in time might be possible in spite of the clinical appearances of the areas being similar. Accordingly multiple biopsies were performed within a few minutes of each other from 6 cases of histologically confirmed carcinoma of the mouth and handled in the manner already described. The results appear in Table 2 and indicate that there is no variation within a tumour where the clinical appearances are constant. Necrotic or grossly infected areas were again avoided in the biopsies and thus a reasonably constant type of cell population was examined. REFSUM & BERDAL (1969) have indicated that they have found topographic variations in the mitotic index in human squamous cell carcinoma but unfortunately gave no details, it is possible that their investigation did not have the same limits as the present one. Similar findings have been reported by IVERSEN (1967) but again no details appeared. SHIRAKAWA *et coll* (1970) in human malignant melanoma discovered variation in the mitotic index between the growing edge of melanoma deposits and the centre but not between similar areas of the tumours. These observations would be in accordance with the present ones and again are a necessary prerequisite for reliable investigations on cell kinetics.

*Mitotic index in simultaneously occurring tumours* This was examined in 6 histologically confirmed squamous cell carcinomas of the mouth (Table 3). While a wide variation between cases exists the mitotic indices in the two separate tumours in the one case appear to be similar. This is of great interest since it implies a common tumour host relationship since the tumours do not have a common origin (with the exception of the last case in Table 3). SHIRAKAWA

Table 4

*Mitotic index (per thousand cells) in infiltrating squamous cell carcinoma and exophytic squamous cell carcinoma of the mouth*

Infiltrating		Papillary	
69/475	16	69/1157	39
69/625	13	69/1286	17
69/657	22	69/ 716	7
69/744	25	69/1445	34
69/857	24	69/1484	22
69/717	18	69/1490	26
70/ 48	41	69/1611	24
Average	22.7	69/1667	20
		69/1683	29
		69/1689	29
		69/1843	32
		Average	25.4

et coll (1970) reported similar mitotic indices in several simultaneously occurring metastases from human malignant melanoma. These workers also stated that the mitotic index and labelling index was lower in infiltrating tumours where there was a chronic inflammatory cell infiltration and in the centre of larger masses. It is suggested that a host response mechanism might be at least partly responsible. The present case with the low mitotic index in both tumours had a considerable inflammatory cell infiltrate mainly of plasma cells as well as of lymphocytes in both tumours. Antilymphocyte serum will increase the growth of tumours in experimental animal systems (WOLF JURGENSEN et coll 1968; DE COSSE & GELFANT 1968) and it has been suggested that the presence of round cell infiltration of melanoma may be associated with a low labelling index (SHIRAKAWA et coll). It is therefore possible that the combination of low mitotic index and round cell infiltration might conceivably be used as a convenient measure of host resistance to malignancy.

The topographic variation in the mitotic index within tumours reported by others has already been noted. It therefore appeared that the same might apply in tumours of grossly different clinical appearances.

Accordingly the mitotic index was estimated in infiltrating squamous cell carcinoma and exophytic squamous cell carcinoma of the mouth. The results are given in Table 4. It is clear that no difference exists in the mitotic index between the two clinical types of tumour. This is unexpected since the blood supply to the papillary type of tumours might be expected to be improved and

thus allow a more rapid cellular turnover and perhaps better access for cell mediated defence mechanism. There appears to be a different biologic background for these two types of tumours since KRISHNAMURTHY (1961) has noted a difference in response to radiation therapy in the mouth. It is of interest that the sections from the case with the papillary growth and low mitotic index revealed infiltration with plasma cells and lymphocytes. The careful correlation of mitotic index, clinical type, assessment of host resistance and longterm response to radiation in this field appears desirable.

### Acknowledgements

The authors take this opportunity of thanking J. G. Burger for permission to publish this paper. The work was supported by the Medical Research Council, the Cancer Research Trust and the Radiotherapy Research Fund of the University of Cape Town.

### SUMMARY

The mitotic index in human squamous cell carcinoma is discussed with reference to diurnal variation, topography and multiple tumours as well as those of different clinical types. A low mitotic index in these tumours was associated with chronic inflammatory cell infiltration.

### ZUSAMMENFASSUNG

Der mitotische Index beim menschlichen Schuppenzellkarzinom wurde im Hinblick auf Tagesgangvariationen, die Topographie, multiple Tumoren, als auch solche von verschiedenen klinischen Typen diskutiert. Ein niedriger Mitoseindex bei diesen Tumoren war mit chronischen entzündlichen Zellinfiltrationen verbunden.

### RÉSUMÉ

L'index mitotique de l'épithélioma malpighien humain est étudié en fonction de la variation diurne, de la topographie et de la multiplicité des tumeurs ainsi que en fonction des différents types cliniques. Un index mitotique faible dans ces tumeurs est associé avec une infiltration cellulaire inflammatoire chronique.

### REFERENCES

- BLUMENFELD C. M. Studies of normal and abnormal mitotic activity. II. The rate and the periodicity of the mitotic activity of experimental epidermoid carcinoma in mice. *Arch. Path.* 35 (1943) 667.
- DE COSE J. J. and GELFANT I. Noncycling tumour cells. Mitogenic response to antilymphocytic serum. *Science* 162 (1968) 698.

- DUBLIN W. B. Absence of daily rhythm of growth of malignant neoplasms. *Northw Med (Seattle)* 43 (1944) 232
- GREGG R. O. and BORDERS A. C. Mitoses in specimens removed during day and night from carcinomas of large intestines. *Arch Path* 30 (1940) 893
- IVERSEN O. H. Kinetics of cellular proliferation and cell loss in human carcinomas. A discussion of methods available for in vivo studies. *Europ J Cancer* 3 (1967) 389
- KRISHNAMURTHY S. Some factors controlling the radioresponse of squamous cell carcinoma of the cheek. *Clin Radiol* 12 (1961) 55
- REFSUM S. B. and BERDAL P. A chemical experimental investigation of the rate of cell proliferation in human malignant tumours. *Acta oto laryng* 67 (1969) 101
- SHIRAKAWA S., LUCE J. K., TANNOCK I. and FREI III E. Cell proliferation in human melanoma. *J clin Invest* 46 (1970) 1188
- WOLF J. J., JORGENSEN P., KOFF A. W., LIPKIN G. and BART R. S. Influence of antilymphocyte serum on malignant melanoma. *J invest Derm* 51 (1968) 441

## METHOD OF STAGING SYSTEM CONSTRUCTION

by

S S KUROHARA, F W GEORGE III, V VONGTANA and J H WEBSTER

In a previous publication the purpose and concepts of constructing staging systems were presented (KUROHARA & GEORGE 1970). A split then lump tabulation procedure was demonstrated to produce an optimal staging system for carcinoma of the corpus uteri recurrent after total hysterectomy. Each level of stage was separated distinctly from each other.

In this paper the same procedure is used with slight modification to demonstrate construction of staging systems for primary adenocarcinoma of the corpus uteri.

*Materials and Methods* In this approach to staging each of the variables or factors customarily known to represent measures of prognosis in a specific variety of carcinoma is discriminated into two or more levels according to survival rates or similar parameters. The population of patients is subdivided into groups accounting for a combination of levels of each of the variables. Subsets of patients with similar survival rates are then combined into fewer categories with distinct differences in rates depending on the clinical characteristics of the carcinoma process as well as on the sample size.

Submitted for publication 15 January 1971

Table 1

*Anatomic sites of involvement according to prognosis. Possible sites or regions of involvement by adenocarcinoma originating in the corpus uteri are indicated in columns two through six.*

Primary corpus	Cervix	Upper vagina	Lower vagina	Pelvis	Bladder or rectum	Distant	Per cent	5 year survival*	
+	—	—	—	—	—	—	61 (725)	→ 61	(725)
+	+	—	—	—	—	—	37 (35)	→ 37	(35)
+	—	+	—	—	—	—	33 (3)	III	(11)
+	+	+	—	—	—	—	13 (8)		
+	—	—	+	—	—	—	0 (10)		
+	+	—	+	—	—	—	0 (2)		
+	—	+	+	—	—	—	0 (2)	4	(68)
+	—	—	—	+	—	—	13 (15)		
+	+	—	—	+	—	—	0 (9)		
+	—	+	—	+	—	—	0 (1)		
+	+	+	—	+	—	—	0 (3)		
+	—	—	—	+	—	—	0 (1)		
+	+	+	+	+	—	—	0 (2)		
+	—	—	—	—	+	—	0 (3)		
+	—	—	—	+	+	—	0 (1)		
+	+	—	—	+	+	—	0 (1)		
+						+	6 (18)		

+ Carcinoma present at site

— Carcinoma not present

For distant spread (last row) + or — are not specified for sites within pelvis

\* Crude 5 year rates are shown for groups of patients with various combinations of sites of involvement found in this series. Groups with small numbers of cases have been combined according to extent of spread and prognosis. Crude rate = number alive/number at risk expressed as percentage (number at risk)

The material consisted of 835 primary cases of adenocarcinoma of the corpus uteri with complete clinical and histopathologic information suitable for this investigation. The patients were seen at the Roswell Park Memorial Institute during 1940 through 1960. None of them was lost to follow up for at least seven years after diagnosis.

Anatomic site of involvement, uterine cavity depth and uterine size were the three commonly used variables in staging of carcinoma of the corpus uteri. Histologic grade and age were also included because they are the next most clinically sensible staging variables to be considered. Other variables were not examined because of the limited number of cases.

In order to show the probabilistic significance of the particularly constructed set of prognostic classes or stages i.e. the chance occurrence of the staging systems in low an algorithm was devised to perform the following operations

- 1 Randomly permute and partition subsets of patients in a  $4 \times 4 \times 2 \times 2$  array consisting of the respective age, histology, uterine size and uterine cavity depth variables as axes for lesions confined to the corpus (Table 1) Because of the small sample size the anatomic dimension was not incorporated into the array i.e. each of the three extracorporeal subgroups was not subdivided according to the above four variables but considered separately in later computations

Two situations of random permutating and partitioning were considered In the first situation the subsets in the four dimensional intracorporeal array were grouped into stage subgroups without regard to their initial positions in the arrays A programmed technique (IBM) was utilized to randomly permute the positions of the subsets and to randomly partition them into subgroups consisting of anywhere from 2 to 22 subsets This procedure could produce a maximum of 33 stage subgroups to a minimum of three However such extreme condition of staging are unlikely to occur

In the second situation the positions of subsets of patients in the multi dimensional array were considered to simulate somewhat in a random fashion the process by which the particular staging systems were constructed (Tables 3 & 4) The array was subdivided into stage subgroups by starting at the origin and taking integer distances along each of the axes in order of variables with decreasing prognostic discrimination i.e. in order of age histology uterine size and uterine cavity depth The first stage group would be located closest to the origin The next one was produced by continuing along axes in the same order etc

When the limits of any of the axes values four for age and histology and two for uterine size and cavity depth were reached these axes were excluded in subsequent partitionings The choice of integer distances to travel along each of the axes was done by the permutation program using integers 0 up to 4 Staging subgroups consisting of less than two subset cells or those with no patients were combined with the next subgroup in the process of partitionings

- 2 Calculate the weighted averages of 5 year survival rates of subgroups of patients, representing those for stages obtained by the above procedures

- 3 Combine the patients with uterine cervix involvement with those of stage subgroups with intracorporeal lesions associated with 5 year survival rates of less than 40 per cent

- 4 Rank the rates from one to the highest integer of stages



5 Calculate the Pearson's linear and Spearman's rank correlation coefficients, Wilcoxon rank sum statistic (Bross 1954) for survival rates against stage ranks, and chi square values (corrected for continuity) for differences between adjacent survival rates

Several criteria for the evaluation of effectiveness of clinical stages were used and tested according to the following statistics: Pearson's and Spearman's correlation coefficients ( $R$  and  $R_s$ ), Wilcoxon statistic ( $W$ ), and each of them multiplied by the number of significantly different ( $\lambda > 3.84$ ) adjacent survival rates plus one. The frequency distribution of each of these six statistics for 20 000 machine constructed staging systems, was compared for the two situations. The Wilcoxon statistic times the number of stage levels with nonoverlapping rates (WND) appeared to be the best measure of effectiveness. For example, one set of rates 37, 53, 62 and 73 per cent, and another 33, 45, 61 and 66 per cent (61 and 66 overlap) yielded  $W$  of 43 and 43, and  $R$  and  $R_s$  of 0.23 and 0.23, whereas WNDs were  $43 \times 4$  and  $43 \times 3$ , respectively.

## Results

Table 1 shows groups of cases subcategorized according to anatomic sites of involvement of organs by carcinoma, listed in increasing order of advancement of disease. Carcinoma begins in the corpus (first column), spreads to cervix (second column) and then to upper vagina, lower vagina, pelvis, bladder, rectum or distant sites (column wise, right and row wise, down). For the six sites or regions to which carcinoma of the corpus uteri may spread there were 64 possible combinations of involvement; however, only 17 of them actually occurred in this investigation. Cases with metastasis outside the true pelvis were considered in one group irrespective of involvement of carcinoma elsewhere in the pelvis.

The largest group consisted of patients with carcinoma confined to the organ of origin with a 5 year survival rate of 61 per cent. The proportion of such cases is large, indicating that this tumor does not have great propensity to spread early. The next largest group consisted of patients with carcinoma spread to cervix. The survival rate has dropped to roughly one half that of the former. The number of cases for groups with combinations of more distant sites of spread is small with inconsistent and generally low rates close to zero. Because of this such cases are combined into a group with upper vaginal involvement and into one with more extensive sites of spread. This arrangement yielded a maximal WND statistic of 353. Thus four prognostic levels of spread of corpus carcinoma are considered: corporeal, cervical, upper vaginal and more extensive.

Table 2

*Age histology uterine cavity depth or uterine size according to prognosis\**

Variable	Level 1	Level 2	Level 3	Level 4	WND statistic
Age (yrs)	< 50 73 (111)*	50-59 62 (203)	60-69 53 (328)	> 70 37 (197)	172
Histology	Adenocarcinoma Grade 0 66 (68)	Adenocarcinoma Grade I 61 (518)	Adenocarcinoma Grade II 45 (83)	Adenocarcinoma Grade III 33 (166)	129
Uterine size	Normal 58 (350)	Large 53 (471)	Very large 33 (18)		8
Uterine cavity depth (cm)	≤ 7 55 (213)	8 54 (261)	9 59 (174)	≥ 10 50 (191)	1

Crude 5 year survival rate per cent (number at risk)

Vertical line indicates cut off points for conversion of uterine cavity depth and uterine size values into binary ones

The prognostic gradient for levels of variables age at diagnosis histologic grades uterine size and uterine cavity depth are given in Table 2. Five year rates for age ranges < 50 50-59 60-69 and ≥ 70 years are 73 62 53 and 37 per cent respectively (WND=172). Though this partitioning of patients into these age groups did not yield the maximum WND value of 180 as for another set it was chosen for convenience. Rates for histologic grades 0 to III are 66 61 45 and 33 per cent respectively (WND=129). Those for uterine sizes N L and VL are 58 53 and 33 per cent (WND=8) and for uterine cavity depths ≤ 7 8 9 and ≥ 10 cm, are 55 54, 59 and 50 per cent (WND=1), respectively. Because the latter two variables are weakly discriminating of prognosis they are demarcated into binary forms. For example uterine sizes above normal values were associated with a crude 5 year rate of 52 per cent as compared to 58 per cent for those of normal size. Uterine cavity depths less than 10 cm were associated with a rate of 56 per cent as compared to 50 per cent for those 10 cm or more.

Table 3 shows in two dimensions the survival rates of 64 possible groups of patients with localized carcinoma according to age histology uterine cavity depth and uterine size. Because of the zero to small numbers of cases in some of the categories the rates appear somewhat inconsistent. However, on close

Table 3

*Combination of age, histology, uterine cavity depth and uterine size according to prognosis*

Histology	Canal depth	Uterine size	Age (yrs)								Row totals	
			< 50		50-59		60-69		> 70			
Adenoacanthoma												
Grade 0	< 9 cm	N	100	(7)*	63	(8)	79	(14)	60	(5)	76	(34)
		L	—	—	60	(5)	100	(6)	33	(3)	71	(14)
	> 9 cm	N	—	—	—	—	—	—	—	—	—	—
		L	50	(2)	75	(4)	75	(4)	—	—	70	(10)
Grade I	< 9 cm	N	81	(21)	75	(59)	61	(77)	46	(46)	64	(203)
		L	—	—	62	(42)	69	(70)	38	(29)	61	(177)
	> 9 cm	N	—	—	—	—	67	(3)	50	(2)	60	(5)
		L	94	(18)	67	(24)	54	(33)	62	(21)	67	(96)
Grade II	< 9 cm	N	67	(3)	78	(9)	70	(10)	38	(13)	60	(35)
		L	60	(5)	50	(4)	67	(6)	33	(6)	52	(21)
	> 9 cm	N	—	—	—	—	—	—	—	(1)	—	(1)
		L	—	—	100	(1)	14	(7)	40	(5)	31	(13)
Grade III	< 9 cm	N	50	(4)	33	(3)	48	(15)	46	(13)	46	(35)
		L	75	(8)	73	(11)	46	(22)	15	(13)	48	(24)
	> 9 cm	N	—	—	—	—	—	—	—	—	—	—
		L	60	(5)	50	(6)	25	(16)	29	(7)	35	(34)
Column totals			81	(98)	68	(176)	59	(283)	42	(164)	60	(291)

\* Crude 5 year survival rate per cent (number at risk)

scrutiny, there are similarities in patterns of survival rates which have been lumped together. Some clinical judgment was used in lumping in order not to cross over excessively between levels of variables to cause confusion of clinical oncologic terms.

The composite tabulation for initial staging definition of corpus carcinoma is given in Table 4. In early lesions young patients (< 50 years) with low grade carcinoma (0 or I) do exceedingly well. Middle aged patients (50-69) with grade 0 carcinoma also do well but somewhat less than the above. Middle aged patients with grade I carcinoma do well but not as well as the above two. Elderly patients ( $\geq 70$ ) with low grade lesions have a moderate degree of

Table 4  
Composite tabulation of stages for corpus adenocarcinoma

Histology or anatomic site	Age (yrs)		
	< 50	50-69	> 70
Grade 0		IB 76 (41)	
	IA 88 (73)*		IIIB 47 (106)
Grade I		II 65 (308)	
Grade II or III	Cavity Depth < 9 cm	IIIA 59 (100)	
	> 9 cm	IIB 34 (35)	IIC 33 (58)
Cervix involved		IIV 37 (32)	
Upper vagina involved		V 18 (11)	
More extensive spread		VB 4 (68)	

Crude 5 year survival rate per cent (number at risk)  
Stages IIA IIB IIC are combined to give a 5 year rate of 34 per cent for 128 cases

prognosis In high grade lesions these patients do worse Patients less than 70 years of age with high grade carcinoma (II or III) do fairly well when the uterine cavity measures 9 cm or less, and poorly when it measures over 9 cm Elderly patients ( $\geq 70$ ) with high grade carcinoma also do poorly Uterine size had the same effect as cavity depth

In lesions not confined to the corpus only the anatomic sites of involvement are used in the definition of stages When carcinoma has extended beyond the corpus down into the cervix survival is poor It is even poorer when the tumour involves the upper vagina Beyond the above anatomic confines, prognosis is close to nil

Fig 1 indicates the survival curves up through five years post diagnosis for stages IA through VB (II levels) as defined in Table 4 Considering the limitations

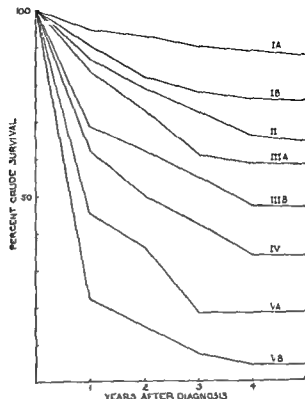


Fig 1 Survival curves for clinical stages IA through VB

of sample size the curves are fairly well separated from each other without any crossing over. However, none of the adjacent 5 year rates were significantly separable from each other. The WND value and the Wilcoxon statistic were the same 139.

Fig 2 shows a plot of survival rates against midpoint of percentage cumulative incidence of stage levels. Because of the overlap between the rates for adjacent stages IA through VB the alphabetized ones have been combined. Stages I, II, III, IV and V revealed no statistical overlap in rates at  $p < 0.025$  with a WND value of 650. A theoretical curvilinear off diagonal line which defines a segment of a circle divides the total sample population space for staging into areas of patients alive beyond five years after diagnosis and dead before. The patients alive make up 54 per cent of the entire series and those dead 46 per cent. As suggested in a previous publication (KUROHARA & GEORGE 1970), an ideal staging system should approximate this line and in addition, produce an even distribution of stages. The actual line fairly well approximates this ideal line, however, it deviates somewhat in the high region near stages I and II. One

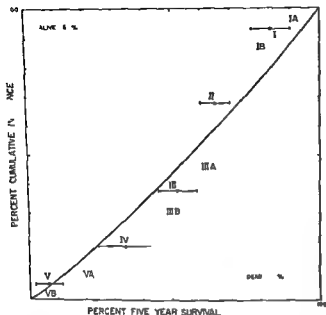


Fig 2 Assessment of constructed staging system in primary adenocarcinoma of the corpus uteri. Horizontal bars denote  $\pm 2$  SE.

reason for this deviation is that stage II consists of a relatively large group of patients 50—69 years of age with grade I lesions. If it were possible to separate this group further prognostically with the five variables employed the actual curve would have been closer to the ideal. Another reason is low incidence of lesions spread outside the corpus. A larger proportion of stage V patients would push the plot of the stage IV group upward into the ideal line. Extracorporeal lesions made up only 14 per cent of this series rather than near 25 per cent in other series.

Thus this procedure yields five prognostically distinct stages defined in the investigation of this case material.

Stage I Carcinoma confined to corpus in patients less than 50 years of age with grade 0 or I lesions or in patients 50 to 69 years with grade 0 lesions.

Stage II Carcinoma confined to corpus in patients 50 to 69 years of age with grade I lesions.

Stage III Carcinoma confined to corpus in patients less than 70 years of age with grade II or III lesions and with uterine cavity depth 9 cm or less or in patients 70 years or older with grade 0 or I lesions. Tumor involves the cervix but not beyond.

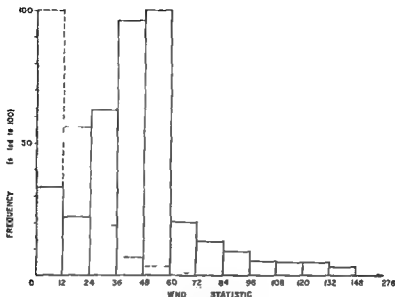


Fig 3 Frequency distribution of WND statistic - Solid line for adjacent position and dotted line for independent position situations

Stage IV Carcinoma confined to corpus in patients less than 70 years of age with grade II or III lesions and with uterine cavity depth greater than 9 cm or in patients 70 years or older with grade II or III lesions

Stage V Carcinoma extending beyond the corpus and cervix

It should be mentioned here that the above definitions of five clinical stages for adenocarcinoma of the corpus uteri, are only adaptable to this series of cases, and are not meant to be applicable to others. Generally applicable staging systems can only be developed from a large number of cases of widely representative data.

Fig 3 indicates the frequency distribution of the WND statistic for 20 000 machine constructed staging systems produced by random partitioning for each of the two probabilistic situations, when subgroup stages of patients according to age histology uterine cavity depth and size were considered independently of position and dependently on adjacent positions in the four dimensional matrix. It is seen that the histogram of the former falls rapidly in an exponential manner from maximal frequency of 0 to 12 WND values to near zero at 60 to 72 the largest value being 156. In the latter there is a peaking of high values between 48 to 60, meaning that consideration of adjacent subgroup stages of patients

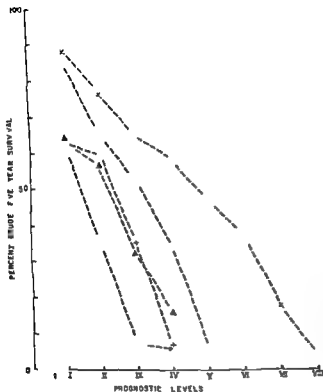


Fig 4 Five year survival rates against stage levels for several staging systems O system A (WND 650) X system B (WND 139) • International Staging System (WND 351) ▲ GUSBERG (WND 288) + HIRABAYASHI (WND 105)

has a better chance of generating more efficient staging systems. The highest WND value was 276. The distributions of the correlation and Wilcoxon chi square values were close to normal however being somewhat skewed toward the left for the latter.

Fig 4 gives the plots of survival rates against one up to eight stage levels for several staging systems as applied to this sample population. The two optimal systems constructed for this series indicated by plots O and X have the highest W and Rs values however the one with less number of stage levels has a higher WND statistic because each level was prognostically distinct from the next ( $p < 0.025$ ). The International Staging System (KOTTMEIER 1963) has a relatively high WND value of 351 but there is essentially no difference in survival rates of stages III and IV. Systems proposed by GRAHAM & HIRABAYASHI (1968) and by GUSBERG (1966) had relatively low WND values of 105 and 288 respectively.



Table 5

*Results of radiation therapy in adenocarcinoma confined to corpus according to stages*

Clinical stage	Treatment groups*		
	Radiation	Surgery	Preoperative
I	III (25)**	71 (17)	85 (72)
II	47 (88)	64 (55)	76 (165)
III	40 (89)	46 (37)	70 (80)
IV***	21 (41)	33 (9)	44 (43)

\* Treatment groups consists of patients treated with irradiation alone with total hysterectomy with or without postoperative irradiation or with preoperative irradiation and total hysterectomy

\*\* Crude 5 year survival rate per cent (number at risk)

\*\*\* Consists of cases with substage lesions IVB and IVC

Table 5 demonstrates the applicability of this or similarly constructed staging systems for the comparison of treatment methods according to 5 year crude survival rates. Patients with stage I lesions respond equally well to each of the treatment methods. In stage II lesions, the result of the preoperative radiation therapy is best, that of the irradiation group is the worst, and that of the surgical group is intermediate. With advancing stage the results of all treatment procedures fall and the differences between them decrease. In stages III and IV radiation therapy before total hysterectomy yield better results than radiation therapy alone or total hysterectomy alone. The results of the latter two treatment methods are similar. The data have been analyzed in detail, according to incidence of carcinoma deaths, of local recurrence rates and techniques of irradiation. These specific results are not included and will be published elsewhere.

### Discussion

A good system of clinical carcinoma staging should group patients with clinically similar tumor as well as host characteristics into distinct prognostic groups for the provision of comparing different methods of treatment. The reason for this is that the make up of patients govern, to a large part the end results of treatments of carcinoma.

For the construction of an optimal system of stages or of prognostic classes knowledge of the survival characteristics of terms or of patient variables used in their definitions, is necessary. Without such knowledge, there is the danger

of mixing terms or variables with different degrees of prognostic distinctions when combining them into the various levels of stages

Survival characteristics in carcinoma have been in decreasing order of usage, the crude 5 year rates, corrected or adjusted five year rates (for age causes of death etc.), crude or corrected survival curves up to five or more years post diagnosis or treatment depending on the follow up duration, and slopes or some other parameter of survival curve functions. The crude 5 year rate was employed in this investigation because of its simplicity and relatively short duration of follow up and because most of carcinoma deaths occurred within five years of diagnosis. Five year rates corrected for deaths due to other causes yielded essentially the same results. More complicated characteristics such as survival curve slopes or functions were not possible to obtain from the limited ample population data.

In staging of corpus carcinoma the patient variables have been most often anatomic sites of involvement less often uterine cavity depth or uterine size, and least often histologic grade. Anatomic sites of involvement have been generally accepted to be a valid concept of measurement of growth and spread for the many types of carcinoma causing the eventual death of patients. Degrees of spread of carcinoma from its site of origin have been found to predict prognosis well, provided that they have been defined optimally.

Levels of spread of carcinoma have generally been described as follows: (1) tumor confined to organ of origin; (2) tumor spread limited to adjacent tissues or organs e.g. to upper vagina or paracervical tissues in gynecologic carcinomas; (3) tumor spread extensively to surrounding regions e.g. to pelvic wall or lower vagina; and (4) tumor spread to distant sites e.g. outside the true pelvis. The degrees of spread of corpus carcinoma is somewhat similar to the above. Although further refinement in degrees of anatomic sites of involvement was attempted this was not found possible in this series of corpus carcinoma since a great majority of cases (86 per cent) had disease in its earliest stage of spread leaving only a small number for such subdivisions. Of the initially defined 16 levels of spread outside the corpus uteri the latter 14 more extensive ones were combined. Thus this variable was assigned only four convenient and realistic degrees of spread of carcinoma with maximal prognostic distinction.

Since corpus carcinoma tends to remain confined within its organ of origin some authors have incorporated uterine cavity depth or uterine size to describe the prognostic behavior of cases with localized disease (HIRABAYASHI & GRAHAM 1968). In this investigation these variables were found to be well correlated with each other and weakly discriminative being applicable only for high grade lesions. Because of greater reliability in measurement uterine cavity depth was employed rather than uterine size. A point of demarcations

between 9 and 10 cm was used to denote small and large uterine cavity associated with tumor size, because the number of cases with depths of 11 cm or more was too small.

Having employed all available clinical variables conceptualizing tumor spread and size, the next most sensible variable for staging would be histologic grade, as has been suggested elsewhere (GUSBERG 1966). In this investigation this variable was found to be more powerful in discriminating prognosis than uterine cavity depth or uterine size.

Age was added as an additional variable because of its relatively strong effect on survival (second to anatomic site). Although survival is expected to fall with age because of increased incidence of other age dependent diseases for some unknown reason it was still possible to discriminate rates between histologic grades even at advanced ages. That is prognosis of elderly patients ( $\geq 70$  years) with low grade lesions (0 or I) were better than those with high grade lesions (II or III).

In order to segregate the large group of patients with carcinoma confined to the corpus, age, histologic grade and uterine cavity depth were employed in combinations. Seven levels of stages were identified for patients with carcinoma confined to the corpus (IA, IB, II, IIIA, IIIB, IVB and IVC). These stages were combined with those spread outside the corpus to yield eight levels of stages for the total series. However, because of limitations in sample sizes, only five prognostically distinct levels of stages were possible.

Non parametric statistical procedures were employed to show the degree of correlation between stage ranks and ranked proportion of cases survived. Both the Spearman rank correlation and the Wilcoxon rank sum statistic indicated similarly the degrees of monotonic increase in survival rates with stage levels. Pearson's coefficient was usually the same as Spearman's but because of uncertainty of normality of data the former was not relied upon. Since prognostic distinctions were not accounted for effectively by the correlation coefficients or by the Wilcoxon statistic this aspect was incorporated by use of the chi square test to distinguish overlap between survival rates of adjacent stages. The Wilcoxon statistic multiplied by the number of prognostically distinct stage groups was found to produce maximal separation between the randomly constructed systems and those constructed by selection of patient characteristics. However this single WND measure is not completely to be relied upon since its large value does not always guarantee good separation of all classes from each other. It is necessary to inspect the number of distinct groups and sometimes the actual graphic plotting of stage levels against survival rates for certain high values obtained. This situation occurred in assessing the International Staging System which yielded a high WND value despite disproportionate

distribution of cases in stage I and poor distinction between stages III and IV

Although it may be argued that this procedure of constructing staging systems is not completely objective and a more mathematical or statistical one should be employed, as of the time of this writing there seemed to have been no good solution. For this purpose a randomization pseudo-permutative technique was employed to show that there would be less than five per cent chance of mechanically producing an equally good staging system. Of 20 000 systems generated, none had a WND statistic and case distribution better than the one constructed.

It should be stated here that problems of grouping individuals into logical subsets have been previously encountered in the field of biology, psychology, anthropology and other related sciences. Approaches undertaken in attempt to solve specific problems in these areas have been generally categorized as frequency curve resolution, factor analysis and hierarchical clustering based upon distance measures (JOYES 1968). Names of some of the various methods using these approaches are discriminant classification, Q and R factor analysis, common factor analysis, multiple factor analysis, numerical taxometrics, taxonomic optimization, pattern analysis, similarity analysis, dissimilarity analysis, profile analysis, agreement analysis, etc.

Although several of the above statistical methods were employed in attempt to construct staging systems, they did not yield results satisfactory to us. Some of the reasons for their inapplicability were as follows: (1) linguistic differences in approach to this problem, (2) theoretical assumptions of properties of data incompatible with facts, (3) requirement of parametricity of data and variable relationships, and (4) indeterminacy in functional relationship between variables in loadings in axis rotations in distance measures in similarity coefficients, etc. without previous information on group membership.

The suboptimal performance of currently proposed staging systems tested on this sample data was due to the use of too few clinical staging information for purposes of simplicity or due to the use of additional appropriate anatomic or histologic information but in combinations inefficient to effectively discriminate prognosis in unselected series having a sizable proportion of elderly patients at high risk to other causes of death.

The International System of Staging employs only anatomic extent of spread for classification. Although simple, this system lumps a disproportionally large number of patients into the first category of stage (roughly 75 per cent in most series). The results of this investigation have demonstrated that patients with lesions still confined to the corpus may be still subdivided into smaller groups having 5 year survival rates ranging from 88 per cent down to 33 per cent. With such heterogeneity of patients grouped within one stage level, comparison

of treatment methods becomes unreliable without the necessity of strict statistical control which would also require a larger number of patients than required for a relatively more homogeneous subpopulation.

To decrease this extreme variation in patient types for lesions localized to corpus, other authors suggested employing uterine cavity depth or uterine size measurements with or without histologic grade to overcome this heterogeneity. HIRABAYASHI & GRAHAM (1968) employed uterine cavity depth of 8.5 cm to segregate these cases. However, they excluded cases dying of other causes and in this way their staging system would be applicable only to patients whose death from carcinoma could possibly be predicted. Though this worked out well in these selected cases, its performance was poor in all cases with localized disease in this investigation.

GUSBERG (1966) divided intracorporeal lesions into these groups: cases with low grade carcinoma in normal sized uterus, those with low grade carcinoma in moderate sized uterus or with high grade carcinoma in normal sized uterus, and those with more advanced degrees of combinations of histologic grade and uterine size. His system yielded a relatively high WND value, however without prognostic distinction between stages I and II groups.

The production of prognostically distinct stages has the importance of minimizing variations in survival rates so that results of different treatment methods for patients within stage groups can be assessed reliably. The use of a poorly constructed staging system permits the physician under usual circumstances to select patients for each of the treatment methods so that the end results are governed by inhomogeneities in prognostically powerful variables rather than the treatment procedures themselves. As has been demonstrated in this investigation as well as by others (GUSBERG 1966, NOLAN et coll. 1967), different treatment methods may be selected for different classes of patients based on histologic grade and uterine size. Hence, towards this end it is necessary to construct efficient staging systems with minimal heterogeneity in powerful biologic prognostic variables within each of the stage groups with whatever applicable objective procedures available.

Finally it should be stated that staging systems assessed to be effective by this or any other quantitative measure available or yet to be developed, should ultimately be judged realistic by experienced clinicians and be compatible with current concepts in clinical oncology. It is believed that if this approach or any other similar one had been utilized previously, much of the numerous ineffective and incompatible staging systems would not have been proposed and many man hours would not have been wasted in utilizing such staging systems for the purpose of reporting and assessing end results of carcinoma treatment.

## SUMMARY

The controversial subject of logical approaches to constructing effective staging systems in carcinoma was presented. As an example a simple but perhaps arbitrary split lump tabulation procedure was applied to the construction of an effective staging system for a series of 835 primary cases of adenocarcinoma of the corpus uteri. The five particular clinical stages constructed by this procedure were prognostically distinct and directly related to crude five year survival rates. It was demonstrated that this staging system was highly efficient relative to those currently proposed and could not have occurred by chance. A generally acceptable system of staging for this type of carcinoma can only be developed by this or other similar methods with a much larger sample of patient data representative of many regions of the world.

## ZUSAMMENFASSUNG

Die kontroverielle Frage logischer Ansätze effektive Stadien Systeme für Karzinome zu konstruieren, wurde dargestellt. Als Beispiel wurde ein einfaches aber vielleicht willkürliches split lump Tabulationsverfahren verwendet um ein effektives Stadien System für eine Reihe von 835 Primärfällen von Adenokarzinomen des Corpus uteri zu konstruieren. Die fünf besonderen klinischen Stadien die durch dieses Verfahren konstruiert wurden waren prognostisch distinkt und standen in direktem Verhältnis zur groben Fünfjahres Überlebensrate. Es wurde nachgewiesen dass dieses Stadien System im Verhältnis zu den bisher verwendeten sehr effektiv ist und nicht zufällig entstanden sein kann. Ein allgemein anerkanntes System der Stadieneinteilung dieses Typus von Karzinom kann nur mit dieser oder anderen ähnlichen Methoden an einer wesentlich grosseren Gruppe von Patientendaten die repräsentativ für viele Gebiete der Welt sind entwickelt werden.

## RÉSUMÉ

Les auteurs présentent le problème controversé que constitue la façon logique d'aborder l'élaboration d'un système efficace de classement des stades du cancer. Comme exemple ils ont appliqué une méthode simple mais peut-être arbitraire à la construction d'un système de classement en stades efficace pour une série de 835 cas primaires d'adenocarcinome du corps de l'utérus. Les cinq stades cliniques particuliers définis par cette méthode ont eu un pronostic différent et directement en rapport avec le taux brut de survie à cinq ans. Il a été démontré que ce classement par stade est très efficace par rapport à ceux qui sont habituellement proposés. Ceci ne peut pas être dû au hasard. Seule cette méthode ou des méthodes similaires appliquées à un beaucoup plus grand nombre de cas provenant de nombreuses régions du monde pourront aboutir à un système de classement en stades qui puisse être accepté de façon générale pour ce type de cancer.

## REFERENCES

- BROSS I. D. J. Is there an increased risk? Fed. Proc. 13 (1954) 815  
 HIRABAYASHI K. and GRAHAM J. M. Classification of carcinoma of the uterine body Surg. Gynec. Obstet. 126 (1968) 75  
 CUSBERG E. M. The problems of staging endometrial cancer. Obstet. Gynec. 28 (1966) 305  
 IBM Applications program manual H20-0205 2 1967 p. 54

- JONES K. J. Computers in behavioral science. Problems of grouping individuals and the method of modality. *Behavioral Sci.* 13 (1968) 496
- KOTTMEIER H. L. The classification and clinical staging of carcinoma of the uterus and vagina. *J. Int. Fed. Gynec. Obstet.* 1 (1963) 83
- KUROHARA S. S. and GEORGE III F. W. Objective procedure of constructing stages in cancer. Its application in recurrent carcinoma of the corpus uteri. *Acta radiol. Ther. Phys. Biol.* 9 (1970) 513
- NOLAN J. F., DOROUGH M. E. and ANSON J. H. The value of preoperative radiation therapy in stage I carcinoma of the uterine corpus. *Amer. J. Obstet. Gynec.* 98 (1967) 663

## ANTIBODIES TO A HeLa CELL LINE IN CARCINOMA OF THE CERVIX UTERI

The effect of radiation therapy

by

NINA EINHORN and J. JOHANSSON

Irradiation of the thyroid gland is followed by a temporary increase in antibodies to the cytoplasmic antigens of the gland lasting about a year (BUCHANAN et coll 1964, O'GORMAN et coll 1964, IRVINE 1964, EINHORN et coll 1965) this is not a manifestation of a general increase in the autoimmune reactivity (JOHANSSON et coll 1968). Surgical reduction in the volume of the thyroid gland does not result in any rise in the antibodies to the cytoplasmic antigens of the thyroid (HJORT & MOGENSEN 1962, EINHORN et coll 1965). An increase in antibodies to the irradiated tissue also occurs after local irradiation of the vagina and uterus (EINHORN et coll 1969). There are indications that the cell mediated reactivity to the irradiated tissue antigens also becomes greater after local radiation therapy: the sensitivity of the lymphocytes to stimulation with thyroglobulin appears to rise after local irradiation of the thyroid gland (EINHORN et coll 1970 b). Local irradiation in 2 cases of Burkitt's lymphoma and 3 cases of nasopharyngeal carcinoma was followed by an increase in antibodies to the Epstein Barr virus associated cell membrane antigens (MA) present in Burkitt's lymphoma cells (EINHORN et coll 1970 a).



The aim of the present investigation was to ascertain the effect of local irradiation on the reactivity of the serum to a carcinoma of the cervix cell line in long term culture — the HeLa cells. Since the patients were followed for 5 years after the treatment it was also possible to examine the correlation of the reactivity of the serum to the clinical course of the malignant disease.

*Case series* The sera were obtained from 84 consecutive patients with carcinoma of the uterine cervix receiving radiation therapy between 1 January and 31 March 1966. Except for the exclusion of patients with known or possible thyroiditis or rheumatoid arthritis, the material was unselected and represented various stages of the disease. The diagnosis was always confirmed by histology.

The first serum specimen was obtained before the first radiation treatment with subsequent specimens at 3 to 8 weeks, 2 to 6 months, 6 to 12 months and 1 and 2 years. Serum from the three first sampling times was available in all 84 patients. Specimens were sometimes not obtained for the 6 to 12 month and 1 to 2 year periods usually owing to the death of the patient.

*Methods* The radial diffusion disc test modification (FAGRAEUS et coll. 1965) of the mixed haemadsorption technique (FAGRAEUS & ESPMARK 1961) was performed on three to six samples from each of the 84 patients. The cell line used for the test were HeLa cells obtained from J. T. Syveton in 1953. Regular clinical follow up examinations were performed usually by one of the authors (N. E.) during the first year at intervals of 1 to 2 months and during the last year at intervals of 6 to 8 months. All the patients could be followed.

The material was divided into two groups: one including patients who developed recurrence or distant metastases and the other regarded as being free from recurrence. The clinical evaluation was sometimes subject to uncertainty. Biopsy specimens were taken only if they were regarded as being in the patient's interest, not all the patients dying during the control period came to autopsy. A few patients presented particular difficulties. Pain and doubtful fibrous palpated in the pelvis were suggestive of a recurrence in one patient, but as aspiration biopsy and further clinical observation disclosed no evidence of residual malignancy the patient was assigned to the no recurrence group. Another patient in whom incisional biopsy 4 1/2 years after treatment confirmed malignancy, was included in the recurrence group. Only patients in whom no recurrence at least 1 year before death occurred were regarded as having died from intercurrent disease, there were 2 such patients. One had committed suicide at 18 months and the other died from ileus at 2 years; neither of them had clinical evidence of the disease during the year preceding death. Autopsy was performed only on the latter, both were considered to have died from intercurrent disease.

Table 1

*Antibodies to HeLa cells before and at various intervals after radiation therapy for carcinoma of the cervix uterus. Number of patients reacting in the mixed haemadsorption test*

	No of patients	Positive serologic reactions titre								
		1/12	1/25	1/50	1/100	1/200	1/400	1/800	1/1600	1/3200
Before radiation therapy	11	7	5	2	1	1	0	0	0	0
Interval after radiation therapy										
3-8 weeks	84	9	5	1	1	1	1	1	1	1
2-6 months	84	14	8	4	4	4	2	1	1	1
6-12 months	71	5	5	3	3	1	1	1	0	1
1-2 years	56	6	4	2	2	2	1	1	0	0
2-3 years	43	5	4	2	1	1	0	0	0	0

A comparison was made of the results of the serologic tests and the clinical development of the disease at about 5 years after treatment. The evaluator responsible for the clinical control of the patients was unaware of the results of the serologic examinations. Five years after the primary treatment 60 of 84 patients were alive and clinically free from recurrence. 2 had died from intercurrent disease and 22 were included in the recurrence group. All but one of the 22 patients with recurrence were dead.

Eighteen of the 22 patients had local recurrence and 4 died with large masses of extra pelvic distant metastases unaccompanied by known intrapelvic tumour changes. Seventeen of the 18 patients with known local recurrence had a large intrapelvic mass considered to be the cause of death. 4 of these patients also had or probably had extrapelvic metastases.

### Results

The results of the serologic tests in relation to the time after irradiation are presented in Table 1. A positive serologic reaction tended to be more frequent at the examination performed 2 to 11 months after radiation therapy than before but the difference is not statistically significant.

All 7 patients in whom antibodies to HeLa cells were present before radiation therapy had no evidence of a growth at the end of the follow up period (Table 2). Antibodies to HeLa cells were present on at least one occasion before or

Table 2

*Relationship between a recurrence and the presence of antibodies to HeLa cells in 84 patients with carcinoma of the cervix uteri*

	Total	Local recurrence		Distant metastases (only)		Total recurrence		No recurrence	
	No	No	Yes	No	Yes	No	Yes	No	Yes
Antibodies before radiation therapy	7	0	0	0	0	0	0	7	0
Antibodies only after radiation therapy	22	2	9	3	14	5	23	17	17
No antibodies before or after radiation therapy	55	16	29	1	2	17	31	33	69

after therapy in 29 patients and 5 of them (17 per cent) developed recurrence. Seventeen patients (31 per cent) had recurrence of the tumour in the group without demonstrable antibodies to HeLa cells.

### Discussion

Two problems were investigated in this material, namely, the change in the antibodies reacting with the HeLa cells after irradiation of carcinoma of the cervix uteri and the correlation between the presence of antibodies to HeLa cells and the clinical development of the disease.

An increase in the antibodies to the epithelium of the portio uteri and to the glandular epithelium of the cervix occurs after local irradiation of the vagina and uterus (EINHORN *et coll.* 1969). An increase in antibodies to the tumour associated antigens after local irradiation has recently been reported in Burkitt's lymphoma and nasopharyngeal carcinoma (EINHORN *et coll.* 1970). An increase in the number of patients whose sera reacted to the HeLa cell line 2 to 6 months after irradiation also occurred in the present series (Table 1), but the difference is not statistically significant.

Seventeen out of 55 patients with no demonstrable antibodies to HeLa cells developed recurrences. None of the 7 patients whose serum taken before therapy reacted to the HeLa cell line had any evidence of recurrence 5 years after radiation therapy (Table 2).

Five of the 22 patients with recurrence had demonstrable antibodies to HeLa cells on at least one occasion after the radiation therapy, manifested in 3 patients

as extrapelvic metastases only. The remaining 17 with no evident reactivity to HeLa cells usually had a local recurrence, only one had had solely distant metastases. The usual cause of death in carcinoma of the cervix uteri is intrapelvic recurrence (HENRIKSEN *et coll* 1949) even in large autopsy materials exclusively extrapelvic tumours have been recorded in only 10 per cent of patients (KJELLGREN 1967).

The fact that the relatively few patients developing remote metastases were mainly (3 out of 4) included among those with antibodies to HeLa cells after radiation therapy suggests that the course of the condition may be influenced in some measure by an enhancement reaction. This should however be confirmed by ascertaining among other things whether the sera of patients with generalized malignancy actually contain antibodies blocking the effect of the lymphocytes on cells of carcinoma of the cervix. Furthermore the immunoglobulin class of the reacting antibodies should be determined and if possible, the antigenic determinants involved should be identified.

The implications of the findings reported are still to be clarified. The reactivity to HeLa cells was usually observed only at low titres (Tables 1 and 2). The HeLa cells were derived from a case of carcinoma of the cervix but it is not known to what extent the original tissue specific antigens were retained after the numerous passages to which this cell line had been subjected. Furthermore some antigenic determinants present in small concentration on the surface of normal cells may be increased in number upon malignant transformation (HAKOMORI & MURAKAMI 1968). For example cytolipin H is assumed to be present on the plasma membrane of HeLa cells (TAL 1965). experimentally prepared ant sera against carcinoma tissue are known to contain antibodies to this glycosphingolipid while ant sera against normal tissue do not (RAPPORT & GRAF 1969). It has not been ascertained whether the reactions against HeLa cells described in this report were so caused and not by organ specific antibodies.

The total series of 84 patients is quite large but it is divided into small groups and the differences between them were not statistically significant. The results presented should therefore be regarded as being preliminary pending the availability of a larger series that has been submitted to serologic examination and followed clinically.

### Acknowledgements

The authors wish to express their thanks to Prof A Fagraeus and Prof J Einhorn for their valuable guidance to Mrs Bibbi Brodin, Mrs Christina Halldin and Miss Anita Östborn for their technical assistance. The project was supported by a grant from the Swedish Cancer Society.

## SUMMARY

Patients with carcinoma of the cervix uteri were examined by the mixed haemadsorption test before and on five occasions following local radiation therapy. All 7 patients in whom antibodies to HeLa cells were present before radiation therapy had no evidence of a growth at the end of the follow up period while five out of 22 patients with antibodies that reacted with HeLa cells after the treatment and 17 out of 54 patients without demonstrable antibodies on any occasion developed a recurrence.

## ZUSAMMENFASSUNG

Patienten mit einem Carcinom des Cervix uteri wurden mit dem mixed haemadsorption test vor und fünf mal nach lokaler Strahlentherapie untersucht. Alle 7 Patienten bei denen Antikörper gegen HeLa Zellen vor der Strahlentherapie vorhanden waren zeigten keine Zeichen eines Wachstums am Ende der Nachuntersuchungsperiode während 5 von 22 Patienten mit Antikörpern die mit HeLa Zellen nach der Behandlung reagierten und 17 von 54 Patienten ohne nachweisbare Antikörper bei allen Untersuchungen erneutes Wachstum aufwiesen.

## RÉSUMÉ

Des malades atteintes du cancer du col de l'utérus ont été examinées par le test d'hemadsorption mixte avant et dans cinq cas après traitement local par les radiations. Les 7 malades chez qui des anticorps aux cellules HeLa étaient présents avant le traitement par les radiations ne présentaient pas de signes de tumeur à la fin de la période de surveillance alors que cinq des 22 malades qui avaient des anticorps qui réagissaient avec les cellules HeLa après le traitement et 17 des 54 malades chez qui on n'avait pas pu mettre en évidence d'anticorps à aucun moment ont présenté une récurrence.

## REFERENCES

- BUCHANAN W, KOUTRAS D, CROOKS J et coll: The clinical significance of the complement fixation test in thyrotoxicosis. *J Endocr* 24 (1962) 115
- EINHORN J, FAGRAEUS A and JONSSON J: Thyroid antibodies after <sup>131</sup>I treatment for hyperthyroidism. *J clin Endocr* 25 (1965) 1218
- — — Thyroid antibodies in euthyroid subjects after iodine 131 therapy. *Radiat Res* 28 (1966) 296
- EINHORN V, JONSSON J and FAGRAEUS A: Immunologic reactions after irradiation of the uterus. *Radiat Res* 40 (1969) 465
- KLEIN G and CLIFFORD P (a): Increase in antibody titer against the EBV associated membrane antigen complex in Burkitt's lymphoma and nasopharyngeal carcinoma after local irradiation. *Cancer* 26 (1970) 1013

- WASSERMAN J and PACKALÉN T (b) Cellular autoimmune reactions following radioiodine treatment for hyperthyroidism *Acta radiol Ther Phys Biol* 9 (1970) 225
- PACKALÉN T and WASSERMAN J Lymphocyte stimulation by thyroglobulin after local irradiation of the thyroid gland in man *Acta radiol Ther Phys Biol* 10 (1971) 481
- FAGRAELS A and ESPMARK Å Use of a mixed haemadsorption method in virus-infected tissue cultures *Nature* 190 (1961) 370
- and JONSSON J Mixed haemadsorption A mixed antiglobulin reaction applied to antigens on a glass surface Preparation and evaluation of indicator red cells survey of present applications *Immunology* 9 (1965) 161
- HAKOMORI S and MURAKAMI W Glycolipids of hamster fibroblasts and derived malignant transformed cell lines *Proc nat Acad Sci (Wash)* 59 (1968) 254
- HENRIKSEN E The lymphatic spread of carcinoma of the cervix and of the body of the uterus A study of 420 necropsies *Amer J Obstet Gynec* 58 (1949) 924
- HJORT T and MOGENSEN F Thyroid auto antibodies *Acta med scand* 171 (1962) 289
- IRVINE W Thyroid auto-immunity as a disorder of immunological tolerance *Quart J exp Physiol* 49 (1964) 374
- JONSSON J, FINHORN N, FAGRAELS A and EINHORN J Organ antibodies after local irradiation *Radiology* 90 (1968) 536
- KJELLGREN O Gynecologisk cancer *Klinik och terapi* (In Swedish) Almqvist & Wiksell Stockholm 1967
- O GORMAN P, STAFFURTH J and BALLENTYNE M Antibody response to thyroid irradiation *J clin Endocr* 24 (1964) 1072
- RAPPORT M and GRAF L Immunochemical reactions of lipids *Progr Allergy* 13 (1969) 273
- TAL C The nature of the cell membrane receptor for the agglutination factor present in the sera of tumor patients and pregnant women *Proc nat Acad Sci (Wash)* 54 (1965) 1318

## AUTOMATIC PRODUCTION OF ISODOSE CURVES

by

OLE KALNES and JENS MUNK

An automatic system for producing isodose curves and data for automatic treatment planning was needed in connection with the installation of a 6 MeV linear accelerator (Varian Clinac 6). A system that measured depth dose curves and dose profiles of radiation fields and stored the results on punched paper tape was therefore designed. From these data isodose curves are produced ready for use by means of a plotter coupled on line to an IBM 1130 computer. Depth dose tables are also evolved and when a larger computer becomes available at the hospital, automatic treatment planning may be based on the field data stored on paper tape.

*Measuring equipment* A block diagram of the measuring system appears in Fig. 1. The measurements are carried out in the water phantom by means of an ionization chamber with an inner diameter of 6 mm. The chamber is run automatically between two end stops at a speed of 2 mm per 4 seconds. As the absorbed dose is proportional to the ionization a depth dose curve along the axis of the field or a dose profile perpendicular to the axis may be measured. The ionization current is determined by means of an electrometer (Keithley), and the output potential of this instrument is converted to a number of pulses

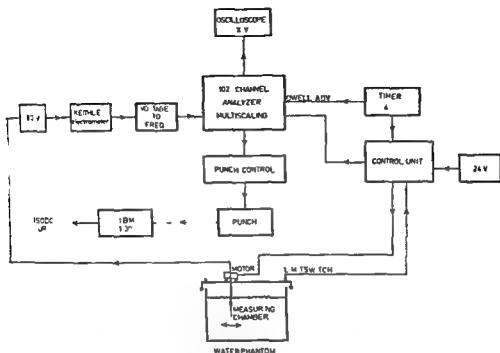


Fig 1 Measuring system for automatic registration of depth dose data and profile data of radiation fields

proportional to the measured ionization by means of a voltage-to-frequency converter (Hewlett Packard). The number of pulses in 4 seconds is counted with a 1024 channel analyzer (TMC) run in the multiscaler mode. The analyzer's memory is divided into four parts each consisting of 256 channels so as to store information of more curves; this means that the curves may be extended to a length of more than 50 cm. The stored information may be displayed on an oscilloscope and if no faults are evident may be punched out on perforated paper tape. About 200 000 pulses are obtained corresponding to the maximum dose of a field with the applied potential-to-frequency conversion, thus about 2 000 pulses represent a one per cent dose.

Due to the dimension of the chamber and its protecting cap as well as to the wall thickness of the water phantom the effective measuring point (i.e. a point placed at a distance of  $0.75 \times$  inner radius of the cylindric chamber from the centre line towards the radiation source) cannot come closer than 2.0 cm from the surface of the phantom. As no measurement is made during the first 2 mm so as to avoid false counts due to the operation of several electric relays etc. the



first measurement is obtained at from 2.2 cm to 2.4 cm which means that the first measuring point is assumed to be 2.3 cm. The measurements are then carried out to a depth of 37 cm.

Dose profiles are normally measured at 4 depths namely 2.1 cm, 12.1 cm, 22.1 cm and 32.1 cm. The end stops for these measurements are symmetrically sited in relation to the central axis and at a distance of an odd number of mm from the axis, all 4 profiles are measured under the same conditions. Again the results are inspected on an oscilloscope after each profile measurement and the 4 profile measurements for a field having been carried out, the complete set of data of the 1024 channel analyzer is punched out.

**Calculation of isodose curves** The isodose curves are calculated by the decrement line principle as suggested by ORCHARD (1964). The assumption is that all points in which a dose is a certain percentage of that on the central axis at the same depth are on a straight line. ORCHARD demonstrated that this is true in a cobalt field and the method was used by several authors to draw isodose curves by hand (NAYLOR & ORMSBY 1968, FELDMAN et coll 1968), it has been used for some time in Odense. ORR et coll (1964) employed the same method for a linear accelerator.

The above principle is not assumed to hold for a whole field in the computer program ISOSE in which isodose curves are calculated from the measurements described but rather for the area between two profiles, i.e. over a depth variation of 10 cm. This assumption will probably be close to reality at all depths greater than 10 cm as the manufacturers of the Varian 6 MeV accelerator have at

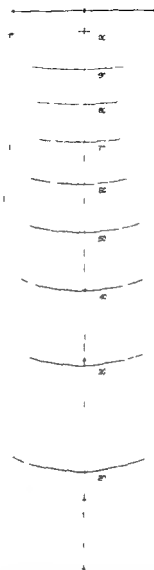


Fig. 2. Isodose curves for a 10 cm  $\times$  15 cm field as drawn by the computer. The unit on the central axis of the field is 5 cm (Scaled down from normal size).

tempted to have a uniform dose over the field at a depth of 10 cm. A certain amount of overcompensation is obtained with a flatness compensator: this gives a uniform dose over the field at 10 cm depth. At depths less than 10 cm the dose at the edge of a broad field may therefore be as much as 5 per cent higher than at the central axis. The assumption of straight decrement lines does not hold in these areas which means that the higher dose at the edges of broad fields do not appear on the isodose curve diagrams.

The depth dose curve is always measured twice to ensure that it is capable of being reproduced: an attempt is made to run the linear accelerator at the same dose rate during the two measurements (see Discussion).

The depth dose curve used in the calculation is a mean value of the two curves. The ratio of the dose at the first measuring point to the dose at the maximum point is given as an input variable and is obtained from the data of HORSBY *et al.* (1967). Four dose profiles across the entire field are measured. Any possible lack of symmetry is however ignored in the treatment planning: therefore the profile in the calculation is the mean value of the two halves.

Isodose curves are drawn by means of decrement line calculations for every one per cent dose change on the central axis. This means for example that the 90 per cent isodose curve will be drawn by means of 10 points in each field half, whereas the 30 per cent curve will be depicted by 70 points in each field half. The points will be connected by straight lines, excepting that the central 10 mm of all isodose curves are drawn perpendicular to the central axis.

*Calculation of isodose curves for fields not measured directly.* The depth dose curves and dose profiles for all usable square fields having been measured, it becomes possible to calculate approximate isodose curves for all suitable rectangular fields. An equivalent square field with the same depth dose curve may be found for any rectangular field (Brit. J. Radiol. (1961) Suppl. No. 10). It is then assumed that the dose profiles for the rectangular field are identical with those for a square field of the same width, and the isodose curves for the rectangular field may thus be calculated. Any discrepancy between these calculated curves and the true measured ones are due to the contribution from the scattered radiation. This will be discussed later.

*The computer program ISOSE: data and results.* The input data necessary for ISOSE consist of a punched card and two punched paper tapes. The card must contain information such as name of the radiation source, skin source distance and field width and height. The starting and end points of the depth dose curve measurement must be given and the dose at the point of the first measurement divided by the maximum dose. The depth of four profiles and the distance from the central axis to the starting position of the measuring point on

these the depth of the dose maximum and a code number determining the amount of plotting to be done are all quantities that are needed. All distances must be in cm. One paper tape must give two depth dose curves, and the other paper tape the four dose profiles. The detailed format of the punched card and the paper tapes appear in an internal report.

The results obtained consist of a control print out on a line printer and an automatic drawing on the plotter. The plotting is governed by the code number. If this is zero then first of all the two original depth dose curves are plotted as dotted lines whereas the mean depth dose curve appears as a full line. The two halves of the profiles are also drawn as dotted lines whereas the mean value is depicted by a full line. The 10 dose curves are presented in Fig. 2. Only the 10 dose curves are plotted if the code number 1 or 2 and in the latter case the 5 per cent curve is omitted.

### Discussion

The measuring equipment described has proved extremely useful in the measurement of radiation fields for radiation therapy. Nevertheless several alterations in the equipment would improve the performance. First of all the ionization chamber with an inner diameter of 6 mm ought to be somewhat smaller. This is only of importance near the edges of the fields. The penumbra of the fields will appear somewhat greater than is actually the case. It would also be convenient if the ionization chamber were to travel at a higher speed so as to make the measurements more quickly. By a change in the gearing the travelling speed of the probe might well be increased by a factor of two combined with a decrease in the measuring interval by the same factor to two seconds. No loss in accuracy due to this would occur.

A most important condition for the successful outcome of the measurements is the constant dose rate from the radiation source during a complete measurement. That this assumption is fulfilled may easily be checked as any change in dose rate would appear as a difference between the two dotted depth dose curves and the two dotted profile half parts, this has been done for all measurements. If the dose rate cannot be kept constant, a reference chamber must be used in connection with a ratio circuit or print-out of the measurements from the two chambers.

As far as the use of the decrement line principle is concerned, this has been proved valid in the two papers previously quoted. The condition is that no overcompensation is used as mentioned earlier. In the case of overcompensation no decrement lines can be drawn which means that the use of the decrement line system is not entirely satisfactory. This limitation is however not serious from a practical point of view.

A great advantage of the method is that any skew in the set up of the measuring system is easily detected by visual inspection of the computer plotted transfer curves. The two half parts of a curve are plotted in the same co-ordinate system and therefore any discrepancy between the planned and the actual radiation axis appears at twice the true size on the computer plot.

The possibility of having to measure only square fields and being able to calculate sufficiently accurate isodose curves for all rectangular fields is most important. Regarding the equivalency of the depth dose curves for square fields with rectangular fields as given in Suppl. No. 10 (Brit. J. Radiol.) it has been proved that agreement with the cobalt 60 table exists for 6 MeV roentgen rays for field dimensions  $10\text{ cm} \times 15\text{ cm}$  and  $6\text{ cm} \times 20\text{ cm}$ .

The error due to the scattered radiation is small in the most important parts of the isodose curves when dose profiles measured on square fields are used for rectangular fields. The five per cent isodose curve is drawn only on fields measured directly as this curve is displaced considerably when the rectangular fields are far from square geometry. Apart from these discrepancies of any importance occur only at the corners of the isodose curves at fair depths. The maximum discrepancy for a  $10\text{ cm} \times 15\text{ cm}$  field measured at right angles to the isodose curves is 1 mm which occurs only at the 10 per cent curve. The maximum discrepancy for a  $6\text{ cm} \times 20\text{ cm}$  field measured as above is 8 mm at the corner of the 20 per cent isodose curve corresponding to about 1 per cent of the maximum dose and 5 per cent of the actual dose. The maximum discrepancy for the 50 per cent curve at the corners is 4 mm corresponding to about 1 per cent of the maximum dose and 2 to 3 per cent of the actual dose. The 10 per cent curve for this elongated field is also displaced up to 4 mm measured at right angles to the central axis.

## SUMMARY

The measuring equipment, the principles and the computer program for the automatic production of isodose curves are described. This method necessitates measurements only of square fields and the computer plotted curves may be used directly in treatment planning. The accuracy obtainable is discussed.

## ZUSAMMENFASSUNG

Die Messausrüstung, die Prinzipien und das Computerprogramm für die automatische Herstellung von Isodosiskurven werden beschrieben. Diese Methode benötigt lediglich Messungen der Quadrätfelder und die vom Computer dargestellten Kurven können direkt für den Bestrahlungsplan verwendet werden. Die zu erreichende Genauigkeit wird besprochen.

## RÉSUMÉ

Les auteurs décrivent l'appareillage de mesure les principes et le programme d'ordinateur pour la production automatique de courbes isodoses. Cette méthode ne nécessite de mesures que pour des champs carrés et les courbes établies par l'ordinateur peuvent être utilisées directement pour établir le plan de traitement. Les auteurs examinent la précision que l'on peut obtenir par cette méthode.

## REFERENCES

- DEPTH DOSE TABLES FOR USE IN RADIOTHERAPY Brit J Radiol (1961) Suppl No 10
- FELDMAN A ANDERSEN J A WEBER F G and WILLIAMS M Construction of isodose lines for  $^{60}\text{Co}$  X rays by the decrement line method Radiology 90 (1968) 369
- HORSBY R J PRICE R H SAUNDERS J E and DINGWALL P W Performance of a 6 MeV Van der Graaf linear accelerator Brit J Radiol 41 (1968) 312
- NAYLOR G P and ORMSBY P L A graphical method for the production of isodose curves from central axis and transverse data Brit J Radiol 41 (1968) 829
- ORCHARD P G Decrement lines a new presentation of data in cobalt 60 beam dosimetry Brit J Radiol 37 (1964) 756
- ORR J S LAURIE J and WAKERFIELD S A study of 4 MeV transverse data and associated methods of constructing isodose curves Phys in Med Biol 9 (1964) 503

## PHYSICAL MEASUREMENTS INCLUDING DEPTH DOSE DATA AND ISODOSE CURVES FOR 8 MV ROENTGEN RAYS

by

S K AGARWAL R V SCHEELE and J WALKER

An Arco Mevatron 8 linear accelerator recently installed (July 1969) at the University of Virginia Hospital varies in a number of ways from other models of linear accelerators in use today. It can be operated at specific electron energies from 3 to 10 MeV, the accelerator rotary drum rotates through more than  $360^\circ$  permitting both arc and full rotational therapy with clockwise and counterclockwise movements, the beam stopper is retractable, a beam bending magnet causes the electron beam to deflect through an angle of  $261^\circ$  towards the target, and there is a facility for a straight through undeflected electron beam. This paper is intended to present the results of physical measurements related to electron peak energy, roentgen ray asymmetry, percentage depth doses and isodose curves which were made while preparing this machine for routine operation producing roentgen rays at 8 MV. The Brit J Radiol Suppl No 10 includes 8 MV percentage depth dose tables which are based on only one set of reported data by NEWBERRY & BEWLEY (1955) while an unpublished report of which we are aware is that of WRIGHT et coll (1969). We hope that this report of our experience with this machine and the results obtained will be of use to others in the future.

Submitted for publication 4 January 1971

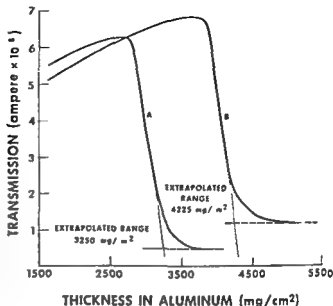


Fig 1 Relationship between the transmission of electrons produced at 6 MeV (A) and 8 MeV (B) settings and the thickness of aluminum absorbers. The extrapolated range is at the intersection of the extrapolated transmission curve with the estimated contribution of background due to bremsstrahlung in the absorber and other causes

**Electron energy calibration** The Arco Mevatron 8 linear accelerator has been designed to operate between 3 and 10 MeV at 1 MeV intervals; however, the machine at this facility has been used to date at only two energies, 6 and 8 MeV. Electron energy calibration is achieved by the range measurement method as this was found to be the quickest and easiest to set up. Relative intensities of electron current are measured by a 1N 2482 Salkes Tarzian diode connected to a Model No 610C Keithley electrometer. The diode detector is set at a distance of 100 cm from the target. Absorption curves of electrons are measured in aluminum (Fig 1) and electron energy is evaluated from the range energy relationship given by KATZ & PENFOLD (1952)

$$R_p = 0.530 T - 0.106$$

$$\text{for } 2.5 < T < 17 \text{ MeV}$$

$R_p$  is the extrapolated range in aluminium ( $\text{g}/\text{cm}^2$ ), for electrons with kinetic energy,  $T$

**Röntgen ray asymmetry** The determination of beam flatness is accomplished using a remote control radiation field scanner, which was manufactured in the department's machine shop and is pictured in Fig 2. This is used in conjunction with the diode detector electrometer combination discussed previously. Its directional response was checked against a Baldwin Farmer substandard dosimeter and found to be within  $\pm 1\%$ . Typical beam flatness curves obtained

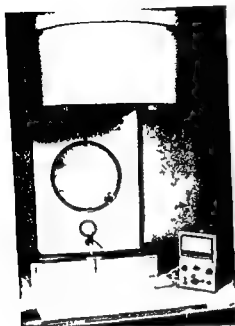


Fig. 2 Remotely controlled radiation field scanner along with the diode detector and Keithley electrometer

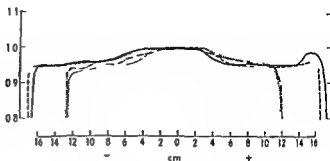
with this measuring system are shown in Fig. 3. The flatness was found to be within  $\pm 3-4\%$  over a  $25\text{ cm} \times 25\text{ cm}$  field with the collimator wide open and is not as good as the manufacturer's specification of  $\pm 2.5\%$  beam flatness over the same field.

**Röntgen ray output.** Output is determined according to the procedure recommended in ICRU Report 10d (1963). For a preset dose at the control console, the output is determined at a depth of 5 cm in a water phantom at a target-to-water surface distance of 100 cm with  $10\text{ cm} \times 10\text{ cm}$  field size at 100 cm. A Baldwin Farmer substandard dosimeter calibrated recently for cobalt 60 gamma rays at the National Bureau of Standards and a Victoreen Radocon 555 equipped with a 100 HA probe are used for these measurements. The Baldwin Farmer readings are corrected for temperature and pressure chamber energy response and multiplied by  $C = 0.94$  (GREEN & MASSEY 1967). The corrected reading is divided by the percentage depth dose at 5 cm depth (89.3%) to yield the dose at the maximum dose depth (2 cm). If the measured output varies from the preset dose by more than  $\pm 2\%$ , the preset dose is changed by adjusting two variable resistors located inside the control console.

**Depth dose measurements.** Central axis depth dose measurements were made employing the diode-detector electrometer measuring system and a large water



Fig 3 Roentgen ray beam flatness curves along the axis parallel to the gantry (—) perpendicular to it (---) and the two diagonal axes of the radiation field (— — — and — — —)



phantom ( $45\text{ cm} \times 54\text{ cm} \times 41\text{ cm}$ ) equipped with a remote control probe moving mechanism (Fig 4)

Linearity of the diode response at various depths within the phantom was checked against the Baldwin Farmer substandard dosimeter. A plastic tank, having thin walled plastic tubes at two depths to provide a waterproof heath for the substandard dosimeter, was employed to determine the dose rates at depths 2, 5, 10, 15 and 20 cm with a  $10\text{ cm} \times 10\text{ cm}$  field size at an SSD of 100 cm. Taking the dose rate at 2 cm to be the maximum percentage depth doses at 5, 10, 15 and 20 cm were determined. These values were compared with those obtained using the diode probe in the large water phantom and were found to be in good agreement.

The phantom water surface was maintained at a constant distance of 100 cm from the target, and the diode was moved vertically until the electrometer registered a maximum reading. The depth at which this occurred was between 1.9 and 2.0 cm and was considered to be 2 cm from the surface. This level rather than the water phantom surface served as a reference for measuring the depths. Measurements were taken for various field sizes at 1 centimeter intervals to a depth of 22 cm and depth dose curves extended to a depth of 30 cm were drawn on semilogarithmic graph paper (Fig. 5). The table of central axis depth doses for the various square field sizes investigated was generated from these curves (Table) and the relationships between percentage depth dose and area of the field at depths of 4, 8, 12, 16, 20 and 24 cm are illustrated in Fig. 6.

*Isodose curves* were determined by employing the same water phantom and remote control moving probe mechanism described above. The probe was moved laterally at various depths ranging from 1 to 22 cm with 1 cm depth increments for depths from 1 to 10 cm and 2 cm increments for depths greater than 10 cm. Readings were taken every 0.5 cm in regions of low dose gradient

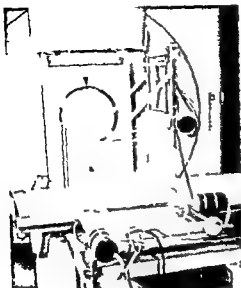


Fig 4 The moving probe mechanism in a large water phantom (46 cm  $\times$  54 cm  $\times$  41 cm) with the remote control unit (manufactured in the machine shop of the department)

and every 0.2 cm in regions of high dose gradient. To check dose rate constancy during measurements, a reading at 2 cm depth was taken after each lateral excursion of the probe had been completed. The dose rate was found to remain constant ( $\pm 0.5\%$ ) throughout the measurements. The data were recorded on large graph paper and converted into percentages by taking the dose rate at 2 cm depth to be 100%. Curves were drawn on semilogarithmic graph paper taking the abscissa as the lateral distance and the ordinate as the percentage dose. Some curves were also generated at a definite position lateral to the central ray taking depth as the abscissa and percentage dose as the ordinate. The points corresponding to the same percentage were plotted on linear graph paper and the resultant isodose curve was smoothed. Isodose curves for 10 cm  $\times$  10 cm, 15 cm  $\times$  15 cm and 7 cm  $\times$  20 cm field sizes are shown in Fig 7.

### Discussion

The electron peak energy, roentgen ray asymmetry for two perpendicular axes, and roentgen output (absorbed dose) are determined on a daily basis and the observations recorded on a log sheet. It has been found that there is no significant day-to-day variation in the electron energy ( $80 \pm 0.2$  MeV) and beam flatness ( $\pm 4\%$ ); however, the output has varied by more than  $\pm 1\%$ . The daily log sheet has proven to be useful in anticipating or detecting faults in the system, e.g., on an occasion when a change in beam asymmetry suggested a fault in the power supply to the steering systems.

1571  
1060106

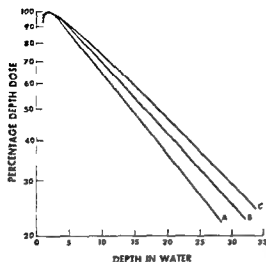


Fig 5 Relationship between the percentage depth dose of 8 MV roentgen irradiation and the depth in water for three field sizes 4 cm x 4 cm (A) 10 cm x 10 cm (B) and 25 cm x 25 cm (C) SSD 100 cm

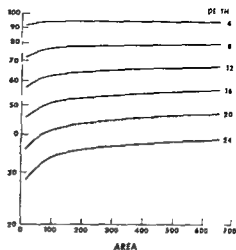


Fig 6 Relationship between the percentage depth dose of 8 MV roentgen irradiation and the area of square fields at depths 4 8 12 16 20 and 24 cm SSD 100 cm

Table

*Percentage depth doses at SSD 100 cm of an 8 MV roentgen ray linear accelerator*

Depth (cm)	Field Size (cm x cm)						
	4 x 4	6 x 6	8 x 8	10 x 10	15 x 15	20 x 20	25 x 25
10	92.5	93.5	94.0	94.4	95.1	96.1	97.0
20	100.0	100.0	100.0	100.0	100.0	100.0	100.0
30	96.4	97.0	97.5	97.5	97.5	97.5	97.5
40	91.6	92.6	93.2	93.7	93.9	94.0	94.2
50	86.9	87.8	88.6	89.3	89.6	89.8	90.1
60	81.5	82.9	84.0	85.0	85.0	85.4	87.0
70	77.2	78.5	79.5	80.4	81.9	82.8	83.9
80	72.2	74.0	75.7	77.0	78.1	79.0	79.4
90	68.2	70.1	71.7	72.9	74.8	75.7	76.0
100	64.7	66.1	67.6	69.0	71.0	72.0	72.9
120	57.1	59.3	61.4	62.7	64.7	65.9	67.0
140	51.0	53.2	55.2	56.7	58.9	60.5	61.7
160	45.6	47.5	49.3	51.0	53.2	55.0	56.9
180	40.5	42.5	44.4	45.9	48.5	50.3	51.5
200	36.0	38.0	40.1	41.6	43.8	45.4	46.7

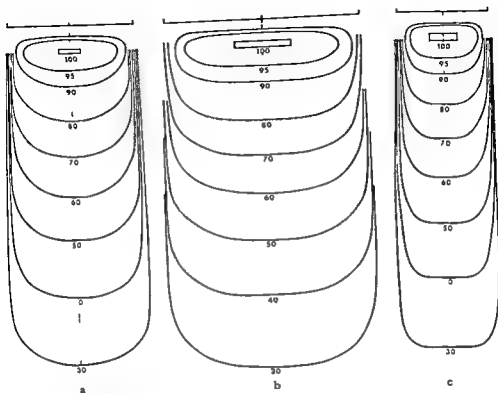


Fig 7 Isodose distributions of 8 MV linear accelerator with percentages based on the point of maximum dose SSD 100 cm Field sizes 10 cm  $\times$  10 cm (a) 15 cm  $\times$  15 cm (b) and 7 cm  $\times$  20 cm (c)

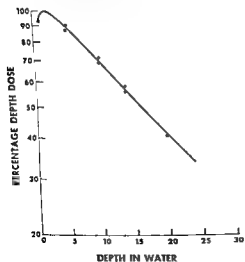


Fig 8 Comparison of the percentage depth doses of 11 MV linear accelerators in the present investigation with those given in Brit J Radiol Suppl No III (●) and those of WRIGHT et coll (○) Field size 10 cm  $\times$  10 cm SSD 100 cm

The half value thickness was found to be 13.1 mm Pb but as the electron peak energy is a better indication of roentgen ray quality at this energy, the daily check of the electron energy is provided for on the daily log sheet.

Our central axis depth dose data are compared in Fig. 11 with the data in Brit. J. Radiol. Suppl. No. 10 and that obtained on a similar linear accelerator (WRIGHT et coll. 1969). Our data for a 10 cm  $\times$  10 cm field size agree with the Brit. J. Radiol. tables within  $\pm 2\%$  and with the data of WRIGHT et coll. within  $\pm 1\%$ . This resemblance confirms our previous observation that the response of the diode used in conjunction with the Keithley electrometer is linear. Isodose curves at this energy are not readily available and therefore no comparison can be made of the shape of the curves. The curves indicate that the optical field is defined by the 50% isodose curve.

### Acknowledgements

This is to acknowledge our thanks to Dr T. E. Keats, Chairman, Radiology Department and Dr W. C. Constable, Director, Radiotherapy Division for their encouragement and valuable advice and discussion in the preparation of this paper, also Mr R. V. Leake, Mr J. E. Smith and Mrs F. C. Acree for their skilled mechanical, technical and clerical assistance. We would like to thank the staff of the Photographic Department of the University of Virginia Medical Center for their help in the preparation of the illustrations.

### SUMMARY

The Arco Mevatron-8 linear accelerator at the University of Virginia designed to operate at 1 MeV intervals between 3 and 10 MeV is being used for roentgen rays produced by electron energies of 6 and 8 MeV. The electron energy, roentgen ray flatness and absorbed dose are determined daily before the commencement of treatment, the energy being measured by extrapolating the electron range in aluminium. Central axis depth doses were measured in water for square fields from 16 to 62.5 cm<sup>2</sup> employing a remote control moving probe mechanism. The same mechanism was used to determine isodose curves. The results compared favorably with the existing data at this energy.

### ZUSAMMENFASSUNG

Es wurde der Arco Mevatron-8 Linear Accelerator der Universität von Virginia, der vorgesehen ist mit 1 MeV Intervallen zwischen 3 und 10 MeV zu arbeiten, für Röntgenstrahlen verwendet, die durch Elektronenenergien zwischen 6 und 8 MeV hervorgerufen werden. Die Elektronenenergie, die Röntgenstrahlen-Abflachung und die absorbierte Dosis werden täglich vor Beginn der Behandlungen bestimmt. Die Energie durch Extrapolation der Elektronenreichweite in Aluminium gemessen. Die Zentralstrahl-Tiefendosen wurden in Wasser für quadratische Felder zwischen 16 und 62,5 cm<sup>2</sup> gemessen, wobei ein Fernkontroll-System mit einem beweglichen Probenmechanismus verwendet wurde. Derselbe Mechanismus wurde verwendet, um Isodosis-Kurven zu bestimmen. Die Ergebnisse stimmen gut mit vorhandenen Daten bei dieser Energie überein.

## RÉSUMÉ

L'accélérateur linéaire Arco-Mevatron 8 de l'Université de Virginie construit pour fonctionner par intervalle de 1 MeV entre 3 et 10 MeV a été utilisé pour la production de rayons de Roentgen au moyen d'énergie d'électrons de 6 à 8 MeV. L'énergie des électrons, l'homogénéité du faisceau de rayons Roentgen et la dose absorbée sont déterminées chaque jour avant le commencement des traitements. L'énergie étant mesurée en extrapolant la pénétration des électrons dans l'aluminium. Les doses en profondeur sur l'axe central ont été mesurées dans l'eau pour des champs carrés allant de 16 à 675 cm<sup>2</sup> en utilisant un mécanisme de sonde mobile télécommandée. Le même mécanisme a été utilisé pour déterminer les courbes isodoses. Les résultats obtenus supportent favorablement la comparaison avec les données existantes pour cette énergie.

## REFERENCES

- DEPTH DOSE TABLES FOR USE IN RADIOTHERAPY Brit J Radiol (1961) Suppl No 10
- GREEN D and MASSEY J B The use of Farmer Baldwin and Victrometer ionization chambers for dosimetry of high energy x radiation Phys in Med Biol 12 (1967) 569
- ICRU Report 10d Clinical dosimetry NBS Handbook No 87 National Bureau of Standards Washington 1963
- KATZ I and PENFOLD A S Range energy relations for electrons and determination of beta ray endpoint energies by absorption Rev mod Phys 24 (1952) 28
- NEWBERRY G R and BEWLEY D K The performance of the medical research council 8 MeV linear accelerator Brit J Radiol 28 (1955) 241
- WRIGHT A E, BLISHONG S C, HILDON P T and BELLINGER D I Calibration of energy and absorbed dose and measurement of dose distribution and tissue air ratios for an 8 MeV linear accelerator Paper presented at the annual meeting of the American Association of Physicists in Medicine at Chicago in 1969 Abstract in Quart Bull of AAPM 1969

## CONCEPTS $W$ AND $G$ USED IN RADIATION DOSIMETRY

### Comments on current definitions

by

CARL A. CARLSSON

The concepts  $W$  and  $G$  are used in radiation dosimetry with ionization chambers and chemical dosimeters respectively. Both concepts give relations between the number of molecules changed and the energy lost by charged particles in the medium.

$W$  is commonly defined as the average energy expended in a gas for the production of an ion pair, and  $G$  as the average number of changed molecules of one type per unit absorbed energy, that is,

$$W = \frac{E}{N} \text{ and} \quad (1)$$

$$G = \frac{M}{E_D}, \quad (2)$$

where  $E$  = energy expended in the dosimeter mass,  $E_D$  = energy absorbed in the dosimeter mass and  $N$  and  $M$  are the number of ion pairs and changed molecules of observed type respectively.

Apart from minor differences in the energy expressions  $W$  seems at the first glance to be the inverse of  $G$ . In the following, fundamental differences between

the two concepts are discussed and attempts are made to give a definition of  $W$  which could be as generally valid as the most accepted definition of  $G$ . Some definitions of these concepts are valid only in a well-determined situation.

### Comparison of $G$ and $W$

Even if the same expression for energy is used, there are still fundamental differences between  $G$  and  $W^{-1}$ .

The number of changed molecules that is created ion pairs included in eq (1) is the result of a fundamental physical process: the ionization. Only ion pairs produced directly by ionizing radiation are included in  $\Lambda$ . Because ion collection is slower than many secondary processes  $\Lambda$  is not necessarily equal to the number of ion pairs observed in an ionization chamber. The number of ion pairs collected may for example be increased by ion producing collisions of excited atoms or be decreased by recombination. Further phenomena influencing the determination of  $N$  are described by PLATZMAN (1961).

As a result of this definition,  $N$  is proportional to the absorbed dose in the gas and independent of the dose rate.

Furthermore, as the molecular changes in an ion chamber are reversible that is the ions are neutralized at the electrodes the ionization chamber has constant properties independent of dose.  $W$  is therefore independent of both dose and dose rate.

On the other hand  $M$  in eq (2) is defined as the observed number of changed molecules of one type. This number may result from a complicated chain of reactions that may vary with both dose and dose rate.

A chemical dosimeter usually changes its composition during the irradiation in an irreversible way. For these reasons the  $G$  value in general varies with both dose and dose rate.

In the discussion only the initial value of  $G$ ,  $G_0$ , is used. This expression is valid at low doses, i.e., as long as the change in the composition of the dosimeter can be neglected. ICRU (1968) has not included  $G$  in their definitions of radiation quantities. In the current literature however,  $G$  is predominantly defined in terms of the energy imparted to matter  $E_D$  (ALLEN 1954, FRICKE & HART 1966, HART et al. 1956, SCHULER & ALLEN 1957) while  $W$  is defined in terms of the initial kinetic energy of the charged particles (ICRU 1968). It is pointed out in the following sections that the definition of  $G$  is generally valid but that the definition of  $W$  can only be applied in some simple irradiation geometries.

**Concept  $G$ .** Throughout this paper the  $G$  value is defined as in eq (2) as the ratio of the average chemical yield (numbers of changed molecules of the observed type  $M$ ) to the energy imparted to the chemical solution,  $E_D$ .  $E_D$  is



In eq. 11, however, the integrals have to be solved only for the kinetic energies present in the fluences of the incident particles. As the dosimeter in this case is homogeneously irradiated the absorbed dose,  $D$  instead of the absorbed energy can be used as a weighing factor

$$\bar{G}_D = \sum_{i=1}^n \frac{D_i}{D} \int_{T_{i,min}}^{T_{i,max}} G_i(T) \frac{D_i(T)}{D} dT \quad (12)$$

For intermediate cases, when all of the charged particles neither are completely stopped by the dosimeter nor traverse it with negligible energy degradation the resulting  $G$ -value can, as before, be related to the fundamental quantity  $G(T)$  by an expression identical to eqs. 8 and 11. The contribution to the absorbed energy must be evaluated for all particle energies present, whether they are initial energies or the results of slowing-down processes.

**Concept II** ICRL 1968 defines II: the average energy expended in a gas per ion pair formed, only for the case of monoenergetic charged particles completely stopped by the gas

$$\bar{II} = \frac{E}{N} \quad (3)$$

where  $E$  is the initial kinetic energy of the charged particles and  $N$  is the average number of ion pairs formed by the charged particles during their slowing-down. Ions produced by bremsstrahlung are counted in  $N$ .

As an alternate definition, ICRL 1968 gives

$$\bar{II} = \frac{E(1-G)}{N(1-G)} \quad (2)$$

where  $G$  is the fraction of the initial kinetic energy of the particle which goes into bremsstrahlung and  $G'$  is the fraction of the ions produced by the total absorption of this bremsstrahlung.

ICRL 1968 has not given a definition applicable when the charged particles are not completely stopped by the dosimeter gas. On the other hand a  $W$  is introduced in connection with Bragg-Gray measurements by ICPL

1964. In this case there is no sense in introducing the kinetic energy of the particle. The absorbed energy seems to be the only appropriate quantity and therefore  $W$  must be defined as

$$W = \frac{E_D}{N} \quad (13)$$

Thus, today, different definitions for  $W$  must be used, depending on the radiation geometry, which is unnecessarily confusing.

From the previous section it can be seen that with the introduction of absorbed energy  $E_D$ , instead of the initial kinetic energy in the definition of  $W$ , eq (15) will be a general definition valid for all irradiation geometries.

With this definition eqs (3–12) are valid for  $W^{1/2}$ .

### Conclusion

The proposed definition  $W = \frac{E_D}{\lambda}$  is applicable for all irradiation geometries

and all detector dimensions. The possibility of expressing  $W$  values valid in one irradiation geometry as a function of local  $W$  values facilitates the use of a  $W$  value determined in one detector in another.

### Acknowledgement

The author wishes to express his gratitude to Dr Niels W. Holm, Prof. Kurt Liden and Gudrun Alm Carlsson, M.Sc., for valuable discussions.

### SUMMARY

The ICRU definition of  $W$ , the average energy expended in a gas per ion pair formed, is applicable only when the charged particles are completely stopped by the gas or under charged particle equilibrium conditions. By changing the definition from  $W = E/\lambda$ , where  $E$  stands for initial kinetic energy, to  $W = E_D/\lambda$ , where  $E_D$  means energy imparted,  $W$  can be used even when charged particle equilibrium does not exist, as in the case of cavity ionization dosimetry. A further advantage of the proposed definition is that  $W$  is closer related to the inverse of the quantity  $G$  used in radiation chemistry, where  $G = M/E_D$  is defined as the average number  $M$  of changed molecules of one type per unit absorbed energy. Fundamental differences between  $W$  and  $G^{1/2}$  are discussed.

### ZUSAMMENFASSUNG

Die ICRU Definition von  $W$ , der mittleren Energie die in einem Gas per gebildetes Ionenpaar verbraucht wird, ist nur dann anwendbar wenn die geladenen Partikel durch das Gas vollständig aufgehalten werden oder unter Gleichgewichtsbedingungen der geladenen Partikel. Durch Änderung der Definition von  $W = E/\lambda$ , wobei  $E$  die initiale kinetische Energie bedeutet zu  $W = E_D/\lambda$ , wobei unter  $E_D$  die absorbierte Energie verstanden wird, kann  $W$  auch dann verwendet werden wenn ein Gleichgewicht der geladenen Partikel nicht vorhanden ist wie bei der Kavitäts Ionisations Dosimetrie. Der Fall ist Ein weiterer Vorteil der vorgeschlagenen Definition ist dass  $W$  enger zu dem umgekehrten Wert von  $G$  related ist der in der Strahlenchemie verwendet wird wobei  $G = M/E_D$  als die mittlere Zahl  $M$  veränderter Moleküle eines Typs per Einheit absorbierter Energie definiert ist. Fundamentale Unterschiede zwischen  $W$  und  $G^{1/2}$  werden diskutiert.

## RÉSUMÉ

La définition donnée par l'ICRU de  $H$  énergie fournie dans un gaz par paire d'ions formé n'est applicable que quand les particules chargées sont complètement arrêtées par le gaz ou dans les conditions d'équilibre des particules chargées. Si on remplace la définition  $H = E/N$  ou  $E$  est l'énergie cinétique initiale par  $H = E_D/N$  ou  $E_D$  représente l'énergie absorbée on peut utiliser  $H$  même quand il n'y a pas d'équilibre des particules chargées comme c'est le cas dans la dosimétrie d'ionisations de cavité. Un autre avantage de la définition proposée est que  $H$  est en rapport plus étroit avec l'inverse de la quantité  $G$  utilisée en chimie des radiations ou  $G = M/E_D$  est défini comme le nombre moyen  $M$  de molécules modifiées d'un type par unité d'énergie absorbée. L'auteur examine les différences fondamentales entre  $H$  et  $G$ .

## REFERENCES

- ALLEN A. O. The yields of free H and OH in the irradiation of water. *Radiat. Res.* 1 (1954) 85.
- FAW R. E. and DONNERT H. J. Radiation effects in chemical dosimetry. *Nucl. Instr. Meth.* 58 (1968) 307.
- FRICKE H. and HART E. J. Chemical dosimetry. *In* Radiation dosimetry Vol. 2, p. 167. Edited by F. H. Attix and W. C. Roesch. Academic Press, New York, London, 1966.
- HART E. J., RAMLER W. J. and ROCKLIN S. R. Chemical yield of ionizing particles in aqueous solutions. Effects of energy of protons and deuterons. *Radiat. Res.* 4 (1956) 378.
- ICRU. Physical aspects of irradiation. Report 10b of the International Commission on Radiological Units and Measurements. NBS Handbook 85. National Bureau of Standards, Washington, 1964.
- ICRU. Radiation quantities and units. Report 11 of the International Commission on Radiation Units and Measurements. Washington, 1968.
- PLATZMAN R. L. Total ionization in gases by high energy particles. An appraisal of our understanding. *Int. J. Appl. Radiat.* 10 (1961) 116.
- ROESCH W. C. and ATTIX F. H. Basic concepts of dosimetry. *In* Radiation dosimetry Vol. 1, p. 1. Edited by F. H. Attix and W. C. Roesch. Academic Press, New York, London, 1968.
- SCHULER R. H. and ALLEN A. O. Radiation chemistry studies with cyclotron beams of variable energy. Yields in aerated ferrous sulfate solution. *J. Amer. Chem. Soc.* 79 (1957) 1565.

## CORRECTION OF ISODOSE-DIAGRAMS FOR $^{60}\text{Co}$ AND 35 MeV ELECTRONS AT PENETRATION OF LUNG TISSUE

by

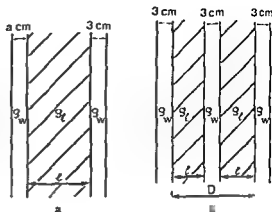
ULLA BRITA NORDBERG

Measurements in a phantom were made to investigate how the course of isodose curves is influenced by the passage of regions having a volume weight of less than  $1 \text{ g/cm}^3$ . This effect is correlated to volume weight to enable a simple approximate calculation of the corrections necessary in routine dose planning. The individual volume weight of normal lung tissue was established for 13 patients.

*Material* The thorax phantom consisted entirely of polystyren. On the entrance side there was a 3 cm thick homogeneous sheet corresponding to the thorax wall and then 11 mm polystyren sheets perforated with holes 3 mm in diameter simulating lung tissue. The sheets were stratified so that small air bubbles of about 3 mm in diameter were formed. Human lung tissue contains alveoli the diameter of which can be up to 1 mm at the most. The phantom had the same chemical composition in its homogeneous part as in its lung simulating part though in the latter the volume weight (in  $\text{g/cm}^3$ ) was lower. Lung volume weight was varied by introducing 1 mm air gaps respectively 1 mm homogeneous sheets between the perforated polystyren sheets thus getting

From the Department of Radiation Physics (Director Prof. K. Liden) University of Lund, Sweden. Submitted for publication 12 March 1971.

Fig 1 Thorax phantom constructions  
 a)  $\rho_w = 1.04 \text{ g/cm}^3$  Phantoms A, B, C and D  $a = 3 \text{ cm}$   $l = 20, 15, 9$  and  $3 \text{ cm}$   $\rho_l = 0.58, 0.42, 0.37$  and  $0.25 \text{ g/cm}^3$  Phantom G  $a = 15 \text{ cm}$   $l = 20 \text{ cm}$   $\rho_l = 0.42 \text{ g/cm}^3$  b)  $\rho_w = 1.04 \text{ g/cm}^3$   $\rho_l = 0.42 \text{ g/cm}^3$  Phantom E  $D = 20 \text{ cm}$   $l = 10 \text{ cm}$   $l = 7 \text{ cm}$  Phantom F  $B = 13 \text{ cm}$   $l = 6 \text{ cm}$   $l = 4 \text{ cm}$



volume weights ( $\rho_l$ ) of 0.32, 0.42 and 0.58  $\text{g/cm}^3$ . For one of the measurements the lung simulating part was made of sawdust, compressed to a volume weight of 0.25  $\text{g/cm}^3$ .

The phantom measurements were made with microionization chambers and with photographic film. Certain measurements referred to were made in a water phantom with a cable connected ionchamber or with Fricke dosimeters. Calculation of absorbed dose from measured ionization for electrons was done by means of a calibration curve drawn from identical depth dose determinations with ionchambers and Fricke dosimeters. The mean electron energy  $E_x$  at a depth of  $x \text{ g/cm}^2$  is assumed to be  $(E_0 - kx) \text{ MeV}$ , where  $E_0$  is the initial electron energy in MeV and  $k = 2 \text{ MeV/g cm}^2$ .

The wall of the microionization chambers was about 0.25  $\text{g/cm}^2$  and required a perspex cap for exposure measurements with  $^{60}\text{Co}$  radiation. A number of chambers provided with caps 0, 0.5, 1.0, 2.0, 2.5 and 3.0 mm thick were irradiated in a thorax phantom having a volume weight of 0.25  $\text{g/cm}^3$ . The absorbed dose was evaluated using the individual chamber constants valid for a 3.0 mm cap. Investigations were made in the thorax phantom at depths of 2.5, 5.0 and 10.0 cm. Absorbed dose determinations with different cap thicknesses were, at all the depths, within  $\pm 3\%$  for 14 measuring chambers at each depth. As a result no caps were used for the measurements in the thorax phantom.

### Method

**Cobalt 60** The central axis depth absorbed dose for the field  $10 \text{ cm} \times 10 \text{ cm}$  at SSD 70 cm was determined with ionchambers for four different types of phantom (A, B, C, D) and for four different lung volume weights (1, 2, 3, 4) (Fig 1 a).

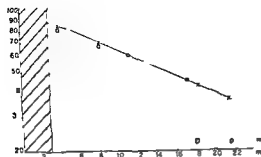


Fig 2 Central axis depth absorbed dose in the phantoms A, B, C and D  $^{60}\text{Co}$  SSD 70 cm  $10\text{ cm} \times 10\text{ cm}$   $\rho_1 = 0.42\text{ g/cm}^3$  Measurement in phantom A ( $\times$ ) B ( $\bullet$ ) C ( $\circ$ ) and D ( $+$ )

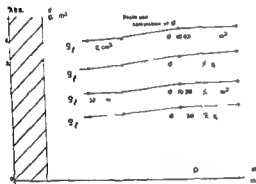


Fig 3 Absorbed equivalent density ( $d$ ) as a function of depth in phantom for different  $\rho_1$   $\bar{d}$  = mean value of  $d$  in the investigated interval

The four phantom types were (A) 3 cm thorax wall (volume weight  $\rho_w = 1.04\text{ g/cm}^3$ ) 20 cm lung tissue 3 cm thorax wall (B) the same as (A) but with 15 cm lung tissue, (C) the same as (A) but with 9 cm lung tissue (D) the same as (A), but with 3 cm lung tissue

The four lung volume weights ( $\rho_1$ ) were (1)  $0.58\text{ g/cm}^3$  (2)  $0.42\text{ g/cm}^3$  (3)  $0.32\text{ g/cm}^3$  (4)  $0.25\text{ g/cm}^3$

Measurements were not made within the thorax walls themselves nor close to the border lines between different volume weights

The absorbed dose distribution perpendicular to the central axis was determined at 6, 10 and 14 cm depths in the thorax phantom with a volume weight of  $0.42\text{ g/cm}^3$ . The same distribution has also been measured in a water equivalent phantom at depths having the same central axis depth absorbed dose as 6, 10 and 14 cm in the thorax phantom. Ionization chambers were used for these measurements

**35 MeV electrons** The central axis depth absorbed dose for the field  $10\text{ cm} \times 8\text{ cm}$  at SSD 110 cm was determined with ionchambers for four different phantom variants and three different lung volume weights. The four phantom

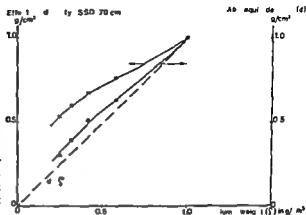


Fig 4 Effective density ( $d$ ) for SSD 70 cm (left curve) and absorption equivalent density ( $d$  right curve) as functions of volume weight ( $\rho$ ) for  $^{60}\text{Co}$

types were the same as for the  $^{60}\text{Co}$  measurements. The depth absorbed dose for the same radiation geometry was determined for one lung volume weight ( $0.42 \text{ g/cm}^3$ ) in two phantom types (E and F) where an extra wall of water equivalent material was placed at different depths in the lung tissue (Fig 1 b) (E) 3 cm thorax wall, 10 cm lung tissue 3 cm extra wall, 7 cm lung tissue 3 cm thorax wall, (F) 3 cm thorax wall, 6 cm lung tissue 3 cm extra wall, 4 cm lung tissue 3 cm thorax wall.

Also the depth absorbed dose for one lung volume weight ( $0.42 \text{ g/cm}^3$ ) was established in a phantom where the anterior thorax wall was only 1.5 cm thick (G in Fig 1 a) (G) 1.5 cm thorax wall, 20 cm lung tissue, 3 cm thorax wall.

Measurements were not made close to the border lines between two volume weights.

The absorbed dose distribution perpendicular to the central axis at a depth of 13 cm in the thorax phantom with lung volume weight  $0.42 \text{ g/cm}^3$  was investigated using film. The optical density of which was evaluated in per cent of the density in the central axis. The density of the film has earlier been proved to be linearly dependent on the absorbed dose in corresponding measurements with film in homogeneous phantom, where film density was correlated with depth absorbed dose measurements.

## Results

**Cobalt 60** Fig 2 gives the  $^{60}\text{Co}$  measurements in the four different phantom types (A B C D) for volume weight  $0.42 \text{ g/cm}^3$ . Due to the measuring errors, only one curve can be drawn which implies that the absorbed dose at a point in the lung tissue is largely independent of the amount of lung tissue behind it. This is also valid for the other volume weights. When  $x$  cm of material,

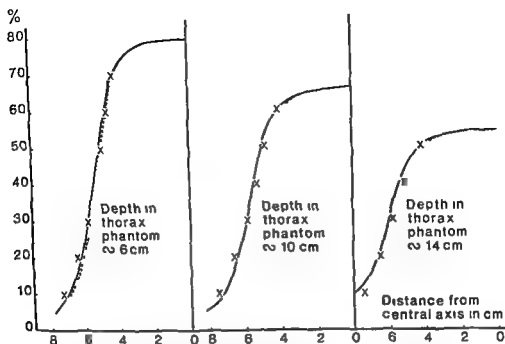


Fig 5 Absorbed dose distribution perpendicular to central axis  $^{60}\text{Co}$  SSD 70 cm 10 cm  $\times$  10 cm  $\rho_1 = 0.42 \text{ g/cm}^3$  Measuring points in thorax phantom (x) distribution in water equivalent material corrected for increased depth (full drawn curve) the same distribution without this correction (dotted curve)

measured along the central axis with broad beam geometry in a phantom, causes the same decrease in depth absorbed dose as  $y$  cm of water with density  $\rho_{H_2O} \text{ g/cm}^3$  the value  $y/x \cdot \rho_{H_2O} \text{ g/cm}^3$  in this paper will be used as the effective density of the material valid for the SSD used. If the radiation beam is parallel, the value  $y/x \cdot \rho_{H_2O} \text{ g/cm}^3$  will be named absorption equivalent density. The inverse square law effect for the valid SSD and for the depth differences between  $x$  and  $y$  can be eliminated. Thus the effective density can be converted into an absorption equivalent density independent of SSD.

Comparing the measured values from Fig 2 with the corresponding central axis data from the Brit J Radiol Suppl No 10 for water an effective lung density valid for SSD 70 cm is obtained. A calculation of an absorption equivalent density is done for four different depths. Fig 3 shows that the absorption equivalent density ( $d$ ) is almost constant regardless of the depth for which the value is calculated. Fig 4 shows the mean value of this density, ( $\bar{d}$ ) corresponding to the value at a depth of 12 cm in Fig 3) as a function of the true volume weight. In the diagram there is also a curve with the effective



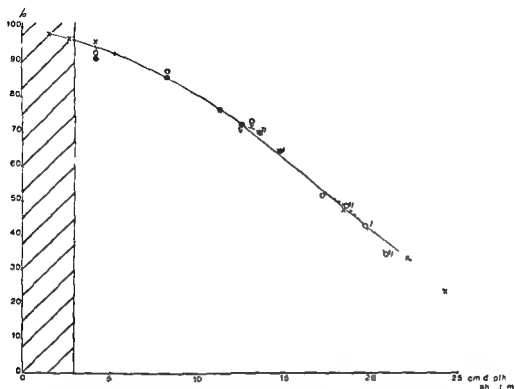


Fig 6 Central axis depth absorbed dose in thorax phantoms A B C and D 35 MeV e SSD 110 cm 10 cm  $\times$  8 cm  $\rho_l = 0.42$  g/cm<sup>3</sup> Measurements in phantom A (x) B (o) C (●) and D (+) Measurements marked 1) were made in the posterior chest wall Mean value of measurement in lung (full-drawn curve)

density valid for SSD 70 cm as a function of the true volume weight. This effective density, arrived at directly from the slope of the depth absorbed dose curve in lung tissue, is the one which is determined at individual exit measurements on patients.

Fig 5 shows the absorbed dose distribution perpendicular to the central axis for depths of 6, 10 and 14 cm in the lung phantom, ( $\rho_l = 0.42$  g/cm<sup>3</sup>) as well as corresponding distribution in water-equivalent phantom at levels having the same depth absorbed dose in the central axis. If a correction for divergence of the latter distribution to corresponding depths in the lung phantom is done, a somewhat wider (2–4 mm) distribution is obtained. The water and lung curves are considered to be in agreement within the measuring errors.

**35 MeV electrons** Fig 6 shows the central axis depth absorbed dose for the field 10 cm  $\times$  8 cm at SSD 110 cm, volume weight 0.42 g/cm<sup>3</sup> and different phantom types (A, B, C, D). The spread in the measuring values for the different

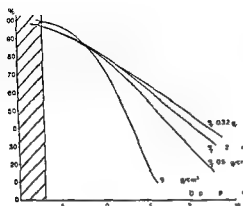


Fig 7

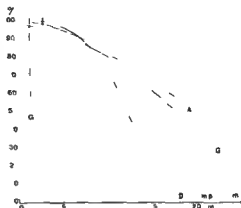


Fig 8

Fig 7 Central axis depth absorbed dose in thorax phantom 35 MeV  $e^-$  SSD 110 cm  $10\text{ cm} \times 8\text{ cm}$   $\rho_1 = 0.58, 0.42$  and  $0.32\text{ g/cm}^3$   $\rho_1 = 1.00\text{ g/cm}^3$  indicates corresponding water curve

Fig 8 Central axis depth absorbed dose in thorax phantom 35 MeV  $e^-$  SSD 110 cm  $10\text{ cm} \times 8\text{ cm}$   $\rho_1 = 0.42\text{ g/cm}^3$  Phantoms A and G

phantom types is greater here than with  $^{60}\text{Co}$ . A mean value curve of the lung measurements was drawn which is later used. The dotted parts of the curve show the course in the posterior thorax wall for the three largest phantom types. The increase in depth absorbed dose immediately within the posterior wall is due to build up of  $\delta$  particles and the decrease at the exit side is due to lack of back scattered electrons. There is a corresponding relation for the other two volume weights.

Fig 7 shows the mean value curve from Fig 6 together with the corresponding mean value curves for volume weights  $0.32$  and  $0.58\text{ g/cm}^3$  and the depth absorbed dose curve in water obtained with Fricke dosimeters; the curves being normalized to the same incident electron fluence. The absorbed dose in the anterior chest wall and in the lung immediately behind this wall was found to be lower than it would be in a homogeneous water equivalent phantom due to lack of back scattered electrons. At about  $5\text{ cm}$  depth in lung tissue, the absorbed dose in the thorax phantom became higher than the absorbed dose in water at the same depth.

Fig 8 shows the depth absorbed dose for volume weight  $0.42\text{ g/cm}^3$  with anterior thorax wall  $1.5$  and  $3\text{ cm}$  respectively. The curves belonging to the different thicknesses have about the same shape.

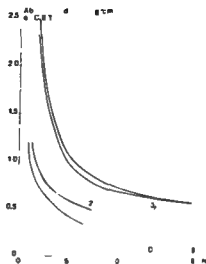


Fig 9 Absorption equivalent density (or CFT) as a function of depth in lung 1) 2 cm chest wall 9 MeV  $\rho_1 = 0.39 \text{ g/cm}^3$  (ALMOND et coll) 2) 2 cm chest wall 1.5 MeV  $\rho_1 = 0.39 \text{ g/cm}^3$  (ALMOND et coll) 3) 3 cm chest wall 35 MeV  $\rho_1 = 0.42 \text{ g/cm}^3$  (present investigation) 4) 1.5 cm chest wall 35 MeV  $\rho_1 = 0.42 \text{ g/cm}^3$  (present investigation)

ALMOND et coll (1967) have made similar depth absorbed dose measurements in lung tissue for up to 18 MeV electrons using a thorax wall of 2 cm (in a few cases 4 cm) together with a true lung volume weight of  $0.39 \text{ g/cm}^3$ . The value  $0.39 \text{ g/cm}^3$  may practically be considered as comparable to  $0.42 \text{ g/cm}^3$  in the present investigation, which is the volume weight of the phantom consisting only of perforated sheets. These depth absorbed doses show the same reduction in relation to water curves at small depths but the deviations are less and extend only about 1.5 cm into the lung tissue.

The depth absorbed dose from the thorax phantom was compared with corresponding values for water equivalent material at different depths. As for  $^{60}\text{Co}$  the effect of inverse square law was eliminated. The absorption equivalent density for volume weight  $0.42 \text{ g/cm}^3$  thus calculated for different depths is shown in Fig 9 as a function of depth in lung tissue together with corresponding results by ALMOND et coll (1967). ALMOND et coll and BOONE et coll (1969) use the expression coefficient of equivalent thickness (CET), which corresponds to the numerical value of the virtual absorption equivalent. This is greater than  $1 \text{ g/cm}^3$  for depths smaller than the depth where the water and lung curves cross each other (see Discussion). The thin wall gives somewhat higher value than the thick wall which has also been accounted for by ALMOND et coll.

The perpendicular absorbed dose distribution at a depth of 6, respectively 10 cm lung tissue (that is 9 respectively 13 cm depth in the phantom) is seen in Fig 10. The distribution in water equivalent material at levels with about

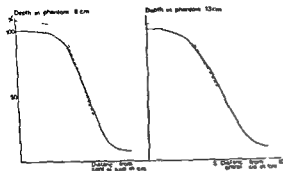


Fig 10 Absorbed dose distribution perpendicular to central axis 35 MeV electrons SSD 110 cm, 10 cm  $\times$  8 cm  $\rho_1 = 0.42$  g/cm<sup>3</sup> Full-drawn curve indicates measured and dashed curve calculated values without correction for divergence

the same depth absorbed dose at the central axis is also given here. Motivation for choosing these levels is presented later on in this paper. The correction for divergence is unimportant and may be ignored. The deviations within the penumbra region can be considered as small for clinical purposes. The distribution in lung tissue is largely unchanged if the posterior thorax wall lies immediately behind the measuring plane or 10 cm away.

### Discussion

For <sup>60</sup>Co the primary absorbed dose contribution at a point in thorax can be calculated from the depth in g/cm<sup>3</sup> using true lung volume weight together with inverse square law correction for the difference between the true depth and the corresponding depth in water. The scatter contribution to the same point decreases with density and the attenuation of this contribution is diminished. The net effect is negative. This decrease in scattering contribution results in a lower total depth absorbed dose than would be expected from depth in g/cm<sup>3</sup> using true lung volume weight. The correction for inverse square law has the same effect. This corresponds to a virtual density greater than the true volume weight. In this investigation the virtual density arrived at directly from measurements is called effective density. If the effect of inverse square law is eliminated it is called absorption equivalent density.

The depth absorbed dose increases with enlarged field size, that is increased scatter contribution. For <sup>60</sup>Co the depth absorbed dose increases for example from 16 cm field to 100 cm field 5, 10 and 15 % at 4, 8 and 12 cm respectively. For 35 MeV electrons the corresponding increase is 4, 26 and 75 %.

It seems reasonable to assume that the ratio between absorption equivalent density and volume weight is near to 1 for small scatter contribution. That is for cobalt absorption equivalent density ought to be near the true volume

weight and be relatively independent of the depth while for electrons a greater and variable difference would be expected.

*Cobalt-60* Fig 3 confirms that the absorption equivalent density for  $^{60}\text{Co}$  is largely independent of the depth for a given volume weight. The ratio between the absorption equivalent density and the volume weight varies according to the left part of Fig 3 for  $^{60}\text{Co}$  between 1.07 and 1.20 within the interval investigated.

The scatter contribution was calculated for the different volume weights from the measured depth absorbed dose curve at 12 cm depth that is at 9 cm depth in the lung tissue. This contribution varied from 72 to 83% of the corresponding contribution in water phantom. In order to see the reduction in direct relation to the volume weight, the same calculations were made for the same depths in  $\text{g cm}^{-3}$  6.8  $\text{g cm}^{-3}$ . The scatter contribution then varied from 60 to 90% of the corresponding contribution in water phantom for change of volume weight from 0.25 to 0.58  $\text{g cm}^{-3}$ .

The value of volume weight for normal lung tissue given by different authors varies between 0.2 and 0.7  $\text{g cm}^{-3}$  (1, 3, 6, 7, 8, 9, 11). However patients who are irradiated in the thorax region often have abnormal lung volume weight.

Measurements on 13 patients with roentgenologically unaffected lung gave effective densities for SSD 70 cm from 0.41–0.74  $\text{g cm}^{-3}$  mean value 0.55  $\text{g cm}^{-3}$ . According to Fig 4 this corresponds to a volume weight of 0.27  $\text{g cm}^{-3}$  which value is in agreement with DAHL & VIKTERLOF's (1955) measurements on calf lung.

In order to correct the absorbed dose of a cobalt treatment according to exit measurements it is not necessary to know the true volume weight of the lung. If, however, such measurements have to be transferred to treatment with another type of irradiation where exit measurements can hardly be done, for example with electrons, it may be necessary to calculate the true volume weight.

*35 MeV electrons* Fig 9 confirms that for 35 MeV electrons, the ratio between absorption equivalent density and volume weight in a thorax phantom varies considerably and is much higher than for  $^{60}\text{Co}$ . For volume weight 0.72  $\text{g cm}^{-3}$  it varies from 2.4 to 1.3 between 5 and 20 cm depth in lung tissue. Measurements for 15 MeV electrons by ALMOND et coll. (1967) give values between 2.8 and 1.3 in the interval 1.5 to 7.5 cm depth in lung tissue. LAUGHLIN (1965) has suggested an absorption equivalent density of 0.5  $\text{g cm}^{-3}$  for normal lung tissue and for 22 MeV electrons (valid for different depths and field size) and volume weight 0.33  $\text{g cm}^{-3}$  that is a ratio of 1.5. LAUGHLIN (1965) also has used a factor of 1.3 together with a volume weight of 0.38  $\text{g cm}^{-3}$  which means the same value of 0.5  $\text{g cm}^{-3}$  for absorption equivalent density. DAHLER et coll. (1969) also recommended this ratio. POHLIT (1969) suggested a depth absorbed dose shift, which gives the ratio of 1.5 without any specifications.

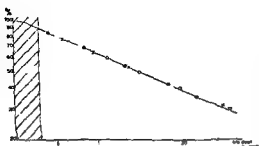


Fig 11 Central axis depth absorbed dose for  $^{60}\text{Co}$  SSD  $\approx 70$  cm  $10$  cm  $\times$   $10$  cm  $\rho_1 = 0.42$  g/cm $^3$  Measured values (O) calculated values using absorption equivalent density  $0.51$  g/cm $^3$  and inverse square law correction (X) calculated values using effective density  $0.67$  g/cm $^3$  (O)

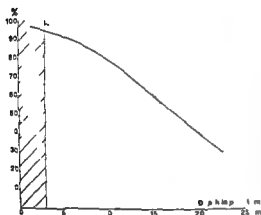


Fig 12 Central axis depth absorbed dose for  $3.0$  MeV  $\times$  SSD  $110$  cm  $10$  cm  $\times$   $8$  cm  $\rho_1 = 0.42$  g/cm $^3$   $d = 0.64$  g/cm $^3$   $d = 0.67$  g/cm $^3$  Full drawn curve indicates measured dashed curve calculated values using absorption equivalent density and inverse square law correction dotted curve calculated values using effective density ( $d$ ) for  $^{60}\text{Co}$  and SSD  $70$  cm

### Clinical application

**Cobalt 60** The investigation shows that the correction of depth absorbed dose data for water when applied to lung tissue can be done by adjusting to depth in g/cm and (1) using an absorption equivalent density followed by a separate inverse square law correction or (2) using an effective density which already includes inverse square law correction for the valid focus distance (Fig 11)

Fig 5 shows that even the distribution perpendicular to the central axis is retained by this method. This method thus permits the transformation of an isodose diagram as a whole into a cross section of the patient. Fig 11 a) shows that the correction can take place with sufficient accuracy parallel to the central axis and not along lines of divergence with sufficient accuracy for SSD  $\geq 70$  cm.

The procedure for drawing a corrected isodose diagram according to alternative (2) is then as follows. A number of lines parallel to the central axis and passing through the entire cross section of the patient are drawn at distances one or two centimetres apart. The thicknesses of different materials along these

Table I

*Measured and calculated depth dose values*

Calculated depth absorbed dose in ° 30 MeV e <sup>-</sup> SSD 110 cm 10 cm × 8 cm	Measured depth absorbed dose		
	$r_1 = 0.58$ g/cm	$r_1 = 0.42$ g/cm	$r_1 = 0.32$ g/cm

From absorption equivalent  
density and inverse  
square law correction

90	86	86	86
80	76	76	76
70	68	68	68
60	60	60	61
50	52	54	55
40	46	48	49
30	39	42	44
20	32	36	38

From effective density for  
 $C_0$

90	85	83	81
80	75	74	71
70	68	66	64
60	60	59	55
50	54	54	52
40	48	48	47
30	42	43	42
20	36	37	37

lines are then determined, each of which is multiplied by the effective density, whereby the depths of the border lines in the cross section measured in g/cm are obtained. The same lines are drawn in the water isodose diagram to be used and the depths in g/cm<sup>2</sup> for the different isodoses (90 % 80 % etc.) are read. A comparison along corresponding lines in the cross section of the patient and in the isodose diagram will give the regions of density in which the different isodose curves lie.

The exact point of intersection between an isodose and the line is then determined in the following way. The depth in g/cm<sup>2</sup> of the border line nearest the isodose in the direction of the beam entrance is subtracted from the depth in g/cm of the same isodose. The resulting difference is then divided by the effective density of the region. The quotient is the distance in cm from the

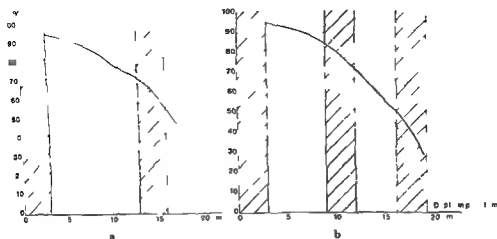


Fig 13 Central axis depth absorbed dose for 35 MeV  $e^-$  SSD 110 cm  $10\text{ cm} \times 8\text{ cm}$   $\rho_1 = 0.42\text{ g/cm}^3$  Full drawn curve indicates measured dashed curve calculated values using effective density for  $^{60}\text{Co} = 0.67\text{ g/cm}^3$  a) Phantom E b) Phantom F

border line mentioned above to the new point of intersection for this isodose on the line investigated. After having established the intersections of the different isodose curves along all the lines, the complete corrected isodose diagram can easily be drawn.

**35 MeV electrons** Fig 9 shows that adjusting according to depth in  $\text{g/cm}^3$  cannot be done with a constant value of the absorption equivalent density if an agreement along the entire depth absorbed dose curve is wanted. On the other hand it is possible to choose a value which gives the least deviation within the most valid depth interval. The dashed curve in Fig 12 was obtained at calculation according to the  $\text{g/cm}^3$  method with constant value for the absorption equivalent density and afterwards correction for inverse square law. This value was chosen so that measuring curve and calculated curve cross each other at 60%. The volume weights of 0.32, 0.42 and 0.58  $\text{g/cm}^3$  thus correspond to the absorption equivalent densities of 0.60, 0.64 and 0.72  $\text{g/cm}^3$  respectively (giving a correct 60% depth absorbed dose) that is essentially higher than for  $^{60}\text{Co}$ .

Correction for inverse square law is of much less importance for SSD 110 cm than for SSD 70 cm. This means that the effective densities for  $^{60}\text{Co}$  (SSD 70 cm) and 35 MeV electrons (SSD 110 cm) ought to be more comparable. The effective densities for  $^{60}\text{Co}$  and for corresponding volume weights are 0.60, 0.67 and 0.76. If these values are used as the effective density for electrons



Table 2

*Deviations between calculated and measured depth absorbed doses*

Calculated depth absorbed dose in 35 MeV $e^-$ SSD 110 cm 10 cm $\times$ 8 cm $\rho_t = 0.42$ g/cm using effective density 0.67 g/cm for $^{60}\text{Co}$	Measured depth absorbed dose in	
	Phantom E	Phantom F
90	84	85
80	74	78
70	69	70
60	63	61
50	58	59
40	50	49
30	41	43
20		36

curves are obtained which for practical purposes show the same approximate agreement with measuring values as those described earlier (Fig. 12)

The calculated curves show the greatest divergence from the measurement curves close to the thorax wall as well as at greater depths in the lung tissue (Table 1). The relative deviation near the bordering surface is relatively low, but after the normalizing point of 60 % it increases.

Fig. 13 shows measured depth absorbed doses calculated according to depth in g/cm using effective density for  $^{60}\text{Co}$  in the phantoms E and F in Fig. 1 b. Table 2 gives deviations between calculated and measured depth absorbed dose in figures. The comparison between Tables 1 and 2 reveals that the deviations are of the same magnitude.

The measured absorbed dose distribution perpendicular to the central axis in lung tissue shows relatively good agreement with the absorbed dose distribution in water equivalent material at the levels which in the approximate depth correction are to agree to the depths in lung tissue (Fig. 10). The measured central depth absorbed doses at the two valid depths were established = 100 %. There is complete agreement only for depths having central axis depth absorbed dose of 60 %. Thus, a normalization at central axis for the measured curve gives 104 and 108 %, respectively, for the calculated curves in the central axis.

Within the limits of error which are seen in Tables 1 and 2, the electron isodoses for SSD 110 cm can be transformed in their entirety parallel to the central axis according to the method given on page 123, using effective density measured for  $^{60}\text{Co}$  and SSD 70.

A few patients were irradiated with a lateral electron field. The measurement

values obtained in the oesophagus show a good agreement with the calculations done in accordance with the above principle

The importance of this simplified isodose correction for electrons from the viewpoint of dosage will be illustrated by two examples

*One field* Assumed that the relevant absorbed dose is 90 %, that is, the area to be irradiated is between 80 and 100 %, the following deviation is obtained for 6 000 rad and a fairly dense lung tissue with a volume weight of 0.42 g/cm<sup>3</sup>. The absorbed dose within the treatment area, calculated according to the method just mentioned lies between 5 330 and 6 670 rad that is the minimal figure lies 400 rad lower than was calculated. At a depth of 15 cm, the calculated absorbed dose is 4 270 and the true one 4 130, a deviation of 140 rad. On the other hand the calculated absorbed dose at 18 cm depth is 2 810, but the true one is 3 310, an error of 500 rad. If no correction of water absorbed dose data is done at all the error at these two depths would however fall at about 3 000 rad. If there is a dense middle wall within the lung tissue, the deviations are largely the same as in the previous case.

*Two opposing fields* A distance between both the opposite entry portals of 20 cm is assumed with 14 cm lung tissue between the lung walls. The calculated absorbed dose summed from both of the fields differs within the entire area with  $\pm 8$  % from the true absorbed dose except for a centimetre close to the surface, where the calculated dose is 15 % too low. If there is a dense middle wall within the lung tissue the figures are somewhat lower, being then 5 and 10 %, respectively.

### Conclusions

The dose absorbed in the tumour and in the healthy tissue of a patient must be as accurately established as possible. Corrections for inhomogeneity are therefore necessary in dose planning programmes. The method described in this paper has been used routinely in our department since 1967 for normal planning mainly performed by radiographers. It will be transferred to our programme for automatic dose planning which is under development.

The investigation has proved that this simple method gives sufficiently accurate results for clinical purposes for both <sup>60</sup>Co gamma and electron beam therapy. For electrons there will still remain a certain small discrepancy between true and calculated values which, however, is quite acceptable in comparison to the errors obtained without any corrections.

Clinical measurements of absorption equivalent density also make it possible to estimate the true lung volume weight of a patient from the phantom data presented in this paper.

## SUMMARY

A simple method for the construction of individual isodose curves in lung tissue for  $^{60}\text{Co}$  and 35 MeV electrons is described. The validity of the method was experimentally verified. A mean volume weight for normal lung tissue was determined for 13 patients.

## ZUSAMMENFASSUNG

Eine einfache Methode individuelle Isodosiskurven im Lungengewebe für  $^{60}\text{Co}$  und 35 MeV Elektronen zu konstruieren wird beschrieben. Die Gültigkeit der Methode wurde experimentell nachgewiesen. Ein mittleres Volumengewicht des normalen Lungengewebes von 13 Patienten wurde bestimmt.

## RESUMÉ

Description d'une méthode simple pour la construction de courbes isodoses individuelles dans le tissu pulmonaire pour le  $^{60}\text{Co}$  et pour les électrons de 35 MeV. La validité de cette méthode a été vérifiée expérimentalement. L'auteur a déterminé pour 13 malades un volume poids moyen pour le tissu pulmonaire normal.

## REFERENCES

- 1 ALMOND P. R., WRIGHT A. F. and BOONE M. L. M. High energy electron dose perturbations in regions of tissue heterogeneity. Part II. Physical models of tissue heterogeneities. *Radiology* 88 (1967) 1146.
- 2 BOONE M. L. M., ALMOND P. R. and WRIGHT A. E. High energy electron dose perturbations in regions of tissue heterogeneity. *Ann. N. Y. Acad. Sci.* 161 (1969) 214.
- 3 DAHL O. and VIKTERLOF K. J. Den fungerande människolungans röntgenabsorption: en undersökning med sikte på djupdosberäkningar och fantomkonstruktioner. (In Swedish) *Nord. Med.* 54 (1955) 1576.
- 4 DAHLER A., BAKER A. M. and LAUGHLIN J. S. Comprehensive electron beam treatment planning. *Ann. N. Y. Acad. Sci.* 161 (1969) 198.
- 5 DEPTH DOSE TABLES FOR USE IN RADIO THERAPY. *Brit. J. Radiol.* (1961) Suppl. No. 10.
- 6 ICRU Report 10d. Clinical dosimetry. NBS Handbook No. 87. National Bureau of Standards. Washington 1963.
- 7 LAUGHLIN J. M. Symposium on high energy electrons. Montreux 1964. p. 262. Proceedings. Springer Berlin 1965.
- 8 — High energy electron treatment planning for inhomogeneities. *Brit. J. Radiol.* 38 (1965) 143.
- 9 LEUNG P. M. K., SEAMAN H. and ROBINSSON F. Low-density inhomogeneity correction for 22 MV X-ray therapy. *Radiology* 94 (1970) 449.
- 10 POHLIT W. Calculated and measured dose distributions in inhomogeneous material and in patients. *Ann. N. Y. Acad. Sci.* 161 (1969) 189.
- 11 SUNDBOM L. Dose planning for irradiation of thorax with  $^{60}\text{Co}$  in fixed beam teletherapy. *Acta radiol. Ther. Phys. Biol.* 3 (1965) 343.

## IMMOBILISATION, COMPENSATION AND FIELD SHAPING IN MEGAVOLT THERAPY

by

N E SØRENSEN and A SELL

This communication deals with attempts made to overcome problems that arise in ensuring that the absorbed dose within the patient is in agreement with the calculated dose plan. The introduction of megavolt apparatus has increased the demand for precision so that the fields may be well defined with consequent reduction both in the integral and unwanted absorbed doses to particularly radiosensitive organs such as the eyes, brain and kidneys.

The reasons for a deviation between the planned and the true absorbed dose may be: (1) The position of the patient changing from treatment to treatment; (2) The body surface not being the same as that of the phantom which is plane and used for measuring the depth dose and isodose curves that form the basis of the calculations; (3) With the field limitation marked directly on the skin, variation during the treatment may still occur from breathing as well as from treatment to treatment because of loss of weight or small differences in the set up; (4) Inhomogeneous tissue (bone, air cavities etc.).

*Positioning of the patient* The most stable and reproducible positions of the patient during treatment are supine and prone, the former being normally preferred. This position permits irradiation of the patient from the front and from the sides and where the treatment unit can be fully rotated and sections of the couch

---

Submitted for publication 12 July 1971

FIG. 1 Treatment shell for a radiation of the oral cavity with parallel opposing fields.



removed or changed to very thin sheets (e.g. mylar folium) from the back as well.

Uniform positioning from treatment to treatment may even be difficult with the patient supine especially in head and neck conditions. Different technical remedies may be used. Shells of plastic or plaster of Paris and tailored for the individual patient are considered to form the most effective immobilisation unit. The cost in money and technician's time in connection with their production has however proved a handicap. Partly individual shells such as front shells in connection with standard back support kits have been employed in some centres. The authors have found these useful, for instance in the treatment of bladder and prostate tumours.

The experimental manufacture of fully individual shells was started in 1964 particularly for the treatment of the head and neck region. A front shell of plastic, and a back shell of plaster were connected by straps with press-studs (Fig. 1). The plastic part was produced in the same way as described by other centres. An impression was taken of the patient with plaster bandages and from this a plaster model was produced. This enabled a plastic shell to be manufactured by a vacuum process on an industrial machine. A difficulty arose in making a suitable back shell of sufficient stability. After several experiments with unsatisfactory results, such a shell was produced from plaster bandages. This combination is still in use.

The back shell is made as follows. The patient is placed on a couch with a surface similar to the treatment couches and pieces of foam rubber of different shapes are used to position the head and arms; this is done with due regard to the treatment and comfort of the patient. A convenient position having been found, the patient, if possible, sits up. Plaster bandages are then applied from the top of the head down to the scapulae. Before the plaster hardens the patient is returned to his original position so that the bandages may be held and moulded by hand as necessary until they harden. The hardening process takes about five minutes.

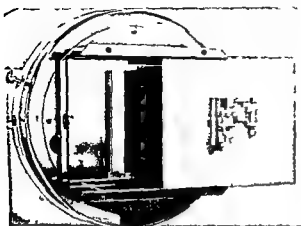


Fig 2 Filter holder for v edge and compensating filters with the v edge filter in its correct position and the compensating filter drawn halfway out

The plaster shell is then extended around the shoulders and the top of the head. A bandage is also applied from the back of the head down over the foam rubber support to the surface of the couch to fix the head at the correct distance. The patient is then removed from the shell and the foam rubber replaced by plaster to form a solid, reproducible support.

This type of back shell has proved to be so effective that where the field size has proved too large to be cut out of the front shell it has been possible to remove the latter during the treatment and only use it during the set up procedure.

The front shell could of course also be of plaster but it was found best to proceed to a plastic shell for the following reasons: (1) It is much more convenient for the patient. (2) If a treatment programme is changed either immediately or later during the treatment a new plastic shell may be made quickly and without inconvenience to the patient. (3) The positive model may be used later for the design of compensating filters and for obtaining exact measurements and contours of the patient. (4) The plastic shell is transparent.

The immobilisation of the patient during treatment is more secure with the shell system. The latter also saves time in the daily set up and thus increases the capacity of the treatment apparatus. Furthermore compensating filters demand that the planning and treatment positions be as nearly the same as possible.

*Compensating filters* Without compensation for missing tissue, problems in the planning of the treatment will always arise. Even with complicated set ups and by making calculations of the dose distribution at several levels it may be impossible to obtain a sufficiently homogeneous absorbed dose within the tumour volume. Individually designed compensating filters make both the set up and the calculation easier.

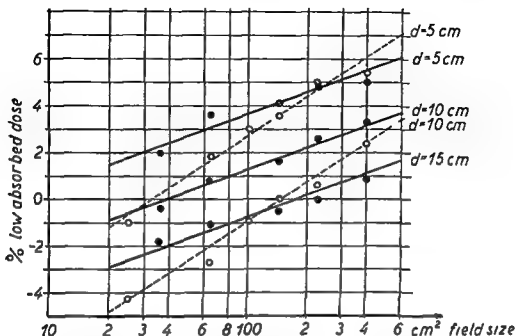


Fig 3 Measured error when compensating for 5 cm missing tissue with  $\frac{5}{\rho_{\text{Al}}} = 1.85 \text{ cm Al}$   
 ○ ○ for  $^{60}\text{Co}$   $\gamma$  rays and ● — ● for 6 MeV roentgen rays for different field sizes and depths (d) in the water phantom. A low absorbed dose means over compensation.

A photographic method that simplifies the design of compensating filters has been described earlier (SØRENSEN 1968). The method may be used both for the system with aluminium columns described by ELLIS et coll (1959) and HALL & OLIVER (1961) and the system with lead sheets described by WILKS & CASBOW (1969). We employ the former system. A filter holder with two frames is mounted on each treatment unit so that it is possible to insert wedge and compensation filters at the same time (Fig 2). The mounting plate for both filters has a slot near one of the corners with which a spring loaded ball in the filter holder engages. This arrangement ensures that the plate is correctly located and at the same time the filter is properly orientated.

To simplify the system it has been decided to use the same columns independent of the machine and the energy. The spectrum of energies includes  $^{60}\text{Co}$   $\gamma$  rays and 6 and 32 MeV roentgen rays. The cross section of the columns is  $0.74 \text{ cm} \times 0.74 \text{ cm}$  (For  $^{60}\text{Co}$  this corresponds to  $1 \text{ cm} \times 1 \text{ cm}$  at the normal treatment distance of 80 cm). By selecting the length of the columns as  $\frac{1}{e} = \frac{1}{2.7} = 0.37 \text{ cm}$

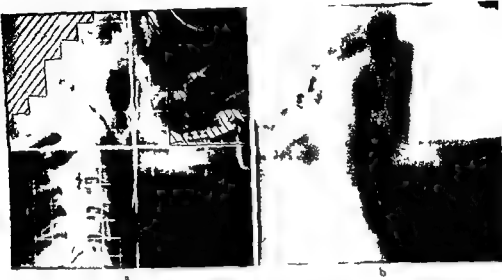


Fig 4 An example of field shaping in the neck region a) Film obtained on the simulator with hatching of the areas to be covered with lead b) Control film taken on the therapy unit with the compensating filter mounted

per cm missing tissue where  $\rho$  indicates the density in  $\text{g/cm}^3$  the system is further simplified as the lengths and sides of the columns then have the same module of

0.37 cm HALL & OLIVER (1961) gave the best length for  $^{60}\text{Co}$  rays as  $\frac{0.88}{\rho}$

The error in using  $\frac{1}{\rho}$  cm was measured by an arrangement described by SUMM (1964) A Mix D block 5 cm thick, was placed in front of a water phantom (50 cm  $\times$  50 cm  $\times$  60 cm) The absorbed dose was measured at different depths and with various field sizes The same measurements were taken without the Mix D block but with one of aluminium corresponding to 5 cm tissue (1.85 cm) placed in the position used for the compensating filters on each machine

The results for the  $^{60}\text{Co}$  rays and 6 MeV roentgen rays appear in Fig 3 For field sizes from 5 cm  $\times$  5 cm to 20 cm  $\times$  20 cm, and depth in the water phantom varying from 5 to 15 cm the absorbed dose varies from 4 per cent high to 6 per cent low For the 32 MeV roentgen rays the technique is used only for field sizes varying between 10 cm  $\times$  10 cm and 14 cm  $\times$  14 cm The absorbed dose was then 5 per cent low at 5 cm phantom depth and between 1 and 2 per cent low at 10 cm and 15 cm depth This has been considered a satisfactory compromise and is used routinely in this department



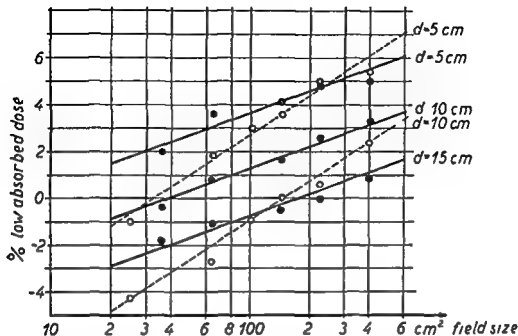


Fig 3 Measured error when compensating for 5 cm missing tissue with  $\frac{5}{\rho_{Al}} = 1.85$  cm Al  
 ○ for  $^{60}\text{Co}$   $\gamma$  rays and ● for 6 MeV roentgen rays for different field sizes and depths (d) in the water phantom. A low absorbed dose means over compensation.

A photographic method that simplifies the design of compensating filters has been described earlier (SØRENSEN 1968). The method may be used both for the system with aluminium columns described by ELLIS et coll (1959) and HALL & OLIVER (1961) and the system with lead sheets described by WILKS & CASEBOW (1969). We employ the former system. A filter holder with two frames is mounted on each treatment unit so that it is possible to insert wedge and compensation filters at the same time (Fig 2). The mounting plate for both filters has a slot near one of the corners with which a spring loaded ball in the filter holder engages. This arrangement ensures that the plate is correctly located and at the same time the filter is properly orientated.

To simplify the system it has been decided to use the same columns independent of the machine and the energy. The spectrum of energies includes  $^{60}\text{Co}$   $\gamma$  rays and 6 and 32 MeV roentgen rays. The cross section of the columns is  $0.74 \text{ cm} \times 0.74 \text{ cm}$  (For  $^{60}\text{Co}$  this corresponds to  $1 \text{ cm} \times 1 \text{ cm}$  at the normal treatment distance of 80 cm). By selecting the length of the columns as  $\frac{l}{\rho} = \frac{1}{2.7} = 0.37 \text{ cm}$

## DIGITAL STEREOSCINTIGRAPHIC EXPERIMENTS WITH A GAMMA-CAMERA

by

E. INGEMAR LARSSON

A number of ideas have been presented in the literature about the problems encountered in distinguishing overlapping information from the information of interest in gamma-camera cinematography. FREEDMAN (1970) proposed a digital method very similar to the method described in the present work. MEHLHERRS (1970-1971) technique is based on analogue read-out but is otherwise principally the same. Theoretical considerations around this problem are presented by CASSEN (1968) and McAFFEE & MOZLEY (1969). The present work is also based in part on the longitudinal section scanning method described by KUHL & EDWARDS (1968). All previously described methods for three dimensional investigations with the gamma-camera except that of CHARKES & SOMERANASIN (1968) however require the use of quite different equipment than is ordinarily employed thus eliminating the possibility of carrying out static or dynamic examinations with conventional depth response. This is also the case with the methods described by ANGER (1968) and MIRALDI & DiCHIRO (1970).

Submitted for publication 21 June 1971

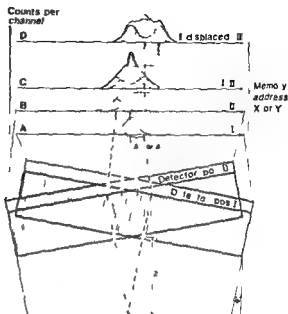


Fig 1 Operating principle for stereoscinigraphy with conventional gamma camera equipment and digital storage facilities. Sections A and B PSF from two sources with detector in positions I and II respectively. Section C Sum of PSF in sections A and B. Section D Sum of PSF in sections A and B with address displacement as shown by arrows between sections B and D.

**Method** A number of experiments which have been carried out for evaluating the stereoscinographic or tomographic possibilities with conventional gamma camera equipment and digital storage facilities are described in the present work (Nuclear Chicago Pho Gamma III Inter technique Bloc d'exploration, BM 96 B, 4096 word memory two Codeur d'amplitude CA 13 B Unite de visualisation RG 96, Calculateur intermediaire, RG 23). The operating principle is illustrated in Fig 1. At the bottom of this figure there are two point sources having an internal distance of  $z$ . These two sources are first detected by the gamma camera crystal with its parallel hole collimator in position I. This means that the central axis of the detector deviates with an angle  $\theta$  from the normal direction of view. The photons from the upper source will be detected by the centre of the crystal and will also be counted in the centre of the memory, which is illustrated with the point spread function (PSF) indicated by the dashed curve in section A of Fig 1. Photons from the lower point source will be counted in channels the mean address of which deviates  $\Delta x$  or  $\Delta y$  which is proportional to  $z \sin \theta$ , from the centre of the memory, as is illustrated by the dashed dotted PSF in section A. This point source will also be detected with a poorer resolution distance as a result of the poorer imaging properties of the parallel hole collimator for sources lying at a greater distance (ÅNGER 1964, LARSSON & LIDEN 1969).

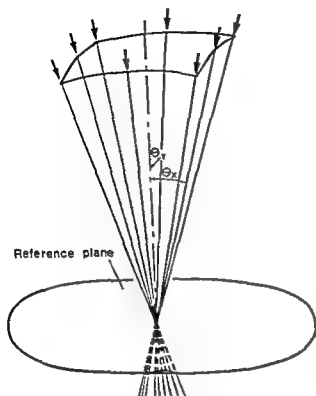


Fig 2 Three-dimensional illustration of the direction of view for the central axis of the detector in eight elementary images. The angles of inclination are  $\theta_1$  and  $\theta_2$ .

With the detector in position II the upper source will still be seen by the centre of the detector and will be registered in the centre of the memory. Photons from the lower point source however will be displaced to the left in the memory compared to position I (section B). Views Nos I and II in sections A and B are stored separately on magnetic tape. They can afterwards be summed into the solid line in section C without any address-modification. Using a certain suppression level indicated by the dotted line in the figure we can now display channels containing pulses the main part of which is obtained from the upper point source.

The solid line in section D also represents a sum of views Nos I and II but all addresses in view No II are shifted in proportion to  $\sin \theta$  as indicated by the arrows from section B to section D. The PSF from the upper source is therefore suppressed or blurred into the separated PSF indicated by the broken line in the same way as the lower source in section C. The view of the lower source is enhanced because the dashed-dotted PSF from sections A and B coincide in the memory.

The views in sections A and B can, of course, be viewed with a stereoscope (CHARLES & SOMEURANASIN 1968) giving a subjectively perceived three dimensional image. Using the digital treatment illustrated here, we can make use of any desired angle of inclination and also extend it in several azimuths in order to avoid false summation of multiple sources as mentioned by McAFFEE & MOZLEY (1969). The size of the angles is partly limited by the reduction of the field of view at greater distances from the collimator.

It is apparent from Fig. 1 that the effect of the earlier explained suppression or blurring is greater the better the resolution one can achieve, because the PSF from different depths will be better differentiated in all sections of the figure. The blurring effect in the planes which are out of focus can also be regarded as a low pass-filtering of the spatial frequency spectrum i.e. a removal of high frequency components.

The problem of selecting a rotation centre close to the organ being investigated is solved by using an index which is mounted in the centre of the collimator. This index points towards the same point on the patient or the phantom in all the individual elementary images. The phantom, or patient must therefore also normally be moved between each exposure.

Fig. 2 shows three dimensionally how the angle of inclination is selected in eight different elementary views. Photons from any point in the shaded plane, hereafter called the reference plane, receive the same memory addresses in all the individual images when using a small angle of inclination. This means that the best focus is achieved in this plane when the elementary images are added without address-modification.

## Results

Focusing to any plane other than the reference plane can be performed using different address-displacements when the elementary images are added. This is illustrated in Fig. 3 shown in the isometric display fashion. In Fig. 3 a and b four cobalt 57 point sources are placed in the reference plane and in Fig. 3 c and d the position of the sources is 12 cm below the reference plane. Fig. 3 a and c are focused on this plane simply by adding all eight elementary images together without any address-displacement.

It is possible to focus to the point sources 12 cm below the reference plane as shown in Fig. 3 b and d if a certain address-modification is applied when the elementary images are added. In Fig. 3 b the individual point spread functions from the eight elementary images are displayed slightly separated and suppressed with a factor of 8 as compared to Fig. 3 a. In Fig. 3 d however the eight PSF from the elementary images coincide in the memory and the resultant images

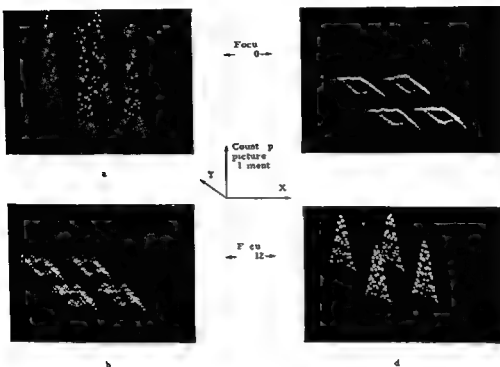


Fig 3 Isometric display of point sources at two different distances a) and d) Sources in plane of best focus b) Sources 12 cm above plane of best focus c) Sources 12 cm below plane of best focus

are therefore enhanced as compared to Fig 3 c. The angle of inclination in this experiment is 10°.

Eight separate elementary images (B—I) are illustrated in Fig 4 a, together with a view in the centre (A) taken without any inclination of the detector, i.e. with conventional depth response. Three digits 0, 7 and 14 drawn with technetium 99m solution are placed in the reference plane and at 7 and 14 cm below that plane respectively. The eight minutes exposure time for the conventional view is now replaced by a one minute exposure of each of the eight elementary images. In this case the angle of inclination is 20°. This relatively large angle makes it easier to see the differences between the separate elementary images giving at the same time a more marked tomographic effect. There is a slight distortion of the projected plane when using this angle. This distortion also limits the angle of inclination in this technique, a limitation which does not exist when using a collimator with parallel holes inclined in relation to the central axis of the detector (FREEDMAN 1970, McAFEE & MOZLEY 1969).

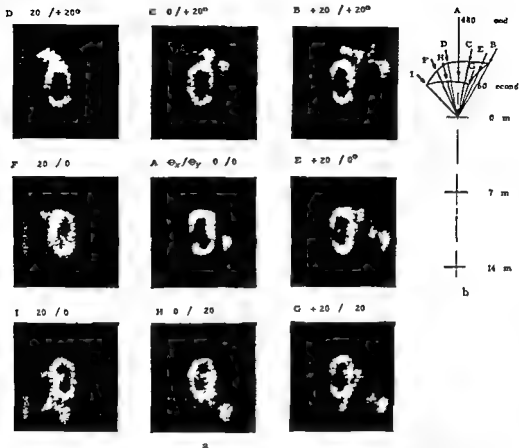


Fig 4 Stereoscintigraphy of three digits 0 7 and 14 drawn with technetium solution and placed 0 7 and 14 cm below the reference plane respectively a) Illustration of the differences in the elementary images (B I) For purpose of comparison image A is taken without inclination b) Directions of detector and exposure times for the eight elementary images and image A

MUEHLEHNER 1970, 1971) The necessity of working at a greater distance from the collimator thereby degrading the overall resolution, is also a limiting factor when setting the angle of inclination

When the elementary images in Fig 4 a are added, it is, however possible to enhance the contrast in the planes selected for best focus because the information from other depths is blurred Identification of the different numbers from the planes selected is possible in Fig 5 a b and c

For purposes of comparison it is here shown that it might not always be necessary to use all of the eight elementary images as in Fig 5 a, b and c, only four are used in Fig 5 d e and f In these four elementary images it should be

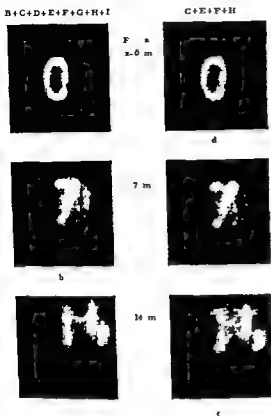


Fig 5 Summation of the elementary images in fig 4 Sum of the eight elementary images with a) 0 in plane of best focus (reference plane) b) 7 in plane of best focus (7 cm below the reference plane) and c) 14 in plane of best focus (14 cm below the reference plane) d) e) and f) The same as for a) b) and c) respectively but only four of the elementary images are used

possible to compensate for the distortion of the projected plane mentioned earlier when the angle of inclination is large. This could be done by a slight adjustment of the gain along the  $x$  or  $y$  axis respectively although this is a complicating factor which has not been used here. Better results are obtained from this comparison when more elementary images are used and distortion of the kind mentioned earlier is negligible.

Fig 6 illustrates that it is more difficult to achieve contrast enhancement with this technique when looking for a region with lower activity concentration than its surroundings. The liver phantom in Fig 6 has a simulated non active lesion placed as illustrated in the cross sectional side view of the phantom. Quantitative information is presented in the lower row of views as isocount levels at 95 90 85 80 and 75 % of the maximum. These levels are produced using repeated exposures on the same polaroid film and calculated settings on the dial determining the suppression level on the RG 96 unit. To overcome the statistical



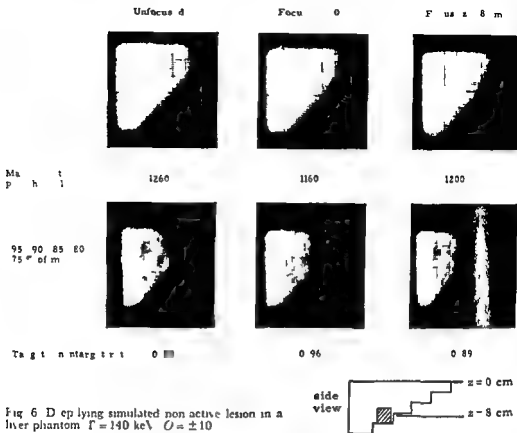


Fig. 6. Displaying simulated non active lesion in a liver phantom  $\Gamma = 140 \text{ keV}$   $O = \pm 10$

fluctuations along the  $z$  levels a nine element smoothing matrix is applied with the aid of the tape recorder RG 23 (LARSSON 1970). The conventional unfocused view has a target to non target ratio of 0.88. Nothing can be said from the unfocused view alone about the depth of the simulated lesion. From the stereo cinigram with focusing to the surface we get the information that it is not close to the surface because it has a poorer target to non target ratio. Focusing to the 8 cm depth gives the actual position of the simulated lesion, because this gives the same target to non target ratio as obtained in the unfocused view. This focusing has, however, very little influence on the maximum number of counts, as this maximum is already from the beginning spread out over a large number of channels. This lack of contrast enhancement can also be explained by the fact that the low pass filtering has no effect on the d.c. component in the spatial frequency spectrum or little influence on the low frequency components.

### Discussion

When applying this method on patients it is desirable to take a view with the conventional depth response. Although this increases the examination time by a factor of 2 the whole procedure with readjustments of patient and detector position can be carried out without making undue demands on the patient.

It has been mentioned that a good resolution is of great importance when applying this or other, similar tomographic techniques. If the spatial frequency spectrum contains only low frequency components the low pass-filtering will have little or no effect as the high frequency components have already been removed at earlier stages. This means that the visibility of the details will be poor in the plane of best focus as well as above or below this plane. The poor high frequency response of all types of imaging devices of this kind complicates tomographic investigations in nuclear medicine. ANGER (1969) has achieved a better resolution by using a converging collimator. Extremely good resolution can be achieved with the pinhole-collimator at small distances (LARSSON & LIDEN 1969), where sensitivity is also highest. These properties could also be used for tomographic purposes as noticed by BECK & ANGER (1969).

### Acknowledgements

This work was supported by grants from John and Augusta Perssons Foundation for Medical Research, Karlskrona, Sweden. The author wishes to express his sincere gratitude to Prof. A. Liden for fruitful discussions throughout the work.

### SUMMARY

A simple and cheap method for stereoscinigraphy using conventional gamma-camera equipment and digital storage facilities is described. Some experimental results are presented and discussed.

### ZUSAMMENFASSUNG

Eine einfache und billige Methode für Stereoscinigraphie unter Anwendung einer konventionellen Gamma-Kamera-Ausrüstung und einem digitalen Speicher wird beschrieben. Einige experimentelle Ergebnisse werden gezeigt und besprochen.

### RÉSUMÉ

Description d'une méthode simple et peu coûteuse pour faire une stéréoscinographie au moyen d'un équipement de gamma-caméra ordinaire et d'un équipement de stockage de données numériques. L'auteur présente quelques résultats expérimentaux et les examine.

## REFERENCES

- ANGER H O Multiplane tomographic gamma ray scanner *In* Medical radioisotope scintigraphy I p 203 IAEA, Vienna 1969
- Scintillation camera with multichannel collimators *J nucl Med* 5 (1964) 515
- BECK R N and ANGER H O Discussion *In* Medical radioisotope scintigraphy I p 216 IAEA Vienna 1969
- CASSEN H Image formation by electronic cross time correlation of signals from angular ranges of unfocused collimating channels *In* Medical radioisotope scintigraphy I p 107 IAEA Vienna 1969
- CHARKES N D and SOMBURANASIN R Stereoscintigraphy *J nucl Med* 9 (1968) 491
- FREEDMAN G S Tomography with a gamma camera *J nucl Med* 11 (1970) 602
- KUHL D H and EDWARDS R Q Image separation radioisotope scanning *Radiology* 80 (1963) 653
- LARSSON I Digital handling och presentation av gammakamerabilder (In Swedish) *Nord Med* 83 (1970) 734
- and LIDEN K Resolution components and differential linearity of gamma camera *In* Medical radioisotope scintigraphy I p 111 IAEA Vienna 1969
- MCAFFE J G and MOZLEY J M Longitudinal tomographic radioisotopic imaging with a scintillation camera theoretical considerations of a new method *J nucl Med* 10 (1969), 654
- MIRALDI F and DICHIRO G Tomographic techniques in radioisotope imaging with proposal of a new device the tomoscanner *Radiology* 94 (1970) 513
- MUEHLLEINER G Rotating collimator tomography *J nucl Med* 11 (1970) 347
- A tomographic scintillation camera *Phys in Med Biol* 16 (1971) 87

## DETERMINATION OF SMALL MASS DIFFERENCES IN ROENTGENOGRAPHY

### II Experimental investigations with a roentgen diffraction apparatus

by

L. HOLLENDER and G. LYSELL

Part I of this series (LYSELL et coll 1968) concerned a theoretic analysis of the relation between the thickness of a given mass and the photographic density of its roentgen image. The following equations were derived

$$d = \frac{(D - D_1) \ln 10}{\gamma_{D_1}(D) (\mu_1 - \mu)} \quad (1)$$

$$d = \frac{D - D_1}{\alpha D (\mu_1 - \mu)} \quad (2)$$

where  $d$  denotes the thickness of the object,  $D$  the photographic density,  $\mu$  the linear attenuation coefficient and  $\gamma_{D_1}(D)$  the rate of change of  $D$  as a function of the logarithm of the exposure and  $\alpha$  a constant. The equations hold good under ideal conditions, i.e., monoenergetic radiation and narrow beam geometry. Such ideal conditions are however rarely available in clinical roentgenography.

Submitted for publication 22 March 1971

There is, on the other hand, a need for quantitative investigations on mineralized tissue in clinical research. The present investigation therefore deals with the determination of the thickness of objects by means of the equations derived in part I first under nearly ideal conditions and secondly, under conditions approaching those prevailing in routine diagnostic work.

*Material and Methods* A Philips roentgen diffraction apparatus PW 1010 equipped with a Philips roentgen diffraction tube with copper target and four mica beryllium windows with two outputs was used. The radiation was transmitted through the nickel filter of the apparatus at 16 kVp and 20 mA and through a 5.97 mm aluminium filter at 54 kVp and 16 mA. All exposures were made in air. Three different exposure times were employed for each combination of tube tension and object thickness.

The objects examined consisted of aluminium foils of different thicknesses. At 16 kVp the foil was about 9  $\mu\text{m}$  thick and of 99.97 per cent purity (according to the manufacturers the impurities were mainly Fe and Si). At 54 kVp a foil was about 100  $\mu\text{m}$  thick both as a single layer and in three layers. The aluminium was of the same quality as that of the thinner foil. Measurements had to be made of the thickness of the various foils, the figures given by the manufacturers being only approximate. The thickness of the thin foil (9  $\mu\text{m}$ ) was measured with a Microcator (C. F. Johansson, Eskilstuna, Sweden), fifteen times in approximately the same area. An extra determination of the true value was also obtained. A piece of aluminium foil was held tightly between perspex plates (135 mm  $\times$  170 mm) and foils of corresponding size cut out. These sheets, twenty in all, were weighed on a Mettler analytical balance, type E5. Each foil was weighed twice and the thickness was calculated from its known area and density (2.7). The thicker foil was measured fifteen times with a Microcator. An independent double determination of the thickness was also made with an Etalon micrometer, the thickness was measured fifteen times.

*Film and Processing* Kodak periapical radiatized dental roentgen films were used. A standardized darkroom procedure is important, as stressed by VAN ALEN (1962) and HENRIKSON (1963) and others who also stated that the film speed increased when the developer recommended by the manufacturer was used instead of that recommended by the American Standards Association (1956). A developing process resembling that employed in routine work was chosen instead of that suggested by the ASA. The films were developed under manual agitation at 18  $^{\circ}\text{C}$  for five minutes in Kodak DX-80. Non-exposed films were always developed together with the exposed films to a certain density of base and chemical fog. After development the films were rinsed in tap water for 10 seconds, fixed in Kodak acid fixer for 10 minutes, washed in running tap water for one hour, and dried at room temperature.

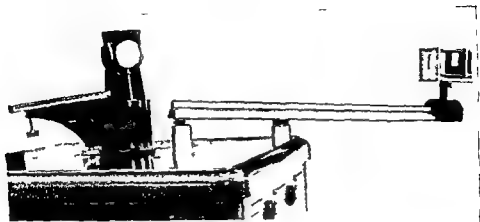


Fig 1 The diffraction apparatus and the optical bench with the device for object and film

*Device for maintaining constant relationship between object and film and irradiation geometry* An optical bench was fixed on the table of the diffraction tube to maintain the positions of object and film in relation to focus constant throughout the investigation. This bench was equipped with a rider carrying three parallel aluminium plates covered with lead (Fig 1). The front and the rear plates were connected by four bars placed parallel to the bench. The middle plate could be moved 100 mm along the four bars and the front plate had a vertical slit opening of  $4 \text{ mm} \times 44 \text{ mm}$  in front of which the object was sited parallel to the plates and covering the upper part of the slit opening. The plate in the middle was equipped with a film holder. The midpoint of the vertical dimension of the midlevel of the slit opening was marked by a small notch in the plate. This notch was clearly evident in the roentgenogram. The film was exposed centrally through the slit opening the exposed area being  $4 \text{ mm} \times 41 \text{ mm}$ . The film holder was placed in its rearmost position, producing a FFD of 1150 mm the OFD was 110 mm. An imaginary ray from the focus through the midpoint of the slit opening ran perpendicular to the foil and the film plane. (Maximum deviation of the roentgen rays in the central parts of the slit opening from this perpendicular line was  $0.1^\circ$  as estimated from repeated measurements and calculations.) The duraluminium plates were perpendicular to the optical bench (Maximum deviations less than  $0.25^\circ$  measured both in horizontal and in vertical planes.) This ensured a reproducible narrow beam geometry.

*Densitometry* An Eel universal densitometer was connected to a controlled power supply Oltronix the density range was 0.4 to 2.0. Each film was measured at a point 3 mm above the mid level of the slit opening i.e. within the area where

Table 1

*True thickness of aluminum foils for 16 kVp radiation determined from measurements with a Microcator and from weighings*

	Microcator measurements	Weighings
n	15	20
M	8.7 $\mu\text{m}$	8.72 $\mu\text{m}$
s	0.14 $\mu\text{m}$	0.24 $\mu\text{m}$
s <sub>M</sub>	0.04 $\mu\text{m}$	0.05 $\mu\text{m}$

Table 2

*True thickness of aluminum foils for 54 kVp radiation determined from measurements with a Microcator and a micrometer*

	Microcator measurements	Micrometer measurements
n	15	15
M	108.5 $\mu\text{m}$	108.3 $\mu\text{m}$
s	0.38 $\mu\text{m}$	1.18 $\mu\text{m}$
s <sub>M</sub>	0.10 $\mu\text{m}$	0.30 $\mu\text{m}$

Table 3

*Linear attenuation coefficients for aluminum at 16 kVp radiation (A) and 54 kVp radiation (B)*

A Thickness of absorber	$\mu_{\text{Al}}$ at 16 kVp ( $\text{cm}^{-1}$ )
All thicknesses	122.3
III Thickness of absorber (mm Al)	$\mu_{\text{Al}}$ at 54 kVp ( $\text{cm}^{-1}$ )
0	2.40
0.1	2.38
0.3	2.36
1	2.30
2	2.18
3	2.07
4	1.95
5	1.84

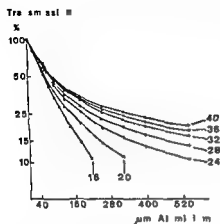


Fig 2 Relative transmission through aluminium of Hs filtered radiation generated at tube tensions from 16 kVp to 40 kVp

the foil was reproduced as well as 3 mm below the mid point, i.e. outside where it appeared. Three measurements were made at each point.

*Determination of characteristic film curves* The practical application of the equations required determination of the characteristic curves of the films. Exposures were made in air with a FFD of 440 mm. The radiation from a 1 mm  $\times$  1 mm focus for the films and the radiation from a 1 mm  $\times$  10 mm focus for an ionization chamber registered the exposure ad modum BJÄRNGÅRD et coll (1959).

Four characteristic film curves were obtained for the 16 kVp radiation and two curves for the 54 kVp radiation. The four curves at 16 kVp were made with films of different emulsion numbers. Films of two of these numbers were used at 54 kVp but no significant differences in the shapes of the characteristic curves could be demonstrated. This implied that variation in radiation energy has no appreciable influence. The characteristic curves indicating the  $\gamma$  values enabled an electronic computer to determine  $\gamma$  values for various combinations of  $D_1$  and  $D$ . For a given value of  $D_1$  a graphic representation of  $\gamma$  was obtained as a function of  $D$ .  $D_1$  was allocated values between 0.1 and 2.0 in steps of 0.1 density units producing 20 curves in all. The  $\gamma$  values were calculated by interpolation between these 20 curves.

The value of the constant  $a$  in eq. (2) is equal to the inclination of the straight line obtained when the logarithm of the photographic density value is given as a function of the logarithm of the exposure values.

*Determination of linear attenuation coefficients* The transmission of the radiation through different layers of aluminium was registered with ionization chambers at different tube tensions. The linear attenuation coefficients were determined from the curves obtained in this way.



Table 4

*Precision of the Eel densitometer estimated from measurements in 9 films of those used for thickness determinations. The photographic density was measured at two points in each film. Ten repeat measurements were made at each point. The precision is given as the standard deviation ( $s$ ) of a single observation.*

Film No	Mean photographic density (base and fog density included)	$s$	$s/s_1$
1	0.470	0.00037	0.00010
	0.510	0.00095	0.00030
2	0.470	0.00067	0.00021
	0.509	0.00082	0.00026
3	0.470	0.00042	0.00013
	0.510	0.00000	0.00000
4	0.787	0.00587	0.00186
	0.871	0.00599	0.00189
5	0.782	0.00472	0.00133
	0.877	0.00258	0.00087
6	1.204	0.00400	0.00126
	1.306	0.00328	0.001037
7	1.196	0.00309	0.000977
	1.314	0.00352	0.001113
8	1.189	0.00311	0.000984
	1.308	0.00145	0.000459
9	1.195	0.00349	0.001104
	1.318	0.00185	0.000585

## Results

**Foil thickness (true values)** These appear in Tables 1 and 2. Although the accuracy of the microcator and the balance, as well as the micrometer was not determined, the mean values of the thicknesses were considered as true, since these measuring devices are practically free from systematic errors and of high precision (balance 0.000065 g, microcator 0.32  $\mu\text{m}$ ) and as there was excellent agreement between the results. The values obtained with the highest precision were selected. Thus at 16 kVp the true foil thickness was 8.7  $\mu\text{m}$  in good agreement with measurements obtained by ERICSSON (1965). The true values at 54 kVp were 108.5  $\mu\text{m}$  and 325.5  $\mu\text{m}$  respectively.

Table 5

*Determination of foil thickness from photographic density measurements 16 kVp radiation. Upper section of foil always covered by 8.7 µm aluminium foil. Distribution of calculated thicknesses at different levels of photographic density*

Thickness range (µm)	Mean photographic density above base and fog								
	0.213	0.422	0.427	0.448	0.672	0.679	1.026	1.401	1.472
7.1-7.5									
7.6-8.0					1				
8.1-8.5					3		1	1	
8.6-9.0			2		7	1	1	2	
9.1-9.5			3		2		3	1	1
9.6-10.0			4	2			4	3	3
10.1-10.5	1	2	1	3	2	2	4	1	3
10.6-11.0		5		3		2	1		
11.1-11.5	3	2		6		3			1
11.6-12.0	1	1				1			
12.1-12.5	4					1			
12.6-13.0	1								
13.1-13.5	2								
n	14	10	10	14	10	10	14	10	10
M	12.0	10.9	9.5	10.8	8.9	10.9	9.7	9.3	10.0
s	0.91	0.45	0.51	0.55	0.87	0.92	0.63	0.65	0.48
se	0.24	0.15	0.16	0.15	0.28	0.29	0.17	0.21	0.15

*Linear attenuation coefficients* The transmission curves are given in Fig. 2. A only one value ( $122.3 \text{ cm}^{-1}$ ), of the linear attenuation coefficient had to be employed for any thickness of aluminium absorber at 16 kVp the radiation could be considered as monoenergetic. At tube tensions above 16 kVp it cannot be so considered. For example transmission measurements at 54 kVp revealed that the attenuation coefficient varied with the absorber thickness. The calculated values are given in Table 3.

*Precision of the measurements of photographic density* Nine films, employed in the determination of foil thickness were used. Ten repeat measurements of the photographic density were made at two points in each film. The precision values are given in Table 4. The accuracy depends on, among other things, the precision of the measuring apparatus (Eel densitometer) and the position of the film in the measuring device. The determinations were made at the different photographic density ranges employed in the investigation. The range of variation of the measurements was small and of similar magnitude at photographic densities above 0.7. The variation at lower densities was significantly smaller.

Table 6

*Determination of foil thickness from photographic density measurements 54 kVp radiation Upper section of slit opening covered by 108.5  $\mu$ m aluminium foil Distribution of calculated thicknesses at different levels of photographic density*

Thickness range ( $\mu$ m)	Mean photographic density above base and fog		
	0.328	0.648	1.243
71—80		2	
81—90		2	
91—100		1	
101—110	1	2	
111—120	2	1	
121—130		4	2
131—140			2
141—150	7	1	2
151—160		1	3
161—170	1		2
171—180	3		
181—190			1
n	14	14	14
$\Sigma$	147.1	109.9	131.6
$\bar{x}$	22.0	26.2	16.3
$s_x$	5.89	7.01	4.3

*Foil thickness (photographic determinations)* Three series of exposures at 16 kVp radiation were made on different occasions. Three levels of photographic density were obtained each time by varying the exposure time. The foil thickness was calculated according to eq. (1); the results are given in Table 5. The standard deviation was always below 10 per cent and usually around 5 per cent. All the mean values were higher than the true value. Absorber thicknesses of 108.5  $\mu$ m aluminium and 325.5  $\mu$ m aluminium respectively were used at 54 kVp. Different values of the linear attenuation coefficient were thus employed (Table 3). The results are given in Tables 6 and 7. The standard deviation of the single observation varied widely (from less than 5 per cent to about 27 per cent). All mean values were with one exception above the true value.

The series at 16 kVp comprising 14 films at each level of photographic density was again measured in the densitometer. The new values served as a basis for calculating foil thickness according to eq. (1) as well as eq. (2). The results are given in Table 8. The photographic densities were of the same magnitude as before (see Table 5). All mean values exceeded the true value.

Table 7

*Determination of foil thickness from photographic density measurements 54 kVp radiation Upper section of slit opening covered by 325.5  $\mu$ m aluminium layer Distribution of calculated thicknesses at different levels of photographic density*

Thickness range ( $\mu$ m)	Mean photographic density above base and fog		
	0.740	0.490	0.956
261—270	1		
271—280			
281—290		1	
291—300	3		
301—310	1	1	
311—320			
321—330	3	1	
331—340	2	3	
341—350	3		1
351—360	2		6
361—370	1	2	
371—380		3	3
381—390		1	2
391—400			1
401—410		2	
n	14	14	13
M	321.9	325.0	368.0
s	28.4	34.5	16.7
%s	7.60	9.23	4.62

The mean values according to eq (1) and eq (2) respectively were of the same magnitude at each level of photographic density in addition these new values for the foil thickness agreed with the means of the first determinations (Table 5)

Fq (2) was also applied in the calculation of the mean thickness of each aluminium foil or combination of foils. This was done by calculating the mean difference in photographic density at each density level and by determining the mean value of the photographic density above base and fog  $\left(\frac{\bar{D}_1 + \bar{D}}{2}\right)$ . The results are given in Table 9. The mean values exceeded the true values in 13 of the 15 cases.

Most roentgen ray sources produce a spatial variation in intensity. Nine films were exposed on various occasions through the slit opening to find out whether

Table 8

*Determination of foil thickness from photographic density measurements 16 kVp radiation Upper section of slit opening covered by 8.7  $\mu$ m aluminum foil Distribution of calculated thicknesses according to eq (1) as well as to eq (2) at different levels of photographic density*

Thickness range ( $\mu$ m)	Mean photographic density above base and fog					
	According to equation (1)			According to equation (2)		
	0.283	0.454	1.024	0.283	0.454	1.024
8.1—8.5						
8.6—9.0			1			1
9.1—9.5			1			1
9.6—10.0	1	2	2	1	4	3
10.1—10.5		4	3		5	6
10.6—11.0		5	6	1	4	2
11.1—11.5	2	2		2		
11.6—12.0	1		1	1		1
12.1—12.5	3			2		
12.6—13.0	2			3		
13.1—13.5	2			1		
13.6—14.0	1			2		
14.1—14.5	2			1		
n	14	13	14	14	13	14
M	12.6	10.6	10.4	12.3	10.3	10.2
s	1.23	0.48	0.73	1.22	0.45	0.72
sM	0.33	0.13	0.26	0.33	0.13	0.19

such variation occurred along the slit opening both exposure time and tube tension were varied. The blackened area of the film was divided by horizontal lines across the image of the vertical slit into eight equal sections a, b, c, d, e, f, g and h. The mid level of the slit was thus marked by a line separating d and e. The photographic density was measured three times in each section. A variation in intensity was found along the slit opening (Table 10), which however was less marked at 54 kVp although the focal spot was the same. Since the foils covered the upper part this variation in intensity tends to increase the difference and consequently tends to give too high a value for the foil thickness.

Experiments were performed to assess the effect of this variation in radiation intensity on foil thickness. Five films were exposed at 16 kVp radiation with the 8.7  $\mu$ m thick aluminum foil covering the upper section and 5 films were exposed with the foil covering the lower section of the slit opening. The results are given in Table 11. Three layers of 108.5  $\mu$ m thick aluminum foils were

Table 9

*Determination of foil thicknesses from photographic density measurements 16 kVp radiation and 54 kVp radiation Upper section of slit opening covered by foils of various thicknesses Eq (2) is applied Mean thicknesses are given at various levels of photographic density*

Tub tension	Mean photographic density above base and fog $\frac{\bar{D} + \bar{D}}{2}$	$\bar{D} - \bar{D}$	Mean thickness of Al foil ( $\mu\text{m}$ )
16 kVp	0.427	0.046	9.5
	0.672	0.067	8.8
	1.401	0.153	9.6
	0.422	0.051	10.6
	0.679	0.082	10.6
	1.472	0.165	9.9
	0.273	0.037	11.9
	0.448	0.033	10.4
	1.056	0.115	9.6
54 kVp	0.328	0.010	137.7
	0.648	0.015	104.6
	1.243	0.040	145.4
	0.240	0.017	322.7
	0.490	0.037	344.0
	0.9.6	0.077	367.0

used at 54 kVp radiation. Four different levels of photographic density were employed with four films at each. Two of these were exposed with the upper section covered and two with the lower section covered by the foils. The results appear in Table 12. With one exception all values for the upper section covered were higher than the corresponding values for the lower section covered.

### Discussion

The variation in thickness at 16 kVp tube tension was generally much lower than 10 per cent indicating that the resolving power of the method is good. The standard deviation was greater at 54 kVp tube tension in one case more than 20 per cent implying that the deviation of a single measurement of a thickness of about 100  $\mu\text{m}$  could exceed 20  $\mu\text{m}$ . The standard deviation of one single

Table 10

*Variation in photographic density at different tube tensions and levels of photographic density along the image of the slit opening uncovered by foils (Mean values based on two determinations)*

Film No	Mean photographic density base and fog included									
	Tube tension 16 kV p					Tube tension 54 kV p				
	1	2	3	4	5	6	7	8	9	10
Section										
a	0.820	0.835	1.194	1.209	1.420	1.421	1.051	1.720	1.748	
b	0.850	0.852	1.230	1.227	1.459	1.461	1.070	1.740	1.776	
c	0.875	0.888	1.262	1.258	1.485	1.500	1.085	1.760	1.780	
d	0.898	0.900	1.293	1.281	1.534	1.521	1.098	1.760	1.780	
e	0.920	0.925	1.337	1.311	1.559	1.563	1.105	1.770	1.800	
f	0.940	0.935	1.359	1.363	1.589	1.589	1.105	1.780	1.810	
g	0.950	0.950	1.390	1.382	1.616	1.619	1.110	1.780	1.820	
h	0.950	0.950	1.427	1.443	1.640	1.637	1.112	1.770	1.825	

measurement was however usually about 10 per cent. This means that at 54 kV p a difference in photographic density of 0.005 at densities around 1.0 cannot be considered as significant although the resolving power must nevertheless be considered as satisfactory. The standard deviation of the mean value is strongly influenced by the number of measurements; quantitative measurements should therefore be based on several independent determinations.

The systematic deviations of the calculated values from the true values call for a few remarks on pertinent sources of error.

1. Different methods were applied in the determination of the 'true' thicknesses. The agreement between the results of the measurements indicates that these values may be considered true, i.e. more accurate than the calculated values.

2. The variation in radiation intensity along the slit opening might explain the systematic discrepancies. It is however, difficult to determine the exact difference in thickness caused by this gradual change in intensity. It appears likely, however, that the systematic deviations from the true value are due mainly to the variation in radiation intensity.

3. Errors in the determination of the linear attenuation coefficients will affect the calculated thickness differences systematically. The values were obtained by attenuation measurements with the same equipment and the same kind of foil. The coefficients may be thus considered free from substantial systematic errors.

Table 11

*Calculated foil thicknesses applying eq (2) at the same level of photographic density when upper and lower section of slit opening respectively was covered by 8.7  $\mu\text{m}$  aluminium foil 16 kVp radiation*

Mean photographic density above base and fog	Foil thickness ( $\mu\text{m}$ )	
	Upper section covered	Lower section covered
1.113	10.4	6.4
	9.8	6.7
	10.5	6.3
	9.3	6.0
	9.9	5.9
Mean	10.0	6.3
Total mean	8.1	

Table 12

*Calculated foil thicknesses applying eq (2) at various levels of photographic density when upper and lower section of the slit opening respectively was covered by 325.5  $\mu\text{m}$  aluminium layer 54 kVp radiation*

Mean photographic density above base and fog	Foil thickness ( $\mu\text{m}$ )	
	Upper section covered	Lower section covered
0.176	334.6	260.4
	308.9	234.3
0.376	342.0	309.5
	297.4	305.4
0.933	416.4	303.7
	378.1	296.5
1.424	280.2	225.4
	293.3	246.9
Mean	331.4	272.8
Total mean	302.1	

4. Determination of  $\gamma$  values should not introduce systematic errors, provided the characteristic curves used for the  $\gamma$ -determination are similar to those for the films and processing procedure employed in the investigation. A FFD of 440 mm was used for obtaining the characteristic curves whereas the distance was 1150 mm when determining the foil thicknesses. Additional experiments revealed



that the effect of this difference was negligible. Application of eq (2) and thus of the constant  $n$  (see Table 8), does not reduce the variation significantly which indicates that the influence of irregular errors in the determination of  $\gamma$  values is small.

5 Variations in thickness and composition of the photographic emulsion cannot be easily controlled or determined. The 2 mm aperture of the densitometer irons out spatial fluctuations of high frequency in radiation intensity and emulsion thickness (BIEDERMANN & FRIESER 1967). The existence of variations in thickness of the photographic emulsion cannot however, be excluded as an important cause of variation in foil thickness obtained within a set of films at the same level of photographic density.

6 The photographic procedure was standardized. The influence may be considered negligible for one series of films exposed and developed on the same occasion.

7 Variation in the photon spectrum exerts an influence on the value of the attenuation coefficient. The systematic deviations of the measured thicknesses from the true values at 16 kVp and at 54 kVp were also the same. There was probably no systematic error in the determination of the linear attenuation coefficients. Random variations will influence the precision.

8 The precision of the densitometer (see Table 4) was good. The accuracy of the measurement was not determined. Thus differences between mean thicknesses at different levels of photographic densities may have been due to errors in the measuring device.

9 The possible influence of scattered radiation was investigated. Six films in the photographic set up were exposed at three different distances: 10, 60 and 110 mm respectively, from an aluminium step wedge covering the slit opening (Fig 1). The calculated thicknesses at 60 and 110 mm for one step were equal, whereas the thickness value was less at 10 mm distance, indicating an influence of scattered radiation. Furthermore the base and fog density measured close to the image of the step wedge was equal to that measured in unexposed films. The influence of scattered radiation for the set up may thus be ignored.

In summary the present roentgenographic method for determining small mass differences may be considered as possessing satisfactory resolving power. The influence of variation in radiation intensity is however, not negligible and should be taken into account. This may be done either by means of a correction equation or by compensatory filters. The method may be improved by the use of special films and densitometers of higher precision. The constant  $n$  seems to be applicable even at differences in photographic densities of the order of 0.5 units.

The detection of a mass difference within an object is a main problem in roentgen diagnosis. The present investigation indicates that the method may be utilized clinically. The next step will consequently be to apply the equations in experiments with a roentgen apparatus employed in clinical roentgen diagnosis.

### Acknowledgement

The authors wish to express their gratitude to Bengt H. A. Marten for valuable support throughout the investigation.

### SUMMARY

The present investigation deals with the determination of the thickness of a mass and the photographic density of its roentgen image by means of the equations previously derived first under nearly ideal conditions and secondly under conditions approaching those prevailing in routine diagnostic work. The variation in thickness at 16 kVp tube tension was generally much under 10 per cent. The standard deviation was greater at 54 kVp tube tension.

### ZUSAMMENFASSUNG

Die vorliegenden Untersuchungen befassen sich mit der Bestimmung der Dicke der Masse und der photographischen Dichte ihrer Röntgenbilder mit Hilfe zuvor abgeleiteter Gleichungen erst unter nahezu idealen Bedingungen und dann unter Bedingungen wie sie bei der routinemässigen diagnostischen Arbeit vorherrschen. Die Variation der Dicke bei einer 16 kVp Rohrensannung war generell unter 10 Prozent. Die Standardabweichung war bei einer 54 kVp Rohrensannung grösser.

### RÉSUMÉ

Ce travail de recherche concerne la détermination de l'épaisseur d'une masse et la densité photographique de son image radiologique au moyen des équations établies précédemment d'abord dans des conditions presque idéales et ensuite dans des conditions voisines de celles qui existent dans le diagnostic radiologique habituel. Pour une tension dans le tube de 16 kVp la variation d'épaisseur est en général très inférieure à 10 pour cent. L'écart standard est plus grand quand la tension du tube est de 54 kVp.

### REFERENCES

- VAN KEN J. A study of some properties of thirty three different dental X-ray films. *Oral Surg.* 15 (1962) 1330.
- AMERICAN STANDARD METHOD FOR THE SENSITOMETRY OF MEDICAL X-RAY FILMS. American Standards Association. New York 1956.

- BIEDERMANN K. und FRIESER H. Die Photometrie des Röntgenfilms. *Röntgen III* 20 (1967) 157
- BJÄRNGÅRD B., HOLLENDER L., LINDAHL B. and SORESSON A. Radiation doses in oral radiography. I. Measurements of doses to gonads and certain parts of head and neck during full mouth roentgenography. *Odont. Revy III* (1959) 355
- ERICSSON B. G. Quantitative microradiography of cementum and abraded dentine. *Acta radiol.* (1965) Suppl. No. 246
- HENRIKSON C. O. The speed and contrast of dental films. *Acta radiol. Diagnosis I* (1963) 66
- LYSELL G., MÅRTENSSON B. K. Å. and ÖRNELL K. Å. Determination of small mass differences in roentgenography. I. Theoretical considerations. *Acta radiol. Ther. Phys. Biol.* 7 (1968) 42

## COMPUTERIZED TREATMENT PLANNING AND INHOMOGENEITIES

by

RICHARD F NELSON

Historically speaking the interest of the physicist and radiation therapist in inhomogeneities and the possible effects that they do or do not have in the patient undergoing radiation therapy is not new. As early as 1920 FAILLA investigated the absorption of gamma rays from a radium source by various tissues. This experiment consisted of using various slices and thicknesses of different tissues as absorbers. The resultant transmission measurements were taken with an electroscope.

One of the first measurements that was taken in cadavers was in 1923 by BORELL in Germany. However in 1934 QUIMBY reported that there was some concern as to whether the previous measurements were actually representative of the true distributions within the patient. In view of this QUIMBY et coll did an experiment using a male cadaver fixed in phenol and glycerine. Unfortunately in today's society it is doubtful whether we would be able to conduct the experiments again. Hence we find ourselves forty years later still trying to approach this problem on a routine basis.

Submitted for publication 29 January 1971. The author is now at Department of Radiological Physics, The Cooper Hospital, Camden, New Jersey.



Fig 1  $^{60}\text{Co}$  treatment plan of urinary bladder using a field size of  $13\text{ cm} \times 10\text{ cm}$  and  $90^\circ$  anterior oscillation and the axis located posteriorly. The dose to the bladder area is very intense with a sharp fall off outside the area.



Fig 2 Dose distribution for unit density calculation of squamous cell carcinoma of the cervix. Field size  $18\text{ cm} \times 20\text{ cm}$  and  $360^\circ$  rotation T/A 0.70.

Today the problem is being approached in a different manner by using predominantly mathematical models. However we still find ourselves going back to the human body to corroborate our results by inserting ionization chambers into various orifices in the body to check the calculations that are made on the patient either manually or with computers. We still find many members who are startled by the dose distributions obtained when all the inhomogeneities that are encountered when the beam traverses the body are taken into consideration.



Fig 3 Same case as fig 2 Dose distribution obtained for 360 rotation when taking into consideration the treatment table Field size 18 cm x 20 cm T/A 0.55

I believe a great impetus was given to us when Mr Watson of IBM backed Tsien's experiment using accounting machines in 1954 (Tsien 1955, 1958). This was one of the first if not the first semi automatic computing systems for external beam treatment planning in radiation therapy. A planar distribution particularly for rotational therapy could be obtained with this system within a realistic period of time and with fairly good accuracy. In 1957 a system for determining the dosage distributions from internal sources was developed (Nelson & Meurk 1958). At this time we realized that we had to begin to take into consideration the various inhomogeneities that existed within the body and also outside the body. It was impractical to think that these systems would be able to do this and also computers became available to some physics and radiation therapy departments. So it has just been in the past decade that we have really been able to use these instruments to obtain dose distributions correcting for inhomogeneities. As of today there have been written many and varied radiation treatment planning programs. Some of the most notable programs would be those of Shalek (1962), Laughlin (1962), Cunningham et coll (to be published), Van de Geijn (1970), Sterling et coll (1961) and others. At the City of Hope National Medical Center we are presently using a modified version of the Memorial Sloane Kettering computer program on an IBM 36091 computer.

A typical printer map using this program is shown in Fig 1. It is from a patient with transitional cell carcinoma of the bladder and shows a distribution obtained by using  $^{60}\text{Co}$  therapy and a field size of 13 cm x 10 cm and oscillating the beam through an anterior arc of 90°. The deepest shade represents the most intense area of radiation.

The first heterogeneity that I would like to present is the treatment table. Experiments have been made where an ionization chamber is centered over the table top and the machine is rotated through an arc of 360°. In this manner, an average table absorption factor per rotation can be obtained. However this does not take into consideration the dose perturbations caused by the table to the

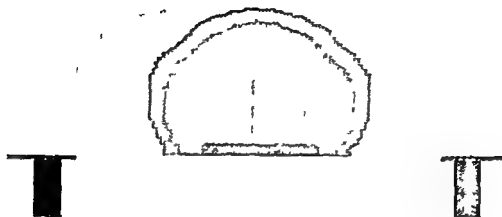


Fig 4 Same case as fig 2 Treatment plan showing uniform pelvic dose when treatment table has been modified. Field size 18 cm  $\times$  20 cm and 360° rotation T/A 0.65

other points of interest in the treatment area. In the following treatment plans the effects of such a table structure and how it can be altered so as to give a more uniform dose throughout the volume of treatment interest will be shown.

A dose map is shown (Fig 2) taking into consideration only the external contour of a patient's pelvis with no heterogeneities. The small light area in the center represents a T/A of 0.69. However, the dark area T/A of 0.7 shows a very uniform distribution within the cervical area of this patient with squamous cell carcinoma of the cervix. The treatment technique used was an 18 cm  $\times$  20 cm field with 360° rotation. However, the patient has to be supported with a table. A representative cross-section of a patient on a Theratron 80 AECL table is shown in Fig 3. As can be seen from this treatment plan, the dosages within the areas of interest are indeed not homogeneous. The patient is being treated using the same technique but taking into consideration the treatment table. The T/A goes from 0.5 to 0.65 within the pelvic area. The hot spots, T/A 0.6 are located over the bladder and on the posterior aspect of the patient including the rectal area. If 4,000 rad were to be delivered to this patient at the T/A of 0.55, the bladder and the rectum would receive approximately 4,700 rad. In view of this, we have modified the table structure so that the patient is supported on a thin mylar sheet stretched between two pieces of a thin aluminum annulus. The same patient is being supported by the modified table top and we have obtained a very uniform dose throughout the pelvic area (Fig 4). Using this technique, the patient received a pelvic dose of 4,000 rad with a small skin and subcutaneous area receiving 4,300 rad.

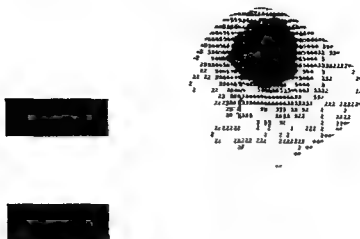


Fig 5 360° rotation plan for marginal recurrence of a cervical node using steel table supports for shielding. Field size 4.5 cm × 13 cm T/A 0.80

In some cases it is desirable to protect certain areas and yet deliver a very intense dose to an adjacent area. We have found that the steel table supports on the Theratron table can be used for such purposes. The treatment plan of a patient with a marginal recurrence of a cervical node is shown in Fig 5. The technique employed for this case was a long but narrow field with 360° rotation. The table supports were used in the geometry shown to obtain a shielding of all the areas but the nodal bed. So it is possible to use to an advantage some of the table structures that normally are considered as a disadvantage.

In the past a patient's treatment plan was normally done in the cross-sectional plane. However, a volume of tissue is being treated and the distribution in the sagittal plane could be very important. Fig 6 is from a patient with a lympho-angiosarcoma of the anterior tongue and soft palate. Shown here are the cross-sectional and the sagittal plane distributions. The treatment technique prepared here was a straight anterior field 14 cm × 10 cm. Obviously this would not be the treatment plan of choice and a distribution in the respective two planes with an anterior and posterior treatment technique with a field size of 14 cm × 10 cm is seen in Fig 7, but weighing the distribution 2:1 anterior and posterior respectively. This patient was to be treated to a dose of 5000 rad to all areas involved using split course therapy. However it was thought that the patient's spinal cord in the neck area would receive at least the same dose of 5000 rad or more and therefore a compensating wedge filter was added to correct for this high dose area. Using this technique the patient received a dose of 5000 to





Fig 6 Distributions in the sagittal plane (left) and the cross sectional plane (right) for an anterior field 14 cm x 10 cm in the tongue and soft palate areas

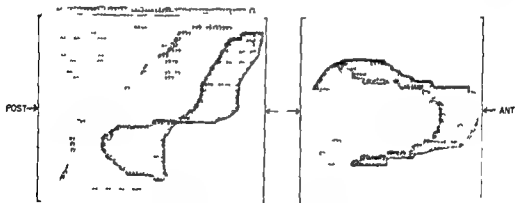


Fig 7 Same case as fig 6 Two plane treatment plan of tongue and soft palate as 5 cm employing anterior and posterior fields 14 cm x 10 cm ratio 2:1 Hot spot in the neck Sagittal plane (left) and cross sectional plane (right) T/A 0.72

5500 rad throughout the tumor volume yet it was considered that the spinal cord received only approximately 4200 rad. So far in this presentation I have discussed and shown only external heterogeneities and the effects that they had on treatment plans, both good and bad.



Fig 8 360° rotation plan of carcinoma of the esophagus taking into consideration lungs ribs vertebral body and treatment table. Field size 7 cm  $\times$  18 cm. Internal and external inhomogeneities.

An area that is of even greater concern is internal inhomogeneities. It is relatively easy to determine the geometries of external inhomogeneities relative to the patient when they are being irradiated. However, the location of internal inhomogeneities is more difficult to determine. Therefore, the axial transverse tomographic unit has been developed and made available now to radiation therapists for the treatment planning of their patients. At the City of Hope, we use a Toshiba axial transverse tomographic unit and a simulator. The collimators of the simulator are placed in a plane so that they duplicate the geometries of our Theratron 80 unit. It has proven very useful and decreases patient set up time. In the same room, located 180° from the simulator is the Toshiba tomograph. This instrument has proven already quite valuable to us; however, great care has to be taken when interpreting the tomograms as it is a new field and they are sometimes difficult to interpret. We have found that the monograph by TAKAHASHI (1969) has proven quite helpful along with his comparison to ECLESIAIMER & SCHIOEMAKER's book (1938).

The area where the greatest number of inhomogeneities and heterogeneities is obtained is in the thorax area, particularly for rotational therapy for carcinoma of the esophagus. The dose distribution obtained when taking into consideration 15 different inhomogeneities is shown in Fig 11. These are the lungs, ribs, vertebral body and, of course, the heterogeneities of the treatment table. It would be physically impossible and unrealistic for an individual to be expected to calculate such a distribution manually taking into consideration all the 15 inhomogeneities and heterogeneities.

A tomogram of a patient (Fig 9) is illustrated with a postsurgical tumor recurrence in the floor of the mouth. From the tomogram, the position of the



Fig. 9. Axial transverse tomogram of the floor of the mouth.

tumor, the mandible and the vertebral column can be seen. The patient contour (Fig. 10) is shown with the interpretation of this axial transverse tomogram. Also placed in the treatment contour is the area that was considered to be possible tumor extension and possible nodal pathways. This patient was treated using lateral opposed fields with a ratio of 2:1, left to right. The left field was 7 cm  $\times$  10 cm and the right was 6 cm  $\times$  10 cm (Fig. 11). This illustrates the increased absorption by the mandible and shows the effect on the treatment when the bone structures are excluded or included in the treatment plan.

In conclusion we are now able to start looking at the distributions within patients as they possibly really exist. This is not on a general view but on each particular patient. Using the simulator, the tomograph and the computer each patient can be evaluated for therapy.

In the very near future many institutions will probably introduce three dimensional distributions. In this manner we will be able to observe the true radiation dosage to tumor and normal tissues. As a result there certainly will be newer and better programs and techniques available and used in patients undergoing radiation therapy. This knowledge added to that through research in the areas of radiation biology, might enable us to understand more about the effects of ionizing radiations on neoplastic diseases. With all this it is entirely possible that we might be able to have better survival rates in 1980 for the different diseases.

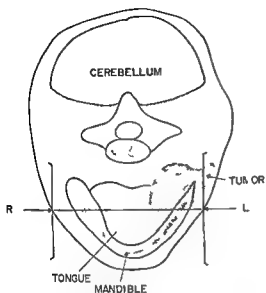


Fig 10 Same case as fig 9 Interpretation of axial transverse tomogram showing tumor area and bones located with in the section

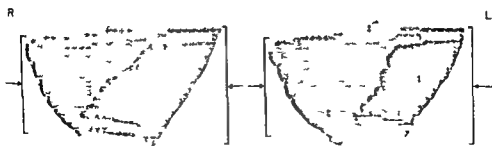


Fig 11 Same case as fig 9 Computer treatment plan showing distribution without (left) and with (right) bone Opposed fields 7 cm  $\times$  10 cm (left) and 6 cm  $\times$  10 cm (right) Ratio 2 : 1

that are treated with radiation therapy than presently exist in 1970. It is only through the cooperation that we get from our colleagues, administrative staffs and industrial companies that makes all these things possible.

### Acknowledgements

The author wishes to thank Dr Mary W. Denk for her help and for presentation suggestions. Computing assistance was obtained from the Health Sciences Computing Facility, UCLA, sponsored by NIH Special Research Resources Grant RR 3.

### SUMMARY

A brief history of the physical measurements is presented. The effects of external heterogeneities and internal inhomogeneities are also shown. A computer program is used to present the various treatment plans in patients undergoing radiation therapy for different neoplastic diseases. The use of the axial transverse tomography is discussed and presented.

### ZUSAMMENFASSUNG

Es wird eine kurze Geschichte der physikalischen Messungen gegeben. Der Effekt der externen Ungleichheiten und internen Inhomogenitäten wird ebenfalls gezeigt. Ein Computerprogramm wird verwendet, um die verschiedenen Behandlungspläne für Patienten, die mit Strahlentherapie wegen verschiedener neoplastischer Erkrankungen behandelt werden, zu zeigen. Die Anwendung der Transversaltomographie wird besprochen und dargestellt.

### RÉSUMÉ

L'auteur fait un bref historique des mesures physiques. Il montre l'influence des hétérogénéités externes et des inhomogénéités internes. Il utilise un programme d'ordinateur pour présenter les différents plans de traitement sur des malades soumis à un traitement par les radiations pour différentes affections néoplasiques. Il étudie et illustre l'utilisation de la tomographie axiale transverse.

### REFERENCES

- BORELL, H. Experimentelle Untersuchungen zur Tiefendosierung harter Röntgenstrahlen mit besonderer Berücksichtigung der Streustrahlung. *Strahlentherapie* 14 (1923) 39.
- CUNNINGHAM, J., SHRIVASTAVA, P. and WILKINSON, J. Computer Calculation of dose within an irregularly shaped beam. To be published.
- EVGLESIMYER, A. and SCHÖENMAKER, D. *A cross section anatomy*. D. Appleton Century Co. New York 1938.
- FAILLA, G. The absorption of radium radiations by tissues. *Amer. J. Roentgenol.* 11 (1920) 215.

- NELSON R and MEURK M Use of automatic computing machines for implant dosimetry  
Radiology 70 (1958) 90
- QUINBY E, COPELAND M and WOODS R The distribution of roentgen rays within the human  
body Amer J Roentgenol 32 (1934) 534
- SHALEK R J and STOVALL M The calculation of isodose distributions in interstitial implanta-  
tions by a computer Radiology 76 (1961) 119
- SILVER W M and LAUGHLIN J S A computer method for radiation treatment planning  
Comm Ass Computing Machinery 5 (1962) 407
- STERLING T, PERRY H and BAHR G A practical procedure for automating radiation treat-  
ment planning Brit J Radiol 34 (1961) 726
- TAKAHASHI S An atlas of axial transverse tomography and its clinical application Springer  
Verlag New York 1969
- THEN K C The application of automatic computing machines to radiation treatment plan-  
ning Brit J Radiol 28 (1955) 432
- A study of basic external radiation treatment techniques with the aid of automatic com-  
puting machines Brit J Radiol 31 (1958) 37
- VAN DE GEYN J A computer program for 3-D planning in external beam radiation therapy  
Computer Programs in Biomedicine (1970) 17

## TREATMENT OF INOPERABLE PULMONARY TUMOURS WITH HIGH-ENERGY ELECTRONS

by

T LANDBERG ULLA BRITA NORDBERG, H OLIVECRONA  
M LINDGREN and H HENRIASON

The prognosis in inoperable carcinoma of the bronchus is poor and little significant improvement appears to have been achieved by the introduction of mega-voltage units for photon irradiation (DE JONG & RENNER 1966, HOLSTI 1967). BELING & EINHORN (1965) gave a one year survival rate of 22 per cent in inoperable patients given curative treatment with  $^{60}\text{Co}$  while DE JONG & RENNER (1966) reported 25 per cent.

Irradiation of pulmonary tumours has commonly been administered with 5 or 6 fractions a week with a daily absorbed dose of 120 to 200 rad in the target (BELING & EINHORN, DE JONG & RENNER, HOLSTI). BELING & EINHORN reported tumour doses of 5 100 to 6 000 rad based on calculations of the absorbed dose from the depth dose tables and measurements of the exit absorbed dose. HOLSTI put the most common minimum tumour dose as 5 000 to 6 000 rad, calculated from individual dose charting. DEELEY (1966) published the results of radiation therapy with an 8 MV linear accelerator in advanced inoperable anaplastic car-

cinoma of the bronchus Of the two dose levels viz 3 000 rad and 4 000 rad, the smaller proved more effective The tumour doses had been calculated for homogeneous water equivalent tissue but it was stressed that the actual doses received had probably been larger than those in the report, later measurements of the exit dose had suggested that even with supervoltage therapy the actual dose received by the bronchial carcinoma could be up to 30 per cent more than that calculated on the assumption of homogeneous water equivalent tissue

ELLIS (1963) stressed the difficulties in comparing absorbed doses gathered from different radiation therapy centres owing to the frequent absence of information as to whether consideration had been given to the tissue inhomogeneity or whether the doses reported were maximum minimum or an average absorbed dose to the target

UHLMANN (1958, 1960) and UHLMANN & OVADIA (1960) described the treatment of lung carcinomas with 20 to 40 MeV electrons from a linear accelerator They stressed that the wide variation in tissue density within the area to be irradiated constitutes a major problem The difference in penetration in the lung parenchyma could not have been compensated for by lowering the electron energy for such reduction would have resulted in undertreatment of parts of the area irradiated They therefore used lucite wedges shaped for each patient and each lesion The authors gave examples of absorbed dose distributions in patients in whom these were used the isodose curves had however apparently been drawn for water equivalent tissue and the wedges appear to have served mainly as contour compensating filters The patients received tumour doses of 6 000 to 7 000 rad, and it was stated that large doses of effective ionizing radiation may be applied with electrons to deep-seated tumours with only a relatively low integral dose to healthy tissue i.e. a dose best tolerated by the patient ZUPPINGER (1962) reported the use of 30 MeV electrons in the treatment of carcinoma of the lung and pleura together with the therapeutic results as discouraging Radiobiologic experiments revealed the RBE value as 0.6 to 0.7 but only provided the single dose applied was not too large and the absorbed dose rate not over 100 rad per minute

ELLIS (1963) stated "Large single doses or large fractions would be more effective in killing a high proportion of cells than small fractions because of the rounded initial shoulder of the cell survival curve and that in dose time relationship it would appear that the number of fractions is more important than the overall time OLIVER (1963) wrote "there appears to be no theoretical advantage in increasing the number of fractions used in a radiotherapy regime but every advantage in using the minimum number of suitably spaced fractions within of course the limitations of other treatment effects (e.g. radiation sickness)



MICELI et coll (1967) reported the results of irradiation with  $^{60}\text{Co}$  of pulmonary carcinoma with large fractions. They gave a daily absorbed dose of 400 to 1 000 rad to the tumour up to a total of 5 000 to 7 000 rad, and reported better survival rates with such a technique than those obtained with daily absorbed doses of only 150 to 250 rad to the tumour. GEST & DELOUCHE (1967) discussed 12 patients with bronchial carcinoma in whom a total of 2 000 rad to the tumour was administered with  $^{60}\text{Co}$  within 24 hours and stressed the good tolerance. LEVITT et coll (1967) reported inoperable squamous cell carcinoma of the lung treated with radiation therapy with  $^{60}\text{Co}$  or a 2 MV Van de Graaff generator. An absorbed dose of 1 800 rad in the tumour was applied in 3 days, and a similar course was started 28 days later. No significant difference in symptomatic response, survival or roentgenologically demonstrable effects was recorded between the patients given the fractionation mentioned and those who had received radiation therapy with routine fractionation. There appeared however to be a less marked effect on the tumour and increased fibrosis in the former group.

SCHUMACHER (1965) and LOERBROKS & SCHUMACHER (1965) reported the use of large fractions thus reducing their total number, in the treatment of inoperable carcinoma of the bronchus with 35 MeV electrons delivered via two portals. Curative treatment in 48 patients was administered with irradiation three times a week with 400 to 500 rad per session to a different field up to a total absorbed dose of 7 000 to 9 000 rad in the target. Palliative treatment in 34 patients was given with 1 000 to 2 000 rad to a field with an interval of 1 to 2 weeks between the consecutive fractions up to a total absorbed dose of 1 500 to 10 000 rad to the target. The survival rate was increased in treated patients as compared with those who had no treatment at all. Two thirds of the patients who had curative treatment and one third of those who received palliative treatment developed radiation pneumonitis which generally appeared one month after the conclusion of treatment. Radiation reactions of the lungs were regarded as the main cause of death in 16 per cent of the 82 patients. The lung reactions occurred more often in patients given large absorbed doses but no correlation was evident between such doses and the frequency of lung reactions. The authors demonstrated the variation in the absorbed dose at the central axis of two opposed beams in water but gave no clinical example of its distribution.

TESCHENDORF & BLEHER (1969) treated 136 patients with lung tumours with 42 MeV electrons. Treatment was given with one ventral and one dorsal oblique field. Eighteen fractions were administered as split course treatment over approximately 30 weeks. The skin reaction was usually only modest. Extensive lung fibrosis was diagnosed in 68 patients and mostly appeared five months after the beginning of treatment. The one year survival rate was 32 per cent (44/136).

This paper concerns a technique for the treatment of lung tumours with high energy electrons and the results obtained with such treatment as well as the calculation and checking of the absorbed dose.

**Material** This consisted of 27 men and 9 women with lung tumours. All the patients had an intrathoracic neoplasm at the beginning of electron therapy, although it failed to exceed a limit corresponding to the largest homogeneous field for a source skin distance (SSD) of 110 cm. Twenty of the patients were over 60 years of age and 2 were under 40. Thoracotomy had been performed in 6 patients at the most three months before the beginning of radiation therapy. Spread of the disease to the prescalene nodes had been proved in 3 and to the mediastinal or hilar nodes in 9 patients. Extrathoracic foci of the disease had been demonstrated in 11 patients before radiation therapy. Operation in 9 patients was contraindicated by impaired ventilation, poor general condition or the proximity of the growth to the trachea. Four patients were considered inoperable because of the anaplastic type of the tumour. The main reason for inoperability in the remaining 23 patients was usually a locally advanced neoplasm or a combination of more than one factor.

The bronchial carcinomas were typed by the KREIBERG (1967) classification. 11 patients had epidermoid carcinoma, 9 small cell anaplastic carcinoma, 10 adenocarcinoma and 2 patients had large cell carcinoma. Four patients had metastases: 2 from a uterine cervical squamous-cell carcinoma, 1 from a uterine sarcoma and 1 from an anaplastic ethmoid carcinoma.

**Method** Thirty-two patients were treated with one ventral and one dorsal opposing field, two of them with a third lateral field as well and 4 patients with only one field. The field sizes were 60 to 180 cm for 22 patients and 200 cm for 14 patients. SSD 110 cm. Maximum electron energy was 20 MeV for one patient treated for subpleural malignancy but 35 MeV for the remaining 35 patients.

A cross section was drawn through the centre of the target with the patient in the treatment position. This section was cranial to Th 6 in 5 patients at the level of Th 6-8 in 27 patients and caudal to Th 8 in 4 patients. Most patients had been examined with transversal tomography. Only an extension of the intrathoracic tumour, which had been demonstrated, was accepted as target. Individual tissue inhomogeneity (lung, bone and sometimes even the tumour) within the treatment region was taken into account in the calculation of the absorbed dose and a complete dose plan was made for the section drawn. The variation, if any, in absorbed dose in a cranio-caudal direction was taken into account in determining the total dose.



Fig 1

Fig 2

Fig 1 Patient No 30 Roentgenogram of ventral field. Plastic catheters with condenser chambers and indicators in the oesophagus and on the dorsum

Fig 2 Patient No 17 Low sensitivity film exposed during irradiation with  $^{60}\text{Co}$ . Plastic catheters with condenser chambers and indicators in the oesophagus and on the dorsum

To enable such individual corrections for tissue inhomogeneity measurements were made in the oesophagus during treatment of each field with electrons as well as during a single treatment of each of the fields with  $^{60}\text{Co}$  at SSD 70 cm, given to allow a more correct calculation of the absorbed dose, the exit exposure was also measured during the  $^{60}\text{Co}$  treatments. A roentgenogram with the field borders and three plastic catheters containing small condenser chambers and steel indicators appear in Fig 1. Two of the catheters each containing six condenser chambers are placed on the back of the patient, and one with eight chambers is introduced into the oesophagus. The positions of the three catheters during treatment with  $^{60}\text{Co}$  were also checked with low sensitivity films exposed during the treatment (Fig 2). Insertion of the catheter into the oesophagus caused at the most only one or two days slight discomfort in swallowing but without any serious complications.

If there were no scatter contribution  $^{60}\text{Co}$  dose curves for water could be moved according to the penetrated thickness in gram per cm and then corrected for different source skin distances by the inverse square law. A lower volume weight, however, affects the scatter contribution in different ways but results in a decreased contribution which has the same effect as virtual increased

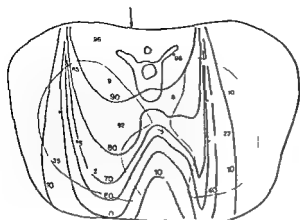


Fig 3



Fig 4

Fig 3 Isodose (curves) calculated by means of  $^{60}\text{Co}$  determined effective density and absorbed dose (points) measured during irradiation with 35 MeV electrons 14 cm  $\times$  14 cm field size and SSD 110 cm in an anatomic thorax phantom

Fig 4 Same case as fig 1 Chest roentgenogram before treatment. Massive atelectasis of right lung

density (NORDBERG 1972) The inverse square law also causes a further increase in the virtual density the smaller the SSD the greater the effect. It seems as if this line of thought would also apply to 35 MeV electrons but the increase in virtual density owing to lack of scatter contribution is much greater than for  $^{60}\text{Co}$ . The increasing effect of the inverse square law is however quite small for SSD 110 cm. The total effects for  $^{60}\text{Co}$  with SSD 70 cm are approximately the same as those for 35 MeV electrons with SSD 110 cm which means that a virtual effective density measured with  $^{60}\text{Co}$  and SSD 70 cm can be used as a mean value to correct the 35 MeV electron isodose curves for SSD 110 cm. The measurements of the exit exposure were used to calculate the individual effective densities (NORDBERG) of the lung and neoplasm and the measurements in the oesophagus were employed mostly for calculating the effective density for bone. Those patients in whom measurements of corresponding densities had been made with both  $^{60}\text{Co}$  and electrons presented good agreement which suggests that the method for determining the individual absorbed dose plan for electron irradiation is acceptable.

Fig 3 was produced with an anatomic thorax phantom in which the above mentioned method was used. The lung of the phantom had a volume weight of 0.25 g/cm<sup>3</sup>, a value corresponding to an effective density of 0.53 g/cm<sup>3</sup> for 35 MeV electrons. This density varies with the depth and 0.53 denotes the



Fig 9

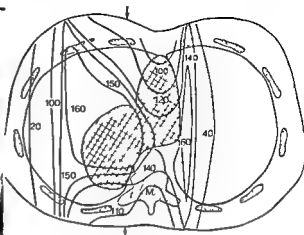


Fig 10

Fig 9 Patient No 15 Chest roentgenogram before treatment Tumour surrounding lung tissue not affected roentgenologically

Fig 10 Same case as fig 9 Absorbed dose distribution as percentage of peak absorbed dose in the central axis Two opposing 14 cm  $\times$  14 cm fields SSD 110 cm and 35 MeV electrons Distance between entrances of beams is 20.3 cm Measured effective density for lung and for bone is 0.41 and 1.0 g/cm<sup>3</sup> respectively

occurred (Fig 7) Displacement of the mediastinum towards the healthy side had also taken place Fig 8 gives the distribution of the absorbed dose with the effects of correction for lung tissue after replanning Furthermore the beam entrances were moved slightly medially because of the mediastinal shift The measured effective lung density was 0.65 g/cm<sup>3</sup> The absorbed dose in the target varied between 100 and 160 per cent of the peak absorbed dose and the absorbed dose in the spinal cord was less than 100 per cent The absorbed dose received by the lung parenchyma around the tumour rose considerably and the absorbed dose in the hilar region on the other side had also risen as an effect of the medial movement of the fields

A frontal chest roentgenogram of patient No 15 at the beginning of treatment appears in Fig 9 A large adenocarcinoma in the right hilum and mediastinal lymph node metastases were demonstrated Roentgenologically the lung tissue outside the tumour was not affected the vertebrae were markedly decalcified Fig 10 presents distribution of the absorbed dose from treatment with two opposing 14 cm  $\times$  14 cm fields, with 35 MeV electrons and a distance of 20.3 cm between the beam entrances The measured effective lung density was 0.41 g/cm<sup>3</sup> and the measured effective density of the vertebrae was 1.0 g/cm<sup>3</sup> The maximum absorbed dose in the target was 160 per cent and



Fig 11

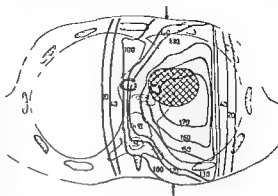


Fig 12

Fig 11 Patient No 19 Chest roentgenogram Tumour near the left hilum and atelectatic changes

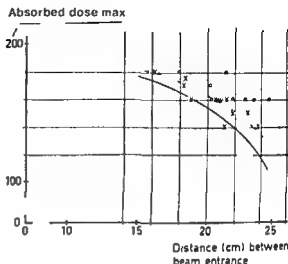
Fig 12 Same case as fig 11 Absorbed dose distribution as percentage of peak absorbed dose in the central axis Two opposing 14 cm x 14 cm fields SSD 110 cm and 35 MeV electrons Distance between entrances of beams is 18.3 cm Measured effective density for lung and for bone is 0.67 and 1.4 g/cm<sup>3</sup> respectively

the minimum 100 per cent. The marked variation in the target absorbed dose in this patient may partly be explained by the fact that the mediastinum was included in the target and partly by the low effective lung density. The average absorbed dose in the spinal cord was less than 110 per cent.

It is apparent from Figs 6, 8 and 10 that if the mediastinum is to be included in the target, the variation in the target absorbed dose will be considerable. Figs 11 and 12 illustrate the more favourable ratio between the absorbed dose to the target and that in healthy tissue in a patient in whom only part of the mediastinum was included in the target.

When the isodose curve indicating the highest absorbed dose level circumscribed an area less than 2 cm or narrower than 1 cm, it was called a 'hot spot' and the next 5 per cent lower dose value was taken as the maximum. Fig 13 gives the maximum absorbed dose (as percentage of peak absorbed dose at the central axis) as a function of different distances between beam entrances in patients treated with the same peak absorbed dose to two opposing fields and with 35 MeV electrons. Distinction has been made between patients in whom the lung tissue surrounding the tumour was not affected (e.g. Figs 9, 10) and those patients in whom the lung tissue around the growth was apparently affected (e.g. Figs 7, 11, 12). The maximum absorbed dose at the central axis in water for 35 MeV electrons (e.g. Figs 4, 6) is also included. Since individual absorbed dose charting is time consuming, the diagram is now used when determining clinically the maximum absorbed dose.

Fig. 13. Maximum absorbed dose (as percentage of peak absorbed dose at the central axis) as function of distance between entrances of beams in patients treated with the same peak absorbed dose to two opposing fields and 35 MeV electrons. Distinction has been made between patients in whom the lung tissue surrounding the tumour was not affected roentgenologically (○ and dotted curve) and those in whom a varying degree of atelectasis was observed (x and dashed curve). Maximum in absorbed dose on the central axis in water is also shown (full drawn curve).



**Dosage:** The peak absorbed dose at the central axis was at each fraction under 500 rad in 4 patients (300 rad in 3 and 400 in 1), 500 in 28 and more than 500 in 4 patients (600 rad in 3 and 750 in 1 patient who was treated with an 8 cm (circular field). Treatment was given three times a week with one field at each fraction.

Full treatment was administered to 32 of the 36 patients in 2 of the 32 as a split course in two series but in the remaining 30 patients in one series. Treatment was stopped in 4 patients in 2 because of lack of response to treatment and in one patient because of progressive generalisation one patient refused further treatment.

Including the treatments given with  $^{60}\text{Co}$  for purpose of calibration but excluding the 4 patients who did not receive full treatment, 7 to 26 (mean 16, median 17) fractions were given over 15 to 95 (mean 38, median 36) days. Total maximum absorbed dose to the target was at least 6300 rad in 15 of the patients and the minimum was at least 5300 rad in 12 patients.

As already mentioned the variation in the absorbed dose in the target is considerable if the mediastinum is included and of 7 patients in whom the difference between maximum and minimum absorbed dose in the target exceeded 1800 rad, 6 had demonstrable tumours in the mediastinum.

The absorbed dose in the spinal cord was smaller than the minimum absorbed dose in the target in 21 of the 30 patients treated with two opposing fields but in 3 it was the same and in 4 patients it was larger. In 11 of these 30 patients the total absorbed dose in the spinal cord exceeded 4700, but was under 7000 rad, given in 16 to 24 (median 18) fractions in 30 to 90 (median 40) days.

Table 1

*Symptoms and signs before treatment and at conclusion of treatment in 36 patients treated with high energy electrons*

Symptoms and signs at beginning of treatment	No of patients	At conclusion of treatment			
		Free of symptoms and signs	Improved	Unchanged	Deteriorated
Cough	27	8	16	3	—
Dyspnea	6	—	4	2	—
Weakness	7	3	1	1	1

*Symptoms and clinical findings during treatment* Of 27 patients who had cough at the beginning of treatment 24 improved (Table 1), and 11 of the were free of symptoms at the conclusion of treatment. Six patients had dyspnea 4 of whom improving. 7 patients complained of considerable weakness 4 of whom improving but one becoming worse.

Symptoms developed during treatment in some patients, namely cough in 1 weakness in 4 and discomfort in swallowing in 6 patients although in none was it necessary to interrupt the treatment. A bigeminal pulse in one patient appeared during treatment but disappeared when the peak absorbed dose per fraction was lowered from 500 to 300 rad. Symptoms or signs of radiation myelitis were never evident.

The tumour was roentgenologically demonstrable at the beginning of treatment in 23 patients. By the end of treatment the tumour had regressed in 20 patients (Table 2) including 2 in whom it was no longer roentgenologically demonstrable. In 23 patients with atelectasis of varying degree the condition regressed in 16 including 7 patients in whom it had entirely disappeared. Pleural exudation was persistent in 2 of 3 patients. Enlarged hilar nodes and widening of the mediastinum had regressed in 1 of 11 patients and 2 of 3 patients respectively. Two patients had cavities but treatment could be given without any special complication.

Sixteen patients had anemia ( $Hb \leq 11$  g/100 ml) during treatment but it was never necessary to interrupt the treatment because of a fall in blood values. Eight patients were febrile at the beginning of treatment but at its conclusion 3 of these were afebrile, 2 subfebrile while 3 patients still had a temperature

*Skin reactions* Three patients had no visible skin reactions at the conclusion of treatment whereas different degrees of skin reaction were evident in 32 patients (1 patient was excluded because some of his treatments were for techni-



Table 2

*Roentgenologic findings before treatment and at conclusion of treatment in 36 patients treated with high energy electrons*

Roentgenologic changes at beginning of treatment	No. of patients	At conclusion of treatment				
		Total regression	Good regression	Some regression	Unchanged	Deteriorated
Tumour	23	2	8	10	3	—
Atelectasis	23	7	4	5	7	—
Pleural exudation	3	—	1	—	2	—
Enlarged hilar nodes	2	—	—	1	1	—
Mediastinal widening	3	—	—	2	1	—

cal reasons given with  $^{60}\text{Co}$ ). Four patients had epidermitis exsudativa, whereas 28 had epidermitis sicca. This latter reaction caused irritation in the form of itching in 3 of the 28, while the other 25 patients experienced little or no discomfort. Fig. 14 includes different types of skin reaction present at the conclusion of treatment, distributed among total peak absorbed doses (rad) at the central axis of the electron beam (excluding any treatment with  $^{60}\text{Co}$  for calibration and any exit absorbed dose from the opposing field, these two doses amounting mostly to 300 rad), and the total number of days of treatment to the field. The individual tolerance apparently varies considerably. Patient No. 33, who received a peak absorbed dose of 7 000 rad in 14 fractions over 35 days to an 8 cm circular field with 35 MeV electrons and 500 rad peak absorbed dose per fraction, had only epidermitis sicca without discomfort at the end of treatment. Patient No. 26, who received a peak absorbed dose of 5 300 rad in 7 fractions over 21 days with a 10 cm  $\times$  11 cm field with 20 MeV and 750 rad peak absorbed dose per fraction, had no skin reaction at all at the end of treatment. The total peak absorbed dose was at least 3 000 rad in 26 of the patients. It was never necessary to interrupt treatment because of skin reactions.

Information was available on the further course of the skin reactions in 21 patients who were followed for at least two months after the conclusion of treatment. The skin reaction in 2 of the 11 became more marked some weeks after the end of treatment, but after a further two weeks the reactions regressed, namely in patient No. 33, who had epidermitis exsudativa, and in patient No. 34

Total peak abs dose  
n rad for electrons

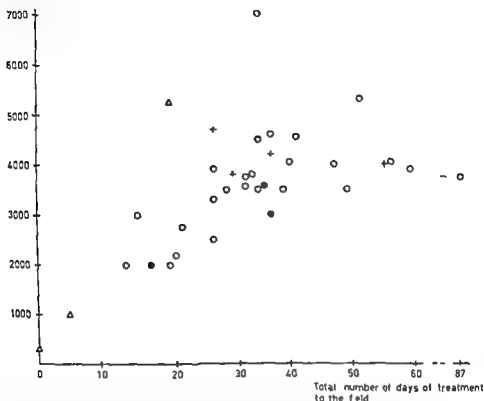


Fig 14 Different types of skin reactions at conclusion of treatment distributed among total peak absorbed dose (rad) in the central axis of the electron field and total numbers of days of treatment of the field + = epidermitis exudativa ● = epidermitis sicca with discomfort ○ = epidermitis sicca without discomfort Δ = no skin reaction

(peak absorbed dose 4500 rad in 9 fractions over 35 days with 30 MeV electrons 14 cm  $\times$  14 cm field and 500 rad peak absorbed dose per fraction) who later had epidermitis sicca with pruritus

In 19 patients (2 with epidermitis exudativa 2 with epidermitis sicca and pruritus and 15 with epidermitis sicca without discomfort) successive regression of the skin reactions occurred after the end of treatment. The reactions had practically disappeared about four weeks later. No data were available about patient No. 26 regarding the further course of the skin reaction and in the remaining patients the follow up was under two months.



Fig 15 Same case as fig 9. Chest roentgenogram six months after treatment. Marked pleural fibrosis with elevation of the diaphragm, displacement of the mediastinum to the right and further widespread changes due to pneumonitis in the right lung (cf fig 9).

*Radiation pneumonitis.* A diagnosis of radiation pneumonitis was made if the patient had increasingly dry cough and roentgen examination of the chest disclosed progressive changes in the pulmonary parenchyma within the treated region which could not reasonably be attributed to growth of the tumour. Pneumonitis was treated with antibiotics and steroids. Fig 15 illustrates pneumonitis in patient No. 15. The film of the chest of the same patient taken before the beginning of treatment appears in Fig 9 and the absorbed dose plan in Fig 10. Treatment was given in two series at the end of the second series of which additional treatment with  $^{60}\text{Co}$  was applied to the mediastinum although this did not affect the lung tissue. The total maximum absorbed dose in the lung tissue was 7100 rad in 16 fractions within 86 days. A roentgenogram six months after the beginning of treatment (Fig 15) revealed pleural fibrosis and elevation of the right dome of the diaphragm as well as displacement of the mediastinum to the right with widespread changes in the lung parenchyma due to pneumonitis. This patient was treated for cough but a later roentgen examination disclosed progression of the fibrosis. Signs of pneumonitis usually appeared 2 to 6 (mean 3.5) months from the beginning of treatment. Twenty-one patients were controlled at least four months after the beginning of treatment. Pneumonitis was diagnosed in 9 of these whereas 12 patients had no symptoms or signs of pneumonitis.

Fibrosis of the lung parenchyma was evident in 13 patients. All had been controlled for at least five months after the beginning of treatment and of 9 patients with a follow up for at least seven months 8 were affected. Of the

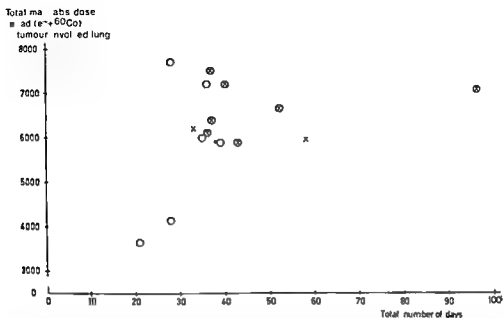


Fig 16 Roentgen examination of chest after conclusion of treatment in 21 patients followed for at least four months after the beginning of treatment. Pneumonitis (×) and no pneumonitis (●) distributed among maximum absorbed dose (rad) in the lung tissue and total number of days. The occurrence of roentgenologically demonstrated fibrosis of the lung parenchyma is also indicated (○).

first mentioned 13 patients. 7 had also displayed symptoms and signs of pneumonitis.

Fig 16 gives the results of roentgenography of the chest after the end of treatment in patients followed for at least four months after the beginning of treatment. The findings consist of radiation pneumonitis or no pneumonitis distributed over total maximum absorbed doses (rad) in the lung parenchyma and total number of days. Fibrosis, if any, of the lung parenchyma is also given. Three patients who had received a total maximum absorbed dose in the lung parenchyma of 4500 rad or less (3700 to 4500 rad) applied in 11 to 14 fractions over 21 to 28 days had no radiation pneumonitis. The remaining 18 patients had had a maximum absorbed dose in the lung parenchyma of at least 5800 rad and in 9 of these radiation pneumonitis was diagnosed. It seems remarkable, however, that 3 patients who had been followed for 5 to 6 months and who had received a total maximum absorbed dose in the lung parenchyma of at least 7200 (7200 to 7700) rad given in 9, 16 and 16 fractions over 28, 53 and 36 days respectively had no symptoms or signs of radiation pneumonitis.

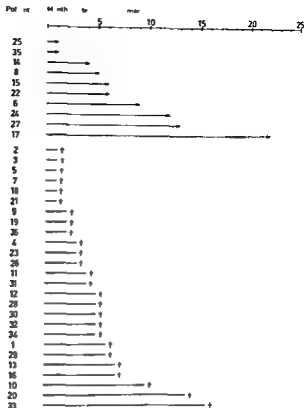


Fig 17 Survival (months) of 36 patients from the beginning of treatment → = living † = dead

Thirteen patients received a considerable absorbed dose to the medial parts of the unaffected lung with consequent radiation pneumonitis in 5, the total maximum absorbed dose in the lung parenchyma on the healthy side had in the 5 patients been 5 600 to 5 900 rad applied in 14 to 26 fractions over 33 to 38 days

*Survival* Fig 17 gives the survival in months after the beginning of treatment. Ten patients were alive 1 to 22 (median 6) months after the beginning of treatment at the end of follow up, 2 of these 10 had generalized disease at the beginning of treatment and remote metastases were later diagnosed in 2 patients. A total of 26 patients had died within 1 to 16 (median 4) months after the beginning of treatment. In 10 of these 26 patients generalization had been diagnosed before the beginning of treatment and 5 later had remote metastases. Eleven patients thus died without clinically demonstrated extra-thoracic spread of the disease. No precise information was available about the

cause of death of 2 of the 11 patients. One patient died from pulmonary embolism following femoral vein thrombosis, autopsy revealed no tumour within the irradiated volume. One patient died from haemoptysis and death could be attributed to local progression of the growth in 3 patients. Acute reaction of the lung parenchyma (perhaps radiation pneumonitis) was evident after the end of treatment in 4 patients and was considered to have contributed to death, two of these acute reactions were however obviously infectious in character. The total maximum absorbed dose in the 4 patients was not particularly large viz 4700, 5800, 6100 and 6500 rad given in 11, 24, 16 and 18 fractions over 24, 59, 36 and 50 days respectively.

A total of 29 of the 36 patients had either been followed for at least a year or died. 5 of the 29 patients were alive twelve months after the beginning of treatment.

No conclusion could be drawn regarding differences in survival in groups with varying reasons for inoperability or in groups of different histologic types. It might be mentioned, however that if patients Nos 25 and 35, who were controlled for only 2 months are excluded 6 of the 13 patients with several reasons for inoperability were alive four months after the beginning of treatment compared with 14 of 21 patients considered inoperable for only one reason (5 out of 8 patients who had been inoperable because of impaired ventilation, poor general condition or location of the tumour close to the trachea and 9 out of 13 patients who had been inoperable because of local spread of the tumour). Of patients with epidermoid carcinoma 5 of 11 patients were alive four months after the beginning of treatment compared with 7 of 9 with adenocarcinoma, 5 of 10 with small cell anaplastic carcinoma and large cell carcinoma and 4 of 6 patients with metastatic pulmonary tumours.

Fifteen patients had received a total maximum absorbed dose of at least 6300 (6300 to 7500) rad given in mean 19 fractions over 46 days to the target. Seven of the 15 patients were alive at the end of the follow up whereas of the 21 patients who had received a smaller maximum absorbed dose (700 to 6100 rad given in mean 13 fractions over 30 days) only 3 were alive. Twelve patients had received a total minimum absorbed dose of at least 5300 (5300 to 6900) rad in mean 19 fractions over 49 days to the target and 7 of the 12 were alive at the end of the control whereas of 24 patients who had received a smaller minimum absorbed dose (700 to 5200 rad in mean 14 fractions over 31 days) only 3 were alive.

The variation in the absorbed dose to the target reasonably well agreed with the range 5300 to 6300 rad in 8 patients still alive at the end of the control. The treatment had in the 4 patients been given in mean 16 fractions over 32 days.

## SUMMARY

Thirty six patients with inoperable pulmonary tumours were treated with high energy electrons. The calculation and checking of the absorbed dose are described. Only mild side effects apart from radiation pneumonitis were observed. Most patients were benefited by the treatment. The investigation indicated that the most useful total absorbed dose to the target may be between 5 300 and 6 300 rad given in sixteen fractions over 32 days.

## ZUSAMMENFASSUNG

Sechszunddrei sig Patienten mit inoperablen Lungentumoren wurden mit hochenergetischen Elektronen behandelt. Die Berechnung und die Kontrolle der absorbierten Dosis werden beschrieben. Nur geringere Nebeneffekte wurden abgesehen von der Strahlenpneumonitis beobachtet. Für die meisten der Patienten war die Behandlung vorteilhaft. Die Untersuchung zeigt, dass die nützlichste totalabsorbierte Dosis am Herd zwischen 5 300 und 6 300 rad in 16 Fraktionen während 32 Tagen gegeben zu sein scheint.

## RÉSUMÉ

Trente six malades atteints de tumeur pulmonaire inoperable ont été traités par les électrons de haute énergie. Les auteurs décrivent le calcul et le contrôle de la dose absorbée. À part la pneumopathie radiothérapique ils n'ont observé que des effets secondaires peu importants. La plupart des malades ont été améliorés par le traitement. Ce travail montre que la dose absorbée totale à la cible qui est la plus utile se situe entre 5 300 et 6 300 rad données en seize fractions sur 32 jours.

## REFERENCES

- BELING U. and EINHORN J. Radiotherapy for carcinoma of the lung. *Acta radiol. Ther. Phys. Biol.* 3 (1965) 281.
- DAHL O. och VIKTERLOF K. J. Den fungerande manniskolungans röntgenabsorption i en undersökning med sikte på djupdosberäkningar och fantomkonstruktion. (In Swedish) *Nord. Med.* 54 (1955) 1576.
- DEELEY T. J. Clinical trial to compare two different tumour dose levels in the treatment of advanced carcinoma of the bronchus. *Clin. Radiol.* 17 (1966) 299.
- ELLIS F. The dose time relationship in radiotherapy. *Brit. J. Radiol.* 36 (1963) 153.
- GEST J. et DELOUCHE G. La radiothérapie concentrée. *Sem. Hop. Paris* 43 (1967) 2057.
- HOLSTI L. R. Roentgen and tele-cobalt therapy of cancer of the lung. *Acta radiol. Ther. Phys. Biol.* 6 (1967) 65.
- DE JONG K. and RENNER K. Zur Behandlung des Bronchialkarzinoms. *Strahlentherapie* 129 (1966) 348.
- KREYBERG L. Histological typing of lung tumours. International histological classification of tumours. No. 1. World Health Organization, Geneva, 1967.
- LEVITT S. H., BOGARDUS C. R. and LADD G. Split dose intensive radiation therapy in the treatment of advanced lung cancer: a randomized study. *Radiology* 88 (1967) 115.

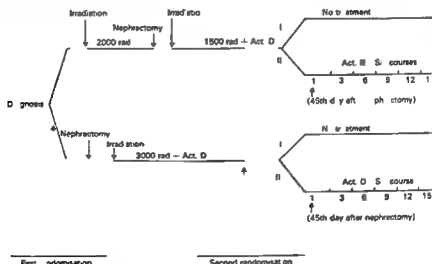
- LOERBROKS B und SCHLMACHER W. Behandlungsergebnisse und intrathorakale Strahlenreaktionen bei der Therapie des Bronchuscarcinoms mit schnellen Elektronen Beitr Klin Tuberk 131 (1965) 131
- MICELI R, CORINALDESI A, BONO F e MORETTI S. Cobaltoterapia a dosi concentrate nei carcinomi polmonari (In Italian.) Radiobiol Radioter Fis med 22 (1967) 139
- NORDBERG U II. Corrections of isodose-diagrams for  $^{60}\text{Co}$  and 35 MeV electrons at penetration of lung tissue. Acta radiol Ther Phys Biol 11 (1972) 113
- OLIVER R. Theoretical implications of cell survival data in relation to fractionated radiotherapy treatments Brit J Radiol 36 (1963) 178
- SCHLMACHER W. Die Therapie des Bronchialkarzinoms. In: Symposium on high energy electrons p 338 Springer Verlag Berlin Heidelberg New York 1965
- TESCHENDORF W und BLEHER E. A. Erste Erfahrungen mit einem 42 MeV Betatron bei der Therapie des Bronchialcarcinoms Rontgenblätter 22 (1969) 432
- UHLMANN E. M. Ein 45 Millionen Volt Linearbeschleuniger als Elektronenquelle für die Behandlung tiefliegender Karzinome Strahlentherapie 106 (1958) 319
- Utilization of high energy-electrons (20—40 MeV) in the treatment of deep-seated cancer. In: Transactions of the 14th international congress of radiology p 826 Georg Thieme Verlag Stuttgart Urban & Schwarzenberg Verlag München Berlin 1960
- and OVADIA J. High-energy electrons in the treatment of malignant tumours of the thorax Radiology 74 (1960) 265
- ZUPFINGER A. Radiation therapy with high speed electrons Radiol Clin 31 (1962) 129



# EUROPEAN TRIAL ON THERAPY OF NEPHROBLASTOMA

The International Society of Pediatric Oncology (SIOP) is planning a trial of the therapy of nephroblastoma (LEMERLE 1971). Considerable agreement exists on the treatment of these tumours the principal methods comprising surgery, radiation therapy and chemotherapy. Certain questions remain unanswered however as to the value of the different forms of administration of the two latter methods which might best be elucidated by clinical trial. Such an investigation has been proceeding in the USA for the last two years and in anticipation of the results SIOP has planned a European trial to cover matters not included in the American work and at the same time to complete the investigation.

The purpose, scope and outlines of the work proposed were discussed and agreed at the SIOP meetings in Madrid (1969), Lyon (1970) and Mainz (1971). The main purpose was to decide (a) whether preoperative and postoperative radiation therapy yield better results than the latter alone and (b) whether multiple courses of actinomycin D therapy are more successful in preventing metastases and recurrences than one single course after surgery. The purpose might be achieved by collecting and analysing the pertinent clinical data. Schedule of the proposed trial.



The reliability of such research obviously depends on the amount of material available for analysis. All those who wish to participate are cordially invited to apply for further information to Dr P. A. Voute, Emma Kinderziekenhuis, Spinozastraat 51, Amsterdam, the Netherlands.

## Reference

- LEMERLE J. Therapeutic trial and prospective study on nephroblastoma: a scheme of the International Society of Paediatric Oncology (SIOP). LICC Bulletin 9 (1971) 4.

## CLINICAL AND CYTOGENETIC INVESTIGATION IN CHILDREN OF PARENTS TREATED WITH RADIOIODINE

by

J EINHORN MAJ HULTEN J LINDSTEN HARRIET WICKLUND and  
P ZETTERQVIST

Some extrathyroid irradiation is always obtained as a side effect of radioiodine therapy. Thus for instance the radiation dose to the gonads for the  $^{131}\text{I}$  isotope is almost independent of age (BUCHAN & BRINDLE 1970) and has been estimated to be 0.5 to 1 rad/mCi (JOHNS & TAYLOR 1958, WEIJDER et coll 1960). An increased frequency of structural chromosome aberrations has been found in lymphocyte cultures from patients after radioiodine therapy (BOYD et coll 1961, MACINTYRE & DOBYNS 1962, NOFAL & BEIERWALTES 1964, OLSH & POMERAT 1964, CANTOLINO et coll 1966). The aim of the present investigation was to determine whether children conceived after a parent had received radioiodine therapy might have a consistent chromosome aberration or an increased frequency of aneuploidy or chromosome breakage. Cytogenetic and clinical examinations were made in 33 such children, 14 of which from 10 families were selected for a more detailed analysis. In four of the families the parent had been given fairly small doses of radioiodine (1.5 to 7 mCi) while large doses had been administered to 6 patients (14 to 175 mCi). The low dose group included a family in which the mother had been treated during

From Radiumhemmet and the Departments of Clinical Genetics and Medical Pediatrics Karolinska Sjukhuset, Stockholm, Sweden. Submitted for publication 16 September 1971.

Table 1

*Number of patients under 40 years of age given radioiodine therapy between 1952 and 1962*

	Males	Females	Total
Hyperthyroidism	28	104	132
Carcinoma of the thyroid	9	28	37
Total	37	132	169

Table 2

*Number of spontaneous abortions and children in patients previously given <sup>131</sup>I therapy: deaths among the children*

	No of patients	No of children				No of spontaneous abortions	
		Before treatment		After treatment		Before treatment	After treatment
		Alive	Dead	Alive	Dead		
<i>Hyperthyroidism</i>							
Males	14	9		7		2	3
Females	72	80	4	22	1	11	6
<i>Carcinoma of the thyroid</i>							
Males	8	9		4		3	—
Females	21	12		9		3	1
Total	115	110	4	42	1	16	10

pregnancy. Cytogenetic analysis of children exposed to ionizing radiation during foetal life have been reported only occasionally (LEJEUNE et coll 1964; MACINTYRE et coll 1965; BLOOM et coll 1967; UCHIDA et coll 1968).

*Material.* All 169 patients who had received radioiodine therapy for hyperthyroidism or carcinoma of the thyroid between 1952 and 1962 and who were less than 40 years old at the time of the treatment were questioned about post treatment pregnancies (Table 1). Information on spontaneous abortions and terminated pregnancies was obtained at personal interviews of 115 patients. These patients had given birth to a total of 157 children: 43 of whom were born after radioiodine therapy to one of the parents (Table 2).

Cytogenetic analyses were performed in 33 of the 43 children (19 girls, 14 boys) of the remaining 10 children: one refused to cooperate while others

Table 3

Results of the cytogenetic analysis in families in which at least 50 cells were analysed in the parent undergoing radioiodine therapy and in the children born subsequently Fp female patient Mp male patient Fc female child Mc male child Fk female control Mk male control The number of aneuploid cells was calculated as the number of centromeres

Family	I therapy		Age at chro-mosome analysis (years)	Total No of cells analysed	Aneuploid		Chro-matid breaks or frag-ments	Chro-mosome breaks isofrag-ments or inter-changes	Cells with breaks/100 cells
	Dose (mCi)	Age (years)			<45	>47			
Hyperthyroidism									
1 Fp	1.5	37	50	100	7	1	3	4	8
Mc	—	—	12	150	2	—	4	15	17
4 Fp	4.0	34	40	100	2	1	1	3	4
Fc	—	—	4	100	2	—	1	—	1
Fc	—	—	3	100	3	—	—	3	3
6 Fp	5.0	26—27	34	100	2	1	1	4	5
Mc	—	—	5	100	3	—	2	1	3
8 Fp	7.0	27	38	100	4	—	2	3	5
Mc	—	—	9	100	2	—	—	4	4
12 Fp	14.0	27—28	36	50	—	—	—	7	14
Fc	—	—	6	50	1	—	1	2	6
Mc	—	—	3	50	3	—	1	2	6
Carcinoma of the thyroid									
17 Fp	50.0	28	32	100	—	—	2	8	11
Fc	—	—	2	100	3	—	1	2	3
18 Mp	70.0	37	41	100	1	—	2	13	15
Mc	—	—	2	100	2	—	1	1	1
19 Mp	70.0	37	36	100	4	—	—	6	6
Mc	—	—	2	100	2	—	3	4	6
21 Fp	70.0	19	23	75	4	—	2	11	15
Fc	—	—	3	61	1	1	—	1	1
Fc	—	—	4	100	3	—	2	—	2
22 Mp	175.0	18	{ 29 32	{ 37 100	{ 5 5	{ — —	{ 2 3	{ 5 3	{ 19 4 } 11
Mc	—	—	7	100	1	—	4	4	8
Mc	—	—	2	100	—	—	4	4	8

Table 3 (cont.)

Family	<sup>131</sup> I therapy		Age at chro- mosome analysis (years)	Total No of cells analysed	Aneuploid		Chro- matid breaks or frag- ments	Chro- mosome breaks isofrag- ments or inter- changes	Cells with breaks/ 100 cells
	Dose (mCi)	Age (years)			<45	47>			
Controls									
<i>Older controls</i>									
23 Mk	—	—	49	50	—	—	—	1	2
24 Fk	—	—	44	50	1	—	2	—	4
25 Mk	—	—	38	50	—	—	—	—	0
26 Fk	—	—	36	50	1	—	2	4	12
27 Fk	—	—	35	50	1	—	—	—	0
<i>Younger controls</i>									
28 Mk	—	—	22	100	1	—	1	2	3
29 Mk	—	—	21	50	—	—	1	—	2
30 Fk	—	—	17	50	2	—	—	1	?
31 Mk	—	—	1	50	1	—	1	1	4
32 Fk	—	—	1	50	2	—	—	—	0

were lost to the investigation because of culture failure. Data on the type of thyroid disorder in the parents, the time and dose of the radioiodine therapy, date of birth of the children and results of the chromosome analysis are presented in Table 3.

Six of the 8 parents with carcinoma of the thyroid and one of the 14 with hyperthyroidism had received supplementary external radiation therapy. The patient with hyperthyroidism (3 Fp) had had surface roentgen treatment (dose unknown) for keloid formation in a scar on the neck. Five parents with thyroid carcinoma (8 Fp, 12 Fp, 16 Fp, 17 Fp, 22 Fp) were irradiated for 3 to 6 weeks with doses ranging from 3500 to 5000 rad to the thyroid region or regional lymph nodes of the neck. One (18 Mp) was operated on for seminoma five months before the radioiodine therapy. <sup>60</sup>Co kilocurie irradiation was given after the operation to the retroperitoneal lymph glands over two fields in addition to radiation treatment over two mediastinal fields and roentgen treatment to the thyroid region. Unlike the external irradiation of the neck, that to the retroperitoneal fields (2000 rad/field) may have contributed significantly to the dose to the gonads, since the frequency of chromosome breakage was however not appreciably higher in this patient than in those

receiving slightly lower or higher doses of  $^{131}\text{I}$ , and since the chromosome abnormalities did not depart from the overall pattern in any other way, the patient was not excluded from the material

Ten families were examined in greater detail. At least 50 and usually 100 cells were analysed both from the treated parents as well as from the 14 children born after the therapy (Table 3). Four of these parents were treated for hyperthyroidism and 11 for carcinoma of the thyroid. The doses ranged from 1.5 to 175 mCi radiiodine. The ages of the 14 children ranged from 2 to 12 years (mean 4.1 years) at the time of the investigation. The total dose to 13 parents was as follows:

Dose of $^{131}\text{I}$ (mCi)	1.5—7	14—70	175
No. of children	4	7	2

In addition a dose of 1.5 mCi was given five months before delivery in Case IMc. This child must therefore have been irradiated in utero and is reported separately.

A control group for the cytogenetic investigation comprised 10 volunteers in apparently sound health (Table 3). Five were 1 to 22 years of age (mean 12 years) and five were 35 to 49 years old (mean 40 years). None of them had undergone treatment with ionizing radiation or had ever been working in a department of therapeutic or diagnostic radiology. In the year preceding the chromosome analysis none had been taking drugs known to induce chromosomal aberrations, had been exposed to diagnostic radiation or had had diseases known to be caused by viral infection. The blood specimens were taken during the same period as the case series.

Examinations of blood groups (ABO, Rhesus, MNS, P, Kell, Duffy & Lewis) and serum protein groups (haptoglobins Gc and Gm) were performed in order to check paternity and, with a consistent chromosome aberration to determine gene location. In those families in which complete information could be obtained (Nos 6, 11, 13, 16, 17, 18 and 20) no parent-child discrepancies were observed.

*Methods.* Each child underwent a careful physical examination by a pediatrician (P.Z.). Lymphocyte cultures were made with minor modifications of the technique of MOORHEAD *et al.* (1960). A micromethod was used when venipuncture was difficult. All cultures were harvested after 72 hours. Colcemid (0.5  $\mu\text{g}$  per ml of culture medium) being added for the last three hours of culture. The cells were stained in acetic orcein and photographed in phase contrast oil immersion with a Zeiss photomicroscope. The chromosome analysis was made in coded slides. Fifteen consecutive cells were photographed when only the karyotype was examined and the photographic enlargements

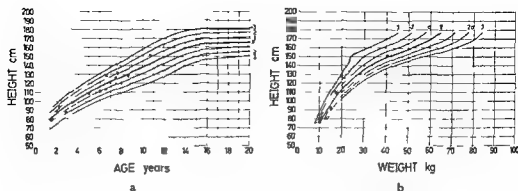


Fig 1 Age height and weight of girls born after one of their parents had had radioiodine therapy. The distribution in the Swedish population is indicated a) Age versus height b) Weight versus height

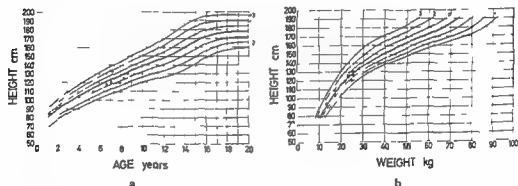


Fig 2 Age height and weight of boys born after one of their parents had had radioiodine therapy. The distribution in the Swedish population is indicated a) Age versus height b) Weight versus height

of the cells were karyotyped independently by two cytologists. One hundred consecutive cells were photographed in the cases selected for more detailed investigation. Each cell in a photographic enlargement was analysed independently by two cytologists for both karyotype and chromosome breakage. The results were compared, controversial cells discussed, and if necessary, rechecked under the microscope. Doubtful abnormalities and gaps in the chromosomes were not scored as aberrations, and only clearly displaced chromosome pieces were scored as fragments or breakages (Figs 1 to 6 and Table 3).

The interpretation of the karyotype was difficult in many cells especially as regards the distinction between structural aberrations and normal variations. Double or enlarged satellites or enlarged short arms on the acrocentric chromosomes were not scored as aberrations even when observed only in a small



Fig 3 461 — mar<sub>1</sub> + Probable deletion of one chromosome No 1 close to the centromere (Nomenclature of the Chicago Conference 1966)



Fig 4 An extra small chromosome similar to the Philadelphia chromosome

proportion of the cells in a single subject. These changes commonly appear in cells of healthy subjects and are regarded as normal variants of unknown or merely hypothetical significance (COURT BROWN 1967). The same applies to the variation in the size of chromosome No 16, one of which is sometimes larger and sometimes smaller than normal. Furthermore, one B chromosome was sometimes difficult to distinguish from one of the C chromosomes, its long arm being relatively short. Chromosomes 1 and 3 are generally almost metacentric. Asymmetry of one of these chromosomes, especially No 1, appears in some cells, probably owing to variations in size or extension of the secondary constriction. Cells with such chromosomes were not scored as abnormal. A variation in the size of the Y chromosome is common in the general population (COURT BROWN 1967). None of the subjects had a short Y chromosome, while the father and son of family No 19 had a rather long Y, similar in size to a D chromosome. Furthermore, the size of the Y chromosome varied among the cells from the father. A somewhat enlarged short arm on a G chromosome in family No 17 was the only so-called variant of the short arm of the acrocentric chromosomes evident in the present investigation. Because of the difficulty in distinguishing certain structural chromosome aberrations and because the scoring was performed according to strict principles, the figures probably underestimate the true frequency of structural abnormalities. The control material was tested blindly by the same rules.



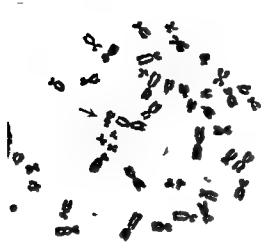


Fig 5 45 X (16 G Dic+) Missing No 16 and a G chromosome one dicentric chromosome



Fig 6 46 XX Isochromatid break on the long arm of chromosome No 2 Gap on No 3 not scored as an abnormality

## Results

### *Clinical observations*

The body height and weight for all 33 children for whom a cytogenetic analysis was performed fell within the normal range of variation (Figs 1 to 4) their physical and mental development was apparently also normal. A perceptible hearing impairment in the eldest son of family No 21 probably had no connection with the radiation therapy to the father, since the mother had several relatives with a similar type of hearing loss. No other malformations were diagnosed in any of these children.

There were three twin pairs among the 43 children. The material is too small to judge whether the frequency of twins after radioiodine therapy was greater than in the general population.

Spontaneous abortions occurred in 16 out of 130 pregnancies (12.3 per cent) before and 10 out of 53 after (18.9 per cent) the radioiodine therapy (Table 2). The mean ages of the treated parent at the end of these pregnancies were 27 and 36 years respectively. These frequencies are lower than those reported by PETTERSSON (1968) in the same age groups in the Swedish population. Four of the 114 children born before (1 out of 30), but only 1 of the 43 children born after radioiodine therapy, died during the follow-up period. These figures are not comparable since the children born before the radioiodine therapy had a longer follow-up period than the others.



Fig 7 46,2(3+C) The simplest interpretation being either trisomy monosomy or a structural rearrangement involving one or 2 C chromosomes

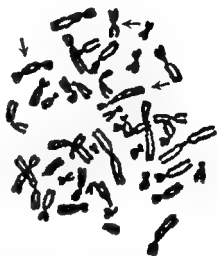


Fig 8 45,16,-C,C,C,-dic+,mar1+,mar1+,mar2+ Multiple changes One number 16 and three C chromosomes missing and replaced by one dicentric one abnormal metacentric and one long sub-metacentric chromosome

### *Cytogenetic analysis*

The results are presented in Table 3 and examples of chromosomal changes scored as normal variations and structural aberrations appear in Figs 1 to 8. The 10 families submitted to a more thorough cytogenetic examination and the 10 controls are reported in greater detail.

**Controls** The mean frequency of cells with breaks in the whole control group was  $2.9 \pm 1.1$  per 100 cells analysed. For the younger (1 to 22 years mean 12 years) and older (35 to 49 years mean 40 years) groups the respective figures were  $2.2 \pm 0.7$  and  $3.6 \pm 2.2$  per cent, the difference being not statistically significant. The frequency of aneuploid cells ranged from 0 to 4 per cent with a mean of  $1.7 \pm 0.5$ . It was numerically higher for the younger ( $2.2 \pm 0.8$  per cent) as compared to the older ( $1.2 \pm 0.5$  per cent) control group, but this difference is also not statistically significant (Tables 4, 5).

**Parents given radioiodine therapy** The frequency of cells with breaks was  $5.5 \pm 0.9$  per cent for the patients with hyperthyroidism who received fairly small doses of radioiodine (1.5 to 7 mCi mean 3.9 mCi). This is not significantly different from the value for the older control group (3.6 cells  $\pm$  2.2 per cent). The mean age was 40 years for the two groups (Table 4).

**Table 4**  
*Cells with chromatid or chromosome breaks*

	No	Cells with break per 100 analysed	
		No	SF
Controls	10	2.9	1.1
Children of parents given I therapy			
Low dose (4 to 7 mCi)	4	2.8	1.0
High (14 to 175 mCi)	9	4.6	0.9
The child irradiated in utero (1.5 mCi)	1	12	
Parents given I therapy			
Low dose	4	5.5	0.9
High	6	12.2	1.5

The frequency of cells with breaks was  $12.2 \pm 1.5$  per cent for the patients with carcinoma of the thyroid in whom larger doses of radioiodine were given (14 to 175 mCi; mean 75 mCi). This was significantly higher ( $p < 0.01$ ) than for the older controls and the whole control group ( $p < 0.01$ ). The mean age of the patients with carcinoma of the thyroid (33 years) was somewhat lower than that of the older controls (40 years). The increased frequency of cells with chromosome aberrations was mainly due to isochromatid breaks and rearrangements rather than to chromatid breaks; the incidence of which was almost the same for the two groups (Table 3).

The frequency of aneuploid cells in the patients receiving radioiodine therapy was  $3.8 \pm 1.0$  per cent. There was no significant difference between those patients given fairly small and those given high doses ( $4.5 \pm 1.2$  and  $3.3 \pm 1.6$  cells per cent respectively). The latter value is not significantly different from that for the older controls or the whole control group ( $1.2 \pm 0.5$  and  $2.2 \pm 0.8$  per cent respectively) (Table 5).

A Philadelphia chromosome-like abnormality was observed in a low proportion of the cells (3 per cent) from the father of family No. 18, but the clinical examination and blood smear disclosed no signs of leukaemia.

The interval from the  $^{131}\text{I}$  treatment to the blood culture ranged from 2 years and 9 months to 11 years and 6 months. There were no evident differences in the frequency of scorable chromosome abnormalities among patients examined at different time intervals after the treatment.

*Children of parents given radioiodine therapy.* The mean frequency of cells with breaks was  $2.8 \pm 0.6$  per cent for the 4 children of parents receiving ■

Table 5  
*Aneuploid cells*

	No	Aneuploid cells per 100 analysed		Age years	
		No	SE	Range	Mean
Young controls	3	22	0.8	1-22	12
Adult controls	3	12	0.5	33-49	40
Children of parents given I therapy					
Low dose (4 to 7 mCi)	4	23	0.3	3-9	6
High (14 to 173 mCi)	9	24	0.6	2-7	3
The child irradiated in utero	1	7		12	
Parents given I therapy					
Low dose	4	43	1.2	34-50	41
High	6	33	1.6	23-41	33

low dose of radioiodine (4 to 7 mCi). The corresponding value for the 9 children of parents given larger doses (14 to 173 mCi) was  $4.6 \pm 0.9$  per cent cells with breaks. Neither of these figures differed significantly from those for the younger controls and the whole control group ( $2.2 \pm 0.7$  and  $2.9 \pm 1.1$  per cent cells with breaks respectively). It is however notable that both children of the only parent receiving more than 100 mCi (173 mCi) recorded a higher number of cells with breaks (8 per 100 analysed) than any of the 16 young controls or children of parents given less than 100 mCi. The probability that this would occur by chance is small ( $p < 0.01$ ).

The child exposed to radioiodine in utero had the highest frequency of cells with breaks, 12 per cent, even though the mother received the lowest dose, 1.5 mCi (Table 4).

The higher frequency of cells with chromosome aberrations in the children was mainly due to lochromatid breaks and rearrangements, and only to a lesser extent to chromatid breaks. The frequency of aneuploid cells in these children was  $2.5 \pm 0.4$  per cent as compared to  $2.2 \pm 0.8$  per cent in the young controls and to  $1.7 \pm 0.5$  per cent (aneuploid) cells in the whole control group (Table 5).

None of the 33 children presented a consistent chromosome aberration. A Philadelphia chromosome like abnormality was observed in 1 out of 100 cells from Case 6 Mc that had no signs of leukaemia.

### Discussion

Radioiodine therapy is commonly applied in the treatment of hyperthyroidism, atoxic goitre not suitable for surgical treatment and carcinoma of the thyroid. Certain risks associated with the administration of radioiodine may already have been evaluated, while others are still difficult to assess despite the availability of large series of patients followed for 20 years or more. The immediate hazards associated with any exacerbation of the clinical signs after radioiodine therapy are small and may be further reduced by applying the appropriate measures (LARSSON 1955, EDENMYR & EINHORN 1966, SÄTERBORG & EINHORN 1966). The frequency of hypothyroidism a long time after the treatment is high (BELING & EINHORN 1961, DUNN & CHAPMAN 1964, GREEN & WILSON 1964) and the probability of recurrence extremely low (CHAPMAN & MALOOF 1955, WERNER et coll 1957, ELLER et coll 1960, BELING & EINHORN 1961). The chance of carcinoma of the thyroid resulting from radioiodine therapy is considered to be practically non-existent in adults (STAFFURTH 1966) but has to be taken into account in children (SHELINE et coll 1962, STARR et coll 1964, KOGUT et coll 1965). The likelihood that radioiodine therapy will induce leukaemia is regarded as negligible except with the doses used in the treatment of carcinoma of the thyroid (POCHIN 1960, WERNER et coll 1961, SEIDLIN 1965).

It is still difficult to estimate the risk of genetic damage associated with radioiodine treatment despite the large number of patients treated. Estimates may be made from the calculated radiation dose to the gonads and extrapolation to other categories of patients exposed to radiation with the same gonadal doses. The largest presumptive control group might be that exposed to irradiation of the gonads in connection with roentgen examinations. Even though the radiation doses in some roentgen examinations (LARSSON 1958) are often comparable with the gonad doses in radioiodine therapy for a small toxic goitre, they are not comparable to the gonad irradiation associated with larger doses of radioiodine. Moreover, the calculation of the radiation dose to the gonads in radioiodine therapy is based on an assumed random distribution of the extrathyroidal radioiodine in the body, whereas in reality this distribution is subject to extremely large individual variations (SEIDLIN et coll 1962, JOHNS & TAYLOR 1958, WEIJDER et coll 1960). It has also been demonstrated that inorganic radioiodine passes into the testicular tubuli and binds with protein in the intertubular fluid, which plays a mechanical role in the transport of sperms. This fluid has also proved to be a rich source of substrate and co-factors involved in the gametogenic function of the testis as revealed by investigations in various animals (PANDE et coll 1966, 1967 a, b). Thus gametogenesis might be affected to a greater extent than computed on the assumption of a random distribution of radioiodine in the body.

The most reliable information on the genetic risks associated with radioiodine therapy will probably be obtained from follow up investigations of several generations of descendants of those who have had radioiodine therapy. Such materials are not yet available and even indirect information on the genetic risk that might be associated with a common form of treatment would therefore be of value (HEDDLE 1969, SOBELS 1969).

No malformations ascribable to mutations resulting from irradiation were found in children born after the parents had received radioiodine doses of up to 175 mCi. Clinically these children did not differ from the general population of the same age as regards weight, height (Fig. 1) and haemoglobin concentration. Nor were any other deviations disclosed by the clinical examination to which all the children were submitted. However, the material is small, and *does not permit of definite conclusions*.

No consistent chromosome aberrations were demonstrated in any of the 33 children. The families submitted to a more detailed cytogenetic analysis are, however, of some further interest. As expected from previous reports, the frequency of cells with breaks was higher in the patients given radioiodine therapy than in the controls (Table 4). It was also higher ( $p < 0.01$ ) in those receiving the greater rather than the smaller, radioiodine doses. The frequency of cells with breaks in the controls was significantly lower than in the patients receiving larger doses of radioiodine ( $p < 0.001$ ) and numerically but not statistically significantly lower than in those given the low doses.

The frequency of cells with breaks in the children born after the parent had received radioiodine therapy seemed to increase with the dose (Table 4). The frequency of cells with breaks in children of parents given a small dose (4 to 7 mCi) did not differ from that of the controls (Table 4). The frequency was higher than for the controls in the children of parents who had had the higher doses (14 to 175 mCi) but the difference in this small series was not statistically significant. In addition, the two children of the parent with the highest dose (175 mCi) had both a higher frequency of cells with breaks than any of the other 16 young persons in this series (11 were children of parents receiving the lower dose and 5 were of the younger controls). No definite conclusions can, however, be drawn from this very small series, especially since the two children came from the same family. It should be mentioned in this connection that chromosome aberrations have been observed in newborn swine after insemination with semen irradiated with roentgen radiation (ZARTMAN et coll. 1969).

Chromosomal aberrations have been observed among survivors exposed in utero at Hiroshima and Nagasaki (BLOOM et coll. 1967). The rather high frequency of cells with breaks in the child exposed to radiation in utero in the

present series is remarkable in view of the small dose of radioiodine received by the mother (1.5 mCi). This frequency remained unchanged for two consecutive examinations at intervals of several months.

### Acknowledgements

The investigation was supported by grants from the Cancer Society of Stockholm and the Swedish Medical Research Council. Part of the cytologic work was performed when one of the authors (M.H.) was a guest of the Euratom Unit for Radiation and Cytogenetics, University of Pavia, Italy. The authors take this opportunity of thanking A. Heiken for performing the blood and serum protein grouping. The technical assistance of Mrs Barbro Hermansson, Miss Kerstin Hansson and Miss Anita Tillberg is gratefully acknowledged. The Colcemid was provided by CIBA.

### SUMMARY

The number of pregnancies and spontaneous abortions were investigated before and after  $^{131}\text{I}$  therapy in 169 patients. Thirty of the 43 children who were born after the parent had received the treatment were examined clinically and cytogenetically and were compared with a control material.

### ZUSAMMENFASSUNG

Es wurde eine Nachforschung bezüglich der Zahl der Schwangerschaften und der spontanen Aborte an 169 Patienten vor und nach der Behandlung mit  $^{131}\text{I}$  vorgenommen. Von 43 Kindern wurden 30 Kinder klinisch und zytologisch untersucht, die alle nach vorheriger Behandlung der Mutter geboren waren. Die Resultate wurden mit normalen Kontrollen verglichen.

### RÉSUMÉ

Les auteurs ont étudié le nombre de grossesses et le nombre d'avortements spontanés avant et après traitement par  $^{131}\text{I}$  chez 169 malades. Trente des 43 enfants nés après traitement de leur mère ont été examinés cliniquement et cytogénétiquement et ont été comparés à une série de témoins.

### REFERENCES

- BELING L. and EINHORN J. Incidence of hypothyroidism and recurrences following  $^{131}\text{I}$  treatment of hyperthyroidism. *Acta radiol.* 56 (1961) 275.
- BLOOM A. D., VERISIE S., KAMADA N. and ISEKI T. Leukocyte chromosome studies of adult and in utero exposed survivors of Hiroshima and Nagasaki. In *Human radiation cytogenetics*, p. 136. Edited by H. J. Evans, W. M. Court Brown and A. S. McLean. North Holland Publishing Company, Amsterdam, 1967.

- and ARCHER P G Cytogenetics of the in utero exposed of Hiroshima and Nagasaki *Lancet* 1968 I p 10
- BOYD E, BUCHANAN W W and LEXNON E Damage to chromosomes by therapeutic doses of radioiodine *Lancet* 1961 I p 977
- BUCHAN R E and BRINDLE J M Radioiodine therapy to out patients—the contamination hazard *Brit J Radiol* 43 (1970) 479
- CANTOLINO E J, SCHNICKEL R D, BALL M and CISAR C F Persistent chromosomal aberrations following radioiodine therapy for thyrotoxicosis *New Engl J Med* 175 (1966) 739
- CHAPMAN E M and MALOOF F The use of radioactive iodine in the diagnosis and treatment of hyperthyroidism: ten years experience *Medicine* 34 (1955) 261
- CHICAGO CONFERENCE Standardization in human cytogenetics *Birth Defects Original Article Series* II 2 The National Foundation New York 1966
- COURT BROWN W M Human population cytogenetics North Holland Publishing Company Amsterdam 1967
- DUNN J T and CHAPMAN E M Rising incidence of hypothyroidism after radioactive iodine therapy in thyrotoxicosis *New Engl J Med* 271 (1964) 1037
- EDMYR F and EINHORN J Complications in radioiodine treatment of hyperthyroidism *Acta radiol Ther Phys Biol* 4 (1966) 49
- ELLER M, SILVER S, YOHALEN S B and SEGAL R L The treatment of toxic nodular goiter with radioactive iodine: 10 years experience with 436 cases *Ann intern Med* 52 (1960) 976
- GREEN M and WILSON G M Thyrotoxicosis treated by surgery or iodine 131 With special reference to development of hypothyroidism *Brit Med J* (1964) p 1005
- HEDDLE J A Radiation induced chromosome aberrations in man: a possible biological dosimeter Pathology Society symposium Human chromosome aberrations induced by radiation: chemicals and viruses *Fed Proc* 28 (1969) 1790
- JOHNS H E and TAYLOR R M Gonadal dose in Canada arising from the clinical use of unsealed radioactive isotopes *J Canad Ass Radiol* 9 (1958) 55
- KOGUT M D, KAPLAN S A, COLLIPP P J et coll Treatment of hyperthyroidism in children: Analysis of forty five patients *New Engl J Med* 272 (1965) 217
- LARSSON L E Radiation doses to the gonads of patients in Swedish roentgen diagnostics *Acta radiol* (1958) Suppl No 157
- LARSSON L G Studies on radioiodine treatment of thyrotoxicosis With special reference to the behaviour of the radioiodine tracer tests *Acta radiol* (1955) Suppl No 126
- LEJEUNE J, BERGER H, ARCHAMBAULT L et coll Mosaïque chromosomique probablement radio-induite in utero *C R Acad Sci (Paris)* 259 (1964) 495
- LITTLEFIELD L G, HOLLOWELL J G and POOL JR W H Chromosomal aberrations induced by plasma from irradiated patients: an indirect effect of X radiation *Radiology* 93 (1969) 879
- MACINTYRE M N and DOBYS B M Anomalies in chromosomes of the circulating leukocytes in man following large doses of radioactive iodine *J clin Endocr* 22 (1962) 1171
- STENCHIVER M A, WOLF B H and HIMPET J M Effect of maternal antepartum exposure to X rays on leukocyte chromosome of newborn infants *Obstet Gynec* 25 (1965) 650
- MOORHEAD P S, NOWELL P C, MELTZMAN W J et coll Chromosome preparations of leukocytes cultured from human peripheral blood *Exp Cell Res* 20 (1960) 613



- NOFAL M and BEIERWALTES W Persistent chromosomal aberrations following radioiodine therapy J nucl Med 5 (1964) 840
- OISHI H and POMERAT C M Chromosomal studies on human leukocytes following treatment with radioactive iodine in vivo and in vitro In Cytogenetics of cells in culture Vol 3 Edited by R J C Harris Academic Press New York and London 1964
- PANDE J K DASGUPTA P R and KAR A M (a) Chemical composition of fluid collected from testis of the Rhesus monkey and goat Indian J exp Biol 5 (1967) 65
- — — (b) Biochemical composition of human testicular fluid collected post mortem J clin Endocr 27 (1967) 892
- CHOWDHURY S R DASGUPTA P R et coll Biochemical composition of the rat testis fluid Proc Soc Exp Biol Med 121 (1966) 899
- PETTERSSON F Epidemiology of early pregnancy wastage Svenska Bokforlaget Norstedt — Bonniers Stockholm 1968
- POCHIN E E Leukaemia following radioiodine treatment of thyrotoxicosis Brit med J (1960) p 1545
- SATERBORG N E and EINHORN J Fractionated  $^{131}\text{I}$  therapy in large toxic goitres Acta endocr (Abh) 51 (1966) 7
- SEIDLIN S M YALOW A A and SIEGEL E Blood radioiodine concentration and blood radiation dosage during  $^{131}\text{I}$  therapy for metastatic thyroid carcinoma J clin Endocr 12 (1952) 1197
- SIEGEL E MELAMED S and YALOW A A Occurrence of myeloid leukemia in patients with metastatic thyroid carcinoma following prolonged massive radioiodine therapy Bull N Y Acad Med 31 (1955) 410
- SIELINE G E LINDSAY S MCCORMACK K M and GALANTE M Thyroid nodules occurring late after treatment of thyrotoxicosis with radioiodine J clin Endocr 22 (1962) 8
- SOBELS F H Estimation of the genetic risk resulting from the treatment of women with iodine Strahlentherapie 138 (1969) 172
- STAFFLUTH J S Thyroid cancer after  $^{131}\text{I}$  therapy for thyrotoxicosis Brit J Radiol 39 (1966) 471
- STARR P JAFFE H L and OETLINGER JR L Late results of  $^{131}\text{I}$  treatment of hyperthyroidism in seventy three children and adolescents J nucl Med 5 (1964) III
- UCHIDA I A HOLLINGA R and LAWLER C Maternal radiation and chromosomal aberrations Lancet 1968 II p 1045
- WEIJDER H L DUGGAN H E and SCOTT D M Total body radiation and dose to the gonads from the therapeutic use of iodine  $^{131}\text{I}$  A survey of 20 cases J Canad Ass Radiol 11 (1960) 50
- WERNER S C COELHO B and OLIMBY E M Ten year result of  $^{131}\text{I}$  therapy of hyperthyroidism Bull N Y Acad Med 33 (1957) 783
- GITTELSOM N M and BRILL A B Leukemia following radioiodine therapy of hyperthyroidism J Amer med Ass 177 (1961) 646
- ZARTMAN M L FECHHEIMER N S and BAKER L N Chromosomal aberrations in cultured leukocytes from pigs derived from N irradiated semen Cytogenetics 8 (1969) 355

## CERVICAL PLEXUS LESIONS FOLLOWING POST OPERATIVE RADIATION THERAPY OF MAMMARY CARCINOMA

by

P WESTLING H SVENSSON and P HELE

Complications following post-operative radiation therapy of primary carcinoma have not been uncommon and have consisted of lesions of the cervical plexus subcutaneous fibrosis in the supraclavicular field and mild lung reactions.

A total of 103 patients with mammary carcinoma were treated during the period March 1963—March 1965 71 with post operative radiation therapy by a standardized  $^{60}\text{Co}$  technique. The object of the treatment consisted in the delivery of a cancerocidal radiation dose to the regional lymph node areas through one parasternal one supraclavicular and one axillary field (Fig 1). The supraclavicular field measured approximately 8 cm  $\times$  12—13 cm with the medial border reaching just over the midline somewhat below the clavicle. The parasternal field was centred about one centimetre lateral to the sternal border and measured about 7 cm  $\times$  12 cm. The beam direction of the supraclavicular field was vertical and to avoid overlap in the border zone the parasternal beam was directed 10° caudally. The axillary field measuring 9—10 cm  $\times$  11—12 cm

This paper was read at the XII International Congress of Radiology Tokyo October 1969. Submitted for publication 12 July 1971.



Fig 1 a) The supraclavicular and parasternal fields b) The axillary field irradiated with the arm elevated

was irradiated with the arm elevated and the central beam positioned in a plane through the centres of the axilla and supraclavicular fields this beam was angled  $30^\circ$  dorsally to the horizontal plane in order to reduce the overlap between the supraclavicular and the axillary beams

A peak dose of 400 rad was given daily to each of the 3 fields for five days a week with a total dose of 4 400 rad per field over 21 to 26 days (average 23 days) two of the three fields being irradiated each day. The isodoses in a plane through the centres of the axilla and supraclavicular region appear in Fig 2. The dose maximum (Fig 2 a) was rather small and located about 4 to 5 cm under the skin but was considered acceptable, further investigations have however indicated that the maximum may be located more superficially in about 70 per cent of patients (Fig 2 b) and may reach 130 per cent. All the patients were treated supine.

Induration of the subcutaneous tissues in the supraclavicular region was observed in 90 per cent of the patients, beginning after an average latency period of 12 months (range 5 to 20 months) with light somewhat tender edema gradually becoming firmer. The induration was not always homogeneous but was nodular to suggest metastases. Fine needle biopsy performed in several patients failed to confirm this possibility.

The first few cases of cervical plexus lesions were evident about a year from the end of therapy although at this time the symptoms consisted only of slight sensory disturbances. Not until about 18 months later were the first obvious motor lesions observed. As soon as it became clear that the symptoms and motor lesions were not caused by metastases around the plexus the method of treatment was changed (see p 214).

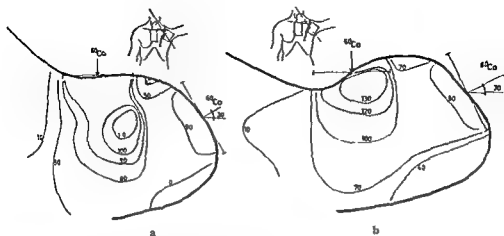


Fig 2 Isodoses in planes through the centres of the axillary and supraclavicular fields a) The resultant maximum dose (110 per cent) lies relatively deeply b) The resultant maximum dose (130 per cent) is situated in the plexus nerve region

The cervical plexus lesions developed in a typical manner starting with sensory disturbances such as irradiating pain numbness of the fingers and paraesthesia. After a period of a few days to about 18 months the sensory symptoms were followed by motor signs (Fig 3) when some relief of pain occurred. Mild cases consisted of slight paresis of one muscle or muscle group while in others complete or nearly complete paralysis of one muscle combined with moderate paresis or normal function in other muscles occurred. Three of the most severe cases had almost complete paralysis of one arm. The distribution of the motor as well as the sensory lesions were thus generally patchy. EMG recordings were usually obtained and presented evidence of conditions ranging from the normal to partial or total denervation, reinnervation signs were sometimes apparent. The motor lesions were often progressive in the first few months later becoming stationary although partial recovery was also observed. The correlation between the latency period and the degree of paresis was negative the longer the period the milder the paresis. Many of the patients had some relief of pain from prednisolone and physiotherapy. Decompressive surgery has been reported by STOLL & ANDREWS (1966) some relief of symptoms occurred but the sensory and motor signs persisted. Resection of a part of the clavicle of a patient of the present material failed to produce a positive result, since the tissues around the plexus nerves were hard it was believed that dissections would carry a definite risk of healing complications including necrosis.

Peripheral nerves are regarded as relatively radiation resistant. Much animal research work has been carried out on the functional and histologic changes in

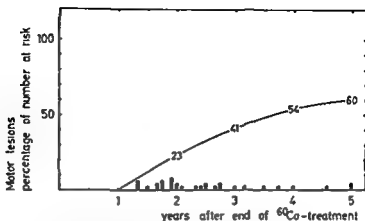
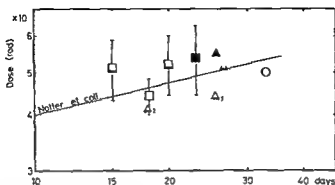


Fig. 3 Cumulative percentage of motor lesions at different times after treatment. Each circle represents one patient. The motor lesions in 23 of 31 patients occurred at 16 to 33 months.

such nerves (BACHOFER *et coll.* 1964; LEBEDINSKY *et coll.* 1963). Most of this work, however, concerns the effect of krad doses observed a short time after the irradiation. Experiments with doses at clinical levels and with longer observation times were made by JANZEN & WARREN (1942). The authors reported no changes in nerves irradiated with doses between 4 000 and 10 000 rad after an observation time of two months. LINDER (1959) observed histologic changes at 3 to 11 months in nerves irradiated with  $3 \times 1\,000$  rad over 6 days. No functional disturbances could be demonstrated, however.

The cervical plexus lesions constituted an unexpected complication and at first suggested malignant infiltration of the nerves. Lesions of this pathogenesis are not uncommon and cases were described by SON (1967) and NISCE & CHU (1968). The symptoms and signs of this syndrome are the same or very similar to those of radiation induced lesions. The effect of radiation therapy (mostly supervoltage) was excellent with relief of pain and recovery of motor function in a fair number of patients. A dosage of 4 000 to 5 000 rad over four weeks was more effective than lower doses. Fibrosis induced by previous radiation therapy or surgery (NISCE & CHU) was often evident and it was sometimes difficult to determine whether the syndrome was caused by a neoplasm or fibrosis or a combination of both. The results of radiation therapy were better in patients without pre-existing fibrosis. Though the possibility of malignant infiltration of the plexus region could not be ruled out in the present material, the repeated negative fine needle biopsies and the subsequent course suggested that the condition was radiation induced. In no patient treated after the beginning of 1962



	Author	Plexus lesions	Field	Radiation	Dose
▲	Still and Andrews	73 /	On 1 side supraclav. dia	4 Mrad / y	500 ad / 25-26 days
▲		15 /			5100 ad / 25-28 days
▲		16 /	(Large)		100 ad / 18 days
▲		10 /	Small 1 side	200 kV H/L 1 mm	4300 ad / 25 day
■	Presley	60 /	Large supraclav. 1 side	60°C	1000-1000 rad / 23 d. yrs
□		14 /	Small 1 side supraclav. 1 side	16 MeV 60°C	5100-800 ad / 15 days
□		16 /		15 MeV 60°C	5000-800 ad / 20 d. yrs
□		None		13 MeV 60°C	4400-400 rad / 18 days
○	Notter et coll	None	Two field supraclav. 1 side	60°C	5000 rad / 30-35 days

Fig 4 Time dose relations

did recurrence occur in the ipsilateral supraclavicular or axillary regions. No instance of plexus lesions was recorded in patients who had no or only slight fibrosis in the supraclavicular region. The nerve lesions were therefore probably caused by pressure exerted by fibrous tissue by interference of the blood supply by this pressure or by direct changes in the small vessels of the nerves.

Radiation induced cervical plexus lesions have been previously described. MUMENTHALER (1964) and STOLL & ANDREWS (1966) reported several cases and MARUYAMA et coll (1967) published a further case. It is also probable that some of the sensory symptoms observed by EDWARDS & WALSTAM (1963) were radiation induced. The present report was communicated to the Swedish Radiotherapy Club in May 1966 and to the Scandinavian Society of Radiology in 1967. NOTTER et coll (1970) published their experiences in a large series of

cases STOLL & ANDREWS described different incidences of plexus lesions with various dose time combinations.

The  $^{60}\text{Co}$  method described was replaced by electron therapy to the supraclavicular and parasternal region in March 1965, the axilla, however, was treated by  $^{60}\text{Co}$  as before. Different time dosage schedules have been employed with this combined electron  $^{60}\text{Co}$  therapy. The data of STOLL & ANDREWS and our own are plotted on a double logarithmic scale in Fig. 4, which also includes the data of NOTTFER *et al.* STOLL & ANDREWS reported a high incidence of plexus lesions (73 per cent), sensory in nature with a minimum plexus dose of 5500 rad + MeV roentgen radiation over 25 to 26 days (11 or 12 sessions). The field was about 5 cm  $\times$  15 cm, much less wide than in the present material, it included the scalene supraclavicular and axillary node areas. With a somewhat lower dose of 5100 rad over 25 to 28 days the incidence of lesions was reduced to 15 per cent. The wide supraclavicular field (maximum 13 cm  $\times$  22 cm) in another group of patients produced an incidence of 16 per cent with a dose of 4100 rad over 18 days. Orthovoltage therapy was given to their fourth group by small fields to the apex of the axilla, the minimum dose associated with neuropathy was 4350 rad over 25 days.

The  $^{60}\text{Co}$  technique described produced a calculated average plexus dose of 5400 rad over 23 days. This dose may have varied by  $\pm 1000$  rad, depending on variations of the addition—by radiation from the axillary beam—to the plexus dose from the supraclavicular field. This calculation was founded on dose measurements and dose plans in the last two to three years in over 100 patients. The motor lesion incidence was high (Fig. 4). The supraclavicular field size with the combined electron  $^{60}\text{Co}$  method (axilla) was greatly reduced, and extended only about 3 to 4 cm above the clavicle. The combined electron (16 MeV)  $^{60}\text{Co}$  dose to the plexus region averaged 5100 rad over 15 days in a first group of patients 28 of whom have been controlled for three years or more. Only 4 patients had relatively mild lesions in spite of the short time factor. In a second group the treatment was somewhat more protracted, the average dose being about 5200 rad over 20 days. 3 of 18 patients observed for three years or more had mild lesions. Finally, the dose was further lowered to 4400 rad over 18 days.

Electron therapy is now applied at 13 MeV, the daily dose being 300 rad for five days a week, the daily (5 days per week)  $^{60}\text{Co}$  dose to the axilla being of the same size. The radiation dose arising from the axillary irradiation is always measured with small thimble chambers placed at several points on the skin including that of the supraclavicular area. If the dose to the latter be relatively high i.e. more than 5 per cent, the back angle is increased from 30° to 40° or in a few cases to 50° to 60°. This method has now been in use for about 35

years, no symptoms of plexus lesions have been reported in 20 patients controlled for nearly this time. NOTTER et coll. observed plexus lesions in 17 per cent of 237 patients with mammary carcinoma treated by  $^{60}\text{Co}$ . Their original technique placed the maximum dose in the axilla, where accordingly fibrosis occurred. The plexus dose in the cases that developed signs of a lesion varied between 4 500 rad over 27 days and 8 100 rad over 21 days. Modification of the technique produced a homogeneous dose distribution and with the present dose level of 5 000 rad over 30 to 35 days no plexus lesions occur. NOTTER et coll. plotted their doses on a double logarithmic dose-time diagram. With the STRANDQVIST (1944) slope for skin reaction they constructed a line that was considered to represent the lowest dose that might induce a motor nerve lesion of the plexus. Only five of their own cases with symptoms fall below this line; the dose level of 5 100 rad over 25 to 28 days of STOLL & ANDREWS lies on the line. The dose level of NOTTER et coll. as well as that of the present authors is clearly below the line. The dose and time factors used by NOTTER et coll. has been employed for some years in many centres.

The slope of the line may be questioned as emphasized by NOTTER et coll. It should be noted that the number of fractions reported by the various authors referred to in Fig. 4 are different. STOLL & ANDREWS usually gave 3 fractions per week and NOTTER et coll. 3 to 5 fractions per week for some time and later 3 fractions per week. The patients of the present series were regularly treated with 5 fractions per week.

It is not possible to draw any definite conclusions since great variations exist in for instance the size of the irradiated volume and the number of fractions used. It appears however probable that the dose of 5 000 rad over 5 weeks in 3 to 5 fractions per week carries a reasonably low risk of serious plexus lesions provided that the irradiated suprascapular volume be moderate. This dose is also probably cancerocidal for most lymph node metastases from mammary carcinoma (GUTTMAN 1966 and others). If less than five weeks be preferred for the post-operative treatment it would seem wise not to exceed 4 500 rad over 20 days.

### SUMMARY

Lesions of the cervical plexus following post-operative radiation therapy for mammary carcinoma are described. The symptoms and signs of these range from slight sensory and motor disturbances to severe paralysis. The literature on the subject is reviewed and the dose-time effect relations are discussed.

### ZUSAMMENFASSUNG

Schädigungen des Nervenplexus des Halses im Anschluss an die postoperative Bestrahlung des Mammakarzinomes werden beschrieben. Die Symptome und Zeichen dieser Schäd-



gungen reichen über leichte sensorische und motorische Störungen bis zur schweren Lähmung. Es werden die Literatur über diese Frage zusammengefasst und die Dosis-Effektverhältnisse besprochen.

## RÉSUMÉ

Les auteurs décrivent les lésions du plexus cervical après radiothérapie post-opératoire pour cancer du sein. Les signes fonctionnels et les signes physiques vont d'un léger trouble sensitif ou moteur jusqu'à une paralysie sévère. Les auteurs passent en revue la littérature qui concerne ce sujet et étudient les relations entre les effets secondaires et la répartition de la dose dans le temps.

## REFERENCES

- BACHOFER C. B., GAUTREUX M. E. and KACAK S. M.: Relative sensitivity of isolated nerves to  $^{60}\text{Co}$  gamma rays. In: Response of the nervous system to ionizing radiation, p. 221. Edited by Th. J. Haley and R. S. Snyder. Little Brown, Boston, 1964.
- EDSVYR F. and WALSTAM R.: Complications in postoperative irradiation of mammary carcinoma. *Acta radiol. Ther. Phys. Biol.* 1 (1963) 397.
- GUTTMAN R. J.: Role of supervoltage irradiation of regional lymph node bearing areas in breast cancer. *Amer. J. Roentgenol.* 96 (1966) 560.
- JANZEN A. H. and WARREN S.: Effect of roentgen rays on the peripheral nerve of the rat. *Radiology* 38 (1942) 333.
- LEBEDINSKY A. V. and NAKHILNITSKAYA Z. N.: Effects of ionizing radiation on the nervous system. Elsevier Publishing Co., Amsterdam-London-New York, 1963.
- LINDER E.: Über das funktionelle und morphologische Verhalten peripherer Nerven längere Zeit nach Bestrahlung. *Fortschr. Röntgenstr.* 90 (1959) 618.
- MARUYAMA Y., MYLREA M. and LOGOTHETIS J.: Neuropathy following irradiation. *Amer. J. Roentgenol.* 101 (1967) 216.
- MUMENTHALER M.: Armplexusparesen im Anschluss an Röntgenstrahlen. *Schweiz. med. Wschr.* 94 (1964) 1069.
- NISCE L. Z. and CHU F. C. G.: Radiation therapy of brachial plexus syndrome from breast cancer. *Radiology* 91 (1968) 1022.
- NOTTER G., HALLBERG O. and VIKTERLOF K. J.: Strahlenschaden am Plexus brachialis bei Patienten mit Mammakarzinom. *Strahlentherapie* 139 (1970) 538.
- SON Y. H.: Effectiveness of irradiation therapy in peripheral neuropathy caused by malignant disease. *Cancer* 20 (1967) 1447.
- STOLL B. A. and ANDREWS J. T.: Radiation induced peripheral neuropathy. *Brit. med. J.* 1966, 1, p. 834.
- STRANDQVIST M.: Studien über die kumulative Wirkung der Röntgenstrahlen bei Fraktionierung. *Acta radiol.* (1944) Suppl. No. 55.
- WESTLING P. and NORDIN G.: Cervical plexus lesions following postoperative total ablation therapy for carcinoma of the breast. (In Swedish.) 28th Congress of Scandinavian Society of Radiology, 1967.
- — — och HELE P.: Cervikalplexusläsioner efter postoperativ strålbehandling vid cancer mammae. (In Swedish.) *Nord. Med.* 80 (1968) 1636.

## VALUE OF PELVIC PNEUMOGRAPHY IN GYNECOLOGIC BRACHYTHERAPY

by

I J WEIGENBERG

One of the hitherto neglected areas of dosimetric consideration in gynecologic brachytherapy is the cervical surface of the uterus. This forms a natural landmark and barrier whose involvement or lack of it is of considerable significance. For this reason dosage at this surface may well be an important parameter of adequate radiation therapy. Thus far a reliable critical dosimetric point or set of points for such therapy have not as yet been defined and in the absence of such knowledge it behooves us to maintain an open and inquiring attitude toward all such pertinent and relevant locations. Although the classic approach to preoperative radiation therapy in endometrial carcinoma has been to pack the uterine cavity with multiple radioactive sources (HEYMAN & BENNER, HEYMAN et coll.) several reports describe comparable satisfactory results using moderate doses of external beam radiation (LAMPE, SALA & DEL REGATO). Investigation of the site or sites of critical dosage and the magnitude of this dose could be of benefit in the evaluation and optimal utilization of each of these modalities.

Submitted for publication 20 January 1971

Pelvic pneumography provides an excellent means of demonstration of the uterine serosal surface. When utilized together with computer calculation of dosage from these implants it can provide accurate dosage information at this surface.

**Method:** Pneumoperitoneum is induced on the operating table. A needle puncture is made in the anterior abdominal wall to the left of the rectus sheath in either the upper or lower quadrants, and 1 000 to 1 500 ml of air or nitrous oxide are injected into the peritoneal cavity. This can be done either before or after the induction of general anesthesia. The peritoneal cavity can also be entered via cul de sac puncture as suggested by LANG, but the present author has found this route to be less reliable than the anterior abdominal approach because of distortion by tumor myomas, atrophy with age, relaxation of the pelvic floor, etc.

Following introduction of the intraperitoneal air the implant is performed in the usual manner. Radiolucent applicators are utilized to the furthest possible extent so as to facilitate localization of the sources for computer dosimetry (WEIGENBERG et coll.). At the time of the implant a metallic skin clip is affixed to the cervix to serve as a roentgenographic marker. Radiographically visible packing is utilized primarily to demonstrate that no vaginal packing has inadvertently become interposed between the applicator and the cervix. Dosage at various points such as the cervix, bladder and rectum may be measured with a probe detector to serve as interim guidance until the computer data are available. A retention catheter containing 5 ml of diatrizoate iothalamate, or other similar urographic contrast medium in the bulb identifies the bladder neck on subsequent roentgenograms.

The patient is taken to the radiology department from the recovery room. The technique described by STEVENS et coll. for pelvic pneumograms is followed wherein the patient is placed in the prone position and the head of the table tilted down 45 degrees so that the gas may rise to the pelvis. Roentgenograms are ordinarily taken with the beam axis vertical and tilted 10, 20 and 45 degrees toward the feet as well as in cross table lateral. The table is then returned to the horizontal position and the patient is turned supine. Stereoscopic roentgenograms which serve as the basis for localizing the sources for computation of dosage (POWERS et coll.) are obtained. A small amount of barium is then run into the rectum and distal sigmoid to identify the relationships of the uterus and applicators to these structures.

The technique for computer dosimetry has been described previously (POWERS et coll.). The sources are spatially localized on a three dimensional coordinate system by stereoscopic roentgenograms. The contribution from each source to a multitude of points in the irradiated volume is then calculated by estimation of

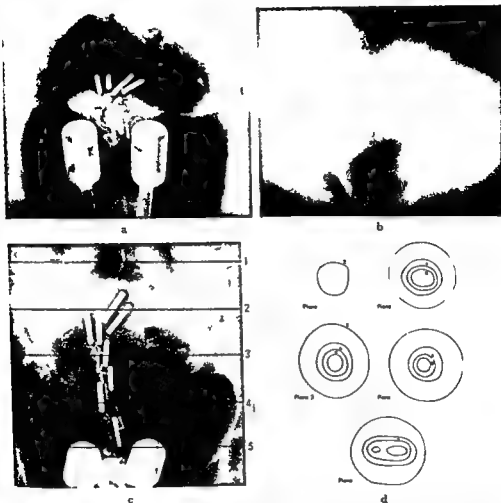


Fig 1 a) b) The uterine fundus is well outlined by the intraperitoneal air. The cervix is marked by two metallic clips and the bladder neck by contrast medium in the bulb of the retention catheter. A small amount of residual barium is still in the rectum. The vaginal packing is indicated by marker c) The planes in which the isodose curves were computed. d) The isodose curves. From the e data it can be seen that with the exposure of 6 200 milligram hours the endometrium received at various points 1 000 to 10 000 rad the serosal surface between 3 000 and 11 000 rad the cervix and vaginal vault 6 000 rad the bladder neck 3 000 rad and the rectum 2 000 rad ● = Point where active portion of the source pierces the plane of computation

the Sievert integral taking into account specific emission of the source the buildup of electron equilibrium absorption within the shield and tissues decay with time and falloff with distance

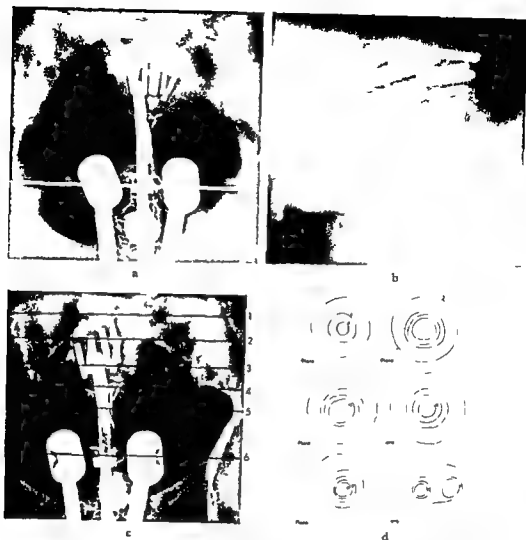


Fig 2 Another similar implant and its associated dose distribution. The various points of interest are indicated as stated in fig 1. The exposure of 6 100 milligram hours in this instance resulted in the endometrial surface receiving between 8 000 and 10 000 rad at various points, the serosa 4 000 to 6 000 rad, the cervix 4 000 to 6 000 rad, and the rectum and bladder neck 3 000 rad each.

### Results

Figs 1 and 2 illustrate representative implants and the attendant dose distributions. The serosal surface of the uterus is well defined by the intraperitoneal air, while the endometrial surface is approximated by the sources. The cervix, bladder neck, rectum, and pelvic wall are demarcated as indicated previously.

ously. The planes of computation are as indicated on the roentgenograms. The five principal planes are perpendicular to the long axis of the implant, with the central plane passing through the computed center of mass of the implant and the others spaced at equal distances as desired. Additional planes of computation may be obtained at will either parallel to these or with the axes rotated. At least one coronal plane, through the long axis is usually obtained. Each of the points of interest demonstrated on the roentgenograms can be localized in relation to the data printout, and dosage at various relevant points determined.

The pneumoperitoneum technique produces minimal discomfort to the patient even when done under local anesthesia, and has been free of morbidity thus far. The only problem encountered has been inadvertent intersutural injection which was subsequently re-ordered without difficulty.

### Discussion

The pneumoperitoneum technique affords a simple, reliable and safe means of determining the dosage at another hitherto neglected and likely important location. In the specific instance of packing the uterine cavity with multiple sources dosimetry has long defied an adequate solution. This has characteristically been estimated by measurement of dosage about phantoms utilizing varying arrangements of sources and multiple small radiation detectors or film (HEYMAN & BENNER, HEYMAN et coll., NOLAN & STEELE). Direct measurements can be made at the time of the implant using a probe detector in the vagina, bladder and rectum, but the use is of limited value (FLETCHER et coll., TRAPPIER).

KARLSTEDT measured at laparotomy and with a probe dosimeter the doses at various points on the uterine surface in 18 patients. With the technique proposed initially by HEYMAN et coll., he found the mean dose at the uterine surface to be 2,200 rad, with large variations between patients and at different points on the surface of the same uterus. Radiation safety considerations as well as the usual clinical practice of allowing an interlude between the implant and hysterectomy would preclude this being accepted as a routine dosimetric procedure. The marked variability furthermore emphasizes the need to determine such doses on an individual basis rather than relying upon standard tables, isodose curves or averages. It is also of interest to note that KARLSTEDT also utilized pelvic pneumography in at least one patient to demonstrate the surprising extent of physiologic variability in the thickness of the uterine wall. With air outlining the serosa and a positive contrast medium in the uterine cavity, the thickness of the uterine wall illustrated was shown to be 17 to 18 mm when the uterus was not distended or subjected to internal pressure and decreased to a thickness varying between 5 and 8 mm when the cavity was packed with Heyman capsules.

- KARLSTEDT K. Carcinoma of the uterine corpus. Factors bearing on the curability. *Acta radiol* (1968) Suppl. No. 282
- LAMPE I. Endometrial carcinoma. *Amer J Roentgenol* 90 (1963) 1011
- LANG E. K. and GREER J. L. The value of pelvic arteriography for the staging of carcinoma of the cervix. *Radiology* 92 (1969) 1027
- LEWIS JR G. C. and RAVENTOS A. Dose distribution during the radium therapy of cervical cancer. *Amer J Obstet Gynec* 82 (1961) 1031
- NOLAN J. F. and STEELE J. P. Carcinoma of endometrium. Measurements of radiation distribution around various multiple capsule applications of radium in irregular uterus. *Radiology* 51 (1948) 166
- POWERS W. E., BOGARDUS JR C. R., WHITE W. and GALLAGHER T. Computer estimation of dosage of interstitial and intracavitary implants. *Radiology* 85 (1965) 135
- SALA J. M. and DEL REGATO J. A. Treatment of carcinoma of the endometrium. *Radiology* 79 (1962) 12
- SCHWARTZ G. An evaluation of the Manchester system of treatment of carcinoma of the cervix. *Amer J Roentgenol* 100 (1969) 579
- SPIRA J. and ARAL I. Radium dosage patterns in the treatment of uterine carcinoma. *Amer J Roentgenol* 105 (1969) 110
- STEVENS M. G. Pelvic pneumography. *Sem Roentgenol* 4 (1969) 252
- , WEIGEN J. F. and LEE R. S. Pelvic pneumography. *Med Radiogr Photogr* 42 (1966) 89
- TESTA E. R. and RUBENFELD S. A critical look at points A and B in the treatment of cancer of the uterine cervix. *Radiology* 94 (1970) 199
- TRAPPIER A. S. Rectum bladder dosimetry in the treatment of 100 cases of cancer of the uterine cervix by intracavitary radium 226 and cobalt 60 teletherapy. *Radiology* 97 (1969) 162
- WEIGENBERG I. J., MARSHALL J. R. and POWERS W. E. Radiolucent intracavitary radiation applicators. Their special usefulness in computer calculated dosimetry. *Amer J Roentgenol* 99 (1967) 881

## HAEMOPOIETIC ASPECTS OF THE CHANGES IN THE NATURAL RADIATION RESISTANCE OF MICE AFTER HYPOXIA

by

M. BERAN and B. TRIBUKAIT

Decreased radiation sensitivity of mice irradiated after hypoxia (TRIBUKAIT & FORSSBERG 1964, TRIBUKAIT 1966, OAKUNEWICK et al. 1968) is connected to the decreased mortality between 8 and 15 days after irradiation with LD<sub>1</sub>—LD<sub>30</sub>/30 exposure range. The favourable effect of hypoxic preconditioning is restricted to a distinct period of 1 to 3 days after hypoxia and the upper limit of the radiation dose in our experimental conditions was 1 000 R <sup>60</sup>Co gamma irradiation.

Irradiation with higher doses resulted in disappearance of the favourable effect of hypoxia preconditioning. Apparently this mechanism is only effective in animals dying from bone marrow depletion and the mortality caused by the intestinal syndrome following higher roentgen doses is not influenced. With doses under 1 000 R the dose profit after hypoxia is about 150 R, this means

Submitted for publication 5 July 1971



that the  $LD_{50}/30$  after hypoxia is about the same as found by SMITH et coll (1969) in investigations on the effect of variations in the size of haemopoietic cell population on the survival of mice. It was postulated (McCULLOCH & TILL 1964) that the survival of animals in the above mentioned dose range is related to the survival of colony forming units (CFU) of the haemopoietic tissue and because of the exponential curve for their killing (McCULLOCH & TILL 1962) in some degree to the size of cell population exposed. However, the evaluation of the size of the CFU pool during the posthypoxic period demonstrated that the survival of animals in our experimental model was not simply related to the size of the CFU pool (BERAN & TRIBUKAIT 1971 b). This may indicate that other factors affecting the radiation sensitivity of CFU, as the proliferative state and environmental conditions, may influence their survival fraction. Furthermore the capacity of CFU for repair of sublethal damage (ELKIND & SUTTON 1960) and rates of proliferation and differentiation of stem cells should be considered if the relationship between radiation effect on the haemopoietic tissue and the response of the whole animal should be established. The aim of this investigation was to evaluate some of these factors in the normal and in the more radiation resistant hypoxia pretreated (HP) mouse.

The experiments presented in this paper were designed to evaluate: (1) the differences in the immediate response of stem cell to irradiation in normal and HP animals; (2) the extent to which the enhanced survival of mice depends on the polycythemic state and (3) kinetic type of repopulation of bone marrow and spleen. The term stem cell is used for a fraction of haematopoietic cells that after transplantation into lethally irradiated recipients is able to form macroscopically visible colonies on the spleen surface. At least a part of these cells usually referred to as colony forming units CFU (TILL & McCULLOCH 1961) possess properties that characterize a multipotent stem cell.

### Materials and Methods

Six week old male albino NMRI mice weighing about 25 g were used in these experiments randomized in control and experimental groups.

*Hypoxic treatment* Hypoxia was obtained in an automatically regulated decompression chamber at a simulated altitude of 6 000 m ( $\approx 354$  mm Hg) as previously described (TRIBUKAIT 1966). The animals were returned to ambient pressure and irradiated at different intervals thereafter.

*Irradiation* The donors of bone marrow in the investigation on the early repair of CFU were irradiated with roentgen rays under the following condi-

tions distance 60 cm, 250 kV 10 mA 2 mm Al, 40 R/min. The other mice were irradiated with the  $^{60}\text{Co}$  unit (distance 90 cm from radiation source, dose rate 80 R/min as measured in air).

*Determination of the radiation sensitivity and early repair of bone marrow CFU* The exocolonizing method of TILL & McCULLOCH (1961) was used. The technique was the same as reported previously (BERAN & TRIBUNAIT 1971 b). The surviving fraction of the CFU was determined after irradiation with doses between 100 and 840 R of  $^{60}\text{Co}$  irradiation. For the determination of the early repair CFU donors were irradiated either with 400 R or with two doses of 200 R separated by different time intervals. Within 30 min after the second dose the donors were killed and pooled bone marrow cell suspension from 4–6 animals was injected intravenously into lethally irradiated (960 R of  $^{60}\text{Co}$ ) recipients. The number of injected bone marrow cells was adjusted to give countable number of colonies in recipient spleens 9 days after transplantation.

*Bleeding procedure* A standard amount of the blood corresponding to 3% of body weight was removed from the infraorbital plexus.

*Transfusion polycythemia* Two intraperitoneal injections of 1 ml of 80% red blood cells suspended in saline were given to each animal on two consecutive days. This procedure resulted in the rise of the haematocrit value to the same extent as produced by hypoxia.

*Measurement of the proliferative state of CFU by suicide technique* The selective elimination of cells in DNA synthesis after in vitro exposure to large doses of tritiated thymidine of high specific activity (BECKER et al. 1965) was used for the determination of the bone marrow CFU fraction in DNA synthesis. At different intervals after hypoxia bone marrow from the femur of at least 4 mice was suspended in Hanks BSS to produce suspensions of approximately  $10^6$  nucleated cells/ml and divided into 2 aliquots. 4  $\mu\text{g}$  of thymidine/ml were added to one and 300–350  $\mu\text{Ci}$  of tritiated thymidine (spec. act. 16–20 Ci/mM) to the other. Both suspensions were incubated for 25 min at 37°C then placed in ice water and diluted to the desired cell concentrations with Hanks BSS containing 4  $\mu\text{g}$  of cold thymidine per ml. Aliquots of both suspensions were injected into the lethally irradiated recipients. After 9 days the recipients were killed, their spleens removed and fixed in Bouin fixative. The number of colonies on the spleen surface was counted. The results were expressed as the percentage of CFU which survived the lethal effect of tritiated thymidine in vitro. The number of CFU in the suspension with cold thymidine was taken to be 100%. The surviving fraction is negatively correlated to the proliferative activity of the cell population investigated.

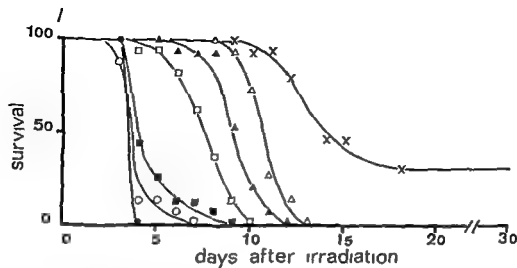


Fig 1 The survival of male NMRI albino mice after irradiation with different doses of  $^{60}\text{Co}$  gamma irradiation. Fifteen mice were irradiated at each dose level ● 1400 ○ 1300 ■ 1200 □ 1100 ▲ 1000 △ 900 × 800 R.

## Results

The survival of normal mice irradiated with different doses of  $^{60}\text{Co}$  gamma irradiation is shown in Fig 1. Doses between 800 and 1000 R, chosen for our survival tests, resulted in the death of mice between 8 and 15 days after irradiation. All mice that died had signs typical for the haemopoietic death. About 10 per cent of the mice survived a dose of 800 R.

*Effect of the physiologic state of the haemopoietic tissue on the 30 day survival.* The posthypoxic period is characterized by a polycythemic state with almost suppressed erythropoiesis. It may be expected that this may result in some diversion of the pluripotent stem cells into the granulocytic pathway with an improvement of survival due to enhanced production of neutrophils. If the radiation resistance after hypoxia is produced by such a mechanism then polycythemia induced by transfusion may produce a comparable effect on the survival. Similar bleeding of posthypoxic mice either before or after irradiation could reverse the resistant state. Bleeding itself may improve survival of some strains of mice if made at a certain time in relation to the irradiation (SUGAHARA et coll 1969, SUGAHARA & TANAKA 1970, MARSH et coll 1968, SMITH & WILLARD 1969) and therefore we tested the effect of bleeding for comparison. The effect of previous treatment of mice by hypoxia, blood transfusion and bleeding on the survival of mice irradiated three days thereafter is presented in Fig 2.

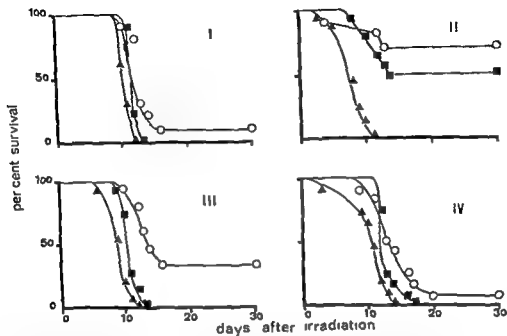


Fig 2 The postirradiation survival of the normal mice (III) and mice irradiated with  $^{60}\text{Co}$  gamma source three days after (I) bleeding (II) ten days of hypoxia and (IV) erythrocyte transfusion. Fifteen mice were used in each group and at each dose level. ○ 800 ■ 900 ▲ 1000 R.

It is clearly evident that neither bleeding nor transfusion induced polycythemia has any effect on the survival. In mice made polycythemic by transfusion the haematocrit values and the suppression of erythropoiesis were approximately the same as in posthypoxic mice. Bleeding reduced the haematocrit values to about 70% of controls one day after the blood was removed. The 30 to 90 days survival of posthypoxic mice irradiated with 900 R was 50 and 42% respectively. 70% of the mice irradiated with 800 R survived both 30 and 90 days.

*Effect of bleeding on the stability of the radiation resistant state of mice irradiated 2 days after hypoxia.* The standard amount of blood was removed from mice irradiated with 900 R either before or after irradiation. The results are presented in Table 1. The bleeding affected to some degree haematocrit and peripheral leucocyte values but did not produce any significant effect on the 30 day survival of posthypoxic animals. No conclusions can be drawn from the slightly decreased survival of mice bled immediately after hypoxia or irradiation as too few animals were used.

Table 1

*The effect of bleeding on the survival, leucocyte counts and haematocrit values of mice irradiated during the period of enhanced radiation resistance two days after hypoxia 900 R  $^{60}\text{Co}$  gamma irradiation*

	No. of animals	30 day survival ( )	Days after irradiation			
			13	27	13	27
			Blood leucocytes*		Haematocrit**	
Normal irradiated mice	12	8/3				
HP mice irradiated 2 days after hypoxia	12	100/0	990 $\pm 203$	5541 $\pm 556$	42.8 $\pm 3.0$	46.1 0.4
HP mice bled immediately after hypoxia and irradiated two days later	12	80/0		7007 $\pm 1317$	35.9 $\pm 2.4$	44.8 0.8
HP mice irradiated two days after hypoxia and bled immediately after irradiation	12	90/0	1685 $\pm 312$	6378 $\pm 649$	34.4 $\pm 3.9$	47.1 0.5
HP mice irradiated two days after hypoxia and bled 5 days later	12	100/0		9404 $\pm 1064$	39.7 $\pm 2.5$	45.9 0.7

\* The number of leucocytes in thousands/ml blood. Mean  $\pm$  SE of at least 8 animals.

\*\* Per cent of whole blood. Mean  $\pm$  SE of at least 8 animals.

*Proliferative state of the CFU in the early posthypoxic period* Proliferative activity of CIU may be of importance for the radiation sensitivity of CFU and consequently for the postirradiation recovery of the haematopoietic systems. The suicide technique permits determination of the number of CFU in the S phase of the cell cycle and from these data the proliferative state of the whole CFU population can be concluded.

Results of two identical experiments are presented in Fig. 3. In the normal bone marrow about 70% of CIU survived the lethal effect of tritiated thymidine *in vitro*. Accordingly 30% of CFU susceptible to  $^3\text{H}$ TdR *in vitro* were in the DNA synthetic phase. This fraction is higher than reported by BECKER *et al.* (1963) and DELAN & FEINENDEGEN (1970). The total number of CIU increased during the early posthypoxic phase (Fig. 3a) which is in

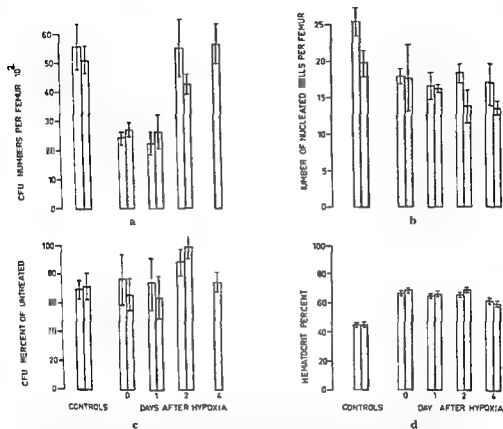


Fig 3 Haemopoietic status of mice at different intervals after hypoxia as compared to control. Open and shaded figures refer to two separate experiments. a) Number of CFU per femur b) Total nucleated cell counts per femur in millions c) Fraction of CFU resistant to  $^3\text{HTdR}$  in vitro d) Haematocrit values indicating the extent of erythropoietic suppression. The values represent mean  $\pm$  SE of 4 to 6 animals.

agreement with our previously published results (BERAN & TRIBUKAIT 1971 b). However the fraction of CFU sensitive to  $^3\text{HTdR}$  in vitro is the same immediately and also one day after hypoxia but lower two days after hypoxia (Fig 3 c).

**Radiation sensitivity of CFU after hypoxia** When looking for the mechanism responsible for the enhanced survival of mice irradiated 2 days after hypoxia we considered the possibility that at this time the surviving fraction of CFU might be higher than CFU in normal mice. Experiments were performed in which the radiation sensitivity of femoral CFU was assessed. The results presented in Table 2 reveal lower surviving fractions at all dose levels in mice

Table 2

*In vivo* radiation sensitivity of CFU in the bone marrow of irradiated normal mice and hypoxia pretreated (HP) mice irradiated 2 days after hypoxia with different doses of  $^{60}\text{Co}$  gamma irradiation. Left part of the table indicates surviving fractions calculated as mean  $\pm$  SE from at least 6 lethally irradiated recipients of bone marrow. Right part of the table presents the computed  $D_{10}$  values

	CFU fraction surviving radiation doses of					D)
	100 R	300 R	410 R	570 R	810 R	
Normal irradiated mice	0.40 $\pm 0.09$	0.30 $\pm 0.04$	0.032 $\pm 0.016$	0.033 $\pm 0.016$	0.0010 $\pm 0.0003$	99 R
HP mice irradiated 2 days after hypoxia	0.41 $\pm 0.07$	0.18 $\pm 0.04$	0.024 $\pm 0.008$	0.008 $\pm 0.002$	0.0007 $\pm 0.0003$	99 R

irradiated 2 days after hypoxia. The computed  $D_{10}$  value was however 99 R for both normal and hypoxia pretreated mice.

*Early repair of the bone marrow CFU.* The sigmoid character of the radiation survival curves for the proliferative capacity of mammalian cells suggested that loss of proliferative capacity involves an accumulation of radiation damage. Using the experimental system in which the radiation dose was given in two fractions, ELKIND & SUTTON (1960) demonstrated that accumulated sublethal damage may be rapidly repaired and that the increased surviving fraction is a function of the time by which the two doses are separated. TEIL & MCCULLOCH (1963) were the first to demonstrate that early repair of radiation damage occurs in colony forming cells irradiated and proliferating *in vivo*. Recently impairment of early repair in CFU of hypoxically irradiated mice has been reported (PHILLIPS & HANNA 1968). The present authors were interested if early repair did not change in hypoxia pretreated animals since this process may contribute to the earlier resumption of the proliferative activity of CFU and influence the speed of repopulation of hematopoietic tissue.

In the control mice and hypoxia pretreated mice used in the experiment the number of CFU per  $10^5$  nucleated marrow cells was  $27.1 \pm 1.9$ . No apparent differences in the characteristics of the early repair of CFU in normal and hypoxia pretreated animals were observed (Fig. 1). The values for posthypoxic animals tended to be slightly lower and the differences were statistically significant at 2 and 11 hours ( $p=0.05$ ) and 18 hours ( $p<0.01$ ) intervals. The maximal repair in both normal and posthypoxic CFU was

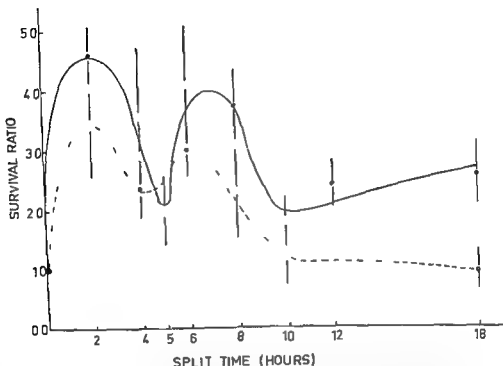


Fig 4 Kinetics of early repair of bone marrow colony forming cells irradiated in vivo with two doses of 200 R of roentgen rays separated by different time intervals. The survival ratio is defined as the ratio of the percentage of surviving CFU after two doses separated by a time interval (abscissa) to the percentage survival for the same total dose given as a single exposure. The mean  $\pm$ SE of the number of CFU counted on spleens of six to eight lethally irradiated syngeneic recipient mice are shown. The dots represent values for control mice and the circles values for mice irradiated two days after hypoxia.

observed at 2 hours split interval minimal repair at 10 and 12 hours dose separation. Then the surviving fraction slowly increased up to 18 hours split interval in the control group but remained the same in hypoxia pretreated mice.

*Postirradiation repopulation of bone marrow and spleen.* Preliminary results have indicated that the decreased radiation sensitivity after hypoxia seems to correlate with the improved repopulation of the bone marrow (BERAN & TRIBUKAIT 1971 b). In this investigation the quantitative evaluation of the repopulation kinetics of the bone marrow and spleen cells of normal irradiated mice and mice irradiated at the time of the maximal radiation resistance was performed.



Fig. 5 The recovery of cell numbers in the spleen of 300 R ( $^{60}\text{Co}$ ) irradiated normal mice ( $\Delta$ — $\Delta$ ) and mice irradiated 2 days after hypoxia ( $\bullet$ — $\bullet$ ). The points represent mean  $\pm$  SE of five to 15 animals.

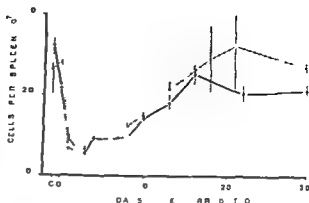
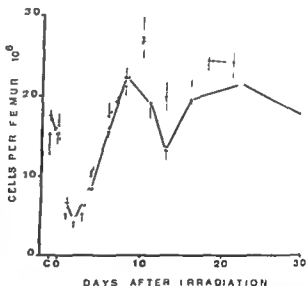


Fig. 6 The recovery of the cell numbers in the femur of 300 R ( $^{60}\text{Co}$ ) irradiated normal mice ( $\Delta$ — $\Delta$ ) and mice irradiated 2 days after hypoxia ( $\bullet$ — $\bullet$ ). The points represent mean  $\pm$  SE of five to six animals.



Two days after hypoxia immediately before irradiation the total number of cells per femur and spleen was slightly lower as compared with the control group. The depletion of cells after 300 R had the same appearance in both groups of animals. The minimal level was reached in both bone marrow and spleen on the second day after irradiation. Onset of repopulation in the spleen (Fig. 5) was first noted on the sixth day after irradiation and no significant differences between the control and posthypoxic mice were observed until 30 days after irradiation. At this time the number of cells was still below the normal level in both groups. The repopulation of the bone marrow (Fig. 6) started on the third day after irradiation and until the eighth day the kinetic

pattern in both normal and posthypoxic mice was identical. Between the sixth and eighth day after irradiation the cell numbers reached the normal level. However, marked differences were noted after the eighth day. While the overall cell proliferation ceased in control mice and the number of cells decreased below the normal level during the next three days, the cell number continued to increase until the tenth day in the posthypoxic mice. After this period the kinetic pattern became the same as in the control mice, however, and for the rest of the observation period the numbers of cells never fell below the normal level and remained significantly higher in posthypoxic than in control mice.

### Discussion

Since there is evidence that CFUs possess different radiation sensitivity depending on their position in the cell cycle (DUPLAN & FEINENDEGEN 1970) and because of the metabolic changes during the posthypoxic period (STREFFER *et coll* 1970) we suggested the possibility that the immediate response of CFU may be different in hypoxia pretreated animals. FRIED *et coll* (1966) reported that immediately after hypoxia the fraction of CFU surviving irradiation decreased and concluded that they are proliferating more rapidly.

Using the *in vitro* suicide technique with tritiated thymidine (BECKER *et coll* 1965) we were unable to detect an increased number of 3HTdR sensitive CFU, immediately nor one day after hypoxia. Two days after hypoxia, when the number of CFU clearly increased in bone marrow, the percentage of CFU in the S phase was lower than in controls. These unexpected results obtained in two separate experiments cannot only be logically explained by the decreased proliferative activity. The well known fact that the CFU does migrate offers an explanation assuming that the increase in CFU numbers is a result of increased migration from the spleen or decreased migration from the bone marrow. This is however only a speculative explanation like others such as a higher susceptibility of CFUs to damage during the preparation of cell suspensions resulting in altered metabolism of cells *in vitro* or shortening of the S phase of the cell cycle.

When the radiation sensitivity of the CFU was measured a somewhat lower surviving fraction of the cells in the more resistant animals was detected at all dose levels but no differences in  $D_{50}$  values could be found. This is in agreement with the results of DUPLAN & FEINENDEGEN (1970) who in spite of the higher radiation sensitivity of CFU in the S phase were not able to detect any difference between the overall sensitivity of CFU in populations with low and high percentages of CFU in the S phase. Similarly investigations on mice recovering from treatment with vinblastine have shown essentially the same

survival fractions of CFU in both treated and untreated mice (SMITH *et coll* 1968)

These results together with those previously reported (BERAN & TRIBLAKIT 1971 b) show no differences between control and HP animals in respect to the size of the CFU compartment and the radiation sensitivity of CFU. This suggests that these factors cannot be responsible for differences in the post-radiation behaviour of the haemopoietic system resulting in survival of animals due to prevention of the bone marrow death. Results of experiments comparing the early repair of CFU pointed in the same direction. In these experiments the capacity of CFU for reparation of the sublethal damage appeared to be rather lower in HP mice. The lower shoulder in the survival experiments of CFU is in conformity with the results.

On the other hand we have previously reported the recovery of higher numbers of nucleated cells from the femurs of mice sublethally irradiated between the first and third day after hypoxia, at the time when the radiation resistance was increased (BERAN & TRIBLAKIT 1971 b) these preliminary results were now confirmed after irradiation with 300 R. Even when the rate of depopulation of nucleated cells after irradiation was the same in controls and in mice irradiated 2 days after hypoxia, the kinetic pattern of repopulation was different. This is in agreement with the view that there is little difference between the early response of strains and species with a low or high LD<sub>50</sub> and that the main difference is found in the rate of restoration of the nucleated cell count (LUDWIG & KORN 1964). In spite of difficulties in the interpretation of the changes in the number of marrow nucleated cells caused by the population heterogeneity and the influence of the posthypoxic polycythemia they indicate some differences in the rate of proliferation of different cell compartments during the recovery process.

The posthypoxic period is characterized by a polycythemic state with almost completely suppressed erythropoiesis. Therefore we tested the possibility that some diversion of the pluripotential stem cell favouring the granulocytopenia may be responsible for the enhanced production of granulocytes, the lack of which is well known to be an important factor in the bone marrow death (BOND *et coll* 1965). Diminished granulocyte response to endotoxin in irradiated bone marrow treated mice in which erythropoiesis has been stimulated before or after irradiation has been interpreted in the sense of a competition on the stem cell level (HELLMAN & GRATE 1967). The experiments with transfusion polycythemia, however, clearly demonstrated that if enhanced survival of the HP mice is related to the haematopoietic system as indicated by the accelerated repopulation of the CFU compartment (BERAN & TRIBLAKIT to be published) and increased granulocytopenia (BERAN & TRIBLAKIT 1972

after irradiation, this in no means a simple function of the polycythemic state

The recovery of the bone marrow of posthypoxic mice is more complete in the postirradiation period during which the survival of mice depends on the function of their haematopoietic system and especially on the neutrophils and platelets balance. This fact may play a significant role for the survival of animals particularly if the difference is due to changes in homeostatic mechanisms resulting in accelerated granulocytic recovery. Indeed the detailed analysis of the whole body granulocytic system has verified that this is the case in HP more radiation resistant animals (BERAN & TRIBUKAIT 1971 a). Since the results presented do not support the idea that this is due to suppressed erythropoiesis possibly on the basis of stem cell competition we suggest that the differences may be due to more complex alterations of haemopoiesis and particularly of the granulocytopoietic system. The explanation of these changes is not possible on the basis of the experiments presented. It is known that in the course of the readaptation of the organism from hypoxia to the ambient pressure, some alterations of the intermediate metabolism which paralleled the survival changes occur (STREFFER et coll 1970) in liver cells. Such types of metabolic changes produced either locally in haemopoietic tissue or outside and mediated by a humoral mechanism may be able to favorably influence the repopulation of haemopoietic tissue without changing the immediate cell response to irradiation. Absence of similar situations in animals made polycythemic by transfusion must explain the inability of the transfusion polycythemia to influence the postirradiation survival of animals.

### Acknowledgements

This investigation was supported by the Swedish Atomic Energy Committee and the Swedish Medical Research Council (Project No. 69-40\ 631 05).

### SUMMARY

The contribution of the haemopoietic tissue to the increased radiation resistance of the mouse after hypoxia preconditioning has been further analysed. Neither the radiation sensitivity nor the early intracellular repair of the stem cells were improved. The significance of the posthypoxic polycythemia for the survival of irradiated mice was tested using animal made polycythemic by transfusion. The erythropoietic suppression per se did not influence the survival. Removal of blood from hypoxia preconditioned mice either immediately after hypoxia or after irradiation did not change the radiation resistance. It is suggested that metabolic changes resulting from hypoxia and subsequent readaptation to the ambient pressure affects the processes of proliferation and differentiation of the haemopoietic tissue.

### ZUSAMMENFASSUNG

Die Bedeutung des haematopoietischen Gewebes für die erhöhte Strahlenresistenz der Maus nach Vorbehandlung durch Hypoxie ist weiter analysiert worden. Weder die Strahlen-

empfindlichkeit der Stammzellen noch deren frühe interzelluläre Erholung sind untersucht. Die Bedeutung der posthypoxischen Polyzythämie für das Überleben der bestrahlten Maus wurde an Tieren geprüft, die durch Transfusion polyzythämisch gemacht worden waren. Die Unterdrückung der Erythropoiese *per se* beeinflusst nicht die Überlebensrate. Auch Blutentnahme von Hypoxievorbehandelten Tieren entweder unmittelbar nach Hypoxie oder nach Bestrahlung verändert nicht die gesteigerte Strahlenresistenz. Es wird vermutet, dass durch Hypoxie hervorgerufene metabolische Veränderungen und die nachfolgende Readaptation an normalen Druck die Prozesse der Proliferation und Differenzierung des hämatopoetischen Gewebes beeinflussen.

## RÉSUMÉ

La contribution du tissu hémo-poïétique à l'augmentation de la radio-résistance de la souris après preconditionnement par hypoxie a été l'objet de nouvelles recherches. Ce preconditionnement n'améliore ni la radiosensibilité ni la réparation intra-cellulaire précoce des cellules souches. L'influence de la polycythémie posthypoxique sur la survie des souris irradiées a été étudiée sur des animaux rendus polycythémiques par transfusion. La suppression de l'érythropoïèse en soi n'a pas d'influence sur la survie. La soustraction de sang sur des souris preconditionnées par hypoxie soit immédiatement après l'hypoxie soit après l'irradiation ne change pas la radio-résistance. L'auteur pense que les modifications métaboliques résultant de l'hypoxie et de la readaptation ultérieure à la pression ambiante modifient les processus de prolifération et de différenciation du tissu hémo-poïétique.

## REFERENCES

- BECKER A. J., McCULLOCH E. A., SIMONOVITSCH L. and TILL J. E. The effect of differing demands for blood cell production on DNA synthesis by haemopoietic colony forming cells of mice. *Blood* 26 (1965) 296.
- BERAN M. and TRIBUKAIT B. (a) The posthypoxic bone marrow and spleen composition. *Scand. J. Haemat.* 11 (1971) 5.
- (b) Changes in the natural radioresistance of the mouse after hypoxia of several days duration: the posthypoxic behaviour of stem cells. *Int. J. radiat. Biol.* 19 (1971) 27.
- Quantitative aspects of postirradiation granulocytic recovery. The influence of erythropoietic suppression due to hypoxia and to hypertransfusion. To be published in *Int. J. radiat. Biol.* 1972.
- BOND V. P., FLIEDNER T. M. and ARCHAMBEAU J. O. Mammalian radiation lethality: a disturbance in cellular kinetics. p. 159. Academic Press, London, New York, 1965.
- DUPLAN J. F. and FFINENDEGEN L. E. Radiosensitivity of the colony-forming cells of the mouse bone marrow. *Proc. Soc. exp. Biol. Med.* 134 (1970) 319.
- ELKIND M. M. and SUTTON H. Radiation response of mammalian cells grown in culture. I. Repair of X-ray damage in surviving chinese hamster cells. *Radiat. Res.* 13 (1960) 303.
- FRIED W., MARTINSON D., WEISMAN M. and GURNEY C. A. Effect of hypoxia on colony-forming units. *Exp. Haemat.* 10 (1966) 22.
- HILLMAN S. and GRATE H. F. Haematopoietic stem cells: Evidence for competing proliferative demands. *Nature* 216 (1967) 63.
- LUDWIG F. C. and KOHN H. I. Quantitative studies on the radiation pathology of the bone marrow of small laboratory animals. II. Marrow response to whole body X-irradiation in rodents of different LD 50. *Radiat. Res.* 31 (1964) 233.

- MARSH I C, BOGGS D R, CHERVENICK P A et coll Factors influencing haematopoietic spleen colony formation in irradiated mice IV The effect of erythropoietic stimuli J Cell Physiol 71 (1968) 63
- McCULLOCH E A and TILL J E The sensitivity of cells from normal mouse bone marrow to gamma irradiation in vitro and in vivo Radiat Res 16 (1962) 822
- Proliferation of haemopoietic colony forming cells transplanted into irradiated mice Radiat Res 22 (1964) 383
- OKUNIEWICZ J P, HARTLEY K M and DARDEN J Comparison of radiation sensitivity, endogenous colony formation and erythropoietic response following prolonged hypoxia exposure Radiat Res 38 (1969) 530
- PHILLIPS T L and HANKS G E Apparent absence of recovery of endogenous colony forming cells after irradiation under hypoxic conditions Radiat Res 33 (1968) 517
- SMITH L H and WILLARD H G Alteration of haemopoietic tissue as a factor influencing radiosensitivity of the mouse Amer J Physiol 216 (1969) 493
- SMITH W W, WILSON S M and FRED S S Kinetics of stem cell depletion and proliferation effect of vinblastine and vincristine in normal and irradiated mice J nat Cancer Inst 40 (1968) 847
- STREFFER CH, TRIBUKAIT B und SCHLAFFERUS S Über die Änderungen der natürlichen Strahlenresistenz der Maus nach mehrtägigem Aufenthalt in Hypoxie Enzymaktivitäten des Tryptophan und Cysteinstoffwechsels Strahlentherapie 139 (1970) 626
- SUGIYAMA T and TANAKA T Effect of bleeding after irradiation on survival of three strains of lethally irradiated mice with different radiosensitivity Int J radiat Biol 18 (1970) 395
- NAGATA H et coll Variation in radiosensitivity of mice in relation to their physiological conditions In Comparative cellular and species radiosensitivity p 30 Edited by V P Bond and T Sugahara Igaku Shoin Ltd Tokyo 1969
- TILL J E and McCULLOCH E A A direct measurement of the radiation sensitivity of normal mouse bone marrow cells Radiat Res 14 (1961) 213
- Early repair processes in marrow cells irradiated and proliferating in vivo Radiat Res 18 (1963) 96
- TRIBUKAIT B Über die Änderungen der natürlichen Strahlenresistenz der Maus nach mehrtägigem Aufenthalt in Hypoxie Überleben und Körpergewicht Strahlentherapie 131 (1966) 371
- und FORSBERG A Änderungen der Strahlenempfindlichkeit der Maus nach vorübergehendem Aufenthalt in Hypoxie Naturwissenschaften 51 (1964) 12

## PREPARATION METHODS OF LIVER AND LUNG RADIOPHARMACEUTICALS WITH $^{86}\text{Sr}^m$ , $^{99}\text{Tc}^m$ AND $^{113}\text{In}^m$

by

P. E. ASARD and INGEBORG BOIS-SVENSSON

Earlier investigations of methods of liver and lung scintigraphy have made use of  $^{197}\text{Au}$  and  $^{125}\text{I}$ . The development of generators during the last few years for short lived isotopes has introduced a need for the development of simple preparation techniques. The use of such isotopes means short measuring time and better information. This depends on the fact that millicurie quantities may be administered, the dose per millicurie being much lower compared to that of conventional isotopes, such as  $^{198}\text{Au}$  and  $^{131}\text{I}$ .

*Liver agents* HARPER (1964) HARPER et coll (1964-1966) were the first to develop a  $^{99}\text{Tc}^m$  compound for liver, spleen and bone marrow gamma imaging. They first used a fat emulsion (HARPER 1964) and later on developed a sulphur colloid (HARPER et coll 1964-1966). The latter was prepared by passing  $\text{H}_2\text{S}$  through acidified pertechnetate solution containing gelatin as stabilizing agent. However the yield from converting  $\text{TcO}_4^-$  to the colloidal form was low and it was necessary to remove the free pertechnetate by passing the solution through an anion exchange resin. A further drawback was the use of the toxic gas  $\text{H}_2\text{S}$ . A modified method for this preparation was published by BLUM (1967).

Another approach to the problem of preparing a technetium colloid was to

---

Submitted for publication 15 June 1971

make a gelatin stabilized colloid by means of antimony sulfide and then label the colloid with technetium (DEGROSSI et coll 1965 GARZON et coll 1965, AKHTAR 1969) The advantage of this method is that the colloid itself may be preformed and stored for a long time before labelling the drawback is the toxicity of antimony compounds

A simplified method of preparing technetium sulphur colloids by forming the colloid of the sulphur liberated from sodium thiosulphate in the presence of hydrogen ions was introduced by STERN et coll (1966) The main disadvantage of the method is that the pH must be carefully adjusted with sodium hydroxide with risks of overshoot errors The same technique was developed by PATTON et coll (1966) who used as carrier perrhenate ( $\text{ReO}_4^-$ ) a homologue to technetium They simplified the preparation technique in that they employed a phosphate buffer instead of sodium hydroxide to adjust the pH This preparation was further modified and tested by LARSON & NELP (1966) and FRENCH (1969) WEBBER et coll (1969) reported that the use of rhenium was not necessary for obtaining a high yield of colloid

GOODWIN et coll (1966) used stable indium as a carrier but also suggested iron in the first attempt to investigate the possibilities of  $^{113}\text{In}^m$  in colloidal form A modified technique and standardization of the indium colloid resulted in a more simplified and reproducible preparation (ADATEPE et coll 1968 POTCHEN et coll 1968) with iron as carrier These authors used a phosphate buffer instead of titrating the pH with NaOH A similar method (BRUNO et coll 1968) involving titration with  $\text{NH}_4\text{OH}$  and with phenol red as the pH indicator have also been investigated The effect of adding iron as carrier raised the uptake in the spleen by increasing the size of particles although the preparation without iron gave as good scintigrams of the liver as with it (COLOMBETTI et coll 1969)

The main use of  $^{87}\text{Sr}^m$  is for bone scintigraphy  $^{87}\text{Sr}^m$  colloids may easily be made (MILERS & HUNTER 1969)

*Lung agents* The preparation techniques for making macroaggregated albumin particles labelled with  $^{99}\text{Tc}^m$  have been based on the tagged albumin then aggregated by heating (GWYTHIER & FIELD 1966 PETERSON & BONTE 1967 SUPREYANT et coll 1969) The main drawback with this preparation technique is that the labelling of albumin is rather complicated A simpler method which gives a high labelling efficiency is first to make a technetium labelled colloid and to this add a certain amount of albumin and aggregate albumin together with the colloidal particles (CRAGEN et coll 1969) The use of preformed albumin microspheres labelled with  $^{99}\text{Tc}^m$  has also been suggested (RHODES et coll. 1969 WAGNER et coll 1969 a b BURDENF et coll 1970 ZOLLE et coll 1970)

A preparation technique for  $^{113}\text{In}^m$  labelled albumin aggregates was published by CISCATO et coll (1969) This is however rather complicated and time con



suming despite the fact it is based on preformed macroaggregates of albumin. The preparation must, for instance, be centrifugalized twice during the labelling procedure. A simpler labelling technique is based on preformed albumin microspheres (ZOLLE et coll 1968, 1970; BLCHMAN et coll 1969; RHODES et coll 1969).

Carbonate particles labelled with  $^{14}\text{C}$  or  $^{86}\text{Sr}^m$  have been described (MYERS & HUNTER 1969) although no details of the labelling procedure were reported.

The trend in published preparation techniques appears to be in the direction of more simplified methods. This must be the tendency so that the risk of making a mistake in the preparation must decrease as the methods become more simplified. It was therefore considered that it might be useful to lay down the criteria from the bacteriologic and radiation protection points of view regarding the procedures: (1) The whole preparation procedure must be performed in one and the same sterile pyrogen free and capped phial. (2) The solutions, sterile and pyrogen free, needed for the preparations must be dispensed in once for all capped phials (which means in kit forms). (3) When adding solutions to the phials, disposable plastic syringes must be used and the number of injections into the phial be kept to a minimum. (4) No pH measurements and titrations must be used. (5) No centrifugation or use of ion exchanged resins must be necessary. (6) It is favourable if the final preparation is capable of being autoclaved.

In addition, the procedure should be uncomplicated and reproducible so that in a busy isotope laboratory it may be performed by a skilled technician or nurse trained in working with radioactive isotopes. It is also of practical value if the preparations are stable at least during one half life of the isotope. Point 6 is further commented on in the discussion regarding the autoclaving of MAA particles.

Simple and reproducible methods of preparing liver and lung scanning agents will be described. Attempts have been made to fulfil the six points mentioned; there was a failure only in preparing a lung agent with  $^{86}\text{Sr}^m$  which cannot be autoclaved. The amount of sulphur in the  $^{99}\text{Tc}^m$  colloid and  $^{99}\text{Tc}^m$  MAA has been reduced and no stabilizers or carriers are included. A new simple method for making macroaggregated albumin particles labelled with  $^{113}\text{In}^m$  and details of  $^{86}\text{Sr}^m$ -compounds are also presented. All compounds have been tested in mice and their stability investigated.

### Preparation techniques

All compounds are made up in 10 ml capped sterile and pyrogen free phials. Disposable plastic syringes are used to add solutions to the phials, all solutions are also sterile and pyrogen free.

**A  $^{99}\text{Tc}^m$  sulphur colloid** (1) Eluate 4 ml  $^{99}\text{Tc}^m$  pertechnetate with saline, inroduce into 10 ml capped phial containing 0.5 ml 0.3 M HCl and shake the bottle (2) Add 0.4 ml Na<sub>2</sub>S<sub>2</sub>O<sub>3</sub> solution (4 mg Na<sub>2</sub>S<sub>2</sub>O<sub>3</sub> per ml) (3) Incubate in a boiling waterbath for 5 min with agitation (4) Add immediately 2.5 ml of a phosphate buffer (Sorensen buffer pH 6.8 containing 9.35 g NaH<sub>2</sub>PO<sub>4</sub> and 9.2 g KH<sub>2</sub>PO<sub>4</sub> per litre) and cool to room temperature (5) Autoclave for 25 min at 1 atm Total volume 7.4 ml Final pH 5.8

**B  $^{99}\text{Tc}^m$  MAd** (1—4) See points A 1—A 4 (5) Add 0.4 ml albumin solution (albumin 2% in sterile water prepared daily) (6) Incubate in a boiling waterbath for 2 min with agitation of the bottle The particles are formed after about one minute (7) Autoclave for 25 min at 1 atm Final volume 7.8 ml Final pH 5.8

(Some particles have the appearances of snow flakes and are rather large they are however easily fragmented by shaking the bottle and by drawing up into the syringe a few times)

**C  $^{113}\text{In}^m$  hydroxide colloid** (1) Eluate the generator with 1 ml 0.04 M HCl (pH = 1.4) into a 10 ml capped phial containing 1 ml phosphate buffer (pH 6.7 53.15 g NaH<sub>2</sub>PO<sub>4</sub> · 2H<sub>2</sub>O and 64.87 g Na<sub>2</sub>HPO<sub>4</sub> per litre) (2) Autoclave for 25 min at 1 atm Total volume 5 ml Final pH 6.4

**D  $^{113}\text{In}^m$  MAA** (1) See point C 1 (2) Autoclave for 10 min at 1 atm (3) Cool the solution and add 0.35 ml albumin solution (albumin 2% in sterile water prepared daily) (4) Autoclave for 25 min at 1 atm Total volume 5.35 ml Final pH 6.4

(Step D 2 may be excluded because the colloid is formed even without heating the solution This form of preparation has been used by the authors for about six months Further experiments have revealed that it is possible to lower the albumin content to 0.5 mg per ml final solution at a pH of 5.6 to 6.0)

**E  $^{86}\text{Sr}$  carbonate colloid** (1) Eluate the generator with 3 ml citric acid 0.005% (adjusted to pH 5 with ammonia) into a 10 ml capped phial containing 1 ml phosphate buffer pH 6.7 (same buffer as for the  $^{113}\text{In}^m$  hydroxide colloid) and 0.2 ml Na<sub>2</sub>CO<sub>3</sub> solution (20%) Shake the bottle (2) Autoclave for 25 min at 1 atm Final volume 4.2 ml Final pH 9.4

**F  $^{86}\text{Sr}^m$  carbonate particles** (1) Eluate the generator with 3 ml citric acid 0.005% (adjusted to pH 5 with ammonia) into a 10 ml capped phial containing 0.2 ml Na<sub>2</sub>CO<sub>3</sub> solution (20%) Shake the bottle (2) Heat the solution to about 40°C in a waterbath and add 0.5 ml SrCl<sub>2</sub> (7 mg/ml) with agitation of the bottle Final volume 3.7 ml Final pH 11.5

Table 1

*Layer scanning agents. The errors indicated are the standard error of the mean*

Colloid	Hours after prep	No of prep	No of mice	Percentage uptake				
				Lung	Liver	Spleen	Kidneys	Heart
Au	—	1	6	0.11 ± 0.03	99.7 ± 0.03	0.57 ± 0.06	0.13 ± 0.04	0.04 ± 0.02
Tc <sup>99m</sup>	0	3	23	1.6 ± 0.2	91.7 ± 0.3	2.4 ± 0.2	1.0 ± 0.1	0.29 ± 0.04
sulfid	6	3	6	1.2 ± 0.2	93.8 ± 0.7	1.8 ± 0.4	1.1 ± 0.2	0.16 ± 0.03
Ir <sup>192m</sup>	0	3	24	0.63 ± 0.08	97.1 ± 0.2	2.4 ± 0.2	0.16 ± 0.02	0.019 ± 0.004
hydroxid	4	3	6	0.48 ± 0.04	97.3 ± 0.3	2.2 ± 0.3	0.09 ± 0.03	0.016 ± 0.004
Sr <sup>90m</sup>	0	3	23	3.1 ± 0.2	30.8 ± 0.6	7.7 ± 0.1	3.4 ± 0.3	0.55 ± 0.07
carbonat	4	2	4	7.4 ± 1.8	83.3 ± 3.3	2.6 ± 0.2	3.8 ± 0.5	1.2 ± 0.3

The main techniques for testing the different preparations have been *in vivo* tests in white mice 0.1 to 0.3 ml being injected intravenously into a tail vein. The mice were killed by either 10 min after injection of the colloids and 2 min after injection of the lung particles. Lungs, liver, spleen, kidneys and heart were dissected out and the total activity in each organ was measured in a well-counter. The total count rate from each organ was summed and from this the percentage uptake in each organ was calculated. (See discussion.)

For the technetium-sulphur colloid the amount of free pertechnetate was estimated with thin layer chromatography in methanol 85% and with an  $R_F$  value of 0.39. The chromatographic plates used (cellulose acetate on an aluminium base) were placed on roentgen films and after identification of the radioactive spots significant parts of the chromatographic plates were cut out and the activity was measured in a well-counter.

The numbers of particles were measured in a Bürker chamber with a projection microscope, after the albumin aggregates had been coloured with Rose Bengal. The sizes of the particles, about 100 each time, were measured with the same microscope; only one dimension was measured so that the largest diameter was obtained. The particle size of the colloids was not measured.

The preparations were stored in a refrigerator at about 4°C in tests of stability.

The isotope generators used in this investigation were delivered from the Radiochemical Centre, Amsterdam, England. All were eluted through 0.22 µm millipore filters mainly to increase the leakage of particles, the mother isotope and other contaminations. It has been disclosed (FRENCH *et coll.* 1969) that a

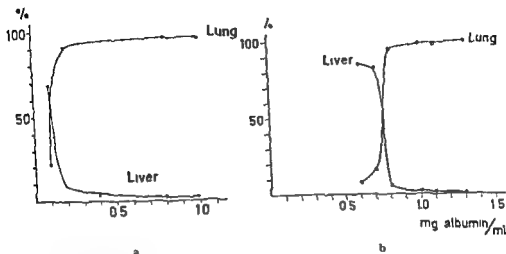


FIG. 1 Percentage uptake in lung and liver for  $^{99}\text{Tc}^{\text{m}}$  MAA (a) and  $^{113}\text{In}^{\text{m}}$  MAA (b) as a function of the quantity of albumin

0.22  $\mu\text{m}$  millipore filter considerably reduces the  $^{113}\text{Sn}$  contamination.  $^{113}\text{Sb}$  could be detected by gamma spectrometry either with a solid state detector or a NaI crystal. The amount of  $^{113}\text{Sn}$  was estimated to be of the order of 10 compared to  $^{113}\text{In}^{\text{m}}$ . No tests on the leakage of  $^{99}\text{Mo}$  and  $^8\text{Y}$  were made.

## Results

**Liver scanning agents.** The results of the tests in mice appear in Table 1. The  $^{198}\text{Au}$  colloid delivered from Amersham has the highest liver uptake and the lowest lung uptake. The spleen and lung uptakes were considerably lower than those of the other colloids investigated. All the colloids made by  $^{99}\text{Tc}^{\text{m}}$ ,  $^{113}\text{In}^{\text{m}}$  and  $^{87}\text{Sr}^{\text{m}}$  have a considerable spleen uptake and the lung uptake is also higher than that of the gold colloid. The kidney and heart activities which mainly reflect the labelling efficiency of the agents are much lower for the gold and indium colloids. The  $^{87}\text{Sr}^{\text{m}}$  colloid gives the highest lung uptake. These experiments establish that the indium colloid has nearly the same properties regarding liver uptake as the gold colloid, the discrepancies lying mainly in the higher lung and spleen uptakes.

The results of the stability tests of the different preparations are presented in Table 1. The  $^{87}\text{Sr}^{\text{m}}$ -colloid seems to be unstable as after four hours the liver uptake is diminished and the lung uptake increases. However the  $^{99}\text{Tc}^{\text{m}}$  and  $^{113}\text{In}^{\text{m}}$  colloids appear to be stable in spite of the absence of stabilizers. No precipitation of these three different preparations occurred during the observed storage time.

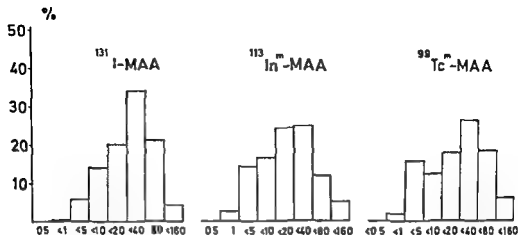


Fig. 2. Particle size distribution for  $^{131}\text{I}$ -MAA,  $^{113}\text{In}$ -MAA and  $^{99}\text{Tc}$ -MAA. Particle size denoted for instance  $<20\ \mu\text{m}$  means particle sizes from 10 to 19  $\mu\text{m}$ .

The amount of free pertechnetate estimated by thin layer chromatography was  $5.2 \pm 0.7$  per cent where the error indicated was the standard error for twelve agents. After 3 hours of storage the mean value for four preparations was  $5.8 \pm 1.6$  per cent. These values are slightly higher than those earlier published (LOPEZ & FRENCH 1969). The results obtained in the experiments in mice also indicated that no increase in free pertechnetate of any significance was obtained as was evident from the values of activity in the kidneys and heart (Table 1).

**Lung scanning agents.** The amount of albumin needed to give a satisfactory lung uptake is evident from Fig. 1 for  $^{99}\text{Tc}$  and  $^{113}\text{In}$ . This indicates that 0.3 mg albumin per ml of the final solution or more is needed for the  $^{99}\text{Tc}$  preparation to give a high lung uptake and low liver uptake. One mg albumin per ml final solution was employed in these experiments. The amount of albumin was higher for the  $^{113}\text{In}$  preparation, more than 0.8 mg albumin per ml final solution being needed (Fig. 1b). 1.3 mg albumin per ml was used in these experiments.

The particle size distribution for the  $^{131}\text{I}$  (Amersham),  $^{99}\text{Tc}$  and  $^{113}\text{In}$  microaggregated albumin appear in Fig. 2. The size distribution (mean value of five preparations) for  $^{113}\text{In}$  is about the same as for  $^{131}\text{I}$ , the difference being that  $^{131}\text{I}$  aggregates have a slightly narrower size distribution. The number of particles per ml and the mean sizes appear in Table 2. The size distribution for  $^{87}\text{Sr}$  carbonate particles is better as the distribution is narrower (Fig. 3).

The results of testing the particles in mice are presented in Table 2. The most suitable agent for the uptake in lung and liver was  $^{113}\text{In}$ -MAA, the particles labelled with  $^{131}\text{I}$ ,  $^{99}\text{Tc}$  and  $^{87}\text{Sr}$  having about the same quality. The stability

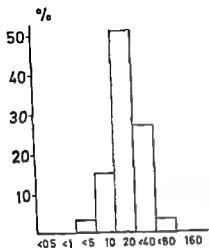


Fig 3 Particle size distribution for  $^{87}\text{Sr}$ -carbonate particles. Particle size denoted for instance < 20  $\mu\text{m}$  means particle sizes from 10 to 19  $\mu\text{m}$ .

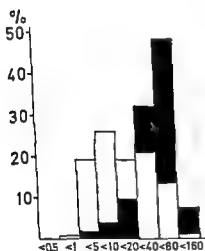


Fig 4 The effect of autoclaving on particle size distribution for  $^{99}\text{Tc}$ -MAA. Particle size denoted for instance < 20  $\mu\text{m}$ , means particle sizes from 10 to 19  $\mu\text{m}$ .  $\square$  before  $\blacksquare$  after autoclaving.

of these compounds was tested in mice and the results are presented in Table 2. These results indicate that a storage time of 6 and 4 hours for  $^{99}\text{Tc}$ -MAA and  $^{113}\text{In}$ -MAA respectively did not affect the quality of the compounds. A decrease in the lung uptake and an increase in the liver uptake after 2 and 4 hours of storage for the  $^{87}\text{Sr}$  carbonate particles indicate however that the compound is not stable.

The  $^{113}\text{In}$ -MAA is prepared by autoclaving the solution after adding the albumin so that the particles form during 20 min at 1 atm. The  $^{99}\text{Tc}$ -MAA particles on the other hand are formed after the albumin has been added by in

Table 2

*Laen<sub>3</sub> scanning agents. The errors indicated are the standard error of the mean*

MAA agent	Hours after prep	Particles ml 10	Mean size $\mu\text{m}$	No of prep	No of mice
I MAA	—	$9.5 \pm 0.4$	$28.7 \pm 3.3$	1	5
$\text{Tc}^m$ MAA	0	$0.3 \pm 0.1$	$52.6 \pm 1.9$	5	24
	8			4	8
$\text{In}^m$ MAA	0	$3.5 \pm 1.0$	$37.0 \pm 1.3$	5	25
	4			3	6
$\text{Sr}^m$ carbonate	0	$2.8 \pm 0.1$	$21.0 \pm 1.3$	5	25
	4			3	6

cubating the solution in a bottle agitated in boiling water for two min. The effect on the particle distribution of autoclaving the  $^{99}\text{Tc}^m$  MAA particles after incubation appears in Fig. 4. This presents the results of five different preparations. The size distribution as expected is changed to larger particle diameters after autoclaving. The mean size before autoclaving is  $19.4 \mu\text{m}$  and after autoclaving becomes  $54.4 \mu\text{m}$ , the number of particles per ml being reduced from 4.8 to 0.7 millions per ml. The effect of autoclaving the solution on the uptake in different organs appears in Table 3: a slight increase in the pulmonary uptake is obtained.

### Discussion

A simplified description of the preparation techniques appears in Fig. 5. This is intended to depict the number of steps with  $^{99}\text{Tc}^m$  and  $^{113}\text{In}^m$  excluding heating and cooling procedures. The methods with  $^{89}\text{Sr}^m$  have the same number of steps as for  $^{113}\text{In}^m$ . The  $^{113}\text{In}^m$ -colloid is the simpler one and in principle merely consists of an elution procedure.

Papers on  $^{99}\text{Tc}^m$  sulphur colloids have mentioned different types of stabilizers being used as gelatin (HARPER et coll. 1966; PATTON et coll. 1966; PERSSON & NAVERSTEN 1970), dextran (LARSON & NELP 1966; DWORIN 1967), carboxymethyl cellulose (CMC) (STERN et coll. 1966), polyvinyl pyrrolidone (GARZON et coll. 1965; SZYMDERA et coll. 1968; EGE & RICHARDS 1969), mannitol (HUNTER 1969) and albumin (WEBBER et coll. 1969). Patient reactions following the technetium sulphur colloid have been observed and the stabilizers included have been blamed for these reactions (SMITH et coll. 1967; BAILEY et coll. 1967).

Table 2 (cont.)

Percentage uptake				
Lung	Liver	Spleen	Kidneys	Heart
95.9 ± 0.4	3.7 ± 0.4	0.09 ± 0.01	0.17 ± 0.02	0.12 ± 0.04
95.7 ± 0.3	3.6 ± 0.3	0.09 ± 0.02	0.43 ± 0.04	0.16 ± 0.03
94.5 ± 0.3	3.9 ± 0.3	0.08 ± 0.02	0.45 ± 0.04	0.11 ± 0.01
98.5 ± 0.2	1.3 ± 0.2	0.04 ± 0.01	0.16 ± 0.02	0.06 ± 0.01
93.3 ± 0.5	1.6 ± 0.3	0.07 ± 0.02	0.22 ± 0.08	0.15 ± 0.04
96.1 ± 0.7	3.3 ± 0.6	0.11 ± 0.02	0.27 ± 0.03	0.24 ± 0.04
91.3 ± 1.7	7.6 ± 1.6	0.28 ± 0.11	0.40 ± 0.06	0.45 ± 0.09

WEBBER *et coll* (1969) stated that if no stabilizer were present in the colloid suspension the amount of free pertechnetate ions increased considerably with time. However LOPEZ & FRENCH (1969) excluded gelatin in making the  $^{99}\text{Tc}^m$  sulphur colloid and at the same time reduced the amount of sodium thiosulfate so as to prevent the precipitation that occurred if the original quantity of sodium thiosulfate were used. The result was less than 2 per cent increase in the free pertechnetate five hours after preparation.

Methods published of preparing  $^{113}\text{In}^m$  hydroxide colloids (GOODWIN *et coll* 1966, ADATEPE *et coll* 1968, BRUNO *et coll* 1968, POTCHEN *et coll* 1968, BURDINE 1969, COLOMBETTI *et coll* 1969, FILBER *et coll* 1969, WAGNER *et coll* 1969, SEWATKAR *et coll* 1970) disclose that gelatin has been used as stabilizer. A trial to exclude stabilizer (gelatin or mannitol) failed (SEWATKAR *et coll* 1970) owing to the lung uptake increasing considerably without them. The present results however indicate that no stabilizer is necessary for the  $^{99}\text{Tc}^m$  sulphur colloid at least if the amount of  $\text{Na}_2\text{S}_2\text{O}_3$  be diminished as suggested by LOPEZ & FRENCH (1969). No stabilizer is needed for the  $^{113}\text{In}^m(\text{OH})_3$  colloid contrary to the opinion of SEWATKAR *et coll* (1970) this holds at least for the storage time investigated.

The quality of radiocolloids used for liver gamma imaging may be mainly expressed as the uptake in the lung as a percentage of the uptake in the liver; a low lung uptake is of course desirable. A comparison with other published tests on lung and liver uptake is presented in Table 4. The conclusion is that the modified substances described in this paper have about the same quality regarding lung and spleen uptake as others that have been published.



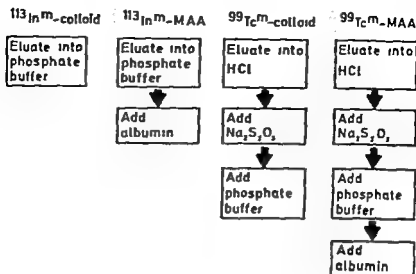


Fig. 5 The number of steps in making liver and lung agents labelled with  $^{113}\text{In}^m$  and  $^{99}\text{Tc}^m$

Table 3

The effect of autoclaving  $\text{Tc}^m$  MAA. The errors indicated are the standard error of the mean for five different preparations with each tested in 120 mice

	Particles ml $\times 10$	Mean size $\mu\text{m}$	Percentage uptake				
			Lung	Liver	Spleen	Kidneys	Heart
Before autoclaving	$4.8 \pm 0.9$	$19.4 \pm 4.9$	$96.3 \pm 0.5$	$2.9 \pm 0.5$	$0.21 \pm 0.07$	$0.47 \pm 0.09$	$0.12 \pm 0.04$
After autoclaving	$0.6 \pm 0.07$	$54.4 \pm 4.4$	$97.2 \pm 0.6$	$2.2 \pm 0.3$	$0.13 \pm 0.06$	$0.37 \pm 0.09$	$0.10 \pm 0.03$

The preparation techniques for  $^{99}\text{Tc}^m$  MAA and  $^{113}\text{In}^m$  MAA are simple and possess the advantage that the same chemicals are used both for the colloids and the corresponding aggregates. The stability of the MAA aggregates are quite satisfactory over at least one half life time of the isotopes. The  $^{87}\text{Sr}^m$  particles seem to be unstable a condition perhaps improved by a stabilizer being added this also perhaps holding for the corresponding  $^{87}\text{Tc}^m$ -colloid. The pH of the  $^{87}\text{Sr}^m$  particle solution was too high and pain reactions occurred in the mice when the lung particles were injected they are thus unsuitable for human use.

Table 4

*Uptake in lung and spleen as percentage of liver uptake for liver scanning agents*

Reference	Type of colloid	Animal	Per cent uptake in lung	Per cent uptake in spleen
LARSON & WELP (1966)	<sup>99</sup> Tc <sup>m</sup> sulfide	Rabbit	3.9	2.6
STERN et coll (1966)	<sup>99</sup> Tc <sup>m</sup> sulfide	Mice	1.4	1.3
COLOMBETTI et coll (1969)	<sup>99</sup> Tc <sup>m</sup> sulfide	Mice	0.6	1.8
FRENCH (1969)	<sup>99</sup> Tc <sup>m</sup> sulfide	Rat	1.5	—
Present authors	Tc <sup>m</sup> sulfide	Mice	1.6	2.5
ADATEPE et coll (1968)	<sup>113</sup> In <sup>m</sup> Fe (OH)	Rat	1.8	1.7
COLOMBETTI et coll (1969)	In <sup>m</sup> (OH)	Mice	0.1	1.5
Present authors	In <sup>m</sup> (OH)	Mice	0.6	2.5
COLOMBETTI et coll (1969)	Au	Mice	0.1	1.1
Present authors	Au	Mice	0.1	0.6

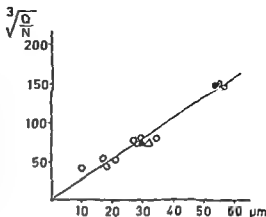
Table 5

*Uptake in liver and spleen as percentage of lung uptake for lung scanning agents (MAA)*

Reference	Type of MAA	Animal	Per cent uptake in liver	Per cent uptake in spleen
BOYD et coll (1969)	<sup>99</sup> Tc <sup>m</sup> Fe(OH)	Rat	1.2	0.1
CRAGIN et coll (1969)	Tc <sup>m</sup> MAA	Mice	1.3*	—
YANO et coll (1969)	Tc <sup>m</sup> Fe(OH)	Rat	8—9.5	—
RHODES et coll (1969)	Tc <sup>m</sup> HSA			
	microspheres	Mice	0.4—2.3	—
Present authors	<sup>99</sup> Tc <sup>m</sup> MAA	Mice	3.8	0.1
			0.5	
ADATEPE et coll (1968)	In <sup>m</sup> (OH)	Rat	10.5	1.0
COLOMBETTI et coll (1969)	In <sup>m</sup> Fe(OH)	Rabbit	2.2	0.18
BUCHANAN et coll (1969)	In <sup>m</sup> HSA			
	microspheres	Mice	0.5	—
RHODES et coll (1969)	In <sup>m</sup> HSA			
	microspheres	Mice	1.4	—
Present authors	In <sup>m</sup> MAA	Mice	1.3	0.04
Present authors	I MAA	Mice	3.9	0.1
			0.5*	
CRAGIN et coll (1969)	I MAA	Mice	0.5	—

\* Denotes calculations based on the specific activity in the organ

Fig. 5 The mean maximum diameter of MAA particles as a function of the square root of  $Q/N$  where  $Q$  (mg ml<sup>-1</sup>) is the quantity of albumin per ml and  $N$  (ml<sup>-1</sup>) the number of particles times 10<sup>3</sup>.  $\Delta$  denotes the mean value of five different batches of <sup>131</sup>I MAA,  $\bullet$ ,  $\circ$  and  $\ominus$  denote the mean value of five different preparations of <sup>99</sup>Tc MAA stored 0, 2 and 4 hours respectively.  $\triangle$  denotes the mean value of five different <sup>113</sup>In MAA agents and  $\circ$  denotes these with albumin ranging from 0.1 to 1.4 mg albumin per ml.



A comparison of other published tests regarding liver uptake for different lung scanning agents appears in Table 5. Our <sup>99</sup>Tc MAA has a slightly higher liver uptake compared to <sup>99</sup>Tc HSA microspheres but much lower than the <sup>51</sup>Cr Fe(OH)<sub>3</sub> reported by YANO et al. (1969). The <sup>113</sup>In MAA preparation has the same quality regarding the liver uptake compared to the <sup>113</sup>In HSA microspheres.

The most critical point in preparing macroaggregated albumin particles is the size distribution and the number of particles per mCi obtained. If the volume of the particles be measured for instance with a Coulter counter (TOW et al. 1966; RICHMOND et al. 1970) the relation between the number of particles per ml ( $N$ ), the quantity of albumin in mg/ml ( $Q$ ) and the mean size of the particles

$R$  ( $\mu\text{m}$ ) is  $R = \sqrt[3]{\frac{Q}{N}}$ .  $R$  is here meant to be the diameter of a sphere with

a volume  $V$  measured by the Coulter counter. When the measurements of the mean maximum diameters of the particles and the corresponding number of particles per ml were estimated it appeared that a relatively small variation of the diameters caused a large variation in the numbers of particles per ml. It was therefore considered that even if only the maximum diameter were measured the relationship between  $R$  and  $Q/N$  would be a cubic function. The maximum

mean diameter  $R$  has been plotted as a function of  $\sqrt[3]{\frac{Q}{N}}$  for different preparations in Fig. 6; this indicates that a straight line may be drawn.

The mean maximum diameter of the particles of the <sup>99</sup>Tc MAA preparations is considerably changed by autoclaving. The size distribution before and after

autoclaving reveals that the number of particles with a diameter less than 20  $\mu\text{m}$  aggregates further during the procedure. However this seems not to change the lung and liver uptake so much as was expected. Tow et coll (1966) have demonstrated that it is possible that the larger particles are fragmented during their passage through the heart and lung vessels before lodging in the smaller vessels. This means that the number of particles injected may be estimated but the true number trapped in the capillary bed cannot be known with the same certainty. The use of preformed albumin microspheres is thus favourable as these particles will not be broken up in the circulation and their number is accurately known beforehand. The labelling procedure is however not so simple as that of the agents presented in this paper.

The autoclaving of the albumin particles especially the  $^{99}\text{Tc}^{\text{m}}$  MAA may be questioned as a risk still exists that the particles depending on their rather large mean size, may be trapped at a precapillary level. This means that point 6 in the introduction must probably be neglected for these types of compounds. The colloid may however be autoclaved and as the albumin may be prepared daily in once for all capped phials under well controlled conditions and the fact that not more than 0.4 ml albumin solution is used the risk of bacterial contamination is negligible.

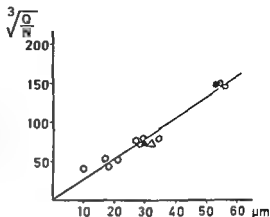
The stability tests of the MAA particles investigated indicate that it is possible to store the particles at least half the time of the short lived isotope. The particles can possibly be stored longer but after a time lapse corresponding to the half decay time the number injected will be double if the same quantity of activity be administered. Taking this into account the specific activity of the final compound limits the storage time.

As was mentioned above the main technique for testing the preparations has been the use of mice. This is a fast and reproducible method and is used as a routine in our laboratory. A test of a substance takes less than half of an hour. The authors have not tried to measure the total activity in the mice and relate the distribution of the activity in different organs to that value. However if this be done the amount of activity in the tail of the mouse must be checked. It has been proved that an imperfect injection may produce activity in the tail vein that cannot be neglected. It means that colloids and particles may be trapped in the vein and may introduce a systematic error in the results.

## SUMMARY

A new and simple method of preparing  $^{113}\text{In}$  MAA is presented together with tests of colloids labelled with  $^{87}\text{Sr}^{\text{m}}$ ,  $^{99}\text{Tc}^{\text{m}}$  and  $^{113}\text{In}^{\text{m}}$  and lung scanning agents labelled with these. No stabilizers are used for the colloids.

Fig. 6 The mean maximum diameter of MAA particles as a function of the square root of  $Q/N$  where  $Q$  (mg ml<sup>-1</sup>) is the quantity of albumin per ml and  $N$  (ml<sup>-1</sup>) the number of particles times 10<sup>3</sup>.  $\Delta$  denotes the mean value of five different batches of <sup>131</sup>I MAA,  $\bullet$ ,  $\circ$  and  $\oplus$  denote the mean value of five different preparations of <sup>99</sup>Tc<sup>m</sup> MAA stored 2 and 4 hours respectively.  $\triangle$  denotes the mean value of five different <sup>113</sup>In<sup>m</sup> MAA agents and  $\circ$  denotes these with albumin ranging from 0.1 to 1.4 mg albumin per ml.



A comparison of other published tests regarding liver uptake for different lung scanning agents appears in Table 5. Our <sup>99</sup>Tc<sup>m</sup> MAA has a slightly higher liver uptake compared to <sup>99</sup>Tc<sup>m</sup> HSA microspheres but much lower than the <sup>99</sup>Tc<sup>m</sup> Fe(OH)<sub>3</sub> reported by YANO et coll (1969). The <sup>111</sup>In MAA preparation has the same quality regarding the liver uptake compared to the <sup>112</sup>In HSA microspheres.

The most critical point in preparing macroaggregated albumin particles is the size distribution and the number of particles per mCi obtained. If the volume of the particles be measured for instance with a Coulter counter (TOW et coll 1966, RICHMOND et coll 1970) the relation between the number of particles per ml ( $N$ ), the quantity of albumin in mg/ml ( $Q$ ) and the mean size of the particles

$R$  ( $\mu$ m) is  $R = \sqrt[3]{\frac{Q}{N}}$ .  $R$  is here meant to be the diameter of a sphere with

a volume  $V$  measured by the Coulter counter. When the measurements of the mean maximum diameters of the particles and the corresponding number of particles per ml were estimated it appeared that a relatively small variation of the diameters caused a large variation in the numbers of particles per ml. It was therefore considered that even if only the maximum diameter were measured the relationship between  $R$  and  $Q/N$  would be a cubic function. The maximum

mean diameter  $R$  has been plotted as a function of  $\sqrt[3]{\frac{Q}{N}}$  for different preparations in Fig. 6. This indicates that a straight line may be drawn.

The mean maximum diameter of the particles of the <sup>99</sup>Tc<sup>m</sup> MAA preparations is considerably changed by autoclaving. The size distribution before and after

- FILBEE J F and MAXWELL I D Technical note Notes on preparation of indium colloids  
Int J appl Radiat 20 (1969) 552
- FRENCH R J The preparation of a technetium colloid and an indium colloid for liver scanning  
Brit J Radiol 42 (1969) 300
- JOHNSON P F and TROTT N G Dosimetry of indium 113m In Medical radioisotope scintigraphy Vol I p 843 IAEA Vienna 1969
- GARZON O L, PALCOS M C and RADICELLA R A technetium 99m labelled colloid Int J appl Radiat 16 (1965) 613
- GOODWIN D A, STERN H S, WAGNER JR H N and KRAVER H H A new radiopharmaceutical for liver scanning Nucleonics 24 (1966) 63
- GWYTHIER M M and FIELD E O Aggregated  $Tc^{99m}$  labelled albumin for lung scintiscanning  
Int J appl Radiat 17 (1966) 485
- HARPER P V Improved liver scanning with 24 hour  $Tc^{99m}$  in fat emulsion J nucl Med 5 (1964) 613
- LATHROP K A and RICHARDS P  $Tc^{99m}$  as a radiocolloid J nucl Med 5 (1964) 382
- — JMIENEX F et coll Technetium 99m sulfur colloid In Radioactive pharmaceuticals p 343 Edited by G A Andrews R M Kinsey and H N Wagner US Atomic Energy Commission CONF 651111 (1966)
- HUNTER JR W W Stabilization of particulate suspension with non antigenic polyhydric alcohols Application to  $Tc^{99m}$  sulfur colloid J nucl Med 10 (1969) 607
- LARSON S M and NELP W B Radiopharmacology of a simplified  $Tc^{99m}$ -colloid preparation for photoscanning J nucl Med 7 (1966) 817
- LOPEZ R B and FRENCH R J Stabilizer free technetium colloid Brit J Radiol 42 (1969) 633
- MYERS W G and HUNTER W W Carbon 11 in bone and lung scanning In Medical radioisotope scintigraphy Vol II p 43 IAEA Vienna 1969
- PATTON D D, GARCIA E N and WEBBER M M Simplified preparation of technetium 99m sulfide colloid for liver scanning Amer J Roentgenol 97 (1966) 880
- PERRON R B and NAVERSTEY Y Technetium 99m sulfide colloid preparation for scintigraphy of the reticuloendothelial system Acta radiol Ther Phys Biol 9 (1970) 567
- PETERSON C C and BONTE F J Technetium 99m macroaggregated albumin A new lung scanning agent Int J appl Radiat 18 (1967) 201
- POTCHEN E J, ADATEPE M, WILCH M et coll Indium 113m for visualizing body organs J Amer med Ass 205 (1968) 208
- RICHMOND D R, TAUBE W N and BASSINGTHWAIGHTE J B Albumin macroaggregates and measurements of regional blood flow Validity and application of particle sizing by Coulter counter J Lab clin Med 75 (1970) 336
- RHODES B A, ZOLLE I, BUCHANAN J W and WAGNER JR H N Radioactive albumin microspheres for studies of the pulmonary circulation Radiology 92 (1969) 1453
- SEWATKAR A B, PATEL M C, SHARMA S M et coll A simple and safer  $In^{113m}$  colloid preparation for scanning the liver Int J appl Radiat 21 (1970) 36
- SMITH E M, SNOOK W M and GILSON A J Letter to the Editor J nucl Med 8 (1967) 896
- STERN H S, McAFEE J G and SUBRAMANIAN G Preparation, distribution and utilization of technetium 99m sulfur colloid J nucl Med 7 (1966) 663
- SUPRENTY E L, WEBBER M M and BENNETT L R Technetium lung scanning Int J appl Radiat 20 (1969) 77

- SZYMEK J, MALINOWSKI A Z, CHEGUILLAUME J et coll. Experience with the preparation and use of  $Tc^{99m}$  sulfide colloid. *Nucl Med* 7 (1968) 388.
- TOW D E, WAGNER JR H N, LOPEZ MAJANO V et coll. Validity of measuring regional pulmonary arterial blood flow with macroaggregates of human serum albumin. *Int J appl Radiat* 96 (1966) 664.
- WAGNER JR H N, STERN H S, RHODES B A et coll. (a) Design and development of new radiopharmaceuticals. *In: Medical radioisotope scintigraphy*. Vol II, p. 3. IAEA, Vienna, 1969.
- , HOSAIN F and RHODES B A. (b) Recently developed radiopharmaceuticals. Ytterbium-169 DTPA and technetium-99m microspheres. *Radiol Clin N Amer* 7 (1969) 233.
- WEBBER M M, VICTORY W and CRAGIN M D. Stabilizer reaction free  $Tc^{99m}$  sulfur suspension for liver, spleen and bone marrow scanning. Technical notes. *Radiology* 92 (1969) 170.
- YANO Y, McRAE J, HONBO D S and ANGER H O.  $Tc^{99m}$  ferric hydroxide macroaggregates for pulmonary scintiphotography. *J nucl Med* 10 (1969) 683.
- ZOLLE J, RHODES B A, BUCHANAN J W and WAGNER JR H N. Properties and uses of radioactive albumin microspheres. *J nucl Med* 9 (1968) 363.
- and WAGNER JR H N. Preparation of metabolizable radioactive human serum albumin microspheres for studies of the circulation. *Int J appl Radiat* 21 (1970) 155.

## EFFECT OF IRRADIATION ON THE RELEASE OF LYMPHOCYTES FROM THE THYMUS

by

ULF ERNSTROM

The involution and regeneration of the lymphoid organs after irradiation have been extensively investigated (MURRAY 1948 SMITH & KIEFFER 1957 HARRIS 1958). Within hours after whole body irradiation the thymus contains pyknotic nuclei and cell debris. Thymic macrophages are activated and during the following days an increasing cellular depletion of the thymic cortex occurs. Regeneration starts after a few more days with an increasing frequency of large lymphocytes and an increased mitotic activity in the thymic cortex. The first recovery of the thymus is incomplete and a second phase of cortical atrophy takes place (KAPLAN & BROWN 1957 HARRIS 1958 CROSS et coll 1964 HARAN GHERA 1965 OSMOND et coll 1966 TARADA et coll 1969). No such cyclic regeneration is reported in other lymphoid organs.

The regeneration of the thymus is accelerated by thigh shielding during the irradiation (KAPLAN & BROWN 1952 OSMOND et coll 1966 BLOMGREN & REVESZ 1968) or by the intravenous injection of bone marrow cells after irradiation (BROWN et coll 1953 BLOMGREN 1969). The second phase of

---

Submitted for publication 21 May 1971



thymic atrophy is also prevented. The transfused bone marrow cells have been traced to the thymus where they proliferate (FORD et coll 1956 GENGOZIAN et coll 1957 FORD & MICKLEM 1963, MICKLEM et coll 1966). Such cells, repopulating the thymus have been proved to be immunologically competent to cause graft versus host reaction (TYAN & COLE 1965 Popp 1961).

The thymus even when irradiated, is important for normal regeneration of the spleen and lymph node tissue and for immunologic restoration (GLOBERSON et coll 1962 MILLER et coll 1963, GLOBERSON & FELDMAN 1964). Whether this influence is hormonal or due to a release of lymphocytes repopulating the spleen and lymph nodes has been much debated.

The aim of the present investigation was to correlate the export of lymphocytes from the thymus during different phases after whole body irradiation with the regeneration of the lymphoid organs. Furthermore the effect of whole body irradiation on the release of thymic lymphocytes was compared with the effect of local irradiation of the thymus. Such a comparison may help to distinguish between a direct effect of radiation on the thymus and an indirect effect.

The present paper demonstrates that gamma radiation causes an early inhibition of the export of lymphocytes from the thymus followed by a successively increasing release of lymphocytes. The results suggest that the second phase of thymic atrophy is due to the increasing thymic export of lymphocytes at a time when the thymic equilibrium between the proliferation and release of cells is disturbed. The existence of a regulatory mechanism in the thymus for the maturation and release of thymic lymphocytes is considered probable.

### Material and Methods

**Animals.** A total of 543 male guinea pigs each with an initial weight of about 250 g was used. The animals were fed on cabbage turnips, carrots and vitamin pellets. They were used in four main experimental groups: (1) investigation of the thymic veno-arterial difference after whole body irradiation (104 animals), (2) investigation of the thymic veno-arterial difference after local irradiation of the thymus (145 animals), (3) investigation of the blood flow through the thymus after whole body irradiation (109 animals) and (4) investigation of the blood flow through the thymus after local irradiation of the thymus (143 animals).

The rest of the animals were non irradiated controls for investigation of the thymic veno-arterial difference (19 animals) and the thymic blood flow (23 animals).

Table 1

*Number of animals used in the quantitative investigations of different lymphatic organs and of the blood*

	Days after irradiation									
	1	2	3	6	9	12	15	18	21	24
Whole body irradiation	10	10	10	10	10	10	11	11	11	11
Local thymus irradiation	15	15	14	14	15	15	15	14	14	14

**Irradiation** This consisted of gamma radiation from a  $^{60}\text{Co}$  therapy unit at a distance of 90 cm. The doses of 150 rad at a dose rate of 75 rad per min given are less than the LD<sub>50</sub> for guinea pigs which for 400 to 500 g animals has been determined to be 250 rad (ELLINGER 1945).

The whole body irradiations were performed on groups of five guinea pigs in well ventilated plastic cages. The local irradiations of the thymus were administered to one animal at a time. Each was placed on its back with the feet immobilized and controlled through a television screen during the irradiation which was restricted to an area of 2 cm<sup>2</sup> of the thymic region.

**Investigation procedure** The day for irradiation is day 0. Different groups of animals were investigated 1, 2, 3, 6, 9, 12, 15, 18, 21 and 24 days after irradiation. The number of animals appears in Tables 1, 4 and 5.

The following investigation procedure was used for the determination of the thymic veno-arterial difference in the number of lymphocytes. The animals were anaesthetized with Nembutal sodium 2.5% (25 to 50 mg/kg body weight intraperitoneally). The thymus was exposed by an incision and the largest of the thymic veins severed; the blood was collected in heparinized pipettes for the counting of the white cells in a Burker chamber and for classification of the lymphocytes by their mitochondrial content in supravital preparations. Slides were prepared with a mixture of Janus green B and neutral red in alcohol for the latter purpose (CULLING 1957). Janus green II is a specific mitochondrial stain (SHOWACRE & DU BUY 1955; COOPERSTEIN et al. 1953). A small drop of blood was applied to the dry slide and a cover glass put on and sealed with wax. The preparations were immediately examined.

The right carotid artery was cut near the origin of the thymic arteries and blood samples were obtained for the same examination as mentioned, which was performed within a minute of the incision of the vein. The artery was then ligated.

*Organ samples* Thymus, spleen, cervical and mesenteric lymph nodes and adrenals were dissected out quantitatively and weighed. The dissections of the lymph nodes were performed by the method of GYLLENSTEN (1953). Samples of the thymus were prepared for histologic examination by fixation in formalin 10 % embedded in paraffin, cut in 5  $\mu$  sections and stained with hematoxylin and eosin.

*Cell counts* For the white cell count in the Burkner chamber 25  $\mu$ l of blood were diluted with 475  $\mu$ l Toisson's solution containing methyl violet for staining of the white cells. Differentiation was made between mononuclear and polynuclear cells.

The supravital preparations of the blood samples were examined in a light microscope at 1 000  $\times$  magnification. The lymphocytes (100 cells per sample) were registered in three classes: cells with 0 to 10, 11 to 20 and over 20 mitochondria. A mitochondrial content (MC) of 0 to 10, 11 to 20 and above 20 mitochondria per lymphocyte was denoted as low, medium and high MC, respectively. The mitochondrial content is correlated to the size of the lymphocytes, a low MC corresponds to small lymphocytes and a high MC to large lymphocytes (WISEMAN 1931, FICHTELIUS & LARSSON 1961, ERNSTROM & LARSSON 1963). The number of lymphocytes in each class was obtained by combination with the white cell count. The number of lymphocytes per  $\mu$ l of blood from the thymic vein and the carotid artery was compared in each animal and the veno-arterial difference registered.

The results were analyzed statistically by Student's *t* test. The comparison between the number of lymphocytes of different categories per  $\mu$ l of blood from the thymic vein and the carotid artery was performed by statistical analysis of all the differences in the individual animals. The *p* values  $< 0.05$ ,  $< 0.01$  and  $< 0.001$  are denoted as almost significant, significant and highly significant respectively.

*Histology* The thymus specimens were investigated in a light microscope. The thickness of the thymic cortex was measured in each specimen by means of an ocular scale. The mean of ten determinations was noted. The density of cells in the thymic cortex was obtained by counting all nuclei within a given area defined by an ocular circle. The thickness of the specimens was 5  $\mu$  and an estimation of the number of cells per unit volume was calculated. No corrections were made for nuclei lying only partly within the specimen. The figures for cell density are thus not exact values but are used for comparisons allowing an estimation of radiation induced changes.

The density of macrophages in the thymus cortex and of the Hassall's corpuscles in the thymus medulla was similarly obtained.

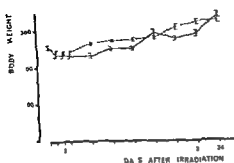


Fig 1

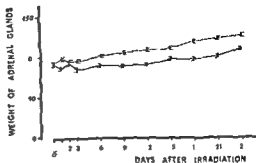


Fig 2

Fig 1 Body weight (g) of guinea pigs at different intervals after 150 rad whole body (—) or local thymus (---) irradiation. Mean  $\pm$  SE.

Fig 2 Weight (mg) of adrenal glands of guinea pigs at different intervals after 150 rad whole body (—) or local thymus (---) irradiation. Mean  $\pm$  SE.

**Thymic blood flow.** The thymic blood flow was determined in a separate experiment by the method of LARSSON (1966). The guinea pigs were anaesthetized with Nembutal and a femoral vein was exposed for the intravenous administration of Heparin (1500 IU per 100 g body weight). The right or left jugular vein was exposed by a 5 cm cervical incision. All small veins emptying into the jugular vein were ligated proximally and distally to the entry of the thymic veins. A heparinized polythene catheter with an outer diameter of 1 mm could easily be introduced through a minor incision in the wall of the jugular vein. The blood from the thymus flowed through the catheter into a small container placed on a Mettler precision balance on which direct continuous readings were made. The distal end of the catheter was sited below the proximal end so that the capillary resistance of the catheter and the siphon effect equalized each other. Vaporization of the blood was prevented by covering the container during the registration. For the experiment to be accepted, a continuous and constant flow was required for at least 20 min, the mean blood flow per min was calculated.

The operations were performed on a heating unit at 35°C. During the registration of the blood flow from the thymus the cervical wound was covered with liquid paraffin at 35°C; this was changed repeatedly for without this procedure, the thymus was chilled and the flow decreased.

**Thymic release of lymphocytes per min.** The export of lymphocytes per min from each thymus was calculated from the blood flow per min and the thymic veno-arterial difference in number of lymphocytes. The standard deviation of

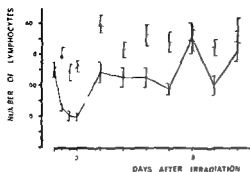


Fig 3

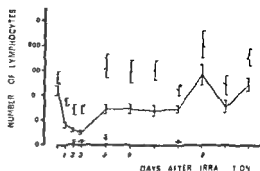


Fig 4

Fig 3 Total number of lymphocytes per  $\mu$ l of blood from the carotid artery of guinea pigs at different intervals after 150 rad whole body (—) or local thymus (---) irradiation. Mean  $\pm$  SE. Marked depression of the lymphocyte count occurred after the former. A peak at 18 days coincided with the second phase of cellular depletion in the thymus.

Fig 4 Number of lymphocytes per  $\mu$ l of blood from the carotid artery of guinea pigs at different intervals after whole body irradiation. Lymphocytes divided into three subpopulations according to their mitochondrial content. Those with low, medium and high mitochondrial content are called small (—), medium sized (---) and large (····) lymphocytes. Mean  $\pm$  SE. Whole body irradiation caused marked depression in the number of small and medium sized lymphocytes, minimal values at 3 days.

the mean product was obtained from the formula

$$S_{\bar{x}\bar{y}} = \pm \sqrt{\bar{r}^2 S_{\bar{x}}^2 + \bar{j}^2 S_{\bar{y}}^2}$$

where  $\bar{r}$  = mean blood flow,  $S_{\bar{x}}$  = standard deviation of  $\bar{x}$ ,  $\bar{j}$  = veno-arterial difference,  $S_{\bar{y}}$  = standard deviation of  $\bar{y}$ .

## Results

### Whole body irradiation

No mortality occurred after whole body irradiation with 150 rad. The weight of the animals decreased during the first 6 days after irradiation ( $-11\%$ ,  $p < 0.01$ ), from the 6th day the body weight increased normally (Fig 1). The weight of the adrenals was almost constant during the experiment (Fig 2).

**Blood.** The total number of blood lymphocytes was markedly decreased early after irradiation, being only 40% of the normal after 3 days ( $p < 0.001$ ). At 6 days the number had returned to normal (Fig 3).

The division of blood lymphocytes into subpopulations disclosed that all categories of lymphocytes were decreased in number during the first days after irradiation (Fig 4). The deficiency was somewhat more marked and persisted

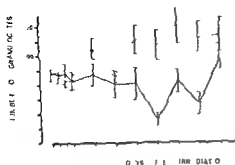


Fig 5

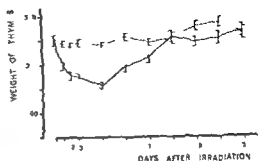


Fig 6

Fig 5 Number of granulocytes per  $\mu$ l of blood from the carotid artery of guinea pigs at different intervals after 150 rad whole body (—) or local thymus (---) irradiation. Mean  $\pm$  SE. Depression of the granulocyte count occurred 12 to 21 days after the former but not after local thymus irradiation.

Fig 6 Weight (mg) of thymus of guinea pigs at different intervals after 150 rad whole body (—) or local thymus (---) irradiation. Mean  $\pm$  SE. A first phase of thymic atrophy occurred at 1 to 12 days and a second phase of atrophy at 18 to 21 days after the former. Little change was evident after local thymus irradiation.

for a longer time among the small lymphocytes of low mitochondrial content.

The granulocytes were essentially unchanged in number until the 15th day after irradiation when they decreased to 31 % of the normal value ( $p < 0.001$ ). The number later increased towards the usual level (Fig 5).

**Thymus weight.** The weight of the thymus was markedly decreased after irradiation ( $p < 0.001$ ) being only 53 % of the normal value after 6 days (Fig 6).

**Thymus histology.** The histology of the thymus cortex was changed by irradiation. An increased number of macrophages thus appeared. They were evident as early as the first day and contained nuclear debris apparently from lymphocytes damaged by the irradiation. Almost normal histology was restored by the third day.

Quantitative morphology with coded slides confirmed the observations described in the thymus cortex and also demonstrated a more prolonged effect of irradiation on thymus morphology. The thickness of the thymus cortex decreased after irradiation being 52 to 60 % of the normal value at 1 to 6 days and 83 to 85 % at 12 to 15 days. At 18 to 24 days the cortex was again thinner 60 to 73 % of the normal value (Table 2). The density of cells per unit volume of thymus cortex was only slightly and statistically not significantly decreased after irradiation (Table 3). The density of macrophages was markedly

Table 2

Thickness of thymic cortex ( $\mu$ ) in non irradiated controls and after whole body and local irradiation of the thymus. Greater cortical atrophy occurred after whole body than after local irradiation. The former caused a second phase of cortical atrophy at 18 to 24 days. Mean  $\pm$  SE.

	Days after irradiation									
	1	2	3	6	9	12	15	18	21	24
Control	263 $\pm$ 11									
Whole body irradiation	136 $\pm$ 5	159 $\pm$ 4	152 $\pm$ 7	132 $\pm$ 4	184 $\pm$ 18	224 $\pm$ 15	216 $\pm$ 14	191 $\pm$ 90	175 $\pm$ 14	157 $\pm$ 14
Local thymus irradiation	207 $\pm$ 11	225 $\pm$ 21	207 $\pm$ 12	218 $\pm$ 16	227 $\pm$ 13	175 $\pm$ 16	211 $\pm$ 17	225 $\pm$ 10	243 $\pm$ 16	229 $\pm$ 22

Table 3

Nucleated cells per unit volume of thymic cortex in non irradiated controls after whole body and local irradiation of the thymus. Only a slight decrease in number of cells occurred after irradiation (cell  $\times 10^4$  per mm<sup>3</sup>). Mean  $\pm$  SE.

	Days after irradiation									
	1	2	3	6	9	12	15	18	21	24
Control	136 $\pm$ 5									
Whole body irradiation	135 $\pm$ 6	129 $\pm$ 5	129 $\pm$ 5	123 $\pm$ 7	122 $\pm$ 5	126 $\pm$ 6	115 $\pm$ 5	140 $\pm$ 4	138 $\pm$ 4	138 $\pm$ 4
Local thymus irradiation	124 $\pm$ 3	127 $\pm$ 5	116 $\pm$ 6	124 $\pm$ 5	116 $\pm$ 4	118 $\pm$ 4	130 $\pm$ 5	115 $\pm$ 6	118 $\pm$ 4	134 $\pm$ 5

increased, the increase being 140 % at 1 day, 110 % at 2 days, 100 % at 3 days and 50 % at 6 days.

The density of Hassall's corpuscles in the thymus medulla was unchanged.

**Thymus blood flow.** The blood flow decreased to a minimal value after 9 days ( $p < 0.001$ ) and then returned to normal (Table 4). When the thymic flow was calculated per mg thymic weight, the changes were less obvious and the only significant change appeared at 9 days (Table 4).

**Thymic veno-arterial difference in number of leucocytes.** The export of cells from the thymus was measured by the thymic veno-arterial difference in the number of cells. The difference in the number of small lymphocytes with low mitochondrial content (MC) decreased after irradiation (Fig. 7). No significant

Table 4

*Decreased thymic blood flow (one lobe) after whole body irradiation with minimal value at 9 days Mean  $\pm$  SE*

	Control Days after irradiation									
	1	2	3	6	9	12	15	18	21	24
Thymic blood flow (ml/min)	49.9	33.6	48.4	39.1	31.9	21.7	32.3	48.8	55.1	53.9
	$\pm 4.3$	$\pm 3.6$	$\pm 6.7$	$\pm 5.8$	$\pm 5.4$	$\pm 4.1$	$\pm 5.1$	$\pm 9.2$	$\pm 8.9$	$\pm 9.4$
Thymic blood flow per mg thymic tissue ( $\mu$ l/min mg)	0.25	0.26	0.37	0.30	0.27	0.14	0.23	0.29	0.31	0.33
	$\pm 0.03$	$\pm 0.02$	$\pm 0.06$	$\pm 0.03$	$\pm 0.04$	$\pm 0.03$	$\pm 0.03$	$\pm 0.04$	$\pm 0.03$	$\pm 0.06$
Number of animals	23	12	12	12	12	8	10	11	11	10

export was demonstrated at 3 days and the decrease from the control value was highly significant. The decreased output persisted for 15 days when the output slowly increased to about the normal value at 24 days.

No significant thymic output of medium sized lymphocytes (with medium MC) is indicated by the thymic veno-arterial difference in normal guinea pigs. However, at 2, 3 and 6 days after irradiation a significant output of such lymphocytes was observed ( $p < 0.01$ ,  $p < 0.01$  and  $p < 0.05$  after 2, 3 and 6 days respectively). Later at 15 and 21 days a similar output of medium sized lymphocytes was registered (Fig. 8).

After the irradiation higher amount of granulocytes occurred in the arterial blood than in the thymic venous blood, indicating an influx of granulocytes into the radiation damaged thymus. This influx was statistically significant 2 days after irradiation ( $p < 0.05$ ).

**Spleen.** The splenic weight markedly decreased ( $p < 0.001$ ) during the first 12 days after irradiation (Fig. 9), the initial weight being regained at 15 days. No second phase of atrophy occurred.

**Lymph nodes.** The weight of the cervical and mesenteric lymph nodes decreased early after irradiation (Figs. 10, 11). The decrease was highly significant and the initial weight was not regained until 15 days after irradiation.



Table 2

Thickness of thymic cortex ( $\mu$ ) in non irradiated controls and after whole body and local irradiation of the thymus. Greater cortical atrophy occurred after whole body than after local irradiation. The former caused a second phase of cortical atrophy at 18 to 24 days. Mean  $\pm$  SE

	Days after irradiation									
	1	2	3	6	9	12	15	18	21	24
Control	263 $\pm$ 11									
Whole body irradiation	136 $\pm$ 5	159 $\pm$ 4	152 $\pm$ 7	137 $\pm$ 4	184 $\pm$ 18	224 $\pm$ 15	216 $\pm$ 14	191 $\pm$ 20	175 $\pm$ 14	157 $\pm$ 14
Local thymus irradiation	207 $\pm$ 11	225 $\pm$ 21	207 $\pm$ 12	218 $\pm$ 16	227 $\pm$ 13	175 $\pm$ 16	211 $\pm$ 17	225 $\pm$ 16	243 $\pm$ 16	279 $\pm$ 27

Table 3

Nucleated cells per unit volume of thymic cortex in non irradiated controls after whole body and local irradiation of the thymus. Only a slight decrease in number of cells occurred after irradiation. Cells  $\times 10^6$  per mm<sup>3</sup>. Mean  $\pm$  SE

	Days after irradiation									
	1	2	3	6	9	12	15	18	21	24
Control	136 $\pm$ 5									
Whole body irradiation	135 $\pm$ 6	129 $\pm$ 5	129 $\pm$ 5	123 $\pm$ 7	127 $\pm$ 5	126 $\pm$ 6	115 $\pm$ 5	140 $\pm$ 6	138 $\pm$ 4	138 $\pm$ 4
Local thymus irradiation	124 $\pm$ 3	127 $\pm$ 5	116 $\pm$ 6	124 $\pm$ 5	116 $\pm$ 4	118 $\pm$ 4	130 $\pm$ 5	115 $\pm$ 6	118 $\pm$ 4	134 $\pm$ 5

increased the increase being 140 % at 1 day, 110 % at 2 days 100 % at 3 days and 50 % at 6 days

The density of Hassall's corpuscles in the thymus medulla was unchanged

**Thymus blood flow.** The blood flow decreased to a minimal value after 2 days ( $p < 0.001$ ) and then returned to normal (Table 4). When the thymic flow was calculated per mg thymic weight, the changes were less obvious and the only significant change appeared at 9 days (Table 4).

**Thymic veno-arterial difference in number of leucocytes.** The export of cell from the thymus was measured by the thymic veno-arterial difference in the number of cells. The difference in the number of small lymphocytes with low mitochondrial content (MC) decreased after irradiation (Fig. 7). No significant

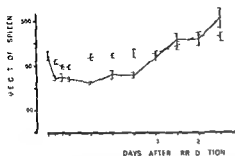


Fig 9

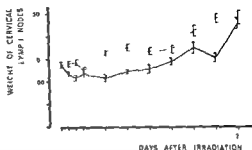


Fig 10

Fig 9 Weight (mg) of spleen of guinea pigs at different intervals after 150 rad whole body (—) or local thymus (---) irradiation Mean  $\pm$  SE A significant depression of the splenic weight occurred after both modes of irradiation but was most marked after the former the splenic regeneration between 12 and 18 days after whole body irradiation coincides with the restoration of the thymic release of small lymphocytes (fig 13)

Fig 10 Weight (mg) of cervical lymph nodes of guinea pigs at different intervals after 150 rad whole body (—) or local thymus (---) irradiation Mean  $\pm$  SE Marked involution of the lymph nodes occurred after the former followed by a slow recovery in weight

**Thymus histology** The thymic cortex decreased in thickness being 79 to 86 % of the normal value at 1 to 6 days after irradiation (Table 2) the normal thickness was not fully restored during the experimental period The density of cells per unit volume of the thymus cortex decreased slightly but not significantly (Table 3) The density of macrophages increased the increase being 70 90 80 and 60 % after 1 2 3 and 6 days respectively

No change in the density of Hassall's corpuscles was registered in the thymus medulla after the irradiation

**Thymus blood flow** The blood flow was decreased to a minimal value 9 days after irradiation ( $p < 0.01$ ) even when calculated per mg thymic weight (Table 5)

**Thymic veno arterial difference in number of leucocytes** The output of small lymphocytes from the locally irradiated thymus was markedly reduced Thus output at 3 days was only 14 % of that of the controls At later intervals after the irradiation the output was larger but increased and decreased irregularly without reaching the normal level (Fig 7)

No output of larger lymphocytes from the thymus has been observed in the normal guinea pig in this and in earlier investigations An export of medium sized lymphocytes (with medium MC) was however observed after local thymus irradiation This was significant as early as the first day after the irradiation and persisted for 15 days (Fig 8)

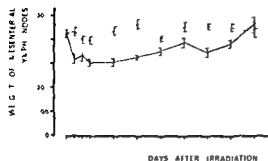


Fig 11

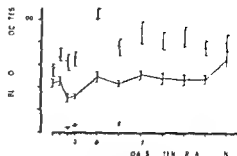


Fig 12

Fig 11 Weight (mg) of mesenteric lymph nodes of guinea pigs at different intervals after 150 rad whole body (—) or local thymus (---) irradiation. Mean  $\pm$  SE. The irradiation and the recovery were similar to that in the cervical lymph nodes.

Fig 12 Number of lymphocytes per  $\mu$ l of blood from the carotid artery of guinea pigs at different intervals after 150 rad local thymus irradiation. The lymphocytes are divided into three subpopulations according to their mitochondrial content. The lymphocytes with low, medium and high mitochondrial content are called small (—), medium sized (---) and large (····) lymphocytes. Mean  $\pm$  SE. The local thymus irradiation caused a depression of the number of small lymphocytes while the counts of medium sized lymphocytes increased. The changes were apparently due to the alterations in the thymic release of lymphocytes after local irradiation (figs 13, 14).

**Spleen.** The splenic weight was reduced 2 and 3 days after the irradiation ( $-15\%$ ,  $p < 0.05$ ). At later intervals the spleen increased in weight in a normal manner (Fig 9).

**Lymph nodes.** Cervical and mesenteric lymph nodes were not significantly decreased in weight by local irradiation of the thymus (Figs 10, 11).

### *Comparison between the effects of the two modes of irradiation*

Neither type of irradiation influenced the general appearance of the animals. The early decrease in body weight was however somewhat more marked after whole body irradiation (Fig 1), similarly, the adrenal weight was lower (Fig 2).

**Blood.** The total number of blood lymphocytes was considerably decreased after whole body irradiation although not following local irradiation of the thymus (Fig 3). Both small and medium sized lymphocytes decreased in number early after irradiation of the whole body (Fig 1). The small lymphocytes in the blood decreased in number at the same time as the medium sized lymphocytes rose by almost the same extent after local irradiation of the thymus (Fig 12).

Table 5

*Change in thymic blood flow (one lobe) after local irradiation of thymus with minimal value at 9 days*  
*Mean  $\pm$  SF*

	Control Days after irradiation										
	1	2	3	6	9	17	15	18	21	24	
Thymic blood flow (l/min)	49.9 ± 4.3	43.8 ± 8.3	44.0 ± 7.0	49.2 ± 7.7	36.3 ± 6.7	30.9 ± 5.4	55.6 ± 7.8	44.3 ± 6.3	41.8 ± 7.2	68.5 ± 10.0	42.8 ± 5.6
Thymic blood flow per mg thymic tissue (μl/min mg)	0.20 ± 0.03	0.22 ± 0.03	0.24 ± 0.03	0.28 ± 0.04	0.19 ± 0.03	0.15 ± 0.02	0.27 ± 0.03	0.23 ± 0.03	0.19 ± 0.03	0.31 ± 0.06	0.24 ± 0.03
Number of animals	23	15	14	15	14	15	14	14	14	14	14

The number of granulocytes fell late after irradiation with lower blood counts after whole body than after local thymus irradiation (Fig. 5)

*Thymus* The weight of the thymus markedly decreased during the first days after whole body irradiation but hardly changed at all after local irradiation. Secondary thymic atrophy appeared 18 and 21 days after whole body irradiation but not after local irradiation (Fig. 6)

The thymus cortical thickness decreased after irradiation, the decrease being more after whole body than after local irradiation (Table 2). A second fall in cortical thickness was registered between 18 and 24 days after whole body irradiation.

The number of thymus macrophages rose much more after whole body than after local irradiation during the first 3 days.

*Thymus blood flow* The blood flow through the thymus decreased after irradiation being minimal at 9 days. The decrease was most obvious after whole body irradiation. No second decrease in the blood flow occurred later (Tables 4, 5).

The thymic blood flow in normal guinea pigs is correlated to the thymic weight (ERASTROM & LARSSON 1970). Similarly the decrease in thymic weight after irradiation was accompanied by decreased thymic blood flow. However, 9 days after both modes of irradiation the thymic blood flow was significantly decreased even when calculated per mg thymic tissue (Tables 4, 5).

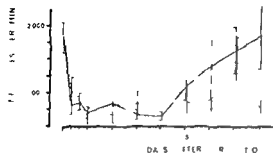


Fig 13

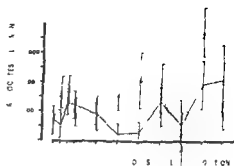


Fig 14

Fig 13 Thymic release of small lymphocytes per min at different intervals after 150 rad whole body (—) or local thymus (---) irradiation based on the thymic veno-arterial differences and the values for the thymic blood flow (fig 7 tables 4 5) Mean  $\pm$  SE Both modes of irradiation caused marked depression of the thymic release of small lymphocytes. The restoration of the release seemed to be more irregular after the latter.

Fig 14 Thymic release of medium sized lymphocytes per min at different intervals after 150 rad whole body (—) or local thymus (---) irradiation based on the thymic veno-arterial differences and the values for the thymic blood flow (fig 8 tables 4 5) Mean  $\pm$  SE Both modes of irradiation caused a significant release of medium sized lymphocytes. This varies irregularly during the regeneration of the thymus.

**Thymic veno-arterial difference in number of leucocytes** The thymic veno-arterial difference in number of small lymphocytes was decreased in the early phase after both modes of irradiation. The export was minimal after 3 days (Fig 7). The difference in the number of medium sized lymphocytes increased more after local thymus than after whole body irradiation. A small migration of granulocytes from the blood into the damaged thymus was observed after both modes of irradiation.

The release of cells per min from each thymic lobe can be calculated from the thymic veno-arterial differences and the thymic blood flow. The calculations must be performed on values from two different groups of animals due to the technique applied. This causes a larger variance in this parameter than in each of the two factors used in the calculation. A comparison of the effect of the two modes of irradiation disclosed an identical decrease in the output of small lymphocytes from the thymus during the first 9 days (Fig 13). Later on during the regeneration of the thymus the release of small lymphocytes increased continuously in the whole body irradiated animals and more irregularly after local thymus irradiation.

A significant release of medium sized lymphocytes occurred after irradiation (Fig 14). This was larger after local than after whole body irradiation.

*Spleen* The splenic weight fell in the early phase after both modes of irradiation ( $p < 0.001$ ) but to a greater extent following whole body irradiation. The difference in effect on the spleen was highly significant. The regeneration was also different. The spleen after local thymic irradiation had regained its weight after 6 days but not until 15 days after whole body irradiation (Fig 9).

*Lymph nodes* Only whole body irradiation caused significant atrophy of the lymph nodes. The weight was lower after whole than after local thymus irradiation also during the regenerative phase (Figs 10-11).

### Discussion

Comparison between the effects of irradiation of the thymus and of the whole body provides information about the direct effect of irradiation on the thymus and the non-thymic factors influencing its involution and the regeneration.

It is firmly established that ionizing radiation inhibits DNA synthesis in living cells (ALTMAN et coll 1970). Total body roentgen radiation depresses DNA synthesis in the thymus within 24 h (HARRINGTON & LAVIE 1955; ORD & STOKEN 1956; NYGAARD & POTTER 1959). During the regeneration of the thymus enhanced RNA synthesis precedes the peak of DNA synthesis and mitosis and the recovery of the thymus weight (THOMPSON et coll 1966). This first phase of recovery is histologically characterized by an increased frequency of large lymphocytes (GREENBERG et coll 1965; BLOMGREN & REYESZ 1968) which represent the precursors of the small lymphocytes (CRADDOCK et coll 1964; METCALF & WIADROWSKI 1966).

Both modes of irradiation in the present experiment resulted in almost complete failure in the export of small lymphocytes from the thymus (Fig 13), suggesting a direct effect of the irradiation. The failing thymic export of small lymphocytes is apparently secondary to cell death and the depressed proliferation of cells in the thymus. Some differences in effect on the thymus of the two modes of irradiation were however recorded even in the early phase of thymic atrophy. Thymic weight, cortical thickness and thymic blood flow thus exhibited larger decreases after whole body irradiation. As existing data indicate that the bone marrow furnishes stem cells that can repopulate the irradiated thymus the differences may be explained by the existence of a passage of stem cells from the non-irradiated bone marrow but no or decreased passage from the irradiated bone marrow. The migration of normal stem cells to the locally irradiated thymus may thus be responsible for the partial protection

from decrease in thymic weight from thymic cortical atrophy and from interference with thymic blood flow. Despite the low dose of radiation used, the whole body irradiation may have changed the release of hormones such as adrenalin and adrenal steroids or other humoral factors. A certain influence of such factors on the results cannot be excluded, even if no adrenal hypertrophy was recorded.

Whole body irradiation probably thus reduces the pool of stem cells outside the thymus. Functioning stem cells may slowly reappear and migrate into the thymus resulting in a return to normal of the thymic proliferation and the release of lymphocytes as described. The venous output of lymphocytes from the thymus was low during the first 12 days post irradiation. Immigrating stem cells may of course have contributed to the low veno-arterial difference in the number of lymphocytes. Later, after 15 days, a significant release of both small and medium sized lymphocytes from the thymus occurred. The release of small lymphocytes then successively increased towards the normal.

The thymus had the fastest regeneration of the lymphoid organs in the first phase of recovery after whole body irradiation as judged by the increase in weight (significant increase from day 6 to day 9, Fig. 6). The recovery of the spleen occurred somewhat later (significant increase from day 12 to day 15, Fig. 9). The increase in splenic weight coincided with the increase in thymic release of small lymphocytes (no significant release 1 to 12 days after irradiation, significant release 15 days afterwards, Fig. 13). An intact thymus is important for the normal regeneration of the spleen after irradiation and the present results suggest that this may be due to the recurrence of the thymic release of small lymphocytes.

The experiments of Cross et al. (1964) with irradiated mice indicated that the thymus *in situ* caused little restoration of the immunologic responsiveness for at least 10 days although when the thymus was present for a longer time rapid recovery occurred. This pattern of time for immunologic restoration correlates well with the present results. It demonstrates the failure of the thymus to export small lymphocytes for 12 days after irradiation and then to release small lymphocytes. This indicates a relationship between cellular passage from the thymus and immunologic restoration.

The thymic regeneration was not complete after the first phase of cellular repopulation. A second phase of thymic atrophy occurred between 18 and 24 days after whole body irradiation with a decrease in weight and cortical thickness but without signs of increased cell death. This second phase of thymic atrophy was not associated with any decrease in the thymic release of small lymphocytes. The second phase of cellular depletion must thus be due to a disturbed equilibrium between the proliferation of cells in the thymus and the

increasing release of lymphocytes from the thymus. The secondary cellular depletion of the thymus is temporarily associated with an increase in homograft rejection and hemagglutinin response to sheep red cells (Cross et coll 1964).

Local irradiation of the thymus produced a disturbed thymic equilibrium. No second phase of thymic atrophy occurred but an irregular thymic release of lymphocytes was evident. The locally irradiated thymus released medium sized lymphocytes which indicates that this occurred before the normal proliferation and differentiation to small lymphocytes had taken place.

The exact mechanism behind the second phase of cellular depletion is not known. The supply of stem cells from the irradiated and perhaps exhausted bone marrow may be deficient in the regenerating thymus. Alternatively the radiation may have caused damage to thymic cells that produce a hormone regulating the proliferation, maturation and release of lymphocytes (GOLDSTEIN et coll 1970). The release of larger lymphocytes after irradiation may be due to such a disturbed thymic regulation. It may also be argued that the radiation may cause a structural disorganization of the thymus, resulting in the venous output of larger lymphocytes. This is however improbable as the thymus morphology was more intact after local than after whole body irradiation and the release of larger cells occurred to the same degree or more after the local thymus irradiation. Finally the release of lymphocytes from the thymus may be regulated by a non thymic factor and due to a deficiency in thymus-derived lymphocytes in non thymic lymphoid tissue. Some evidence of the existence of such a feed back between the spleen and the thymus has been reached in experiments with splenectomized guinea pigs (ERNSTROM & SANDBERG 1970).

### Acknowledgements

The author is indebted to Prof Bernhard Tribukait for his help and advice with the irradiations and to Miss Kersti Granlöf and Mrs Lena Hedman for their technical assistance. This work was supported by the Swedish Cancer Society. Grant No 69 169.

### SUMMARY

The thymic release of small lymphocytes in the blood was markedly depressed after both whole body and local thymus gamma irradiation in a material of 543 guinea pigs. This was followed by their successively increasing release. The importance of the thymus even when irradiated in the regeneration of the spleen and lymph node tissue as well as in immunologic restoration is discussed.



## ZUSAMMENFASSUNG

Die Abgabe von kleinen Lymphozyten vom Thymus in das Blut war nach sowohl Ganzkörper als auch lokaler Bestrahlung mit Gamma Strahlen bei einem Material von 543 Meer-schweinchen wesentlich herabgesetzt. Diesem Abfall folgte eine nach und nach ansteigende Abgabe. Die Bedeutung der Thymus auch bestrahlt während der Regeneration der Milz und von Lymphknotengewebe ebenso wie bei der immunologischen Wiederherstellung wird besprochen.

## RÉSUMÉ

La libération par le thymus de petits lymphocytes dans le sang est nettement diminuée sur une série de 543 cobayes après irradiation totale du corps et irradiation localisée au thymus par le rayonnement gamma. Ce phénomène est suivi d'une augmentation ultérieure de la libération de petits lymphocytes. L'auteur examine l'influence du thymus même quand il est irradié sur la régénération de la rate et du tissu ganglionnaire lymphatique ainsi que sur la restauration immunologique.

## REFERENCES

- ALTJAN, K. J., GERBER, G. B. and OKADA, S. Radiation biochemistry, Vol. 1 Cells and tissues. Press, New York and London 1970.
- BLOMGREN, H. The influence of the bone marrow on the repopulation of the thymus in  $\gamma$ -irradiated mice. *Exp. Cell Res.* 58 (1969) 353.
- and REVEZ, L. The effect of bone marrow protection on the cellular composition of irradiated mouse thymus. *Exp. Cell Res.* 53 (1968) 261.
- BROWN, M. B., KAPLAN, H. S., WEYMOUTH, P. P. and PALL, J. Effect of intravenously injected bone marrow cell suspensions on thymic regeneration in irradiated C57 black mice. *Science* 117 (1953) 693.
- COOPERSTEIN, S. J., LAZAROW, A. and PATTERSON, J. W. Studies on the mechanism of Janus green B staining of mitochondria. II. Reactions and properties of Janus green B and its derivatives. *Exp. Cell Res.* 5 (1953) 69.
- CRADDOCK, C. G., YAKA, G. S., FUKUTA, H. and VANSLAGER, L. M. Proliferative activity of the lymphatic tissues of rats as studied with tritium labeled thymidine. *J. exp. Med.* 120 (1964) 389.
- CROSS, A. M., DAVIES, A. J. S., DOE, B. and LELCHERS, E. Time of action of the thymus. *Nature Lond.* 203 (1964) 1239.
- CULLING, C. F. S. Handbook of histopathological technique. First edition, p. 344. Butterworth & Co. London 1957.
- ELLINGER, F. Lethal dose studies with  $\gamma$  rays. *Radiology* 44 (1945) 125.
- ERNSTROM, U. and LARSSON, B. Influence of thyroxine on the mitochondrial contents of thymic and lymph node cells. *Acta path. microbiol. scand.* 59 (1963) 301.
- — Determination of thymic blood flow in guinea pigs of different ages. *Acta path. microbiol. scand. Section A*, 78 (1970) 366.
- and SANDBERG, G. Influence of splenectomy on thymic release of lymphocytes into the blood. *Scand. J. Haemat.* 7 (1970) 343.
- FICHTELTUS, K. E. and LARSSON, S. E. Blood lymphocytes in supravital and dried smear preparations studied with mitochondrial stain. *Acta anat. (Basel)* 44 (1961) 60.

- FORD C. E. and MICKLEM H. S. The thymus and lymph nodes in radiation chimaeras *Lancet* 1963 I p 359
- HAMERTON J. L. BARNES D. W. H. and LOUITT J. F. Cytological identification of radiation chimaeras *Nature (Lond.)* 177 (1956) 457
- GENGOPIAN N. URSO J. E. CONGDON C. C. et coll. Thymus specificity in lethally irradiated mice treated with rat bone marrow *Proc Soc exp Biol (N.Y.)* 96 (1957) 714
- GLOBERSON A. and FELDMAN M. Role of the thymus in restoration of immune reactivity and lymphoid regeneration in irradiated mice *Transplantation* 2 (1964) 212
- FIORE DONATI L. and FELDMAN M. On the role of the thymus in recovery of immunological reactivity following  $\gamma$  irradiation *Exp Cell Res* 28 (1962) 455
- GOLDSTEIN A. L. ASANUMA Y. and WHITE A. The thymus as an endocrine gland: properties of thymosin: a new thymus hormone *Recent Progr Hormone Res* 26 (1970) 505
- GREENBERG L. J. COLE L. J. and MARTIN R. L. Enzyme activity changes and cell volume distribution in mouse thymus after  $\gamma$  irradiation *Radiat Res* 26 (1965) 413
- GYLLENSTEN L. Influence of thymus and thyroid on the postnatal growth of the lymphatic tissue in guinea pigs *Acta anat. (Basel)* (1953) Suppl. No. 18
- HARAN GHERRA V. The effects of ionizing radiation on growth and regeneration of internal thymus grafts in mice *Radiat Res* 20 (1963) 442
- HARRINGTON H. and LAVIK P. S. The differential effect of  $\gamma$  irradiation on the incorporation of various precursors into rat thymus deoxyribonucleic acid *Arch Biochem* 54 (1955) 6
- HARRIS I. F. Changes in thymus and lymph node activity and alterations in bone marrow lymphocyte levels during recovery of the guinea pig from whole body irradiation *Brit J exp Path* 39 (1958) 557
- KAPLAN H. S. and BROWN M. B. Effect of peripheral shielding on lymphoid tissue response to irradiation in C57 black mice *Science* 116 (1952) 195
- Radiation injury and regeneration in lymphoid tissues *In: The leukemias: Etiology, patho-physiology and treatment* p. 163 Edited by J. W. Rebusck, F. H. Bethell and R. W. Monto Academic Press New York 1957
- LARSON B. A quantitative estimation of the venous output of lymphocytes from the thymus in guinea pigs *Acta path microbiol scand* 67 (1966) 586
- METCALF D. and WLADEWSKI M. Autoradiographic analysis of lymphocyte proliferation in the thymus and in thymic lymphoma tissue *Cancer Res* 26 (1966) 483
- MICKLEM H. S. FORD C. E. EVANS E. P. and GRAY J. Interrelationships of myeloid and lymphoid cells: studies with chromosome marked cells transfused into lethally irradiated mice *Proc roy Soc B* 165 (1966) 78
- MILLER J. F. A. P. DOAK S. M. A. and CROSS A. M. Role of the thymus in recovery of the immune mechanism in the irradiated adult mouse *Proc Soc exp Biol (N.Y.)* 112 (1963) 785
- MURRAY R. C. The spleen. The thymus *In: Histopathology of irradiation* p. 243 and 446 Edited by W. Bloom, McGraw Hill New York 1948
- NIGGAARD O. F. and POTTER R. L. Effect of  $\gamma$  radiation on DNA metabolism in various tissues of the rat. I. Incorporation of  $C^{14}$  thymidine into DNA during the first 24 hours postirradiation *Radiat. Res* 10 (1959) 462
- ORD M. G. and SROKEN L. A. The effects of  $\gamma$  and  $\beta$  radiation on nucleic acid metabolism in the rat *in vivo* and *in vitro* *Biochem J* 63 (1956) 3
- OSMOND P. G. ROYLANCE P. J. LEE W. R. et coll. The effect of unilateral limb shielding on the haemopoietic response of the guinea pig to gamma irradiation (150 r) *Brit J Haemat* 12 (1966) 365

- POPP R. A. Repopulation of thymus by immunologically competent cells derived from donor marrow. *Proc Soc exp Biol (N Y)* 108 (1961) 561
- SHOWACRE J. L. and DE BUY H. G. On the enzymic nature of mitochondrial characterization by Janus green II and the detection of Krebs-cycle dehydrogenases with Janus green B. *J nat Cancer Inst* 16 (1955) 173
- SMITH C. and KIEFFER D. A. Studies on thymus of the mammal. V. Regeneration of irradiated mouse thymus. *Proc Soc exp Biol (N Y)* 94 (1957) 601
- TAKADA A. TAKADA Y. HUANG C. C. and AMBROS J. L. Biphasic patterns of thymus regeneration after whole body irradiation. *J exp Med* 129 (1969) 445
- THOMPSON J. S. SEVERSON C. D. and REILLY R. W. The effect of estradiol and irradiation on the nucleic acid metabolism of the thymus, spleen, lymph node and liver of mice. *Radiat. Res* 29 (1966) 537
- TYAN M. L. and COLE L. J. Bone marrow as the major source of potential immunologically competent cells in the adult mouse. *Nature (Lond)* 208 (1965) 1233
- WISEMAN H. H. Criteria on the age of lymphocytes in the peripheral blood. *J exp Med* 54 (1931) 271

## REDUCTION IN STRONTIUM ABSORPTION IN PREGNANT LACTATING AND SUCKLING RATS

by

**K. KOSTIAL, N. GRUDEN, A. DURAKOVIĆ, V. JUVANČIĆ and I. SIMONOVIC**

Previous work has indicated that the absorption of radioactive strontium from the gut may be reduced by various dietary additives. The best results were obtained by increasing the calcium phosphate and alginate content of the diet (KOSTIAL et coll 1967 a). This also proved successful in reducing strontium absorption from the intestine in lactating rats (KOSTIAL et coll 1969 a) without interfering with its greatly increased absorption due to lactation (KOSTIAL et coll 1969 b, DURAKOVIĆ & KOSTIAL 1969). The addition of sodium alginate to the milk of artificially fed suckling rats also caused a reduction in the absorption of strontium from the gastrointestinal tract without interfering with the high absorption of calcium (KOSTIAL et coll 1969 a).

The purpose of the present work was to estimate the absorption of calcium and strontium from the intestine over the entire reproductive period (pregnancy and lactation) as well as to evaluate the effect of dietary additives on strontium absorption during this period. We also tried to obtain more data on the effect

of dietary additives on strontium absorption from the gut in 5–7 day-old rats by using a simpler experimental technique than in the previous experiments (KOSTIAL *et al.* 1969 a)

The results obtained indicate that alginates may be successfully used for reducing strontium absorption without affecting the higher calcium absorption during the reproductive period and at a very early age

### Methods

*Determination of strontium and calcium absorption in pregnant rats* The absorption of calcium and strontium was determined in two groups of pregnant albino rats fed on a normal diet during the earlier (7–10th day) and later (16–19th day) stages of pregnancy and in another group of pregnant rats given a diet with calcium, phosphate and alginate additives during the later stage of pregnancy. The absorption of these cations was also determined in two groups of virgin rats fed on normal and experimental diets respectively. The rats were between 15 and 16 weeks old at the time of mating. The beginning of pregnancy was determined from daily evaluation of vaginal smears. The number of animals in each group varied from 5 to 11.

The calcium, strontium and phosphorus content of the control diet was 1.2 g, 1.86  $\mu$ g and 0.8 g per 100 g dry food respectively. The addition of calcium as chloride, phosphates as potassium dihydrogen phosphate and alginates as sodium alginate (Manuocol SS(LD)2 Alginate Industries Ltd, London) to the control diet increased the calcium phosphate and alginate content of the experimental diet to 2.1 g Ca, 1.1 g P and 10 g alginates per 100 g dry food. Both diets were fed *ad libitum*. The food consumption was determined during the earlier and later stages of pregnancy over a period of three days while keeping the animals in metabolic cages for measuring the absorption of calcium and strontium from the intestine. The calcium, strontium and phosphate content of the diet was determined by standard methods (COMAR 1965; HARRISON 1958; LUCENA CORNE & PRATT 1957).

Carrier free  $^{45}\text{Ca}$  or  $^{47}\text{Ca}$  or  $^{86}\text{Sr}$  as supplied from the Radiochemical Centre, Amersham, England, were given to animals in drinking water for two days. About 0.5  $\mu\text{Ci}$  of calcium-47 and 0.3  $\mu\text{Ci}$  of strontium-86 were added to 10 ml of drinking water containing about 10 mg of calcium per 100 ml; no additional carrier was therefore required. The water bottles were supplied with stainless steel balls to prevent spillage of the radioactive solution. The amount of radioisotope received by each animal was calculated from the difference between the weight of the radioactive solution at the beginning and end of the two-day period. The percentage of radioactivity recovered in the carcass, urine and feces

under such experimental conditions amounted to 95 per cent with an average standard error of 3—4 per cent. The technique used produced the same results as in experiments in which radioactive isotopes were added to the diet so that uniform mixing of the radioactive isotopes in the drinking water with the calcium and strontium in the diet was assumed. The animals were killed 24 hours later by an overdose of ether. All animals were in metabolic cages over this period and separate collections of urine were made.

The carcass of the mother rat (the gastrointestinal tract removed), the uterus with fetuses and the pooled three day urine samples were ashed in a muffle furnace. Calcium-47 and strontium-89 in dissolved samples were determined in a well type scintillation counter connected to a single channel analyzer (HOSTIAL *et coll* 1964). Calcium-45 precipitated as oxalate was estimated in an end window counter. All results were expressed as percentages of the oral dose. The absorbed dose was recorded as the sum of the radioactivity in the carcass, fetuses and urine in pregnant animals and in the carcass and urine in controls.

The experimental methods used were essentially the same as in the previous work in lactating animals (HOSTIAL *et coll* 1969 a, b).

*Determination of calcium and strontium absorption in new born rats* The experiments in young rats were performed by a similar experimental technique of artificial feeding as described in our previous paper (HOSTIAL *et coll* 1967 b). The baby rats 5—6 days old were fed artificially for 8—10 hours on cow's milk with tracer amounts of  $^{45}\text{Ca}$  and  $^{89}\text{Sr}$  and additives of calcium phosphate and alginates. After this artificial feeding period they were returned to their mothers and killed 40 hours later. The baby rats were fed by means of the dropper, each receiving about 18 drops in a volume of 0.4 ml. The control group had cow's milk with  $\text{CaCl}_2$  and  $\text{KH}_2\text{PO}_4$  additives to reach the normal calcium and phosphate content of rat's milk (400 mg Ca and 230 mg P per 100 ml of milk) (SPRAY 1950). The experimental group received an additional amount of sodium alginate OG 1 (HUMPHREYS 1967) of 2 g per 100 ml. Radioactive calcium and strontium were determined in dissolved ashed samples of the carcass in the same way as in the mother rats.

## Results

The results of calcium and strontium absorption in pregnancy are presented in Table 1 and Figs 1 and 2 together with the previous data obtained during the earlier (2—5th day) and later (14—17th day) stages of lactation for rats on control (HOSTIAL *et coll* 1969 b; ĐERADJIC & HOSTIAL 1969) and experimental diets (HOSTIAL *et coll* 1969 a). All experiments were performed by practically the same experimental technique.

Table 1

*Calcium and strontium absorption from the intestine in pregnant, lactating and virgin rats on control and experimental diet. Each value represents the arithmetic mean and standard error of the mean.*

Experimental group	Diet	No. of anim.	Amount of food consumed g/day	Dietary Ca % 100 g
7-10th day of pregnancy	Control	11	17.1 $\pm$ 0.7	1.900
Virgins	Control	8	16.1 $\pm$ 1.0	1.900
16-19th day of pregnancy	Control	10	20.6 $\pm$ 0.5	1.200
	Alginate	5		2.100
Virgins	Control	10	16.1 $\pm$ 1.0	1.900
	Alginate	8		2.100
2-5th day of lactation	Control	12	24.5 $\pm$ 0.8	1.00
Virgins	Control	12	16.1 $\pm$ 1.0	1.00
14-17th day of lactation	Control	27	30.9 $\pm$ 1.2	1.900
	Alginate	16		100
Virgins	Control	41	16.1 $\pm$ 1.0	1.100
	Alginate			400

The daily calcium and strontium intakes appear in columns 4 and 7 of Table 1. The values were calculated from the result of daily food consumption (column 2) and the calcium 1.2 g, 2.1 g and 2.4 g per 100 g of food, respectively, and strontium (18  $\mu$ g per 100 g) content of the diet. The daily calcium and strontium absorptions from the intestine are presented in columns 8 and 9 and were calculated from the daily intake values and the percentage radioactive calcium and strontium absorptions (columns 5 and 8).

The results obtained during the earlier and later phase of pregnancy and lactation in animals on experimental diets presented in Table 1 are always followed by data obtained in virgin control animals on control and experimental diet for the same time intervals.

Food consumption appears gradually to increase during the reproductive period, being only slightly higher during pregnancy to reach the highest values during the later phase of lactation. All virgin rats consumed approximately the same amount of food on control and experimental diets so that the same figure of 16 gr per day was used for calculations in Table 1. The percentage calcium absorption was also higher in pregnancy, reaching the highest values toward the end of the lactation. The increase in the percentage strontium absorption during

Table I (cont.)

Daily Ca intake mg	Ca Ca absorption	Daily Ca absorption mg	Daily Sr intake μg	Sr * absorption	Daily absorption μg
205	16.9±0.7	34.7±1.4	318	8.1±0.3	25.6±0.9
193	13.9±1.1	27.0±2.2	300	8.6±1.0	25.7±3.0
248	16.4±0.4	40.5±1.0	383	7.0±0.2	26.8±0.8
433	10.6±0.3	45.9±1.3	383	2.6±0.1	9.8±0.4
103	13.7±0.5	26.4±0.9	300	6.0±0.2	18.0±0.7
338	8.8±0.6	29.8±1.9	300	2.2±0.2	6.6±0.5
294	18.7±1.1	54.9±3.3	456	7.4±0.6	33.8±2.1
193	12.4±1.3	22.1±2.8	300	6.4±0.8	19.3±2.2
371	29.5±1.3	109.3±5.0	575	10.7±0.6	61.4±3.5
142	14.2±0.5	105.4±3.9		2.9±0.2	16.6±1.2
194	11.4±0.5	22.2±1.0	300	5.0±0.4	14.8±1.0
381	7.4±0.4	28.4±1.4	300	2.3±0.2	7.2±0.7

the reproductive period was always less marked. The percentage radioactive calcium absorption was always lower in animals on experimental diets but the daily absorption of calcium from the gut remained practically unchanged. The percentage strontium absorption and the daily strontium absorption, in rats on experimental diet was however always decreased.

The results in Fig. 1 demonstrate the increase in the amount of strontium absorbed from the intestine over the reproductive period. Pregnant and lactating animals with calcium phosphate and alginate additives in the diet maintained however the same level of strontium absorption from the gut as the rats in the control group.

The results presented in Fig. 2 disclose the high increase in the absorption of calcium from the gut during the reproductive period compared to the virgin controls. The addition of calcium phosphates and alginates to the diet failed to prevent the increased absorption of calcium during the reproductive period.

The selective action of these dietary additives on strontium absorption from the gut during the reproductive period caused a great reduction in the  $^{85}\text{Sr}/^{45}\text{Ca}$  or  $^{45}\text{Ca}$  ratio in the carcass of the mother, fetus and suckling (Fig. 3). The values were corrected for the calcium content of the diet.



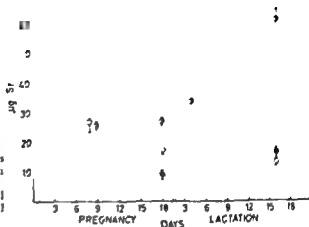


Fig. 1. Intestinal absorption of strontium in pregnant and lactating rats on control diet (○) and diet with calcium phosphate and alginate additives (●) as compared to intestinal absorption in virgin rats on control diet (○). Mean  $\pm$  SE.

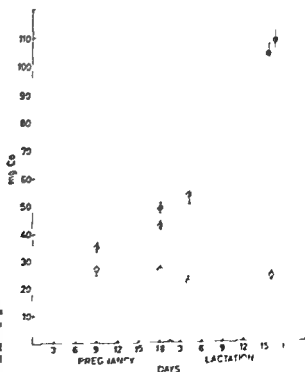


Fig. 2. Intestinal absorption of calcium in pregnant and lactating rats on control diet (○) and diet with calcium phosphate and alginate additives (●) as compared to intestinal absorption in virgin rats on control diet (○). Mean  $\pm$  SE.

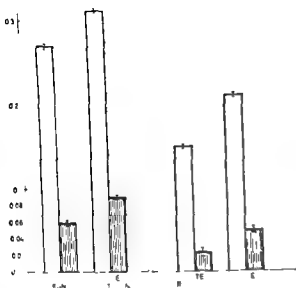


Fig 3 Ratio of radioactive strontium to calcium in the carcass of the mother (to the left) and fetuses or sucklings (litter) (to the right) during the later stage of pregnancy and lactation in animal on control diet (open fields) and diet with calcium phosphate and alginate additives (hatched fields) Mean  $\pm$  SE

*The effect of dietary additives on strontium and calcium absorption in newborn rats* The retention of radioactive calcium and strontium in the carcass in sucklings fed artificially on milk with and without alginate additives appears in Table 2. The previous data obtained in 10 day feeding experiments are presented in the same table for comparison (KOSTIAL et coll 1969 a). Both sets of the results are in good agreement. The addition of alginates to milk caused a decrease of about 50–60 per cent of the radiostrontium retention without influencing the high calcium absorption from the intestine.

### Discussion

The data of calcium requirements during the reproductive period are usually calculated from the amount of calcium provided by the mother for the fetus or infant and from calcium losses in the mother's urine presuming an intestinal absorption rate of 25 per cent (WHO Technical Report Series 1962, 1965). The authors have however previously been able to indicate both with *in vitro* and *in vivo* techniques that the absorption rate from the intestine greatly increases in lactating rats. This increased absorption is assumed to be mainly due to an increased passive transport of these ions but also to an enhanced active transport of calcium through the intestine (KOSTIAL et coll 1969 b). The changes in the alimentary tract of lactating animals observed by other authors provide

Table 2

*Influence of alginate additives on the retention of  $^{45}\text{Ca}$  and  $^{90}\text{Sr}$  by 5-7 day-old rats fed artificially on rats milk for 1 and 10 days*

Milk (mg 100 ml)			Days of artificial feeding	No. of rats	Retention in carcass percentage oral dose mean $\pm$ SE			
Ca	P	Alg			Sr	$^{45}\text{Ca}$	$^{90}\text{Sr}$	Ca
400	230	—	1	136	63.50 $\pm$ 0.84	67.11 $\pm$ 0.80	0.977	0.004
400	230	2.000	1	86	26.31 $\pm$ 0.58	60.60 $\pm$ 1.70	0.439	0.007
400	230	—	10	36	69.99 $\pm$ 0.76	73.52 $\pm$ 0.84	0.96 $\pm$ 0.01	
400	230	2.000	10	36	33.96 $\pm$ 0.57	71.79 $\pm$ 1.22	0.41 $\pm$ 0.04	

morphologic and histologic bases for explanation of these results (BOYSE *et coll* 1966). The present experiments reveal that an increased absorption of calcium through the gut wall starts by the pregnancy period and reaches maximum values during the later phase of lactation. The rats do balance their higher needs for calcium by increasing their consumption in food during the reproductive stage. The present results of food consumption are in good agreement with data published by KUMARASAN & TURNER (1968) for pregnant and by ANDERSON & TURNER (1963) for lactating rats.

The absorption of strontium is also increased during the reproductive period although not to the same degree as that of calcium.

Several other changes in calcium metabolism due to pregnancy and lactation may also affect the deposition of strontium in bone. The acceleration of calcium turnover (STERNBERG 1968; STERNBERG *et coll* 1969) may cause the removal of bone seekers incorporated in the deeper parts of the bone before the reproductive period. This has been demonstrated for radiostrontium in various experimental investigations (MOMILOVIĆ *et coll* 1969; KOLLMER & KRUGEL 1964; RONNBACK *et coll* 1968) and constitutes another way in which radioactive strontium may be transferred to the fetus and in nursing mothers to their infants.

The best way of avoiding radiostrontium uptake in the fetus and suckling would be to prevent radiostrontium absorption from the mother's intestine during pregnancy and lactation. This might justify the use of dietary additives as a means of decreasing radioactive strontium retention in both mother and offspring during the reproductive period. Alginates have already been successfully employed in human subjects and experimental animals for reducing radiostrontium absorption from the intestine (HARRISON *et coll* 1966; HERS & KAMMERTON 1965). An addition of calcium phosphates and alginates to the diet has been proved to be the most effective method of lowering radiostrontium retention in experimental animals (KOSTIAL *et coll* 1967a). Rats fed on diets with alginate additives for one year developed no changes in food consumption

growth rate or calcium and phosphate content in their skeletons (HARRISON 1967). Similar results were obtained in rats fed calcium phosphate and alginate supplemented diets for six months in our experiments (SLAT & KOSTIAL 1967).

The present data on the effect of these dietary additives in pregnancy fully confirm the previous results obtained during the lactation period, they indicate a successful means of decreasing radiostrontium absorption from the intestine without influencing the greatly increased calcium absorption from the gut during the reproductive period. Their inclusion results in a three to four times lower intestinal strontium absorption and in a four to six times decreased strontium to calcium ratio in the carcass of the mother, fetus and suckling.

The other possible way of decreasing strontium absorption from the gut in artificially fed infants or animals would be a direct addition of alginates to the milk. The present and previous results indicate that the addition of alginates to the milk reduces strontium absorption from the gut by 50–60 per cent without decreasing the very high calcium absorption. Alginates seem to be the only additive to the milk that causes a decrease in strontium absorption since an increased calcium or phosphate content in the milk had no effect on strontium metabolism in new born rats (KOSTIAL et coll 1967 b KOSTIAL et coll 1969 a).

### Acknowledgements

The authors wish to express their thanks to the MRC Radiobiological Research Unit, Harwell for the supply of sodium alginate (OGI) and to Messrs M. Buben, M. Landeka and M. Vnucec for their skilful technical assistance. This work was supported by a grant from the Federal and Republic Scientific Research Council, Belgrade and Zagreb.

Some of the results were briefly presented at the Fourth Yugoslav Symposium on Radiological Protection Basko Polje 1969 and the Second International Congress of the International Radiation Protection Association Brighton 1970.

### SUMMARY

The absorption of oral radioactive calcium and strontium was determined during the earlier and later stages of pregnancy and lactation in rats. A gradual increase in their absorption from the gut occurred, maximum values being reached at the end of lactation. The addition of alginates to the milk of new born rat fed artificially decreased the absorption of strontium without affecting that of calcium.

### ZUSAMMENFASSUNG

Die Absorption oral verabreichten radioaktiven Calciums und Strontiums wurde während der früheren und späteren Stadien der Gravidität und Laktation bei Ratten bestimmt. Ein gradueller Anstieg der Absorption vom Darm trat auf maximale Werte wurden am Ende der Laktation erreicht. Der Zusatz von Alginaten zur Milch von künstlich ernährten neugeborenen Ratten verminderte die Absorption von Strontium ohne die des Calciums zu beeinflussen.

## RÉSUMÉ

L'absorption de calcium et de strontium administrés par voie buccale a été étudiée pendant les premiers et les derniers stades de la gravidité et de la lactation chez des rates. On observe une augmentation graduelle de leur absorption intestinale, les valeurs maximales étant atteintes à la fin de la lactation. L'addition d'alginate au lait donné à des rats nouveaux nés alimentés artificiellement a diminué l'absorption du strontium sans modifier celle du calcium.

## REFERENCES

- ANDERSON R. R. and TURNER C. W. Feed consumption during lactation in Sprague Dawley Ratsmeyer rats. *Proc Soc exp Biol (NY)* 113 (1963) 334.
- BLANJA M., MOMČILOVIĆ B., HARMUT M. et coll. Some parameters of calcium metabolism in lactation measured by  $^{45}\text{Ca}$ . *Jugoslav Physiol Pharmacol Acta* 5 (1969) 393.
- BOYNE R., ILLI B. I. and ROSS I. The surface area of the intestinal mucosa in the lactating rat. *J Physiol (Lond)* 183 (1966) 570.
- COMAR C. L. *Radioisotopes in biology and agriculture* p. 220. McGraw Hill, New York, 1965.
- DLAKOVIĆ A. and KOSTIAL A. The influence of early lactation on intestinal absorption of calcium and strontium. *Jugoslav Physiol Pharmacol Acta* 5 (1969) 397.
- FELI B. F., CAMPBELL R. M. and BOYNE R. Observations on the morphology and nitrogen content of the alimentary canal in breeding hill sheep. *Res Vet Sci* 5 (1964) 17.
- HARRISON G. E. Estimation of strontium in biological material by means of a flame spectrophotometer. *Nature* 182 (1958) 792.
- Absorption of strontium in rats on alginate supplemented diet. *In: Diagnosis and treatment of deposited radionuclides* p. 333. Excerpta Medica Foundation, Amsterdam, 1967.
- HUMPHREYS E. R., SUTTON A. and SHEPHERD H. Strontium uptake in rats on alginate supplemented diet. *Science* 132 (1966) 655.
- HESP R. and RAMSBOTTOM B. Effect of sodium alginate in inhibiting uptake of radio strontium by the human body. *Nature* 208 (1965) 1341.
- HUMPHREYS E. R. Isolation of an oligoguluronide from sodium alginate. *Carbohydr Res* 4 (1967) 507.
- KOLLMEYER W. F. und KRUGEL H. Das biologische Verhalten von Radiostrontium bei Ratten im Verlauf der Laktation. *Int J radiat Biol* 9 (1965) 369.
- KOSTIAL A., VOJNOVIĆ S., GRUDEN V. and LUKIĆ A. Skeletal uptake of calcium-47 and strontium-85 as influenced by the phosphorus content in the diet. *In: Bone and teeth* p. 111. Pergamon Press, London, 1964.
- MALJKOVIĆ T., KADIĆ M. et coll. (a) Reduction of the absorption and retention of strontium in rats. *Nature* 215 (1967) 189.
- SIMONOVIC I. and PIŠONIC M. (b) The effect of calcium and phosphates on gastrointestinal absorption of strontium and calcium in new born rats. *Nature* 215 (1967) 1181.
- DLAKOVIĆ A., SIMONOVIC I. and JUVANČIĆ V. (a) The effect of some dietary additives on calcium and strontium absorption in suckling and lactating rats. *Int J radiat Biol* 12 (1969) 563.
- GRUDEN V. and DLAKOVIĆ A. (b) Intestinal absorption of calcium 47 and strontium-85 in lactating rats. *Calc Tiss Res* 4 (1969) 13.

- KUMARESAN P and TURNER C W Effect of pregnancy on food consumption and mammary gland in rats *Proc Soc exp Biol (N Y)* 129 (1968) 957
- LUCENA CONDE F and PRATT L A new reagent for the colorimetric and spectrophotometric determination of phosphorus arsenic and germanium *An Chim Acta* 16 (1957) 473
- MONCILOVIC M, ĐURAKOVIĆ A and KOSTIAL K Mobilizacija radioaktivnog stroncija iz skeleta u laktaciju (In Yugoslav) *Zbornik radova IV jugoslovenskog simpozijuma o radiološkoj zaštiti* p 154 1969
- RONNBACK C, NELSON A and NILSSON A Influence of lactation on retention of radiostrontium in mice *Acta radiol Ther Phys Biol* 7 (1968) 330
- ŠLAT B and KOSTIAL K Effect of food with calcium phosphate and alginate additives on calcium and strontium metabolism II Yugoslav congress of occupational medicine Split 1967
- SPRAY C M A study of some aspects of reproduction by means of chemical analysis *Brit J Nutr* 4 (1950) 354
- STERNBERG J Tissue deposition of radionuclides during pregnancy *In* *Diagnosis and treatment of deposited radionuclides* p 91 Edited by H A Hornberg *Excerpta Medica* Foundation Amsterdam 1968
- LEGARE J M and MARCIE B Radiocontamination of the environment and its effects on the mother and fetus II Kinetic studies with labeled bone seekers in pregnant and lactating rats *Int J appl Radiat* 20 (1969) 81
- WORLD HEALTH ORGANIZATION Technical Report Series 230 1962
- Technical Report Series 302 1965

## Books received

We acknowledge with thanks under this heading books received for review. We trust this will be regarded as a sufficient mark of appreciation of the courtesy of the sender. Reviews of selected items will appear as soon as an opportunity affords.

- ACKERMAN L A and DEL REGATO J A. Cancer: Diagnosis, treatment and prognosis. C. V. Mosby Company, Saint Louis 1970.
- BASIC RADIATION PROTECTION CRITERIA. NCRP Report 39. National Council on Radiation Protection and Measurements, Washington 1971.
- BRITTON K E and BROWN N J C. Clinical radiography. Lloyd-Luke, London 1971.
- (THE) CLINICAL MANAGEMENT OF ADVANCED BREAST CANCER. Edited by C A F Joslin and E N Gleave. Tenovus Workshop Publications, Cardiff 1970.
- COMPUTERS IN RADIOLOGY. Edited by R De Haene and A Wambersie. S Karger, Basel 1970.
- DENOIX P. Treatment of malignant breast tumours. RRCR 31. Springer Verlag, Berlin 1970.
- ECOLOGY OF THE CANCER PATIENT. Edited by J E Healey. Interdisciplinary Communications Associates, Washington 1970.
- HENDEE W R. Medical radiation physics. Year Book Medical Publishers, Chicago 1970.
- INTERNATIONAL ENCYCLOPEDIA OF PHARMACOLOGY AND THERAPEUTICS. Volumes 1 and 2. Radiocontrast agents. Edited by P K Knöfel. Pergamon Press, Oxford 1971.
- KAMATH P R. The environmental radiation surveillance laboratory. World Health Organization, Geneva 1970.
- LACARDE C, CHALVERONE J et HOERNI B. La maladie de Hodgkin. Masson & Cie, Paris 1971.
- MITCHELL J S. Cancer—'if curable why not cured?' W. Hefser and Sons, Cambridge 1971.
- MODAN B. The polycythemic disorders. Charles C Thomas, Springfield, Illinois 1971.
- OLIVER R. Principles of the use of radio-isotope tracers in clinical and research investigations. Pergamon Press, Oxford 1971.
- PACK G T and ISLAM A H. Tumors of the liver. RRCR 26. Springer Verlag, Berlin 1970.
- PRECAUTIONS IN THE MANAGEMENT OF PATIENTS WHO HAVE RECEIVED THERAPEUTIC AMOUNTS OF RADIONUCLIDES. NCRP Report 37. National Council on Radiation Protection and Measurements, Washington 1970.
- PROTECTION AGAINST IONIZING RADIATION FROM EXTERNAL SOURCES. ICRP 15. Pergamon Press, Oxford 1970.
- PROTECTION OF THE PATIENT IN X-RAY DIAGNOSIS. ICRP 16. Pergamon Press, Oxford 1970.
- PROTECTION OF THE PATIENT IN RADIONUCLIDE INVESTIGATIONS. ICI 14. Pergamon Press, Oxford 1971.
- QUANTITATIVE ORGAN VISUALIZATION IN NUCLEAR MEDICINE. Edited by P J Kennel and F M Smith. University of Miami Press, Coral Gables 1971.
- RADIATION PROTECTION INSTRUMENTATION AND ITS APPLICATION. ICRU Report 20. International Commission on Radiation Units and Measurements, Washington 1971.
- RADIATION QUANTITIES AND UNITS. ICRU Report 19. International Commission on Radiation Units and Measurements, Washington 1971.
- STRAUB C P. Public health implications of radioactive waste releases. World Health Organization, Geneva 1970.
- WAKABAYASHI M. High dose rate intracavitary radiotherapy using the Ralston H. Wando. University School of Medicine, Sapporo 1971.

## DETERMINATION OF DOSE DISTRIBUTION IN THE PELVIS BY MEASUREMENT AND BY COMPUTER IN GYNECOLOGIC RADIATION THERAPY

by

I JOELSSON B I RUDEN A COSTA ANDREE DUTREIX and J C ROSENWALD

The distribution of doses in the female pelvis about the radiation sources used for treatment of carcinoma of the uterine cervix has been investigated with various methods during the last three decades. Reconstructural techniques were for example employed by LEDERMAN & LAMERTON (1948) with excellent results but were too tedious for routine use. Isodose rate curves determined by measurements around the applicators combined in idealized geometry have been superimposed on roentgen films of the pelvis and thereby related to frontal and lateral projections of the pelvic anatomy (WALSTAM 1954). This method offers a general appreciation of the distribution of dose rates. Clinical experience at Radiumhemmet has revealed that routine dose rate measurements along the anterior and posterior contours of the tumor may be used as a guide for the determination of treatment and its duration in the individual patient. Unexpectedly high dose rates or the observation of the maximal dose rate at an inappropriate location

From the Department of Gynecology (Director Prof H L Kottmeier) Radiumhemmet and the Department of Clinical Radiation Physics (Director Prof R Walstam) National Institute of Radiation Protection Stockholm Sweden and Unite de Radiophysique (Madame Andree Dutreix) Institut Gustave Roussy Villejuif France. This work was supported by grants from the Cancer Society of Stockholm and the King Gustaf V Jubilee Fund. Submitted for publication 30 December 1971.



indicate that the irradiators are incorrectly placed and that reinsertion is advisable. Together with information on the extent of the tumor and on the distances from the uterine cervix to the bladder, the rectum and the pelvic wall, these measurement data combined with knowledge of the dose rate distribution about the irradiators form the basis of the individualized dose planned intracavitary treatment. The measured dose rates may also be used for the characterization of treatment by defining a reference dose rate curve on the periphery of the tumor.

A more complete specification of treatment requires dose rate measurements close to the applicators combined with dose assessments in the lateral parts of the pelvis. KOTTMEIER (1951) utilized an ionization chamber for dose rate measurements at the pelvic wall during the procedure of extraperitoneal lymphadenectomy, the radium irradiators being *in situ* during surgery. Thermoluminescent dosimeters have now become available in sizes and shapes that make them suitable for dose determinations in the pelvic veins (TJERNBERG *et coll.* 1968, JOHANSSON *et coll.* 1969, JOELSSON *et coll.* 1970). This technique makes it possible to ascertain the integrated dose for the treatment time, thereby nullifying the effect of an inconstant relationship between the location of the irradiators and the anatomy of the patient.

Methods for calculating the dose distribution about intracavitary irradiators with the help of a computer have been introduced in several centers (ADAMS & MEURA 1964, SELLING *et coll.* 1967, POWERS *et coll.* 1965, BALTER *et coll.* 1966, SHALEK & STOVALL 1966, DUTREIX 1967, ROSENWALD & DUTREIX 1970). The isodose curves about any combination of irradiators may thus be defined and depicted with great saving of time. The computer may be programmed to deliver anatomy related isodose curves for every plane of interest, such as the frontal, oblique through the iliac lymph nodes and the transverse plane through the center of the tumor.

No investigation appears to have been published on the accuracy in clinical practice of the computerized calculation of pelvic dose distribution. This work was therefore designed with the aim of comparing such calculations with dose measurements in the same parts of the pelvis during intracavitary treatment by the Stockholm technique performed at Radiumhemmet. The calculations were undertaken by computer at Institut Gustave Roussy.

### Clinical material

Ten patients, 32 to 72 years of age, with carcinoma of the uterine cervix, stage Ib—IIa, were investigated. The Stockholm technique was used for the intracavitary irradiation, which was always performed before the external beam treatment. The patients were so selected that the combination of a given intra-

uterine cylinder and a flat box like vaginal irradiator was considered to represent their optimal treatment. The cylinder was loaded with an activity of 70 mg radium, its diameter being 8 mm, total length 75 mm and active length 55 mm. The total filtration was equal to 1.5 mm Pt. The box was loaded with 9 radium needles, total activity 72 mg; it measured 11 mm  $\times$  45 mm  $\times$  45 mm, the active surface being 26 mm  $\times$  35 mm. The walls of the box were of polymethyl methacrylate. The total filtration was equal to 0.5 mm Pt. The same cylinder and box were used for the treatment of all the patients. The irradiators were kept in place by inserting a gauze tampon packed into the vagina. The tampon also had the effect of increasing the space between the irradiators and the rectum.

As a basis for the computerized calculation of doses, the location of the irradiators in the pelvis was documented in a p and cross-table lateral roentgenograms. The films were always taken 3 to 4 hours after the irradiators had been applied, by which time the patient had recovered from the anesthesia. A specially constructed cassette holder was always used and was fitted with lead indicators in the top and bottom as well as in the side walls. The information derived from the analyses of the projection of the crosses in the film was used in correcting for the position of the diagnostic source (ROSENWALD & DUTREIX 1970).

*Dose rates close to the irradiators* were measured along the anterior contour of the uterine cervix with the dose rate detector in the urinary bladder and the urethra and along the posterior contour of the uterine cervix with the detector in the rectum. A Siemens Gammameter was used with the CdS crystal mounted in the end of a slightly curved rigid brass sound of 7 mm diameter. This enabled the detector to be approximated closely along the outer contour of the tumor by compressing the intervening tissues. Doses were measured with the patient in the lithotomy position according to a schedule that allowed, after temperature correction, a persistent probable error of method of  $\pm 10$  per cent (JOELSSON & BACKSTROM 1969).

In addition to the determinations with the Siemens Gammameter, doses in the vicinity of the applicators were sometimes measured with thermoluminescent dosimeters loaded into teflon catheters; these were introduced into the urinary bladder, urethra and rectum.

*Doses at a distance from the irradiators* were measured with lithium fluoride LiF (Harshaw extruded rods, 6 mm long and 1 mm in diameter) loaded into presterilized teflon catheters introduced into the external and common iliac veins by a technique commonly used for venous catheterization. Lead spacers had been placed between the dosimeters to allow, after phlebography, a precise roentgenologic determination of the location of each numbered LiF rod in relation to the pelvis. The dosimeters were left in situ during the whole course of treatment.

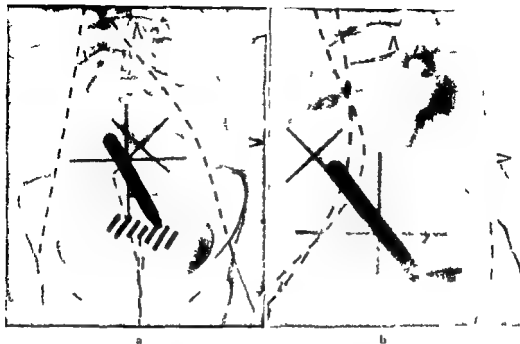


Fig 1 a) Ap and b) lateral projections of combination of vaginal and uterine irradiators. Input data on the anatomy of the pelvis and the geometry and location of the radiation sources were obtained from these films. LiF dosimeters in teflon catheters have been inserted into the pelvic veins and the bladder and rectum. The dosimeters served as reference points for computer calculated doses.

### The thermoluminescent technique

The influence of various heating procedures on the precision of the thermoluminescent technique has recently been investigated with LiF discs (CARLSSON 1969). Maximal precision ( $\sigma \approx 0.3$  per cent) was achieved if so-called pre-annealing was avoided and the dosimeters were heated only during the read-out cycle. The resultant distribution of the electron traps means however that fading exerts much influence. The 20 to 30 hour exposure of the dosimeters in the experiments necessitated additional heat treatment to avoid the effect of fading, even though this impaired the precision ( $\sigma \approx 1.5$  per cent). Before exposure the dosimeters were kept for 1 hour at  $400^\circ\text{C}$  and for 24 hours at  $80^\circ\text{C}$ . Before the read-out they were held for 15 minutes at  $80^\circ\text{C}$ .

The dosimeters were calibrated with a  $^{60}\text{Co}$  beam, the calibration constants  $C_i$  being  $C_i = 1/\lambda_i$ , where  $\lambda_i$  is the thermoluminescent signal from dosimeter number  $i$ . These calibration constants express the variation in the sensitivities of the dosimeters around a common mean  $\lambda$ . Even though  $\lambda$  changes,  $C_i$  remains

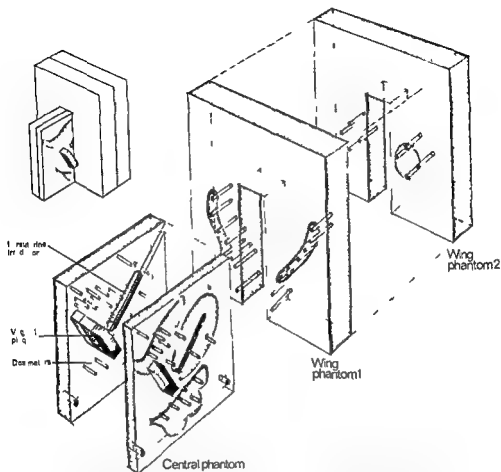


Fig 2 Phantom designed to allow comparison between measured and calculated doses in a situation involving a constant relationship between the radiation sources and the dosimeters. The separate parts of the phantom and the way they are combined during measurements.

constant for each dosimeter provided all the dosimeters are subjected to exactly the same heating and cooling procedure (MARTENSSON 1969). Four dosimeters from each series were recalibrated each time during the measurements while the individual calibration constants were checked after every second measurement. The observed variation of the calibration constants was 1.5 per cent. The LiF dosimeters were divided from the beginning into one series for the vessels on the right side of the pelvis, another for those on the left side and a third series for the bladder and rectum. Each dosimeter always had the same location in the teflon catheters and in the body.

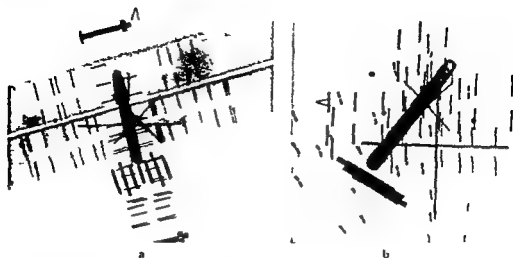


Fig 3 Roentgenograms of the phantom in a) a p and b) lateral projections used to determine the coordinates of the radium needles and the LiF dosimeters

### Dose computation

The calculation of doses by computers was performed at Institut Gustave Roussin with the CUGYLC program and a Univac 1107 computer (Centre de calcul de l'INSERM) with a curve plotter. Input data regarding the anatomy of the pelvis and the geometry and location of the radiation sources were obtained from a p and cross-table lateral roentgenograms with a curve tracer (Fig 1). The origin of the three dimensional coordinate system in which the positions in space of the end points of the radium sources and of the reference points were determined was chosen to coincide with the anatomic center of the pelvis as defined by ROSENWALD & DUTREIX (1970). The filtration factor of the individual source was taken into account in the program but no special allowance was made for the influence of oblique incidence. Tissue attenuation was corrected by the formula of MEISBERGER et coll (1968). Exponential attenuation was considered to occur at distances of more than 10 cm from the sources. Originally the program allowed only the drawing of isodose curves in arbitrarily chosen frontal, sagittal and transverse planes through the pelvis as well as in the plane through the iliac lymph nodes. In addition doses could now be computed at a number of reference points, formed by the LiF dosimeters in the pelvic veins, the urinary bladder and the rectum. Opaque spherical balls on a rod graduated in centimeters and placed in the lumen of the rectum also served the same purpose.

### Phantom measurements

Measurements were undertaken with a polystyrene phantom immersed in a water bath to compare measured and calculated doses in a situation involving a constant relationship between sources and dosimeters. Determinations were made in 48 locations at various distances from the same cylinder and box as were used in the series of patients. The irradiators were combined in the phantom in a geometry that represented an average application in the 10 patients as judged from their localization roentgen films. The phantom was designed so that the LiF rods could be placed in a manner that simulated the middle part of the common iliac veins and the middle part of the external iliac veins. In addition LiF rods were arranged in the sagittal plane through the irradiators at distances from the radiation sources that represented the base of the bladder and the anterior rectal wall (Fig. 2). The phantom incorporated opaque material to simulate the bony landmarks of the human pelvis used in the determination of the anatomic origin. Roentgen films taken with the same technique as in the series of patients could therefore be utilized to indicate the coordinates of the radium needles and the LiF rods (Fig. 3). Additional measurements were made in the identical phantom with teflon substituted for these lead rods. The latter experiments served for investigating the influence of the lead indicators upon the magnitude of absorbed doses in the LiF detectors.

### Results

*Doses in the urinary bladder* The clinically significant dose rates along the anterior surface of the uterine cervix with the detector of the Siemens Gammameter introduced into the urinary bladder varied between 86 and 146 rad/h mean 110 rad/h. (The values represent the mean of the three highest dose rates measured on consecutive centimeters.) Where LiF dosimeters loaded into a teflon catheter were introduced into the bladder through the urethra their positions assumed in the localization roentgen films corresponded to calculated dose rates of between 40 and 50 rad/h. The depth dose curve in the ventral direction derived from the computer print-out of the dose rate distribution in the midsagittal plane through the pelvis revealed that the individual distance between the detector of the Siemens Gammameter and the LiF dosimeters at the moment of roentgen exposure ranged from 15 to 20 mm. As the catheter holding the dosimeters in the bladder floated during the course of treatment the relationship between the dosimeters and the radium sources was inconstant. Thus the absorbed doses measured with LiF detectors integrated over the whole course of

Table 1

Measured radiation doses during one course of intracavitary radium treatment in various parts of the veins in rad as mean values and limits of determination in ten patients. Because of anatomic inequalities the right and left sides of the pelvis are considered separately.

	Common iliac vein			External iliac vein		
	Cranial	Middle	Caudal	Cranial	Middle	Caudal
Right side						
Mean	210	190	370	500	540	450
Limit	145-350	110-250	160-530	230-1000	300-900	275-765
Left side						
Mean	245	305	450	580	660	530
Limit	185-350	145-410	245-775	240-1200	280-1440	280-1000
Left/Right side						
Right side	$\times 100$	+17	+60	+22	+16	+22
						+18

Table 2

Computer-calculated radiation doses during one course of intracavitary radium treatment in various parts of the pelvic veins in rad as mean values and limits of determination in ten patients.

	Common iliac vein			External iliac vein		
	Cranial	Middle	Caudal	Cranial	Middle	Caudal
Right side						
Mean	255	290	430	550	540	4
Limit	240-290	160-415	225-600	275-915	375-800	375-540
Left side						
Mean	360	450	565	685	740	540
Limit	330-325	200-780	370-1195	270-1145	295-1795	280-850
Left/Right side						
Right side	100	+41	+55	+31	+25	+37
						-

treatment corresponded to only 70 to 80 per cent of the doses computed from the position of the LaF rods during the roentgen exposure.

*Doses in the rectum.* The clinically significant dose rates along the posterior contour of the uterine cervix measured with the detector of the Siemens Gammameter introduced in the rectum varied between 58 and 100 rad/h mean 80 rad/h. (The values are the mean of the three highest consecutive dose rates observed at centimeter intervals.) The doses calculated by

Table 3

*Differences between computer-calculated and measured doses as percentages of the latter in various parts of the pelvic veins. The figures represent means of individual differences*

	Common iliac vein			External iliac vein		
	Cranial	Middle	Caudal	Cranial	Middle	Caudal
Right side						
Mean	+31	+49	+19	+11	+1	-3
Limit	+50	+66	+46	+32	-37	+38
	and -24	and +33	and -76	and -72	and -20	and -32
Left side						
Mean	+50	+48	+30	+19	+10	+7
Limit	+89	+150	+150	+76	+39	+10
	and +10	and +8	and -20	and -17	and -20	and -23

the computer at reference points represented by spheres of the rod placed in the rectal lumen or by the LiF dosimeters in the same position, varied between 25 and 65 rad/h mean 50 rad/h. Judging from individual dose rate differences between measurements (Siemens Gammameter) and calculations at the reference points the discrepancy proved to be 1 to 19 mm mean 9 mm. The position of the rod in the rectum as indicated by localization films differed negligibly from the average location during treatment; the doses measured with the LiF dosimeters were equal to those calculated.

*Doses in the pelvic veins.* The doses absorbed in the common iliac and external iliac veins measured with intravascularly inserted LiF dosimeters were referred to different parts of the veins using the information gained by phlebography (Table 1). Anatomic asymmetry made it necessary to consider the right and left sides separately. On the right side the mean doses in the common iliac vein given in a caudal direction proved to be 210, 190 and 370 rad; in the external iliac vein the doses also in a caudal direction were 500, 540 and 450 rad. The doses on the left side amounted to 245, 305 and 450 rad in the common iliac vein and 580, 660 and 530 rad in the external iliac vein. The maximal difference (+60 per cent) between the left and right sides was observed in the middle part of the common iliac vein. The interindividual variations were marked—for example a dose in the cranial part of the external iliac vein of 1200 rad in one case and 260 rad in another one.

The doses in the different portions of the common iliac and external iliac veins were also calculated by computer with the LiF dosimeters as reference



points in the computer program (Table 2). The differences between the calculated and the measured dose as percentages of the latter were +31, +49 and +19 per cent in the common iliac vein on the right side. The corresponding differences in the external iliac vein were +11, +1 and -3 per cent. On the left side the differences in the common iliac vein were +50, +48 and +30 per cent and in the external iliac vein +19, +10 and +7 per cent (Table 3).

*Doses in the pelvic phantom.* LiF dosimeters surrounded by lead indicators were employed to measure absorbed doses five times in the phantom for each of the locations corresponding to the common and external iliac veins, the bladder base and the anterior rectal wall. These determinations indicated that close to the irradiators as well as at a distance from them the average variation amounted to 6, with a maximum of 12 per cent.

The a.p. and cross-table lateral roentgen films of two of these measurements served as a basis for the calculation of doses by computer. In the separate locations the differences between calculated and measured dose values as a percentage of the latter, were as follows: for the common iliac veins, average 5, maximum 14 per cent; for the external iliac veins, average 6, maximum 15 per cent; for the locations equivalent to the bladder base and the rectal wall, average 5, maximum 9 per cent; for the points on the long axes of the radium needles in the vaginal box the differences were greater and averaged about +20 per cent.

The measured doses used in the comparison with the computer data were also compared with measured values, obtained with teflon in place of the lead indicators surrounding the LiF rods. The differences between measurements performed with and without lead indicators did not exceed 12, mean 5 per cent in any location.

### Discussion

Computers are used as a routine in many centers nowadays to calculate the actual anatomy related dose distribution in the pelvis with a combination of intrauterine and vaginal irradiators. The results of such calculations have not been compared with the results of measurements in the same locations in various parts of the pelvis. Earlier investigations have indicated, however, that the location of the radiation sources as established from one sequence of roentgen projections is not representative of their position during the whole course of treatment, especially if the sources be made heavy by encapsulation in stainless steel (JOELSSON & BÄCKSTRÖM 1970). If dosimeters remain in place during the whole course of treatment, any effect of an inconstant location of the radiation sources will be accounted for in the measured values. This holds true for the

dosimeters introduced in the pelvic veins, where they are kept in a fixed position. Difficulties are however encountered in the long term measurement of doses in the urinary bladder and in the rectum. Here, on the other hand, dose rate measurements have proven clinical significance (GRAY & KOTTMEIER 1957, KOTTMEIER & GRAY 1961). Close correlations have also been found between the computer calculated and the measured dose rates at the bladder wall and the rectal mucosa (DOBROWOLSKI *et coll.* 1972). Calculated values may be considered to afford an accurate description of the dose distribution at a specific moment during treatment except along the long axis of a radium needle where the effect of oblique filtration is neglected.

Ten patients with tumors in moderately advanced stages were treated with the Stockholm method in this investigation. Even though this method emphasizes individualization the treatment in stages Ib and IIa is fairly standardized. Data representing the average dose distribution in the pelvis may therefore be regarded as indicating an optimal dose distribution since it has been established that this technique is capable of yielding a high 5 year survival rate (Annual Report on the Results of Treatment in Carcinoma of the Uterus and Vagina, Vol. 14 1967).

The measurement of doses in various portions of the pelvis with the thermoluminescent technique and LiF rods served as a basis for the comparisons with the computerized calculation of doses. In phantom measurements the average difference between repeated dose determination, was 6 per cent. It had been demonstrated previously that the variability of the calibration constants was 1.5 per cent when compared with a mean for all the dosimeters used. The difference in precision may be explained by the difficulty even in phantom experiments of obtaining a constant relationship between irradiators and dosimeters.

The LiF rods were interspaced with lead indicators for the identification of each numbered dosimeter during the clinical measurements. A problem has been whether or not the presence of lead by producing a characteristic radiation may influence the dose measured with the adjacent dosimeter. Measurements in the phantom gave no conclusive answer: the difference between doses measured with a dosimeter flanked and unflanked respectively, by lead lay within the experimental error.

With the phantom measurements in mind the doses in various parts of the pelvis calculated by the computer were compared with the results obtained with LiF dosimeters. Good agreement was observed in the external iliac veins on both sides: the differences exceeding 10 per cent only in the cranial parts of the veins. The mean of the individual differences increased at greater distances from the irradiators. The calculated values were larger than the measured ones in the common iliac veins on both sides where the highest mean difference amounted

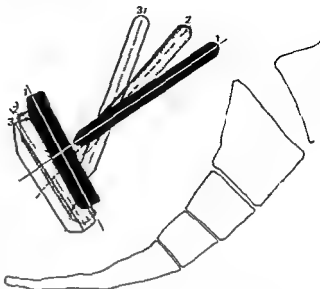


Fig. 4 The location of the radiation sources according to localization films exposed 2 hours (irradiators in black) 12 hours (irradiators in half tones) and 24 hours (irradiators in white) after the application. The intrauterine cylinder has rotated around the axis of symmetry and assumed a more oblique position. The angle between the cylinder and the box has become acute. The irradiators have moved in a caudal as well as a dorsal direction.

to 50 per cent. A difference of as much as +150 per cent was noted in the middle part of the common iliac vein in one patient and amounted to +10 per cent in 2 other patients.

Several factors may be responsible for the difference observed between calculated and measured doses in the pelvic side wall. It would appear that the most important factor is the unstable relationship during treatment between the radiation sources and the anatomic structures. The roentgen projections on which the computerized calculations are based depict the situation at one particular moment. In order to reduce any effect of anesthesia upon the tone of the pelvic musculature and thereby upon the position of the irradiators, the localization films were not exposed until the patient was fully awake. Despite this, repeat exposures during the latter part of treatment sometimes revealed that the position of the irradiators gradually changed in a caudal as well as a dorsal direction (Fig. 4). The intrauterine cylinder was found to rotate around the axis of symmetry and thereby assumed a position in the transverse rather than in the transverse-oblique plane through the body. This might augment the dose to the cranial portions of the vessels. The discrepancy between the calculated and measured values could be qualitatively explained almost always by the effect of such a movement.

It is suggested that light weight irradiators are best for retaining position during lengthy periods. Support for this contention was attained from an analysis of roentgenograms taken at intervals during more than 30 hours of treatment with cesium sources mounted in plastic tubing attached to a vaginal mould.

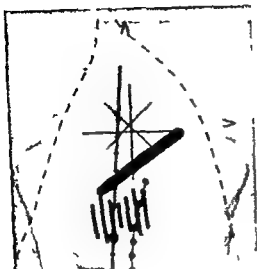


Fig 5 Intracavitary applicators with the intrauterine cylinder in a markedly asymmetric position

The first thing in the interpretation of localization films is to define the projection of the anatomic origin in the pelvis. Experience has established that the caudal end points of the sacro iliac joints, the cranial domes of the acetabular structures and in the lateral view the promontory of the sacrum are easily identified and make suitable landmarks. The next task is to determine the coordinates denoting the ends of the radium needles in the cylinder and vaginal box (7 needles). The distortion due to an oblique direction of the diagnostic roentgen beam is automatically corrected and selective magnification factors are applied for structures dispersed throughout the depth of the patient. The computer program also includes a calculation of the error in the determination of coordinates: data from the frontal film being compared along the longitudinal axis of the patient with those from the lateral film. A discrepancy of up to 4 mm is considered to be acceptable: the error in this series never exceeded 2 mm. The influence of an error in the determination of coordinates upon the calculated dose varies with the distance between the reference point and the radiation source. If this be about 3 cm, an error of only 0.3 mm will distort the calculated dose by more than 2 per cent.

The intrauterine cylinder used in the treatment of the patients in this series represented the original design while the vaginal box had been reconstructed in that the stainless steel enclosure was replaced by polymethyl metacrylate: this was necessary for identification of the individual needles in the box. The dose in the computer program is overestimated in the direction of the long axis of the needles. Such an overestimation was observed in the phantom experiments for

the positions in the direction of the axes of the radium needles. This may sometimes have played a part also where the intrauterine cylinder was placed markedly asymmetrically (Fig 5).

The calculated doses include a correction for tissue attenuation, assuming no inhomogeneity. It has been suggested that gas in the bowel interposed between the radiation sources and the points of interest, may disturb the correspondence between calculated and measured dose values in the pelvis. This is not likely, however, as the effect of tissue attenuation would be reduced by the presence of gas to less than allowed for in the calculation. The experimental results point to the opposite.

The dose rates in the close vicinity of the irradiators were measured regularly with the Siemens Gammameter. The position of the probe during the measurement of clinically significant dose rates could not be documented and consequently the results failed to lend themselves to comparisons with calculated doses. The doses in the bladder and rectum were sometimes measured with LiF dosimeters introduced in teflon catheters. There are reasons to believe that such a catheter floats, at least in the urinary bladder, and that dose values calculated from the position of the LiF rods as determined from localization films would differ considerably from those measured during the whole of treatment. This was verified regarding the urinary bladder, but the doses calculated at the reference point in the rectum were remarkably close to those measured with the LiF dosimeters in the rectal lumen. In both the bladder and the rectum the distance was estimated between the location of the flexible catheters and that imposed upon the dose detector of the Siemens Gammameter during the measurement procedure. The distance was up to 20 mm in the bladder as well as in the rectum. This is due to the fact that dose rate measurements according to the Stockholm technique define the dose rate at the contour of the tumor rather than that within the bladder or rectum.

The results of this investigation indicate that there is good agreement between measured and calculated doses in the vicinity of as well as at a distance from radiation sources in situations involving a stable relationship between the sources and the reference points. It seems that the differences observed between calculated and measured doses in the clinical series were due to movement of the heavy irradiators during treatment lasting as long as 24 hours. The computer calculation with such applicator systems provides information about the dose distribution around the radiation sources but caution must be exercised when applying the data to the designation of a treatment dose at specific anatomic points. For other types of applicators and especially if the relationship between radiation sources and pelvic anatomy be checked for constancy during the whole of treatment computerized dose calculations may be suggested.

## SUMMARY

The correspondence between doses in various parts of the pelvis as measured with LiF dosimeters or calculated by means of a computer was investigated. Close correlation of dose values along the external iliac veins with a discrepancy for those along the common iliac vein were evident. The discrepancy may be explained by the movement in caudal and dorsal direction of the heavy radium irradiators during lengthy periods of treatment.

## ZUSAMMENFASSUNG

Die Übereinstimmung zwischen den Dosen in verschiedenen Teilen des Beckens mit LiF Dosimetern gemessen oder mit Hilfe eines Computers berechnet wurde untersucht. Eine enge Korrelation langs der externen Venae iliacae mit einer Diskrepanz für solche Werte langs der Vena iliaca communis war offenbar. Der Unterschied kann durch die Bewegung in kaudaler und dorsaler Richtung der schweren Radiumirradiatoren während längeren Behandlungszeiten erklärt werden.

## RÉSUMÉ

Les auteurs ont étudié la correspondance entre les doses dans différentes parties du bassin selon qu'elles sont mesurées par des dosimètres à LiF ou qu'elles sont calculées par un ordinateur. Ils ont trouvé une bonne corrélation le long des veines iliaques externes mais une discordance pour les doses situées le long de la veine iliaque interne. La discordance peut s'expliquer par le mouvement de l'irradiateur à radium dans la direction caudale et dorsale pendant de longues périodes de traitement.

## REFERENCES

- ADAMS G. D. and MELER V. L. The use of a computer to calculate isodose information surrounding distributed gynecological radium sources. *Phys in Med Biol* 9 (1964) 533.
- Annual report on the results of treatment in carcinoma of the uterus and vagina. Fourteenth Vol. Statements of results obtained in 1951 to 1960 inclusive. Edited by H. L. Kottmeier. P. A. Norstedt & Soner Stockholm 1967.
- BALTER S., FREED B., RAGAZZONI G., SILVER W. and LALCHLIN J. S. An extension of the Memorial system for implant dosimetry. *Radiology* 87 (1966) 475.
- CARLSON C. A. Thermoluminescence of LiF: dependence of history. *Phys in Med Biol* 14 (1969) 107.
- DOBROWOLSKI F., BENNINGHOFF D. and VACIRCA S. Intercomparison of dosimetry in the rectum and bladder. Paper read at the Annual Meeting of the American Radium Society 1972.
- DUTREIX A. Utilisation d'un ordinateur pour la dosimétrie en curiethérapie. *Ann Phys Biol* 2 (1967) 139.
- GRAY M. J. and KOTTMEIER H. L. Rectal and bladder injuries following radium therapy for carcinoma of the cervix at the Radiumhemmet. *Amer J Obstet Gynec* 74 (1957) 1294.
- JONSSON I. and BACKSTROM A. Dose rate measurements in bladder and rectum. Intracavitary

- radiation of carcinoma of the uterine cervix *Acta radiol Ther Phys Biol* 7 (1969) 343
- — Applicators for remote afterloading technique for optimum pelvic dose distribution in carcinoma of the uterine cervix *Acta radiol Ther Phys Biol* 9 (1970) 233
- — LAGERGREN C and DIEHL J Dose distribution from intracavitary radium and supplementary external irradiation with regard to topography of lymph nodes in carcinoma of the uterine cervix *Acta radiol Ther Phys Biol* 9 (1970) 33
- JOHANSSON J M LINDSKÖLD B Å A and NYSTROM C E Pelvic dosimetry during radiotherapy of carcinoma of the cervix uteri *Acta radiol Ther Phys Biol* 8 (1969) 360
- KOTTMEIER H L Studies of the dosage distribution in the pelvis in radium treatment of carcinoma of the uterine cervix according to the Stockholm method *J Fac Radiol (Lond)* 2 (1951) 312
- and GRAY M J Rectal and bladder injuries in relation to radiation dosage in carcinoma of the cervix A five year follow up *Amer J Obstet Gynec* 82 (1961) 74
- LEDERMAN M and LAVERTON L F Dosage estimation and distribution in the radium treatment of carcinoma of the cervix uteri *Brit J Radiol* 21 (1948) 11
- MARTENSSON K A Thermoluminescence of LiF A statistical analysis of the influence of preannealing on the precision of measurement *Phys in Med Biol* 14 (1969) 11
- MEISBERGER L L KELLER R and SHALEK R J The effective attenuation in water of the gamma rays of gold 198 iridium 192 cesium 137 radium 226 and cobalt 60 *Radiology* 90 (1968) 90
- POWERS W E BOGARDUS JR C R WHITE W and GALLAGHER T Computer estimation of dosage of interstitial and intracavitary implants *Radiology* 85 (1965) 135
- ROSENWALD J C et DUTREIX A Etude d'un programme sur ordinateur pour le calcul des doses en curiethérapie gynécologique *J Radiol Électrol* 51 (1970) 651
- SHALEK R J and STOVALL M A The computation of dosage in interstitial and intracavitary radiation therapy *J chron Dis* 19 (1966) 519
- SNELLING M D ELLIS R F and JANESON D G Calculations of intracavitary and interstitial dose distributions by computer *In Progress in radiology* Vol 2 p 1709 ICA No 105 Excerpta Medica Foundation Amsterdam 1967
- IJFRBERG B JOHANSSON J M och LINDSKÖLD B Thermoluminescensdosimetri vid radiologisk behandling av gynekologisk cancer klinisk tillämpning, (In Swedish) *Nord Med* 80 (1968) 1537
- WALSTAM R The dosage distribution in the pelvis in radium treatment of carcinoma of the cervix *Acta radiol* 42 (1954) 237

## GENERAL EQUATION FOR THE CALCULATION OF NOMINAL STANDARD DOSE

by

R. L. DIXON

In order to compare the biologic effect on normal tissue of various dose time fractionation regimes in radiation therapy ELLIS (1968 1969 1971) has suggested the use of a nominal standard dose (NSD). The NSD is essentially a parameter which defines a particular iso-effect surface in a three dimensional space having axes dose time number of fractions. If the same NSD is achieved by different dose time fractionation schedules the damage to normal tissue is presumably the same. There is ideally a single value for the NSD which represents connective tissue tolerance but which may vary from center to center — depending on dosimetry and judgement (as to what is clinically tolerable). In reality tolerance will depend on the location and the size of the volume treated and hence one might have several NSDs — each one being appropriate for the treatment of a specific disease (or a class of diseases). According to ELLIS one should compute the NSD for one or more treatment regimes which represent in one's own judgement connective tissue tolerance and then adopt the average value as the tolerance NSD for one's own center. The NSD is then no longer a

---

Submitted for publication 5 July 1971



variable. Once the tolerance NSD is established one no longer computes the NSD for a given treatment schedule but rather a ret dose (ELLIS et coll 1969) which is computed as a partial tolerance (ELLIS 1969). If the ret dose is less than the NSD the given schedule does not achieve full tolerance.

The calculation of NSD (or ret dose) for a single course of treatment is quite simple however for a split course where there is a gap (or gaps) in the treatment or where the dose per fraction is changed during a single course of treatment the calculation is somewhat more complicated. In the examples of split course calculations previously given in the literature (ELLIS 1968, 1969, WINSTON et coll 1969), the NSD representing tolerance is presumed known and the number of fractions or the dose per fraction are then adjusted until the treatment schedule attains the specified NSD. These are specific numerical examples and no general equation has been derived for such calculations. Several of the examples available involve the use of a slide rule (WINSTON et coll 1969) which tends to obscure the reasoning used in the calculations.

In this paper a general equation is derived which can be used to calculate the NSD (or ret dose) for any situation, and which is readily suitable for computer calculations of these quantities. A simple FORTRAN program for these calculations is described. We use this program routinely (as part of a larger program for calculation of depth dose and treatment time) in order to evaluate the proposed treatment schedule for each patient—the ret dose being printed out on the patient's treatment record. Our main program which calculates and prints the entire treatment record for the patient is interlocked so that an 'unreasonable' ret dose cannot be given.

*Calculation of nominal standard dose* If the dose per fraction remains the same throughout the course of treatment, and the fractions are (more or less) evenly spaced in time the NSD may be calculated from the formula

$$NSD = \frac{D}{N_0 + T_{90}} \quad (1)$$

where  $N$  is the number of fractions,  $T$  is the time in days between the first and last fraction and  $D$  is the total absorbed dose delivered. In actual practice a fixed number of fractions are given per week, and hence  $T$  and  $N$  are not independent variables. For a given number of fractions, the exact value of  $T$  will depend on the day of the week the first fraction is given, however, the average value of  $T$  (for an arbitrary starting day) may be approximated by (WINSTON et coll 1969)

$$T = 6N^{1/3} \quad (2)$$

**Table**  
*Fractionation scheme*

No of fractions/week	$k$
5 (Mon - Fri)	0.89
4 (M T Th F)	1.13
3 (M W F)	1.51
2 (T Th)	2.29
1	4.61

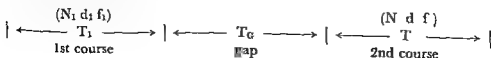
where  $k$  depends on the number of fractions per week and takes the values given in the Table. If we combine eqs (1) and (2), we obtain

$$NSD = N^{0.6957} k^{-0.11d} \quad (3)$$

where  $d = D/N$  is the dose per fraction.

The calculation of the NSD for a split course of treatment is somewhat more complicated. If there are gaps in the treatment, eq (1) no longer applies (nor does it apply if the dose per fraction or the number of fractions/week are changed during a course of treatment containing no gaps). The proper way to calculate the NSD for a split course is to use the concept of partial and residual tolerance (ELLIS 1968, 1969). For example, if the NSD representing tolerance is 1.760 ret (corresponding to 6,000 rad given in 30 fractions, 5 times per week over 6 weeks), then an incomplete treatment of 3,000 rad given in 15 fractions results in a partial tolerance of  $(15/30) \times 1.760 = 880$  ret (and not 1,133 ret as computed from eq (3)). The residual tolerance is then  $1.760 - 880 = 880$  ret. In the examples of split course calculations previously given in the literature (ELLIS 1968, 1969; WINSTON et al. 1969), the NSD representing tolerance is presumed known and the number of fractions or the dose per fraction are then adjusted until the specified NSD is attained. It is therefore necessary to invert this reasoning in order to obtain the (unknown) NSD for a specified treatment schedule. This is precisely the problem that would face a (hypothetical) therapy center which treated all patients with split courses in trying to establish their own tolerance NSD.

We will consider, for simplicity, a split course having a single gap as illustrated schematically below.



The total course consists of  $N_1$  fractions given in  $T_1$  days using  $f_1$  fractions/week and  $d_1$  rad/fraction followed by a gap of  $T_r$  days, followed by  $N$  fractions given in  $T$  days using  $f$  fractions/week and  $d$  rad/fraction. We assume that the NSD which represents full tolerance is specified (from our point of view we are starting with the desired answer). In order to reach full tolerance (in the absence of any gaps) at the dose/fraction and number of fractions/week specified in the first course we would require  $N_1$  fractions, where  $N_1$  is found by solving eq. (3) for the number of fractions required to reach the specified NSD, i.e.,

$$N_1 = \text{NSD}^{1/2} K_1^{0.1/2} d_1^{-1/2} \quad (4)$$

where  $K_1$  depends on  $f_1$  according to the Table. The partial tolerance at the end of the first course is then  $(N_1/N_1) \text{NSD}$ . The partial tolerance at the end of the gap is somewhat smaller, due to recovery (or repair) during the resting period and is given by

$$PT = \frac{N_1}{N_1} \text{NSD} \left( \frac{T_1}{T_1 + T_r} \right)^{0.11} \quad (5)$$

The residual tolerance is then

$$RT = \text{NSD} - PT \quad (6)$$

The number of fractions that would be required to reach full tolerance (starting from the first day and with no gap) at the rate specified in the second course is

$$N = \text{NSD}^{1/2} K^{0.1/2} d^{-1/2} \quad (7)$$

The number of fractions required to deliver the residual tolerance in the second course and thus bring the split course treatment up to full tolerance is given by  $(RT/\text{NSD})N$ . If we require this number of fractions to be equal to the number of fractions specified for the second course i.e.

$$N = \left( \frac{RT}{\text{NSD}} \right) N \quad (8)$$

then our calculation is self-consistent. That is, the second course — as specified — is exactly what is required to bring the treatment up to full tolerance. If we then combine eqs. (4)–(8) and solve for the NSD explicitly, we obtain an equation which represents the NSD for a split course treatment, namely

$$\text{NSD} = \left[ \left( \frac{N_1^{0.6} d_1}{K_1^{0.11}} \right)^{1/2} \left( \frac{T_1}{T_1 + T_r} \right)^{0.11} + \left( \frac{N^{0.6} d}{K^{0.11}} \right)^{1/2} \right]^{2/0.7} \quad (9)$$

This equation is also valid if there is no gap ( $T_r = 0$ ) but the course is split in the sense that the dose/fraction or the number of fractions/week is different for the two parts of the treatment. It is easy to show that eq. (9) reduces to eq. (3)

in the proper limit viz,  $T_G = 0$ ,  $K_1 = K_2 = K$  and  $d_1 = d = d$  Eq (9) is therefore generally applicable

For a course with two gaps i.e. three courses one can show by similar reasoning that the equation for the NSD is

$$\text{NSD} = \left\{ \left[ \left( \frac{N_1^{0.6357} d_1}{K_1^{0.11}} \right)^{1.53} \left( \frac{T_1}{T_1 + T_{G1}} \right)^{0.11} + \left( \frac{N^{0.6357} d}{K^{0.11}} \right)^{1.53} \right] \left( \frac{T_1 + T_2 + T_{G1}}{T_1 + T_2 + T_{G1} + T_G} \right)^{0.11} + \left( \frac{N^{0.6357} d_3}{K^{0.11}} \right)^{1.53} \right\}^{0.6357} \quad (10)$$

The generalization required for any number of courses is then obvious

It is necessary to point out that we have assumed the treatment to be a complete treatment and the NSD thus calculated represents in our judgement full tolerance for that particular treatment. Tolerance in this sense will depend on the location of the irradiated volume as well as the size of the volume e.g. when treating a large volume in the abdomen one usually must treat to a smaller NSD than would be used to treat a small volume in an extremity

*Calculation of ret dose* Once the NSD which represents connective tissue tolerance has been established then all treatment schedules can be referred to this tolerance NSD for purposes of comparison. That is one calculates a ret dose for a given treatment schedule — the ret dose being calculated as a partial tolerance. For an uninterrupted course of treatment the ret dose is computed as follows. If  $N$  is the number of fractions required to reach full tolerance and  $N$  fractions are given the ret dose is

$$\text{ret dose} = \left( \frac{N}{N} \right) \text{NSD} = \text{NSD}^{-0.53} N^{1.53} K^{-0.13} \quad (11)$$

where eq (3) has been used to compute  $N$ . It is evident that two different centers will compute different ret doses for precisely the same treatment schedule if they have chosen different tolerance NSDs. In fact the ratio of ret dose to NSD will be different as is evident from eq (11). (The two centers will however compute the same NSD for the same treatment schedule.)

For the split course treatment previously considered the ret dose is given by

$$\begin{aligned} \text{ret dose} &= \text{NSD} \left[ \frac{N_1}{N_1} \left( \frac{T_1}{T_1 + T_G} \right)^{0.11} + \frac{N}{N} \right] \\ &= \text{NSD}^{-0.53} \left[ \left( \frac{N_1^{0.6357} d_1}{K_1^{0.11}} \right)^{1.53} \left( \frac{T_1}{T_1 + T_G} \right)^{0.11} + \left( \frac{N^{0.6357} d}{K^{0.11}} \right)^{1.53} \right] \quad (12) \end{aligned}$$



## RÉSUMÉ

L'auteur présente une équation générale qui peut être utilisée pour calculer la dose standard nominale ou la dose ret pour tout plan de traitement si compliqué soit-il. Il donne un programme d'ordinateur pour ces calculs.

## REFERENCES

- ELLIS F The relationship of biological effect to dose time fractionation factors in radiotherapy. In Current topics in radiation research, Vol IV p 357 Edited by M Ebert and A Howard North Holland Amsterdam 1968
- Dose time and fractionation A clinical hypothesis Clin Radiol 20 (1969) 1
  - Nominal Standard Dose and the Ret Brit J Radiol 44 (1971) 101
  - WINSTON B M FOWLER J F and DEGRINDER W L Three or five fractions per week Treated on alternate treatment days Brit J Radiol 43 (1969) 715
- LIVERAGE W E A critical look at the Ret Brit J Radiol 44 (1971) 91
- WINSTON B M ELLIS F and HALL E J The Oxford NSD calculator for clinical use Clin Radiol 20 (1969) 8

## SELENIUM LABELLED TOLUIDINE BLUE AS AN AGENT FOR PARATHYROID SCANNING

### Theoretic considerations

by

T G BRIEN

Radioisotope scintillation scanning was first introduced as a medical diagnostic aid in the middle nineteen fifties. Since that time it has become a useful technique for the investigation of disorders of many organs particularly brain, thyroid, lungs, kidney, liver and bone. Two organs in which scintillation scanning has met with less success are the parathyroids and pancreas mainly because of the lack of a radiopharmaceutical which localizes sufficiently selectively in these organs.

Currently the radiopharmaceutical used for scanning the pancreas and parathyroids is  $^{75}\text{Se}$  selenomethionine, a  $^{75}\text{Se}$  analogue of the natural sulfur containing amino acid methionine. First introduced by PORCUPA in 1963 this compound has been used by a number of workers for scanning both pancreas and parathyroids. The results however have been far from encouraging (McGOWAN *et al.* 1968) having reviewed the literature of parathyroid scanning and reported a further eight cases concluded we think that selenomethionine  $^{75}\text{Se}$  is not sufficiently selectively concentrated in the parathyroid glands and that real progress in the scanning of these glands will depend upon the discovery of a more suitable radioactive compound. GARROW & SMITH (1968) considered a theoretic model of the process whereby selenomethionine is con-

concentrated in the parathyroids and concluded that it is not to be expected that the normal parathyroids will ever be demonstrable by the selenomethionine scanning technique even though the main difficulty in surgery of the parathyroids lies in the necessity to detect and identify not only the tumor or tumors but the remaining normal glands (DAVIES 1959). In 1967 POTCHEN et coll described 40 cases in only 24 of which the scan correlated with the surgical findings. They described the results as encouraging albeit frustrating. Similarly DI GIULIO & MORALES (1969) found that Se methuonine scanning identified the abnormal gland in only 13 of 23 patients with surgically proven parathyroid adenoma. They concluded that scanning was of little diagnostic use in patients with small adenomas (less than 2 g) and in patients with hyperplasia or with adenomas or hyperplastic glands lying in the thorax. Pancreatic scanning has proved somewhat more successful but there again many difficulties arise. Selenomethuonine is also taken up by the liver which due to its greater size accumulates more radioactivity than the pancreas. When the two organs overlap pancreatic identification is either interfered with or completely blocked. SODEE (1964) reported a series of 251 pancreatic scans and despite difficulties of interpretation successfully predicted carcinoma in 24 of 26 proven cases. In 151 cases later diagnosed as normal the scan interpretation was also normal. In 145 MELMED et coll (1968) also reported a high correlation between the scan and the ultimate diagnosis. They correctly predicted the result in 37 out of 40 consecutive cases both normal and pathologic.

Despite these good results the interpretation of pancreatic scans presents many difficulties even to experienced clinicians particularly when there is a generalized reduction in uptake of the radioisotope (AGNEW et coll 1967). Attempts at improving the results have ranged from methods aimed at increasing uptake by pancreatic stimulation (KING et coll 1966) to scanning liver and pancreas with two different isotopes and using electronic devices to subtract the liver scan from the superimposed liver pancreas scan to give an image of the pancreas alone (COTTRALL et coll 1968). Another technique employed has been the direct injection of selenomethuonine into the pancreatic artery (REUTER & COHN 1969) a method which has been shown to improve the pancreas/liver ratio of radioactivity (KUPIC & KASENTER 1969).

Nevertheless the limitations of selenomethuonine as a pancreatic scanning agent have prevented it from achieving its hoped for potentiality. Indeed CHARLESWORTH et coll (1970) have shown that with present methods small and hence resectable tumors of the pancreas cannot be detected.

*Toluidine blue* KLOPPER & MOE (1966) observed that when toluidine blue was administered intravenously to dogs it concentrated in the parathyroids, pancreas and gastric corpus staining these organs a distinct blue color. This



observation has later been confirmed (HURVITZ et coll 1967, KEAVENY & LITZGERALD 1968)

This dye has also been used to locate and identify parathyroid glands at surgery (KEOPFER & MOR 1966, KEAVENY & LITZGERALD 1968, YIACER & KREMENTZ 1969) and to detect a tumor of the pancreas (KEAVENY et coll 1971)

It soon became obvious, that if a suitable radioactive label could be incorporated within the toluidine blue molecule, without altering its ability to concentrate in the organs mentioned, a desirable scanning agent could be produced. The first attempt at producing a radioactive form of toluidine blue was by BRIEN & KEAVENY (1968) who labelled the dye with  $^{131}\text{I}$  and achieved a parathyroid to thyroid ratio of 2.97 in a dog, 20 minutes after injection. Further work, however, failed to improve this ratio which was approximately the same as that obtainable with scleromethuonine (BRIEN, unpublished observations). ARONER et coll (1969) also prepared  $^{131}\text{I}$  toluidine blue and measured its concentration in various organs in the rat. They found a parathyroid to thyroid ratio of 3.0 after five minutes but reported that the parathyroid uptake fell rapidly thereafter. They concluded that the labelled dye did not remain in the parathyroids for a sufficiently long period to render it a useful agent for external scintillation scanning.

Another attempt to produce a labelled version of toluidine blue using  $^{99}\text{Tc}$  pertechnetate failed because the material obtained was in an aggregated form and over 70 per cent of the injected dose accumulated in the liver (YEN et coll 1968).

Since the molecule of toluidine blue contains a sulfur atom within its ring structure of the molecule it was thought that replacement of this sulfur atom by a radioactive selenium atom could result in a molecule with the requisite biologic and functional properties.  $^{75}\text{Se}$  has an adequately long half life (121 days) and emits only gamma rays, the principal energies being 110 keV, 270 keV and 230 keV. These energies are all suitable for use with standard scintillation scanners.

*Calculation of theoretic specific activities and gland concentration of  $^{75}\text{Se}$  toluidine blue.* In order to evaluate the usefulness of  $^{75}\text{Se}$  toluidine blue as a scanning agent for the parathyroids the following calculations were made.

Molecular weight of  $^{75}\text{Se}$  toluidine blue is 300; molecular weight of selenium is 79.

Specific activity of  $^{75}\text{Se}$  after four weeks irradiation is 6.2 mCi/g (Radiochemical Manual). Specific activity of  $^{75}\text{Se}$  toluidine blue is  $79 \div 6.2 = 12.75$

mCi/g. If the tissue concentration in the parathyroids after a 100 mg/kg dose is 90  $\mu$ g toluidine blue/g parathyroid (KANG & Di GRULIO 1968) then the radioactive concentration is

$$\frac{1.63 \text{ mCi}}{\text{g}} \times \frac{90 \text{ } \mu\text{g}}{\text{g}} = 0.15 \text{ } \mu\text{Ci/g tissue}$$

Alternatively, if  $^{75}\text{Se}$  labelled toluidine blue can be synthesized using commercially available  $^{75}\text{Se}$  with a specific activity of 1 mCi/g selenium (Radiochemical Centre Amersham) then the specific activity of the  $^{75}\text{Se}$  toluidine blue could be

$$\frac{1 \times 79}{300} = 0.26 \text{ } \mu\text{Ci/g}$$

and the tissue concentration in the parathyroids would be

$$\frac{260 \text{ } \mu\text{Ci}}{1000 \text{ } \mu\text{g}} \times \frac{90 \text{ } \mu\text{g}}{\text{g}} \text{ or } 23.4 \text{ } \mu\text{Ci/g}$$

Although there is evidence to suggest that radioactivation might prove a simple and convenient method of preparing  $^{75}\text{Se}$  labelled toluidine blue from the non labelled molecule (McCONNELL et coll 1962 BADIELLO & BRECCIA 1966) the length of time required to irradiate the material to an adequately high specific activity would appear excessively long. It is suggested therefore that the more practical approach would be *ab initio* synthesis of the molecule using relatively high specific activity  $^{75}\text{Se}$ .

Given a reasonable high specific activity  $^{75}\text{Se}$  toluidine blue it still remains to be shown that sufficient radioactivity will be concentrated in a parathyroid gland to permit its demonstration by conventional scanning techniques. GARROW & SWITH (1968) determined that it was necessary for a point source to contain at least 0.5  $\mu$ Ci of  $^{75}\text{Se}$  in order to be visible on scan with the conditions they used. Assuming that a 1 g adenoma effectively represents a point source then a tissue radioactivity of 0.5  $\mu$ Ci/g would be necessary to permit demonstration of the gland. McGEOWN et coll (1968) using phantom tumors in a radioactive solution simulating an evenly distributed background found that for a 1 ml tumor a minimum activity of 0.16  $\mu$ Ci was necessary to allow detection when the background was one third this level. On the other hand Di GRULIO & BIERWALTES (1964) in similar experiments found a detection limit of 0.02  $\mu$ Ci in a 1 ml tumor again with a background of one third the tumor level. These latter figures agree fairly well with their own data on the tissue activity of parathyroid glands excised after administration of  $^{75}\text{Se}$  methionine (0.005 to 0.043  $\mu$ Ci/g) and also with that of McGEOWN et coll (0.012 to 0.021  $\mu$ Ci/g).

Although this evidence from  $^{75}\text{Se}$  methionine phantom investigations appears to be somewhat conflicting there is no doubt that a 1 g parathyroid adenoma

should be readily demonstrated at a tissue radioactivity concentration of 1  $\mu\text{Ci/g}$ .

According to the data of KANG & DI GIULIO (1968) a dose of 10 mg of toluidine blue per kg body weight results in a concentration of 90  $\mu\text{g}$  of dye per gram of parathyroid tissue. In order to achieve a radioactive concentration of 1  $\mu\text{Ci/g}$  parathyroid the necessary specific activity of toluidine blue would be 1  $\mu\text{Ci}/90 \mu\text{g}$  or 0.011  $\mu\text{Ci}/\mu\text{g}$ . The total dose to a 70 kg man would then be  $10 \times 70 \times 1000 \times 0.011 = 7700 \mu\text{Ci}$ .

This would appear to be an unacceptably high dose of radioactivity to administer in a diagnostic test considering that the generally accepted dose of Se methionine is 200 to 250  $\mu\text{Ci}$ .

An alternative method of approach is to calculate the percentage of the administered dose which is concentrated in parathyroid tissue. Using the same data as above the dose to a 70 kg man is  $10 \times 70 = 700 \text{ mg}$ . The parathyroid concentration is 90  $\mu\text{g/g}$  tissue. Therefore the per cent dose/g tissue is

$$\frac{90 \times 100}{700 \times 1000} = 0.013 \text{ \% / g}$$

This is about the same as that found after Se methionine (McGROW *et coll*)

Since toluidine blue has a much larger molecular weight than methionine (306 vs against 117) the incorporation of one labelled atom of selenium into each molecule would result in a much higher specific activity for selenomethionine than for seleno-toluidine blue. Thus if the same percentage of the administered dose of each is incorporated into parathyroid tissue a higher concentration of radioactivity would be expected in the case of selenomethionine. Thus it would appear that on a molar basis selenomethionine is in fact concentrated to a greater extent in the parathyroids than is toluidine blue. However the average parathyroid to thyroid ratio of radioactivity is about 3 after Se methionine administration (DI GIULIO & MORALES 1969; McGROW *et coll* 1968). After toluidine blue this ratio rises to 10 (KANG & DI GIULIO 1968). Since the background activity registered by the scintillation counter would thus be decreased the absolute level of activity necessary for demonstration of the parathyroids would also be decreased. This factor was taken into account by KANG & DI GIULIO when they estimated that for a 70 kg man 350  $\mu\text{Ci}$  of  $^{125}\text{I}$  labelled toluidine blue would be sufficient to demonstrate a 0.3  $\mu\text{Ci/g}$  parathyroid at a tissue concentration of 0.03  $\mu\text{Ci/g}$ , this figure of 0.03  $\mu\text{Ci/g}$  being their measured level of radioactivity in excised parathyroid after Se methionine.

Another factor which needs to be taken into account is the fact that the permissible dose of Se methionine is limited by its long biologic half life in man which has been variously reported as being as low as 23 and as high as



Scan of parathyroid phantom containing four mock tumors 1—1  $\mu\text{Ci}$  in 1 ml 2—0.3  $\mu\text{Ci}$  in 0.3 ml 3—0.5  $\mu\text{Ci}$  in 1 ml 4—0.5  $\mu\text{Ci}$  in 0.5 ml

144 days (SODEE 1964 PENNER 1966). Although there is to date no published data on the biologic half life of toluidine blue in man the impression gained from clinical investigations is that the figure is of the order of days rather than weeks.

This is supported by the findings of MORTENSEN & McRAE (1970) that no residual toluidine blue could be found in any organ of dogs who had received intravenous injections of the dye forty eight hours previously. From the radiation dosimetry point of view therefore the acceptable dose of  $^{75}\text{Se}$  labelled toluidine blue might well be considerably greater than that for  $^{75}\text{Se}$  methionine. The final answer to this question however will probably have to await the production of the labelled molecule for metabolic radiotracer investigations.

*Experimental.* In order to evaluate the level of activity which would be required and the minimum size of parathyroid detectable a number of experiments were carried out using a phantom model of the parathyroids. This phantom consisted of a circular dish 12 cm in diameter in which were placed four small flat bottomed test tubes arranged in a square of side 4 cm. These test tubes contained a solution of  $^{75}\text{Se}$  of the following volumes and concentrations.

Tube	Volume	Concentration
1	1 ml	1 $\mu\text{Ci}/\text{ml}$
2	0.3 ml	1 $\mu\text{Ci}/\text{ml}$
3	1 ml	0.5 $\mu\text{Ci}/\text{ml}$
4	0.5 ml	1 $\mu\text{Ci}/\text{ml}$

The circular dish was filled with a solution of 100 ml of  $^75\text{Se}$  at a concentration of  $0.1 \mu\text{Ci/ml}$ .

The phantom was scanned using a Nuclear Chicago Pho-Dot scanner using a 19 hole collimator at a speed of 10 cm/min and a suppression factor of 80 per cent. The result is shown in the Figure. All four tumors are clearly seen and some indication of their relative sizes can also be deduced.

### Conclusion

If  $^75\text{Se}$  labelled toluidine blue with a specific activity of  $0.01 \mu\text{Ci}/\mu\text{g}$  can be synthesized and if this compound retains the biologic properties of toluidine blue it should concentrate sufficiently selectively in the parathyroids to prove a useful scanning agent for these glands. Tumors down to 300 mg or less in size should be adequately demonstrated instead of the 1 to 2 g limit currently obtainable with  $^75\text{Se}$  methionine. Some indication of tumor size may also be possible.

### Acknowledgement

The author wishes to thank Mr P. Coughlan, Physicist, St. Anne's Hospital, Dublin for scanning facilities. This work was supported by a grant from the Irish Cancer Society.

### SUMMARY

The usefulness of radioactive labelled analogues of toluidine blue as scanning agents for pancreas and parathyroids is considered with particular reference to the minimum size of parathyroid adenoma likely to be demonstrated. It is concluded that a selenium labelled analogue of toluidine blue should prove a better scanning agent for parathyroids than selenomethionine and that with appropriate specific activities adenomas of 300 mg or less could be detected.

### ZUSAMMENFASSUNG

Die Anwendbarkeit radioaktiv gezeichneter Analoge von Toluidin Blau als Substanzen für das Scanning des Pankreas und der Parathyreoidea wird erwogen besonders in Hinblick auf die geringste darstellbare Grösse des Adenoms der Parathyreoidea. Man kommt dazu dass ein Selenium-gezeichnetes Analog von Toluidin Blau sich mehr als Scanning Substanz der Parathyreoidea eignet als Selenmethionin und dass mit geeigneten spezifischen Aktivitäten Adenome von 300 mg oder weniger nachgewiesen werden könnten.

### RÉSUMÉ

L'auteur étudie l'utilité d'analogues marqués radio-activement de bleu de toluidine utilisés pour la scintigraphie du pancréas et des parathyroïdes. Il a étudié en particulier les dimensions minimales du plus petit adénome parathyroïdien que ces corps permettraient de mettre en évidence. Il conclut qu'un analogue du bleu de toluidine marqué au sélénium pourrait être un meilleur agent scintigraphique pour les parathyroïdes que la sélénométhionine et que avec des activités spécifiques appropriées on pourrait détecter des adénomes de 300 mg ou moins.

## REFERENCES

- AGNEW J A, MCCARTHY D M, MELMED R N and BOUCHIER I A D Count rate analysis as an adjunct to the Se selenomethionine pancreas scan *Brit J Radiol* 42 (1969) 762
- ARCHER E G, POTCHEN E J, STÜDER R and SEGEL H Distribution of <sup>75</sup>Se toluidine blue in the rat (abstract) *J nucl Med* 10 (1969) 386
- BADIELLO R e BRECCIA A Preparazione di selenotrea Se per atti azione neutronica e sua decomposizione radiologica (In Italian) *Ric Sci* 36 (1966) 335
- BRIEN T G and KEAVENY V Iodinated toluidine blue A potential agent for parathyroid scanning *Int J appl Radiat* 19 (1968) 820
- CHARLSWORTH D, TESTA H J, PULLAN B R and TORRANCE B Radioisotope scanning in the diagnosis of pancreatic disease *Brit J Surg* 57 (1970) 413
- COTTRALL M F, BURN G and FIELD E O Localization in scintiscanning using two isotopes *Int J appl Radiat* 19 (1968) 523
- DAVIES D R Discussion on parathyroid disease *Proc roy Soc Med* 52 (1959) 995
- DI GIULIO W and BEIERWALTES W H Parathyroid scanning with selenium 75 labelled methionine *J nucl Med* 5 (1964) 417
- and MORALES J O The value of selenomethionine Se scan in preoperative localization of parathyroid adenomas *J Amer med Ass* 209 (1969) 1873
- GARROW J H and SMITH R The detection of parathyroid tumors by selenomethionine scanning *Brit J Radiol* 41 (1968) 307
- HLRVITZ R J, HLRVITZ J S and MORGENTHAU L In vivo staining of the parathyroid glands and pancreas *Arch Surg* 95 (1967) 274
- KANO G H and DI GIULIO W Potential value of toluidine blue analogs as parathyroid scanning agents *J nucl Med* 9 (1968) 643
- KEAVENY T V and FITZGERALD P Selective parathyroid staining *Lancet* 1968 II p 284
- , TAYES R and BELZER F O A new method for intra-operative identification of insulinomas *Brit J Surg* 58 (1971) 235
- KINO E R, SHARPE A, GRUBBS W et coll A study of the morphology of the normal pancreas using Se<sup>75</sup> methionine photoscanning *Amer J Roentgenol* 96 (1966) 657
- KLOPPER P J and MOE R E Demonstration of the parathyroids during surgery in dogs *Surgery* 59 (1966) 1101
- KUPIC E A and KASENTER B A Experimental pancreatic scanning Preliminary results using intra arterial Se selenomethionine and hormone stimulation *Radiology* 93 (1969) 1376
- MCCONNELL K P, MAUTNER H G and LEDDICOTTE G W Radioactivation as a method for preparing Se labelled selenium compounds *Biochim Biophys Acta* 59 (1962) 217
- MCGROWN M G, BELL T K, SOYANVO M A O et coll Parathyroid scanning in the human with selenomethionine *Se Brit J Radiol* 41 (1968) 300
- MELMED R N, AGNEW J E and BOUCHIER I A D The normal and abnormal pancreatic scan *Quart J Med* 37 (1968) 607
- MORTENSEN R A and McRAE J Toluidine blue-O and its analogs as parathyroid and pancreatic scanning agents *Arch Surg* 100 (1970) 710
- PENNER J A Investigation of erythrocyte turnover with selenium 75 labelled methionine *J Lab clin Med* 67 (1966) 427
- POTCHEN E J Isotopic labelling of the rat parathyroid as demonstrated by autoradiography *J nucl Med* 4 (1963) 480

- WATTS H G and AWWAD H K Parathyroid scintiscanning Radiol Clin N Amer 5 (1967) 267
- RADIOCHEMICAL MANUAL Second edition Radiochemical Centre Amersham 1966
- REITER S R and COHN H J Selective administration of selenomethionine Radiology 97 (1969) 158
- SONDEE H D Radioisotope scanning of the pancreas with selenomethionine Radiology 83 (1964) 910
- YEAGER R M and KREMNETZ E T Toluidine blue in identification of parathyroid glands at operation Ann Surg 169 (1969) 829
- YEH S H DELAHAY J E and KRIS J P Tc 99m labelled toluidine blue B for liver scintillography Int J appl Radiat 19 (1968) 885

## INCIDENCE OF PULMONARY CARCINOMA IN ICELAND BETWEEN 1931 AND 1964

by

GISLI FR. PETERSEN

The National Hospital of Iceland — Landspítalinn — was opened in December 1930 and in 1959 the author published a review of the cases of pulmonary carcinoma observed between 1931 and 1957. The present report is a continuation of the earlier one and includes material up to and including 1964. The cases have been assembled not only from Landspítalinn but also from the Reykjavík City Hospital and St. Joseph's Hospital. Only those cases in which the diagnosis had been fully established by histologic examination at autopsy, biopsy or by cytology were accepted in accordance with the requirements of the UICC. Five cases have been included, however, in which the clinical and roentgenologic diagnosis seemed to be beyond doubt although no biopsy had been carried out and in 30 cases the diagnosis was based solely on the autopsy findings. In Iceland all autopsies and biopsies are performed at the Institute of Pathology at the University and the relevant histologic material from the Institute was re-examined and classified for this investigation (J. Hallgrímsson).

This report was presented as a part of the Gosta Forssell Memorial Lecture given at the first meeting in Reykjavík, Iceland of the Nordic Society of Medical Radiology in June 1971. Submitted for publication 11 October 1971.



Table

*Pulmonary carcinoma diagnosed during the period 1931 to 1964 Sex and age distribution*

Age	30-39		40-49		50-59		60-69		70-79		80+		Total		Both sexes
	M	F	M	F	M	F	M	F	M	F	M	F	M	F	
1931-1944			1		4	1							5	1	6
1945-1949			2		3	1	2	1	1				6	2	10
1950-1954	2		1		5	3	4	2	1				13	5	18
1955-1959	2	1	5	1	12	4	6	5	3	2	2		30	13	43
1960-1964	1	1	6	1	22	4	15	8	4	6	4		48	24	72
Total	5	2	15	2	44	13	27	16	8	2	4		101	45	146

The Cancer Registry in Iceland was opened in 1954. The cases registered include those in which the diagnosis was based solely on the clinical findings or the death certificate and where histologic confirmation was consequently lacking. The number of cases of pulmonary carcinoma on the register is a little over 25 per cent higher than in the present material. It may probably be assumed that some of the cases that were not verified histologically really were cancer cases, and the incidence figures that emerge in the present material ought therefore to be lower than the true figure.

In addition to the aim of obtaining information on the incidence of pulmonary carcinoma and its sex and age distribution, an attempt was made to obtain a complete a clinical and roentgenologic evaluation of the cases as possible from the beginning. All case records, roentgen films and lung reports, including those made before the patients had developed any symptoms, were investigated in order to determine, if possible, the earliest roentgen signs and the incidence of the different findings at roentgen examination.

The age and sex distribution in the 146 patients is given in the Table. Only 6 cases, 5 men and 1 woman, were diagnosed during the first period, which included 14 years from 1931 to 1944. The later periods cover 5 years. The number of cases was nearly twice as high in the second and third periods, and in the fourth and fifth period an increase of just over 67 per cent is noted. A considerable increase had thus taken place during the period covered by the investigation.

The average annual incidence per 100 000 men and women separately is indicated in Fig. 1. In the first period, during 1931 to 1944, the incidence was just under 0.5. In 1945 to 1949 the figure for the men was 2.1. It increased rapidly and during the 1950 to 1954 and 1955 to 1959 periods it more than doubled, to 7.1. In the final period, 1960 to 1964, it increased by 18 per cent, to 10.5. For the

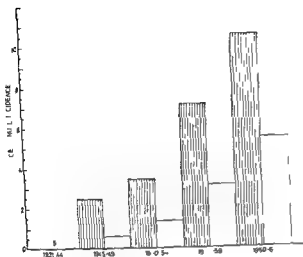


Fig 1 Incidence of pulmonary carcinoma per 100 000 inhabitants between 1931 and 1964 Hatched field represent men and unfilled women

women the annual incidence was only 0.6 per 100 000 between 1945 and 1949. A considerable increase even more marked than in the men is noted for this category also: during the 1955 to 1959 and 1960 to 1964 periods the figure rose by 74 per cent to 5.4.

According to the UICC's report the annual incidence of pulmonary carcinoma in Denmark for the period covering 1958 to 1962 was 40.6 for men and 7.5 for women per 100 000. In Norway the incidence for the years 1959 to 1961 was 17.6 for men and 4.2 for women. In the same period the incidence in Sweden was 22.7 for men and 6.2 for women and in Finland 60.2 for men (the highest figure among the Nordic countries) and only 5.0 for women.

In comparison the incidence of cases per 100 000 was much lower in Iceland than in the above mentioned countries. The figure for men in Iceland for 1960 to 1964 was 10.5 whereas it was twice as high in Norway and Sweden, four times as high in Denmark and six times as high in Finland. For women on the other hand the incidence in Iceland was not much lower than in the other Nordic countries. It should however be pointed out that the number of patients increases annually and the 1959 to 1961 period for the Nordic countries is thus not wholly comparable with the 1960 to 1964 period for Iceland.

The table also shows that most of the men (46 or 44.2 per cent) belonged to the 50 to 59 year age group. The number of women was highest in the 60 to 69 year age group (16 or 35.6 per cent). In the 70 to 79 year group there were 9 men and 8 women (8.6 and 17.8 per cent respectively).

Table

*Pulmonary carcinoma diagnosed during the period 1931 to 1964. Sex and age distribution*

Age	30-39		40-49		50-59		60-69		70-79		80+		Total		Both sexes
	M	F	M	F	M	F	M	F	M	F	M	F	M	F	
Sex															
1931-1944			1		4	1							5	1	6
1945-1949			2		3	1	2	1	1				8	2	10
1950-1954	2		1		5	3	4	2	1				13	5	18
1955-1959	2	1	5	1	12	4	6	5	3	2	2		30	13	43
1960-1964	1	1	6	1	22	4	15	8	4	6		4	48	24	72
Total	5	2	15	2	40	13	27	16	8	11	4		101	45	146

The Cancer Registry in Iceland was opened in 1954. The cases registered include those in which the diagnosis was based solely on the clinical findings or the death certificate and where histologic confirmation was consequently lacking. The number of cases of pulmonary carcinoma on the register is a little over 25 per cent higher than in the present material. It may probably be assumed that some of the cases that were not verified histologically really were cancer cases, and the incidence figures that emerge in the present material ought therefore to be lower than the true figure.

In addition to the aim of obtaining information on the incidence of pulmonary carcinoma and its sex and age distribution, an attempt was made to obtain a complete a clinical and roentgenologic evaluation of the cases as possible from the beginning. All case records, roentgen films and lung reports, including those made before the patients had developed any symptoms, were investigated in order to determine, if possible, the earliest roentgen signs and the incidence of the different findings at roentgen examination.

The age and sex distribution in the 146 patients is given in the Table. Only 6 cases, 3 men and 3 women, were diagnosed during the first period, which included 14 years from 1931 to 1944. The later periods cover 5 years. The number of cases was nearly twice as high in the second and third periods, and in the fourth and fifth period an increase of just over 67 per cent is noted. A considerable increase had thus taken place during the period covered by the investigation.

The average annual incidence per 100,000 men and women separately is indicated in Fig. 1. In the first period, during 1931 to 1944, the incidence was just under 0.5. In 1945 to 1949 the figure for the men was 2.4. It increased rapidly and during the 1950 to 1954 and 1955 to 1959 periods it more than doubled to 7.1. In the final period, 1960 to 1964, it increased by 48 per cent to 10.5. For the

the most common site of the disease. Infiltration had occurred in and beside the hilus in 59 cases (50 per cent) and in the middle or peripheral parts of the lungs in 45 cases (37.8 per cent). Bronchial stenosis in association with segmental or lobar atelectasis was present in 69 cases (58 per cent). This is a high proportion and suggests that the correct diagnosis had been made comparatively late in this material. Exudative pleurisy was the dominant roentgen change in 11 cases (9.2 per cent). Pleural thickening and apical lung changes with fibrosis are observed relatively often in association with pulmonary carcinoma. Such lung changes were noted in 32 per cent. In some, it was doubtless remains of a tuberculous infection.

Pulmonary tuberculosis has been considered by some investigators to be one of the irritative factors that might have a pathogenetic connection with pulmonary carcinoma. In the present material there were 10 cases (6.7 per cent of the whole series) with concurrent tuberculous pulmonary changes, in 2 instances with cavities.

The histologic classification of the material followed that recommended by WHO. In 13 cases (8.7 per cent) no classification could be made. However, in the other 136 cases epidermoid carcinoma was noted in 17.4 per cent, anaplastic small cell carcinoma in 33.6 per cent, adenocarcinoma in 22.1 per cent, and large cell carcinoma in 16.8 per cent. One case was considered to be a carcinoid tumour (bronchial adenoma) when the histologic material was re-examined.

This result is remarkable, seeing that epidermoid carcinoma constituted only 17.4 per cent of the cases when a figure of around 50 per cent was to be expected according to other statisticians. Instead, anaplastic carcinoma and large cell carcinoma together accounted for 50 per cent of the cases.

In the 59 cases in which the tumour was situated in the hilar region or centrally, 45.8 per cent had anaplastic small cell carcinoma and 16.9 per cent epidermoid carcinoma. But among the 45 cases with the tumour in the middle parts of the lungs or at the periphery, nearly one third (31.1 per cent) had adenocarcinoma and 26.7 per cent epidermoid carcinoma. Anaplastic and large cell carcinoma together accounted for nearly 33 per cent (15.6 and 17.8 per cent respectively).

### Conclusion

It has been found that the incidence of pulmonary carcinoma is relatively low, but a high proportion of cases are women. The histologic distribution is also unusual, since only about 17 per cent of cases consist of epidermoid carcinoma, whereas anaplastic and large cell carcinoma together account for nearly 50 per cent of the cases.

## SUMMARY

The incidence of pulmonary carcinoma in Iceland between 1931 and 1961 has been investigated. It has been found to be relatively low but a high proportion of cases are women.

## ZUSAMMENFASSUNG

Es wurde das Vorkommen von Lungenkarzinomen auf Island zwischen 1931 und 1961 untersucht. Dieses war relativ niedrig jedoch war ein hoher Anteil der Fälle Frauen.

## RÉSUMÉ

L'auteur a étudié la fréquence du cancer pulmonaire en Islande entre 1931 et 1961. Cette fréquence est relativement basse mais l'auteur a trouvé une forte proportion de cas féminins.

**NINTH SYMPOSIUM  
NEURORADIOLOGICUM  
GOTHENBURG  
24—29 August 1970**

The majority of the papers presented at the Symposium dealt with the diagnostic aspects of radiology and are published in separate issues. The following papers belonging to the therapy and biology sections have been submitted for publication in *Acta Radiologica*. The titles of all the papers read at the Symposium are also published and arranged in alphabetical order according to first author's name.

ANDERSSON B, LARSSON B, LENSJELL L, MAIR W, REYED B, SOLRANDER P and WENNERSTRAND J	Histopathology of late local radiolesions in the goat brain (published in <i>Acta radiol Ther Phys Biol</i> 9 (1970) 385)	
DAHLIN H, ROANDER KERSTIN and SVEDBERG J	On the selection of dose distributions in clinical cerebral radiosurgery (not received)	—
DAHLSTROM A, HAGGENDAL J and ROENGRE B	The effect of X irradiation on monoamine con- taining neurons in the rat hypothalamus (not received)	—
COLD L, H A, KIEFFER S A, D'ANGIO G J, FALLON V T and LONG D M	Current status of intrathecal radiogold in the treatment of medulloblastoma	329
HAMBERGER A, BLOMSTRAND S and ROSENGREN B	The effect of X irradiation on respiration and protein synthesis in neuronal and glial cell frac- tions (not received)	—

HARIRI N I AKSU Y FALAKALI S and TUNGER O I	Attempt to modify the ionizing radiation induced histopathologic effects on the central nervous system by reserpine administration	341
KIRSCH W M SCHULZ H FUCHS H and NAKANE P	Effect of ionizing radiation on nuclear energy transduction in normal and neoplastic glia—A quantitative cytochemical investigation	349
LARSON B LEKSELL L and WENNERSTRAND J	Techniques for irradiation of small intracranial structures through the intact skull (not received)	—
LARSON B LIDEN A and SARBY B	Quantitative study of stereotaxic radiolesions (not received)	—
VASCULE CL T	Recherches cliniques et expérimentales sur l'ac- tion de petites doses de radiations ionisantes ap- pliquées sur le SNC (not received)	—
WILSON G H BYFIELD J and HANAFER W A	Atrophy following radiation therapy for centr nervous system neoplasms	361

## CURRENT STATUS OF INTRATHECAL RADIOGOLD IN THE TREATMENT OF MEDULLOBLASTOMA

by

L. H. A. GOLD, S. A. KIEFFER, G. J. D'ANCIO, V. T. FALLON and D. M. LONG

The medulloblastoma is a highly radiosensitive tumor of childhood occurring in the cerebellum. The standard treatment regimen of these patients has been surgical removal of the primary tumor followed by irradiation of the entire cerebrospinal axis and supplemental irradiation to the posterior fossa. Survival following this regimen has been quite poor. According to BLOOM *et coll* (1969) the main cause of death is recurrence of the primary tumor. Excluding postoperative deaths, MCFARLAND *et coll* (1969) have calculated a 40 % mortality in one year and a 75 % mortality within three years in a recent extensive review of the literature. Better survival has been reported by PATERSON (1963) and JENKIN (1969). The latter reports a 62 % three year survival and a 53 % five year survival.

Exfoliated cells from the primary tumor disseminate readily via the cerebrospinal fluid pathways resulting in so-called drop metastases along the spinal axis. MCFARLAND *et coll* (1969) calculated a 33 % incidence of metastases outside the posterior fossa of which the vast majority were to the spinal axis.

The high incidence of metastatic deposits along the spinal axis and the frequency of recurrence of the primary tumor suggest that the standard treatment regimen is inadequate. A therapeutic dilemma arises when the tolerance of the



central nervous system to external radiation has been reached and the patient requires further treatment to eradicate spinal axis metastases. A possible solution to this problem has been proposed utilizing a  $\beta$  emitting radionuclide ( $^{198}\text{Au}$ ) intrathecally (D'Angio et coll 1968, KIEFFER et coll 1966, 1969). Radioactive colloidal gold is primarily a  $\beta$  emitter with an average range of under 500 microns and could potentially eradicate nests of tumor cells a few cell layers thick while sparing the underlying central nervous system parenchyma. Because of its short range radiogold has no significant effect on tumor masses with any bulk. Therefore implants visible at myelography must be treated first with external radiation until disappearance. Following this, intrathecal radiogold can be administered.

KIEFFER et coll (1966, 1969) reported on laboratory studies in 19 dogs following intraventricular injection of colloidal radiogold. The dogs were sacrificed at various time intervals up to eighteen months. Gross and microscopic examinations demonstrated no parenchymatous changes in the brain or spinal cord but many animals demonstrated perivascular round cell infiltration in the leptomeninges. Autoradiograms showed a rapid and fairly even distribution of the radioactive colloid over the leptomeningeal surfaces of the spinal cord and cauda equina. Based on these findings a treatment regimen was designed to evaluate the clinical effect of intrathecal radiogold in the management of patients with medulloblastoma.

### Treatment regimen

The following regimen was designed and followed as closely as clinical exigencies permitted in the management of all patients investigated. Radical tumor excision with removal of all grossly identifiable neoplasm if possible is utilized as the primary treatment. Cerebrospinal fluid shunts are employed when necessary. A myelography is performed as soon after posterior fossa exploration as clinical considerations permit. If negative 3500 rad are delivered to the entire intracranial contents and spinal canal in three weeks using  $^{60}\text{Co}$  external teletherapy. A single spade shaped posterior head and pine portal is supplemented by an opposing anterior skull field. In an effort to prevent local tumor recurrence an additional 1500 rad is delivered to the posterior fossa through opposing lateral portals in one and one half weeks. Following this another myelography is performed employing a sufficient volume of Pantopaque to demonstrate completely the spinal subarachnoid space particularly on its posterior aspect where implants are most likely to occur. If the myelography reveals no visible tumor deposits the Pantopaque is completely withdrawn and radiogold is administered intrathecally. If myelography demonstrates drop metastases local

external radiotherapy is employed until the metastatic deposits are no longer visible at myelography. When the tumor mass has disappeared, radiogold is then inserted intrathecally. Another similar procedure is followed if metastases are identified at the first myelography. This has been described in a previous report (D'Angio et coll.)

The radiogold is introduced intrathecally following the myelography with the patient in the prone position and tilted head down at an angle sufficient to insure cephalad flow of the radiogold (usually 45 to 60 degrees). Ten to fifteen mCi of  $^{198}\text{Au}$  mixed with 3 to 5 ml of cerebrospinal fluid are introduced. No barbotage is used for reasons discussed elsewhere (Kieffer et coll. 1966). The patient remains tilted head down for 15 minute periods in the prone, supine, and both lateral decubitus positions. External monitoring with a suitable hand held survey meter is performed to document cephalad migration of the radioactive gold. The patient then is returned to the ward where he remains in the prone, supine, and right and left lateral decubitus positions for 1/2 hour in each position.

Three courses of intrathecal radioactive gold are given at approximately six week intervals, each course preceded by myelography. Assuming an even distribution along the meningeal surfaces, each course of radiogold gives an estimated 3 000 rad to a layer of tissue 100 microns beneath the meningeal surfaces (D'Angio et coll.). Only if the myelography is negative is the radiogold administered. If metastases are seen at myelography, the patient receives additional local external radiation (usually 1 000 to 1 500 rad in 10 to 14 days) to the region of metastasis. Another myelography is performed and if the tumor has disappeared, radiogold is introduced in the belief that any remaining tumor deposits must be extremely small and thus amenable to treatment with radioactive gold.

Large volumes of Pantopaque have been employed for myelography in order to demonstrate completely the spinal subarachnoid space on both its anterior and posterior aspects. The average volume of contrast medium used on the younger patients was 24 ml with a range of 12 to 36 ml.

### Clinical data

Fourteen patients with histologically proven medulloblastoma have been treated at the University of Minnesota Hospitals. There were 10 males and 4 females in the group. The average age of the patients was 8 years with a range from 2 1/2 to 17 years. Thirty-four gold insertions were done altogether.

The intrathecal administration of radioactive gold produced relatively few and minor immediate complications. The most common reaction was a mild fever (in seven patients) which occurred a few hours after the myelography and radiogold insertion. The fever was rarely greater than 38.5° C and usually

Table 1  
*Medulloblastoma survival rate (Life Table Method)*

Periods after diagnosis (yrs)	Alive at beginning of interval	Died during interval	Withdrawn during interval	Projected proportion surviving	Standard error
0-0.5	12	1	0	0.92	0.08
0.5-1.0	11	0	0	0.92	0.08
1.0-1.5	11	1	1	0.83	0.11
1.5-2.0	9	0	0	0.83	0.11
2.0-2.5	9	1	2	0.73	0.14
2.5-3.0	6	0	2	0.73	0.14
3.0-3.5	4	0	3	0.73	0.14

disappeared within 24 hours. Six patients had mild back pain at or near the lumbar puncture site. Six complained of headache and four of nausea and vomiting. These complaints were all mild and transient and cleared within 24 to 36 hours. One patient had a mild transient meningismus.

There were no postoperative deaths in this series. Gross survival data are given utilizing the Life Table Method (CUTLER & EDERER 1958) (Table 1). Two patients were eliminated from the survival data since both were operated upon and treated with radiation at another hospital. Neither received radiogold in the initial postoperative period according to protocol. They were seen six to nine months later at the University of Minnesota Hospitals with metastases and were obviously poor candidates for treatment. There is an 83% estimated two year survival rate with a standard error of 11%. The estimated three year survival rate is 73% with a standard error of 14%. The standard errors are large because of the small number of patients in this series. It remains to be seen whether survival figures based on longer follow up will be different from the best results previously reported where the treatment regimen did not include intrathecal radiogold (JENKIN PATERSON).

Two of the 5 patients who died have been mentioned in brief above. One had malignant cells in the blood and metastases in the spinal canal. He eventually died with brain metastases but without clinical evidence of recurrence in the cerebellum. A detailed history of the clinical course of the other case (who also presented with spinal axis metastases) has been given in a previous report (MARTIN ET COLL 1966). A third patient (Case 1) had a very rapid and fulminating course terminating in death 5 months after operation. He did not receive external radiation to the spinal axis and was given only one course of radioactive gold. He developed spinal axis metastases within 2 months of opera-



Fig 1 Myelography demonstrates a complete block at Th11 to Th12 multiple metastases below the block not suspected clinically. External radiation produced complete resolution of the metastases (Reproduced with permission from Amer J Roentgenol 97 (1966) 980)

tion (see Case Report). The other two patients died 2 years and 1 1/2 years respectively after operation with systemic metastases: one had bone metastases and clinical evidence of recurrent cerebellar tumor while the other had bone and spinal cord metastases. Unfortunately post mortem examination was not obtained in the two cases.

Five patients in the series had metastases to the central nervous system. Two had metastases to the brain (proven in one case at autopsy and presumed in the second on the basis of clinical findings, a positive brain scan and EEG findings) and all 5 had spinal axis metastases. One of the patients with spinal axis metastases is still alive 5 years following operation; however he has recently demonstrated malignant cells in the cerebrospinal fluid. The other 4 patients have died.

Three patients had metastases to bone and all have died. One patient had mixed osteoblastic and osteolytic bone metastases. The lytic lesions occurred in the pelvis and femora while the blastic metastases were in the ribs and vertebrae. The other two patients had lytic lesions in the bone.

**Myelography.** Serial follow up myelography was an integral part of the protocol. Sixty-two examinations were performed on the fourteen patients. Large volumes of Pantopaque were utilized in order to completely fill the thecal sac and rule out the possibility of small posterior placed metastases escaping detection. Spinal axis metastases were detected by myelography in 5 patients. In two pa-

gent in total of 4 metastases were found at myelography which were not suggested clinically. Figs 1, 2a and c, emphasizing the importance of cerebral volume myelography in the care and evaluation of these patients. Myelography demonstrated an appearance compatible with arachnoiditis in 2 patients. One of the 6 showed evidence of arachnoiditis at L5-S1 the site of a metastatic deposit previously treated with external radiation which had disappeared. The other patient (case 2) had myelographic evidence of arachnoiditis involving the entire lumbar spinal canal following his treatment course. He developed a very severe cauda equina syndrome with paraplegia and loss of bladder and bowel control. Operation demonstrated severe arachnoiditis with marked thickening of the dura, matting of the nerve roots and cystic changes in the arachnoid (see Case Report).

### Case reports

**Case 1.** A 3-year-old boy was seen initially because of difficulty in maintaining his balance and falling to his right. Five days prior to admission he became drowsy and began vomiting. Physical examination revealed papilledema and impaired coordination of the upper extremities. A ventriculography demonstrated a mass in the 4th ventricle. Posterior fossa exploration revealed a medulloblastoma.

Postoperatively the patient was treated with  $^{60}\text{Co}$  external teletherapy to the skull 3000 rad in 3 weeks. No radiation was given to the spinal canal. A myelography was performed and the patient was given 10 mCi of intrathecal radioiodine.

He returned 2 months later with ataxia, loss of bladder control, insomnia and irritability. Myelography demonstrated diffuse metastases throughout the subarachnoid space appearing as if the spinal cord was encased in tumor. CSF protein was 300 mg. The patient was given local external  $^{60}\text{Co}$  teletherapy to the lumbosacral region (1000 rad in 10 days) which was then followed by an additional 1000 rad in 10 days to the entire spine. Nevertheless he continued to do poorly with treatment. A brain scan showed a focus of increased activity in the left temporal region and the clinical picture progressed to diffuse brain stem involvement. The patient expired 5 months after operation. Autopsy revealed metastases in the pons, medulla and left temporal lobe and recurrent tumor in the cerebellum. The entire spinal cord was encased in a thick sheath of neoplasia.

This patient was one of the first of this series to be treated and it was thought that with a negative myelography intrathecal radioiodine alone would be sufficient to prevent metastases without external radiation to the spine. His rapidly deteriorating course indicated that external radiation of the cerebrospinal axis is essential in the treatment of these patients and this was included in the regimen for all other cases.

**Case 2.** A 10-year-old boy presented with severely diminished visual acuity, bilateral ataxia and papilledema. A preoperative ventriculography revealed a midline cerebellar mass. Posterior fossa exploration revealed a cerebellar medulloblastoma but excision of the tumor was incomplete.

Postoperatively the patient was treated with external  $^{60}\text{Co}$  irradiation receiving 4000 rad to the skull in 14 days. No irradiation was given to the spinal axis at this time.



Fig 2 a) Three metastases that were not suggested clinically are seen in the lumbar region at myelography b) A myelogram showing irregularity of thecal sac and thickened nerve roots indicating arachnoiditis c) Clinically unsuspected metastases at Th3 to Th4 and Th9 to Th10 at myelography d) Repeat myelogram after further external radiation shows severe arachnoiditis with irregularity of the thecal sac and thick matted nerve roots

Two months later the patient had a myelography which revealed metastases in the lower lumbar region (Fig 2 a) which were unsuspected clinically. 3,900 rad of  $^{60}\text{Co}$  teletherapy were given to the cervical and thoracic spine and posterior fossa in 4 weeks. An additional 4,000 rad were then given to the lumbosacral area in 4 1/2 weeks. A repeat myelography however showed persistence of the intradural metastases and a further 1,500 rad were given to the lumbosacral spine. A third myelography was negative and 10 mCi of radiogold were injected intrathecally. This was repeated six weeks later. Over a period of 4 months the patient had received a total of 5,500 rad of  $^{60}\text{Co}$  teletherapy to the lumbosacral region.

Twenty-one months after operation the patient gradually developed signs and symptoms of the cauda equina syndrome with loss of bowel and bladder control and pain, paresthesias and progressive weakness of both lower extremities. An electromyogram was interpreted as consistent with the cauda equina syndrome. Myelography demonstrated thickening and irregularity of nerve roots and irregularity of the thecal sac in the lumbosacral region (Fig 2 b). Surgical exploration revealed markedly thickened leptomeninges. The nerve roots were thickened, irregular and matted together. Posteriorly there were cystic pouches of arachnoid in which were trapped globules of Pantopaque.

Eighteen months after his first negative myelography and 27 months after his posterior fossa exploration routine repeat myelography revealed clinically unsuspected metastases in the upper and lower thoracic region (Fig 2 c). Further local external  $^{60}\text{Co}$  radiation to the thoracic spine (1,500 rad over 12 days) resulted in disappearance of the myelographic filling defects. A myelography 7 months later again demonstrated severe lumbar arachnoiditis (Fig 2 d).

At the present time the patient is alive five years following surgery. He is paraplegic and has ascending sensory and motor deficits which are now located in the upper cervical region. A recent analysis of his cerebrospinal fluid showed malignant cells.

**Case 3** A 4 year-old girl was in good health until two weeks prior to admission when she fell down and struck her head. Skull films demonstrated widening of the sutures in

dicating increased intracranial pressure. A ventriculography revealed a posterior fossa tumor and a medulloblastoma was found at operation. Postoperatively the patient was given 3500 rad of  $^{60}\text{Co}$  irradiation to the skull and spinal canal in 4 weeks and an additional 1500 rad to the posterior fossa in 10 days.

Two and one half months after operation a complete myelography was negative and 10 mCi of  $^{197}\text{Au}$  were instilled into the subarachnoid space. 6 weeks later another negative myelography was followed by 12 mCi of intrathecal radiogold. A third myelography in another 6 weeks was also negative and 10 millicuries of radiogold were instilled intrathecally.

At the present time the patient is doing extremely well 31 months after operation with only a mild residual cerebellar ataxia.

### Cauda equina syndrome

One severe complication has occurred in 5 patients in this study which was not anticipated. This is the development of the cauda equina syndrome (C.E.S.) which is characterized by leg and back pain, weakness and paresthesia of the lower extremities and loss of bowel and bladder control.

All five patients have manifested varying degrees of pain in the back and legs and weakness of the lower extremities, as well as hyporeflexia. Three patients experienced paresthesia in the legs and three had varying degrees of loss of bladder and bowel control. Two patients had metastases to the cauda equina demonstrated myelographically prior to the administration of radiogold but the other three had no such pre-existing abnormality.

Two of the 5 patients with the C.E.S. subsequently died of disseminated tumor. One had a clinical C.E.S. which completely cleared after intrathecal chemotherapy suggesting that the signs and symptoms were due to metastases which were too small to be seen at myelography. This patient eventually developed widely disseminated metastases and died. Unfortunately, no autopsy was performed. The other patient had spinal axis metastases at his initial myelography thus accounting for the C.E.S. when it was first detected. His symptoms and signs improved with external radiation but were never completely resolved. At myelography several months later arachnoiditis was seen in the lower lumbar and sacral regions. It was not clear at that time whether recurrent tumor, vertebra post radiation effect or all three were responsible for the recurrent signs and symptoms.

Case 2 had a very severe C.E.S. which appeared 1 year after his spinal axis metastases were brought under control. At the present time he is completely paraplegic with loss of bladder and bowel control and a slowly ascending level of sensory and motor impairment in the cervical region. The other two patients have a mild to moderate C.E.S. Neither had any additional irradiation nor did they have clinical or myelographic evidence of metastases.

Table 2  
*Medulloblastoma Cauda equina syndrome*

External radiation to lumbosacral spine		Intrathecal radiogold		Spinal axis metastases at myelo- graphy	Arachnoidi- tis at my- elography	Extra- the- cal Panto- paque
Total (rad)	Time	No of courses	Time			
3 500	4 wks	3	3 mo	—	—	+
10 535	15 mo	3	4 mo	+	+	+
5 500	4 mo	2	2 mo	+	+	+
3 500	5 wks	3	3.5 mo	—	—	+
3 500	4 wks	3	3 mo	—	—	+

All 5 patients with the cauda equina syndrome had some extravasation of Pantopaque from the subarachnoid space during repeat myelographies. Two patients had myelographic evidence of arachnoiditis.

### Discussion

In the 5 patients there seem to be at least six factors that could account for the development of the CES: tumor implants per se; tumor implants treated with external radiation therapy and leading to an irregular theca (cicatrix) before treatment with radiogold; high dose external radiation; arachnoiditis; trapped and extrathecal Pantopaque; and intrathecal radiogold (Table 2).

Two patients never developed spinal axis metastases. Thus they received only the standard 3 500 rad of external radiation therapy to the lumbosacral region prior to the instillation of radiogold. The CES developed thereafter. In another patient the CES cleared completely after chemotherapy, suggesting that it was due to spinal axis metastases too small to be demonstrated at myelography. One patient had spinal axis metastases adequate in degree and location to account for the CES. In addition he had unusually high dose external radiation to the spinal axis (10 535 rad in 15 months). Case 2 is worthy of more extended discussion. He received high dose external radiation to the lower spinal region (5 500 rad in 4 months). The spinal axis metastases cleared, but myelography demonstrated arachnoidal adhesions with consequent trapping of Pantopaque globules. He developed the CES approximately one year after external radiation therapy, and intrathecal radiogold had produced clearing of the spinal axis metastases. It was not known whether his signs and symptoms were caused by residual or recurrent tumor, radiation damage, or arachnoidal adhesions. con-



sequently a laminectomy was performed. The nerve roots were found to be markedly thinned and tightly bound in arachnoidal adhesions. The operative findings suggest that a vicious cycle of events had been initiated: cicatrix formation after successful treatment led to arachnoiditis. This combination led to damage and consequent narrowing of the strands of the cauda equina which became encaased within arachnoidal pockets. The intrathecal radiogold like the Pantopaque tended to become loculated within these pockets so that a high dose was delivered to thinned nerve roots. A major portion of each strand of the cauda equina thus was within range of the electrons bombarding the circumference from all sides. The periphery of the nerve root thus received doses in the thousands of rad leading to narrower roots and more arachnoiditis and setting the stage for more severe damage at the time of the next radiogold instillation. In addition extrathecal Pantopaque might have increased the arachnoiditis and helped to perpetuate the cycle.

The common and probably crucial factor to all the patients who developed the CES was intrathecal radiogold. Undoubtedly, the other factors played a role and aided in the development of the CES, an irregular theca due to arachnoiditis secondary to previous tumor irradiation and loculated Pantopaque could only make matters worse by trapping the radiogold.

It is important to realize however that radical treatments for lethal lesions sometimes produced regrettable complications. Permanent eradication of drop metastases in patients with medulloblastoma seldom is achieved by standard regimens of therapy. One case died of the complications of the disease but had no residual intraspinal tumor at autopsy. The other patient with proven spinal metastases at myelography is alive 5 years after operation, albeit he suffers from a very severe CES and has recently demonstrated malignant cells in the cerebrospinal fluid.

We now believe that this complication can be avoided in most if not all patients by the simple maneuver of placing the patient in a 60° to 90° head-down position at the time the radiogold is introduced. This posture is maintained for a minimum period of one hour while the other rotary positions described elsewhere are assumed. In this way most of the radionuclide has an opportunity to flow away from the lower lumbar region. Only the residual activity (estimated to be about 50% at one hour) is available in the lumbosacral theca for deposition on the cauda equina. Twelve additional patients with medulloblastoma have been treated at another institution by one of us (G.D.A.) during the past two years using this modification. No instance of the CES has been encountered as yet in this group although another child with acute leukemia who received only one instillation of radiogold has developed leg weakness of unknown etiology at this writing.

Electromyograms and nerve conduction velocity measurements of the peroneal and tibial nerves were performed on at least two occasions on three patients and once in one patient (Case 2) with the cauda equina syndrome. In two cases the needle electrode examination revealed irritability of units expressed as repetitive discharges but only in one muscle of each patient. The case most severely affected clinically (Case 2) showed evidence of partial denervation in all muscles tested in both lower extremities and in the paraspinal muscles. The nerve conduction velocity values were within the normal range in all nerves tested of each patient except for a slightly low value (36 m/s) in the right peroneal nerve of Case 2. This degree of reduction in conduction velocity is not unusual when proximal disorders have resulted in severe peripheral denervation.

The electromyogram can provide some indication of early neurogenic damage to anterior horn cells or nerve roots. When the denervation is more clinically manifest the test may be useful in ascertaining the distribution of the process. Electromyography performed at regular intervals may be of value in following patients treated with intrathecal radiogold to detect early manifestations of the cauda equina syndrome possibly before it becomes evident clinically.

Routine myelography using a large volume of contrast medium in order to outline completely the anterior and posterior aspects of the subarachnoid space would seem to be an extremely important adjunct to patient management. In two cases nine clinically unsuspected metastases were revealed by myelography. Considerable care should be used in performing the myelography. Children should be heavily sedated to avoid the problems of extravasation of Pantopaque.

## SUMMARY

Fourteen patients with proven medulloblastoma have been treated with external irradiation followed by intrathecal radiogold. When two patients who presented late after development of widespread metastases are omitted the estimated two year and three year survival is 83 % and 73 % respectively. Late development of the cauda equina syndrome was seen in 5 patients. The complex causes leading to this complication are discussed.

## ZUSAMMENFASSUNG

Vierzehn Patienten mit einem nachgewiesenen Medulloblastom wurden durch externe Bestrahlung gefolgt von intrathecalem Radiogold behandelt. Wenn zwei Patienten ausgeschlossen wurden, die zu spät nach Entwicklung allgemeiner Metastasen eingelesen waren, beträgt die berechnete Zweijahres- und Dreijahres-Überlebensrate 83 bzw. 73 %. Eine späte Entwicklung des Cauda equina Syndroms wurde bei 5 Patienten beobachtet. Die komplexen Ursachen, die zu dieser Komplikation führen, werden besprochen.

## RÉSUMÉ

Quatorze malades atteints de médulloblastome vérifié ont été traités par irradiation externe suivie d'injection sous arachnoïdienne d'or radioactif. Si on ne tient pas compte de deux malades qui se sont présentés longtemps après le développement de métastase disséminées, les taux de survie à deux ans et à trois ans sont estimés respectivement à 83 % et 73 %. On a observé chez 5 malades l'apparition tardive d'un syndrome de la queue de cheval. Les auteurs examinent les causes complexes qui conduisent à cette complication.

## REFERENCES

- BLOOM H J G, WALLACE E N K and HENK J M. The treatment and prognosis of medulloblastoma in children. *Amer J Roentgenol* 103 (1969) 43.
- CUTLER S M and EDERER F. Maximum utilization of the life table method in analyzing survival. *J chron Dis* 8 (1958) 699.
- D'ANGIO G J, FRENCH L A, STADLAN E M and KIEFFER S A. Intrathecal radioisotopes for the treatment of brain tumors. *Clin Neurosurg* 15 (1968) 228.
- JFANKIN R D T. Medulloblastoma in childhood. *Canad med Ass J* 100 (1969) 51.
- KIEFFER S A, D'ANGIO G J and NOWAK T J. Laboratory studies of intrathecal radiogold with a new rationale for its use. *Radiology* 87 (1966) 1120.
- STADLAN E M and D'ANGIO G J. Anatomic studies of the distribution and effects of intrathecal radioactive gold. *Acta radiol Ther Phys Biol* 11 (1969) 27.
- MARTIN JR C F, GEDDOLDS E and D'ANGIO G J. Residual radiopaque bolus in managing intraspinal neoplasms. *Amer J Roentgenol* 97 (1966) 980.
- Mc FARLAND D H, HORWITZ H, SAENGER E L and BAHR G K. Medulloblastoma: A review of prognosis and survival. *Brit J Radiol* 42 (1969) 198.
- PATERSON R. Treatment of malignant disease by radiotherapy. Second edition. p 41. The Williams & Wilkins Co. Baltimore 1963.

FROM THE DEPARTMENTS OF PHYSIOLOGY, PATHOLOGY AND MORPHOLOGY, EGE  
UNIVERSITY MEDICAL FACULTY, BORNova IZMİR TURKEY

---

## ATTEMPT TO MODIFY THE IONIZING RADIATION INDUCED HISTOPATHOLOGIC EFFECTS ON THE CENTRAL NERVOUS SYSTEM BY RESERPINE ADMINISTRATION

by

N İ HARIRI İ ALSU S FALAKATI and O İ TUNÇER

As supervoltage irradiation now allows the delivery of greater depth doses reports of injuries are again increasing in frequency and so-called radioreistant structures are being recognized as vulnerable. More knowledge of the hazards and benefits of irradiation therapy is essential to its progress and increasing effectiveness (RUBIN & CASARETT 1968).

The challenging task of identifying the significant variables governing neural participation in radiation effects has only started. Radiation destruction of vascular and glial tissues within the nervous system may alter the metabolic processes essential for neural activity thereby altering the structure and function of neurons. It is apparent that better resolution of the duality now postulated for radiation effects on the nervous system must be obtained. Although attention has been focussed on function and behaviour morphologic alterations may constitute the most obvious effect of irradiation. Its effects on neural tissues may be largely a result of vascular alterations although evidence exists that they are exerted on neurons. The relative contributions of vascular and late effects represent major

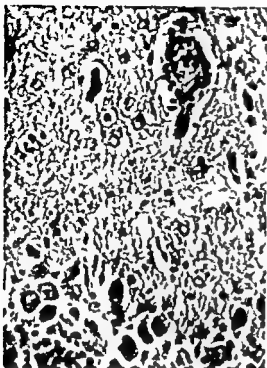


Fig 1 4 hours after irradiation Perivascular infiltration Haematoxylin-eosin  $\times 350$

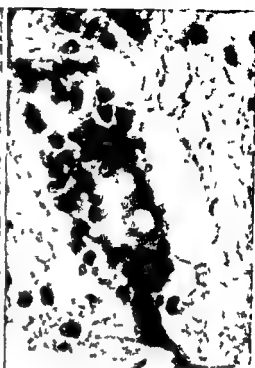


Fig 2 48 hours after irradiation Perivascular infiltration hyaline thrombus Haematoxylin-eosin  $\times 800$

problems that have not been resolved. The application of newer biophysical and histochemical techniques for the subcellular analysis of neural and vascular tissues can be expected to yield a better understanding of the mechanism involved in these structural changes (KIMELDORF & HUNT 1965).

**Material and Methods** The head of rabbits anaesthetized with 50 mg/kg Nembutal Sodium were irradiated (220 kV, 15 mA, 1 mm Cu filter) trans-temporally. The actual irradiation doses were 320 R/min to the upper surface and 160 R/min to the lower surface of the head. Each side was irradiated for seven minutes. The animals were sacrificed at the 1st, 2nd, 3rd, 5th, 7th and 8th post irradiation days. Some animals survived 10 to 12 days after irradiation. The brains were fixed in 10% buffered formaldehyde and eight standard sections cut (THOMPSON 1966). After paraffin embedding 3 to 5  $\mu$  histologic sections were cut and stained by haematoxylin-eosin and modified Ridley methods. The same experimental procedures were repeated in the reserpine (Serpasil CIBA) at 0.5 mg/kg 24 hours and 0.5 mg/kg 5 hours before irradiation. pre-

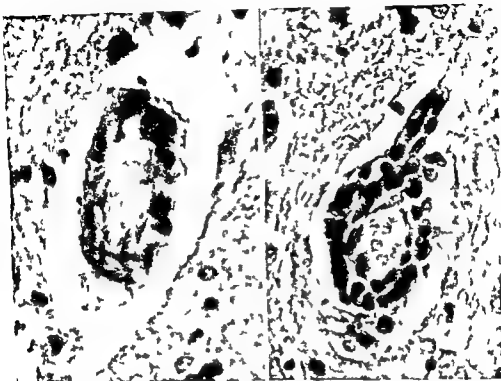


Fig 3 24 hours after irradiation Endothelial proliferation Haematoxylin eosin  $\times 880$

Fig 4 24 hours after irradiation Perivascular infiltration Haematoxylin eosin  $\times 880$

treated animals. The sections were studied microscopically and the results were compared. A general classical autopsy was carried out to investigate the possible cause of death.

### Results

Vascular effects such as hyperemia, teleangiectasis, endothelial swelling and proliferations, perivascular fibrosis and hyaline thrombus as well as gliosis, focal necrosis were observed (Figs 1, 2, 3, 4, 5). Beside the vascular and glial changes such as intranuclear and intracytoplasmic vacuolation, protoplasmic swelling, disintegration, darkly staining and condensation of neurofibrils, apparent, topographic localization and condensation of Nissl bodies especially in the pons, midbrain and bulb were observed (Figs 7, 9, 10, 11). The animals that were pre-treated with reserpine presented almost no vascular alterations although after the 12th post irradiation day some regressive changes occurred at the neurons, i.e. intranuclear and intracytoplasmic vacuolation, cytolysis and disintegration of neurofibrils. It was concluded that reserpine was protective against



Fig. 5



Fig. 6

Fig. 5 24 hours after irradiation. Teleangiectasis and hemorrhage. Haematoxylin-eosin  $\times 200$ .

Fig. 6 A multipolar ganglion cell 24 hours after irradiation. Intranuclear and intracytoplasmic vacuolation, chromatolysis, neurofibrillar disintegration and peripheral condensation of neurofibrils. Haematoxylin-eosin  $\times 2200$ .

radiation damage. The results of general autopsy indicated that peripheral collapse was almost always the possible cause of death. One case had focal necrosis in the adrenal cortex and 2 cases presented evidence of bronchopneumonia.

### Discussion

Radiation destruction of vascular and glial tissues within the nervous system may subsequently alter the metabolic processes essential for neural activity (KIMLIDORF & HUNT 1965). These responses of interstitial and vascular connective tissue are more marked, more permanent and more progressive as the radiation dose is increased. All these changes are non-specific (not unique to radiation). The interstitial fibrosis and the fibrosis of small blood vessels can



Fig 7 Multipolar ganglion cell 48 hours after irradiation. Intranuclear vacuolation, diffuse chromatolysis and cytolysis. Haematoxylin-eosin  $\times 200$ .



Fig 8 8 days after irradiation. Intranuclear vacuolation and chromatin condensation in astrocytes. Silver impregnation  $\times 560$ .

stitute a premature increase in the histohematic connective tissue barrier (the barrier between the blood and the dependent parenchymal tissue cells). It is through the  $e$  that diffusion of nutrients and gases must take place and a premature advance in the development of arteriocapillary fibrosis, both of which are progressive processes in normal aging (CASARETT 1963).

An attempt has been made in the present investigation to modify the ionizing radiation induced alterations on the central nervous system by the administration of reserpine. Basically, reserpine exerts important effects on behaviour and autonomic functions. It is believed by some workers that its ability to cause the release and inhibit the binding of amines such as serotonin and norepinephrine rests on the role of altered amine metabolism and furthermore that the effects of reserpine vary greatly. The Brodie hypothesis has at any rate stimulated enormous amount of work in this field. It suggests that the depressant effects of reserpine may be due to serotonin release although just how such release produces autonomic effects of behaviour is not clear. The continued production of the amine



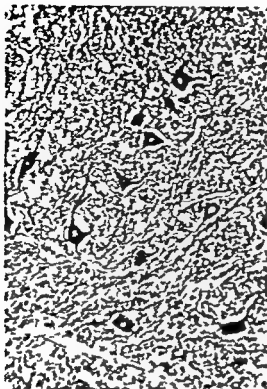


Fig. 9. Multipolar ganglion cells of a rabbit that was pre-treated with reserpine 12 days after irradiation. Only slight regressive changes such as intracytoplasmic vacuolation and condensation of Nissl bodies. Silver impregnation  $\times 40$ .



Fig. 10. Multipolar ganglion cells of a rabbit that was pre-treated with reserpine 15 days after irradiation. Haematoxylin-eosin  $\times 40$ .

without an effective binding mechanism in the cell may suggest a positive role for increased serotonin levels as the mediator of reserpine. It is possible, however, that the depletion of serotonin also is of some importance in this connection. Although these speculations may seem of academic interest only, it should be recognized that attempts at correlating behaviour and brain chemistry are of great moment and justify the elaboration of working hypotheses (GOTT 1961).

Biochemical research in the field of mental illness during the last decade was greatly stimulated by observations indicating that biogenic amines, such as indolamines and catecholamines, may serve as neurotransmitters in brain function. This hypothesis was supported by the fact that many psychotropic agents like psycho-genics, tranquillizers and antidepressants interfere with the metabolism or the actions of biogenic amines (BRUCE 1963).



Fig. 11. Multipolar ganglion cell 13 days after irradiation. Neurofibrillar condensation. Beginning of intranuclear and intracytoplasmic vacuolation. Silver impregnation  $\times 560$ .

Starting from the point that histochemical techniques may be expected to yield a better understanding in radiation induced alterations and that some agents interfere with brain metabolism a series of experiments was planned to investigate the possible radiation protection effects of these agents (i.e. meprobamat, reserpine, adrenaline, acetylcholine, mescaline, etc.). The research is still in progress. Apart from the investigation of the effects of the other agents the extent of the radiation protective action of reserpine on the following will be determined: (1) monoamines of the central nervous system (a sensitive fluorescence method will be used); (2) electrophysiologic changes in the brain; (3) the changes in the DNA and RNA content of the brain neural cells; (4) the histopathology of the glial and neural cells by means of electron and light microscopy.

### Acknowledgement

The investigation was partly supported by the International Atomic Energy Agency.

### SUMMARY

Biochemical research in the field of mental illness has been greatly stimulated by observation that biogenic amines may serve as neurotransmitters in brain function. A series of experiments has been planned to investigate the possible radioprotective actions of psychotropic agents that interfere with the metabolism or action of biogenic amines. Reserpine is supposed to act as a radiation protectant.

## ZUSAMMENFASSUNG

Die biochemische Forschung auf dem Gebiet der Geisteskrankheiten ist wesentlich durch die Feststellung, dass biogene Amine als Neurotransmitter Substanzen an der Hirnfunktion teilnehmen können, stimuliert worden. Es ist eine Reihe von Versuchen geplant worden, die möglichen strahlenschutzende Wirkungen psychotroper Substanzen, die auf den Metabolismus oder die Wirkung von biogenen Aminen einwirken, zu untersuchen. Es wird angenommen, dass Reserpin als Strahlenschutzsubstanz wirksam ist.

## RÉSUMÉ

Le fait que les amines biogéniques peuvent servir de neuro transmetteurs dans la fonction cérébrale a beaucoup stimulé la recherche biochimique dans le domaine des maladies mentales. Les auteurs ont établi le projet d'une série d'expériences pour étudier les actions radio-protectives possibles des agents psychotropes qui influent sur le métabolisme ou l'action des amines biogéniques. Ils supposent que la reserpine agit comme radio protecteur.

## REFERENCES

- LEPINE G. C. Metabolism of biogenic amines and psychotropic drug effects in schizophrenic patients. *In* Progress in brain research, Vol. 16. Horizons in neuro-psychopharmacology, p. 81. Elsevier Publishing Co. Amsterdam, London, New York 1965.
- CATAPRATT G. W. Concept and criteria of radiobiological aging. *In* Cellular basis and aetiology of late somatic effects of ionizing radiation, p. 163. Academic Press, London and New York 1963.
- GOTTLIEB A. Medical pharmacology. *In* Principles and concepts, p. 163. C. V. Mosby Co., St. Louis 1961.
- KIMELDORF D. J. and HUNT L. L. Ionizing radiation. *In* Neural function and behavior, p. 296. Academic Press, New York and London 1965.
- RIDLEY A. Silver staining of nerve endings in human digital glabrous skin. *J. Anat.* 104 (1965) 41.
- RUBIN I. and CATAPRATT G. W. Clinical radiation pathology. Preface. W. B. Saunders Co. Philadelphia, London and Toronto 1968.
- THOMSON S. W. Selected histochemical and histopathological methods, p. 31. Charles C. Thomas, Springfield 1966.

## EFFECT OF IONIZING RADIATION ON NUCLEAR ENERGY TRANSDUCTION IN NORMAL AND NEOPLASTIC GLIA

A quantitative cytochemical investigation

by

W. M. KIRSCH, D. SCHULZ, E. FUCHS and P. NAKANE

The initial intracellular biochemical disturbance induced by ionizing radiation in tissue is poorly understood. This fact has been emphasized repeatedly (ALEXANDER 1960; UENO 1958) with the conclusion that the initial step of radiation damage remains to be determined. Ambiguity characterizes the many reported attempts to determine immediate intracellular radiochemical lesions primarily because of limitations in quantitating biochemical events in discrete subcellular compartments or organelles. These difficulties can be readily appreciated in view of conventional cell fractionation methods consisting of the homogenization of ischemic tissue in water. This approach, though convenient, imposes unavoidable analytical artefacts to include (1) inevitable tissue autolysis and anoxia during specimen preparation, (2) extraction of important small molecular weight substrates and enzymes, and (3) inevitable cross-contamination of one subcellular organelle with another. In an attempt to reduce these artefacts to a minimum and examine immediate radiochemical effects in as close to newly imposed steady state bioenergetic conditions, we have developed a new method for subcellular fractionation of nuclei from normal and neoplastic neural tissue.

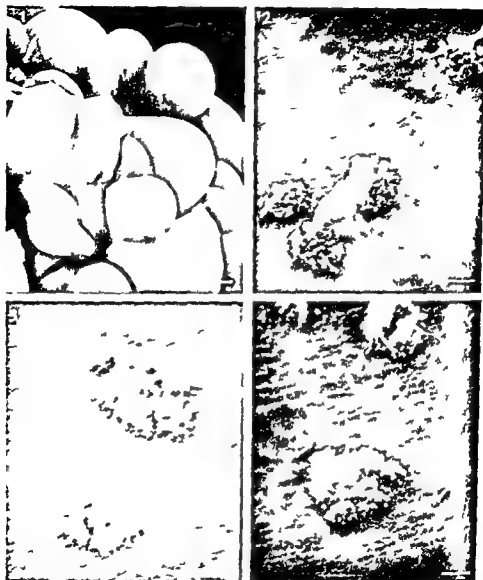


Fig. 1. Montage of representative fields of isolated glioblastoma nuclei and chromosomes isolated by our nonaqueous method. White line in lower right hand corner of each photograph represents 1  $\mu$ . 1—1 bulk collection of glioblastoma nuclei showing clean surface characteristics. 1—2 through 4 are chromosomes prepared from glioblastoma cells in culture in partial mitotic synchrony secondary to double thymidine blockade. A wide variety of mitotic stages are represented. 1—2 lower left anaphase; upper right metaphase. 1—3 4  $\times$  metaphase plates. 1—6 late metaphase. 1—7 anaphase and 1—8 highly extended chromatin — presumably interphase fiber.

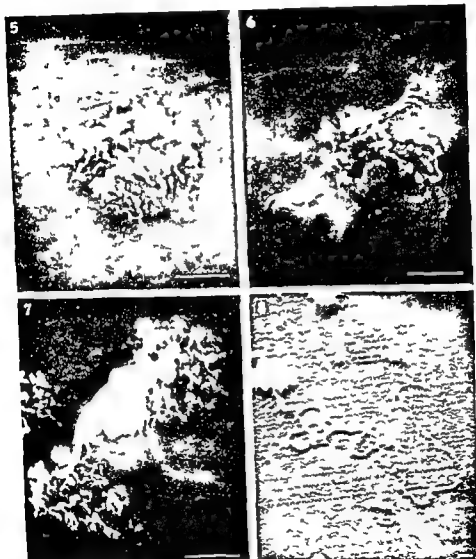


Fig 1 (For legends on opposite page)

(KIRSCH et coll 1970 KIRSCH et coll 1971) This report deals with the use of the method for the elucidation of early radiochemical effects in nuclei and cytoplasm with particular emphasis on nuclear energy transduction. Inferences regarding the latter have been delineated by measuring the changes in steady state compartmental concentration of substrates with bioenergetic potential in response to ionizing radiation.

In brief, the nuclear isolation method permits an examination of the substrate concentration gradient between nucleus and cytoplasm within a few seconds after exposure to ionizing radiation, or at any other appropriate time interval, on the basis of quick freezing fixation.

### Material and Methods

Experiments on murine brain and glioblastoma have been conducted as follows. Six week old mice received 500 rad of irradiation from conventional orthovoltage equipment (250 kV, 30 mA, 1 mm Cu + 1 mm Al) to the head with the remainder of the body shielded. Within five to ten seconds after the completion of brain irradiation, the mice were decapitated, and the severed heads either immediately frozen or allowed to incubate in an ischemic state for one minute prior to freezing. Freezing of the severed heads was accomplished in Freon 12 ( $\text{CCl}_2\text{F}_2$ ) chilled to its freezing point ( $-156^\circ\text{C}$ ) by liquid nitrogen. Brain rendered ischemic for one minute and then frozen has expended endogenous glycolytic energy reserves in a closed anaerobic system (Lowry et coll. 1964). Brains from control, non irradiated mice were prepared by freezing in an identical fashion. In the case of irradiated glioblastoma, cell cultures of the chemically induced murine glioblastoma grown to log phase were irradiated with 300 rad of ionizing radiation (same radiation parameters as for murine brain) while at a temperature of  $37^\circ\text{C}$ . Within five seconds after radiation exposure the incubation media was quickly poured off, cells washed twice with isotonic saline, and the cultures quickly frozen. Control, non irradiated cells were treated identically.

After fixation of tissue by quick freezing brains were dissected from the frozen, decapitated heads at  $-30^\circ\text{C}$  and both brain and tissue culture material lyophilized under rigidly controlled conditions at  $-25^\circ\text{C}$ . Conditions for lyophilization are crucial to permit subcellular fracture of tissue along the nuclear cytoplasmic junction. Cell disruption for nuclear liberation is accomplished by sonication and heating of the lyophilized tissue in viscous neutral hygroscopic media (glycerol) at  $2^\circ\text{C}$ . Nuclear pellets are prepared by centrifugation in a gradient composed of glycerol and 3-chloro-1,2 propanediol resulting in a supernatant band composed of cytoplasmic and membrane constituents virtually free of nuclei. Lyophilized nuclei isolated by this method are devoid of contaminating endoplasmic reticulum and contain a complement of labile water soluble components (cations and important glycolytic substrates such as phosphocreatine (PCr), adenosine triphosphate (ATP), glucose 6 phosphate (G 6 P) and lactate). The latter have been measured by the fluorometric methods of Lowry et coll. Fig. 1—1 is a scanning electron micrograph displaying a typical nuclear



Fig. 2. Transmission electron micrograph of lyophilized glioblastoma nuclei (from cell culture) isolated by this non aqueous method. One micron signified. No contaminating endoplasmic reticulum, prominent nucleoli, intact inner nuclear membrane.

preparation from murine glioblastoma grown in tissue culture. As an aside it should be noted that the method has been extended to permit the isolation of glioblastoma chromosomes in the lyophilized state (KIRSCH et coll. 1971). Fig. 2 is a transmission electron micrograph of isolated glioblastoma nuclei demonstrating the absence of contaminating external nuclear membrane or contiguous endoplasmic reticulum. Fig. 3 is a scanning electron micrograph of an isolated glioblastoma cell nucleus at high magnification.

### Results and Discussion

Nuclear preparations from brain and glioblastoma satisfy accepted biochemical criteria for purity, and as such are amenable to the determination of the steady state levels of important high energy intermediates. The supernatant fraction after centrifugation, appears as a discrete band in the centrifuge tube and is assayed to give a provisional estimate of substrate content in the cytoplasm. An aliquot of the broken cell suspension or glycerol homogenate has been assayed





Fig. 3 High magnification view of isolated glioblastoma nucleus demonstrated by scanning electron microscopy. Magnification signified by micron marker on photograph.

prior to centrifugation in order to give an overall picture of substrate content. Information is obtainable in the following form: Substrate concentration in homogenate (H), cytoplasm (C), and nuclei (N) expressed as  $\mu\text{M}/\text{mg}$  protein. In the case of glioblastoma in tissue culture, only zero time ( $O_t$ ) values have been determined: zero time signifying that the substrate concentrations in homogenate, cytoplasm and nuclei have been compared in control and irradiated tissue culture preparations immediately after radiation exposure. In the case of murine brain these substrate concentrations have in addition been determined after one minute of ischemia in a closed anaerobic system. Since the murine brain is functioning in a closed anaerobic system it is forced to rely on glycolysis for the generation of ATP. An estimate of the energy potential in nuclear and cytoplasmic compartments has been made by summing the known energy equivalents of ATP (2~P per equivalent) and PCr (1~P per equivalent) expressed as concentration. This estimate in the case of glioblastoma is only a part of the total energy reserve since glycogen and glucose were not measured, and is thus an approximation of the energy charge in the adenylate pool only. In the case of brain where glucose determinations have been performed a closer approximation to the total energy charge could be calculated. For the purposes of this report only ATP and PCr~P equivalents have been calculated for both brain and glioblastoma. An extensive discussion of the derivation and rationale of the calculation of energy charge has been presented by KIRSCH (1965) and LOWRY et al. (1964).

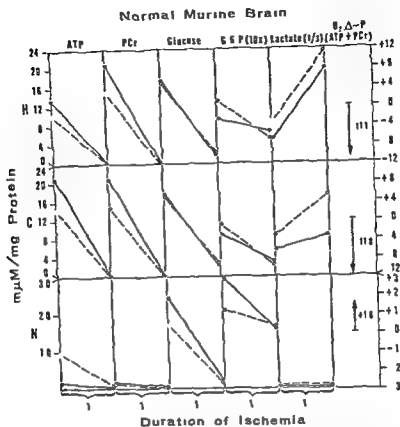


Fig 4 Immediate and ischemic changes in substrates of glycolysis in murine brain with and without exposure to ionizing irradiation. Scale for homogenate (H) cytoplasm (C) and nuclear (N) substrate concentrations (ATP, PCr, glucose, G-6-P and lactate) on left; calculated change in energy charge (ATP + PCr)  $\sim$   $\equiv$  equivalents (7) expressed on right. Changes in irradiated brain plotted with broken line and open circles whereas controls are represented by continuous line and closed circles. Duration of ischemic incubation one minute in all cases. Substrate and energy equivalents ( $\sim$  P) expressed as mM/mg protein. Values are the average of at least four and in many cases more individual determinations.

The nuclear energy charge of normal murine brain and glioblastoma responds differentially to ionizing irradiations (Figs 4, 5). The immediate response of normal murine brain to 500 rad of irradiation is an immediate and significant lowering of total steady state energy reserves, particularly ATP and PCr. This reduction occurs predominantly in brain cytoplasm, presumably secondary to a disturbance in mitochondrial energy transduction. In contrast to cytoplasm, brain nuclei exhibit a modest, but definite, increase in the level of energy reserves.

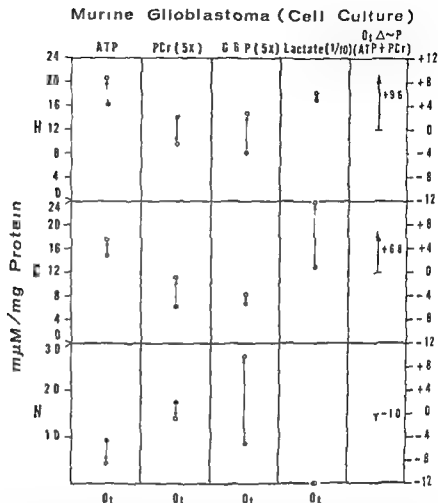


Fig 8 Immediate changes in steady state concentration of major substrates of glycolysis in cultured murine glioblastoma after exposure to ionizing irradiation Scale for homogenate (H) cytoplasm (C) and nuclear (N) substrate concentrations (ATP PCr G6P and lactate) on left calculated change in energy charge (ATP + PCr) ~ P equivalents on right Arrow indicates direction of zero time change in various cytologic compartments Closed circle represents control non irradiated values and open circle irradiated tissue values Determinations are the average of at least four separate samples in each case

after irradiation The latter may be related to a disturbance in the nuclear utilization of nucleotide triphosphates for biosynthetic purposes perhaps RNA biosynthesis Consistent with these observations is an elevation of zero time

steady state lactate levels in brain cytoplasm. The latter indicates an irradiation induced immediate activation of glycolysis in the cytoplasmic compartment — an expected response to an impairment of mitochondrial energy transduction. Once glycolysis has been activated, the rate during the first minute of ischemia is identical in control and irradiated animals (Fig. 4).

Opposite immediate irradiation effects occur in the intracellular compartments of tissue culture preparations of glioblastoma cells. A slight but definite increase in ATP is found in glioblastoma cytoplasm immediately after exposure to irradiation (Fig. 5). This increase in adenylate charge could be due to either an increase in ATP production, or a decrease in ATP utilization in response to radiation. It appears on the basis of substrate evidence that cytoplasmic glycolysis (a metabolic feature characteristic of many malignant tumors — including the glioblastoma) in both normal and neoplastic tissue is activated immediately by irradiation. Substrate evidence for this contention can be summarized as follows: levels of (1) glucose 6 P, the initial step in glycolysis and (2) lactate, the final metabolic end product are markedly increased in tumor cytoplasm within seconds of radiation exposure. The other possible explanation which cannot be excluded by this data, is that ATP expenditure in cytoplasm for synthetic or ionic gradient maintenance is suppressed by irradiation leading to a secondary rise in steady state values. In contrast however the adenylate charge in the tumor nucleus conventionally thought of as the most radiosensitive subcellular organelle, is reduced as an immediate response to irradiation. One important implication of this observation is that a radiosensitive hitherto unrecognized unique nuclear ATP energy generating system is present within the tumor cell nucleus which is damaged immediately by irradiation. The presence and significance of a system of this nature in neoplastic tissue has been speculated upon in previous publications (KIRSCH *et coll.* 1967; HENDLE & KIRSCH 1971).

Since the nuclei isolated by this non aqueous technique are susceptible to assay for cation concentration in addition to measurements of labile substrates preliminary experiments have been conducted to determine shifts in ionic concentration gradients in brain as an immediate effect of irradiation and ischemia (Table). Though this data must be interpreted with caution certain interesting provisional observations are possible. The total  $\text{Na}^+$  and  $\text{K}^+$  content of brain as determined in the homogenate is in good agreement for previously reported dry weight values in brain (HANDBOOK OF BIOLOGICAL DATA 1956). Of considerable interest is the  $\text{Na}^+/\text{K}^+$  ratio of 15 in normal brain nuclei indicating a sodium rich nuclear compartment. The immediate effect of irradiation on brain nuclei is to virtually halve the  $\text{Na}^+/\text{K}^+$  ratio to 8 despite an elevation in nuclear energy reserves. This effect is paradoxical and not subject to ready explanation since ischemia alone — an event which is known to reduce total cellular energy re-

Table

*The immediate effect of irradiation on the intracellular cation distribution in murine brain. All values expressed as mEq/g protein. H, C, N refer to glycerol homogenate, cytoplasm and nuclear fraction respectively.  $O_t$  and 1 min refer to time of anaerobic incubation prior to rapid freezing of tissue.  $Na^+$  and  $K^+$  determinations performed by flame photometry on lyophilized samples. Results are the average of at least two and in many cases three or more determinations on separate samples.*

	Normal brain ( $O_t$ )	Ischemic brain (1 min)	Irradiated brain ( $O_t$ )	Irradiated ischemic brain (1 min)
H $Na^+$	0.80	0.55	0.71	0.72
H $K^+$	0.75	0.79	1.12	0.99
C $Na^+$	1.01	1.51	0.76	0.46
C $K^+$	0.87	0.92	0.99	0.75
N $Na^+$	5.45	3.20	2.00	1.81
N $K^+$	0.36	0.40	0.23	0.26

serves — is also associated with a lowering of the intranuclear  $Na^+/K^+$  ratio. The combination of irradiation and ischemia resulted in the lowest nuclear  $Na^+/K^+$  ratio. The significance of a high intranuclear concentration of  $Na^+$  in normal brain is unclear: either the nucleus has direct connections with the extracellular space or there is a preferential  $Na^+$  binding to negatively charged nuclear constituents.

This innovation in cellular microsurgery opens new and potentially rewarding experimental avenues for research in radiobiology. It is now possible to dissect the initial effects of radiation induced lesions in specific subcellular compartments, with special attention to intranuclear biochemical events. Most importantly, these techniques permit a comparative examination of the influence of therapeutic agents such as ionizing radiation or radiosensitizers, on nuclear energy transduction in normal and neoplastic cells. Though the general pattern of injury subsequent to exposure to ionizing irradiation is relatively well understood, there is no question that a new approach is required for elucidation of immediate lesions secondary to irradiation. We have presented data obtained by the application of a new method for the evaluation of early or initial chemical lesions secondary to the *in vivo* exposure to irradiation. The experimental approach presented offers a potential avenue for resolving this problem of the nature of the early radiation lesion.

### Acknowledgement

This investigation was supported by Veterans Administration Grant 3 72 and an Institutional Grant of the National Cancer Institute and the Donald Jay Bartuska Brain Tumor Research Fund. Dr Nakane is a career development awardee (CA 46728).

### SUMMARY

This investigation compares the immediate effects of ionizing irradiation upon measured energy reserves (ATP PCr) in subcellular compartments of normal murine brain and glioblastoma in cell culture. Determination of these effects is made feasible by application of a new method for tissue fixation employing rapid freezing lyophilization, and subsequent isolation in high purity of lyophilized nuclei. The immediate effect of irradiation on normal murine brain is a significant lowering of steady state cytoplasmic ATP, enhanced cytoplasmic glycolysis with minimal changes in the nuclear energy charge. These results are to be contrasted with immediate irradiation effects in the glioblastoma, namely a slight rise in cytoplasmic ATP but loss of nuclear energy reserves. The latter observation implies the presence of a radiosensitive ATP generating system in glioblastoma nuclei.

### ZUSAMMENFASSUNG

Diese Untersuchung vergleicht die unmittelbaren Wirkungen ionisierender Strahlung auf die gemessenen Energiereserven (ATP PCr) in den subcellulären Kompartiments des normalen murinen Gehirns und des Glioblastoms in der Zellkultur. Die Bestimmung dieser Effekte wird durch eine neue Methode zur Gefixation ermöglicht, wobei das Gewebe rasch gefroren, gefriergetrocknet und anschliessend die gefriergetrockneten Nuclei in hoher Reinheit isoliert werden. Der unmittelbare Effekt von Strahlung auf das normale murine Gehirn ist eine signifikante Erniedrigung des Steady state ATP des Cytoplasmas, eine gesteigerte cytoplasmatische Glykose mit minimalen Änderungen der Energie Ladung im Zellkern. Diese Ergebnisse stehen im Gegensatz zu den unmittelbaren Strahleneffekten auf das Glioblastom, nämlich einem leichten Anstieg des cytoplasmatischen ATPs aber einem Verlust der Energiereserven des Zellkerns. Letzgenannte Beobachtung bedeutet das Vorhandensein eines Strahlensensiblen ATP bildenden Systems in den Nuclei des Glioblastoms.

### RÉSUMÉ

Ce travail compare les effets immédiats d'une irradiation ionisante sur les réserves d'énergie mesurées (ATP PCr) dans les compartiments subcellulaires du cerveau normal du rat et dans le glioblastome en culture cellulaire. La mesure de ces effets est rendue possible par l'application d'une nouvelle méthode de fixation tissulaire employant une congélation rapide, la lyophilisation et l'isolement ultérieur de noyaux lyophilisés de grande pureté. L'effet immédiat de l'irradiation du cerveau normal du rat est une baisse significative de l'ATP cytoplasmique en état stable, une augmentation de la glycolyse cytoplasmique avec des modifications minimes de la charge d'énergie nucléaire. Ces résultats s'opposent aux effets immédiats de l'irradiation du glioblastome, à savoir une légère élévation de l'ATP cytoplasmique mais une perte des réserves d'énergie nucléaire. Ce dernier fait implique la présence dans les noyaux de glioblastome d'un système générateur d'ATP radio-sensible.

## REFERENCES

- ALEXANDER P The nature of radiation damage at the subcellular level *In* Third Australasian Conference on Radiobiology Butterworths London and Sydney 1960
- HANDBOOK OF BIOLOGICAL DATA p 70 Edited by W S Spector W B Saunders Co Philadelphia and London 1956
- HENDREE W R and KIRSCH W M Effects of ionizing radiation upon normal and neoplastic neural tissue *In* The experimental biology of brain tumors Edited by W M Kirsch E Paoletti and P Paoletti Charles C Thomas Springfield Illinois 1971
- KIRSCH W M Substrates of glycolysis in intracranial tumors during complete ischemia *Cancer Res* 25 (1965) 432
- SCHULZ D and LEITNER J W The quantitative histochemistry of the experimental glioblastoma Glycolysis and growth *Acta histochem* 28 (1967) 51
- LEITNER J W GAINES M SCHULZ D LASHER R and NAKANE P Bulk isolation in non aqueous media of nuclei from lyophilized cells *Science* 168 (1970) 1592
- SCHULZ D W NAKANE P and LASHER R Isolation and characterization of glioblastoma nuclei and chromosomes in the lyophilized state *J Neurosurg* 34 (1971) 301
- LOWRY O H PASSONNEAU J V HASSELBERGER F V and SCHULZ D W Effect of ischemia on known substrates and cofactors of the glycolytic pathway in brain *J biol Chem* 239 (1964) 18
- UNITED NATIONS SCIENTIFIC COMMITTEE ON THE EFFECTS OF ATOMIC RADIATION United Nations Organization New York 1958

## ATROPHY FOLLOWING RADIATION THERAPY FOR CENTRAL NERVOUS SYSTEM NEOPLASMS

by

G H WILSON, J BYFIELD and W N HANAFEE

Patients who have received radiation therapy for central nervous system neoplasms often present with a recurrence of symptoms following their therapy. The radiation therapist is under pressure to give further therapy on the assumption that the symptoms are related to regrowth of the neoplasm. It has been pointed out by others (LEE & ADAMS 1968, VERITY 1968) that patients with radiation damage may have symptoms which suggest regrowth of tumor. Reevaluation by neuroradiologic examination is essential to determine if there is a recurrence or if the symptoms are related to radiation damage. In some of the cases it will be possible to demonstrate atrophic changes at encephalography. If the patient has also been operated upon, post-operative adhesions may contribute to the symptoms and it may not be possible to distinguish surgical damage from radiation damage at encephalography.

### Material

This is a retrospective investigation of the encephalographic films of 40 patients who had received radiation therapy for lesions of the skull or its contents and were evaluated for evidence of recurrent tumor or evidence of radiation damage. Of these patients 21 had a surgical exploration prior to irradiation. Twenty-one also had been examined encephalographically before the radiation therapy and the films were available for comparison. The time interval from end of irradiation to the encephalographic examination varied from four weeks in a patient



with temporal astrocytoma to 13 years in a patient with an ependymoma of the fourth ventricle. It is obvious that this is a selected group since not all patients receiving radiation therapy for lesions of the skull or its contents underwent follow up encephalography.

The primary pathology in the 40 patients is shown below (one patient was irradiated for both eosinophilic adenoma and medullary glioma)

Histiocytosis of calvarium	2
Sarcoma of calvarium	1
Pituitary tumor	12
Empty sella	1
Optic nerve ectopic pinealoma	1
Hypothalamic glioma	1
CPA metastasis	1
Glomus jugulare	2
Brain stem glioma	7
Medulloblastoma	2
Fourth ventricle ependymoma	1
Cerebellar astrocytoma	2
Pinealoma	2
Glioma roof of third ventricle	1
Cerebral hemisphere astrocytoma	5

There were 12 pituitary tumors, seven chromophobe adenomas and five eosinophilic adenomas. Of the 12 pituitary tumors, ten had visual fields recorded prior to irradiation. Five patients had abnormalities of their visual fields: four with chromophobe adenomas and one with eosinophilic adenoma. The ten patients all had visual fields recorded prior to their post radiation encephalography and the same five patients had abnormal visual fields, either unchanged or worse. One patient who was treated for pituitary tumor probably had an empty sella prior to the irradiation. She received irradiation on the basis of a ballooned sella and poorly documented visual field cut. There were six brain stem gliomas and five tumors of the cerebral hemisphere. The remainder of the lesions varied widely in type and location.

### Results

The post radiation encephalography revealed atrophy in 17 cases, residual tumor in 18. Residual tumor was diagnosed whenever there was a space occupying mass which may or may not have changed in size following radiation therapy. Atrophy was diagnosed whenever there was less than the normal amount of brain substance as evidenced on the films by enlargement or abnormal

position of the gas containing spaces. Atrophy was particularly evident when the brain stem had been included in the treatment field (Fig. 1). Two cases had both residual tumor and evidence of atrophic changes in adjacent brain tissue.

In two cases changes occurred other than atrophy or residual tumor: one case of obstructive hydrocephalus following meningitis and one case of post-operative adhesions. In two cases no encephalographic abnormality was demonstrated, one of these had been irradiated for brain stem glioma and the other an acromegalic, had no evidence of suprasellar extension at pre-radiation encephalography.

The atrophic group as seen below included all of the eosinophilic adenomas except the one which had no suprasellar extension before or after radiation. All but one of the cerebral hemisphere tumors were also in the atrophic group.

Eosinophilic adenomas	4
Chromophobe adenoma	1
Cerebral hemisphere gliomas	3
Pinealoma	1
Medulloblastoma	1
Ependymoma, fourth ventricle	1
Brain stem gliomas	3
Histiocytosis	1
Glomus jugulare	1
CPA metastasis	1

The group with residual tumor (see below) included all but two of the chromophobe adenomas, both of the cerebellar astrocytomas and two of the brain stem gliomas.

Chromophobe adenomas	5
Hypothalamic glioma	1
Cerebral hemisphere glioma	1
Pinealoma	1
Ectopic pinealoma	1
Glioma, roof of third ventricle	1
Cerebellar astrocytomas	2
Glioma of fourth ventricle	1
Brain stem gliomas	2
Glomus jugulare	1
Sarcoma of calvarium	1
Histiocytosis	1

Of the 18 patients having a diagnosis of residual tumor, six had surgical and three autopsy confirmation.



Fig. 1. A 41-year-old female seven years post irradiation for glomus jugulare tumor. Trembling of left side of face, tremor of all extremities and a tendency to fall to the left for three weeks prior to encephalogram. a) Lateral tomogram. b) Enlarged fourth ventricle with diminished caliber of the lower pons.



Fig. 2. An acromegalic 36-year-old male five years post irradiation. Recurrence of headaches and elevation of blood pressure. a) Brow-up lateral tomogram. Reversal of anterior third ventricle in normal position ( $\rightarrow$ ). Sulcus arachnoid gas is almost completely filling the enlarged sella. There is a thin strip of pituitary tissue posteriorly. b) Brow-up anteroposterior tomogram through floor of sella. There is a thin strip of pituitary tissue ( $\leftarrow$ ) between the gas-filled intra-sellar space and the lower floor of the enlarged sella ( $\rightarrow$ ).

### Discussion

ROBERTSON (1967) has illustrated a post-radiation encephalogram of an acromegalic which demonstrated gas in the pituitary fossa and at subsequent surgical exploration the pituitary fossa was found to be empty and no tumor



Fig. 3 A 5 year-old male received radiation therapy on three occasions over a period of six years on the basis of an enlarging sella and visual problems; the last irradiation was four years prior to encephalography. Brow up lateral tomogram: extensive destruction of floor of sella with the third ventricle extending into the enlarged pituitary fossa.

It has been LEE & ADAMS included a similar case in their discussion of the empty sella syndrome. Five of the eosinophilic adenomas and one of the chromophobe adenomas in the present series demonstrated this type of change. Four of the eosinophilic adenomas showed varying degrees of arachnoidal gas in the sella (Fig. 2). One of the eosinophilic adenomas and one of the chromophobe adenomas had the third ventricle protruding into the sella (Fig. 3). These cases of empty sella are secondary to the treatment and differ from the empty sella described by KAUFMAN (1968) and by GABRIELE (1968) which is not associated with tumor.

MATSON (1969) reported an average survival time for patients with brain stem glioma of less than one year and stated that should any patient with a clinical diagnosis of brain stem glioma still be alive as long as 18 months after diagnostic investigation and surgical exploration is indicated as some other lesion is probably present. In EVANS (1969) experience the reverse has been true: in his opinion if post radiation encephalography does not demonstrate regression of the tumor then another diagnosis should be entertained. ROBERTSON (1967) has illustrated three cases of brain stem gliomas with post radiation encephalography: one case examined ten months following irradiation demonstrated a return to normal appearance; a second case examined 15 months post irradiation demonstrated atrophic changes. Two patients in the present series demonstrated residual tumor at three and five years respectively after radiation; two patients examined at two months and 21 months respectively following radiation showed a return to normal appearance and two patients examined at one and two years post irradiation had atrophic changes (Fig. 4).

ROBERTSON described one patient with cerebellar astrocytoma who was examined 12 years following radiation therapy with the finding of atrophic changes at

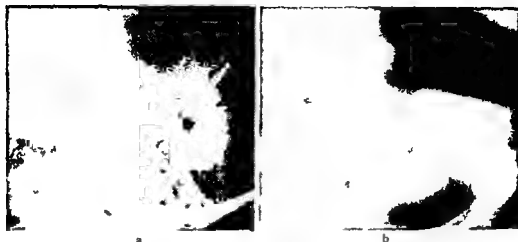


Fig 4. A 9-year-old female with blindness and optic atrophy two years following completion of irradiation for pontine glioma. a) Upright lateral view prior to radiation therapy. The pontine cistern is compressed, the aqueduct stretched and elevated, and the fourth ventricle compressed. b) Upright lateral tomogram after irradiation. Enlarged fourth ventricle, prominent cerebellar folia, and marked reduction in size of brain stem.



Fig 5. A 29-year-old male. A needle biopsy of a grade II astrocytoma in the left temporal lobe was performed four months prior to the encephalography. Irradiation completed four weeks prior to the encephalograph. a) Brow-up AP view, marked enlargement of left temporal horn. b) Brow-down half axial view, enlargement of trigone on left.

encephalography. Two years later surgical exploration demonstrated radionecrosis and regrowth of tumor. Both cerebellar astrocytomas in the present series showed evidence of residual tumor at post-radiation encephalography.

ROBERTSON found that there was reduction in the size of the cerebral hemisphere evidenced by enlargement of the ventricle following roentgen therapy in spite of roentgenographic evidence of residual tumor. Of those patients in the

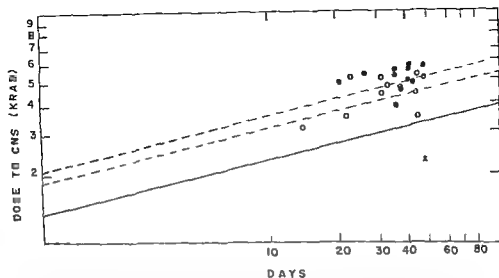


Fig 6 Radiation dose in 23 patients plotted on a Strandquist graph which includes three recommended lines aimed at preventing radiation damage. The upper curve is that recommended by BODEN (1950) for the prevention of radiation myelitis. The middle curve is that of LINDGREN (1958) who was concerned primarily with cerebral necrosis. The lower curve is that of PALLIS et coll (1961) below which only one well documented case of myelitis has been reported. Open circles patients with encephalographic evidence of residual tumor. Closed circles atrophy group (one case as an  $\times$ ). All but two of the atrophy group are above LINDGREN's line and one of these is above PALLIS line. The one case below PALLIS line as a brain stem glioma (Fig 4). (BODEN's curve is in roentgens)

present series that received irradiation to the cerebral hemispheres five revealed evidence of atrophy without roentgen evidence of residual tumor (Fig 5) and four showed evidence of residual tumor with no significant atrophic changes.

Of the patients in this series with atrophic changes for whom adequate information was available concerning their radiation therapy nine were considered to have received only moderate doses of radiation and two had received what we considered a low radiation dose. Only two in this group were considered to have received more than a moderate tumor dose. However when plotted on a Strandquist graph the radiation dose appears more significant (Fig 6). Surprisingly the patient in whom the radiation dose seemed least significant had marked atrophic changes at encephalography (Fig 4).

## SUMMARY

When symptoms do recur following irradiation it is important to keep in mind the possibility of radiation damage rather than a recurrence of tumor as a cause for the symptoms regardless of the dose delivered particularly when such radiosensitive areas as the brain

stem are included in the treatment field. It is essential that the patient be re-evaluated by neuroradiologic investigations to determine if in fact the symptoms are related to radiation damage.

## ZUSAMMENFASSUNG

Wenn nach einer Bestrahlung Symptome wiederauftreten, ist es wichtig, die Möglichkeit eines Strahlenschadens als Ursache der Symptome eher als das Wiederauftreten des Tumors zu erwägen, unabhängig von der verabfolgten Dosis, besonders wenn derartig strahlenempfindliche Gebiete wie der Hirnstamm im bestrahlten Feld gewesen sind. Es ist wichtig, dass der Patient erneut neuroradiologisch untersucht wird, um festzustellen, ob die Symptome tatsächlich auf einen Strahlenschaden zurückzuführen sind.

## RÉSUMÉ

Quand des symptômes réapparaissent après l'irradiation, il est important de penser que la cause des symptômes peut être une radio lésion plutôt qu'une récurrence de tumeur, quelle que soit la dose délivrée, en particulier quand des régions radiosensibles comme le tronc cérébral sont comprises dans le champ de traitement. Il est essentiel de faire de nouveaux examens neuroradiologiques pour déterminer si, en réalité, les symptômes sont dus à une radio lésion.

## REFERENCES

- BODEN G. Radiation myelitis of the brain stem. *J. Fac. Radiol.* 2 (1950) 79.
- EVANS R. A. Brain stem gliomas. Presented at third annual Leo G. Rigler radiology symposium on pediatric neuroradiology. UCLA School of Medicine, Los Angeles, California, November 8—9, 1969.
- GABRIELE O. F. The empty sella syndrome. *Amer. J. Roentgenol.* 104 (1968) 168.
- KAUFMAN B. The empty sella turcica. A manifestation of the intrasellar subarachnoid space. *Radiology* 90 (1968) 931.
- LEE W. M. and ADAMS J. E. The empty sella syndrome. *J. Neurosurg.* 28 (1968) 351.
- LINDGREN M. On tolerance of brain tissue and sensitivity of brain tumours to irradiation. *Acta radiol.* (1958) Suppl. No. 170.
- MATSON D. D. *Neurosurgery of infancy and childhood*. 2nd Ed. Charles C. Thomas, Springfield, Illinois, 1969.
- PALLIS C. A., LOUIS S. and MORGAN R. L. Radiation myelopathy. *Brain* 84 (1961) 460.
- ROBERTSON E. G. *Pneumoencephalography*. 2nd Ed. Charles C. Thomas, Springfield, Illinois, 1967.
- VERITY G. L. Tissue tolerance, central nervous system. *Radiology* 91 (1968) 1221.

## INTRACAVITARY RADIUM TREATMENT OF MALIGNANT TUMOURS OF THE URINARY BLADDER

by

M PEDERSEN and S E HERTING

The literature has from the beginning of this century contained publications dealing with the intraluminal treatment of malignant diseases of the urinary bladder with radioactive isotopes a form of therapy that has been considerably increased by their production in atom piles. The isotopes used have been in the form of interstitially implanted radioactive media tantalum wires (WALLACE et coll 1952 BLOOM 1960) radon seeds (POOLE WILSON 1950) gold grains (HODT et coll 1952) and radium needle implantations (VAN DER WERF MEISSING 1965 1969) as well as by the intravesical instillation of radioactive solutions with or without a container of Na and Ba isotopes (WALTON & SINCLAIR 1952) and Au and Co-isotopes (ELLIS & OLIVER 1955 MÜLLER 1949 MEHLEN 1962). Radium and cobalt sources in a balloon have also been placed centrally in the bladder (FRIEDMAN & LEWIS 1949 1958 SELL & JØRGENSEN 1962, SELL 1967).

The treatment results of most of these different treatment techniques have been difficult to evaluate and compare partly because of the absence of common rules of tumour classification and partly because of the selection of patients.

From the Radium Centre and the Institute of Pathology Odense Sygehus Denmark.  
Submitted for publication 27 september 1971



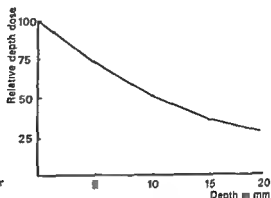


Fig 1 Percentage depth dose in the bladder wall from a central radium source

which presumably has often been a radical one although this is difficult to estimate from the figures. During the last years these methods of treatment especially after the introduction of high voltage therapy in the treatment of carcinoma of the bladder have been on the decline.

The principles, the practical performance, the advantages and disadvantages, complications and fields of indication have been presented in detail by WALLACE 1959. SELL & JØRGENSEN in a preliminary publication described the principles in the treatment of growths of the bladder with intracavitary radium by a modified Walter Reed technique. The results of this treatment in 50 cases of benign and malignant tumours (SELL) failed to reach those obtained by FRIEDMAN & LEWIS (1948, 1958) who in a similar number of cases in all stages from A to D<sub>2</sub> (MARSHALL'S classification 1956), obtained a 5 year crude survival rate of 56 per cent. This appeared to be a high goal to reach in this condition.

The present investigation was undertaken to deal with the results and complications in the treatment of 165 cases of malignancy and to throw further light on the usefulness of the method. Forty of these cases were part of the material published by SELL. The tumours have been reclassified, following the recommendations of the UICC, by the TNM system. They have also been graded according to the principles laid down by BERGQUIST et al (1965) with a grading of malignancy from 0 to IV.

*Method.* This was described in detail by FRIEDMAN & LEWIS (1958) and SELL & JØRGENSEN. The principle consists in irradiating the bladder from the inside by means of a radium source placed centrally in the balloon of a Foley catheter 24 — 26. The balloon is distended to a volume of 40 ml and produces a relatively stable means of placing the radium source in the center of the bladder at a distance of about 4 cm from the wall, this is of course provided the lumen

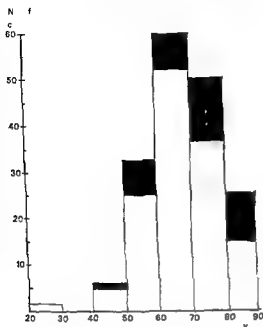


Fig 2 Age distribution at the time of treatment Men white column Women black column

of the bladder is not filled with any mass that displaces the balloon with the radium source. The essential part of the original Walter Reed technique consisted in stinging the catheter through a cystotomy. Large tumour processes could thus be removed and symmetric and central location of the radium source with homogeneous irradiation of the mucosa secured, furthermore, by reducing the masses underdosage of the deepest layers of the tumour could be avoided. Only in a few of the present cases was the catheter introduced through a cystotomy; it was usually passed up the urethra and its final position controlled by cystography after the instillation of a few ml of contrast medium.

The dose to the balloon surface and the mucosa for 120 hours is approximately 3 500 rad for a 20 mg source. The treatment was usually administered in two sessions of 120 hours each with an interval of 14 days to give a total dose to the mucosa of 7 000 rad/25 days. Because of the rapidly decreasing depth dose (Fig 1) the total dose to tumour cells lying 10 to 12 mm under the mucosa will be only 3 500 rad and at a depth of 20 mm about 1 700 to 1 800 rad/25 days.

The intention of the treatment was merely palliative in some of the cases. These were treated at one session with a total dose of 3 500 rad/5 days. The source was occasionally placed eccentrically in the balloon e.g. in growths at base of the bladder with possible invasion of the prostate.

Table 1  
*Distribution of growths and histologic type*

	Transitional cellular	Planocellular	Other histology
Men	120	9 (6.5 %)	2
Women	25	9 (26 %)	1
Ratio Men/Women	4.8/1	1/1	

*Material* Most of the cases were admitted from surgical departments in the district for radiation therapy but some 5 per cent were resident outside this area and were admitted specifically for treatment in a period when high-voltage therapy for carcinoma of the bladder had not become general. The cases were selected primarily from those in which (1) surgical treatment was unsuitable, especially those with large tumours in which the alternative would be cystectomy or extensive electrocoagulation (2) in biologically inoperable cases in which the risk of operation was considered too great, and (3) in cases in which the treatment was clearly palliative especially in those with large bleeding tumours. Only in a few cases was the treatment part of a prescheduled treatment plan. The treatment was given to only 12 cases with no residual malignancy, the remainder not having undergone radical operation or no operation at all. An obvious selection of cases in the direction of a bad risk material thus occurred with a large proportion of widespread and multiple tumours and a heavy load of patients in poor general condition.

A total of 181 cases were treated in the period 1958 to 1965. Eight have been omitted from the investigation because of the absence of histologic confirmation and a wrong diagnosis. 8 cases had no malignancy of the bladder and were omitted as well. Malignancy was present in 165 cases, 131 of which were men and 34 women, a ratio of 3.8/1. Sixty-nine patients were over 70 (42 per cent) and 120 patients were over 60 (72 per cent), the average age for men was 67.8 and for women 63.5 years (Fig. 2).

The distribution of growths by histologic type (Table 1) indicates a surprisingly high incidence of the planocellular variety. These were mostly of low differentiation and carried a bad prognosis because of which they have in the following tables and figures been separated from those of the pure transitional cell type.

Only one case of adenocarcinoma and one of leiomyosarcoma were registered.

All the histologic slides have been revised by one of the authors (S.E.H.) for grading of malignancy by the principle laid down by BERGQUIST *et coll.* (1965). The distribution of planocellular carcinomas and transitional cell

Table 2

*Distribution of tumours of different histology and grading in tumour categories T 1 s to T 4*

TNM category	Transitional cell tumours			Tumours of other histology		
	II	III	IV	Plano	Adenoc	Sarcoma
T in s tu	21	5	0	0	0	0
T 1	10	36	5	3	0	0
T 2	3	19	2	4	0	0
T 3	2	13	13	7	1	0
T 4	1	7	8	4	0	1
Total	37	80	28	18	1	1

carcinomas grade II to IV in the clinical tumour categories T 1 s to T 4 appears from Table 2, while Table 3 presents the percentage of grades II to IV in each tumour category. As expected tumours of grade II dominate categories T 1 s and T 1 while this grade of differentiation seldom appears in tumours of deeper infiltration. In one instance however a grade II tumour was in category T 4 in 2 cases in category T 3 and in 3 cases in category T 2.

Tumour classification was carried out according to the principles laid down by the UICC by means of the TNM system based on cystoscopy, biopsy and bimanual palpation under general anaesthesia. Evaluation of the N factor has not been possible and lymphography not performed. Only in the palliative treatment group have distant metastases been demonstrated and then only in 10 cases.

All the cases were confirmed histologically by biopsy. P staging from histologic slides obtained at operation was possible in 82 cases. Ninety four cases were operated upon but in 12 of these no material for histologic examination was available. Where the clinical evaluation of tumour category has been uncertain the case has been placed in the lowest of the two possible categories, risking rather an understatement than overstatement of tumour category and thereby a displacement of treatment results in a favourable direction.

The treatment must be characterised as palliative in 8 cases classified as category T 3 and in all cases of category T 4. Ten of these had distant metastases at the beginning of treatment and in nearly all palliative cases the doses were reduced to half the usual. The 29 cases appear in some tables as a palliative treatment group.

The cases may in principle be divided into two large groups. One group consisting of 71 cases were not subjected to any surgical treatment before radium

Table 3

*Percentage of tumours of grades II to IV in tumour categories T<sub>1</sub> s to T<sub>4</sub> in 145 transitional cell carcinomas*

TNM category	Transitional cell tumours ( )			Total number
	II	III	IV	
T <sub>1</sub> in situ	81	10	0	26
T <sub>1</sub>	20	70	10	51
T <sub>2</sub>	12	80	8	24
T <sub>3</sub>	8	46	46	28
T <sub>4</sub>	6	44	50	16

Table 4

*Distribution by primary conditions and recurrences*

Primary cases 125	<div> <div>Curative Treatment 165</div> <div>Palliative Treatment</div> </div>	130	No surgery	50 pat
			Surgery + Radium	<div>radical op 12 pat</div> <div>conservative op 74 pat</div>
		29	No surgery	21 pat
			Surgery + Radium	<div>radical op 0 pat</div> <div>conservative op 8 pat</div>
Recurrences 40				

therapy apart from biopsy the other group of 94 cases had some surgical treatment before the radium therapy, the treatment being radical in only 12 patients. Eleven cases had resection of the bladder, 3 of these resections being radical. In 9 cases the treatment was performed transurethrally as electrocoagulations and electroresections, in no instance radical. Operation in the remaining 74 cases was performed transcscally with cystotomy as electrocoagulation, resections and extirpations, in only 9 cases radical.

Radium treatment following operation was administered two to three weeks later except in a few cases when the first treatment was received in immediate connection with the operation.

The distribution of 165 cases by primary conditions and recurrences, curative and palliative treatment and surgery and no surgery grouping appears in Table 4.

### Results

All the cases have been followed for at least 5 years. A total of 144 of the initial 165 cases have been controlled without loss for 7 years. The data were obtained on a fixed date 31 December 1970, and at annual controls where

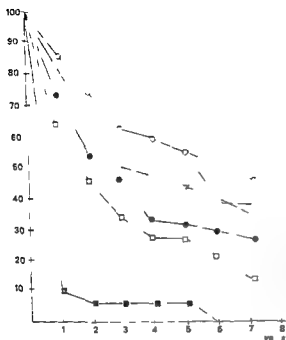


Fig 3 Crude survival rates in 165 cases of carcinoma of the bladder of all histologic types and grades. Last part of curve for T1s has been computed because a rapid fall in observations between 5 and 7 years deforms the curve (Correction stippled line) ○ T1s × T1 ● T2 □ T3 ■ T4

cystoscopy and exploration were performed under general anaesthesia. Only for the patients of tumour category T1s has it been necessary to compute the 7 year survival rate as a large drop in observations between the fifth and seventh year distorts the survival curve (Fig 3). The survival rates enumerated in tables and figures are crude survival rates (CSR). Five of the 53 patients surviving five years without recurrence had been subjected to surgical treatment in the period between the radium treatment and 5 year observation, the CSR in reality being 5 year recurrence free.

Twenty-one patients died without recurrence before the end of the 5 year observation. Cystoscopy at the most three months before death had failed to demonstrate any sign of residue or recurrence. The tables and figures have not been corrected for this rather large proportion of deaths without recurrence, a correction that might seem reasonable in a population of such high average age.

The CSR for cases in tumour categories T1s to T4 appear in Fig 3. For categories T1s and T1 the initial steep decline in the survival curve ends at the third year and for categories T2 and T3 at the fourth year. Ninety

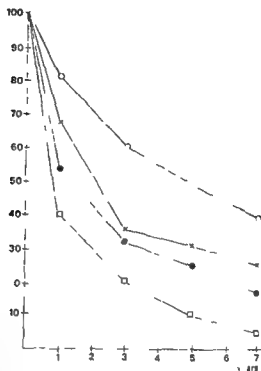
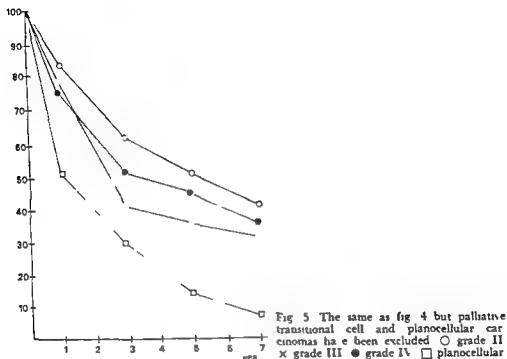


Fig. 4 Crude survival rates in 163 cases of transitional cell and planocellular carcinomas of the bladder according to histology and grade. One adenocarcinoma and a leiomyosarcoma are excluded. ○ grade II, × grade III, ● grade IV, □ planocellular.

per cent of the 29 patients in category T 4 were dead at the end of the first year, only one patient in this category survived 5 years.

By way of comparison Fig. 4 gives the CSR for cases with tumours of different grades of differentiation: transitional cell carcinomas and planocellular carcinomas. An adenocarcinoma and a leiomyosarcoma of category T 3 and T 2 are not included, both the patients being dead at the end of the first year. The considerably better prognosis in grade II tumours is evident. Fifty six per cent of these tumours belonged to tumour category T 1 & 2. When all the cases are placed under one heading there appears to be little significant difference in the CSR for those with growths of grade III and IV, in spite of the fact that 75 per cent of grade IV tumours were in categories T 3 and T 4, the corresponding figure for grade III being only 25 per cent. When palliative cases are excluded, i.e. all cases of T 4 and 8 of those in T 3, the situation is reversed, the grade IV tumours now having a slightly better 5 year CSR than those of grade III (Fig. 5).

The difference in the CSR between grade III and the low differentiated grade IV tumours is not significant, the slightly better prognosis for the latter in those



cases that were subjected to curative treatment and in which adequate tumour doses could be obtained might indicate a higher radiation sensitivity

The poor prognosis in planocellular carcinomas is noteworthy. Only 2 of 18 patients survived for five years, one dying without recurrence after six years, the other from distant metastases but without vesical recurrences seven years after the radium treatment.

The distribution of cases into primary cases and recurrences was 125/40. The representation of palliative cases in these two groups was 25 per cent in each, the rate of planocellular carcinomas being the same and the distribution of cases in tumour categories and grades identical. Nevertheless there was considerable difference in the CSR in the groups. The 5 year CSR for 104 primary cases treated with a curative intention was 42 per cent, while the corresponding figure in recurrences was 28 per cent; this last group consisted however only of 32 cases and the difference in CSR is not statistically significant.

The treatment results in cases of transitional cell and planocellular carcinomas treated with radium alone and with a combination of surgery and radium are



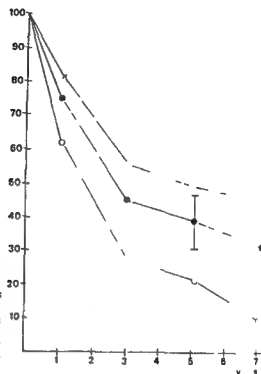


Fig 6 Crude survival rates in 136 cases of transitional cell and planocellular carcinomas of the bladder treated with radium alone and with surgery and radium. Palliative cases have been excluded.  $2 \times SD$  has been marked.  $\times$  surgery + radium (86 cases).  $\circ$  radium alone (50 cases).

presented (Fig 6). Palliative cases have been excluded. A total of 136 cases was treated: 50 with radium alone and 86 with radium and surgery, the first group including 8 planocellular neoplasms, the last 7 tumours of this histology. The distribution of tumour categories was, however, to the prejudice of the non-operated group, this carrying a heavy load of T 3 tumours of 15/50, i.e. 30 per cent, while only 12/86 of the operated group belonged to this category, i.e. 14 per cent. Bearing this difference in selection in mind, the 5 year CSR in the operated group is significantly better. Radically and unradically operated cases were not distinguished since their prognosis did not differ (Fig 6).

The total 5 year CSR in cases with transitional cell tumours treated with radium alone was 16 per cent. When the intention of the treatment was cure, the figure rose to 24 per cent. A 5 year CSR of 51 per cent was reached when the radium treatment was preceded by surgery. The results with this combined treatment are nearly identical in tumour categories I, II, III and IV, and not much worse in T 3 (Table 5). The number of solitary tumours in the operated group was substantially higher and, as earlier mentioned, this group included fewer cases of T 3.

Table 5

Five year crude survival rates in 145 transitional cell carcinomas of the bladder curative and palliative cases according to treatment group. The fractions under the headings T1s to T4 indicate the 5-year survivors/the number of cases treated

	Number	Curative treatment				5-year CSR curative	Palliative treatment		5 year CSR total
		T1s	T1	T2	T3		T3	T4	
		26	51	24	20		8	21	
No surgery	61	5/10	4/16	0/5	1/11	10/42 (24 )	0/7	0/12	10/61 (16 )
Surgery with residue	73	7/14	15/27	9/18	4/9	33/68 (51 )	0/1	1/4	36/73 (49 )
Surgery without residue	11	1/2	4/8	0/1	0	5/11 (43 )	0	0	5/11 (45 )

The grave outlook for patients in the palliative group is illustrated by the fact that 50 per cent of these were dead 3 months after treatment and 90 per cent after one year.

As in other published results of treatment of carcinoma of the bladder this material has indicated a better prognosis for papillomatous than for solid tumours of the transitional cell type and the 5 year CSR for solitary tumours clearly separates them from multiple tumours (Table 6). A significant difference within 95 per cent confidence limits between solitary and multiple papillomatous tumours (61 and 33 per cent 5 year CSR respectively) and between papillomatous and solid tumours (43 and 18 per cent 5 year CSR respectively) was recorded in the whole material. Out of 145 transitional cell tumours, 42 were of the solid type and of these 42 only 3 growths were of grade II differentiation.

Ninety one patients had recurrence locally in the bladder or distant metastases within the first 5 years after radium treatment. With the exception of 5 patients the e were all dead before 5 years had elapsed after treatment. 50 per cent having died after 2 years and 75 per cent after 3 years. Surprisingly the time of recurrence and death seem independent of category in T1s to T3 tumours, while 90 per cent of patients with T4 tumours were dead after about a year.

Nine cases with recurrence had cystectomy between 1 and 3 years after treatment by radium. This was followed in one case by fatal complications but by none in the others. None of these patients lived more than 2 years after operation.

The immediate mortality following treatment by radium is hard to evaluate. Only 2 patients died during the treatment these from pneumonia and heart

Table 6

*Five year crude survival rates according to type and multiplicity of transitional cell tumours. Fractions indicate number of 5-year survivors/total number of group. Planocellular tumours and tumours of other histology are not included*

	Solitary	Multiple	5 year CSR
Papillary	22/36 (61 %)	21/64 (33 %)	43/100 (43 %)
Solid	7/29 (24 %)	1/16 (6 %)	8/45 (18 %)
5 year CSR	29/65 (44 %)	22/80 (27 %)	

failure 11 patients died within a month of treatment and within two months a total of 22 patients was dead half of these belonging to the palliative treatment group

**Complications** The evaluation of complications in intracavitary radium treatment has been made difficult by the fact that in 94 cases a mixture of post operative and postactinic sequelae arose. Infection of the bladder has often been present before the treatment a fact that presumably plays a certain role, especially in the development of immediate reactions, and possibly in late sequelae as well these latter may of course mask a recurrence.

Immediate complications have consisted of more or less marked symptoms of cystitis with dysuria and spasm. These have usually been relieved by suitable analgesics often of the morphine type and psychosedatives such as largactil. Some infection of the urinary tract has usually occurred and has been treated with antibiotics. Only rarely have the immediate complications been so marked as to warrant discontinuation of the treatment. This material has not produced evidence of any connection between the severity of immediate complications and the length of interval between surgery especially electrocoagulation and the treatment by radium. Neither have any differences in immediate reactions been noticed between cases treated with radium alone and those undergoing surgery followed by radium. On the other hand the immediate as well as late complications have been most marked where radium has been used in the treatment of recurrences, especially in cases earlier subjected to multiple electrocoagulations.

Late sequelae were registered in 39 cases although they appeared in 12 of these in close relation to recurrences one to three years after the radium. The

Table 7

*Late sequelae in 165 patients treated with intracavitary radium for malignancy*

Complications	No. of cases	Treatment
Severe cystitis	8	Prednisone (8)
Severe cystitis and constricted bladder	14	Cystectomy (8) Ileum and bladder (1) Prednisone (5)
Severe cystitis and necrosis	8	Cystectomy (1) Resection (1) Prednisone (6)
Calculus	5	Lithotripsy (3) Prednisone (2)
Urethral stricture	6	Bougie treatment (5) No treatment (1)
Total number	41 cases/39 patients (25 )	
Without recurrence	29 cases/27 patients (16 )	

dominating complication was severe radiation cystitis with severe inflammatory changes, bleeding in the mucosa and layers of fibrinous incrustations in more marked cases with necrosis, usually at the site of the primary tumour even ending in fibrosis of the bladder wall and with a decrease in vesical volumes of 50 to 100 ml.

Severe radiation cystitis occurred in 30 cases (Table 7). This in 14 cases produced a constricted bladder and in 8 cases necrosis. Prednisone or triamcinolone and antibiotics always formed the primary treatment. Cystectomy had to be done in 8 cases with a constricted bladder but was never fatal: it was planned in a further case but was not performed because of a large inoperable recurrence. Treatment with prednisone rendered 5 cases relatively symptom free. Necrosis was an indication for cystectomy in one case, in another resection of the bladder was done and 6 cases presented no indications for operative treatment. Of 9 patients in whom cystectomy was performed because of complications 6 survived for five years without recurrence, 2 died without recurrence and 1 patient died 2 1/2 years after cystectomy from distant metastases from a grade II tumour category T<sub>1</sub>s.

The total number of complications amounted to 41 in 39 cases out of 165 treated (or 25 per cent) (Table 7). Twelve cases had symptoms of cystitis in close relationship to recurrence and it seems reasonable to subtract these so as to leave a rate of complications of 27/165 (16 per cent). Approximately half

these cases were subjected to surgical treatment. Operative treatment of complications in no instance led to a fatal outcome.

No renal complications have been recorded in this material.

### Discussion

The results presented seem substantially inferior to those obtained by FRIEDMAN & LEWIS (1958). The 5 year CSR for all cases of transitional cell carcinoma is 51/145 (35 per cent). This figure does not include the planocellular carcinomas whose prognosis is extremely poor with a 5 year CSR of 2/18 (11 per cent), a survival rate that corresponds with that obtained with other treatment procedures, including cystectomy.

In considering a group that may reasonably be compared to the one of FRIEDMAN & LEWIS the cases treated by combined surgery and intracavitary radium may be selected. Of 84 patients with transitional cell carcinoma treated with a combination of surgery and radiation therapy, 41 or nearly 50 per cent, lived for 5 years without recurrence. These were nearly evenly distributed in the tumour categories T 1 s to T 2 (Table 5). It seems fair to assume that the improvement in possibilities for a central symmetric placing of the radium catheter and the reduction in tumour masses obtained by operation has played an essential role in securing more homogeneous irradiation of the bladder wall and higher doses to peripheral parts of the tumour.

Treatment with intracavitary radium without preceding surgery has had little success. Of 61 cases with transitional cell carcinomas so treated only 10 lived for 5 years i.e. 16 per cent. The selection of cases for this treatment was heavy, nearly 50 per cent of the growths being of category T 3 and T 4 in contrast to a corresponding figure of 16 per cent for the operated group. But even if these advanced tumours of category T 3 and T 4 be ignored it is obvious that only in category T 1 s have the results obtained by radium treatment alone been equal to those secured by combined treatment, with a 5 year CSR of 50 per cent. The results have been considerably inferior in the categories T 1, T 2 and T 3. The distribution of tumours of grades II, III and IV has been equal but in the non-operated group an overweight of multiple tumours was evident. It seems reasonable to assume that the results would have been better in this group if the original Walter Reed technique with application of the radium catheter through a cystotomy had been used, or, at any rate, certain tumour ablation surgery had been performed before the introduction of the catheter.

The importance of grade of cell differentiation in assessing treatment results and procedures is hard to evaluate from this material. The prognosis in grade II tumours is significantly better than in grade III and IV tumours. This is in good agreement with the fact that grade II tumours in only 44 per cent of cases

were invasive, while the corresponding figures in grades III and IV were 94 and 100 per cent respectively. This investigation has demonstrated no significant difference in the treatment results between grade III and grade IV tumours but the relatively small figures prevent any realistic evaluation. It must be stressed however, that in spite of the fact that 75 per cent of grade IV tumours were in categories T 3 and T 4, while only 25 per cent of grade III tumours were in these categories the 5 year CSR for these grades did not differ significantly.

The classification of tumours by the TNM system seems to work well. A close relationship between the 5 year CSR and T category was evident. Grading of the tumours by their differentiation is of the greatest help in distinguishing between grade II tumours and those of grades III + IV and of lesser significance in distinguishing grade III and grade IV tumours at any rate when the treatment consists of a combination of surgery and radiation therapy. The authors suggest that the most accurate representation of a vesical tumour would be obtained by a combination of TNM staging, a cytologic grading by the BERGQUIST method and a classification of the growths into papillomatous and solid differentiated and undifferentiated tumours according to the IOU system.

### Conclusion

Intracavitary treatment by radium may be eliminated as a reasonable choice among a multitude of irradiation procedures when the tumor is of category T 3 or T 4. These growths are usually of such magnitude and extend extravasically that the rapid fall in the percentage depth dose will produce a low tumour dose in peripheral tumour areas with a considerable risk of underdosage. Furthermore these advanced tumours are often associated with metastases to regional glands on the pelvic wall glands that will be markedly underdosed. Only in palliative cases can intracavitary treatment be considered.

Leaving out of account the complications and considering the treatment results alone intracavitary radium treatment seems very suitable for the treatment of tumours of category T 1 s with or without preceding surgery. The results in category T 1 are best when the treatment is combined with surgery transvesical and transurethral and the same seems to obtain in tumours with superficial muscular invasion category T 2 and even in cases of deep muscular invasion category T 3, but without large extravasical masses. The 5 year CSR for these three tumour stages in the present material has been 55, 45 and 40 per cent respectively when the treatment has been a combination of radical or conservative surgery and radium.

The treatment results are as in all forms of treatment of vesical malignancy best when the tumour is solitary and especially when it is papillomatous. The

limitation of the irradiation methods based on implantation techniques tantalum wire implantation and radium needle implantation is the magnitude of the masses, most authors considering a diameter of 4 to 5 cm as the maximum safety margin. Many of the so called solitary tumours of the present series have had a diameter exceeding this, suggesting that intracavitary radium treatment may be a reasonable alternative to implantation. High voltage, external treatment would here most often be the method of choice easily obtainable as it is in most centres nowadays. Complications must however be considered. These are rather heavy in intracavitary treatment but the question arises as to whether these are not acceptable if a higher cure rate be obtainable. External high voltage therapy of vesical tumours is not without sequelae although these seem fewer (EdsMYR et coll 1967) and of another type, especially when arising from the intestinal tract. The good results obtained in carcinoma of the uterine cervix with combined radium and external high voltage therapy suggest that a similar combination might be a possibility worthwhile investigating in carcinoma of the bladder, as an alternative to primary cystectomy. The consequence of such a treatment would doubtless be a number of secondary cystectomies because of complications although this might not be an unreasonable price to pay if the result were higher cure rates for this very malignant condition.

The results presented were obtained in cases which because of the selection, must be characterized as bad risks and are likely the minimum obtainable with this treatment procedure. No doubt better results would be obtained in a fair clinical trial and it seems reasonable to believe that the frequency of complications could be substantially diminished if the radium therapy were combined with careful conservative surgery and antibiotic treatment before, during and after radium therapy.

### SUMMARY

The results and complications in the treatment of 165 cases of malignant disease of the bladder by radium alone and combined with surgery have been investigated. The importance of the tumour grading and the selection of the patient are considered. The advantages of the use of intracavitary radium as opposed to high voltage therapy is discussed. The five year survival rate rose to about 50 per cent with radium treatment preceded by surgery.

### ZUSAMMENFASSUNG

Die Ergebnisse und Komplikationen der Behandlung von 165 Fällen einer malignen Erkrankung der Blase durch Radium alleine oder in Kombination mit Chirurgie wurden untersucht. Die Bedeutung der Grad Einteilung der Tumoren und der Selektion der Patienten wird hervorgehoben. Die Vorteile der Verwendung der intrakavitären Radiumbehandlung gegenüber der Hochvolttherapie wird besprochen. Die 5 Jahres Überlebensrate stieg mit der Radiumbehandlung nach vorhergehender chirurgischer Behandlung auf etwa 50 Prozent.

## RÉSUMÉ

Les auteurs ont étudié les résultats et les complications dans le traitement de 163 cas d'affection maligne de la vessie par le radium seul et associé à la chirurgie. Ils examinent l'importance de la détermination du grade de la tumeur et de la sélection des malades. Ils étudient les avantages de l'emploi du radium intracavitaire comparé au traitement par les haut voltage. Le taux de survie à 5 ans s'est élevé à environ 50% des cas traités par le radium après traitement chirurgical.

## REFERENCES

- BERGQVIST A, LJUNGLIST A and MOBERGER G. Classification of bladder tumours based on the cellular pattern. *Acta chir scand* 130 (1965) 371
- BLOOM H J J. Treatment of carcinoma of the bladder. *Brit J Radiol* 33 (1960) 392
- FOSMYR F, JACOBSSON F, DAHL O and WALSTAM H. Cobalt 60 teletherapy of carcinoma of the bladder. *Acta radiol Ther Phys Biol* 6 (1967) 81
- ELLIS F and OLIVER R. Treatment of papilloma of bladder with radioactive colloidal gold. *Au 198 Brit med J* 1 (1955) 136
- FRIEDMAN M and LEWIS L G. A new technique for the radium treatment of carcinoma of the bladder. *Radiology* 53 (1949) 342
- Irradiation of carcinoma of the bladder by a central intracavitary radium and cobalt 60 source (the Walter Reed technique). *Amer J Roentgenol* 79 (1958) 6
- HODG H J, SINCLAIR W K and SMITHERS D N. A gun for interstitial implantation of radioactive gold grains. *Brit J Radiol* 25 (1952) 419
- MARSHAL V F. Bladder tumours. A symposium. Lippincott Philadelphia 1956
- MEISEN P P. Die intravesicale Radiokobalt Behandlung beim Harnblasenkarzinom. *Dtsch med Wschr* 87 (1962) 1496
- MÜLLER J H. Über die multiplen Anwendungsmöglichkeiten eines langlebigen künstlichen radioaktiven Isotops (60-Co) in flüssiger Form für die Strahlentherapie maligner Tumoren. *Schweiz med Wschr* 79 (1949) 547
- POOLE WILSON D S. The treatment of carcinoma of the bladder. *Brit J Urol* 22 (1950) 414
- SELL A. Intracavitary radium therapy of bladder tumours. *Dan med Bull* 14 (1967) 21
- and JØRGENSEN B. Intracavitary radium therapy of bladder tumours. *Dan med Bull* 9 (1962) 189
- UICC. Classification of malignant tumours. Union International Contre le Cancer. Geneva 1968
- WALLACE D M. Tumours of the bladder. Vol 2 p 257. Livingstone London 1959
- WALLACE R J, STAPLETON J E and TURNER R C. Radioactive tantalum wire implantation as a method of treatment for early carcinoma of the bladder. *Brit J Radiol* 25 (1952) 471
- WALTON R J and SINCLAIR W A. Radioactive solutions (Na 24 and Ba-82) in the treatment of carcinoma of the bladder. *Brit med Bull* 8 (1952) 158
- VAN DER WERF MESSING B. Treatment of carcinoma of the bladder with radium. *Clin Radiol* 16 (1965) 16
- Carcinoma of the bladder treated by suprapubic radium implants. *Europ J Cancer* 5 (1969) 277



## RADIOLOGIC PULMONARY CHANGES FOLLOWING COBALT 60 TREATMENT OF MAMMARY CARCINOMA

by

S. HAGEN and A. KOLBENSTVEDT

Patients with mammary carcinoma treated by irradiation may develop changes in the lungs and pleurae the frequency and localization of which will depend on the dose and type of irradiation. The percentage of patients with visible changes reported in the literature varies from 7 per cent (Chu et coll. 1955) to 40 per cent (Ross 1956). This paper deals with these changes as revealed in routine chest roentgenograms during follow up of a group of patients treated by cobalt 60.

*Material* Eighty three patients with histologically proven mammary carcinoma were given postoperative cobalt 60 during the period January 1968 — June 1969. All patients had been treated by radical mastectomy and staged I and II (Stage I: no metastases; Stage II: metastases of the axillary lymph nodes. No evidence of metastases elsewhere). Thirteen patients were later excluded due to absence of follow up films four months or more after the end of treatment.

The irradiation was as follows. The upper field was inclined 15° laterally to avoid the deeper midline structures; the medial border lay 1 cm to the unaffected side of the midline while that of the lower field was at the midline, the border

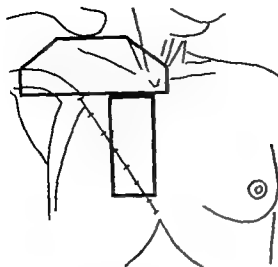


Fig 1 Fields used in postoperative cobalt 60 treatment of mammary carcinoma stages I and II

between the two fields was situated 1 cm below the jugular notch (Fig 1). Daily doses of 300 R at the 100 per cent level were delivered to each field. The total doses (100 per cent level) were 6 000 R in 66 patients, 5 700 R in 3 patients and 4 800 R in 1 patient. The treatment time was 25 to 42 days (85 per cent within 26 to 34 days).

Three patients were aged between 30 and 39, 18 between 40 and 49, 22 between 50 and 59, and 27 between 60 and 69 years.

Roentgen examination of the chest was performed in all patients before treatment and in 22 patients at the end of treatment. The later follow up films, 121 in all, were obtained 7 weeks to 30 months from the end of treatment.

The patients were classified in four groups according to the severity of the pulmonary changes: (1) No changes; (2) slight changes; (3) moderate changes mainly in the medial part of the upper zone; no shrinkage; (4) marked changes involving a large part of the upper zone with considerable pulmonary shrinkage.

### Results

Post irradiation roentgenographic changes were observed in 61 patients (87 per cent). Nine (13 per cent) patients were classified as negative, 16 (23 per cent) as having slight changes, 30 (43 per cent) moderate, and 15 patients (21 per cent) as having marked changes.

No changes were evident in any of the roentgenograms obtained at the end of the treatment, which varied from 25 to 42 days.



Fig. 2. Typical development of post irradiation changes. Left lung: a) before treatment; b) 7 weeks after the end of postoperative cobalt 60 treatment of mammary carcinoma. The indefinite infiltration represents radiation pneumonitis; c) d) 5 and 19 months after treatment. Filariosis with gradual shrinkage towards the mediastinum.

The initial changes and their further development appear in Fig. 2. At about 2 months an indefinite fan shaped infiltration with its apex pointing towards the hilum appeared; this subsequently changed to radiating strands suggesting fi



FIG 3 Right lung a) Before treatment b) c) 4 and 16 months after postoperative cobalt 60 treatment for carcinoma of the right breast. The radiation fibrosis extends below the hilum following the border of the parasternal field.

brosis. Shrinkage gradually followed so that the lateral border of the infiltration moved medially and was situated along the upper mediastinum. Such shrinkage may lead to elevation of the hilum and the diaphragm. Compensatory emphysema of the lower part of the lung has been observed as well. The fibrosis may sometimes extend below the hilum parallel to the mediastinum (Fig 3) following the lateral border of the parasternal field of treatment. Pleural effusion was not observed whereas pleural thickening was common. During the relatively short

Age	40	49	50	59	60	6
#	18		22		27	
Distal to 50						0
40	0		0			
30	x		x			
20	Δ					
10			Δ		x	
0					Δ	

Fig. 4 Relationship between severity of radiation fibrosis and age. Negative Δ slight x moderate 0 marked ●



Fig. 5 Lateral tomogram of lung with radiation fibrosis. The changes in the posterior part of the upper lobe are more marked than in the anterior part, contrary to what could be expected from the dose distribution.

observation time no changes were evident in the bones within the irradiated areas. The four degrees of radiation changes were plotted against the age groups to check the relationship between the extension of the fibrosis and the age of the patients (Fig. 4).

### Discussion and Conclusion

The pathology of pulmonary lesions due to irradiation was described by ENGELSTAD in 1934 (rabbit lung) and in 1940 (human lung). The lung reaction has a characteristic history in which four stages may be distinguished: 1) An initial stage starting one or two hours after irradiation and lasting one or two



FIG. 6. Left lung: a) Pulmonary radiation fibrosis extending to the periphery of the apex; b) A radiation induced pneumothorax during subsequent surgical intervention. No pleural adhesions to prevent the lung from collapsing. The homogeneous infiltration at the apex (→) represents radiation fibrosis; c) Re-expansion of the lung. The radiation fibrosis resumes its original appearance.

days (2) A latent stage with a duration of two to three weeks (3) The main stage characterized by inflammatory or degenerative changes and alveolar peribronchial and perivascular exudation. These changes reach their maximum one or two months after the irradiation (4) A regeneration stage in which the exudative changes are gradually replaced by proliferation of connective tissue.

The present roentgen findings correspond with ENGELSTAD's description of the main and regeneration stages (Fig. 2). The indefinite infiltration is referred to as radiation pneumonitis in the literature (EGER & GREGL 1965, NOTTEP *et coll.* 1970). This pneumonitis corresponds in time to ENGELSTAD's main stage while the later fibrotic appearance represents the regeneration stage. The earliest changes in the material were observed 7 weeks after the end of treatment which for this patient lasted for 32 days. BATE & GUTTMANN (1957) in a series of patients treated in a similar way described the development of radiation fibrosis from a few weeks to a few months after the conclusion of radiation therapy.

The shrinkage of the fibrotic tissue towards the mediastinum may lead to a reduction of the affected area as seen in the roentgenogram. It is important not to misinterpret this as resolution and disappearance of the affected zone.

The longest observation time of any patient of the present material was 30 months and signs of radiation fibrosis may still be demonstrated. ROSS (1956) described changes in a lung 7 years after irradiation which were misinterpreted as tuberculosis. The roentgenologic evidence of fibrosis with shrinkage (visible fibrous strands, elevation of the hilum and diaphragm and compensatory emphysema) indicate that the lesions may be irreversible. Extension of the radiation fibrosis late in the development has been unusual. If such increase seems to occur other causes, e.g. metastases or inflammatory conditions, may be indicated. The location of the fibrosis does not correspond exactly to the fields irradiated, except occasionally in the parasternal field (Fig. 3). The fan-shaped infiltration seems to follow one or more pulmonary segments from the hilum to the periphery rather than the border of the field. Ordinary lateral roentgenograms fail in the main to reveal such changes; some of the patients were therefore examined by lateral tomography. This usually disclosed more marked changes in the posterior than the anterior part of the upper lobe (Fig. 5), contrary to what would be expected from the dose distribution. No certain explanation of this observation can be given. It is possible that anatomic factors such as the bronchial and vascular supply may have been of importance.

The most obvious post-irradiation change in many roentgenograms has been pleural thickening. Pleural effusion has not been observed. ENGELSTAD (1934) stated that the pleurae were radiation resistant. Several authors have stressed the absence of free effusion (WARREN & GATES 1940, LOUGHIEFF & MACGILLIVRE 1960). BACHMAN & MACKEN (1959) however, reported an effusion in 5 per cent of their patients. Extension of the pulmonary fibrosis to the periphery of the lung does not necessarily result in pleural adhesions. In one patient with such changes a pneumothorax was accidentally induced during subsequent surgical intervention. No adhesion was present to prevent the lung from collapsing; the partially collapsed lung with a homogeneous infiltration at the apex, representing

radiation fibrosis appears in Fig 6 McINTOSH & SPITZ (1939) stated that the lungs of elderly subjects with arteriosclerosis were especially prone to radiation pneumonitis and permanent fibrosis CATTERALL & OGILVIE (1959) observed a decrease in diffusing capacity after radiation especially in elderly patients A similar relationship was evident in the present material when the severity of radiation fibrosis was plotted against the age groups (Fig 4) The older the patient, the greater the risk of gross radiologic changes although these are not necessarily excluded by youth

## SUMMARY

Seventy patients with stage I and stage II mammary carcinoma were treated by radical mastectomy followed by irradiation with cobalt 60 Routine follow up chest films revealed post radiation changes in 61 patients (87 per cent) It appears that the changes may end as an irreversible fibrous stage and that they are more marked in the higher age groups

## ZUSAMMENFASSUNG

Siebzig Patienten mit einem Brustkrebs im Stadium I und II wurden durch radikale Mastektomie mit nachfolgender Bestrahlung mit Cobalt 60 behandelt Routinekontrollen der Brust zeigten bei 61 Patienten (87 Prozent) strahlenbedingte Veränderungen Es scheint als ob diese Veränderungen in einem irreversiblen fibrosen Stadium enden und dass diese in den höheren Altersgruppen starker ausgeprägt sind

## RÉSUMÉ

Soixante dix malades atteintes de cancer du sein au stade I et II ont été traitées par mastectomie radicale suivie d'irradiations par le cobalt 60 Les examens de contrôle systématique des poumons ont montré des lésions post radiothérapeutiques chez 61 malades (87 pour-cent) Il semble que ces lésions peuvent aboutir à une fibrose irréversible et qu'elles sont plus marquées dans les groupes d'âge élevé

## REFERENCES

- BACHMAN A L and MACKEN K. Pleural effusions following supervoltage radiation for breast carcinoma Radiology 72 (1959) 669  
BATE D and GUTTMANN H. Changes in lung and pleura following radiotherapy for carcinoma of the breast Radiology 69 (1957) 372  
CATTERALL M and OGILVIE C M. The effects of radiation on pulmonary function Acta Unit Cancer 15 (1959) 485  
CHU F C H, PHILLIPS R, NICKSON F J and McPHEE J G. Pneumonitis following radiation therapy of cancer of the breast by tangential technique Radiology 64 (1955) 642



- EGER W. und GREGL A.: Die Strahlenpneumonitis Hippokrates Verlag Stuttgart 1965
- ENGELSTAD R. B.: Über die Wirkungen der Röntgenstrahlen auf die Lungen Acta radiol (1934) Suppl. No. 19
- Pulmonary lesions after roentgen and radium irradiation Amer J Roentgenol 43 (1940) 676
- LOUCHED M. N. and MACLURE G. H.: Irradiation pneumonitis in the treatment of carcinoma of the breast J Canad Ass Radiol 11 (1960) 1
- MCINTOSH H. C. and SPRY S.: A study of radiation pneumonitis Amer J Roentgenol 41 (1939) 603
- NOTTER G., LINDFELL D. and VIKTORLOF K. J.: Strahlenreaktion in Lungen und Pleura bei Mammakarzinompatienten Fortschr Röntgenstr 112 (1970) 571
- ROSS W. M.: The radiotherapeutic and radiological aspect of radiation fibrosis of the lungs Thorax 11 (1956) 241
- WARREN S. and GATES O.: Radiation pneumonitis and pathological observations Arch Path 30 (1940) 440

## INTRAARTERIAL DISTRIBUTION OF COLLOIDAL BISMUTH COMPOUNDS INJECTED IN MAN

by

G LUNDELL

A considerable amount of the  $^{212}\text{Bi}$  acetate in saline injected intravenously intraarterially is absorbed during its first capillary passage (LINHORN et al 1964). The distribution of four bismuth compounds has been examined, special attention being paid to the possibility of their accumulation in tumours situated distally to the site of their arterial injection. Colloidal compounds of bismuth have been proposed for systemic and local use in the treatment (KAHN 1958, VAN DER WERFF 1958, 1965, MATTHEWS 1962) and diagnosis (VAN DER WERFF 1966, GERIARD et coll 1964) of malignant tumours. It has also been suggested that the accumulation of colloidal solutions with certain properties may have therapeutic implications for the administration of compounds of short lived isotopes in perfusion therapy (BROWNELL et coll 1960).

The four compounds of  $^{212}\text{Bi}$  used in the investigation were the acetate in isotonic saline and in 5 per cent glucose, the nitrate in dilute  $\text{HNO}_3$  and the sulphide in human albumin. The activity ranged from 0.5 to 1 mCi/ml.

*Material* The case material and the compounds used are presented in Table

Table

*The patients examined after injection of various  $^{212}\text{Bi}$  compounds into an iliac artery*

Clinical No.	Sex	Age	Disease	Compound used	Activity injected (MCi)
1	M	1	Osteogenic sarcoma in lower part of left femur	Bi acetate in saline	7.0
2	M	17	Wing sarcoma in left femur	Bi acetate in saline	1.0
3	M	13	Osteogenic sarcoma in middle of left tibia	Bi acetate in saline	1.00
4	M	67	Carcinoma of bladder no skeletal metastases	Bi acetate in glucose	1.00
5	F	61	Mammary carcinoma with metastases in femur	Bi nitrate in dilute $\text{HNO}_3$	0.00
6	M	62	Carcinoma of bladder no metastases	Bi nitrate in dilute $\text{HNO}_3$	0.00
7	M	70	Carcinoma of mouth and lower lip no metastases	Bi sulphide in 2% human albumin	0.00
8	F	57	Myeloma in left leg	Bi sulphide in 2% human albumin	0.00

**Methods** The bismuth compounds were injected into the left or right external iliac artery by the percutaneous technique, the injection was made on the affected side when a tumour was present.

The examination was carried out as whole body scanning and by profile diagram measurement. The IKB whole body scintigraph (JONSSON et al. 1957) was used at a detector speed of 600 mm/min, a line space of 21 mm and a scale factor of 20 or above. In view of the high energy of the gamma radiation from  $^{212}\text{Bi}$ , a focusing collimator was incorporated and beneath which a specially designed extra lead shield was mounted: this produced a shielding of at least 10 cm of lead in all directions except at the collimator opening. The detector consisted of a thallium activated sodium iodide crystal 3 inches (7.6 cm) thick and 3 inches (7.6 cm) in diameter, the scanner was equipped with a single channel pulse height analyzer. The measurement was begun from the head downwards within 1.5 hours of the injection of the radioactive compound and repeated at different intervals up to 4 days.

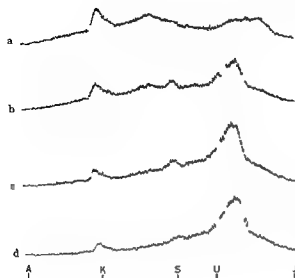


Fig 1 Case 1 Osteogenic sarcoma of the left femur Profile scanning Measurements at 9.5 min (a) 30.5 (b) 52.5 (c) and 57.5 (d) h after the injection of  $^{204}\text{Bi}$  acetate in saline Levels indicated A — ankle K — knee S — symphysis U — umbilicus J — jugulum.

## Results

$^{204}\text{Bi}$  acetate in saline Cases 1, 2 and 3 High counting rates were recorded initially in order of diminishing activity the tumour area, adjacent areas distal to the injection site, thorax and the abdomen (Figs 1 a, 2 a). The accumulation in the tumour area diminished rapidly in the first few hours after the injection and a transfer of activity towards the abdominal region occurred (Figs 1 b, c, 2 b, c).

$^{204}\text{Bi}$  acetate in glucose Case 4 Carcinoma of bladder with no signs of leg involvement. Two hours after the injection an accumulation of the isotope decreasing peripherally appeared in the leg on the side of the injection; this was also evident in the thorax and upper abdominal region (Fig 3 a). Only an extremely small amount of activity remained in the leg at 19 hours (Fig 3 b).

$^{204}\text{Bi}$  nitrate Cases 5 and 6 The distribution and time sequence were similar to those for the acetate in glucose.

$^{204}\text{Bi}$  sulphide Cases 7 and 8 Ninety minutes after the injection no accumulation of the compound was evident in the leg on the side of the injection either in the myeloma case (Case 8) or in the one with no leg involvement (Case 7). Most of the activity was in the upper abdominal region corresponding to the area of the liver (Figs 4, 5).

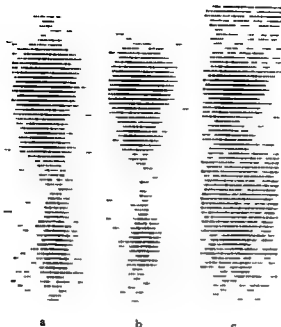


Fig 2 Case 3 Osteogenic sarcoma of the left tibia. Scintigraphy Scanning started 2.5 (a) 8 (b) and 25.5 (c) h after the injection of  $^{204}\text{Bi}$  acetate in saline. The isotope accumulation in the middle part of the left tibia was greatest at the examination 2.5 h after the injection following which there was a rapid decrease. Levels indicated: K — knee S — symphysis J — jugulum.

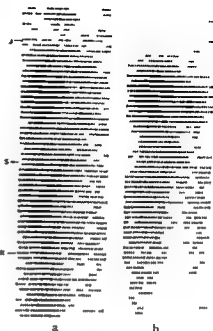


Fig 3 Case 4 Scintigraphy Scanning started 2 (a) and 19 (b) h after the injection of  $^{204}\text{Bi}$  acetate in glucose revealed an initial accumulation in the right femur and to a lesser extent in the right tibia. No signs of tumour involvement of leg.

## Discussion

During the first passage through the vascular system much of the bismuth acetate in saline or in glucose and the bismuth nitrate injected were probably filtered off by the capillary system and remained in the tissues in the region. In view of the nature of the changes in the leg the series is too small and lacking in homogeneity to permit any definitive conclusions regarding the differences between the four compounds of bismuth. The most stable of them, the sulphide, would however seem to be transported more rapidly to the liver and spleen. The reason for this is probably that the three less stable compounds soon form larger aggregates in the blood, most of them then being removed from the circulation by filtration in the capillary system. The redistribution of the colloid toward the abdominal region is probably due to a gradual breakdown of the aggregates that are then accumulated in the reticuloendothelial system and possibly also excreted by the kidneys.

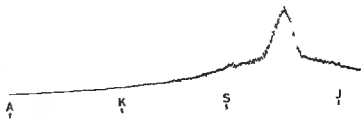


Fig 5

Fig 4 Case 7 Scanning started 1 h and 40 min after the injection of  $^{200}\text{Bi}$  sulphide in 2 per cent human albumin. No tumour of the leg

Fig 5 Case 7 Profile scanning Measurement 1.5 h after the injection

Fig 4

As all the compounds investigated remained for only a short time even in highly vascular tumours (Cases 1 2 3) they seem unsuitable for intraarterial therapy the redistribution to other organs occurs too soon

### Conclusions

Various  $^{200}\text{Bi}$  compounds were injected into the external iliac artery in 5 patients with skeletal tumours in one leg and in 3 patients without signs of tumour involvement of the legs. A fair amount of the acetate and nitrate preparations persisted in the leg distally to the site of injection. It is suggested that this was probably due to filtration during the first capillary passage. The cases with a tumour situated distal to the artery into which the acetate or nitrate was injected was however redistributed rapidly to the liver spleen and lungs. The accumulation in the tumours was of too short a duration to provide favourable conditions for selective radiation therapy by the intraarterial injection of an isotope compound with a half life period of  $^{200}\text{Bi}$ .

### SUMMARY

The requirements for the use of various compounds of  $^{200}\text{Bi}$  for selective radiation therapy by intraarterial injection were examined in 8 cases in which the isotope was injected into an iliac artery. An accumulation in the tumour area was obtained with some of the compounds. Redistribution occurred so rapidly however that the technique must be considered unsuitable for intraarterial isotope therapy.

## ZUSAMMENFASSUNG

Die Forderungen für die Anwendung verschiedener Verbindungen von  $^{210}\text{Bi}$  für die selektive Radiotherapie durch intraarterielle Injektion wurden in 8 Fällen untersucht in denen das Isotop in die A. iliaca injiziert wurde. Mit einigen der Verbindungen wurde eine Akkumulation im Tumorgebiet erreicht. Die Redistribution war jedoch so rasch, dass die Technik für die intraarterielle Isotoptherapie als ungeeignet betrachtet werden muss.

## RÉSUMÉ

L'auteur a examiné sur 8 cas où l'isotope a été injecté dans une artère iliaque les conditions requises pour l'emploi de différents composés de  $^{210}\text{Bi}$  pour la radiothérapie sélective par injection intra artérielle. Certains des composés se sont accumulés dans la région tumorale. La redistribution était cependant si rapide que cette technique ne convient probablement pas pour le traitement intra artériel par les isotopes.

## REFERENCES

- BROWNELL G. L., ELLETT W. H., OJEMANN R. G. and SWEET W. H. The use of short-lived isotopes in the perfusion therapy of isolated organs. *Strahlentherapie* (1960) Sonderband 45, p. 126.
- EINHORN J., ENGSTEDT L., FRANZEN S. and LUNDELL G. Distribution of colloidal Bismuth intravenously and intraarterially administered in man. *Acta radiol. Ther. Phys. Biol.* 2 (1964) 443.
- GERHARD H., GABRIEL E., MUNDINGER C. und WALDBAUER H. Neuere Untersuchungen über die Tumoranreicherung radioaktiver Schwermetallisotope ( $^{210}\text{Bi}$ ,  $^{210}\text{Po}$  und  $^{210}\text{Pb}$ ). In: *Radionuklide in der klinischen und experimentellen Onkologie*, p. 229. F. K. Schattauer Verlag, Stuttgart, 1964.
- GRAUL E. H. und HUNDENHAGEN H. Tierexperimentelle Untersuchungen mit  $^{210}\text{Bi}$  in öle suspension. *Atompraxis* 4 (1958) 324.
- JOHNSON L., LARSON L.-G. and RAGNARSSON I. A scanning apparatus for the localization of gamma emitting isotopes in vivo. *Acta radiol.* 47 (1957) 217.
- KAHN H. Die Ablagerung von aktivem Wismut in malignen Tumoren. *Strahlentherapie* 37 (1930) 751.
- Behandlung maligner Geschwülste mit radioaktivem Wismut (Radium F). *Dtsch. med. Wschr.* 50 (1930) 2131.
- MATTHEWS C. M. E. Irradiation of lymph nodes. *Clin. Sci.* 22 (1962) 209.
- PASSALACQUA F. Verteilungsprüfungen von verschiedenen Radio-Wismut Verbindungen  $^{210}\text{Bi}$  bei normalen und splenektomierten Ratten. *Strahlentherapie* 102 (1957) 606.
- SOLLMAN T. and SEIFTER J. The toxicity of bismuth salts by intravenous injection. *J. Pharmacol. exp. Ther.* 72 (1941) 39.
- VAN DER WERFF J. TH. Radiowismut in der Therapie. *Atompraxis* 4 (1958) 319.
- Radioactive bismuth  $^{210}\text{Bi}$ . Experimental studies and clinical applications. *Acta radiol.* (1963) Suppl. No. 243.
- Gamma encephalography with radioactive bismuth. 206. *Acta radiol. Ther. Phys. Biol.* 4 (1965) 403.

# EFFECT OF SUBCUTANEOUS FAT ON BONE MINERAL CONTENT MEASUREMENTS WITH THE 'SINGLE-ENERGY PHOTON ABSORPTIOMETRY TECHNIQUE

by

LOUIS ZERTZ

The single energy photon technique of CAMERON et coll (1963 1968) is presently used by a considerable number of laboratories for the measurement of bone mineral content in humans (Proceedings of bone measurement conference 1970) The expression used in this determination of bone mineral content is generally of the form

$$M = K \left[ \delta \sum_{i=1}^n \ln \left( \frac{I_0^*}{I} \right)_i \right]$$

$\delta$  is the distance traversed in an integration interval  $K$  a proportionality constant

$$\left[ \delta \sum_{i=1}^n \ln \left( \frac{I_0^*}{I} \right)_i \right]$$

---

Submitted for publication 14 December 1971



## ZUSAMMENFASSUNG

Die Forderungen für die Anwendung verschiedener Verbindungen von  $^{210}\text{Bi}$  für die selektive Radiotherapie durch intraarterielle Injektion wurden in 8 Fällen untersucht in denen das Isotop in die A. iliaca injiziert wurde. Mit einigen der Verbindungen wurde eine Akkumulation im Tumorgebiet erreicht. Die Redistribution war jedoch so rasch, dass die Technik für die intraarterielle Isotoptherapie als ungeeignet betrachtet werden muss.

## RÉSUMÉ

L'auteur a examiné sur 8 cas où l'isotope a été injecté dans une artère iliaque les conditions requises pour l'emploi de différents composés de  $^{210}\text{Bi}$  pour la radiothérapie sélective par injection intra artérielle. Certains des composés se sont accumulés dans la région tumorale. La redistribution était cependant si rapide que cette technique ne convient probablement pas pour le traitement intra artériel par les isotopes.

## REFERENCES

- BROWNELL G L, ELLETT W H, OJEMANN R G and SWEET W H. The use of shortlived isotopes in the perfusion therapy of isolated organs. *Strahlentherapie* (1960) Sonderband 45 p 126.
- EINHORN J, ENOSTEDT L, FRANZEN S and LUNDELL G. Distribution of colloidal Bismuth intravenously and intraarterially administered in man. *Acta radiol Ther Phys Biol* 2 (1964) 443.
- GERHARD H, GABRIEL E, MUNDINGER C und WALDBAUR H. Neuere Untersuchungen über die Tumoranreicherung radioaktiver Schwermetallisotope ( $\text{Hg}$ ,  $\text{Bi}$  und  $\text{Cu}$ ). In: *Radionuklide in der klinischen und experimentellen Onkologie* p 229. F. K. Schattauer Verlag Stuttgart 1964.
- GRALL E H und HUNDESHAGEN H. Tierexperimentelle Untersuchungen mit  $\text{Bi}$ -Kohle suspension. *Atompraxis* 4 (1958) 324.
- JONSON L, LARSSON L G and RAGNHULT I. A scanning apparatus for the localization of gamma emitting isotopes in vivo. *Acta radiol* 47 (1957) 217.
- KAHN H. Die Ablagerung von aktivem Wismut in malignen Tumoren. *Strahlentherapie* 37 (1930) 751.
- Behandlung maligner Geschwulste mit radioaktivem Wismut (Radium E). *Dtsch. med. Wschr.* 50 (1930) 2131.
- MATTHEWS C M E. Irradiation of lymph nodes. *Clin. Sci.* 22 (1962) 209.
- PASSALACQUA F. Verteilungsprüfungen von verschiedenen Radio-Wismut Verbindungen  $^{210}\text{Bi}$  bei normalen und splenektomierten Ratten. *Strahlentherapie* 102 (1957) 606.
- SOLLMAN T and SEIFTER J. The toxicity of bismuth salts by intravenous injection. *J. Pharmacol. exp. Ther.* 72 (1941) 39.
- VAN DER WERFF J TH. Radiowismut in der Therapie. *Atompraxis* 4 (1958) 319.
- Radioactive bismuth  $\text{Bi}$ . Experimental studies and clinical applications. *Acta radiol* (1965) Suppl. No 243.
- Gamma encephalography with radioactive bismuth 206. *Acta radiol Ther Phys Biol.* 4 (1966) 403.

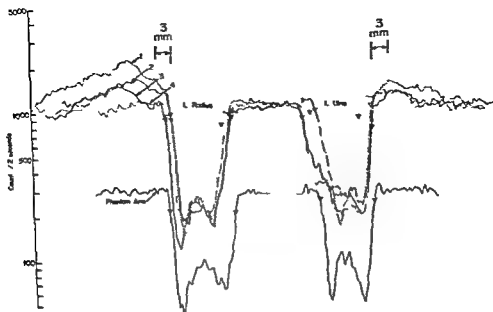


Fig 1 Midshaft scans of human phantom left arm and the left arms of individuals with varying degrees of adipose tissue. Weight, height and Ponderal Index are (1) 105.8 kg 1.7 m 10.833 (2) 114 kg 1.67 m, 11.330 (3) 60.8 kg 1.57 m 11.720 (4) 49 kg 1.55 m 10.809. The measurements are taken with the arm rigidly clamped in a plastic box containing Super Stuf. The scans of the four individuals are adjusted vertically so that the scans in the region between the radius and ulna approximately downward and the ulna is artificially placed to the right of its actual scan position to avoid confusing the various scans.

1.0 and its linear absorption coefficient as measured with rays from a tin filtered  $^{125}\text{I}$  source (ca 27.4 keV) differs by no more than 2 per cent from that for the TEL. Linear scans across the forearm were carried out at about 1/3 the distance up from the distal to the proximal end of the radius. The long term precision in per cent standard deviation for measuring integral values in human forearm bones was found to be about  $\pm 2$  per cent (ZERR).

An estimate of the error involved in ignoring the fat component was made by determining the integral value for scans of a bone reference standard kindly supplied by CAMERON'S Laboratory (WITT et al. Fig 3) with and without varying configurations of subcutaneous fat in the path. The coefficient of variation in measuring the integral value of the standard in water was less than 1 per cent. The bone standard plus fat were always immersed in 8 cm of water. The dimensions and absorbance of the large simulated bone in the standard approxi-

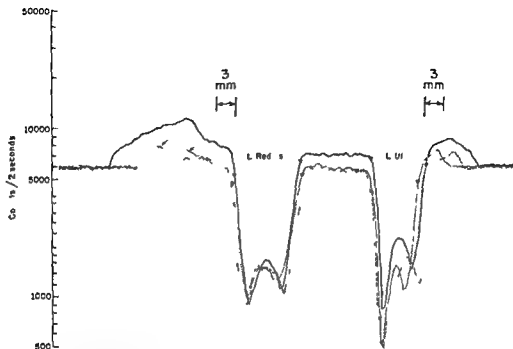


Fig 2 Midshaft left arm scans of the individual designated (1) (2) and (3) of Fig 1. The measurements are taken with arm immersed in water. The scans are plotted directly from the data with no displacement as in Fig 1.

mates those of the midshaft radius. The beef fat employed in these studies was found difficult to accurately shape or measure. Therefore the shapes and the dimensions of fat configurations are only approximate.

### Results

A comparison of the scan of a fat free phantom arm to several human arms in Fig 1 shows an increased transmitted intensity toward the arm edges which can be seen to be larger the smaller the ponderal index (HUNTER 1969)  $R_o$  where

$$R_o = \frac{\text{height in cm,}}{\sqrt[3]{\text{weight in kg}}}$$

and a low ponderal index indicates greater obesity. Subjects 2 and 3 in Figs 1 and 2 have approximately the same increase in transmitted intensity over the  $I_o^*$  level. There is no significant change in transmitted intensity when the beam enters the phantom arm from the tissue equivalent material (Super Stuff) until the bone is reached.

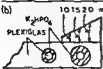
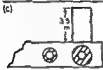
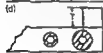
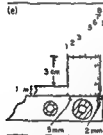
CONFIGURATION OF FAT	10 <sup>4</sup> BASED ON THE MEAN OF SIX VALUES		
	BETWEEN BONES (a)	REGION BEYOND EXTERNAL EDGE (b)	REGIONS ON BOTH SIDES OF BONE (c)
(a) APPROXIMATELY UNIFORM THICKNESS OF 2.5 cm	+1	+1	+1
(b) 	-9	+3	-3
(c) 	-32	-32	-32
(d) 	1 -6 2 -9 4 -15	+2 +5 +15	-2 -1 +1
(e) 			+1 -7 -4 +3 +8 +7 +10 +1

Fig 3 Per cent error in the determination of the integral value for different arbitrarily chosen configurations of fat. The bone standard plus fat are immersed in 8 cm of water

Scans with the arms immersed in water (Fig 2) show that the fractional increases in transmitted intensity at the edges of the arm were approximately the same while the shape of the hump of increased transmission was slightly different for the two cases. This suggests that the distribution of fat in soft tissue of the arm is the primary cause for a greater transmission than is expected for soft tissue plus tissue equivalent material. The replacement of each centimeter of water by subcutaneous beef fat resulted in a 20 per cent increase in transmitted intensity. Based on these data we estimate that individual 1 in Figs 1 and 2 has a peak thickness of a little less than 4 cm of fat lateral to the radius and a thickness of about 1 cm between the radius and ulna. These estimates are to be accepted as very approximate and are used only as a guide in selecting fat thicknesses to be used in the examinations outlined in Fig 3.

Table

*Integral values (mm) for radius and ulna using different methods to obtain  $I_0^*$ . Forearm constraint and tissue equivalent material*

Individual in Figs 1 and 2	1			
	SS/PB*		WJ**	
	Radius	Ulna	Radius	Ulna
Method employed to obtain $I_0^*$				
a) Mean between radius and ulna	17.7 -12	18.5 -9	17.7 -7	12.5 -7
b) Mean of six successive counting intervals starting on the third interval from the edge of the radius (ulna) away from the ulna (radius)	22.9 +14	22.5 +11	20.2 +6	14.7 +9
c) Mean of six intervals three on each side of radius (ulna) starting on the third interval from the edges of the bone	20.1	20.3	19.0	13.3
d) Value taken at a point outside the bone 3 mm from the edge of the radius (ulna) away from the ulna (radius)	23.3 +16	22.6 +11	20.5 +8	14.7 +7
e) Value taken at a point outside the bone 3 mm from the edge of the radius (ulna) toward the ulna (radius)	17.5 -13	18.9 -7	17.7 -7	12.1 -7

\* Super Stuff in plastic box

\*\* Water immersion

The errors resulting from the presence of the different configurations of fat shown in Fig. 3 were determined. The maximum fat thickness used was less than that estimated to be present in the individual designated 1 in Figs 1 and 2. The integral values obtained for the scans of the various fat configurations are dependent on the manner in which the  $I_0^*$  values are determined. The  $I_0^*$  was determined in three different ways. The method designated between bones used 11 intervals starting from the third from the edge of the large simulated bone going toward the smaller simulated bone. That designated region beyond external edge uses six intervals on the opposite side starting with the third from the edge and regions on both sides of the edge refers to the mean of six intervals three on each side starting on the third interval from the edges. The distance traversed in one counting interval was 0.549 mm.

Table (cont.)

2				3			
SS/PB		WI**		SS/PB		WI**	
Radius	Ulna	Radius	Ulna	Radius	Ulna	Radius	Ulna
20.3	17.7	18.1	16.4	16.7	14.9	16.2	12.8
-1	-6	-3	-6	-8	-5	-6	-8
21.3	20.5	19.8	19.1	19.7	16.6	17.8	15.0
+4	+8	+6	+9	+8	+6	+3	+8
20.5	18.9	18.6	17.5	18.2	15.7	17.2	13.9
20.9	21.2	19.7	19.0	19.8	16.4	17.7	15.5
+9	+12	+6	+9	+9	+4	+3	+12
20.0	18.3	18.1	16.5	16.8	14.1	16.6	12.6
-1	-3	-3	-6	-8	-10	-3	-9

The per cent error was determined from the ratio of the integral values obtained with the fat present to that obtained when water replaces fat. The integral values for the standards immersed in water agree with those reported by other laboratories for the same type of standards (ZERTZ & FRED WITT et coll.). The errors obtained for configurations (b) and (d) of Fig. 3 are found to be a minimum when the  $I_0^*$  is based on the average of the transmitted intensity immediately adjacent to the two edges of the bone. For this reason only this averaging method of obtaining the  $I_0^*$  which for future reference will be called double-edge averaging was used to investigate the error for the different configurations of (e) in Fig. 3. The errors found in (a) of Fig. 3 show that a uniform thickness of fat introduces no appreciable error with the different methods used to determine  $I_0^*$ . For a fat configuration similar to that of (c) of Fig. 3 which is unlikely to occur in a human forearm the large error found is independent of the manner in which the  $I_0^*$  is determined. For a step type configuration which may be close to what occurs in some human arms as suggested in the scan of individual 1 (Fig. 2) even the method of double-edge averaging

which results in a minimum error still gives a value which deviates considerably from the actual or true integral value for certain positions of the step

The integral values were determined for the radius and ulna of individuals 1, 2 and 3 (Figs 1-2) on the basis of five different methods for obtaining  $I_0^*$ . The integral values for the arm in Super Stuff and in water are not directly comparable since the scans in the two cases were inadvertently at slightly different positions on the arm

The double edge averaging technique for obtaining  $I_0^*$  results in a calculated value which is closest to the true integral value but even this value could be off by 3 per cent or considerably more from the true value for possible configurations of fat in obese individuals. Let us assume that double edge averaging results in the most accurate determination of bone mineral content in obese individuals. Calculated per cent deviations from this best integral value can be determined and are given under the integral values of the Table

### Discussion

It is clear from the Table that the method employed for determining  $I_0^*$  has a considerable effect and whether compression is or is not used on the arm has some slight effect on the value obtained for the bone mineral content of the arm of obese individuals. Using water immersion, where there is no compression of the arm does not in all cases diminish the deviations from the best integral value for the different techniques used to obtain  $I_0^*$ . It does for the radius measurement of individual 1 but increases it slightly in the cases of the radius of individual 2 and the ulna of individual 3

The data given in the Table suggest that considerable variation in the bone mineral content measurement of human arms is possible with a single energy photon absorptiometric bone mineral analyzer if different techniques are used to determine  $I_0^*$ . The magnitude of this variation could be evaluated by measuring the bone mineral content on the same obese individual with two instruments which use the two different techniques for determining  $I_0^*$ , i.e. the double-edge averaging and the method designated (d) in the Table. The latter technique is presently being used in the Norland-Cameron bone mineral analyzer employed in some laboratories

The single-energy photon absorptiometric technique gives a precision in determining the integral value of about  $\pm 2$  per cent (Zeitz) for forearm bones for all individuals regardless of degree of obesity. Therefore the method of photon absorptiometry is a very useful tool for serial examinations of bone mineral content of the forearm bones. Further work is required if one is to determine the accuracy of serial examinations on individuals where there is a

drastic change in the subcutaneous fat content of the arm in the course of the investigation

With relatively large differences in results possible with different instruments for obese individuals it would seem advisable in reporting results to explicitly and carefully define the method employed to obtain the integral value and to give the proportionality factor used to obtain the absolute bone mineral determination from the integral value

We are presently considering possible approximate corrections related to the obesity of the individual as well as attempting to determine if there is an obesity index level below which the error in the determination of bone mineral content remains below a fixed preassigned value such as 2 or 3 per cent

### Acknowledgements

The author wishes to thank Drs J S Laughlin and H Q Woodard for suggestions and discussions during this investigation and Mr M Mason for his valuable technical assistance. This work was supported in part by A E C Contract AT (30-1) 910 and by N C I CA08748

### SUMMARY

Investigations of bone phantoms with fat configurations suggest that mineral content measurements of the forearm bones by the single energy photon absorptiometric technique could be in appreciable error for certain marked fat configurations. Actual profiles of transmitted intensity for the mid forearm of obese individuals indicate that the bone mineral content determinations on these individuals could differ for different absorptiometric instruments. Because of these possible differences it is suggested that the method employed to obtain the integral value be explicitly and carefully defined.

### ZUSAMMENFASSUNG

Untersuchungen von Knochenphantomen mit Fettkonturen lassen vermuten, dass Messungen des Mineralgehaltes mit der monoenergetischen Photonen Absorptionstechnik für gewisse ausgeprägte Fettkonturen mit einem wesentlichen Fehler behaftet sein können. Aktuelle Profile der durchgelassenen Intensität vom mittleren Unterarm fetter Personen deuten darauf hin, dass Bestimmungen des knöchernen Mineralgehalts dieser Personen mit verschiedenen Absorptionsinstrumenten unterschiedliche Ergebnisse geben können. Wegen dieser möglichen Differenzen wird daran erinnert, dass die verwendete Methode mit der der Integralwert erhalten wird, ausführlich und sorgfältig präzisiert werden soll.

### RÉSUMÉ

Des recherches faites sur des fantômes osseux entourés de masses grasses font penser que les mesures du contenu minéral des de l'avant bras par la technique absorptiométrique de photons d'une seule énergie pourraient donner une erreur appréciable pour certaines masses grasses volumineuses. Les profils d'intensité transmise pour le milieu de l'avant



bras d'individus obèses montrent que les mesures du contenu minéral de l'os chez ces individus peut différer suivant les différents instruments absorptiométriques. En raison de ces différences possibles l'auteur propose que la méthode employée pour obtenir la valeur intégrale soit explicitement et soigneusement définie.

## REFERENCES

- CAMERON J. R. and SORENSON J. Measurement of bone mineral in vivo. An improved method. *Science* 142 (1963) 230.
- MAZES R. B. and SORENSON J. A. Precision and accuracy of bone mineral determination by direct photon absorptiometry. *Invest. Radiol.* 3 (1968) 141.
- GOODMAN L. J. A modified tissue equivalent liquid. *Health Phys.* 16 (1969) 763.
- HUTER N. L. Ponderal index and height. *Amer. J. phys. Anthro.* 31 (1969) 171.
- Proceedings of bone measurement conference May 22–23 1970. USAEC Report CONF 700515.
- SORENSON J. A. and MAZES R. B. Effects of fat on bone mineral measurement. USAEC Report CONF 700515 (1970) 255.
- SPIERS F. W. Effective atomic number and energy absorption in tissues. *Brit. J. Radiol.* 19 (1946) 52.
- WITT R. M., MAZES R. B. and CAMERON J. R. Standardization of bone mineral measurements. USAEC Report CONF 700515 (1970) 303.
- ZEITZ L. Unpublished data.
- and FREED B. Design and calibration of Sloan Kettering Institute osteodensitometer. USAEC Report CONF 700515 (1970).

## CARCINOMA OF THE THYROID IN CHILDREN AND YOUNG ADULTS

A review of 32 patients

by

BERTA JEREB and T LOWHAGEN

Several extensive investigations of carcinoma of the thyroid in children have been published (KENNEDY 1935 DAILEY & LINDSAY 1950 DUFFY & FITZGERALD 1950 HARE & NEWCOMB 1950 WARD 1955 EXEIBY & FRAZELL 1969 WENSHIP & ROSSVOLL 1969). This is a rare disease so that case series at the various institutions have been small and the experience of the condition somewhat limited. The present investigation was directed at the pertinent clinical data in 32 patients of 20 years or under in whom the treatment consisted in operation sometimes supplemented by radiation therapy and thyroid hormone medication.

*Material* A total of 1 024 patients with carcinoma of the thyroid were treated during the period 1916—1967. Thirty four of these were twenty years old or under, the first being admitted in 1929 and the last in 1967. Two of the 34 patients had to be excluded: one because the malignancy was not confirmed at the review of the histology and the other because the slides were missing. The first patient exhibited clinical signs of thyrotoxicosis and at the survey a diagnosis of benign hyperplasia of the thyroid epithelium was made.

Submitted for publication 16 November 1971

Table 1

*Clinical staging of carcinoma of the thyroid*

	No palpable nodes (N0)	Homolateral lymph node metastases (N1b)	Bilateral lymph node metastases (N2b)	Fixed nodes (N3)	Total
Single tumour confined to the gland (T1)	2	6	2*	1	11
Multifocal tumours or deformity of gland goitre (T2)	3	5*	1	—	15
Attachment to surrounding structures (T3)	4	1	—	1	6
Total	15	12	3	2	32

\* One patient with metastases in the lung

Table 2

*Treatment of carcinoma of the thyroid*

	Visible tumour removed in toto	Visible remnants of tumour left behind	Total
Operation	8	6 (+1)*	15
Operation + radioiodine	3	5	8
Operation + external irradiation	—	6	6
Operation + external irradiation + radioiodine	—	3	3
Total	11	20 (+1)*	31 (+1)*

\* Died at the operation

The series of thyroid carcinomas thus consisted of 32 patients — 21 girls and 11 boys — 8 aged 7 to 10, 10 aged 11 to 15 and 14 aged 16 to 20 years.

The follow up time since initial treatment was in 30 of the 32 patients more than five years and in 21 patients more than ten years. The first evidence of the condition in 21 of the patients was advancing goitre or a nodule in the thyroid, in 3 patients enlarged cervical lymph nodes and in 3 patients cough, respiratory distress or hoarseness. The duration of these signs and symptoms before admission ranged from one month to 19 years, with an average of 2 years. Goitre and hypothyroidism had been present at birth in 3 patients.

Table 3  
*Surgical methods in carcinoma of the thyroid*

	Total	Thyroidectomy		No of patients
		Subtotal	Total + subtotal	
Unilateral				
with neck dissection	1	—	—	1
without neck dissection	3	4	—	7
Bilateral				
with neck dissection	6	2	8	14
without neck dissection	2	3	4	9
Total	12	9	10	31*

\* One patient died from haemorrhage during the operation

Clinical staging was performed in retrospect from data obtained at the time of admission. A summary of this staging is presented in Table 1.

**Treatment** All the patients were operated upon and 17 received radiation therapy consisting of external irradiation or radioiodine at various times after wards (Table 2). Thirty-one patients were put on permanent thyroid medication after the operation or postoperative irradiation in 3 patients treated in the early fifties this was delayed for 4 to 5 years.

As the patients had been operated upon at different hospitals and over a long period of time the surgical approach was by no means uniform (Table 3). In general the more advanced the tumour the more aggressive was the surgery. Total thyroidectomy of both lobes was performed in 8 patients. The neck dissection was radical in 5 patients and partial in the rest. It was known in 20 patients that not all the visible tumour had been removed. Tissue in the cervical region accumulating radioiodine was evident after operation in all 26 patients in whom scanning was performed. In 6 of these patients the neoplasm was considered to have been completely removed though only in 3 of them was total thyroidectomy performed. An accumulation of radioiodine was present in 24 patients in the postoperative scan in the thyroid region and in 2 patients in metastatic lymph glands.

Radiation therapy was given to 17 patients in 14 of whom part of the growth had been left behind at operation. Only 3 patients under 15 years of age received external irradiation and only one was given radioiodine. The modalities used for the postoperative external irradiation were conventional 200 kV roentgen units 1 patient telecobalt 3 or 5 units 4 patients <sup>60</sup>Co short distance unit 3 patients

Table 4

*Histologic findings on review of 32 young patients treated for carcinoma of the thyroid*

Histologic type	No. of patients	Lymph node metastases
Papillary carcinoma	30	18
Medullary carcinoma with amyloid stroma	1	1
Indeterminate	1	—
Total	32	19
Percentage		59

The absorbed dose obtained in the tumour tissue could not be accurately calculated in retrospect for the last two modalities and was therefore only estimated. The method of treatment has been described elsewhere (JACOBSSON 1954). Doses of the order of 5 000 to 6 000 rad were estimated at the surface and at a depth of 2 cm in the thyroid region and on both sides of the neck. The dose applied with conventional roentgen radiation was 2 000 to 3 000 rad. Due to the retrospective determination there have been variations in the order of  $\pm 20$  per cent in the estimated doses. One patient received external conventional roentgen radiation for recurrences. Radioiodine alone was given to 7 patients in whom a postoperative uptake was evident in the cervical scan; in 2 others radioiodine was administered for local recurrence and in 2 more for pulmonary metastases.

Radioiodine was given as a single dose (50 to 80 mCi) to 6 patients and in 5 of these was repeated until there was no further uptake, bringing the total dose up to 100 to 400 mCi.

An attempt has been made to evaluate in retrospect from the medical documentation whether the patients were hypothyroid or euthyroid—adequately substituted. This retrospective evaluation is naturally unreliable but has nevertheless been considered more comprehensive than an estimation from the dosage of thyroid hormone administered.

**Histology.** Tissue sections were available for review from 31 primary tumours and in one from recurrences. The carcinomas were reclassified in accordance with the recommendations of the American Thyroid Association. All the growths with papillary or mixed papillary and follicular structures were labelled papillary carcinoma.

Thirty carcinomas were of this type (Table 4) although only a few had pure papillary appearances, most of them being of the mixed kind. Of the remaining

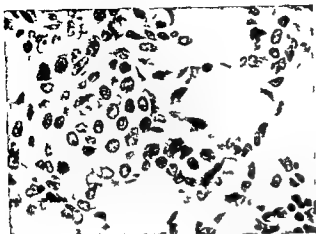


Fig 1 Medullary carcinoma with amyloid deposits (Case 1)

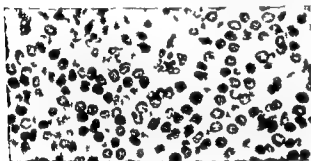


Fig 2 Small celled rather monomorphic poorly differentiated carcinoma. Several mitoses present (Case 2)

2 tumours one was a medullary carcinoma with amyloid deposits (Fig 1). The other could not be classified according to the recommendations of the American Thyroid Association and was therefore listed as indeterminate. The slides from recurrences — the only ones available for scrutiny — revealed a solid tumour made up of fairly small monomorphic cells in solid and suggested trabecular formations (Fig 2). Mitotic figures were numerous. A marked tendency for invasion of the surrounding structures was evident. No retrogressive changes such as necrosis or cyst formation were present. The histogenesis of the tumour could not be established from the sections of the extrathyroidal growing recurrences. However, it was considered that the growth most likely arose from the thyroid gland. The histologic review disclosed lymph node metastases in 18 of the 30 patients with papillary carcinoma and in the one patient with medullary carcinoma.

Attempts were made to group the patients with respect to the presence of single or multiple carcinoma foci in the thyroid gland from surgical and original histologic reports. The multifocal form was tentatively recorded in 13 patients but

Table 5

*Four patients with carcinoma of the thyroid recurrences*

Sex	Age (years)	Histologic findings	Stage	Treat- ment begin	Treatment	Recur- rence year location	Treatment of recurrence
M	15	Papillary type multifocal tumours lymph node metastases	T1N1b	1955	Total + subtotal resection neck dissection right (not radical)	1962 lymph node thyroid	Extirpation + thyroid hormone
F	8	Papillary type	T2N0	1955	Bilateral subtotal resection	1960 thyroid	Bilateral total thyroidectomy + thyroid hormone
M	9	Papillary type	T2N0	1960	Subtotal + total resection thyroid hormone	1962 thyroid	Total resection right + neck dissection + radioiodine + thyroid hormone
F	11	Papillary type lymph node metastases	T1N2b	1967	Bilateral total thyroidectomy neck dissection bilateral (not 'radical') thyroid hormone	1968 lymph node 1969 lymph node	Extirpation Extirpation + radioiodine + thyroid hormone

after a critical review of the histologic slides available in this retrospective investigation it became apparent that it was impossible to distinguish between the true multifocal form and more or less confluent intrathyroidal tumour spread. Moreover, the considerable difference in the number of sections from one case to another made it impossible to draw valid conclusions.

### Results

Thirty of the 32 patients treated were alive and well with no signs of a recurrence at the end of this investigation. Follow up times (after initial treatment) for survivors without disease were as follows: More than 15 years 6 patients, more than 10 years 19 patients, more than 5 years 28 patients and more than 3 years 30 patients. The histories of the 2 patients who died are briefly as follows:

*Case 1* Boy, aged 11 years, with advanced malignancy of the thyroid gland and several fixed cervical lymph node metastases. Surgical exploration revealed an extensive firm tumour that encircled the trachea, involved the carotid vessels and extended down into the



Fig 3 Girl aged 12 on admission. Metastases of carcinoma of the thyroid

jugulum. During the operation uncontrollable bleeding into the mediastinum led to death. Histologic examination of the surgical specimen disclosed medullary carcinoma with amyloid deposits (Fig 1).

*Case 2* Girl aged 10 years operated on in 1926 for an egg sized tumour which was not radically removed. The histologic diagnosis at that time was trabecular adenoma with transition into malignancy. Owing to recurrences resection and external irradiation were performed in 1928, 1932, 1933, 1935 and 1945. General skeletal metastases developed in 1947 and led to death in 1949. At no time did the patient receive thyroid hormone medication. The slides from recurrences — the only ones available for re-examination — failed to indicate the type of tumour but it was possibly a variant of poorly differentiated follicular carcinoma of the thyroid (Fig 2).

Fifteen patients received no postoperative irradiation. Recurrences in 4 of these developed some time after treatment (Table 5). One of the 17 patients treated with radiation therapy in addition to operation is dead, no local recurrences were recorded.

Two girls aged 20 and 12 years operated on in 1956 and 1967 respectively had pulmonary and regional lymph node metastases on admission. The former were diagnosed by roentgen examination and accumulation of radioactive iodine in the thoracic region appeared in the scans (Figs 3, 4). The tumours were of the papillary type and visible remnants were left at the operations which were followed by postoperative radioiodine therapy and thyroid hormone medication. Thirteen and three years respectively after the operation no local recurrences or metastases were evident (Fig 5).

*Late complications* Five patients suffered permanent postoperative damage. 2 had unilateral paresis of the recurrent nerve and 3 patients had insufficiency of the parathyroid glands necessitating permanent substitution therapy. Four of the 5 patients underwent total thyroidectomy and one patient subtotal unilateral resection. Cervical dissection had been performed in all the patients.



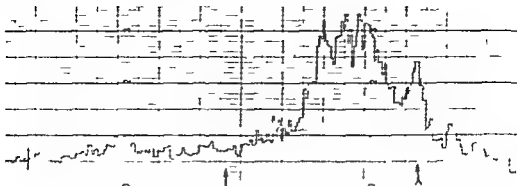


Fig. 4 Same case as in fig. 3. Profile diagram before treatment. Uptake of  $^{131}\text{I}$  in the lung. Umbilicus ( $\rightarrow$ ) and jugulum ( $\rightarrow$ ) levels indicated.

Eight of the 9 patients given external irradiation are still alive. Where a conventional roentgen unit was used only slight atrophy and hyperpigmentation of the irradiated skin was produced. Seven patients treated with the short distance gamma beam of the teleradium or the  $^{60}\text{Co}$  decacurie unit developed atrophy of the irradiated skin with telangiectases and fibrosis of the subcutaneous tissue. One of these patients had chronic ulceration of the skin requiring a skin graft. Another had a stricture in the lower portion of the hypopharynx probably due to the radiation therapy, as well as slight dysphagia. A third patient suffered minor trauma shortly after the radiation treatment which resulted in fracture of the clavicle with a subsequent pseudoarthrosis. This patient complained of paraesthesia in the right arm probably due to previous irradiation of the right supraclavicular area but as she had also undergone neck dissection on the same side this may have been a contributory cause of the nerve condition.

Eleven patients treated with radioiodine had no damage that could be attributed to this kind of therapy. Eight patients treated between the ages of 14 and 20 are now of fertile age. Three female patients all unmarried have normal menstrual periods. Four with 2 and one patient with 3 healthy children received between 50 and 100 mCi radioiodine.

### Discussion and Conclusion

The prognostic significance of age in carcinoma of the thyroid is well established (KENNEDY 1935, HORN & DULL 1954, SLOAN 1954, WARD 1955, WINSHIP & ROSSVOLL 1969) and was confirmed in this investigation. In only one of the 32 patients aged 20 years or under was this condition the direct cause of death.

The neoplasms were in all but two of the patients who died well differentiated papillary carcinomas. Whether this high incidence of well differentiated growths



Fig 5 Same case as in figs 3 and 4. After application of 120 mCi  $^{131}\text{I}$  and thyroid medication. No evidence of metastases.

in young patients can alone account for the favourable outcome cannot be decided from the analysis but this response to the treatment of recurrences and metastases would seem to suggest that other factors are also involved. A locally advanced stage of the tumour recurrence and metastases did not necessarily diminish the chances of survival in this series nor did a non radical surgical procedure. All the patients in whom visible remnants were left behind at the operation survived even when no postoperative irradiation was given. All 5 of the patients with such remnants and receiving only postoperative radioiodine therapy survived without recurrence in 4 of these patients the follow up time was longer than 10 years.

Other investigations indicate that where no operation is performed or where tumour residues are left behind at operation radiation therapy improves the prognosis (SHELVE *et coll* 1966, SMEDAL *et coll* 1967, TUBIANA *et coll* 1969). Our experience on this point may be inconclusive but the favourable results were obtained when radioiodine therapy was given after conservative surgery. External radiation treatment incurs a considerable risk of late radiation sequelae radioiodine treatment however failed to produce demonstrable damage to the patient.

None of the patients in whom the results of treatment were unsatisfactory had adequate hormonal medication. The patient who died had never received thyroid medication it was administered to 2 patients with recurrences only when these actually appeared and in a third patient the dose of medication was kept low. A fourth patient who was found at operation to have carcinoma of the regional lymph nodes had had adequate hormone medication and was also receiving continuous steroid therapy for asthma.

The treatment of the patients comprising this series varied, as did the stages of the conditions. Whether the good results can be ascribed to effective operations, supplemented in 12 cases by radiation therapy, or to the thyroid hormone medication cannot be decided from the data available. It is however notable that of the 4 patients not given a thyroid hormone as immediate postoperative treatment one died from carcinoma and 2 patients developed recurrences or late metastases. The medication thus seems to be a prime prognostic factor (CRILE 1957, THOMAS 1957).

### Acknowledgements

The authors welcome this opportunity of thanking Prof. J. Einhorn, Prof. L. G. Larsson and H. Wijnblad, who treated most of the patients for their advice and help. Prof. R. Walstam greatly facilitated this investigation by estimating the radiation dosages. The work was supported by the Swedish Cancer Society.

### SUMMARY

The treatment of carcinoma of the thyroid in 32 patients of twenty years of age or under during the period 1929—1967 is described. The clinical features, result and complications are dealt with in turn. Factors bearing on the course of the condition are discussed and proposals concerning its management are offered.

### ZUSAMMENFASSUNG

Die Behandlung des Schilddrüsenkarzinomes bei 32 Patienten, 20 Jahre alt oder jünger während der Periode 1929—1967 wird beschrieben. Die klinischen Eigenschaften, Ergebnis und Komplikationen werden nacheinander besprochen. Faktoren, die den Verlauf dieser Erkrankung beeinflussen, werden diskutiert und Vorschläge für deren Behandlung werden vorgelegt.

### RÉSUMÉ

Les auteurs décrivent le traitement du cancer de la thyroïde chez 32 malades âgés de 20 ans ou de moins de 20 ans au cours de la période 1929—1967. Ils examinent les signes cliniques, les résultats et les complications. Ils étudient les facteurs qui ont une influence sur le cours de la maladie et font des suggestions concernant son traitement.

### REFERENCES

- AMERICAN THYROID ASSOCIATION. President T. Winship, Washington D. C. Secretary W. M. McConahy, Mayo Clinic, Rochester, Minnesota, U.S.A.  
CRILE, G. JR. The endocrine dependency of certain thyroid cancers and the danger that hypothyroidism may stimulate their growth. *Cancer* 10 (1957) 1119.

- DAILEY M E and LINDSAY S Thyroid neoplasms in youth *J Pediat* 36 (1950) 460
- DUFFY M J and FITZGERALD P J Cancer of the thyroid in children A report of 28 cases *J clin Endocr* 10 (1950) 1296
- EKELBY P E and FRAZELL E L Carcinoma of the thyroid in children *Surg Clin N Amer* 49 (1969) 249
- HARE H I and NEWCOMB R V Carcinoma of the thyroid in children A ten year follow up *Radiology* 51 (1950) 401
- HAYLES A B KENNEDY R L J and BEAHR O H Management of the child with thyroidal carcinoma *J Amer med Ass* 173 (1960) 211
- HORN R C and DILL J A Carcinoma of the thyroid A re-evaluation *Ann Surg* 139 (1954) 35
- JACOBSSON G Treatment of carcinoma of the thyroid *Acta radiol* 41 (1954) 169
- KENNEDY R L J Carcinoma of the thyroid gland in children *J Pediat* 7 (1935) 631
- KLOPP C T ROSVOLL R V and WINSHIP T Is destructive surgery ever necessary for treatment of thyroid cancer in children? *Ann Surg* 165 (1967) 745
- POCHIN E E MYANT N B and CORBETT M D Leukemia following radioiodine treatment of hyperthyroidism *Brit J Radiol* 29 (1956) 31
- SHELLE G E GALANTE M and LINDSAY S Radiation therapy in the control of persistent thyroid cancer *Amer J Roentgenol* 97 (1966) 923
- SLOAN L W Of the origin characteristics and behavior of thyroid cancer *J clin Endocr* 14 (1954) 1309
- SVEDAL M I SALTZMAN F A and WEISSNER W A The value of 2 MV roentgen ray therapy in differentiated thyroid carcinoma *Amer J Roentgenol* 99 (1967) 352
- THOMAS C M Hormonal treatment of thyroid cancer *J clin Endocr* 17 (1957) 232
- TUBIANA M LALANNE C M BERTHON C MONYER J P and GÉRARD MARCHANT R Results obtained with radiotherapy in cases of thyroid cancer *In* Thyroid cancer UICC Monograph series Vol 12 Edited by Chr Hedinger Springer Verlag Berlin Heidelberg New York 1969
- UICC T N M Classification of malignant tumours Geneva 1968
- WARD R Cancer of the thyroid in children *Amer J Surg* 90 (1955) 338
- WINSHIP T and ROSVOLL R V Cancer of the thyroid in children *In* Thyroid cancer UICC Monograph series Vol 12 Edited by Chr Hedinger Springer Verlag Berlin Heidelberg New York 1969

## VIRUS PARTICLES IN RELATION TO RADIATION INDUCED CHANGES IN THE THYMUS OF C<sub>3</sub>H MICE

by

H. JARPLID

Thymic lymphoma in mouse strains with low spontaneous frequency of leukaemia e.g. C<sub>3</sub>H and C<sub>3</sub>H may generally be induced by suitably fractionated irradiation (KAPLAN & BROWN 1952, GROSS et coll 1959). In C<sub>3</sub>H mice this mode of irradiation leads also to disorders in the diphasic regeneration of the thymus (JARPLID 1968). Radiation induced leukaemia has been transmissible with non-cellular material (GROSS 1958, LIEBERMAN & KAPLAN 1959) and virus particles have been demonstrable in thymic lymphoma which developed after irradiation (GROSS & FELDMAN 1968, LAGERLOF 1968). Acutely radiation damaged thymus has also proved to contain morphologically demonstrable virus particles (GROSS & FELDMAN 1968). Little, however, is known about the exact site of the virus particles within the thymus nor of how the occurrence of particles is related to the various phases of regeneration of the thymus and to the induction of thymic lymphoma.

*Material and Methods:* Fractionated whole body irradiation was given to 79 female C<sub>3</sub>H mice. A total dose of 550 R was divided between four equal exposures and given every fifth day beginning at an age of  $25 \pm 2$  days.

Submitted for publication 19 October 1971

The animals were irradiated in a plastic wheel as described earlier (JARPLID 1968). The roentgen apparatus used, Muller MG 300 was operated at 260 kV and 9.5 mA. The radiation was filtered by 0.5 mm Cu and 0.5 mm Al. An extra filter of Cu was used with a HVL of 1.9 mm Cu at the periphery and a HVL of 2.2 mm Cu at the centre. The focal distance was 45 cm and dose rate 74 R/min.

*Morphologic investigation.* Eighteen fractionated irradiated mice were killed for histologic and electron microscopic investigation in groups of 4 to 5 at 3, 10, 17 and 24 days after the last fraction. Twelve untreated animals served as controls and were autopsied in groups of 3 at corresponding times. All animals were killed by cervical dislocation. The thymic lobes were excised and one part of each lobe was fixed in Stieve's fluid for light microscopy and the other part was prepared for electron microscopy. Conventional histologic methods were used and the sections were stained with Ehrlich's haematoxylin and eosin. The specimens for electron microscopy were fixed in a formaldehyde-glutaraldehyde solution according to KARNOVSKY (1965) for at least 24 hours and postfixed in 2.67 per cent osmium tetroxide buffered with *s*-collidine (BENNET & LUFT 1959) for 1 hour. The fixations were performed at 4°C. The material was dehydrated in ethanol and embedded in Epon (LUFT 1961). One  $\mu$  sections were stained with 0.2 per cent toluidine blue for light microscopy (BJORKMAN 1962). Sections about 700–800 Å thick were collected on 300 mesh copper grids and stained with uranyl acetate in methanol (STEMPAK & WARD 1964) for 5 minutes and subsequently with 0.2 per cent lead citrate (VENABLE & COGGESHALL 1965) for 1 minute. These sections were examined in a Siemens Elmiskop I A at 60 kV. Specimens from both cortex and medulla of each thymic lobe were examined by light microscopy as well as by electron microscopy.

*Non cellular extracts.* Fifty-nine mice which had received fractionated irradiation were killed in groups of 10 to 33 at 3, 10 and 17 days after the last exposure. Non cellular extracts were prepared from the excised thymus glands according to HARAN-GIERA (1966). The extracts were injected intraperitoneally into newborn syngenic mice or into thymic grafts under the kidney capsule in previously thymectomized and whole body irradiated (400 R) young adult syngenic mice.

## Results

*The epithelial cells* of the thymus could be identified by their tonofilaments and desmosomes (Fig. 1). The general ultrastructural appearance of these cells however was somewhat varying. They had rather large and often oval nuclei with finely dispersed chromatin and one or more prominent nucleoli. The cyto-



Fig. 1. Epithelial cell from thymic medulla 17 days after fractionated irradiation. Centrally a cluster of vacuoles (V) containing virus particles (VP). Tonofilaments (T) in a cytoplasmic extension. Inserted field shows tonofilaments (T) and desmosome (D).

plasma was prominent, often with long extensions between other cells. The amount of ribosomes was moderate. The tonofilaments often appeared near the nucleus and at the periphery of the cell where they sometimes were inserted into desmosomes connecting adjacent epithelial cells. The amount of mitochondria varied. At one side of the nucleus the cytoplasm of the epithelial cells often contained a cluster of vacuoles (Fig. 1); these varied in form and size, measuring up to  $3.5 \mu$  in diameter. The vacuoles were surrounded by a membrane, sometimes with microvillous projections into the lumina. In these lumina an amorphous material of moderate density and sometimes virus particles were found.

Virus particles were only found in the epithelial cells of the thymic medulla; no particles were seen in the thymic cortex. In untreated control mice a few single particles were found within vacuoles of epithelial cells in the thymus from 2 of 12 animals investigated. In irradiated mice the particles most frequently

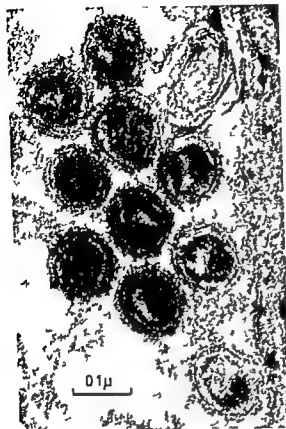


Fig. 2. Detail from fig. 1. Enveloped virus particles with relatively electron-dense capsids.

appeared in the cytoplasmic vacuoles (Fig. 1) but in a few cases within the cytoplasmic matrix i.e. together with ribosomes or budding from endoplasmic reticulum. The appearance of the virus particles was similar to that described for murine leukaemia viruses (type A and C particles; BERNHARD & GUERY, 1958).

Most of the virus particles appearing in the cytoplasmic vacuoles lay free within the lumen (Figs 1 to 3). These particles seemed to have an envelope with a diameter of 100–110 *mμ*; the diameter of their capsids was 50–60 *mμ*. Some of these particles had an electron-lucent centre and have been described as enveloped A particles (DE HARVEN, 1968). Other particles had a more electron-dense centre (C type particles). In a few cases enveloped A particles were seen to bud from the vacuole membrane. In the cytoplasmic matrix the particles generally appeared as doughnut-shaped capsids (naked A particles; DE HARVEN,



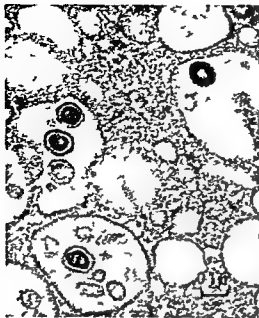


Fig 3 Epithelial cell from thymic medulla 3 days after irradiation. Enveloped virus particles with electron lucent centres (enveloped A particles) in cytoplasmic vacuoles

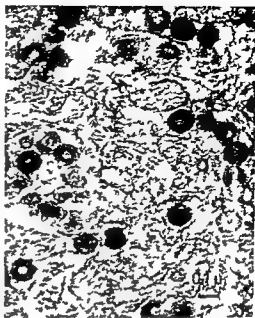


Fig 4 Epithelial cell from thymic medulla 3 days after irradiation. Virus particles with doughnut shaped capsids and electron lucent centre (naked A particles) in the cytoplasm

Fig 4) with an external diameter of 80—90 m $\mu$  and an internal diameter of 40—50 m $\mu$ . The centre of the capsid i.e. the nucleoid, was electron lucent. The particles appeared in diffuse groups or as single scattered particles. Some of the particles were budding from intracytoplasmic membranes which seemed to take part in the formation of a viral envelope (Fig 5). Some virus particles were also budding into the cisternae of endoplasmic reticulum (Fig 6).

*Virus particles in relation to time after irradiation.* As seen in Table 1 a moderate to large number of particles were found in about half the number of cases investigated 3, 10 and 17 days after the last irradiation. After 24 days however no more than a few virus particles were found in each case. On each occasion of examination most of the virions were enveloped A particles or C particles.

Non-cellular extracts were prepared from thymus 3, 10 and 17 days after irradiation. The injection of these extracts into thymic grafts in pretreated mice or into newborn mice did not result in any case of lymphoma within 24 months after injection.



Fig 5 Epithelial cell from thymic medulla 24 days after irradiation. Budding of a circular virus capsid from an intracytoplasmic membrane

*Virus particles in relation to thymic histology.* Three days after the last irradiation the thymus was in the first phase of lymphocyte depletion (JARPLID 1968) with a moderate loss of weight. On the tenth day the thymus was at the maximum of the first phase of regeneration. As seen in Table 1 there seemed to be no difference in frequency of observed virus particles between 3 and 10 days after treatment in spite of the difference in histology between these two occasions. The single thymic lobes from ten animals which were autopsied 17 and 24 days after the last irradiation were classified histologically according to JARPLID. The different histologic appearances of the thymic lobes were briefly: Normal histology. Cortical thinning: the cortex had an irregular thin and less dense appearance than normal. Uniform depletion: the content of lymphocytes in cortex and medulla appeared to be of equal order of magnitude. Cortical inversion: the appearance of the medulla was manifestly unchanged whereas the cortex was almost entirely lacking in lymphocytes. Regeneration: immature lymphoid cells with fine chromatin structure in large nuclei and with basophil cytoplasm formed a broad, mitosis-rich cortex.



Fig. 6. Epithelial cell from thymic medulla 24 days after irradiation. Virus particles within and budding into a cisterna of endoplasmic reticulum. Tonofilaments (T).

As seen in Table 2 there was an abundance of virus particles in one normal lobe and in one lobe with cortical thinning. One lobe in regeneration had a moderate number of particles whereas only a few or no particles were observed in the other lobes. In four cases the thymus had a similar histologic appearance in both lobes. In one of these there were many particles in one lobe and only a few in the other. In two other cases there were a few or a moderate number of particles in one lobe and none in the other. The fourth case had no particles in either lobe. In three mice the thymus was in a state of histologic asymmetry (JARPLID) i.e. one lobe had a normal histology or was in a regeneration phase while the other was the site of depletion of different degrees: cortical thinning, uniform depletion or cortical inversion. Two of these three asymmetric cases had a few virus particles in each lobe. The last asymmetric thymus had one normal lobe with many virus particles and one lobe with cortical thinning and only a few virus particles.

### Discussion

Virus particles were found in epithelial cells of the thymic medulla both in untreated control animals and in irradiated animals. Thus a few single particles were seen within vacuoles of the epithelial cells in 2 out of 12 control animals examined.

Table 1

Frequency of virus particles in the thymus in relation to time after end of fractionated irradiation. Approximate average number of virus particles per grid square: 0 no particles observed; + 1 to 10 particles (few); ++ 11 to 20 particles (moderate); +++ more than 20 particles (abundant).

Days after irradiation	Frequency of particles				
3	+++	+++	++	0	
10	+++	++	+	0	
17	+++	++	+	+	0
24	+	+	+	0	0

Table 2

Frequency of observed virus particles in single thymic lobes in relation to histologic changes of the same lobe 17 to 24 days after the end of fractionated irradiation. Approximate average number of virus particles per grid square: 0 no particles observed; + 1 to 10 particles (few); ++ 11 to 20 particles (moderate); +++ more than 20 particles (abundant).

Histology	Frequency of virus particles				
Normal	+++	0			
Cortical thinning	+++	+	+	+	0
Uniform depletion	+	+	0	0	0
Cortical inversion	+	+			
Regeneration	++	+	+	0	

Virus particles occurred to a moderate average extent after 3, 10 and 17 days after the end of irradiation but fell after 24 days to at most a few particles per grid in irradiated animals. This tendency to a reduced frequency of particles with time may perhaps be related to the reduced infectivity found by HARAN-GIERA (1966) with non-cellular material from thymus and bone marrow of C57BL mice later than 10 days after irradiation. In the electron microscopic investigation by GROSS & FELDMAN (1968) on irradiated C57BL mice virus particles were also found in occasional thymus examined after 8, 15 and 22 days while a thymus examined on day 23 contained no particles.

As already noted the various times of observation 3, 10, 17 and 24 days after irradiation represent four different phases in the development of thymic injury. These various phases are characterized by morphologic differences localized to the cortex, whereas the appearance of the medulla showed no major changes. During the depletion phase the cortex is narrower and thinner than normal while during the regeneration phase it has a more normal breadth and contains an abundance of fairly large lymphoid cells of blast-like appearance. Despite



Fig. 7. Radiation induced thymic lymphoma. Budding virus particles within the cytoplasm of a lymphoma cell.

this morphologic difference there was no appreciable difference in the occurrence of virus particles between the first depletion and regeneration phases and between them and the second depletion phase. During the second regeneration phase, on the other hand, a reduction in the number of virus particles took place.

The occurrence of virus particles accordingly does not appear to be related to the morphologic appearance of the thymic cortex, which also seems to be evident from the limited material in which the frequency of particles has been investigated in respect of the histologic appearance of single thymic lobes (Table 2). An abundance of particles occurred only in a lobe with cortical thinning and in a lobe with normal morphologic appearance. The majority of other lobes showed few or no virus particles. Three of four cases with similar histologic appearance in the two lobes within the same thymus differed in respect of the occurrence of virus. Conversely two cases of three with histologic asymmetry had a similar number of particles within both lobes. The explanation may lie in the fact that virus particles were in no case found in the thymic cortex. As already noted, all particles were instead localized in epithelial cells in the morphologically less changeable medulla. This, however, does not contradict the theory advanced by HAPLAN (1961) that lymphoblasts in a regenerating thymus are target cells for an activated or liberated virus. A wider understanding of this problem, however, requires a greater knowledge of the normal functions and mutual relations of the various kinds of cells in the thymus.

The attempt to test the leukaemogenic properties of the virus particles occurring during the thymic regeneration has hitherto had a negative result. A corresponding investigation has, however, been successful on  $C_{57}$ Bl mice when filtrate from thymus was mixed with filtrate from bone marrow (HARAN GHERA 1966) but not when thymus filtrate alone was tested 2 or 7 days after the end of irradiation (HARAN GHERA & PELED 1967). It has earlier been mentioned that radiation induced thymic lymphoma in  $C_{3}H$  or  $C_{57}$ Bl mice may contain virus particles (GROSS & FELDMAN 1968, LAGERLOF 1968) and that such tumours may be transmitted with non cellular material (GROSS 1958, LIEBERMAN & KAPLAN 1959). In the present investigation the thymus was investigated in one case with generalized thymic lymphoma in respect of the occurrence of virus particles. Apart from a moderate number of particles in intracytoplasmic vacuoles a few particles were found also in the cytoplasmic matrix of lymphoma cells in the cortex (Fig. 7). After injection of leukaemia virus virus particles occur in the thymus both extracellularly and intracellularly and both in lymphocytes and epithelial cells (CARNES et al. 1968, RICH & JOHNS 1968). After leukaemogenic irradiation particles were found in the present investigation only in epithelial cells of the medulla. Even if the number of virus particles in the thymus increases after irradiation, the significance of virus particles for the induction of thymic lymphoma in these mice still appears to be unclear.

### Acknowledgement

The author is indebted to B. M. Svedenstam and J. Thörn for their excellent technical assistance.

### SUMMARY

The occurrence of virus particles in the thymus after fractionated leukaemogenic irradiation was investigated in respect of the various phases of the thymic regeneration. The significance of virus particles for the induction of thymic lymphoma was discussed.

### ZUSAMMENFASSUNG

Das Auftreten von Viruspartikeln im Thymus nach fraktionierter Leukämie hervorrunder Bestrahlung wurde im Hinblick auf die verschiedenen Phasen der Thymusregeneration untersucht. Die Bedeutung der Viruspartikel für die Induktion des Thymuslymphoms wird diskutiert.

### RÉSUMÉ

L'auteur a étudié la présence de particules virales dans le thymus après irradiation fractionnée leucémogène en fonction des différentes phases de la régénération thymique. Il étudie l'influence des particules virales dans l'induction d'un lymphome thymique.

## REFERENCES

- BENNETT H. S. and LUFF J. H. S. collidine as a basis for buffering fixatives. *J. biophys. biochem. Cytol.* 6 (1959) 113.
- BERNHARD W. et GLERIN M. Présence de particules d'aspect viral dans les tissus tumoraux de souris atteintes de leucémie spontanée. *C. R. Acad. Sci. (Paris)* 248 (1958) 160.
- BJORKMAN N. Low magnification electron microscopy in histological work. *Acta morph. neerl. scand.* 4 (1962) 344.
- CARNES H. W., LIEBERMAN M., MARCHILDON M. and KAPLAN H. S. Replication of type C virus particles in thymus grafts of  $C_{3H}$  mice inoculated with radiation leukemia virus. *Cancer Res.* 28 (1968) 98.
- GROSS L. Attempt to recover filtrable agent from X-ray induced leukemia. *Acta haemat.* 19 (1958) 353.
- and FELDMAN D. G. Electron microscopic studies of radiation induced leukemia in mice. Virus release following total body X-ray irradiation. *Cancer Res.* 28 (1968) 1677.
- ROSWIT B., MADA E. R. et coll. Studies on radiation induced leukemia in mice. *Cancer Res.* 19 (1959) 316.
- HARAN GHIERA N. Leukemogenic activity of centrifugates from irradiated mouse thymus and bone marrow. *Int. J. Cancer* 1 (1966) 81.
- and PELFD A. The mechanism of radiation action in leukaemogenesis. Isolation of a leukaemogenic filtrable agent from tissues of irradiated and normal  $C_{3H}$  mice. *Brit. J. Cancer* 30 (1967) 730.
- DE HARVEN E. Morphology of murine leukemia viruses. In: *Experimental leukemia*. Chapter 4, p. 97. Edited by M. A. Rich. Appleton-Century-Crofts, New York, 1968.
- JARPLID B. Radiation induced asymmetry and lymphoma of thymus in mice. *Acta radiol.* (1968) Suppl. No. 279.
- KAPLAN H. S. The role of cell differentiation as a determinant of susceptibility to virus carcinogenesis. *Cancer Res.* 21 (1961) 981.
- and BROWN M. B. A quantitative dose response study of lymphoid tumor development in irradiated  $C_{3H}$  mice. *J. nat. Cancer Inst.* 13 (1952) 185.
- KARNOVSKY M. J. A formaldehyde-glutaraldehyde fixative of high osmolality for use in electron microscopy. *J. cell Biol.* 27 (1965) 137.
- LACERLOF B. The ultrastructure of virus- and radiation induced thymomas of  $C_{3H}$  mice. *Acta path. microbiol. scand.* 74 (1968) 495.
- LIEBERMAN M. and KAPLAN H. S. Leukemogenic activity of filtrates from radiation induced lymphoid tumors of mice. *Science* 130 (1959) 387.
- LUFF J. H. Improvements in epoxy resin embedding methods. *J. biophys. biochem. Cytol.* 9 (1961) 409.
- RICH M. A. and JOHNS L. W. Quantitative distribution of virions in virus induced murine leukemia. *J. nat. Cancer Inst.* 41 (1968) 1463.
- STENPAK G. and WARD T. An improved staining method for electron microscopy. *J. cell Biol.* 22 (1964) 697.
- VENABLE J. H. and COGGESHALL R. A. A simplified lead citrate stain for use in electron microscopy. *J. cell Biol.* 25 (1964) 407.

## LATE EFFECTS OF IRRADIATION ON THE THYROID GLAND IN MICE

### I Irradiation of adult mice

by

G WALINDER

The experiences gained during the past twenty years with radiation induced neoplasms in animal and human thyroid glands have enabled the following three conclusions to be drawn (1) The doses required to produce a certain frequency of thyroid neoplasms are much higher after the administration of  $^{131}\text{I}$  than after roentgen irradiation (see reviews by DONIACH 1963 McCLELLAN et coll 1963 and SAENGER et coll 1963) (2) Increased growth of the thyroid epithelium potentiates markedly the carcinogenic effects of irradiation in the gland (see review by LINDSAY 1969) (3) The thyroid glands of young individuals (children) are more sensitive to the carcinogenic action of irradiation than are those of adults (see reviews by DOLPHIN 1968 and HEMPELMANN 1969)

The first of the three points is a general observation and applies not only to neoplasms but also to more acute effects such as the radiation induced mitotic death observed in thyroid epithelium (WALINDER & SJODEN 1971 WALINDER 1972) The difference in effectiveness between irradiation with roentgen rays and with  $^{131}\text{I}$  for inducing neoplasms is probably mainly the result of dose rate depend

Submitted for publication 14 February 1972



ence, as is the case with acute radiation effects (WALINDER et coll 1972) The third point is probably largely a consequence of point (2) (WALINDER & SJODEN)

It is important to bear these three points in mind when the risk of thyroid damage is being assessed and when adequate protective measures are being decided upon for a population that has either already been exposed to radioactive fallout or is likely to be so The decision as to when and to what extent measures for the protection of a civilian population in a fallout area are to be put into effect must in the light of the aforementioned point (3), be primarily based on an assessment of the risks to the unborn (pregnant women) and to young children Besides the differences in radiation sensitivity, the consequences of the radioiodine incorporations will be especially dangerous for foetuses and young children because the doses on exposure to the same amounts of activity will be higher in the smaller thyroid glands of the young than in the thyroids of adults (CONARD et coll 1970)

The significance of the above mentioned three conclusions has been investigated earlier with respect to the acute effects in mice (WALINDER 1971 WALINDER & SJODEN 1971 WALINDER 1972, WALINDER et coll 1972) Corresponding investigations on the radiation effects in mouse thyroids one to two years after the exposures will be reported in the present paper, as well as in part II (WALINDER & SJODEN to be published) The section now presented deals with mice given  $^{131}\text{I}$  injections or subjected to roentgen irradiation at an adult age

### Material and Methods

Male CBA mice were used for the experiments The mice irradiated with  $^{131}\text{I}$  received the nuclide by injection at 110 to 113 days of age As half the radiation dose is delivered within 4 days and 90 per cent within 12 days it may be said that the mice had in practice been irradiated at the age of 110 to 125 days The animals that received roentgen irradiation were exposed at 123 to 130 days of age The management of the animals and the technique employed for the radioiodine injections and the roentgen irradiation have been described earlier (WALINDER 1971 WALINDER & SJODEN) In order to avoid as far as was possible any biased influence from factors possibly connected with the position of the mice the cages were moved to various places in the room at different times after the exposures

Seven hundred mice were irradiated by injection of 1.5, 3.0 and 4.5  $\mu\text{Ci}$  of  $^{131}\text{I}$  or by roentgen irradiation with 500, 1000 and 1500 R The roentgen irradiation was localized to the thyroid by shielding the rest of the body with lead

Because of the secondary radiation, however, the dose to the hypophysis was approx 10 per cent of the dose to the thyroid (WALINDER & SJODEN)

*Histologic investigations* The mice were killed with chloroform at 680 to 730 days of age and their body and thyroid weights were determined. A few moribund animals were killed at age 580 to 680 days. The parietal bone was removed in all animals, so that the hypophysis was visible and in this condition the skull was placed in formaldehyde solution (neutral). After fixation for some time, the hypophysis was removed and weighed. Overweight hypophyses ( $> 6$  mg) were set aside for histologic examination and were sectioned and stained with PAS-Orange G (Tripas) (PEARSE 1968).

All thyroids and macroscopically observable tumours in other organs were examined at a preliminary histologic analysis: the tissues having first been fixed in neutral formaldehyde or in Steeve's fluid (ROMEIS 1948) and stained with haematoxylin and eosin (H & E) by the method described by ROMEIS. In those cases in which nodules and tumours were found (or had been directly visible in the operating microscope) the serial sectioning was continued over the whole lobe and the cervical lymph nodes were taken out and examined in the microscope. The staining with H & E was then supplemented with van Gieson's stain (ROMEIS) and with the periodic acid Schiff stain (PAS) according to the Hotchkiss technique (PEARSE). Another more detailed analysis of the frozen carcasses ( $-20^{\circ}\text{C}$ ) of these mice was also undertaken.

This method of selection may have resulted in a few small thyroid tumours being overlooked but because of the relatively large number of mice in the different groups, as well as of the fact that the tumours were usually so large that they also occupied central parts of the lobes and furthermore were as a rule directly visible in the operating microscope, a statistically acceptable comparison figure could be obtained for the number of tumours in the different groups.

*Definitions* To make strict distinctions between hyperplasia and benign and malignant tumours by morphologic methods is impossible. Instead it is necessary to rely wholly upon certain definitions based on experience. The criteria applied for distinguishing an adenomatous goitre nodule from true adenomas in the present investigation were based on the definitions set up by WARREN & MEISSNER (1953).

Adenomatous goitre nodule	True adenoma
Multiple nodules	Solitary nodule
Poor encapsulation	Good encapsulation
Variable structure	Uniform structure
Comparable growth pattern in adjacent gland	Different growth pattern in adjacent gland
No compression of adjacent gland	Compression of adjacent gland

The interpretation of whether an observed tumour was malignant or not was based on current morphologic criteria, namely, invasive ability, cellular atypia (e.g. polyploidy), and mitotic frequency.

*Measurement of cell survival in the thyroid* By allowing the mice to have access for 12 days before irradiation to drinking water containing 0.1 per cent propylthiouracil (PTU), and then injecting  $10 \mu\text{Ci}$  tritiated thymidine ( $^3\text{H}$  TdR) the remaining DNA bound tritium activity in the thyroid may be regarded as a value for the cell survival in the gland (WALINDER 1972, WALINDER & WALINDER 1971).

The following experiment was carried out in order to investigate the cell survival in irradiated and unirradiated CBA mice. Two hundred male mice were divided up into 4 groups, with 50 animals in each, and were treated according to the schedule given below.

Date of treatment	24.12—5.1	4.1	11.1—26.1	25.1
Group 1	PTU		Iodine low diet	
Group 2	PTU		Iodine low diet	$3 \mu\text{Ci } ^{131}\text{I}$
Group 3	PTU	$^3\text{H}$ TdR	Iodine low diet	
Group 4	PTU	$^3\text{H}$ TdR	Iodine low diet	$3 \mu\text{Ci } ^{131}\text{I}$

The mean dose to the central parts of the thyroid lobes in the mice in groups 2 and 4 was 14 000 rad which meant that the dose at the periphery was 5 600 rad (WALINDER 1971). One day after the injection of radioiodine the iodine deficient diet ( $< 0.1 \mu\text{g}$  I per g food pellet) was exchanged for a normal diet (circa  $20 \mu\text{g}$  I per food pellet). The iodine content of the diet was determined by activation analysis. Ten mice from each group were killed with chloroform 1, 7, 30, 92 and 182 days after the injection of  $^{131}\text{I}$ . Details concerning the treatment of the thyroid glands and the measuring technique for determination of the tritium activity in the tissue have been reported in an earlier paper (WALINDER 1972).

Twenty mice, 10 of which had been treated simultaneously with, and in the same way as the mice in group 1 and the other 10 similarly to those in group 2 were killed 156 days after the radioiodine injection for quantitative analysis of the different thyroid components and for measurement of the 24 hour uptake of  $^{131}\text{I}$  ( $0.2 \mu\text{Ci } ^{131}\text{I}$  injected intraperitoneally 24 hours before the mice were killed). The technique used for the activity measurements as well as the morphometric methods, have been described earlier (WALINDER 1971, 1972).

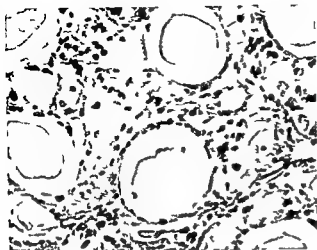


Fig 1 Degenerative changes in the thyroid tissue of a 710 day old CBA mouse injected with 4.5  $\mu$ Ci  $^{131}\text{I}$  at 110 days of age (H & E  $\times 780$ )

## Results

### *Thyroid and hypophysis weights*

Irradiation of the thyroid gland led after about two years to marked degenerative changes (Fig 1) and a significantly lower glandular weight than was found in the controls (Table 1)

As was the case with the acute radiation effects in the thyroids of CBA mice (WALINDER & SJÖDEN) the dose needed to produce a certain degree of growth inhibition was higher when  $^{131}\text{I}$  injections were given than after roentgen irradiation. This difference seemed to increase slightly with increasing doses to the thyroid (Table 1)

There was a positive correlation between the hypophysis weight and the doses to the thyroid. With an assumed linear regression the correlation coefficient was +0.182 in both the  $^{131}\text{I}$  and the roentgen experiments, a value that was significantly separated from 0 ( $p < 0.01$  in both cases). Hypophyses which had proved at the histologic examination to contain tumours were not included in this analysis. Such glands may reach weights of over 25 mg.

### *Cell survival in irradiated thyroids*

The results obtained for cell survival in irradiated and unirradiated thyroids are presented in Tables 2 and 3. They were similar to those observed earlier in C57Bl mice (WALINDER & WALINDER). A rapid decrease in the tritium activity in the thyroids between the seventh and thirtieth day after the  $^{131}\text{I}$  injection (Table 2) indicated a period of increased cellular mortality. Following this

Table 1

*Weights of body, thyroid and hypophysis in 680 to 730 day old CBA mice irradiated at around 4 months of age (According to ICRU Handbook 85 1 R=0.95 rad)*

Group No	Source of irradiation	Amount of I injected $\mu$ Ci	No of surviving mice	Total dose (rad)		Body weight g	Thyroid weight mg ( $\pm$ SE)	Hypophysis weight mg ( $\pm$ SE)
				Centre	Periphery			
1	—	—	100	—	—	31.9	11.81 $\pm$ 0.17	1.87 $\pm$ 0.09
2	I	1.5	93	5.400	2.200	31.2	5.95 $\pm$ 0.15	2.01 $\pm$ 0.08
3	I	3.0	88	11.000	4.400	30.8	4.00 $\pm$ 0.10	2.11 $\pm$ 0.09
4	I	4.5	80	16.000	6.400	30.5	3.75 $\pm$ 0.11	2.23 $\pm$ 0.10
5	Roentgen	—	96	475	475	31.7	10.46 $\pm$ 0.18	2.04 $\pm$ 0.11
6	Roentgen	—	95	950	950	31.3	8.60 $\pm$ 0.15	2.09 $\pm$ 0.10
7	Roentgen	—	84	1.430	1.430	30.1	4.39 $\pm$ 0.12	2.15 $\pm$ 0.10

period, the decrease in activity proceeded at a much slower rate. The values in Table 2 even indicate that the triium content in the thyroids then fell more slowly than in the controls, which would suggest that the irradiated thyroid cells gradually developed a longer life cycle than the unirradiated cells.

The increased cell death that occurred during the first month after the  $^{131}\text{I}$  injection did not cause a corresponding decrease in thyroid weight. Such a decrease occurred later, however, becoming significant between the third and fifth month after injection of the radioiodine (Tables 2, 3). The iodine uptake decreased at approximately the same rate as the fall in the thyroid weight (Table 3). The percentage proportions of colloid, epithelium, mesenchymal tissue and blood were largely the same in both irradiated and unirradiated glands, but the number of epithelial cells was much smaller in the irradiated glands. The mean volume in the epithelial cells was larger in the irradiated glands.

### *Histologic observations*

**Hypophysis tumours.** Irradiation of the thyroids led not only to an increase in hypophyseal growth but also to the development of tumours in the hypophysis, particularly in those mice which had received the highest doses to the thyroid. The tumours were usually of the angular type, which is typical of TSH cells (Fig. 2 a). They contained no acidophilic cells whatever, and normal hypophysis tissue could only be observed in thin peripheral layers (Fig. 2 b). In exceptional cases trabecular and more pleomorphic tumour types were seen (Fig. 2 c, d).

Table 2

Thyroid weights and remaining tritium activity in irradiated and unirradiated thyroids at different times after injection of  $3 \mu\text{Ci } ^{125}\text{I}$  (Dose to lobe centres 14 000 rad Dose to periphery of gland 5 600 rad)  
CPM = counts per min as measured in a scintillation counter

No. of days after injection of $^1\text{I}$	Thyroid weight mg ( $\pm$ SE)	Mean activity of tritium in thyroid CPM
Controls		
1	$4.1 \pm 0.2$	1 039
7	$4.1 \pm 0.2$	1 124
30	$4.4 \pm 0.1$	1 034
97	$7.7 \pm 0.4$	831
187	$11.7 \pm 0.5$	706
Mice injected with $^1\text{I}$		
1	$4.2 \pm 0.3$	1 085
7	$4.1 \pm 0.2$	1 167
30	$4.4 \pm 0.2$	825
97	$6.6 \pm 0.3$	687
187	$7.9 \pm 0.4$	613

Table 3

Iodine uptake and weights of components in  $^{125}\text{I}$  irradiated ( $3 \mu\text{Ci}$ ) and in unirradiated thyroid glands 156 days after injection of the radioiodine. Figures within brackets denote weights of respective components in per cent of total thyroid weight. The 24 hour uptake is significantly lower in the irradiated than in the unirradiated glands but taken per mg of tissue the uptake is approximately the same  $0.30 \pm 0.05\%$  per mg in the controls and  $0.26 \pm 0.02\%$  per mg in the irradiated mice.

	Mice injected with $3 \mu\text{Ci } ^1\text{I}$	Unirradiated controls
No. of mice	10	10
Dose to lobe centres rad	14 000	—
Body weight g	40.2	38.8
24 hour uptake	$1.7 \pm 0.2$	$3.2 \pm 0.3$
Thyroid weight mg	$7.2 \pm 0.4$	$10.9 \pm 0.6$
Colloid mg ( )	5.3 (74.0)	8.1 (74.4)
Epithelium mg ( )	1.1 (15.1)	1.7 (15.5)
Stroma and blood mg ( )	0.78 (10.9)	1.1 (10.1)
No. of epithelial cells	$0.50 \times 10^6$	$1.2 \times 10^6$
Mean volume per epithelial cell $\text{mm}^3 \times 10^{-6}$	$2.11 \pm 0.09$	$1.44 \pm 0.04$

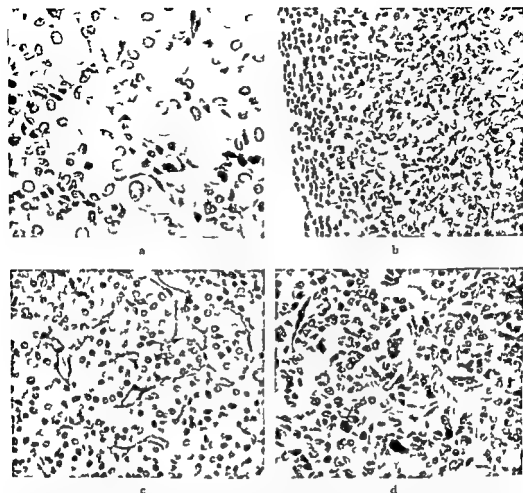


Fig 2 Hypophysis tumours in mice whose thyroids had been irradiated when they were about 4 months old a) The angular cell type (TSH cells) occurring most commonly in these tumours (Tripas  $\times 450$ ) b) A narrow peripheral zone of normal tissue enclosing the tumour (Tripas  $\times 280$ ) c) Occasionally solid masses of cells with discrete lobulation (c) (Tripas  $\times 280$ ) and areas of pleomorphic cells (d) (Tripas  $\times 280$ ) are seen in these tumours

**Thyroid tumours** The increase in thyroid weight observed in the aging CBA mouse is largely a result of increasing colloid goitre. The follicular enlargement is particularly noticeable in the central parts of the thyroid lobes, which thereby gradually lose their functional activity (WALINDER et coll 1971). The follicles are still active at the periphery, particularly at the apices of the lobes, and as the mouse grows older increasing hyperactivity leading to hyperplasia (Fig 3a) and hyperplastic nodules (Fig 3b) may be observed in the central areas.



Fig 3 Nodule development in CBA mice over 700 days of age a) Typical peripheral hyperplasia in an unirradiated gland (H & E  $\times 50$ ) b) Two nodule variants in hyperplastic thyroid tissue with follicular and papillary infolding respectively (H & E  $\times 125$ ) c) A later stage of a nodule probably hyperplastic in origin of the same type as that in (b) in a mouse injected with 15  $\mu$ Ci  $^{131}\text{I}$  at 117 days of age (H & E  $\times 100$ )





Fig. 4. A microfollicular adenoma from a 720 day old mouse injected with  $3 \mu\text{Ci } ^{131}\text{I}$  at 11<sup>o</sup> days of age (H. & E.  $\times 100$ ).

The two most common forms of nodules in such hyperplastic regions may be seen in Fig. 3 b. The process begins as a rule with vacuolation and fragmentation of the colloid in a follicle, accompanied by papillary and microfollicular infoldings. This development continues until all colloid has disappeared from the lumen of the follicle, resulting in the formation of cystic nodules. Nodule formation did not go beyond this stage in the control mice in the present investigation. In the irradiated thyroids, however, the whole of the old follicle had sometimes become filled with cells and the nodule was often encapsulated and because of continued cellular growth was pressing on the surrounding tissue. Fig. 3 c is a photomicrograph of a nodule, mainly of papillary type, in a relatively advanced stage of development.

The borderline case illustrated in Fig. 3 c was classified as a papillary adenoma on the basis of the definitions used in this investigation. In addition to papillary tumour structures the most common histologic types of benign tumour observed in this material were follicular (Fig. 4) and trabecular (Fig. 5) in structure. Two of these three types were often observed in one and the same tumour. In such cases the classification was based on the dominant structure in the tumour.

The five tumours classified as malignant all displayed a fairly high degree of differentiation of follicular type, although the tumour illustrated in Fig. 6, with its diffuse infiltration of surrounding tissue, suggests an anaplastic tendency. The capsular and intravascular infiltrations consisted of ovoid and hypercellular tumour masses of organoid pattern (Fig. 7). A section from a follicular carcinoma with marked cellular atypia is shown in Fig. 8.

No metastases were observed. Table 4 gives the incidence of neoplasia in the material.

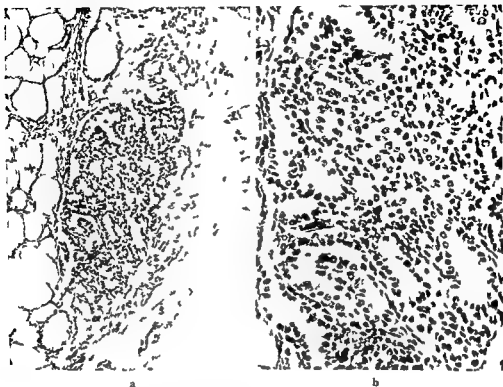


Fig 5 A trabecular adenoma in a 730 day old mouse injected with 4.5  $\mu$ Ci  $^{131}\text{I}$  at around 110 days of age. The tumour is almost wholly without colloid (van Gieson  $\times 110$ ) b) An enlarged view of the same adenoma ( $\times 290$ )

### Discussion

*Reliability of the values obtained* The thyroid and hypophysis weights in Tables 1 to 3 are given as  $\pm$  standard errors of the mean. For errors of this type to be capable of giving any indication of the reliability of the measurement values it is necessary that the values should be randomly distributed and thus that no experimental group has been subject to any systematic source of error. Such a prerequisite is strictly speaking seldom at hand in animal experiments and especially not when it is a question of long term experiments. From a purely statistical standpoint even a roentgen dose of 500 R (475 rad) seemed to give a significantly lower thyroid weight than was obtained in the controls (Table 1). It is doubtful however whether this slight difference in the thyroid weights was biologically significant. The risk of a biased environmental influence in the different groups had it been true been obviated to some extent by moving the cages

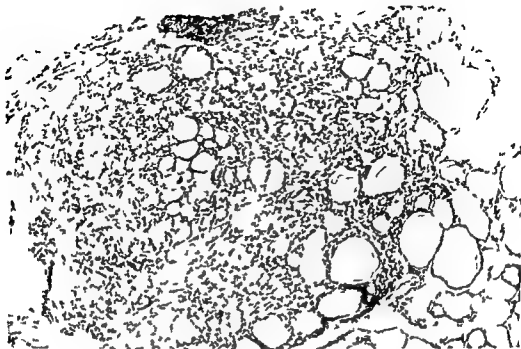


Fig. 6. Infiltrating thyroid carcinoma in a mouse roentgen irradiated at 4 months of age with 1500 R (H & E  $\times 110$ ).

repeatedly to different parts of the room, but in an experiment extending over a long period it is probably not possible completely to eliminate by such simple measures the effect of cage factors and other parameters of relevant significance.

Every value for the tritium activity in the thyroids given in Table 2 was obtained from two samples each containing 5 glands. It is therefore not possible to state any value for a standard error in this case. It might perhaps be said that in both groups of animals the values obtained 1 and 7 days after the injection of  $^{125}\text{I}$  suggested that the tritium activity in mouse thyroids still unaffected by radiation gave a standard error value of approximately 2 per cent of the measurement value. Twelve days treatment with PTU or 3 ATA (3-amino triazole) gives a tritium activity of between 1000 and 1200 cpm in the thyroid of the CBA mouse (WALINDER 1972) and of the C57Bl mouse (WALINDER & WALINDER). This constancy in the measurement values from experiments carried out on different occasions indicates that the incorporation of  $^3\text{H}$ -TdR in the goitrogen-challenged mouse thyroid is a fairly exact mechanism. The difference in the rate at which the activity decreased in the thyroids in the two groups of

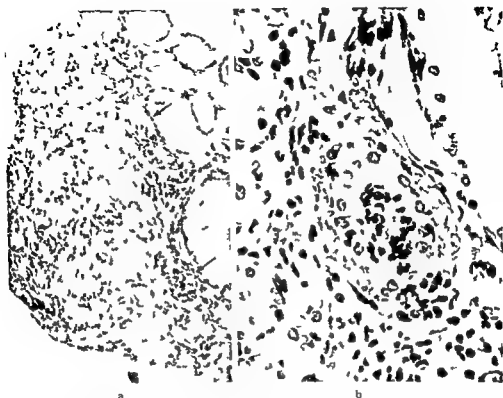


Fig 7 a) Thyroid carcinoma in a mouse roentgen irradiated at 4 months of age with 1500 R. Arrows point to invasion of blood vessels H. & E.  $\times 125$  b) An enlarged view of the lower invasion ( $\times 500$ )

mice in Table 2 would accordingly seem to permit fairly far reaching conclusions to be drawn concerning the effect of radiation on cell survival in the glands.

The morphometric methods used for determining the relative proportions of different thyroid components and the number of epithelial cells in the gland revealed in all instances lower scattering among the individual measurement values than in the case of the thyroid weight. The highest scattering obtained in the measurement values among the mice in one and the same experimental group referred to the percentual proportion of colloid in the thyroid, since the variations in the weight of the glands depend mainly on differences in their colloid content. The smallest thyroid (6.6 mg) among for instance the irradiated mice presented in Table 3 contained 73.1 per cent colloid while the largest (8.4 mg) contained 74.8 per cent colloid. The colloid values in the other mice lay between the two figures which thus means that the percentual difference between the colloid values was much smaller than the corresponding difference be-

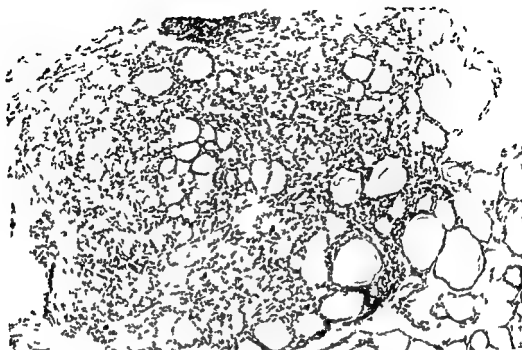


Fig. 6. Infiltrating thyroid carcinoma in a mouse roentgen irradiated at 4 months of age with 1500 R (H & E  $\times 110$ )

repeatedly to different parts of the room but in an experiment extending over a long period it is probably not possible completely to eliminate by such simple measures the effect of cage factors and other parameters of relevant significance.

Every value for the tritium activity in the thyroids given in Table 2 was obtained from two samples each containing 5 glands. It is therefore not possible to state any value for a standard error in this case. It might perhaps be said that in both groups of animals the values obtained 1 and 7 days after the injection of  $^{125}\text{I}$  suggested that the tritium activity in mouse thyroids still unaffected by radiation gave a standard error value of approximately 2 per cent of the measurement value. Twelve days treatment with PTU or 3 ATA (3-amino triazole) gives a tritium activity of between 1000 and 1200 cpm in the thyroid of the CBA mouse (WALINDER 1972) and of the C57Bl mouse (WALINDER & WALINDER). This constancy in the measurement values from experiments carried out on different occasions indicates that the incorporation of  $^3\text{H}$  TdR in the goitrogen challenged mouse thyroid is a fairly exact mechanism. The difference in the rate at which the activity decreased in the thyroids in the two groups of

Table 4

*Tumour frequency in 680 to 750 day old CB-1 mice irradiated at approximately 4 months of age. The carcinoma displayed relatively high differentiation and was mainly of the follicular type*

Group No	No of surviving mice	Source of irradiation	Dose (rad) to thyroid lobes		Adenoma				Carcinoma	Total
			Centre	Edge	Foll	Pap	Trab	Total		
1	100	—	—	—	0	0	0	0	0	0
2	93	1 15 $\mu$ Ci	5 400	2 200	2	1	1	4	0	4
3	88	1 30 $\mu$ Ci	11 000	4 400	2	1	1	4	1	5
4	80	1 45 $\mu$ Ci	16 000	6 400	7	0	—	14	1	15
Total	261	1	5 400— 16 000	2 200— 6 400	11	2	9	22	2	24
5	96	Roentgen 500 R	475	475	2	0	0	2	0	2
6	93	Roentgen 1 000 R	950	950	3	0	1	4	0	4
7	84	Roentgen 1 500 R	1 430	1 430	6	1	3	10	3	13
Total	273	Roentgen	475—1 430		11	1	4	16	3	24

irradiation. A similar explanation has been advanced by GREIG (1965) to explain the hypothyroidism that is often observed in patients a few years after treatment with  $^{131}\text{I}$  for thyrotoxicosis. He considered that this late hypothyroidism is a consequence of a radiation induced deterioration in the reproductive integrity of the thyroidal epithelium. Auto-immunologic factors probably also play a part in encouraging increasing hypothyroidism especially in persons suffering from thyrotoxicosis (JOHANSSON et coll 1968; LINDELL et coll to be published). That irradiation of the thyroid actually does produce a protracted deterioration of the reproductive integrity of the thyroid epithelium has been demonstrated by AL HINDAWI & WILSON (1965) in rats: a radiation induced inhibition of growth stimulated thyroid growth could be observed during the entire period of the experiment in other words for up to one year after the exposure. The hypofunction in mouse thyroids gives rise to increased TSH production which is reflected in hypophyseal enlargement increasing with the size of the radiation dose and in hypophyseal tumours of the TSH cell type. This increased TSH pressure leads to hyperplasia in the c parts of the thyroid which are still functionally active and finally to the formation of thyroidal nodules and neoplasia.

Between the third and fifth month after a  $^{131}\text{I}$  dose of 14 000 rad to the central parts of the thyroid a thyroid weight significantly lower than that found in the controls was obtained. When the observation period is continued until the mice are two years old the difference in weight is significant already after a  $^{131}\text{I}$  dose of 5 400 rad (to the centre of the lobes) and a roentgen dose of 1 000 R (possibly already after 500 R). The difference observed earlier (WALINDER & SJÖDEN) between the effectiveness of short term roentgen irradiation and of irradiation of  $^{131}\text{I}$  in causing inhibition of goitrogen stimulated growth, seems to apply also to inhibition of the slow regeneration of the thyroidal epithelium.

*Radiation induced neoplasia in the thyroid* Many adenomas undoubtedly develop from hyperplastic nodules in the way seen in Fig 3. Probably there are other lines of development as well. In some of the irradiated thyroids there were perfollicular agglomerations of rapidly proliferating cells which could in many cases have been pre stages to tumours. The papillary adenoma illustrated in Fig 3c however probably developed from an earlier cystic nodule through continuous progressing papillary infoldings.

The radiation induced carcinogenicity depends to a high degree on the growth of the thyroid (FLUTH 1957, LINDSAY 1969). The frequency of carcinoma increases when growth is stimulated and a decrease can be brought about through the administration of desiccated thyroid powder (LINDSAY). Malignant tumours may be produced even in animals in which thyroid carcinoma cannot be induced by a  $^{131}\text{I}$  injection alone if the  $^{131}\text{I}$  irradiation is combined with subsequent goitrogenic challenge of the gland (DOVIACH 1963, MORRIS 1965). A similar phenomenon has been observed in human subjects who received roentgen irradiation over the cervical region and later developed hyperthyroidism (DOVIACH et al. 1966). In these patients the occurrence of thyroid tumours seems to have been much higher than in those in whom irradiation of the thyroid is not followed by hyperplasia in the gland tissue or in whom the gland tissue has become atrophied. The frequency of thyroid carcinoma is, as mentioned earlier, also higher in children given roentgen irradiation over the neck region at an early age than in adults who have received the same treatment (HEMPELMANN 1969).

The fact that it has been possible to produce malignant tumours in the thyroid of the CBA mouse after a single injection of  $^{131}\text{I}$  is remarkable. The only other animal in which this has definitely proved to be possible hitherto is the Long Evans rat (LINDSAY). In the case of the CBA mouse it would seem reasonable in the light of what has been said above to assume that the obviously strong TSH pressure on the thyroid gland brought about by the normal age dependent thyroidal development in these mice in association with the radiation damage

produces a combination effect which in other animals can only be achieved through combined irradiation and experimentally provoked thyroïdal growth. The Long Evans rat also displays characteristic features that might possibly be of significance in causing malignant thyroid tumours to develop in this strain after single  $^{131}\text{I}$  injections. The normal occurrence of thyroid tumours is very high in the Long Evans rat (LINDSAY & NICHOLS 1969). These spontaneously occurring tumours are however of a different type (medullary carcinomas) from those that are induced by radiation (mainly follicular and papillary tumour types). Contrary to the findings in other animal species (including other rat strains) no significant reduction in thyroid weight has been obtained in the Long Evans rat one year after exposure, not even after fairly high  $^{131}\text{I}$  doses, although decreased follicular diameters and distinct variability in cellular and nuclear size have been observed. Even a dose as low as  $1 \mu\text{Ci } ^{131}\text{I}$  — a dose that is not capable of producing any signs whatever of histologic changes of the type seen after higher doses — has given rise to thyroid carcinoma in the Long Evans rat (GOLDBERGER *et coll.* 1964).

The total integrated dose of  $^{131}\text{I}$  needed to give rise to a certain tumour incidence is higher than the roentgen dose required to give the same effect. The difference in effectiveness seems to be almost twice as high as in the case of the long term effect on the thyroid weight. Although the perithyroidal tissue may have been damaged severely by the roentgen irradiation, that the blood and lymph supply to the thyroid may have been changed and thereby have contributed in producing the effect, the difference in effectiveness between the two types of irradiation is probably to be explained mainly by dose rate dependence as was the case with the acute effects (WALINDER & SJÖDEN, WALINDER *et coll.* 1972). It is thus not possible, either in the case of effects on the thyroid epithelium or of radiation induced tumours, to draw direct conclusions concerning the  $^{131}\text{I}$  risks from experiments with roentgen irradiation without taking differences in dose rate into consideration. This conclusion is valid not only in comparisons between short term external irradiation and  $^{131}\text{I}$  irradiation but also in comparisons between the effects of radioiodine nuclides with different physical half lives.

The tumour frequency does not, according to the evidence in Table 4, appear to be linearly dose dependent. However, as only three doses were given in each experimental group, it was not possible to obtain statistical confirmation of this non linearity.

## SUMMARY

The thyroid gland of CBA mice was irradiated by injection of  $^{131}\text{I}$  or by local roentgen irradiation, and the effect on the survival and regeneration of the epithelial cells as well



as the frequency of thyroidal neoplasia were investigated. The irradiation gave rise to initial cell death and to inhibition of the epithelial regeneration. This process led to an increased production of TSH (reflected in increased hypophyseal weight and adenomas of the TSH cell type) and after a time in hyperplastic thyroidal nodules which in some cases developed into neoplasms.

## ZUSAMMENFASSUNG

Die Thyreoidea von CBA Mäusen wurde durch Injektion von  $^{131}\text{I}$  oder lokale Röntgenbestrahlung bestrahlt. Es wurden der Effekt auf das Überleben und die Regeneration der Epithelzellen sowie die Frequenz der Neoplasmen der Thyreoidea untersucht. Bestrahlung führte zu einem initialen Zelltod und zur Hinderung der epithelialen Regeneration. Dieser Prozess führte zu einer gesteigerten TSH Produktion, die sich in einem Anstieg des Gewichts der Hypophyse und Adenomen von TSH Zell Typ widerspiegelte sowie nach gewisser Zeit zu hyperplastischen Knoten der Thyreoidea, aus denen sich in einigen Fällen Neoplasmen entwickelten.

## RÉSUMÉ

La grande thyroïde de souris CBA a été irradiée par injection de  $^{131}\text{I}$  ou par irradiation locale par les rayons Roentgen et l'effet de ces irradiations sur la survie et sur la régénération des cellules épithéliales ainsi que la fréquence de néoplasie thyroïdienne ont été étudiées. Cette irradiation entraîne une mort cellulaire initiale et une inhibition de la régénération épithéliale. Ceci a causé une augmentation de la production de TSH (traduite par l'augmentation du poids de l'hypophyse et par des adénomes de type à cellule TSH) et a provoqué au bout d'un certain temps l'apparition de nodules thyroïdiens hyperplasiques qui dans certains cas se sont transformés en néoplasmes.

## REFERENCES

- AL HINDAWI A Y and WILSON G M: The effect of irradiation on the function and survival of rat thyroid cells. *Clin. Sci.* 28 (1965) 555.
- CONARD C A, DOBINS M H and STROW W W: Thyroid neoplasia as late effect of exposure to radioactive iodine in fallout. *J. Amer. med. Ass.* 214 (1970) 316.
- DOBIACH I: Effects including carcinogenesis of  $^{131}\text{I}$  and x rays on the thyroid of experimental animals. A review. *Health Phys.* 9 (1963) 1357.
- , EADIE D G A and HOPE STONE H F: The development of multiple thyroid adenomata in primary hyperthyroidism in previously irradiated thyroid glands. *Brit. J. Surg.* 53 (1966) 681.
- FURTH J: Discussion of problems related to hormonal factors in initiating and maintaining tumor growth. *Cancer Res.* 17 (1957) 454.
- GOLDNER R C, LINDSAY M, NICHOLS C W and CHAIKOFF I L: Induction of neoplasms in thyroid glands of rats by subtotal thyroidectomy and by injection of one microcurie of  $^{131}\text{I}$ . *Cancer Res.* 24 (1964) 32.
- CRITCH W R: Radiation thyroid cells and  $^{131}\text{I}$  therapy. A hypothesis. *J. clin. Endocr.* 25 (1965) 1411.

- HEMPELMANN L H Radiation exposure and thyroid cancer in man *In* Thyroid cancer p 103 Edited by C E Hedinger Springer Verlag Berlin 1969
- JONSSON J EINHORN N FAGRELS A and EINHORN J Organ antibodies after local irradiation *Radiology* 99 (1968) 536
- LINDSAY S Ionizing radiation and experimental thyroid neoplasms A review *In* Thyroid cancer p 161 Edited by C E Hedinger Springer Verlag Berlin 1969
- and NICHOLS C W Medullary thyroid carcinoma and parathyroid hyperplasia in rats *Arch Path* 88 (1969) 402
- — and CHAIKOFF I L Induction of benign and malignant thyroid neoplasms in the rat *Arch Path* 81 (1966) 308
- LUNDELL G and JONSSON J Thyroid antibodies and hypothyroidism in  $^{131}\text{I}$  therapy for hyperthyroidism To be published in *Acta radiol Ther Phys Biol*
- MCLELLAN R O CLARKE W J RAGAN H A et coll Comparative effects of  $^{131}\text{I}$  and x irradiation on sheep thyroids *Health Phys* 9 (1963) 1363
- MORRIS H P Experimental thyroid tumors *In* The Thyroid Brookhaven Symposia in Biology No 7 p 192 Upton New York 1955
- PEARSE A G E Histochemistry Volume 1 Third edition Appendix 10 p 659 J A Churchill Ltd London 1968
- ROMEIS B Mikroskopische Technik Leibniz Verlag Munchen 1948
- SAENGER E L SPLITZER R A SIERLING T D and KERETAKES J G 'Carcinogenic effects of  $^{131}\text{I}$  compared with x irradiation—A review *Health Phys* 9 (1963) 1371
- WALINDER G Determination of the  $^{131}\text{I}$  dose to the mouse thyroid *Acta radiol Ther Phys Biol* 10 (1971) 558
- Quantitative effects of  $^{131}\text{I}$  on different tissue components in foetal and goitrogen challenged mouse thyroids *Acta radiol Ther Phys Biol* 11 (1972) 1
- and SJODEN A M Effect of irradiation on thyroid growth in mouse foetuses and goitrogen challenged adult mice *Acta radiol Ther Phys Biol* 10 (1971) 479
- — Late effects of irradiation on the thyroid gland in mice II Irradiation of mouse foetuses To be published in *Acta radiol Ther Phys Biol* 11 (1972)
- and WALINDER E Effects of  $^{131}\text{I}$  on the cellular survival in mouse thyroids *Acta radiol* (1971) Suppl No 310 p 235
- JONSSON C J and SJODEN A M Dose rate dependence in the goitrogen stimulated mouse thyroid A comparative investigation of the effects of roentgen  $^{131}\text{I}$  and  $^{132}\text{I}$  irradiation *Acta radiol Ther Phys Biol* 11 (1972) 24
- SJODEN A M and JONSSON C J Aging processes in the thyroid gland of the CBA mouse *FOA Reports* Vol 5 No 7 (1971)
- WARREN S and MEISSNER W A Tumors of the thyroid gland *In* Atlas of tumor pathology Section IV Fasc 14 Armed Forces Institute of Pathology Washington D C 1953

# EFFECT OF 180 MeV PROTON OR $^{60}\text{Co}$ GAMMA RADIATION ON THE INCORPORATION OF $^3\text{H}$ -IODO-2'- DI OXYURIDINE INTO INTESTINAL AND SPLEEN DI OXYRIBONUCLEIC ACID OF MICE

by

A. J. JOHANSSON and H. LARSSON

The classical observation (LILLER & HERVEY 1942) that ionizing radiation inhibits the synthesis of deoxyribonucleic acid has been confirmed by many workers as evident for example in the review by MITCHELL (1966). Most investigations have been concerned with the effects of roentgen and gamma radiation while corpuscular radiations have been included to a much less extent. It was considered interesting to compare in the therapeutic dose range the effects of high-energy proton and gamma radiation on the synthesis of DNA.  $^3\text{H}$ -I-5-iodo-2'-deoxyuridine ( $^3\text{H}$ -IUdR) was chosen as a labelled DNA precursor, the incorporation of IUdR into DNA is known to occur in microorganisms and mammalian cells in culture as well as *in vivo* (cf. PRUSOFF 1963).

This work was supported by the Swedish Atomic Research Council. Submitted for publication 13 January 1972.

### Material and Methods

*Animals* Male NMRI mice of about 30 g were kept on ordinary laboratory diet and water ad libitum

*Proton irradiation* was administered with the external proton beam of the Uppsala synchrocyclotron under conditions that have previously been described in greater detail (cf LARSSON 1967). The dose rate was 120 to 350 rad per minute. The mouse in a thin plastic tube was placed longitudinally in the about 10 cm wide beam with the head towards the accelerator. The part of the beam cross-section used was uniform to within  $\pm 10$  per cent.

*Gamma irradiation* was administered with a freely radiating  $^{60}\text{Co}$  source (KJELL & LARSSON 1960) at a dose rate of 56 rad per minute as measured by ferrous sulphate dosimetry (SPRUE & WOODS 1964). The mice were placed vertically in plastic tubes with 2 mm walls and kept rotating at a radius of 40 cm from the gamma source as well as around their own axis.

*Sham irradiation* Control mice were confined in plastic tubes for about the same period as the irradiated mice and then injected with  $^1\text{IUdR}$  in groups of six after 2, 8 or 24 hours. The results from the 2 and 8 hours groups taken together provided a four hour control. Ten non-treated mice were regarded as the control for the 72 hour group.

*Administration of  $^1\text{IUdR}$*  In the irradiation experiment  $10\ \mu\text{Ci } ^1\text{IUdR}$  (Radiochemical Centre, Amersham) in 1 ml isotonic saline with  $0.1\ \mu\text{mol}$  non-radioactive IUdR per ml (synthesized according to PRUSOFF 1959) was injected 2, 4, 8, 24 or 72 hours after the irradiation.

The mice were killed by cervical dislocation 90 minutes after injection. The distribution of the radioactivity of  $^1\text{IUdR}$  was investigated by intraperitoneal injection three times at four hour intervals, the mice being killed 24 hours after the last injection.

*Preparation of tissues* The spleen, the small intestine from about 10 cm below the pyloric sphincter to the ileocecal sphincter and the large intestine were quickly removed, the contents of the latter being flushed out with ice cold isotonic saline. A jejunal specimen was fixed for histology in ethanol mixed with acetic acid (3:1), the remaining parts of the intestine and the spleen being frozen on solid  $\text{CO}_2$  and stored at  $-20^\circ\text{C}$  until analysed.

*Extraction of DNA* After thawing the intestine was opened, the mucosa scraped off with a glass slide and DNA extracted by a modified Schneider procedure. The tissue was homogenized in 10 ml isotonic saline in a Potter Elvehjem glass-glass-homogenizer placed in an ice bath and mixed with an equal

Table 1

*Distribution of activity of  $^{125}\text{I}$  in fractions from tissues of mice following three injections of  $^{125}\text{I}$ UdR at four hour intervals with a total dose of 10  $\mu\text{Ci}$  per mouse. The mice were killed 24 hours after the third injection*

Fraction	Mucosa from small intestine			Mucosa from large intestine		
	c p m	Per cent	SE	c p m	Per cent	St
Acid soluble	930	0.9	0.2	390	2.6	1.3
Nucleic acid	103 200	95.5	0.7	14 100	93.3	2.6
Protein	3 930	3.6	0.7	620	4.1	1.3

volume 0.4 N  $\text{CHIO}_4$  (PCA), it was then stored in the cold for at least 30 minutes, centrifuged (10 min, 1 200 g) also in the cold, and washed twice with 5 ml 0.2 N PCA. The three supernatants were pooled together to give the acid soluble fraction. Nucleic acids were extracted by 10 ml 0.5 N PCA at 90° C for 60 minutes, centrifuged and washed twice with 5 ml 0.5 N PCA. The supernatants were pooled together to give the nucleic acid fraction. The residue, the protein fraction, was dissolved in 10 ml 2% NaOH at 90° C for 10 minutes. The extraction procedure was investigated by 2 ml aliquots of homogenized mucosa from the small intestine, previously treated with cold PCA and uniformly suspended in 0.5 N PCA in a Potter Elvehjem homogenizer, being left in closed test tubes at 90° C for various periods.

**Nucleic acid estimation.** DNA was estimated by the diphenylamine method modified by BURTON (1956) with calf thymus DNA (Sigma Chem. Co.) as a standard. The absorbency was measured in a Zeiss PMQ II spectrophotometer at 600 nm.

**Radiometry.** The activity of  $^{125}\text{I}$  in 1 ml samples was measured in a well type NaI(Tl) crystal with 0.2  $\mu\text{Ci}$   $^{125}\text{I}$ UdR prepared on the day of injection as a standard. The counting rate of the sample divided by that of the standard and by the optical absorbency at 600 nm was used as a measure of the specific activity of the DNA samples.

**Autoradiographic technique.** The fixed portion of the jejunum was embedded in Histowax (Matheson Coleman and Bell m.p. 56 to 58° C) and sectioned transversely at 5  $\mu\text{m}$ . The slides were immersed in cold trichloroacetic acid for 20 min, stained by the Feulgen technique after hydrolysis 2 min in 1 N HCl at 60° C. This short period of hydrolysis was chosen in order to reduce the loss of radioactivity from DNA (LAW & MAURER 1965). Autoradiographs were pro-

Table 2

*Distribution of activity of  $^1\text{H}$  in fractions from tissues of mice killed 90 minutes after an injection of  $10\ \mu\text{Ci } ^{125}\text{IUdR}$*

Fraction	Mucosa from small intestine			Mucosa from large intestine			Spleen		
	c p m	Per cent	SE	c p m	Per cent	SE	c p m	Per cent	SE
Acid soluble	38 000	26.4	1.9	18 400	56.2	2.6	22 100	31.3	3.2
Nucleic acid	100 800	10.1	1.8	13 600	41.7	2.6	44 800	63.6	3.0
Protein	5 080	3.5	0.2	680	2.1	0.4	3 580	5.1	0.2

pared by the dipping technique (MESSIER & LEBLOND 1957) using Ilford K5 emulsion in water (1:1) the emulsion was dried at ordinary room temperature and exposed for a period equivalent to a 14 day exposure starting on the day of injection. The slides were developed in Kodak D 19B for 2 min, dipped in 1% acetic acid for 10 s and fixed in Kodafix for 5 min.

**Grain counting.** Analysis was restricted to crypts available for examination from base to top. Beginning with the Paneth cells at the base of the crypt, the cells were numbered consecutively up to the level of the cryptovillal junction and the grains over each nucleus counted. For each mouse 20 crypts were scored with a Leitz Ortholux microscope equipped with a  $90\times$  objective for oil immersion and a  $12.5\times$  ocular. The grain counts were corrected for background i.e. by the grain counts in the same specimen over an equal number of villous nuclei.

Three zones in the intestinal crypt of the mouse starting from the cryptovillal junction have been defined (THRASHER & GREULICH 1965). Zone 1 with minimum proliferation (7 cells), zone 2 with maximum proliferation (7 cells) and zone 3 containing the Paneth cells at the base of the crypt (4 cells). The cells in the present work were scored from the base of the crypt i.e. cells numbered 1 to 4 belonged to zone 3, cells numbered 5 to 11 to zone 2 and cells numbered 12 to 18 to zone 1.

## Results

**Distribution of radioactivity after injection of  $^1\text{H}$  IUdR.** The fate of  $^1\text{H}$  after injection of  $^1\text{H}$  IUdR is illustrated in the series of experiments presented in Tables 1 and 2. Approximately 95 per cent of the total radioactivity of the mucosa of the small and large intestine was present in the nucleic acid fraction 24 hours

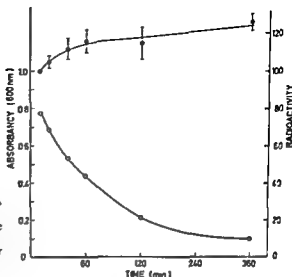


Fig. 1. Extraction of DNA by 0.5 N PCA at 90°C from mucosa of the small intestine of mice as determined by the diphenylamine method and radioactivity. Mean of six experiments. Standard error of mean for the  $^{125}\text{I}$  activity determination. ○ Absorbancy, ● radioactivity.

after injection. Ninety minutes after injection, about 70 per cent of the total radioactivity of the small intestine was present in the nucleic acid fraction; the corresponding values for the large intestine and the spleen being 42 and 64 per cent, respectively. Only 2 to 5 per cent of the total radioactivity were evident in the protein fraction.

*Extraction of DNA from the intestinal mucosa and the destruction of deoxyribose.* The procedure of extraction of DNA was investigated in an experiment performed with homogenated mucosa from the small intestine previously treated with cold PCA. The results are summarized in Fig. 1. The radioactivity is expressed as a percentage of the radioactivity in the soluble fraction at 10 minutes extraction, the time at which maximum absorption with diphenylamine appeared. The exponentially occurring destruction of deoxyribose (cf. LOWTRUP, 1962) would be expected to reduce the absorbancy at an increased extraction time. DNA hydrolysis was, however, still contributing to increased radioactivity in the soluble fraction.

*Biochemical investigation of incorporation of  $^3\text{H}$  IUdR into DNA after irradiation.* A depression of  $^3\text{H}$  IUdR incorporation into the DNA occurred after irradiation. This followed a similar pattern in all the organs examined (Figs. 2, 3, 4), i.e. a fast decrease in incorporation soon after irradiation followed by some hours of heavily depressed DNA synthesis and a recovery period with a more or less marked overshoot. The DNA content of the spleen was much reduced (Fig. 5) to the extent that the depression of DNA synthesis calculated was affected. The

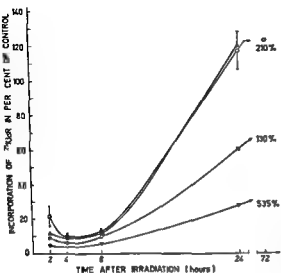


Fig 2 Incorporation of  $^1$  IUdR into DNA in mucosa of the small intestine of mice after irradiation. Each point represents the mean of six mice (2, 4, 8, 24 h) or 3 mice (72 h). Standard error of mean for 200 rad: ○ 200, □ 400, ▽ 800 rad (protons) and ▲ 400 rad ( $^{60}\text{Co}$  gamma).

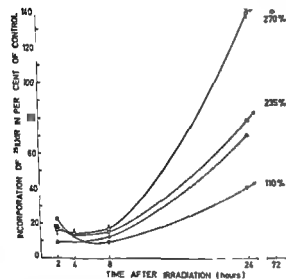


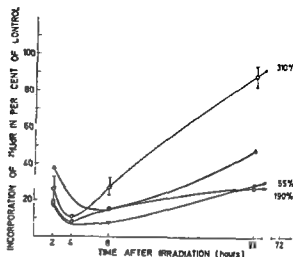
Fig 3 Incorporation of  $^1$  IUdR into DNA in the mucosa of the large intestine of mice (See also legend to fig 2): ○ 200 rad, □ 400 rad, ▽ 800 rad (protons) and ▲ 400 rad ( $^{60}\text{Co}$  gamma).

corresponding decrease in the DNA content in the small intestine was not so obvious (cf MOLE & TEMPLE 1959 NYGAARD & POTTER 1960)

*Autoradiographic investigation of incorporation of  $^1$  IUdR into DNA of small intestine* The grain count in the control group was 445 for 160 cells of the zone of Paneth cells 1 868 for 280 cells of the zone of maximum cellular



Fig 4 Incorporation of  $^3\text{H}$  IUDR into DNA of the spleen from mice (See also legend to fig 2)  $\circ$  200  $\square$  400  $\text{---}$  800 rad (protons) and  $\blacktriangle$  400 rad ( $^{60}\text{Co}$  gamma)



proliferation and 818 for 280 cells of the zone of minimum cellular proliferation (Table 3). Twenty four hours after irradiation at 800 rad (p) or 400 rad (r) a significant difference between the results obtained by biochemical and autoradiographic methods was evident. A corresponding difference was not present 24 hours after 200 rad (p) or 400 rad (p). The most marked difference was recorded at 72 hours after 800 rad (p) and a lengthening of the crypt particularly of the zone of maximum cellular proliferation, in this case containing more than 7 cells appeared to have occurred.

### Discussion

Apparently  $^3\text{H}$  IUDR is a specific DNA precursor with little labelling in the acid soluble and protein fractions as also noted by other authors (FOX & PRUSOFF 1963; HUGHES *et al.* 1964). HUGHES *et al.* stated chemical artifact due to the incorporation into substances other than DNA have not been found and iodide is apparently the only by product of concern. Injected IUDR is catabolized to uracil and iodide with a half life in the blood of 3 min (HUGHES *et al.*); most of the iodide appears in the urine (PRUSOFF *et al.* 1960).  $^3\text{H}$  thymidine is favoured for incorporation into the DNA of the small intestine of mice by a factor of 1.5 (FOX & PRUSOFF 1963) to 3.6 (DETHLEFFSEN 1970).

Although the DNA of the small intestine seems to be easily extracted as compared with the DNA of the liver (LOWTRUP 1962) extraction for 60 min proved necessary. There was still some indication that insoluble DNA containing  $^3\text{H}$  IUDR was contaminating the protein fraction since a decrease in  $^3\text{H}$  activity after

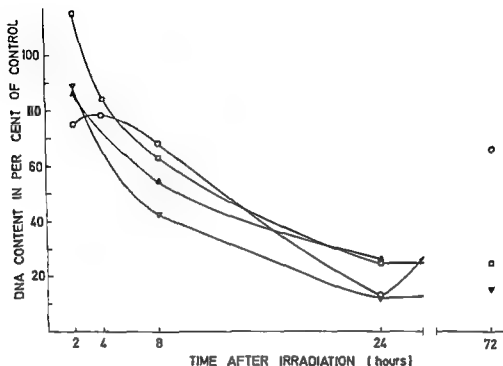


Fig 5 The DNA content of the spleen of mice after irradiation. Each point represents the mean of six mice (2 4 8 24 h) or 3 mice (72 h) ○ 200 □ 400 △ 800 rad (protons) and ▼ 400 rad ( $^{60}\text{Co}$  gamma)

irradiation, not only in the nucleic acid fraction but also in the protein fraction was evident. The diphenylamine reagent reacts mainly with the purine moiety (DISCHE 1960) which is easier to extract than the pyrimidines (LORING 1960).

Irradiation results in a heavy reduction of  $^1\text{I}$ UdR incorporation into DNA which is more marked than when  $^3\text{H}$  thymidine is used. The depression of DNA synthesis observed to be close to its maximum as early as 2 hours after irradiation may be observed soon after irradiation. The incorporation of  $^3\text{H}$  thymidine determined by the grain count per labelled cell in the ileum of the mice drops to one half of its normal values within about 30 min after 800 rad of 240 kV roentgen radiation (SHERMAN & QUASTLER 1960). The incorporation of thymidine  $2\text{-C}^{14}$  into DNA in the spleen of the rat is depressed to 45 per cent at 10 to 20 min after irradiation at 400 rep (370 rad)  $^{60}\text{Co}$  gamma radiation (NIELSEN & POTTER 1962). A still faster effect (3 min) has been reported (ORD &

Table 3

*Incorporation of  $^{125}\text{IUdR}$  into intestinal DNA following 180 MeV proton (p) or  $^{60}\text{Co}$  gamma ( $\gamma$ ) irradiation. Results expressed as percentage of control. The grain count in the control groups 10 mice were. For the zone of minimum cellular proliferation 818 (SE=131) for the zone of maximum cellular proliferation 1868 (SE=209) for the zone of Paneth cells 445 (SE=78) and for the 3 most labelled cells in the crypt 1541 (SE=124)*

No of mice	Dose (rad)	Hours after irradiation	Biochemical method		Autoradiographic method							
			Per cent	SE	Zone of min cell prol		Zone of max cell prol		Zone of Paneth cells		3 most labelled nuclei	
					Per cent	SE	Per cent	SE	Per cent	SE	Per cent	SE
11	200(p)	24	118	11	107	28	123	17	158	28	144	17
6	400(p)	24	61	12	36	8	54	6	76	8	67	1
11	800(p)	24	28	3	15	1	38	3	63	8	67	1
6	400( $\gamma$ )	24	120	13	65	15	92	11	107	11	100	10
3	200(p)	72	211		160		153		245		141	
3	400(p)	72	131		171		139		207		136	
3	800(p)	72	535		323		189		331		187	

STOCKFEN 1957) This initial phase of the change observed must be due to radiation effects upon cells in S phase (SHERMAN & QUASTLER) The mitotic figures disappear at once after about 300 rad and return to normal frequency after a time lag of up to 40 hours depending on the experimental conditions (KNOWLTON & HEMELMANN 1949 LEISHER & BAUMAN 1968 DEVIK 1968) The mitotic count fails to give information on the rate of cell production unless the mitotic duration is known DEVIK (1971) estimated the mitotic rate in the small intestine of unirradiated mice and in other mice at 1, 2 and 3 days after 1 000 R of 250 kV roentgen radiation to be 2.1, 0.8, 2.6 and 7.0 mitoses per hour per 100 cells respectively and the duration of mitoses to be 1.25, 3.75, 0.67 and 0.6 hours respectively The  $G_1$  period is about 3 hours (range 1 to 9 hours) in the small intestine of mice (CAMERON 1971) so the effect of a mitotic block on DNA synthesis would appear from 3 hours presuming no change in the length of the  $G_1$  period occurred It is possible that the prolonged effect on the synthesis of DNA is a consequence of the mitotic block but damage of the synthesis mechanism seems also to interfere since the grain count per labelled cell is extremely low The recovery period may reflect two events a repair of the damaged DNA synthesis system and a recovery from the mitotic block The sedimentation pattern of DNA from *E. coli* B/r is changed after roentgen irradiation which prob-

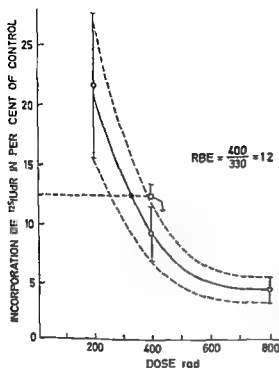


Fig 6 Incorporation of  $^3\text{H}$  IUdR into intestinal DNA of mice 2 hours after irradiation (cf fig 5). Third degree polynomials were fitted to the points indicating results of proton irradiation (open rings) and to those corresponding to the standard error. The RBE was estimated at the level of 400 rad  $^{60}\text{Co}$  gamma irradiation (open square).

ably reflects a repair process in which broken pieces of DNA are rejoined (McGRATH & WILLIAMS 1966).

Radiation may reduce the DNA content in a proliferating organ by killing the cells and reducing the DNA synthesis. These effects were much evident in the spleen (Fig 5). A decrease of the DNA content of up to 50 per cent within 2 days after 400 R of 245 kV roentgen radiation also occurs in the small intestine of the rat (NYGAARD & POTTER 1960). MOLE & TEMPLE (1959) using the DNA content in the intestine as a quantitative index of damage and recovery after irradiation reported a loss of about 20 per cent of total DNA 24 hours after 300 R roentgen radiation. DEVIK (1971) observed a decrease in the number of cells in the section of one crypt at a maximum of about 33 per cent 1 day after doses up to 700 R 250 kV roentgen radiation and an increase of about 35 per cent at 3 days. An autoradiographic method in which grain counts over individual cells are recorded cannot be disturbed by the decrease in the DNA content and change in cell number. The difference in the results of the autoradiographic and biochemic measurements was less than expected considering the change in the DNA content and cell number known to occur (NYGAARD & POTTER 1960; MOLE & TEMPLE 1959; DEVIK 1971). The cells that die after irradiation in the

small intestine are mostly crypt cells (WARREN & WHIPPLE 1922, MONTAGNA & WILSON 1955) and the decrease in DNA content will be correlated to the number of cells that can synthesize DNA. Other changes in the crypt cells, such as nuclear enlargement (McGRATH & CONGDON 1959), may also interfere with the autoradiographic results.

The calculation of the relative biologic effectiveness (RBE) defined as the ratio of the dose of  $^{60}\text{Co}$  gamma radiation to produce a given effect and the dose of proton radiation to lead to the same effect was restricted to the small intestine and the group killed 24 hours after irradiation. Cell death and other secondary effects seemed to be of little importance at that time. The RBE and its standard error were calculated from the data in Fig. 6. It was assumed that the RBE was constant in the dose interval investigated (300 to 400 rad). The calculated RBE for protons under the experimental conditions described is  $1.2 \pm 0.3$ . The mean linear energy transfer ( $\text{LET}_d$ ) for 180 MeV protons ( $0.5 \text{ keV}/\mu$ ) and  $^{60}\text{Co}$  gamma radiation ( $0.3 \text{ keV}/\mu$ ) is similar so that the pattern of the primary radiochemical events should be about the same. The fact that the dose rate for  $^{60}\text{Co}$  gamma radiation is 56 rad per minute and for proton radiation 100 to 300 rad per minute ought to be of minor significance. HORNSEY (1970), for example, reported a dose rate dependence in the survival of crypt cells as well as in the  $\text{LD}_{50}$  for mice irradiated with electrons at 5 krad/min or 500 rad/min. The  $\text{LD}_{50}$  was 1330 rad for mice irradiated at 6 krad/min and 1458 rad when the dose rate was 500 rad/min. The corresponding  $D_0$  values for the crypt cells were 125 and 160 rad respectively. The high dose rate was more effective in producing cell death and killing the mice.

The pulsation of the proton beam (JUNE et al.) should be unimportant as at the actual dose rates interaction between reactive species produced along different proton tracks is unlikely to occur.

## SUMMARY

The incorporation of  $^3\text{H}$ -Iododeoxyuridine into the intestinal and splenic DNA of mice was investigated by biochemical and autoradiographic methods after  $^{60}\text{Co}$  gamma and 180 MeV proton irradiation.  $^3\text{H}$ -IUDR proved to be a specific precursor for DNA. A marked decrease occurred similar to the results obtained by biochemical and autoradiographic techniques.

## ZUSAMMENFASSUNG

Der Einbau von  $^3\text{H}$ -Iododeoxyuridin in die DNS des Darms und der Milz der Maus wurde nach  $^{60}\text{Co}$  Gamma- und 180 MeV Protonen Strahlung mit biochemischen und autoradiographischen Methoden untersucht.  $^3\text{H}$ -IUDR erwies sich als spezifische Vorstufe der DNS. Ein starker in ihren Ergebnissen für die biochemische und autoradiographische Technik ähnlicher Abfall im  $^3\text{H}$ -IUDR Einbau trat nach Bestrahlung auf.

## RÉSUMÉ

L'incorporation de  $^3$  Iododeoxyuridine dans l'ADN intestinal et plasmique de souris a été étudiée par des méthodes biochimiques et autoradiographiques après irradiation par le rayonnement gamma du  $^{60}\text{Co}$  et par irradiation protonique de 180 MeV. La  $^3$  IUDR s'est révélée être un précurseur spécifique de l'ADN. L'irradiation provoque une nette diminution semblable aux résultats obtenus par des méthodes biochimiques et autoradiographiques.

## REFERENCES

- BURTON K. A study on the conditions and mechanism of the diphenylamine reaction for the colorimetric estimation of deoxyribonucleic acid. *Biochem J* 62 (1956) 315.
- CAMEROV I. L. Cell proliferation and renewal in the mammalian body. In: *Cellular and molecular renewal in the mammalian body* p. 45. Edited by I. L. Cameron and J. D. Thrasher. Academic Press, New York, London, 1971.
- DETHLEFSEN L. A. Reutilization of  $^{125}\text{I}$  5-Iodo-2'-deoxyuridine as compared to  $^3\text{H}$  thymidine in mouse duodenum and mammary tumor. *J. nat. Cancer Inst.* 44 (1970) 827.
- DEVIK F. Quantitative cellular aspects of the epithelium of the small intestine of mice following total body irradiation: cell death, mitosis and chromosome aberrations. In: *Effects of radiation on cellular proliferations and differentiation* p. 531. IAEA, Vienna, 1968.
- Intestinal cell kinetics in irradiated mice. A quantitative investigation of the acute reaction to whole body roentgen irradiation. *Acta radiol. Ther. Phys. Biol.* 10 (1971) 129.
- DISCHE Z. Color reactions of nucleic acid components. In: *The nucleic acids*, Vol. 1. Edited by E. Chargaff and J. N. Davidson. Academic Press, New York, 1960.
- EULER H. v. und HEVESY G. Wirkung der Röntgenstrahlen auf den Umsatz der Nukleinsäure im Jensen Sarkom. *Kgl. Danske Videnskab. Selskab. Biol. Medd.* 17 (1942) 3.
- FOX B. W. and PRUSSOFF W. H. The comparative uptake of  $^3\text{H}$  labelled 5-iodo-2'-deoxyuridine and thymidine  $^3\text{H}$  into tissues of mice bearing hepatoma. *Cancer Res.* 25 (1965) 234.
- HORNSEY S. Differences in survival of jejunal crypt cells after radiation delivered at different dose rates. *Brit. J. Radiol.* 43 (1970) 802.
- HUGHES W. L., CONNORFORD S. L., GITLIN D., KRUEGER R. C., SCHULTZE B., SHAH V. and REILLY P. Deoxyribonucleic acid metabolism in vivo. I. Cell proliferation and death as measured by incorporation and elimination of iodo-deoxyuridine. *Fed. Proc.* 23 (1964) 640.
- JUNG B., RIKNER H. G. and SJOOREN O. On the production and monitoring of broad homogeneous radiation fields of high-energy protons. With special reference to the spatial and temporal dose distribution. To be published in *Acta radiol. Ther. Phys. Biol.*
- KIVELL P. O. and LARSSON B. On the arrangement of freely radiating gamma ray sources. *Riso Report* 16 (1960) 9.
- KNOWLTON JR. V. P. and HEMPELMANN L. H. The effect of x rays on the mitotic activity of the adrenal gland, jejunum, lymph node and epidermis of the mouse. *J. cell comp. Physiol.* 33 (1949) 73.
- LANG W. and MAURER W. Zur Verwendbarkeit von Feulgengefärbten Schnitten für quantitative Autoradiographie mit markiertem Thymin. *Exp. Cell Res.* 39 (1965) 1.
- LARSSON B. Radiological properties of beams of high-energy protons. *Radiat. Res.* (1967) Suppl. No. 1, p. 304.

- LESHIER ■ and BAUMAN J Recovery of reproductive activity and maintenance of structural integrity in the intestinal epithelium of the mouse after single-dose whole body  $^{60}\text{Co}$ -gamma ray exposures *In* Effects of radiation on cellular proliferation and differentiation p 507 IAEA Vienna 1968
- LORING H S Hydrolysis of nucleic acids and procedures for the direct estimation of purine and pyrimidine fractions by absorption spectrophotometry *In* The nucleic acids Vol I Edited by E Chargaff and J N Davidson Academic Press New York 1960
- LOWTRUP S Chemical determination of DNA in animal tissues *Acta biochim pol* ■ (1962) 411
- MCGRATH R A and CONGDON C C X-ray induced abnormal differentiation of epithelium of the small intestine of the mouse *Int J radiat Biol* 1 (1959) 80
- and WILLIAMS R W Reconstruction *in vivo* of irradiated *Escherichia coli* deoxyribonucleic acid: the rejoining of broken pieces *Nature* 212 (1966) 534
- MESNIER H and LEBLOND C P Preparation of coated radioautographs by dipping sections in fluid emulsion *Proc Soc exp Biol (N Y)* 96 (1957) 7
- MITCHELL J Some aspects of the effects of radiations on the metabolism of tissues and tumours *In* Encyclopedia of medical radiology Vol II Part I p 355 Edited by A Zuppinger Springer Verlag Berlin Heidelberg 1966
- MOLE R H and TEMPLE D M The DNA content of the small intestine as a quantitative measure of damage and recovery after whole body irradiation *Int J radiat Biol* 1 (1959) 28
- MONTAGNA W and WILSON J W A cytologic study of the intestinal epithelium of the mouse after total body x irradiation *J nat Cancer Inst* 15 (1955) 1703
- NYGAARD O F and POTTER R L Effect of x irradiation on DNA metabolism in various tissues of the rat II Recovery after sublethal doses of irradiation *Radiat Res* 12 (1960) 120
- — Effect of x radiation on DNA metabolism in various tissues of the rat IV Early effect *Radiat Res* 16 (1962) 243
- ORD M G and STOCKER L A The effect of x radiation on rat thymus nucleic acids at short intervals after exposure *in vivo* *In* Advances in radiobiology p 65 Edited by C C DeHevesy A G Forsberg and J D Abbatt Oliver and Boyd Edinburgh 1957
- IRUSOFF W H Synthesis and biological activities of iododeoxyuridine: an analog of thymidine *Biochim biophys Acta (Amst)* 32 (1959) 295
- A review of some aspects of 5 Iododeoxyuridine and azauridine *Cancer Res* 23 (1963) 1246
- JAFFE J J and GLUTHER H Studies in the mouse of the pharmacology of 5 iododeoxyuridine: an analogue of thymidine *Biochem Pharmacol* 3 (1960) 110
- SHIRMAN I G and QUASTLER H DNA synthesis in irradiated intestinal epithelium *Exp Cell Res* 19 (1960) 343
- SPINCKS J W T and WOODS R J An introduction to radiation chemistry Chapter 4 John Wiley & Sons New York 1964
- THIRASHIR J D and GRELICH R C The duodenal progenitor population II Age related changes in size and distribution *J exp Zool* 159 (1965) 385
- WARRIN S L and WHIPPLE G H Roentgen ray intoxication II A study of the sequence of clinical anatomical and histological changes following a unit dose of x rays *J exp Med* 30 (1922) 203

## RETENTION OF $^{125}\text{I}$ GIVEN AS $^{125}\text{I}$ -5 IODO-2- DEOXYURIDINE TO MICE AFTER 180 MeV PROTON OR $^{60}\text{Co}$ GAMMA IRRADIATION

by

H. J. JOHANSON

Iodine labelled thymidine analogues for example  $^{125}\text{I}$  5 iodo-2 deoxyuridine ( $^{125}\text{IUdR}$ ) are specific precursors for DNA and their only labelled catabolic products of significance appear as  $^{125}\text{I}$  (HUGHES et coll 1964). To prevent accumulation of  $^{125}\text{I}$  in the thyroid after the injection of  $^{125}\text{IUdR}$  into mice NaI may be introduced into the drinking water from the day before injection. Most of the  $^{125}\text{I}$  is then excreted in the urine (PRUSOFF et coll 1960). This technique has been used in combination with whole body counting to investigate the effect of irradiation on  $^{125}\text{I}$  retention in whole mice and in cotton rats after the administration of  $^{125}\text{IUdR}$  (GITLIN et coll 1962, O'FARRELL & DUNAWAY 1969). GITLIN et coll reported a 50 to 60 per cent depressed retention of  $^{125}\text{I}$  given as  $^{125}\text{IUdR}$  even after 25 or 50 R 250 kV roentgen irradiation. The  $^{125}\text{I}$  retention after  $^{125}\text{IUdR}$  injection probably reflected quantitatively the  $^{125}\text{IUdR}$  incorporation into DNA. JOHANSON & LARSSON (1972) stated that the  $^{125}\text{IUdR}$  incorporation into DNA of the intestine and spleen of mice was much depressed after proton and

This work was supported by the Swedish Atomic Research Council and the Swedish Cancer Society. Submitted for publication 13 January 1972.



gamma irradiation. The aim of the present investigation was to compare by whole body measurements the effects of 180 MeV proton and  $^{60}\text{Co}$  gamma radiation on the incorporation and retention of  $^3\text{H}$  I given as  $^3\text{H}$  IUdR. It was also hoped to elucidate the possible use of such labelled DNA precursors that can be used for whole body scintigraphic investigations of cellular kinetics.

### Materials and Methods

*Animals* Female NMRI mice weighing 20 to 25 g were given water and food ad libitum. 0.1% NaI was added to the drinking water from 24 hours before injection of  $^3\text{H}$  IUdR.

*Irradiation* The mice were irradiated in plastic tubes. Gamma irradiation was administered 40 cm from a freely radiating  $^{60}\text{Co}$  gamma source under conditions previously described (JOHANSON & LARSSON). The dose rate was 46 rad per minute as measured by Fricke dosimetry (SPINKS & WOODS 1964). Proton irradiation was given with the 180 MeV proton beam from the Uppsala synchrocyclotron as previously described (JOHANSON & LARSSON). The control mice were sham irradiated under conditions similar to the gamma irradiation.

*Administration of  $^{3\text{H}}$  IUdR* Two hours after irradiation the mice were given  $0.08\text{ }\mu\text{Ci } ^3\text{H}$  IUdR (Radiochemical Centre, Amersham) per gram body weight intraperitoneally in isotonic saline at a specific activity of  $100\text{ }\mu\text{Ci}/\mu\text{mol}$  and then placed three in a cage (floor area  $450\text{ cm}^2$ ). The litter was changed near the middle of the period between injection and killing to decrease external contamination.

*Radiometry and organ preparation* The  $^3\text{H}$  I activity of the whole mice was determined twenty hours after injection of  $^3\text{H}$  IUdR with a 3' (7.6 cm) NaI(Tl) crystal with an 1.5' (3.8 cm) well and  $0.1\text{ }\mu\text{Ci } ^3\text{H}$  in mice geometry as a standard. The mice were killed by cervical dislocation within an hour of whole body counting and the small intestine and spleen prepared for  $^{125}\text{I}$  activity determination. The retention of  $^{125}\text{I}$  was calculated as a percentage of the dose injected and further expressed as a percentage of that of the control.

### Results

The effect of irradiation of the  $^3\text{H}$  I retention is presented in Figs 1, 2 and 3. At low doses (40 rad for spleen also 80 rad) the  $^{60}\text{Co}$  gamma radiation seems to affect the  $^3\text{H}$  I retention with higher efficiency than the 180 MeV protons; this effect was observed in the organs examined (Figs 2-3) as well as in the whole

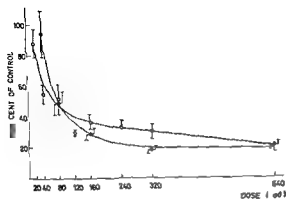


Fig 1 Retained  $^{125}\text{I}$  activity in irradiated mice 20 hours after injection of  $^{125}\text{I}$  IUdR or  $^{60}\text{Co}$  gamma. ● Proton. Each point represents the average of 6 mice  $\pm$  SE.

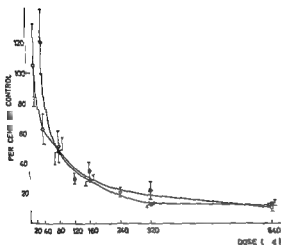


Fig 2 Retained  $^{125}\text{I}$  activity in the small intestine of irradiated mice 20 hours after injection of  $^{125}\text{I}$  IUdR or  $^{60}\text{Co}$  gamma. ● Proton. Each point represents the average of 6 mice  $\pm$  SE.

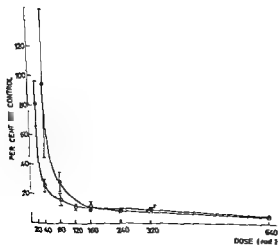


Fig 3 Retained  $^{125}\text{I}$  activity in the spleen of irradiated mice 20 hours after injection of  $^{125}\text{I}$  IUdR or  $^{60}\text{Co}$  gamma. ● Proton. Each point represents the average of 6 mice  $\pm$  SE.

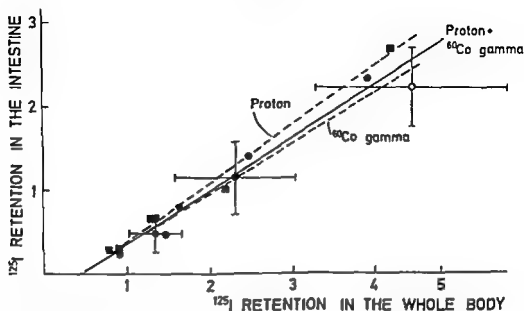


Fig. 4. Regression of  $^{125}\text{I}$  activity retained in the small intestine as a function of the  $^{125}\text{I}$  activity remaining in the whole body 70 hours after injection of  $^3\text{I}$ UdR. ○ Control, ■ Proton, ●  $^{60}\text{Co}$  gamma.

body (Fig. 1). In the dose interval of 80 to 640 rad  $^{60}\text{Co}$  gamma and proton  $\gamma$  radiation had similar effects on the  $^{125}\text{I}$  retention in the small intestine, the small differences being within the experimental error. The same effects occurred in the spleen at doses between 160 and 640 rad. At 160 and 320 rad, however, the protons appeared to be more effective in affecting the  $^{125}\text{I}$  retention in the whole body. The most marked decrease of  $^{125}\text{I}$  retention occurred in the spleen after irradiation with 160 rad or more.

The  $^{125}\text{I}$  retention in the whole body is compared to that in the small intestine and the spleen in Figs. 4 and 5. The  $^{125}\text{I}$  retention in the small intestine and spleen should be a better measure of the  $^3\text{I}$ UdR incorporation into DNA than the  $^{125}\text{I}$  retention in the whole body. Extrapolation in Fig. 4 gives about 0.4 per cent of the injected dose retained in the whole body when no  $^{125}\text{I}$  remained in the small intestine.

### Discussion

The  $^{125}\text{I}$  retention proved to be 4.5 per cent in the unirradiated mice at 20 hours after the  $^3\text{I}$ UdR injection. About 0.4 per cent of this amount was probably due to contamination of the skin as indicated in Fig. 4 as well as in the work

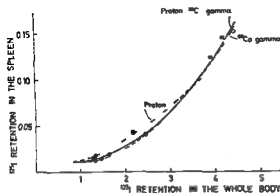


Fig 5 Regression of  $^1\text{I}$  activity retained in the spleen as a function of the  $^1\text{I}$  activity remaining in the whole body 20 hours after injection of  $^1\text{I}$  UdR ○ Control. ■ Proton ●  $^{60}\text{Co}$  gamma

of HUGHES et coll (1964) The remaining 4.1 per cent were probably mostly incorporated into DNA of proliferating tissues. In 6 week-old mice, 3 per cent of the injected  $^{131}\text{I}$  given as  $^{131}\text{I}$ UdR were retained at 20 hours after injection (HUGHES et coll). Since these authors used younger mice than those of the present work a higher  $^{131}\text{I}$  retention would be expected. The corresponding retention in cotton rats was 3 per cent at 2 days after injection (O'FARRELL & DUVAL WAT).

Incorporation of  $^1\text{I}$  UdR into DNA in proliferating tissues after irradiation has previously been investigated by the extraction and determination of the specific activity (JOHANSON & LARSSON). This method indicated that  $^1\text{I}$ UdR incorporation into DNA of the small intestine was depressed to 22 per cent of the control 2 hours after proton irradiation at 200 rad and to 9 per cent after 400 rad. No significant differences were evident in the results obtained by autoradiographic and biochemical methods at the above doses at 24 hours after irradiation. Interpolation in Fig 2 gives a  $^1\text{I}$  retention in the small intestine of 23 per cent of the control after proton irradiation at 200 rad and about 13 per cent at 400 rad. It would appear that similar results may be obtained by evaluating the effects on the small intestine of irradiation with these three independent methods. A similar comparison of the results of the spleen experiments reveals more diverse results probably due to the fact that a marked decrease in the DNA content of the spleen occurs after irradiation (cf JOHANSON & LARSSON). This decrease reflects a similar decrease in the cell content.

The two types of radiation seem similarly to affect the  $^1\text{I}$  retention in the dose range 80 to 640 rad (160 to 640 rad for the spleen). The RBE for 180 MeV protons of  $1.2 \pm 0.3$  from previous work on the incorporation of  $^1\text{I}$  UdR into intestinal DNA at two hours after irradiation (JOHANSON & LARSSON) appears to be in conformity with the present investigation.

The large differences at doses of 40 rad (and 80 rad for the spleen) are surprising. Figs 1, 2 and 3 indicate however, large standard deviations so that the individual variation was considerable. The possible effect of stress due to differences in the irradiation techniques cannot be excluded.

The findings have a bearing upon the problem on how to find suitable labelled precursors for diagnostic investigations of cellular proliferation in man. Only limited possibilities exist of labelling natural precursors of DNA with gamma or positron emitting nuclides. Although formate labelled with  $^{11}\text{C}$  (positron emitter 0.97 MeV, half life 20.5 min) can now be produced and labelling of thymidine with  $^{11}\text{C}$  is under investigation (STENSTROM 1971), the low  $^{11}\text{C}$  activities available and the short half life become limiting factors. Labelled base analogues have to be used for external detection. Iododeoxyuridine seems to be the most useful.  $^{125}\text{I}$ UdR and  $^{131}\text{I}$ UdR, which are commercially available and for example  $^{125}\text{I}$ UdR or  $^{131}\text{I}$ UdR may all be possible alternatives.  $^{131}\text{I}$  has a half life of 13.0 hours disintegrated by electron capture resulting in even gamma rays (0.159 MeV).  $^{131}\text{I}$  is a beta emitter with a half life of 2.3 hours gamma rays of various energies are also emitted. The short half life of  $^{131}\text{I}$  will result in radiation exposure levels that cannot exceed a small percentage of those from  $^{125}\text{I}$  in procedures completed during one day (MYERS 1963).  $^{131}\text{I}$  can be produced by cyclotron from  $^{130}\text{Te}$  or  $^{238}\text{U}$  to give acceptable activities and rather pure  $^{131}\text{I}$  (HUFF et al. 1968; LEBOWITZ et al. 1971).  $^{131}\text{I}$  generators are commercially available.  $^{125}\text{I}$ UdR or  $^{131}\text{I}$ UdR may be a valuable tool in medical diagnosis for examining cellular proliferation in man. Thymidine is incorporated preferentially over IudR by a factor 2 to 3 (FOX & PRUSOFF 1965; DETHLEFSEN 1970). On the other hand the reutilization of IudR is less than that of thymidine.

## SUMMARY

The effect of 180 MeV proton and  $^{60}\text{Co}$  gamma radiation on  $^{131}\text{I}$  retention 90 hours after  $^{131}\text{I}$ UdR injection was investigated in the whole mouse, the small intestine and the spleen. The RBE for 180 MeV protons of  $1.2 \pm 0.3$  from previous work seemed to be confirmed. Labelled precursors for diagnostic examinations of cellular proliferation in man are discussed.

## ZUSAMMENFASSUNG

Die Wirkung von 180 MeV Protonen — und  $^{60}\text{Co}$  Gamma Strahlung auf die  $^{131}\text{I}$  Retention 90 Stunden nach  $^{131}\text{I}$ UdR Injektion wurde an der ganzen Maus, am Dunndarm und an der Milz untersucht. Der RBE-Wert für 180 MeV Protonen von  $1.2 \pm 0.3$  von früheren Untersuchungen scheint bestätigt zu sein. Geeignete Vorstufen für diagnostische Untersuchungen der Zellproliferation beim Menschen werden diskutiert.

## RÉSUMÉ

L'effet des protons de 180 MeV et de la radiation gamma du  $^{60}\text{Co}$  sur la retention de  $^1\text{I}$  20 heures apres injection de  $^1\text{I}$  UDR a ete etudie sur la souris entiere l'intestin grele et la rate LEBR pour les protons de 180 MeV evalue a  $1.2 \pm 0.3$  dans un travail precedent parait confirmee L'auteur examine l'interet des precursurs marques pour les examens diagnostiques de la proliferation cellulaire chez l'homme

## REFERENCES

- DETHLEFSEN L A Reutilization of  $^{125}\text{I}$  5-iodo-2-deoxyuridine as compared to  $^3\text{H}$  thymidine in mouse duodenum and mammary tumor J nat Cancer Inst 44 (1970) 827
- FOX B W and PRUSOFF W H The comparative uptake of  $^1\text{I}$  labelled 5-iodo-2-deoxyuridine and thymidine  $\text{H}^3$  into tissues of mice bearing hepatoma 129 Cancer Res 25 (1965) 234
- GITLIN D COMMERFORD S L AMSTERDAM E and HUGHES W L X rays affect the incorporation of 5-iododeoxyuridine into deoxyribonucleic acid Science 133 (1962) 1074
- HUGHES W L COMMERFORD S L GITLIN D KRUETER R C SCHULTZE B SILAH V and REILLY P Deoxyribonucleic acid metabolism in vivo I Cell proliferation and death as measured by incorporation and elimination of iododeoxyuridine Fed Proc 23 (1964) 640
- HUFF H B ELDRIDGE J S and BEAVER J E Production of iodine 123 for medical applications Int J appl Radiat 19 (1968) 345
- JOHANSON K J and LARSON H Effect of 180 Mev protons or  $^{60}\text{Co}$ -gamma radiation on the incorporation of  $^1\text{I}$  5-iodo-2-deoxyuridine into intestinal and splenic deoxyribonucleic acid of mice Acta radiol Ther Phys Biol 11 (1972) 452
- LEBOWITZ E GREENE M W and RICHARDS P On the production of  $^{125}\text{I}$  for medical use Int J appl Radiat 22 (1971) 489
- MYERS W G Comparisons of  $^{125}\text{I}$ ,  $^{131}\text{I}$  and  $^{132}\text{I}$  for in vivo and in vitro applications in diagnosis In VIIth international congress of internal medicine Vol II Edited by E Wollheim and B Schlegel Georg Thieme Verlag Stuttgart 1963
- O FARRELL T P and DEWAY P B Effects of acute ionizing radiation on the incorporation of  $^{125}\text{I}$  UDR by cotton rats *Sigmodon hispidus* Radiat Res 38 (1969) 109
- PRUSOFF W H JAFFE J J and GUTHER H Studies in the mouse of the pharmacology of 5-iododeoxyuridine an analogue of thymidine Biochem Pharmacol 3 (1960) 110
- SPINKS J W F and WOODS R J An introduction to radiation chemistry Chapter 4 John Wiley & Sons New York 1964
- STENSTROM T Personal communication (1971)

## EFFECT OF INCORPORATED $^{90}\text{Sr}$ ON COLONY FORMING UNITS OF BONE MARROW AND SPLEEN IN MICE

by

V SVOBODA and V KLENFR

Reports on investigations of the long term effect of ionizing radiation on hematopoiesis are not numerous. LAMERTON (1962) observed the response of peripheral rat blood elements and hematopoietic tissues to continuous external gamma irradiation at dose rates of from 176 to 4 rad per day and reported that 50 rad was the highest daily dose at which the peripheral blood count was steadily maintained. BLACKETT (1967) stated that under similar conditions of irradiation production of erythrocytes remained normal in rats, an ability explained by TARBUTT (1969) as due to changed cellular kinetics of the erythroid precursors. TWENTYMAN & BLACKETT (1970) applied continuous irradiation (40 rad/day) in mice and demonstrated that although the erythropoietic system did not break down it failed to prevent a considerable degree of anemia caused by increased blood loss from thrombocytopenia. The histologic changes in bone marrow in mice produced by  $^{90}\text{Sr}$  were described by NILSSON (1970). The kinetic investigation by FRIDÉ et coll. (1966) dealt with the relation of the spleen stem cell compartment to the bone marrow damaged by  $^{90}\text{Sr}$  radiation.

The present work was directed to the stem cell compartment in marrow hematopoiesis in mice surviving for a long period after  $^{226}\text{Ra}$  incorporation. Predominantly alpha particles participate in the biologic effect. The distribution of radium is not uniform in the bone; the arrangement of the bone structures delimiting the marrow spaces differs in various types of bones and need not even be the same in the various parts of a single bone. Furthermore the incorporated nuclide induces also the rearrangement of the bone tissue. The situation is further complicated by the retention of a fraction of radium daughters. These conditions suggest that data may be obtained on the changes in the stem cell compartment as a whole although it may be extremely difficult to analyse such findings in relation to the spatial dose distribution in the bone marrow volume.

The colony forming units of medullar and splenic hematopoiesis in irradiated mice and controls were assessed by the method of TILL & McCULLOCH (1961) the basis being the accepted view that these units have the properties of the hematopoietic stem cells that form the spleen colonies of clonal cell populations. Stem cells in the present report are the self replicating cells capable of progressive differentiation into one or more types of mature cells.

*Material and Methods* The experiment was carried out in female random bred mice of H strain caged in groups of five under standard conditions.  $^{226}\text{Ra}$  was injected intraperitoneally (0.03  $\mu\text{Ci/g}$  body weight) in a group aged 10 weeks mean weight 25 g another group with the same parameters being kept as a control. The mice were killed at intervals of 5, 9, 14, 18 and 37 weeks after injection, and at which peripheral blood counts and blood smears were carried out and the whole body activity was measured. The right femora were dissected, the bones ground in a mortar (CARSTEN & BOND 1968) and the pooled marrow cells washed in 10 ml Tyrode solution. The suspension obtained afforded the optimal number of bone marrow cells to comply with the experimental intentions.

The spleens were removed and homogenized in a tuberculin syringe with 3 ml Tyrode solution the homogenate being filtered through a nylon gauze with further Tyrode solution to make up a volume of 50 ml. The suspensions were prepared under aseptic conditions at a temperature of melting ice. The cellularity of the pooled spleens was determined.

Recipients of the same origin, sex and weight and aged 10 weeks were irradiated with a TUR roentgen unit in a rotating plastic box with a homogenized field under monitoring control with a chamber Integratron—Victoreen. The mice were exposed to 800 R whole body irradiation at a rate of 60 R/min, a HVL of 1.0 mm Cu and a focus-object distance of 50 cm. The endogenous spleen colonies amounted to less than 0.5 colony per spleen. One group of mice received 10 nucleated bone marrow cells in a volume of 0.2 ml intravenously and in another



Table 1

*Colony formation and spleen  $^{59}\text{Fe}$  uptake after injection of bone marrow and spleen cells of tested mice ( $n=5$ )*

Weeks after $^{\text{a}}$ Ra application	Group of tested mice	No. of recipient mice		No. of colonies per 10 bone marrow cells administered (mean $\pm$ SE)	No. of colonies per 10 spleen cells administered (mean $\pm$ SE)	Per cent 18 hour $^{59}\text{Fe}$ uptake into recipient spleens	
		Bone marrow	Spleen cells			After 10 bone marrow cells administered (mean $\pm$ SE)	After 10 <sup>6</sup> spleen cells administered (mean $\pm$ SE)
5	Controls	19	16	21.5 $\pm$ 1.5	26.4 $\pm$ 2.0	2.9 $\pm$ 0.3	3.8 $\pm$ 0.3
	Ra	8	16	14.0 $\pm$ 1.8**	36.6 $\pm$ 1.8	1.7 $\pm$ 0.2**	4.7 $\pm$ 0.3
9	Controls	19		19.7 $\pm$ 0.9		2.4 $\pm$ 0.2	
	Ra	20	18	16.1 $\pm$ 0.9*	30.9 $\pm$ 1.6	1.3 $\pm$ 0.1**	2.9 $\pm$ 0.3
14	Controls		27		35.9 $\pm$ 1.3		3.8 $\pm$ 0.3
	Ra		17		33.6 $\pm$ 1.5		3.3 $\pm$ 0.3
18	Control	11	11	24.7 $\pm$ 1.2	40.0 $\pm$ 2.2	2.6 $\pm$ 0.2	3.5 $\pm$ 0.3
	Ra	18	17	16.1 $\pm$ 1.4**	25.3 $\pm$ 1.7	1.8 $\pm$ 0.2*	1.9 $\pm$ 0.2
37	Controls	19	21	18.5 $\pm$ 0.8	21.9 $\pm$ 0.7	2.0 $\pm$ 0.2	1.5 $\pm$ 0.1
	Ra	19	20	14.9 $\pm$ 0.9**	19.3 $\pm$ 1.3	1.6 $\pm$ 0.1	1.7 $\pm$ 0.1

\* Significantly different from control value at 95% level.

\*\* Significantly different at 99% level (t test).

group 10<sup>6</sup> spleen cells were injected under the same conditions. The animals were killed by transection of the cervical cord on the ninth day, 18 hours before which 1  $\mu\text{Ci}$  of  $^{59}\text{Fe}$  was injected intraperitoneally. The spleens that were removed were fixed in Bouin's solution, the relative activity being ascertained from the incorporated  $^{59}\text{Fe}$  (SMITH 1964 a, b). The colonies were counted at double magnification at 24 hours. The control experiment was performed under the same conditions. The number of colony forming units in the femoral bone marrow or the spleen were reached from the cellularity and colony forming ability (KOSOFF et coll. 1970). The results were statistically evaluated.

## Results

Double the number or even more marrow cells and double the number of colony forming units were obtained in the femora of intact animals by the above technique as compared with flushing only the shaft cavity (cf. PLAYFAIR & COLE

Table 2

*Peripheral blood counts femoral and spleen cellularity and total colony forming units of tested mice*

Weeks after $^{226}\text{Ra}$ injection	Group of tested mice	Erythrocytes/mm <sup>3</sup> (mean $\pm$ SE) $\times 10^6$	Leucocytes/mm <sup>3</sup> (mean $\pm$ SE) $\times 10^3$	Nucleated marrow cells per femur $10^6$	Nucleated cells per spleen $10^6$	Total colony forming units per femur $10^3$	Total colonies forming units per spleen $10^3$
5	Controls	$10.1 \pm 0.6$	$12.8 \pm 0.8$	31.8	183	6.8	4.8
	Ra	$9.6 \pm 0.5$	$9.3 \pm 0.8$	34.0	122	4.8	5
9	Controls	$10.9 \pm 0.4$	$17.0 \pm 1.1$	43.4	16	8.5	
	Ra	$10.0 \pm 0.1$	$14.0 \pm 0.7$	32.7	233	5.2	7.2
14	Controls	$9.9 \pm 0.5$	$12.0 \pm 2.5$		123		4.4
	$^{226}\text{Ra}$	$10.0 \pm 0.3$	$11.5 \pm 1.0$		5		7.3
III	Controls	$10.9 \pm 0.4$	$14.0 \pm 1.1$	30.1	83	8.9	3.9
	Ra	$10.2 \pm 0.4$	$11.8 \pm 0.7$	27.4	115	4.3	2.9
37	Controls	$10.2 \pm 0.5$	$10.5 \pm 1.8$	44.2	81	8.2	1.8
	Ra	$9.5 \pm 0$	$8.2 \pm 0.7$	28.4	150	4.3	7.9

1965). About  $30$  to  $40 \times 10^6$  marrow cells per femur and about  $20$  spleen colonies per  $10^6$  applied marrow cells were recorded CARSTEN & BOND 1968 also obtained a greater yield of colony forming units if they prepared the cellular suspension by chapping and washing off the bones.

The number of macroscopic spleen colonies and the  $^{59}\text{Fe}$  uptake in the spleens of recipients after the intravenous injection of  $10^6$  marrow cells and  $10^6$  spleen cells are presented in Table 1. The number of colonies per  $10^6$  marrow cells in mice given  $^{226}\text{Ra}$  during the experimental period was lower than in the control groups the ratio of these values remaining however comparable. The corresponding results were obtained by measuring the  $^{59}\text{Fe}$  uptake in spleens colonised by irradiated bone marrow cells.

After injection of  $10^6$  spleen cells from  $^{226}\text{Ra}$  treated mice the yield of spleen colonies was the highest in the first interval and decreased in further intervals whereas the number of colonies in the controls rose. The  $^{59}\text{Fe}$  incorporation into the spleens of recipients given spleen cells from  $^{226}\text{Ra}$  exposed mice was also higher in the first interval and subsequently decreased below the control values.

Further data in tested animals are summarized in Table 2. The colony forming units in femora of mice given  $^{226}\text{Ra}$  amounted to 48 to 69 per cent of the control values which corresponded to the decreased stem cell compartment. At the

Fig 1 Femoral bone marrow (solid line bar) and spleen (black bar) cellularity of  $^{226}\text{Ra}$  treated mice as percentage of control values (broken line bar) in the respective intervals

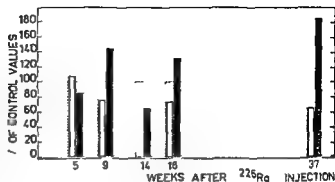
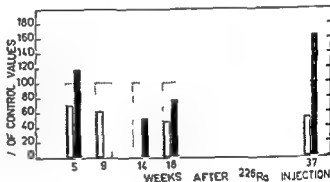


Fig 2 Colony forming units of femoral bone marrow (solid line bar) and spleen (black bar) of  $^{226}\text{Ra}$  treated mice as percentage of control values (broken line bar) in the respective intervals



beginning of the experimental series the femoral marrow cellularity in the radium treated mice failed to differ from the control value in the intervals that followed the number of marrow cells in intact mice increased and reached the level of forty million while in those given  $^{226}\text{Ra}$  it amounted to thirty million. At the 9th, 18th and 37th week after radium injection the femoral marrow cells in the tested mice were reduced to 74, 73 and 65 per cent of the controls. The femoral marrow cells in intact animals amounted to  $1.1 \times 10^6$  per gram body weight, this being in good agreement with the results reported by Bozzini et al. (1970); this figure in  $^{226}\text{Ra}$  treated mice was  $0.88 \times 10^6$  cells per gram body weight, the difference being statistically significant ( $p < 0.05$ ). The bone marrow in mice given radium was thus hypoplastic and this condition was maintained during the whole experimental period.

The cellularity of the spleen in  $^{226}\text{Ra}$  treated mice changed only slightly in the first two intervals, exceeding even in the 9th week the respective control value and decreasing to a minimum in the 14th week. The number of spleen cells again increased in the subsequent intervals so that in the 37th week it was double the

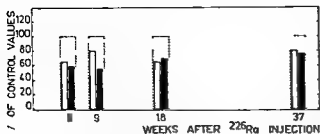


Fig 3 Spleen colonies (solid line bar) and spleen  $^{59}\text{Fe}$  uptake (black bar) in recipient mice after administration of 10-nucleated bone marrow cells of  $^{226}\text{Ra}$  treated mice expressed as percentage of control values (broken line bar)

compared with the controls. The colony forming units in spleens of animals exposed to radium changed in a similar manner.

The cellularity of the femoral bone marrow and of the spleen in mice with  $^{226}\text{Ra}$  is presented in Fig 1 as a percentage of the control values. The colony forming units appear in Fig 2. The continuous decrease of cellularity and slower disappearance of the units from the control spleens with age were noteworthy. Likewise as in the experiments reported by COGGLE & PROUKAKIS (1970) neither the number of femoral marrow cells in ageing mice nor the size of the stem cell compartment as determined by an exocolonizing assay, decreased.

### Discussion

The radiation effect upon femoral hematopoiesis in the period of 5 to 37 weeks following the intraperitoneal administration of  $0.75 \mu\text{Ci } ^{226}\text{Ra}$  per mouse was manifested by diminution of the stem cell compartment. A less significant decrease of bone marrow cellularity also occurred while the number of peripheral erythrocytes and leucocytes was fully compensated during the entire period of observation.

The  $^{59}\text{Fe}$  incorporation into spleens of mice receiving bone marrow cell suspension from those exposed expressed as percentages of control values has been compared with the decrease in the colony forming units similarly recorded (Fig 3). The results in the first two intervals may suggest a decreased erythroid differentiation. Nevertheless this comparison as a whole does not definitely indicate a change in the differentiating capacity of stem cells continuously irradiated by incorporated  $^{226}\text{Ra}$ . No evidence on a different sensitivity of perhaps already committed elements with maintained repopulating ability appears to exist.

BLOOM (1948) observed after the intraperitoneally injected radium in the range of 0.17 to  $1.0 \mu\text{Ci/g}$  body weight a maximal depletion of marrow cells in the metaphyses and epiphyses of the femora of mice, as well as in regions with trabecular bone and large endosteal surfaces as well as along the endosteum of the

shaft. It is probable that even with the smaller activities injected a greater hazard to the marrow cells exists in these critical paraendosteal volumes than in the remaining bone marrow. Assuming that the distribution of stem cells in the bone marrow be uniform, the decrease in the femoral colony forming units observed in the present experiment is inadequate for the size of the critical volume. This suggests that more stem cells are available close to the endosteum.

Due to the known effect of bone seeking nuclides upon bone tissue, the possibility that depletion of the mesenchymal cells of this tissue participates at least indirectly in the diminution of the hematopoietic stem cell compartment cannot be excluded. This conception is to a certain extent supported by the recent findings of PATT & MALONEY (1970) and FONG *et coll.* (1971). These authors proved that the regenerative process in bone marrow after localized depletion originates in uncommitted mesenchymal cells in the connective tissue of the Haversian canals of the adjacent bone. No less interesting were the investigations by CROSBY (1970), TAVASSOLI & CROSBY (1970) and AMSSEL *et coll.* (1969) which demonstrated that the stroma cells of bone marrow transplanted into extramedullary sites have the properties of primitive cells. This would appear to be similar to the behaviour of the above mentioned mesenchymal cells in bone tissue.

The colony forming units and cellularity in mice exposed to  $^{226}\text{Ra}$  were changed in the same way as reported by FRIED *et coll.* (1966) who investigated mice given  $^{90}\text{Sr}$ . These changes may be understood as manifestations of compensatory blood forming activity in an irradiated organ following the impairment of bone marrow hematopoiesis. The importance of the spleen as a source of compensatory hematopoiesis with an increasing  $^{90}\text{Sr}$  dose is obvious (NILSSON, 1971). Considering that the irradiation from  $^{226}\text{Ra}$  incorporated in mice failed to change the peripheral blood count for a considerable time, it would appear that effective reparatory and compensatory mechanisms did much to neutralize the damage to the bone marrow.

### Acknowledgements

The authors wish to thank Mrs R. Housová and Mrs Z. Kotásková for their technical assistance.

### SUMMARY

Data on hematopoiesis in mice were obtained over a period of 5 to 37 weeks after the intraperitoneal injection of  $^{226}\text{Ra}$ . The repopulation ability of bone marrow cells as measured by the  $^{59}\text{Fe}$  uptake in the recipient spleens changed in step with the colony forming units. The effects on the latter and the cellularity of the spleen may express the reaction of the irradiated organ to impairment of the blood forming capacity of the marrow.

## ZUSAMMENFASSUNG

Daten zur Hamatopoese der Maus während einer Zeit von 5 bis 37 Wochen nach intra peritonealer Injektion von  $^{226}\text{Ra}$  wurden erhalten. Das Repopulationsvermögen von Knochenmarkszellen gemessen durch die  $^{59}\text{Fe}$  Aufnahme der Milz von Rezipienten folgte den Veränderungen der koloniebildenden Einheiten. Der Effekt auf letztere und die Zellularität der Milz mögen die Reaktion des bestrahlten Organismus auf die herabgesetzte Blut bildende Kapazität des Knochenmarks zum Ausdruck bringen.

## RÉSUMÉ

Les auteurs ont étudié l'hématopoïèse de souris au cours d'une période de 5 à 37 semaines suivant l'injection intra péritonéale de  $^{226}\text{Ra}$ . L'aptitude au repeuplement des cellules de la moelle osseuse mesurée par la fixation de  $^{59}\text{Fe}$  dans les rates receveuses change en fonction des unités formatrices de colonies. Les effets sur le repeuplement et sur la cellularité de la rate peuvent exprimer la réaction de l'organe irradié à la diminution du pouvoir hématopoïétique de la moelle.

## REFERENCES

- ANSEL S, MANTATIS A, TAVASSOLI M and CROSBY W H. The significance of intramedullary cancellous bone formation in the repair of bone marrow tissue. *Anat Rec* 164 (1969) 101.
- BLACKETT N M. Erythropoiesis in the rat under continuous irradiation at 45 rads/day. *Brit J Haemat* 13 (1967) 915.
- BLOOM M A. Bone marrow. In: *Histopathology of irradiation from external and internal sources* p. 162. Edited by W. Bloom. McGraw Hill, New York, 1948.
- BOZZINI C E, BARRIO RENDO M E, DEVOTO F C H and EPPER C E. Studies on medullary and extramedullary erythropoiesis in the adult mouse. *Amer J Physiol* 219 (1970) 724.
- CARSTEN A L and BOYD V P. Viability of stored bone marrow colony forming units. *Nature* 219 (1968) 1082.
- COOGLE J E and PROUKAKIS C. The effect of age on the bone marrow cellularity of the mouse. *Gerontologia* 16 (1970) 25.
- CROSBY W H. Experience with injured and implanted bone marrow. Relation of function to structure. In: *Hemopoietic cellular proliferation* p. 87. Edited by F. Stohlman Jr. Grune and Stratton, New York, 1970.
- FONG PH L, MALONEY M A and PATT H M. Origin of repopulating cells in a mechanically depleted medullary cavity as determined by studies with marrow transplants. *Blood* 37 (1971) 413.
- FRIED W, GURNEY C W and SWATEK M. The effect of Strontium-89 on the stem cell compartment of the spleen. *Radiat Res* 29 (1966) 50.
- KNOSE H W, FRIED W, GREGORY S et coll. Effect of a noncellular spleen-derived factor on recovery of hematopoietic stem cells from irradiation. *J Lab clin Med* 76 (1970) 584.
- LAMERTON L F. The response of the blood forming tissues of the rat to continuous irradiation at various dose rates. In: *Some aspects of internal irradiation* p. 269. Edited by T. F. Dougherty. Pergamon Press, New York, 1962.

- NILSSON A. Pathologic effect of different doses of radiostrontium in mice. Changes in the haematopoietic system. *Acta radiol Ther Phys Biol* 9 (1970) 528
- Pathologic effect of different doses of radiostrontium in mice. Development and incidence of leukaemia. *Acta radiol Ther Phys Biol* 10 (1971) 115
- PATT H. M. and MALONEY M. A. Reconstitution of bone marrow in a depleted medullary cavity. In: *Hemopoietic cellular proliferation* p. 56. Edited by F. Stohlman Jr. Grune and Stratton, New York, 1970.
- PLAYFAIR J. H. L. and COLE L. J. Quantitative studies on colony forming units in isogenic radiation chimeras. *J. cell comp. Physiol* 65 (1965) 7
- SMITH L. H. a) Uptake of  $^{59}\text{Fe}$  by spleens of lethally irradiated mice given isologous bone marrow. *Ann. N.Y. Acad. Sci.* 114 (1964), 586
- (b) Marrow transplantation measured by uptake of  $^{59}\text{Fe}$  by spleen. *Amer. J. Physiol* 206 (1964) 1244
- TARBUTT H. G. Cell population kinetics of the erythroid system in the rat. The response to protracted anaemia and to continuous gamma irradiation. *Brit. J. Haemat.* 16 (1969) 9
- TAVASSOLI M. and CROSBY W. H. Bone marrow histogenesis. A comparison of fatty and red marrow. *Science* 169 (1970) 291
- TILL J. E. and MCCULLOCH E. A. A direct measurement of the radiation sensitivity of normal mouse bone marrow cells. *Radiat. Res.* 14 (1961) 213
- TWENTYMAN P. R. and BLACKETT N. M. Red cell production in the continuously irradiated mouse. *Brit. J. Radiol.* 43 (1970) 898

## INVOLUTION AND RECOVERY OF THE THYMUS AND SPLEEN OF THE MONGOLIAN GERBIL FOLLOWING ROENTGEN IRRADIATION

by

J. L. MONTGOMERY and R. C. RILEY

The lymphatic organs of various strains and species of laboratory mammals have been noted to exhibit similar radiation sensitivities (BLOOM 1954) even when their radiation sensitivities are somewhat different when acute lethality is used as an endpoint. According to BOYD et al. (1965) the LD<sub>50/30</sub> values for most laboratory animals fall between 450 R (guinea pig) and 800 R (hamster). Most quantitative investigations on lymphatic tissue radiation sensitivity have utilized mice which have LD<sub>50/30</sub> values in the range of 600 R to 700 R. JACOBSON, McDERMOTT & RILEY (1971) have reported that the Mongolian gerbil *Meriones unguiculatus* has an LD<sub>50/30</sub> of approximately 1100 R.

In these experiments we have taken advantage of the high LD<sub>50/30</sub> of the gerbil to examine radiation induced lymphatic tissue involution and recovery over a range of doses not possible with more radiation sensitive animals. The response of the gerbil lymphatic tissue is compared to published values for mice.

Submitted for publication 14 December 1971



Table 1  
Body weights following irradiation

Day	Expt	Average body weights (g)						
		0 R	100 R	200 R	400 R	800 R	1200 R	1600 R
1	1	68.5		66.0	66.8	64.6	61.6	
	2	60.6	60.9					
2	1	63.5	69.6	65.8	69.6	61.6	66.5	60.6
	2	58.8	59.1					
3	1	66.0	69.4	63.5	59.6	65.8	68.2	
	2	55.2						55.1
5	1	67.8	70.6	68.4	66.4	64.1	57.1	59.7
8	1	67.1		68.1	67.2	70.9	62.0	
	2	46.2	48.8					44.9
14	1	66.5		71.3	78.0	65.5		
	2	56.6	56.5	61.0				
	3	61.0				64.0		

It was thus possible to determine whether or not the sensitivity of the spleen and thymus is actually constant regardless of the animal irradiated.

### Methods and Materials

**Radiation conditions** Exposures were performed utilizing a General Electric Maxitron 300 constant potential therapy apparatus operated at 300 kVp and 20 mA with 2 mm Cu added filtration. The first half value layer of the beam was 1.7 mm Cu and the second 3.1 mm Cu. The dose rate measured under conditions of maximum backscatter at a target midline distance of 71 cm was 82 R/min  $\pm$  5 per cent.

The animals were exposed in groups of eight or nine in a 25 cm  $\times$  25 cm lucite chamber 3 cm deep. Different doses were obtained by varying the exposure time. All animals including the sham irradiated controls were returned in the exposure chamber for a time equal to that necessary for the highest dose.

**Animals** Approximately three hundred male gerbils 100 to 105 days old were exposed to doses ranging from 100 R to 1600 R (Expt 1). The animals were housed four per cage provided with wood shavings as bedding and fed an ad libitum diet of Purina mouse chow, sunflower seeds, carrots and water.

Table 2

Thymic weights following irradiation mg per 100 g body weight (mg %)  $\pm$  SE

Day	Expt	0 R	100 R	200 R	400 R	800 R	1200 R	1600 R
1	1	110.5 $\pm$ 8.8		74.7 $\pm$ 9.8	75.4 $\pm$ 5.0	72.4 $\pm$ 3.9	73.8 $\pm$ 3.0	
	2	74.6 $\pm$ 10.0	61.9 $\pm$ 5.5					
7	1	91.8 $\pm$ 8.7	89.7 $\pm$ 4.2	72.5 $\pm$ 5.3	51.3 $\pm$ 2.5	31.8 $\pm$ 2.9	29.1 $\pm$ 2.1	26.9 $\pm$ 0.9
	2	64.9 $\pm$ 7.3	65.0 $\pm$ 10.4					
3	1	111.6 $\pm$ 11.2	63.3 $\pm$ 6.0	67.6 $\pm$ 7.4	49.6 $\pm$ 5.1	24.7 $\pm$ 1.1	21.5 $\pm$ 1.8	
	2	68.6 $\pm$ 8.1						15.4 $\pm$ 2.1
5	1	98.6 $\pm$ 6.6	77.8 $\pm$ 6.9	82.4 $\pm$ 5.5	63.5 $\pm$ 5.4	30.7 $\pm$ 2.1	18.7 $\pm$ 2.4	16.5 $\pm$ 0.5
8	1	116.5 $\pm$ 8.2		99.6 $\pm$ 8.2	75.8 $\pm$ 3.9	42.5 $\pm$ 3.0	21.8 $\pm$ 1.9	
	2	70.0 $\pm$ 7.3	59.1 $\pm$ 9.4					
14	1	102.2 $\pm$ 4.9		108.5 $\pm$ 4.6	86.3 $\pm$ 3.3	77.4 $\pm$ 9.3		
	2	72.4 $\pm$ 7.3	101.3 $\pm$ 6.7	96.7 $\pm$ 7.7				
	3	89.5 $\pm$ 11.0				56.1 $\pm$ 9.0		

Table 3

Splenic weights following irradiation mg per 100 g body weight (mg %)  $\pm$  SE

Day	Expt	0 R	100 R	200 R	400 R	800 R	1200 R	1600 R
1	1	77.7 $\pm$ 5.1		53.8 $\pm$ 2.7	57.5 $\pm$ 2.9	55.1 $\pm$ 3.1	57.9 $\pm$ 4.7	
	2	68.4 $\pm$ 3.2	53.1 $\pm$ 4.8					
2	1	89.8 $\pm$ 5.6	65.7 $\pm$ 2.1	62.1 $\pm$ 2.6	52.6 $\pm$ 3.1	52.5 $\pm$ 2.8	50.3 $\pm$ 2.5	49.5 $\pm$ 2.2
	2	111.2 $\pm$ 8.6	57.6 $\pm$ 5.0					
3	1	85.1 $\pm$ 3.3	64.3 $\pm$ 4.5	53.9 $\pm$ 2.1	55.4 $\pm$ 3.8	42.5 $\pm$ 2.2	41.6 $\pm$ 2.3	
	2	76.0 $\pm$ 6.9						39.9 $\pm$ 4.7
5	1	86.0 $\pm$ 4.4	70.4 $\pm$ 3.3	67.4 $\pm$ 3.4	53.5 $\pm$ 2.5	46.9 $\pm$ 1.6	46.2 $\pm$ 2.9	44.3 $\pm$ 1.7
8	1	86.8 $\pm$ 3.2		105 $\pm$ 8.0	61.0 $\pm$ 3.6	45.3 $\pm$ 2.1	40.8 $\pm$ 2.6	
	2	67.6 $\pm$ 3.5	57.5 $\pm$ 3.9					
14	1	85.2 $\pm$ 1.4			69.1 $\pm$ 3.6	88.3 $\pm$ 7.0		
	2	80.0 $\pm$ 4.1	84.6 $\pm$ 7.5	180 $\pm$ 4.7				
	3	74.6 $\pm$ 2.0				65.2 $\pm$ 5.2		

On days 1, 2, 5, 8, and 14 after exposure 5 to 8 animals from each dose group were weighed, killed by cervical dislocation, and their spleens and thymuses removed and weighed to the nearest 0.1 mg. Deaths in the 1200 R and 1600 R groups precluded measurements at both these dose levels 14 days after

Fig 1 Thymic weight loss and recovery after whole body irradiation of the gerbil ○ 100 R ● 200 R □ 400 R ▲ 800 R ■ 1200 R △ 1600 R

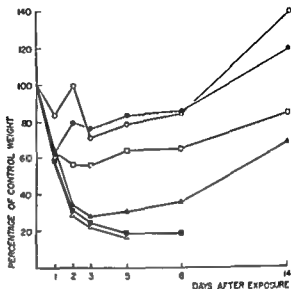
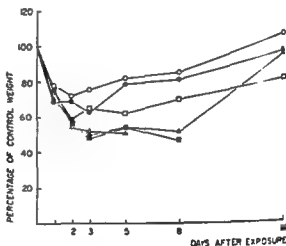


Fig 2 Splenic weight loss and recovery after whole body irradiation of the gerbil ○ 100 R ● 200 R □ 400 R ▲ 800 R ■ 1200 R △ 1600 R



exposure and 11 days after exposure to 1600 R. In each case where additional animals were added (Expt 2 and Expt 3) sham irradiated control animals were included for comparison and conditions were identical to those described above.

## Results

Body weights of all groups are presented in Table 1 and thymic and splenic weights (each in mg/100 g of body weight) are presented in Tables 2 and 3 respectively. The involution and recovery of the lymphatic organs with time are

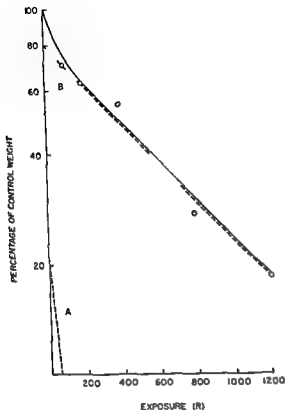


Fig 3 Maximum involution of the thymus of irradiated gerbils. The solid line represents thymic weight which has been divided into a sensitive component (broken line A) and an insensitive component (broken line B). Per cent weight in component A 20 (66) component B 80 (34) and thymic weight 100 (100) ED<sub>50</sub> in component A 50 R (69 R) component B 560 R (317 R) and thymic weight 400 R (90 R). Values in parenthesis are comparable values for the mouse taken from KALLMAN & KORNY (1955 a).

presented as percentage of control weights in Fig 1 (thymus) and Fig 2 (spleen)

**Thymus** One day after exposure the thymic weights in all groups (except 100 R groups) were reduced similar amounts to approximately 62 per cent of the control weights. Two days after exposure a recovery in weight was seen at 200 R, a slight additional decrease at 400 R and a similar decrease in weight to approximately 32 per cent of control weight, in the 800 R, 1200 R and 1600 R groups. Three days after exposure additional involution (again approximately equal) was seen in the 800 R, 1200 R and 1600 R groups only. Five days after exposure recovery was evident in the 800 R, 400 R, 200 R, and 100 R groups. This recovery continued through the eight day observation period and by the fourteenth day was extensive with the thymic weights of the 100 R and 200 R groups being larger than those of the control group. Additional weight loss was seen at 1200 R and 1600 R on day 5. On day 11

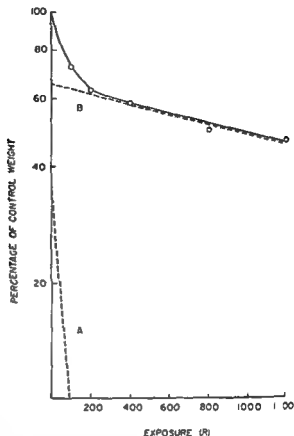


Fig. 4. Maximum involution of the spleen of irradiated gerbils. The solid line represents splenic weight which has been divided into a sensitive component (broken line A) and an insensitive component (broken line B). Per cent weight in component A 35 (5%) component B 65 (48) and splenic weight 100 (100). ED<sub>50</sub> in component A 50 R (82 R) component B 2060 R (498 R) splenic weight 900 R (177 R). Values in parenthesis are comparable values for the mouse taken from HALLMAN & KOUSS (1955).

many animals were dead and the remainder moribund in the 1600 R group. No recovery was apparent in the 1200 R group at that time. Maximum involution of each dose group is plotted in Fig. 3 for doses to 1200 R. The 1600 R group was not included since the animals were moribund and a portion of the maximum involution was probably due to the poor condition of the animals.

The solid line in Fig. 3 (thymic involution) has been divided into two components: A, a radiation sensitive and B, an insensitive component. The sensitive component comprises only 20 per cent of the weight and has an ED<sub>50</sub> (50 per cent depression) of approximately 50 R. The insensitive component comprises 80 per cent of the weight and has an ED<sub>50</sub> value of 560 R. The ED<sub>50</sub> value for total weight loss was found to be 400 R.

**Spleen.** One day after exposure the splenic weights of all groups had decreased to approximately the same level (69 to 78 per cent of control weight). On the second and third day the 100 R and 200 R groups decreased slightly whereas

the 800 R, 1 200 R and 1 600 R groups decreased approximately equal amounts to 55 to 59 per cent of control weight on day 2 and 49 to 53 per cent on day 3. As with the thymus no recovery was seen in the 1 200 R and 1 600 R groups through their abbreviated observation periods. At 800 R no additional decrease in weight was seen five or eight days after exposure but recovery was extensive by the fourteenth day. At 400 R and below, recovery in splenic weights were observed by the fifth or eighth days after exposure and were approaching or exceeding (100 R) control weights by the fourteenth day. Maximum levels of depression in the splenic weights are plotted in Fig. 4. The spleen like the thymus appears to consist of a radiation sensitive and an insensitive portion.  $ED_{50}$  values of 50 R (component A) 2 060 (component II obtained by extrapolation) and 900 R (splenic weight) were obtained from analysis of Fig. 4.

### Discussion

Involution of the thymus and spleen following exposure to ionizing radiation is the result of damage to two populations of cells: the small mature lymphocytes which normally have no further capacity for cell division and the dividing large and medium size lymphocytes. The sensitive components in Fig. 3 (thymus) and Fig. 4 (spleen) are due to the killing and removal of the small lymphocytes. The sequence of events involved are rapid and not dependent upon cell division. The sensitive components of both the thymus and spleen are considerably smaller than the comparable components in the mouse. In the gerbil they comprise approximately 20 per cent (thymus) and 35 per cent (spleen) of the total organ weights; in the mouse these components have been reported to comprise 66 per cent (thymus) and 52 per cent (spleen) of the organ weights (KALLMAN & KOHN 1955 a, b). The radiation sensitivity of this component in the gerbil ( $ED_{50}$  of 50 R) is similar to that reported by KALLMAN & KOHN for the mouse (thymus = 69 R, spleen = 82 R). Examination of data on mice obtained in our own laboratory indicate values very similar to theirs for both amount and sensitivity of this component (MONTGOMERY *et al.* 1969). It is our conclusion that whatever other differences may exist in tissue radiation sensitivities from animal to animal, the small lymphocytes are of similar sensitivity.

The second or insensitive component in the gerbil comprises 80 per cent by weight of the thymus and 65 per cent of the spleen compared to 34 per cent and 48 per cent in the mouse. Although the sensitive component was at least as sensitive as the same component in the mouse, the insensitive component showed  $ED_{50}$  values of 560 R (thymus) and 2 060 (spleen), vastly greater than the reported values for mice of 317 R for the thymus and 498 R for the spleen.

It would seem then, that when dividing cells are considered, radiation sensitivity can vary considerably depending upon a number of factors including division rates and position in the cell cycle. This would appear to be the case in the spleen and thymus as in other cell systems.

It is interesting to note the manner in which involution occurs, with time after exposures (Figs 1-2). All organs decrease in size at about the same rate regardless of dose, until recovery becomes a significant factor. That is, the rate of weight loss does not seem to be dependent upon dose, but the amount of weight loss is directly related to dose.

The weights of the thymus and spleen at any time after radiation exposures are of course the net result of radiation damage and tissue recovery. Even at the time of maximum weight losses some recovery has undoubtedly occurred and recovery is under way. Recovery can be seen to occur by two to three days after exposure at lower doses and at least by the fifth to eighth day at 800 R. Through 800 R recovery is rapid and extensive by the end of the fourteenth day. Only in the 1200 R and 1600 R groups is recovery not apparent. In these groups however, death precluded measurements over the entire experimental period.

It is of interest to note that even at a dose of 800 R which would be lethal to most animals the recovery by fourteen days is almost to the control level. Experiments are under way to examine the radiation response of other gerbil tissues and determine to what extent radiation resistance occurs at the tissue level in this relatively radiation resistant animal.

## SUMMARY

Young male gerbils were exposed to 100 R to 1600 R. Thymic and splenic weights were determined 1, 2, 3, 5, 8 and 14 days after exposure. Although the rate of involution of these organs appeared to be independent of dose, the degree of weight loss was directly related to dose. Maximum weight loss compared to dose was found to be a two component function for both organs. The sensitive component in each case had an  $ED_{50}$  (50 per cent weight loss) of 50 R, similar to that for the same component in mice. The second or insensitive components were much more resistant than the comparable components in mice, yielding  $ED_{50}$  values of 560 R (thymus) and 2060 R (spleen).

## ZUSAMMENFASSUNG

Junge männliche Springmause wurden mit 100 bis 1600 R bestrahlt. Das Thymus- und Milzgewicht wurden 1, 2, 3, 5, 8 und 14 Tage nach der Bestrahlung bestimmt. Obwohl die Geschwindigkeit der Involution dieser Organe unabhängig von der Dosis zu sein scheint, stand das Ausmass des Gewichtsverlustes in direkter Beziehung zur Dosis. Der maximale Gewichtsverlust bezogen auf die Dosis war für beide Organe eine zwei Komponenten

**Funktion** Die sensitive Komponente in jedem Fall hatte eine  $ED_{50}$  (50 % Gewichtsverlust) von 50 R ähnlich der von Mäusen. Die zweite oder unempfindliche Komponente war wesentlich resistenter verglichen mit der von Mäusen mit  $ED_{50}$  Werten von 560 R (Thymus) und 2 060 R (Milz).

## RÉSUMÉ

De jeunes gerboises males ont été exposés à des doses de 100 R à 1 600 R. Les poids du thymus et de la rate ont été mesurés 1, 2, 3, 5, 8 et 14 jours après l'exposition au rayonnement. Bien que la vitesse d'involution de ces organes apparaissent indépendante de la dose, l'importance de la perte de poids était directement en relation avec la dose. La perte de poids maximale comparée à la dose s'est révélée être une fonction à deux composantes pour ces deux organes. La composante sensible dans chaque cas avait une  $ED_{50}$  (50 pour cent de perte de poids) de 50 R semblable à celle de la même composante chez les souris. La seconde composante ou composante peu sensible était beaucoup plus résistante que les composantes comparables chez les souris donnant des valeurs  $ED_{50}$  de 560 R (pour le thymus) et de 2 060 R (pour la rate).

## REFERENCES

- BLOOM W. Histological changes after irradiation. In: Radiation biology, Vol. 1, Part II, p. 1104. Edited by A. Hollaender. McGraw Hill Book Co. New York, 1954.
- BOND V. P., FLIEDNER T. M. and ARCHAMBEAU J. O. Mammalian radiation lethality. A disturbance in cellular kinetics. Academic Press, New York, 1965.
- JACOBSON A. P., McDERMOTT K. A. and RILEY R. C. Mortality and body weight changes in the Mongolian gerbil after cobalt 60 gamma irradiation. *Int. J. Radiat. Biol.* 19 (1971) 247.
- HALLMAN R. F. and KOHN H. I. (a) The reaction of the mouse thymus to X-rays measured by changes in organ weight. *Radiat. Res.* 2 (1955) 280.
- (b) The reaction of the mouse spleen to X-rays measured by changes in organ weight. *Radiat. Res.* 3 (1955) 77.
- MONTGOMERY J. L., STRAUB R. F. and SHELLABARGER C. J. The relative biological effectiveness of 22 GeV protons for thymic and splenic weight loss in mice. *Int. J. Radiat. Biol.* 15 (1969) 491.



## EFFECTS OF FRACTIONATED DOSES OF ELECTRONS ON HUMAN SKIN

by

S. BELLETTI and G. LUNFI

Recent data on the survival and recovery of mammalian cells (BARRANDSEN *et coll.* 1963, HEWITT & WILSON 1959, KALLMAN *et coll.* 1964, SHINO & MFTALLI 1966) have indicated that the dose-time relationship for a given fractionation schedule may be more specifically expressed by the relationships between (1) the total dose and the dose per fraction (i.e. total dose/number of fractions) and (2) the total dose and the time interval between repeated equal fractions.

The work of FOWLER *et coll.* (1965) on pig skin erythema and desquamation revealed that the dose value per fraction plays a greater role than the time interval between fractions. The variation in total dose with total fractionation time is small but not negligible and has been discussed by ELLIS (1967), FOWLER (1965, 1968) and SERINE & HOLMBERG (1968). The present clinical investigation takes into account only the first of the two relationships leaving aside time factors such as the interval of time between fractions and the total fractionation time.

---

Submitted for publication 28 June 1971

*Material* The investigation was based on the evaluation and comparison of early and late skin reactions. Patients with mammary carcinoma undergoing radiation therapy after surgical treatment were examined over a period of eight months. The effects of different dose fractionation schedules were evaluated by comparing skin reactions of both parasternal sides of the same patient. Irradiation was carried out with 15 MeV electron beams to 4 cm  $\times$  12 cm areas.

*Dosimetry* was performed by means of an ionisation and extrapolation chamber (BELLETTI & TORNIELLI 1964) whereas the dose distribution on both parasternal sides was determined by photographic films.

*Evaluation of skin reaction* The right parasternal side of each patient was used as a control field and irradiated according to a constant fractionation schedule. The comparison between two different fractionation schedules was carried out on the same patient. This was to avoid variability due to the differing sensitivities of different patients as indicated by varying magnitudes of reactions or differing times of their appearance.

Early skin reactions were evaluated by three different stages of erythema: initial, florid and purple, numbered 1, 2 and 3 respectively. The most reliable evaluation was obtained when the erythema reached the second stage: initial and purple erythema lead sometimes to equivocal conclusions. Among the late reactions were the appearance of dyschromias, skin atrophy, teleangiectasis and sclerosis of the subcutaneous tissues. Early reactions were checked 20 to 24 hours after each fraction, whereas late reactions were controlled weekly, starting 3 to 4 months after the end of radiation therapy. Experience in the use of electrons together with that of other authors (TRUCCINI 1960) established that for electrons the erythema characteristics of the doses given appear within 24 hours without the necessity of waiting a greater length of time. The evaluation of early and late reactions was carried out independently by 4 to 5 different observers. The indications supplied by the majority of the observers were considered valid.

*Fractionation schemes* Only the influence of the dose per fraction was intended to be taken into account leaving out the influence of the time interval between fractions.

Fractions of varying doses (150, 250, 300 rad) were delivered to the left parasternal side and a constant fraction of 200 rad to the right parasternal side (Table 1). Daily doses up to those values are commonly used in clinical practice and are given for five days a week with the usual interval of two days between each cycle of five irradiations. The investigation also took into account higher dose values per fraction (400, 600, 1000 rad). The time interval of such high doses (and for the 300 rad doses) was increased to 2, 3 and 7 days respectively.

Table 1  
*Fractionation schemes*

Dose per fraction (rad/interval)		No. of patients
Left parasternal side	Right parasternal side	
150 daily	700 daily	12
250 daily	700 daily	10
300 daily	200 daily	12
300/2 days	200 daily	8
400/2 days	200 daily	10
600/3 days	200 daily	8
1 000/7 days	200 daily	4

Table 2  
*Method of obtaining the value of the fractionation factor*

No. of patients	Dose to right side	Dose to left side	Ratio
1	$a_1$	$b_1$	$b_1/a$
"	$a_2$	$b$	$b_1/a_2$
3	$a$	$b_2$	$b_1/a$
"	$a_n$	$b_n$	$b_n/a_n$

$$\text{Fractionation factor of } \lambda \text{ rad/day} = \frac{\sum_{i=1}^n b_i/a_i}{n}$$

in order to avoid overdose reactions. This procedure also allowed useful information on the use of high doses in the clinical field to be obtained.

Late reactions were investigated at 90 and 120 days from the end of treatment by varying, within the usual therapeutic dose range, the total dose for the 200 rad/day scheme (on the right parasternal side). This represented the reference fractionation and held constant the total dose for the various fractionation schemes under test (on the left parasternal side). Several groups of patients were selected for every fractionation scheme with a total constant dose on the left side for each group but variable from group to group (300 to 200 rad/day in four groups of patients with total doses constant for each group of 3 500, 3 600, 3 900, 3 300 respectively) (Tables 3-4). The two total doses for every group of patients that will eventually induce the same late reaction on both sides may be estimated

**Fractionation factor** The ratio between the two doses found to be necessary to produce equivalent effects in both the test fields of a given patient yields an index of the relative efficiency of the two fractionation schemes in causing the early or late reactions. One of these fields received the fractionation under test and the other the 200 rad/day reference fractionation. A series of values of this ratio (each one pertaining to a single patient) is obtained from each group of patients treated with the same fractionation scheme. The average is a dose modifying factor due to fractionation; this will be termed fractionation factor for brevity.

The method of obtaining the value of the fractionation factor appears in Table 2 (200 rad/day right side compared to  $\infty$  rad/day left side).

Dose  $a_n$  and  $b_n$  refer either to the appearance on both sides of an equal grade of erythema (stages 1-2-3) during treatment or to the appearances of a similar type of late reaction on both sides 90 to 120 days from the end of treatment. The values of  $a$  and  $b$  for erythema and late reactions due to the different fractionation schedules are reported, together with the resulting values of the fractionation factor in Tables 3 and 4.

It is necessary to remember that late reactions are associated with alterations not only in the epidermis or dermis but also in the underlying subcutaneous tissues. The appearance of these alterations after a given dose treatment does not follow constant progression and association because of different individual sensitivity. A particularly late reaction was not therefore considered but since the comparison was performed in the same patient the two different fractionations and the two different total doses were assumed to be equivalent when the late reaction appeared to be the same on both sides of the patient.

## Results

The data for early and late reactions appear together in Fig. 1 although for convenience they will be discussed separately.

**Erythema** The values of the fractionation factor for erythema were plotted against the dose per fraction: the daily dose of 200 rad per fraction was used as reference (Fig. 1, Table 1). A continuous curve was drawn up to the experimental point at 400 rad and extended as a original/broken curve at higher doses since reliable fractionation factors for erythema are not available at these levels. In fact, the values obtained at doses higher than 400 rad per fraction may be unavoidably affected by the large difference in total dose between two successive numbers of fractions. For instance, with the 600 rad per dose fractionation method the progression is 600, 1200, 1800, 2400 rad ( $b$  in Table 2) which, compared to the progression of the 200 rad per dose in standard frac-

Table 3

The dose values for erythema in the three stages of intensity initial florid and purple (stage 1 2 3) in both parasternal fields. Each line and each comparison is derived from one patient. The stage the dose in both fields and the dose ratio are indicated for each patient. The values of the fractionation factors also appear.

200/day—150 day				200 day—250/day				200/day—300/day			
Stage	Right side dose	Left side dose	Ratio	Stage	Right side dose	Left side dose	Ratio	Stage	Right side dose	Left side dose	Ratio
III	2 000	2 400	1 200	2	2 400	2 000	0 833	2	2 700	2 200	0 815
2	2 700	2 850	1 295	2	2 000	2 000	1 000	III	1 800	1 500	0 833
2	1 400	1 800	1 285	3	3 200	3 000	0 937	3	2 600	2 400	0 923
3	3 200	3 600	1 125	3	3 000	2 800	0 933	1	1 000	900	0 900
2	2 000	2 250	1 125	1	1 200	1 000	0 833	2	3 000	2 400	0 800
2	2 200	2 400	1 070	2	2 200	2 000	0 909	1	1 000	900	0 900
2	1 600	2 100	1 312	2	1 800	1 750	0 972	2	2 800	2 400	0 857
2	2 000	2 250	1 125	3	2 600	2 500	0 961	1	1 200	900	0 750
1	1 000	1 200	1 200	2	2 000	1 750	0 875	2	2 900	2 700	0 931
3	3 200	3 600	1 125	2	2 200	2 000	0 909	2	2 900	2 400	0 827
1	1 200	1 500	1 250					1	1 500	1 200	0 800
2	2 200	2 700	1 227					2	2 300	2 100	0 913
Fractionation factor 1 191 ± 0 072				Fractionation factor 0 916 ± 0 056				Fractionation factor 0 854			

Mean fractionation factor between 200/day—300/day and 200/day—300/2 days is 0 840 ± 0 038

tionation ( $a$  in Table 2), produces values of  $b/a$  ratio separated by a large interval the error affecting the fractionation factor already significant for the 400 rad fractionation method would then become so large as to deprive the calculated value of its meaning (Fig 1)

**Late reactions** The fractionation factors for late reactions appear in Fig 1. It was impossible to calculate the error of the experimental points since with the staging method it would have needed an impractically large number of patients to obtain sufficient fractionation factors. Research was therefore limited to one value of the fractionation factor for every patient, following the staging technique mentioned above. The spread of values is indicated in Table 4.

A comparison between fractionation factors for erythema and late reaction discloses a similar trend so that it appears that the fractionation factor is the same in the case of early and late reactions. This finding agrees with that of FOWLER *et al.* (1963 1965) in pig skin. On this assumption the curve of

Table 3 (cont.)

200 rad/day—300 ? days				300 rad/day—400 ? days				300 rad/day—600 3 days			
Stage	Right side dose	Left side dose	Ratio	Stage	Right side dose	Left side dose	Ratio	Stage	Right side dose	Left side dose	Ratio
1	1 300	1 050	0 810	1	1 000	800	0 800	?	3 000	—	—
1	1 000	900	0 900	3	1 800	1 700	0 667	3	2 200	1 800	0 820
2	1 800	1 500	0 833	2	1 400	1 700	0 857	2	2 000	1 200	0 600
1	1 200	900	0 750	1	1 400	1 200	0 857	2	2 200	1 200	0 681
										1 800	0 818
2	2 400	1 800	0 750	2	2 000	1 600	0 800	2	2 200	1 200	0 681
										1 800	0 818
2	2 000	1 800	0 900	1	1 700	800	0 667	3	2 600	—	—
?	1 600	1 200	0 750	?	2 000	1 400	0 700	2	1 800	1 200	0 667
3	2 800	2 400	0 857	2	1 600	1 200	0 750	3	2 800	—	—
				3	2 000	1 600	0 800				
				3	2 600	2 000	0 769				
Fractionation factor				Fractionation factor							
0 818				0 767 = 0 0 0							

erythema was extrapolated up to 1 000 rad per fraction making use of the fractionation factors for late reaction obtained at higher doses

Knowledge of the average value of the dose causing erythema for a given fractionation scheme enables the results to be plotted as a curve on which the erythema dose was plotted against the number of fractions. The average value of the erythema dose measured in 64 patients on the right hand parasternal control side was 2 100 rad for a fractionation method of 200 rad/day i.e. 10.5 fractions of 200 rad each given daily. This value and the fractionation factors in Fig. 1 produced an iso-effect curve for 15 MeV electrons referring to a 4 cm × 12 cm area (Fig. 2 curve 1). A reference curve S has been plotted on the same graph: this represents the iso-effect curve for erythema obtained by STRANDQVIST with conventional roentgen radiation. Although no correction for dose or RBE has been applied the absolute values of the two curves are in reasonable agreement (assuming an RBE for the electrons of less than unity would bring them into better agreement), although their shapes appear to be different. The value of 1 350 rad is the extrapolated equivalent dose for erythema obtained by drawing curve 1 (Fig. 2).

Table 4

*The pairs of total doses that induce equivalent reactions at 90 to 120 days from the end of treatment are given for late reactions. The dose range produced matched reactions in both parasternal fields: the values of the resultant fractionation factor are stated.*

	200/day - 300/day			200/day - 400/2 days		
	Right side dose	Left side dose	Ratio	Right side dose	Left side dose	Ratio
	4 200	3 600	0.857	4 200	3 200	0.761
	4 400	3 600	0.818	4 400	3 200	0.727
	4 600	3 900	0.847	4 200	3 200	0.761
	4 000	3 300	0.825			
Dose	4 000 -	3 300 -		4 000 -	3 200 -	
Range	4 600	3 900		4 600	3 600	
Fractionation factor	0.836 $\pm$ 0.018			0.749 $\pm$ 0.030		

### Conclusions

A comparison between the two effect curve for erythema obtained in the present series of experiments and the theoretic curves derived from research in experimental radiation biology is interesting. Such curves were previously obtained and analysed by FOWLER & STERN (1963). These authors, on the basis of mammalian cell survival curve reported by HEWITT & WILSON (1959), PUCK & MARCUS (1956), ELKIND & SUTTON (1960), BARENDSEN et al. (1960) used values of  $D_0$  and  $n$  of 130 rad and 2.8, respectively. It has moreover been noted (NIAS 1963) that small variations in these values introduce insignificant changes in the iso effects curve.

The curves used by FOWLER & STERN have been plotted for this comparison in Fig. 3. It should be noted that the ordinate of this graph is the ratio  $D_n/D_1$  (where  $D_1$  represents the dose necessary to obtain certain effects with a single fraction and  $D_n$  is the total dose for  $n$  fractions) and this is plotted against the number of fractions  $n$ . This plot takes into account only the shape of the curve without consideration of the actual dose value given by  $D_1$ . Only two of the iso-effects curves drawn by FOWLER & STERN appear in Fig. 3, curve a with a  $D_1$  of 1 040 rad and curve b with a  $D_1$  of 1 500 rad. These values of  $D_1$  appear

Table 4 (cont.)

200/day - 1000/3 days			200/day - 1000/7 days		
Right side dose	Left side dose	Ratio	Right side dose	Left side dose	Ratio
4 000	3 000	0.750	3 200	2 000	0.625
4 200	3 000	0.714			
3 800 - 4 600	3 000		3 200 - 3 800	3 000	
0.737 ± 0.025			0.675		

to allow a comparison to be made with an iso effect curve for erythema. Curve 1 in Fig. 3 is that obtained by the present authors and curve S represents the results of STRANDQVIST. It may be deduced from the data in Fig. 2 that curves 1 and S demand that the values of  $D_1$  should be 1 350 rad and 1 000 rad respectively and that the experimental and theoretic values of  $D_1$  are thus almost equal.

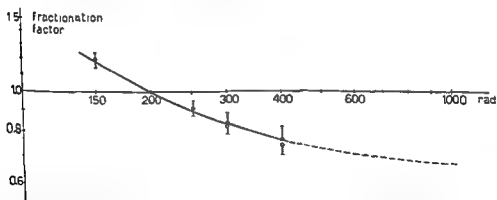


Fig. 1. Fractionation factor plotted against the dose per fraction (reference fractionation 200 rad per fraction 3 days/week). Closed circles indicate the value of the fractionation factor for 1st erythema with open circles as late reactions.



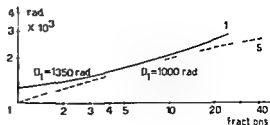


Fig. 2. Erythema dose plotted against the fraction number. Curve 1: Present results (15 MeV electron on 4 cm  $\times$  12 cm area). Curve 5: Strandqvist's erythema curve.

FOWLER & STERN have suggested that no such curve obtained in the clinical field may be explained by survival curves having values of  $D_0$  and  $n$  like those appearing in radiobiologic research. The curve obtained in the present series of experiments is however in good agreement with the theoretic curve b, moreover this curve was obtained with a  $D_1$  of 1500 rad, almost equal to the experimental value of  $D_1$ .

The different time interval between fractions when 400, 600, 1000 rad per fraction were given make it likely that the value of  $D_1$  obtained in the experiments was higher than the true value because of the intervening recovery phenomena. If  $D_1$  were lower the curve would considerably steepen and so would approximate curve b even more closely owing to the high values of the abscissa.

It is suggested that the good agreement between the experimental data and the theoretic curve is due to the substitution in the clinical field of the relationship dose against the number of fractions for the relationship of dose against time. Furthermore it may be caused by the removal through direct comparison of two adjoining sides of the same patient of the errors resulting from a comparison of patients of different sensitivity. Of course, the errors inherent in investigations in

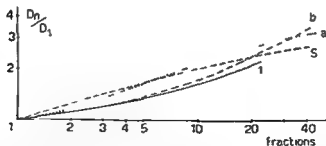


Fig. 3. Ratio  $D_n/D_1$  plotted against the fraction number for present results for Strandqvist's erythema curve and for certain theoretic curves as follows: Curve 1: Erythema curve present results (15 MeV electrons 4 cm  $\times$  12 cm area). Curve S: Strandqvist's erythema curve (from FOWLER & STERN). Curve a: Theoretic curve deduced from a survival with  $D_1 = 130$  rad,  $n = 2.8$  considering  $D_1 = 1500$  rad (from FOWLER & STERN).

human subjects may raise some doubts about the conclusion drawn, especially when the changes in the values considered are not particularly high.

It may be concluded that the method allows a strict evaluation of the different types of fractionation schedules with the dose values most commonly employed in clinical radiation therapy (150 200 300 rad every 24 hours). On the other hand for doses of 400 600, 1 000 rad for which the time between fractions had been increased — different influence of recovery factors was probably present. Although it would appear that the results obtained are reasonably reliable even for higher dose values it must be recognised that the influence of recovery factors has still been insufficiently evaluated. This problem therefore requires further consideration.

### Acknowledgements

The authors are grateful to Prof J F Fowler Prof M Pionente and Prof G Silini for their great help.

### SUMMARY

The authors have evaluated several types of dose fractionation in patients treated after amputation of the breast for carcinoma and irradiated with 15 MeV electron beams to bilateral parasternal lymph nodes. Reactions observed in the same patient with different types of fractionation are plotted and the resulting curves compared with results reported by other workers.

### ZUSAMMENFASSUNG

Die Verfasser haben verschiedene Typen von Dosis Fraktionierung bei Patienten bei denen nach Amputation der Brust wegen eines Karzinoms bilateral die parasternalen Lymphknoten mit 15 MeV Elektronenstrahlen bestrahlt waren beurteilt. Die Reaktionen die beim selben Patienten mit verschiedenen Typen der Dosis Fraktionierung beobachtet wurden werden graphisch dargestellt und die erhaltenen Kurven mit den von anderen Untersuchern beschriebenen Resultaten verglichen.

### RÉSUMÉ

Les auteurs ont étudié différents types de fractionnement de la dose chez des malades traités après amputation du sein pour cancer et irradiés par des faisceaux d'électrons de 15 MeV sur les ganglions lymphatiques parasternaux des deux côtes. Les réactions observées chez la même malade avec les différents types de fractionnement sont mises en graphique et les courbes résultantes sont comparées avec les résultats présentés par d'autres auteurs.

## REFERENCES

- BARENDSEN G W, BELSKER T J L, VERGROESEN A J and BUDKE L. Effects of different ionizing radiations on human cells in tissue culture II Biological experiments Radiat Res 13 (1960) 841
- , WALTER H M D, FOWLER J F and BEWLEY D K. Effects of different ionizing radiations on human cells in tissue culture III Experiments with cyclotron accelerated alpha particles and deuterons Radiat Res 13 (1963) 106
- BELLETTI S and TORNIELLI G. Una camera di ionizzazione ad estrapolazione per dosimetria  $\gamma$  e  $\beta$  (In Italian) Radiol med 9 (1964) 900
- ELKIND M M and SYTON H. Radiation response of mammalian cells grown in culture Radiat Res 13 (1960) 556
- ELLIS F. Modern trends in radiotherapy Vol I chapter 2 Edited by T J Deeley and C A P Wood Butterworths London 1967
- FOWLER J F. The estimation of total dose for different numbers of fractions in radiotherapy Brit J Radiol 38 (1965) 365
- The rationale of dose fractionation In Frontiers of radiation therapy and oncology Vol III Karger Basel 1968
- and STERN H E. Dose time relationship in radiotherapy and the validity of cell survival curve models Brit J Radiol 36 (1963) 163
- , MORGAN R L, SILVESTER J A et coll. Experiments with fractionated  $\gamma$  ray treatment of the skin of pigs. Fractionation up to 5 days Brit J Radiol 38 (1965) 278
- FRIEDMAN M and PEARLMAN A W. Time-dose relationship in irradiation of recurrent cancer of the breast. Iso-effect curve and tumor lethal dose Amer J Roentgenol 73 (1955) 986
- HEWITT H H and WILSON C W. A survival curve for mammalian leukaemia cells irradiated in vivo (implication for the treatment of mouse leukaemia by whole body irradiation) Brit J Cancer 13 (1959) 69
- KALLMAN R F, SILINI G and FRINDEL E. Recuperation in mammalian cell systems as revealed by radiation dose fractionation Jap J Genet 40 (1964) 207
- NIAS A H W. Some comparisons of fractionation effects by erythema measurements on human skin Brit J Radiol 36 (1963) 183
- PICK F T and MARCUS P I. Action of  $\gamma$  rays on mammalian cells J exp Med 103 (1956) 603
- SILINI G and HORNSEY S. Effetto dei neutroni e dei raggi  $\gamma$  sulle cellule dei tumori di Ehrlich (In Italian) Tumori 1 (1964) 3
- and METALLI P. Preliminary results from a split dose experiment on late effects of ionizing radiation in the mouse. Data on life span shortening In Radiation and ageing p 207 Taylor & Francis London 1966
- SPRING E and HOLMBERG P. Evaluation of experimental irradiation fractionation with the single hit multi target model Acta radiol Ther Phys Biol 7 (1968) 207
- STRANDQVIST M. Studien über die kumulative Wirkung der Röntgenstrahlen bei Fraktionierung. Erfahrungen aus dem Radiumhemmet an 280 Haut- und Lippenkarzinomen Acta radiol (1944) Suppl No 55
- TRONIER H. Bestimmung der Hautfarbe unter besonderer Berücksichtigung der Erythem und Pigmentmessung Strahlentherapie 121 (1963) 392
- TRUCCHI O. L'eritema da elettroni veloci (In Italian) Nunt radiol (Roma) 11 (1960) 922

## THYROID RADIONUCLIDE UPTAKE MEASUREMENTS

Report of a panel of experts of the International Atomic Energy Agency

Tests of thyroid function based on measurements of the uptake of radioiodine by the gland (thyroid uptake tests) constituted one of the first diagnostic applications of radioactive tracers and have been widely used in the diagnosis and investigation of thyroid diseases. In 1960 the International Atomic Energy Agency (IAEA) invited a group of consultants to draw up a standardized procedure for such uptake measurements. The recommendations of this group herein referred to as the 1960 recommendations related primarily to measurements of the uptake of  $^{131}\text{I}$  24 hours after its oral administration—the basis of the thyroid uptake most commonly performed in 1960—and were published in a number of scientific journals (IAEA 1961, 1962).

During the ensuing decade thyroid uptake tests underwent considerable development. New radionuclides were utilized, new instruments and techniques for the measurement of uptake were devised, and an increasing emphasis was placed on tests based on uptake measurements made relatively soon after administration of the radioactive tracer. Parallel development took place in tests involving the use of radionuclides but based on measurements of parameters other than uptake. In view of these advances, IAEA decided in 1970 to convene a second panel of experts to review the status of thyroid uptake tests and to update and where necessary amend the 1960 recommendations.

The Panel, whose report follows, met at IAEA Headquarters, Vienna, from 17 to 21 May 1971. It comprised Dr W. B. Alexander (U.K.), Prof. C. Beckers (Belgium), Dr B. Bok (France), Dr H. I. Glass (U.K.), Dr S. Grebe (Federal Republic of Germany), Mr C. C. Harris (U.S.A.), Prof. R. Hofer (Austria), Prof. H. Kakehi (Japan), Dr M. P. Koenig (Switzerland), Dr P. Parakevoulakis (U.S.A.), Dr J. G. Shimmings (U.K.) and Dr H. N. Wellman (U.S.A.). Drs G. Gomez Crespo and E. Komarov attended the meeting.

as representatives of the World Health Organization Prof K. E. Scheer and Drs E. H. Belcher and R. G. Daou of the IAEA Secretariat also participated. Drs Belcher and Daou acting as Scientific Secretaries.

## 1 Clinical Requirements for uptake tests

### 1.1 General considerations

1.1.1 The panel recognized that whilst thyroid uptake tests have been widely practised in the diagnosis and investigation of thyroid disorders no single test of thyroid function is applicable in all circumstances (FRAGU *et coll* 1971). There is increasing evidence that the best screening tests for hypo or hyperthyroidism are those related to the level of circulating thyroid hormone or more specifically to the level of free thyroxine—for example a determination of serum thyroxine in conjunction with an *in vitro* tri-iodothyronine uptake test (GREFE & DOFFP 1970, 1971). Thyroid uptake tests remain valuable however whenever detailed investigation of the thyroid function is required. They are also useful in the follow up of drug treated hyperthyroid patients and patients with non-toxic goitre and in the determination of dosage for radioiodine therapy.

1.1.2 The panel noted that whereas paragraph 4.2 of the 1960 recommendations states 'Uptake measurements of less than 2 hours are not recommended as a routine procedure' uptake tests based on such measurements being described as early tests based on much earlier measurements are now widely practised. The advent of such tests has rendered the word early a subject of confusion. The panel therefore recommended that the designation early uptake tests should henceforth be restricted to tests based on measurements made up to about 30 minutes after intravenous administration of the tracer such as those made with  $^{99}\text{Tc}^{\text{m}}$  in the form of pertechnetate the uptake of which reflects principally the iodide trapping function of the thyroid. Tests made at 2 hours or later such as those made with radioisotopes of iodine in the form of iodide the uptake of which reflects principally the iodine binding function of the thyroid progressively modified by secretion of thyroid hormone should be designated late uptake tests.

1.1.3 A list of the radionuclides in current use in thyroid uptake tests and their more important physical characteristics is given in the Table. The panel drew attention to the fact that preparations of radionuclides used in uptake tests should conform to specifications for the quality control of pharmaceutical preparations laid down in the International Pharmacopoeia (WHO 1967, 1971) and in national pharmacopoeias. The choice of radionuclide, the administered radioactivity and the time at which uptake is measured will be influenced by clinical considerations (e.g. type of disease to be recognized, resulting radiation dose to the patient, type of therapy to be prescribed) as well as by the measurement equipment available. The need to perform other simultaneous or subsequent tests (e.g. tri-iodothyronine suppression test, thyroid scan) will also influence the choice of radionuclide, the administered radioactivity and the time at which uptake is measured.

### 1.2 Early uptake tests

The panel noted the increasing emphasis being placed on early uptake tests based on measurements made up to about 30 minutes after intravenous administration of  $^{99}\text{Tc}^{\text{m}}$  in the form of pertechnetate. In most clinical situations the results of early uptake tests

**Table**  
*Radionuclides used in thyroid uptake measurements*

Rad o nuclide	Type of tran sition**	Half life	Energies of princ pal radiations (keV) (with mean numbers per disintegration)**			Resulting radiation dos to adult thyro d (mrad/ $\mu$ Ci administered)***
			Particles	Photons		
$\text{Fe}^m$	IT	6 h	Conv	119 (0.09)	140 (0.88)	0.2
$^{131}\text{I}$	EC	13 h	Conv	127 (0.13)	159 (0.83)	16
					rtg 27-31 (0.87)	
I	EC	60 d	Conv	33 (0.08)	35 (0.07)	1.120
				31 (0.11)	rtg 27-31 (1.36)	
I	$\beta^-$	80.5 d	$\beta^-$	192 (0.90)	640 (0.07)	1.520
				95 (0.07)	360 (0.83)	
I	$\beta^-$	2.3 h	$\beta^-$	836 (0.18)	1398 (0.09)	17
				669 (0.06)	1280 (0.06)	
				607 (0.09)	955 (0.21)	
				412 (0.20)	773 (0.83)	
				337 (0.18)	671 (0.07)	
				305 (0.05)	668 (0.99)	
				266 (0.08)	630 (0.08)	
				234 (0.16)	670 (0.08)	
					573 (0.17)	

IT isomeric transition

EC electron capture

\* mean energies

Conv conversion electron

Data from DILLMAN (1969-1970)

\* Data from GOOLDEN et al (1968). The calculations are based on a maximum uptake of 30% of a gland mass of 25 g and equivalent radius of 1.81 cm, a biologic half life of 138 days and a half period of uptake of 5 hours. The value is assumed free of  $^{131}\text{I}$  and other radionuclides impurities.

with  $^{99m}\text{Tc}$  correlate well with those of late uptake tests and the two are of approximately equal value for the recognition of hyperthyroidism (SIMPSON et al 1967). Early uptake tests with  $^{99m}\text{Tc}$  are unique in that during therapy with anti-thyroid drugs of the thiouracil type they give results which reflect the underlying functional state of the thyroid gland as distinct from the rate of thyroid hormone production. This is because the early uptake of  $^{99m}\text{Tc}$  reflects principally the iodide trapping function of the thyroid whilst these anti-thyroid drugs affect the later iodine binding functions. A further advantage of  $^{99m}\text{Tc}$  is that its use makes it possible to perform an uptake measurement and a thyroid scan with a radiation dose to the patient about 1/1000 of that from  $^{131}\text{I}$ . These tests are unsuitable however for the diagnosis of hypothyroidism.

### 1.3 Late uptake tests

The panel noted that in contrast to early uptake tests late uptake tests based on measurements made 2 hours or more after administration of the tracer have undergone little development in recent years. Such tests can be used for the diagnosis of both hypo- and hyperthyroidism but their main value lies in the diagnosis of the former condition for which purpose they cannot be replaced by early uptake tests. They find a further application in the determination of dosage for radioiodine therapy.

### 1.4 Stimulation suppression and discharge tests

The panel noted that these variants of simple uptake tests may be based on either early or late uptake measurements or both. Suppression tests can successfully be based on  $^{99}\text{Tc}^{\text{m}}$  uptake measurements even at low uptake levels (GOOLDEN *et coll* 1971). However  $^{99}\text{Tc}^{\text{m}}$  is unsuitable for discharge tests and only radioiodine should be used for this purpose.

### 1.5 Factors influencing the results of thyroid uptake tests

The panel drew attention to a number of clinical conditions and extraneous factors which can influence and so lead to the misinterpretation of the results of uptake tests. A brief summary of these conditions and factors is given below.

#### *Causing increased uptake*

Stimulation of the hypothalamus—pituitary feedback mechanism

- 1 after therapy with antithyroid drugs of the thiouracil type which lead to low levels of circulating thyroid hormone
- 2 after subtotal thyroidectomy or radioiodine therapy
- 3 after recent therapy with glucocorticoids

Decrease of extrathyroidal or intrathyroidal iodide pool

- 1 during or after low dietary intake of iodine or in other iodine deficiency states
- 2 after subtotal thyroidectomy or radioiodine therapy

#### *Causing decreased uptake*

Depression of the hypothalamus—pituitary feedback mechanism

- 1 during therapy with thyroxine tri-iodothyronine or thyroid extracts
- 2 during prolonged therapy with salicylates phenylbutazone and related drugs at high dosage

Increase of extrathyroidal or intrathyroidal iodide pool

- 1 during high dietary intake of iodine
- 2 during therapy with iodine containing drugs
- 3 after administration of iodine containing roentgen contrast media

When the measured uptake expressed as a percentage of the administered tracer is difficult to interpret determination of the absolute iodine uptake in  $\mu\text{g/h}$  may prove helpful (ALEXANDER *et coll* 1967 BECKERS *et coll* 1967 1969 WOLFF 1969).

## 2 Early uptake measurement techniques

### 2.1 Choice of radionuclide

The panel noted that since pertechnetate is trapped by the thyroid in a similar manner to iodide but is not organically bound the uptake of  $^{99}\text{Tc}$  administered in this form

provides an index of the iodide trapping function of the gland independent of its iodine binding function (DEGROSSI et coll 1965 ARATIS & RICHARDS 1968). The uptake is progressively affected by the return of the radionuclide to the circulation from the thyroid but a single measurement of uptake at 20 minutes has been shown to give a satisfactory index of trapping (ANDROS et coll 1965 SHIMMINS et coll 1967 DE GARRETA et coll 1968 SHIMMINS et coll 1969). Kinetic investigations with radioiodine in the form of iodide can be used to determine both iodine trapping and binding but these require sequential measurements extending over at least 2 hours the period needed in order to obtain data which accurately define the shape of the uptake curve (ROBERTSON et coll 1971). Such investigations have so far been carried out with  $^{131}\text{I}$ . The isotope  $^{131}\text{I}$  has more suitable physical characteristics for the purpose but is not yet generally available.  $^{127}\text{I}$  and  $^{129}\text{I}$  are less satisfactory (GOOLDEN et coll 1968 WELLMAN et coll 1971).

## 2.2 Choice of measurement technique

2.2.1 The panel noted that the basic problem in early uptake measurements is the correction of the data for the effect of extrathyroidal radioactivity which may be of the same order as that in the thyroid itself (HILDITCH et coll 1967). Such corrections are most readily applied if the uptake is measured by means of a moving detector or stationary-detector imaging device the output of which is in digital form (SHIMMINS et coll 1967 DE GARRETA et coll 1968). As regards moving-detector devices either a single or dual-detector scanner may be used (WILLIAMS et coll 1972). Profile scanning techniques can also be used to obtain data which can be analyzed so as to take into account the extrathyroidal radioactivity (TOMMEL & GALT 1971). If only an indication of changes in uptake relative to an earlier value is required as in the follow up of patients undergoing drug treatment for hyperthyroidism in whom large changes in uptake reflect the course of treatment simple measurements of uptake with a fixed detector such as is used in late uptake measurements may be sufficient (SHIMMINS et coll 1971). For quantitative  $^{99}\text{Tc}^m$  measurements the following technique (WILLIAMS et coll 1972) which makes use of a single-detector scanner can be expected to yield satisfactory results.

2.2.2 *Administration of tracer* An amount of 0.5–1 mCi of  $^{99}\text{Tc}^m$  in the form of pertechnetate is administered by intravenous injection. The injection should be completed in less than 10 seconds to minimize errors in timing.

2.2.3 *Measurement of injected radioactivity* The count corresponding to the injected radioactivity may be determined by measuring with a scaler the counting rate due to the injected radioactivity in the injection syringe placed at a known distance from the detector of the scanner the collimator being removed for this measurement. Alternatively an aliquot of the dose solution may be scanned in a suitable phantom. If the former procedure is adopted it may be necessary to use a shield or employ other means to ensure that the measured counting rate is not excessive. Whichever procedure is adopted care must be taken that errors are not introduced by changes in technique (e.g. by using a different type of syringe). An appropriate calibration factor must be introduced into the subsequent calculations.



**2.2.4 Time of measurement of uptake** The most suitable time for measurement of uptake is 20 minutes at which time uptake will usually have reached a maximum. Conditions are accordingly arranged so that the interval between the injection and the mid time of the scan is 20 minutes.

**2.2.5 Measurement of uptake** Uptake is measured by counting the individual dots on a scan of the thyroid region. Any moving detector scanner normally used for thyroid imaging and equipped with a dot tapper is suitable for such measurements. The only operating condition which normally has to be changed is the dot factor which should be adjusted so that the individual dots are clearly visible. The detector resolution (full width at half maximum) should be better than 10 mm in the focal plane of the collimator which should lie about 2.5 cm below the skin of the patient. The scan area should be not less than 15 cm × 15 cm. The scanner speed and line spacing should be arranged so that the scan is completed in less than 5 minutes. The pulse height analyzer should be set to accept events within the entire total absorption peak (120–170 keV). It should be noted that these operating conditions may not be suitable for conventional scanning so that a further scan under different conditions may be necessary if an image is required for diagnostic purposes.

**2.2.6 Correction of data for extrathyroidal radioactivity** The scan is divided into two or more areas, one of which contains the entire thyroid image and the total number of dots in each area is counted by means of a simple hand-operated counter. The corrected dot count due to the thyroid is then determined by subtracting from the dot count in the area containing the thyroid image that in neighbouring area(s) above or below this area due allowance being made for the relative sizes of the areas. The extrathyroidal area(s) should be chosen to exclude the region of the submandibular salivary glands and any other regions of high radioactivity. Corrections for extrathyroidal radioactivity based on measurements over the thigh or on the use of lead filters should not be used in this technique.

**2.2.7 Calculation of results** The determination of uptake requires the expression of the dot count due to the thyroid, corrected for extrathyroidal radioactivity, in terms of the count corresponding to the injected radioactivity. Corrections must be applied for the depth of the thyroid in the neck of the patient and for the physical decay of the tracer between the time when the injected radioactivity is measured and the time when the scan is performed. Provided that the depth of focus of the collimator is adequate it is not necessary to make individual corrections for variations in thyroid depth, it being sufficient to use an average depth of 2.5 cm for this purpose. The time spent over each area within which dots are counted must be known. If necessary, corrections for variation in scanning speed should be applied. Since some dots due to radioactivity in the thyroid lie far outside the thyroid image, the corrected count will vary slightly with the size of the chosen area containing the thyroid image. If a calibration curve relating the corrected count to the size of this area is prepared, a correction may be applied for this effect, otherwise relative errors of up to 10 per cent may be introduced (WILLIAMS *et al.* 1972). The percentage uptake is calculated from the relationship

$$U = \frac{100 D (\lambda - RB)}{Ck e^{-\lambda t}}$$

where

- $U$  = uptake (per cent injected radioactivity)  
 $D$  = dot factor  
 $A$  = dot count in area containing thyroid image  
 $N$  = ratio of area containing thyroid image to extrathyroidal area(s)  
 $E$  = dot count in extrathyroidal area(s)  
 $C$  = counting rate due to injected radioactivity in injection syringe  
 $K$  = ratio of dot count from scan of given radioactivity in suitable phantom multiplied by dot factor to counting rate due to same radioactivity in injection syringe (calibration factor)  
 $f$  = correction for radioactive decay between time of measurement of injected radioactivity and time of scan

### 3 Late uptake measurement techniques

#### 3.1 Introduction

Techniques for late uptake measurements were the subject of the 1960 recommendations which related primarily to measurements of the uptake of  $^{131}\text{I}$  with a single fixed detector 24 hours after administration of the tracer. The panel discussed the continuing applicability of these recommendations and while recognizing that radionuclides other than  $^{131}\text{I}$  and techniques for the measurement of uptake other than those using a single fixed detector are now also employed in late uptake tests considered that the general principles of the 1960 recommendations hold good in the situations to which these recommendations are relevant. Though not universally adopted the recommendations still seem desirable and useful as a means of promoting systematic and disciplined measurements. The panel drew attention however to a number of points in the recommendations where there have been changes in validity, emphasis or applicability.

#### 3.2 Choice of radionuclide

The panel noted that  $^{131}\text{I}$  is still the most widely used radionuclide for late uptake tests. A tracer dose of up to  $10\ \mu\text{Ci}$  of  $^{131}\text{I}$  as specified in the 1960 recommendations is still appropriate for uptake measurements on adults but is not suitable for children because of the high radiation dose to the patient with this radionuclide. Oral administration of an aqueous solution of  $^{131}\text{I}$  in the form of sodium iodide is still the preferred means of administration, though capsules containing  $^{131}\text{I}$  may be used. With the latter it is important that the amount of stable iodide in the capsule and its contents should not exceed  $1\ \mu\text{g}$ . Because of its shorter half life and other physical characteristics  $^{131}\text{I}$  can be administered in comparable amounts with much lower radiation dose to the patient and whilst this radionuclide is not yet generally available it could be used with considerable advantage in late uptake tests (GOOLDEN et coll 1968, WELLMAN et coll 1969, 1971). The radiation dose to the patient with  $^{131}\text{I}$  is also much less than with  $^{131}\text{I}$  but the short half life of  $^{131}\text{I}$  contra-indicates its use for uptake measurements later than 24 hours after administration (GOOLDEN et coll 1968). Moreover the high energies of its gamma photons necessitate the use of cumbersome detectors with heavy collimators. The isotope  $^{125}\text{I}$  is not in widespread use for uptake measurements largely because of the low energies of its x-ray and gamma photons (GOOLDEN et coll 1968). The mean radiation dose to the patient with  $^{125}\text{I}$  is also lower than that with  $^{131}\text{I}$  but its biologic effects may be disproportionate to the actual absorbed dose (FEINENDEGEN et coll 1971, FEIGE et coll 1971, LEWIS et coll 1971).

### 3.3 *Choice of measurement technique use of single fixed detector*

3.3.1 The panel noted that the use of a single fixed detector as specified in the 1960 recommendations remains the most widely used technique for late uptake measurements.

3.3.2 The panel noted that the 1960 recommendations allowed the use of a scintillation counter or a Geiger Muller counter as the detector and did not insist on the use of an energy selective counting technique. Since these recommendations were written there has been a widespread increase in the use of scintillation counter systems incorporating facilities for energy selective counting for uptake measurements. In photo peak or total absorption peak counting the role of the neck phantom in simulating radiation scattering conditions in the neck of the patient is less significant and the configuration of the phantom is less critical. The 15 cm × 15 cm phantom specified in the 1960 recommendations and the 12.7 cm × 12.7 cm phantom specified by the Oak Ridge Institute of Nuclear Studies (BRICER 1959) may then be equally acceptable. Indeed under these conditions a neck phantom is not necessary at all as long as an appropriate factor is used to correct the data for attenuation of primary gamma photons in the neck tissues.

3.3.3 The panel noted that the statement in the 1960 recommendations that the volume of the standard should be comparable to the volume of an average sized thyroid gland (30 ml) had met with criticism particularly in countries where capsules were in widespread use. There appears to be no universally acceptable configuration for the standard. Provided that an energy selective counting technique is employed moderate changes in its size or shape do not significantly affect the accuracy of measurement. A standard in the form of a capsule may then be quite acceptable. There is a need however for special procedures for measurements on children. For such purposes the use of a smaller standard in an adult neck phantom is not satisfactory.

3.3.4 The panel considered that the minimum detector crystal size (2.5 cm × 2.5 cm) and the collimator characteristics specified in the 1960 recommendations are still appropriate. Collimators designed to meet these specifications with  $^{131}\text{I}$  cannot however be expected to have a corresponding performance with radionuclides emitting photons of higher energy (e.g.  $^{137}\text{I}$ ).

3.3.5 The panel noted that whilst the lower sensitivity of the Geiger Muller counter makes it unsuitable for routine uptake measurements it is still useful for measurements on patients undergoing radioiodine therapy.

3.3.6 The panel recognized that correction of the measured uptake for the contribution from extrathyroidal radioactivity is necessary in uptake measurements at 24 hours but becomes progressively less important with the passage of time and may be unnecessary at 24 hours. Two methods for estimating this contribution are in current use: measurement of thigh radioactivity as described in the 1960 recommendations and measurement of neck radioactivity with a lead block (B filter) covering the thyroid as specified by the Oak Ridge Institute for Nuclear Studies (BRICER 1959). Both have been found satisfactory provided energy-selective counting techniques are employed (GOMEZ CRESPO & VETTER 1966).

### 3.4 *Other measurement techniques*

3.4.1 The panel recognized that since the 1960 recommendations were drawn up several other acceptable but somewhat more elaborate techniques for late uptake measurements have been developed. However these techniques require equipment which may only be available in certain centres and they are only recommended for use in special investigations.

**3.4.2 High sensitivity techniques** The panel recognized that it is most desirable to limit the radiation dose to the patient in tests on children and pregnant women. This may be achieved by the use of high sensitivity measurement techniques involving the use of large scintillation counters placed close to the neck in a favourable geometric relationship with the thyroid (WELLMAN et coll 1967 SCHULTZ & ROLLO 1970). A further gain in sensitivity is achieved if the measurements are carried out inside a whole body counter shield (LALZER & EISENBLOD 1963). By these means the amount of tracer to be administered may be reduced by a factor of 1000. The same techniques may be applied in the measurement of small amounts of radioiodine in accidentally or occupationally exposed individuals. However the sensitivity of the detector system used is dependent on the depth of the thyroid in the neck, and a correction for depth must be made to each individual measurement. One method devised for making such corrections involves measuring the counting rate with the detector system at two different distances from the body surface (SCHULTZ & ROLLO 1970). Another involves measuring in two different regions of the photon spectrum (WELLMAN et coll 1967 ESPINASSE et coll 1969).

**3.4.3 Scintigraphic techniques** Techniques analogous to those described for early uptake measurements using a moving-detector or stationary detector device the output of which is in digital form may be used for late uptake measurements (HILGREN et coll 1967 TALICE 1969). With such measurements these techniques offer the advantage that it is usually possible to obtain a satisfactory image concomitantly with the uptake measurement.

**3.4.4 Profile scanning and whole body counting techniques** Profile scanning and whole body counting techniques also find applications in late uptake measurements in particular in patients with thyroid carcinoma in whom uptake may occur in metastases remote from the thyroid region (TOTHILL & GALT 1971).

A limited number of sets of the working papers considered by the panel are available on request from the Medical Applications Section, International Atomic Energy Agency, P. O. Box 990, A-1011 Vienna, Austria.

## SUMMARY

This report was drawn up by a panel of twelve experts convened by the International Atomic Energy Agency in May 1971 to review the status of tests of thyroid function based on measurements of the uptake of a radioactive tracer by the gland (thyroid uptake tests). The report updates and where necessary amends the recommendations of a group of consultants convened by the Agency in 1960 to draw up a standardized procedure for thyroid radioiodine uptake measurements. A distinction is made between early uptake tests based on measurements made up to 30 minutes after administration of the tracer which reflect primarily the iodine trapping function of the thyroid gland and late uptake tests based on measurements made 2 hours or more after its administration which reflect primarily the iodine binding function of the gland. The usefulness of tests of each type is assessed, their requirements are detailed particularly as regards choice of radionuclide and choice of measurement technique and consideration is given to clinical conditions and extraneous factors which can lead to the misinterpretation of the results obtained.

## ZUSAMMENFASSUNG

Dieser Bericht wurde von einer Gruppe von zwölf Experten verfasst die auf Einladung der Internationalen Atomenergie Organisation im Mai 1971 den derzeitigen Stand der für die Schilddrüsenfunktion verwendeten und auf der Messung der Speicherung von radioaktiven Indikatoren in der Drüse (Schilddrüsen Speichertest) beruhenden Tests überprüfte. Der Bericht ergänzt und revidiert die Empfehlungen die eine von der IAEA im Jahre 1960 einberufene Expertengruppe zur Festlegung eines Standardverfahrens zur Messung radioaktiver SchilddrüsenSpeicherung ausgearbeitet hatte. Es wird unterschieden zwischen initialen Aufnahmetests welche auf Messungen beruhen die innerhalb 30 Minuten nach Verabreichung des Indikators durchgeführt werden und hauptsächlich die Jodidspeicherefunktion der Schilddrüse wiedergeben und Spataufnahmetests welche auf Messungen beruhen die zwei oder mehr Stunden nach Verabreichung erfolgen und hauptsächlich die Jodbindungsfunktion der Drüse wiedergeben. Die Zweckmassigkeit der beiden Tests wird diskutiert ihre Voraussetzungen im Detail angeführt besonders was die Wahl der Radionuklide und der Messtechnik betrifft. Klinische Bedingungen und aussere Faktoren die zu einer möglichen Fehlinterpretation der Ergebnisse führen können werden behandelt.

## RÉSUMÉ

Le present rapport a été rédigé par un groupe de douze experts qui s'est réuni en mai 1971 sous les auspices de l'Agence internationale de l'énergie atomique pour étudier l'état des connaissances touchant les examens de la fonction thyroïdienne fondés sur la mesure de la fixation d'un radionucléide par la glande (tests de fixation thyroïdienne). Le rapport met à jour en le modifiant parfois les recommandations d'un groupe de consultants qui avait été organisé par l'Agence en 1960 afin d'élaborer une méthode normalisée de mesure de la fixation du radioiode par la thyroïde. Il établit une distinction entre les tests de fixation précoces fondés sur des mesures effectuées jusqu'à 30 minutes après administration de l'indicateur qui correspondent essentiellement à la captation de l'iodure par la thyroïde et les tests de fixation tardifs fondés sur des mesures effectuées 2 heures ou plus après administration de l'indicateur qui correspondent essentiellement à la fixation de l'iode par la glande. Le rapport analyse l'intérêt de ces sortes de tests, précise les critères auxquels ils doivent satisfaire, notamment le choix du radionucléide et celui de la méthode de mesure et indique les conditions cliniques et les facteurs étrangers qui peuvent mener à une interprétation erronée des résultats obtenus.

## REFERENCES

- ALEXANDER W. D., KOUTRAS D. A., HARDEN R. McG. and WAYNE E. J. Quantitative studies of iodine metabolism in thyroid diseases. *Quart J Med* 31 (1962) 281.
- ANDROS G., HARPER P. V., LATHROP K. A. and McCARDLE R. J. Pertechnetate 99m Tc localization in man with applications to thyroid scanning and the study of thyroid physiology. *J clin Endocr* 25 (1965) 1067.
- ATKINS H. L. and RICHARDS P. Assessment of thyroid function and anatomy with technetium 99m as pertechnetate. *J nucl Med* 9 (1968) 7.
- BECKERS C., BARZELATTO J., STEVENSON C., GIANETTI A., PARDO A., BOBADILLA E. and DE VISSCHER M. Endemic goitre in Pedregoso (Chile). II. Dynamic studies on iodine metabolism. *Acta endocr (Kbh)* 54 (1967) 591.

- VAN YPERSELE DI STRIHOU C COCHE E TROCH R and MALVAET P Iodine metabolism in severe renal insufficiency *J clin Endocr* 29 (1969) 293
- BRUCER M Thyroid radioiodine uptake measurements A standard system for universal intercalibration USAEC Rep ORINS 19 (1959)
- DE GARRETA A C GLASS H I and GOOLDEN A W G Measurement of the uptake of  $^{131}\text{I}$  by the thyroid *Brit J Radiol* 41 (1968) 896
- DEGROSS O GOTTA H OLIVARI A PECORINI V and CHWOJNIK V Possibilities of using  $^{99\text{m}}\text{Tc}$  in place of radioiodine in thyroid function studies *Nucl Med (Stuttg)* 4 (1965) 383
- DILLMAN L T Radioactive decay schemes and nuclear parameters for use in radiation-dose estimation Medical Internal Radiation Dose Committee Pamphlet No 4 *J nucl Med* 10 (1969) Suppl No 2 p 5
- Radioactive decay schemes and nuclear parameters for use in radiation-dose estimation Part 2 Medical Internal Radiation Dose Committee Pamphlet No 6 *J nucl Med* 11 (1970) Suppl No 4 p 5
- ESPINASSE P CHASTANIER P and LAHVEGHE B Thyroid uptake measurement using iodine 125 and iodine 131 *Phys in Med Biol* 14 (1969) 27
- FEIGE Y GAVRON A LUBIN E LEWITUS Z BEN PORATH M GROSS J and LOEWINGFR E Local energy deposition in thyroid cells due to the incorporation of  $^{131}\text{I}$  *In Biophysical aspects of radiation quality* p 383 IAEA Vienna 1971
- FEINENDEGEN L E ERTL H H and BOND V P Biological toxicity associated with the Auger effect *In Biophysical aspects of radiation quality* p 419 IAEA Vienna 1971
- FRAU P THOLIN A BAZIN J P et TUBIANA M Comparaison de la valeur diagnostique de différents tests fonctionnels thyroïdiens Intérêt de l'utilisation des fonctions discriminantes *Ann Endocr (Paris)* (in press)
- GOMEZ CRISPO G and VETTER H The calibration and standardization of thyroid radioiodine uptake measurements *Int J appl Radiat* 17 (1966) 531
- GOOLDEN A W G GLASS H I and SILVESTER D J The choice of a radioactive isotope for the investigation of thyroid disorders *Brit J Radiol* 41 (1968) 20
- and WILLIAMS E D The use of  $^{99\text{m}}\text{Tc}$  for the routine assessment of thyroid function *Brit med J* 4 (1971) 396
- GREBE S F und DOEPP M Der Nachweis des wirksamen Jodhormonspiegels im Blut mit dem T7 index *Ges f Nuklearmed* Mitt 3 (1970)
- The determination of thyroxine in blood with the T3 and T4 test value *Int J appl Radiat* (in press)
- HILDITCH T E GILLESPIE F C SHIMMINS J HARDEN R MCG and ALEXANDER W D A study of extrathyroidal neck radioactivity using a radioisotope scanner *J nucl Med* 8 (1967) 810
- IAEA Calibration and standardization of thyroid radioiodine uptake measurements Recommendations drawn up at a consultants meeting convened by the International Atomic Energy Agency Acta isotop (Padova) 1 (1961) 309 Minerva nucl. 5 (1961) 4 *Brit J Radiol* 35 (1962) 205 *Int J appl Radiat* 13 (1962) 167 *Acta über radiol-cancer* 17 (1962) 183 *Acta radiol* 100 (1962) 233 *Ann radiol* 5 (1962) 731 *J belge Radiol* 45 (1962) 511
- LAUER G R and EISENBUD M Low level *in vivo* measurements of iodine 131 in humans *Health Phys* 9 (1963) 401
- LEWITUS Z BEN PORATH M FEIGE Y LUBIN E RECHNIG J and LAUR V Differences in the radiobiological action of  $^{131}\text{I}$  and  $^{125}\text{I}$  in the thyroid cell *In Biophysical aspects of radiation quality* p 405 IAEA Vienna 1971

- ROBERTSON J W K SHIMMINS J HORTON P W LAZARUS J H and ALEXANDER W B  
Determination of the rates of accumulation and loss of iodide and of protein binding of iodine in the human thyroid gland *In* Dynamic studies with radioisotopes in medicine p 199 IAEA Vienna 1971
- SCHULTZ A G and ROLLO F D A method for measuring radioiodine uptake which corrects for thyroid depth *J nucl Med* 11 (1970) 508
- SHIMMINS J G HARDEN R McG and ALEXANDER W D Loss of pertechnetate from the human thyroid *J nucl Med* 10 (1969) 637
- HILDITCH T HARDEN R McG and ALEXANDER W D Thyroidal uptake and turnover of the pertechnetate ion in normal and hyperthyroid subjects *J clin Endocr* 28 (1967) 575
- ALEXANDER W D McLARTY D G ROBERTSON J W K and SLOANE D  $^{99m}\text{Tc}$  per technetate for measuring thyroid suppressibility *J nucl Med* 12 (1971) 51
- TAUXE W N Estimation of thyroid uptake from digitized scintiscan matrices *J nucl Med* 10 (1969) 258
- TOTTHILL P and GALT J M Quantitative profile scanning for the measurement of organ radio activity *Phys in Med Biol* 16 (1971) 625
- WHO Specifications for the quality control of pharmaceutical preparations International pharmacopoeia 2nd ed WHO Geneva 1967 2nd ed Suppl WHO Geneva 1971
- WELLMAN H N MACK J F and SODD V J Production and clinical development of a new ideal radioisotope of iodine iodine 123 *In* Frontiers in nuclear medicine p 19 Springer Verlag Berlin 1971
- — SAENGER E L and SODD V J Study of the parameters influencing the clinical use of  $^{123}\text{I}$  (abstract) *J nucl Med* 10 (1969) 381
- KEREIAKES J G YEAGER T B KARCHES G T and SAENGER E L A sensitive technique for measuring thyroidal uptake of  $^{131}\text{I}$  iodine *J nucl Med* 8 (1967) 86
- WOLFF J Iodide goiter and the pharmacological effects of excess iodide *Amer J Med* 47 (1969) 101
- WILLIAMS E D GLASS H J GOOLDEN A W G and SATYANANTH S Comparison of two methods of measuring the thyroidal uptake of  $^{99m}\text{Tc}$  *J nucl Med* 13 (1972) 159

## INFLUENCE OF IONIZING RADIATION ON CILIARY CELL ACTIVITY IN THE RESPIRATORY TRACT

by

K. FUJIMURA, C. H. HAKANSSON and N. G. TOREMÄLM

Treatment of malignancy of the mucous membrane of the air passages with ionizing radiation is becoming increasingly more common. This is especially true of mantle irradiation for Hodgkin's disease and bronchial carcinoma which despite improved diagnostic possibilities is still often discovered at such a late stage in its development that radical surgery is impossible. Treatment of such cases by irradiation has been used in spite of the poor prognosis (DEELEY *et coll* 1968) and undesirable side effects (FERNHOLZ & MÜLLER 1969) including fibrosis of the interstitial tissue (DEELEY 1967, HOLSTI & VUORINEN 1967) and decreased pulmonary air entry (JENNINGS & ARDEN 1961, BRADY *et coll* 1965, BOUSLEY *et coll* 1970) as well as atrophic bronchitis. Temporary or permanent changes in the coating of the mucous membrane affect the production of secretion and ciliary function (RUCKES & HOLLSTEIN 1968).

The purpose of the present investigation was experimentally to test *in vitro* the effects of ionizing radiation on the function of the tracheal mucous membrane. This first report will deal with the variations that arise in the beat frequency of the cilia as the dosage of irradiation is increased. The effects of

From the Department of Radiation Therapy, University Hospital, Lund, and the Department of Otorhinolaryngology, Malmö Allmänna Sjukhus, Malmö, Sweden. Submitted for publication 29 November 1971.





A light wire was mounted above a point on the monitor where focussing on the surface reflexes was possible the variations in light intensity were registered with a phototube that further conducted the signals to an integration unit. Clear signals were obtained by the screening of those above 25 Hz which lie outside the range of ciliary frequencies by means of an electrode filter (Krohn Hite type 3550). The signals were then fed into a mingograph (Elema Schonander Mingograf 34 No 140) which has both a direct writing and amplifier output. One channel was used for direct reading of the frequency, the outputs of this channel being fed into the data collector (Medicord Lyrec, Denmark) where they were again removed and conducted back to the Mingograf output with a given time delay and with greater amplification of the oscillations. The amplification proved suitable for comparison with the direct registration. The signals were conducted back further to the data collector from the amplifier of this latter channel and then to an amplifier with an oscilloscope for checking the amplitude (DISA DC-Amplifier 51B01) and to an electronic calculator (Hewlett Packard 5233L). The final stage was to a Facit punch tape for automatic frequency analysis on a data machine. A digital analogue converter (Hewlett Packard 580A) and an ink writer which is necessary for making adjustments may also be included in the system for checking purposes. A converting unit was connected to the system between the frequency counter and the punch tape (omitted however from Fig 1).

The experiments were performed at a temperature of 30° C. The humidity was kept as near 100 per cent as possible to avoid drying out of the mucous membrane. The temperature was checked at the inlet of the humid air into the chamber inside the trachea and at the air outlet the humidity was controlled by means of a psychrometer (Ellab Copenhagen type B19).

The trachea specimen was irradiated by means of a Philips contact therapy apparatus. Factors 50 kV, 2 mA, FSD 40 mm, dose rate 34 R rad/s.

The direct manual analysis was carried out as follows. The frequency and the variations in frequency (cf. HALLANSSON & TOREMÄLM 1971) were counted each second for a period of one minute at five minute intervals during the entire experiment which lasted two to three hours. The mean value of these countings being given as the mean value of the frequency for each five minute period. The mean values for each fifteen minute period together with the standard deviation were considered best suited for accompanying the illustrations now presented.

## Results

*Control experiments* In vitro experiments are always subjected to a decay of the physiologic functions starting at the time of deprivation of the blood supply. The intracellular oxygen is consumed within seconds but for a long period the

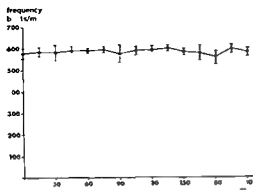


Fig 2 Ciliary beat frequency during constant external conditions. Control experiments

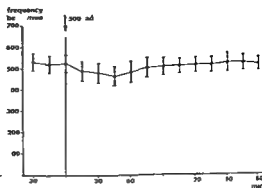


Fig 3 Effect on beat frequency of 500 rad

ciliae surrounded by mucus and moistened air are beating and the underlying smooth muscles change their tone. It is therefore necessary to follow the physiologic activity after preparation in order to determine the suitable duration of an experiment.

The mean values of the ciliated cell frequency during three and a half hours together with the standard deviations are presented in Fig 2, the frequency is between 563 and 598 beats per minute. The frequency usually changes continuously (FUJIWARA *et al.* 1972). The constancy, however, as a whole of the beating ability is proof that frequency may be used as an objective and reliable measure for at least 3 hours. The duration of the experiments was therefore limited to this time.

*Irradiation experiments* The frequency was measured 15 to 30 minutes before irradiation to ensure a steady state being gained.

*Irradiation with 500 rad* The beat frequency per minute before irradiation in this group was  $525 \pm 41$  SD (ME  $100 \pm 3\%$ ) (Fig 3). Irradiation with 500 rad caused the frequency to decrease gradually and fall to a low value of  $472 \pm 44$  per second (ME  $90 \pm 6\%$ ) at 45 minutes. It then began to recover and returned to normal at 105 minutes. The slopes of the initial decrease and increase of beat frequency were  $-0.5$  and  $+0.38$  respectively.

*Irradiation with 3 000 rad* The beat frequency in this group before irradiation was  $509 \pm 29$  (ME  $100 \pm 4\%$ ) (Fig 4). After the exposure of the trachea a decrease in the frequency was immediately observed, the slope being  $-2.5$ . The lowest value was obtained at 60 minutes ( $427 \pm 31$ ) (ME  $77 \pm 6\%$ ), after which it recovered until complete restoration was obtained at 135 minutes.

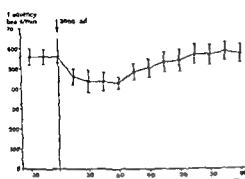


Fig 4 Effect on beat frequency of 3 000 rad

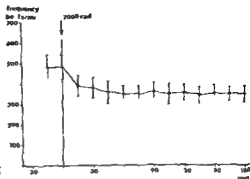


Fig 5 Effect on beat frequency of 7 000 rad

The slopes of increase were calculated to  $+0.4$ . The decrease in beat frequency was more rapid and the total depression effect was higher than that of the group irradiated with 500 rad. Recovery was achieved at a later time.

*Irradiation with 7 000 rad.* The beat frequency before the irradiation was  $486 \pm 58$  per minute (ME  $100 \pm 4\%$ ) (Fig 5). It reached a minimum value of about  $359 \pm 57$  per minute (ME  $74 \pm 6\%$ ) at 45 minutes after irradiation and then held almost constant values of  $350 \pm 53$  (ME  $72 \pm 6\%$ ) to  $358 \pm 45$  (ME  $74 \pm 5\%$ ) per minute. No recovery was observed at 3 hours.

A rapid decrease in the beat frequency was obtained immediately after irradiation, the slope of decrease in this group being almost the same as for the one irradiated with 3 000 rad ( $-2.5$ ).

### Discussion

A temporary reduction in the ciliary beat frequency in a tissue culture of the trachea of an ox after roentgen irradiation with 10 HFD, corresponding to 3 000 to 4 500 rad, was reported by UMEDA (1927). The beat frequency reached the initial value after one hour and continued for at least 8 days. HEINE (1936) performed *in vitro* experiments with roentgen irradiation of the trachea of the rabbit. He stated "11 200 rad was required before any gross effect upon the viability of the ciliated epithelium could be noticed. The author concluded "ciliated epithelium will stand an enormous amount of intense roentgen ray exposure with a maximum of viability."

The present results point at an immediate response with a reversibility to the initial value within one hour and a half for up to 3 000 rad absorbed dose.

## ZUSAMMENFASSUNG

Der Effekt von Röntgenbestrahlung auf die ciliare Bewegungsfrequenz der Trachea des Kaninchens wurde *in vitro* mit einer Lichtreflex-Methode untersucht. Kleine Dosen verursachten lediglich vorübergehende Veränderungen der Schlagfrequenz der Cilien während mit grossen Dosen die Bewegungen vollständig und permanent zum Stillstand gebracht wurden.

## RÉSUMÉ

Les auteurs ont étudié les effets de l'irradiation par les rayons roentgen sur la fréquence des mouvements ciliaires de la trachée de lapin *in vitro* par une méthode d'étude des réflexes à la lumière. Les petites doses ne produisent que des modifications temporaires dans la fréquence des battements des cils mais avec les fortes doses les mouvements sont complètement et définitivement arrêtés.

## REFERENCES

- BOLSHY S. F., HELGASON A. H. and NORTH L. B. The effect of radiation on the lung and bronchial tree. *Amer. J. Roentgenol.* 108 (1970) 284.
- BRADY L. W., GERMON P. A. and GANDER L. The effects of radiation therapy on pulmonary function in carcinoma of the lung. *Radiology* 85 (1965) 130.
- DEELEY T. J. The treatment of carcinoma of the bronchus. *Brit. J. Radiol.* 40 (1967) 801.
- and RICE EDWARDS J. M. Radiotherapy in the management of cerebral secondaries from bronchial carcinoma. *Lancet* 1968 I p. 1209.
- FERNHOLZ H. J. und MÜLLER G. Ergebnisse und Komplikationen der Telekobalttherapie beim Bronchialkarzinom. *Strahlentherapie* 137 (1969) 381.
- FUJIWARA K., HÄKANSSON C. H. and TOREMÄLM N. G. Studies on the physiology of the trachea. VI. Interaction between ciliary beat frequency and transport of secretions. *Ann. Otol.* 81 (1972) 212.
- GOLDBABER G. and BACK A. Studies on radiosensitivity of animal cells *in vitro*. II. Radio sensitivity of muscular and ciliary movement. *Proc. Soc. exp. Biol. (N.Y.)* 48 (1941), 150.
- HÄKANSSON C. H. and TOREMÄLM N. G. Studies on the physiology of the trachea. I. Ciliary activity indirectly recorded by a new light beam reflex method. *Ann. Otol.* 74 (1965) 954.
- — Ciliary activity recorded by TV monitor and phototube. *Acta oto-laryng.* 71 (1971) 508.
- HEINE L. H. The effect of radiation upon ciliated epithelium. *Ann. Otol.* 45 (1936) 60.
- HENSHAW P. S. Peculiar growth lesions in frogs induced by irradiation of sperm cells with X-rays. *J. nat. Cancer Inst.* 3 (1943) 409.
- HOLSTI L. H. and VORONEN P. Radiation reaction in lung after continuous and split-course megavoltage radiotherapy of bronchial carcinoma. *Brit. J. Radiol.* 40 (1967) 280.
- JENNINGS F. L. and ARDEN A. Development of experimental radiation pneumonitis. *Arch. Path.* 71 (1961) 437.
- OCHI D. Studies on the cellular effects by radiations. I. Effects on the cilia movements of  $\beta$  ray irradiation of human and rabbit epithelial cells *in vitro*. *Nippon Acta radiol.* 19 (1959) 135.
- RAJEWSKY M. F. *In vitro* studies of cell proliferation in tumours. *Europ. J. Cancer* 1 (1965) 281.
- RUCKES J. und HOLLSTEIN H. Morphologische Befunde an Trachea und Bronchien nach Betatronbestrahlung von Bronchialkarzinomen. *Strahlentherapie* 136 (1968) 515.
- UMEDA T. The action of light X-ray and radium on the movement of ciliated epithelium (a study in tissue culture method). *Acta derm. (Kyoto)* 10 (1927) 603.

FROM THE DEPARTMENTS OF RADIATION THERAPY (DIRECTOR PROF M LINDGREN) PATHOLOGY (DIRECTOR PROF C M AHLSTRÖM) AND RADIATION PHYSICS (DIRECTOR PROF K. LIDÉN), THE UNIVERSITY HOSPITAL LUND SWEDEN

---

## RADIATION SENSITIVITY OF TISSUES IRRADIATED DURING MANTLE TREATMENT OF HODGKIN'S DISEASE

by

T. LANDBERG, L. BALDETORP, L. G. LINDBERG and GUDRUN SVANEN TAPPER

Mantle treatment has been widely used in recent years for extended field irradiation of supradiaphragmatic Hodgkin's disease. It is hoped that this technique will produce better results than the involved field technique. The value of such improvement may however possibly be reduced by an increased frequency and severity of late adverse effects of radiation, since the mantle field usually includes much more tissue than the involved field treatment.

LANDBERG *et al.* (1971) in a preliminary report reviewed the literature and described some of the side effects of mantle treatment. The sequelae that have attracted most interest are those due to irradiation of the lung tissue, the heart and pericardium, the nervous system and the bone marrow, and to some extent the mucous membranes, the thyroid and connective tissue.

This paper reports autopsy findings in different organs within the irradiated volume in two cases that had received mantle treatment with a split-course technique for Hodgkin's disease. It also reviews the radiation sensitivity of some of these tissues.

---

Submitted for publication 20 April 1972

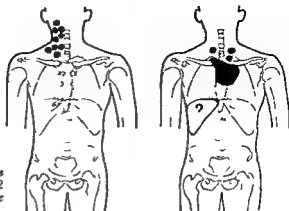


Fig 1 Clinical location of Hodgkin's disease in Case 1 (left) and Case 2 (right) at the beginning of mantle treatment

**Material and Methods** A total of 38 patients received mantle treatment for Hodgkin's disease during the period February 1967 to August 1970. In 32 of these the condition was local, whereas in 6 patients the lesions were widespread. The treatments were given according to the principles described by SVAIRY, TAPPER & LANDBERG (1971). Radiation doses are expressed as absorbed dose (rad) with cobalt 60. For 170 kV roentgen rays (HVL 1.0 mm Cu) the absorbed dose is calculated with RBE for cobalt 60 = 0.85.

Five of the 38 patients had died by August 1970. This report is based on 2 of these patients in whom autopsy was performed.

### Case reports

**Case 1** Female, aged 20 years, who had been operated upon four years earlier for a tumour of the right lung; this was radically excised and proved to be a fibroxanthoma. The present series of examination was undertaken as she had become aware of lumps on the right side of the neck. Biopsy of a node revealed Hodgkin's disease type mixed cellularity. Roentgenography of the chest with tomography of the mediastinum seven months later, apart from postoperative pleural changes, revealed nothing abnormal. Roentgenography of the skeleton, lymphography and phlebography of the inferior vena cava were negative. The bone marrow of the manubrium sterni was normal. Scintigraphy of the liver and spleen revealed no changes. Blood values were normal. Clinically the disease at that time was confined to the lymph nodes on the right side of the neck (Fig 1).

Radiation treatment was given for about three months with the mantle technique with  $^{60}\text{Co}$  in two series. However, for technical reasons, part of the absorbed dose to the right side of the neck was administered with 170 kV roentgen rays. Two thirds of the total absorbed dose was delivered in the first series and the interval between the two series was 33 days. One of the two fields was irradiated at each fraction. The variation in the absorbed dose to the target was smoothed out at the end of the treatment by successive reduction in the field sizes; this dose to the target being 3 800 to 4 600 rad in 23 to 32 fractions over 37 to



Fig. 2 Case 1. Seven months after the beginning of mantle treatment the patient had signs of radiation pneumonitis. New parenchymatous changes paramediastinally within the irradiated lung tissue. Hila retracted upward and trachea displaced to right. Pleural reaction around apex of right lung and slight pleural changes of left lung ventro-basally.

77 days. The absorbed dose in the spinal cord was 3 700 to 4 300 rad and shielded lung tissue received an absorbed dose of 400 to 700 rad.

Seven months after the beginning of mantle treatment the patient had signs of radiation pneumonitis confirmed by roentgenography of the chest (Fig. 2). There was also evidence of pleural thickening on the right side, upward retraction of the pulmonary hilum and displacement of the trachea to the right. The patient was given steroids and broad spectrum antibiotics. Roentgen examination a month later revealed no change in the paramediastinal lung fibrosis or the shrinkage in the superior mediastinum. The radiation pneumonitis ran a protracted clinical course but six months later the patient no longer had symptoms. Spirometry had not been performed immediately before the mantle treatment but eight months later revealed moderately decreased maximal voluntary ventilation suggesting restrictive changes. Apart from evidence of radiation oesophagitis for the first three months after the treatment swallowing was no longer difficult.

About a year later the condition of the patient deteriorated and she developed recurrent fever and anemia. Involvement of the liver and spleen was discovered and there was tachycardia. Electrocardiography revealed a R/S ratio exceeding 1.0 in lead V<sub>1</sub>, which might have denoted right ventricular hypertrophy. The blood pressure was 120/70 mm Hg, no clinical signs of pericarditis. Treatment with Vinblastine was started three months after this but had to be stopped before completion because of pancytopenia. Chest films (Fig. 3) then disclosed moderate shrinkage of the upper parts of the lungs with upward retraction of the





Fig 3 Case 1. Lighten months after beginning of mantle treatment. Treatment for 2 months with Vinblastine. Much paramediastinal pulmonary fibrosis and increasing contraction in the upper part of the mediastinum with marked upward retraction of the hila and displacement of the trachea to the right. Apical changes compared with Fig 2 unaltered.

hila. The marked pleural reaction around both apices persisted. The patient had no signs of adverse radiation effects on the central nervous system or the peripheral nerves. She received blood transfusions and treatment with Procarbazine was started after a few weeks; steroids were also given. Her condition however deteriorated rapidly and she died 19 months after the beginning of the mantle treatment.

Lesions of Hodgkin's disease were present in the lung tissue, liver, spleen and lymph nodes in various regions at autopsy. They were also evident in the bone marrow. Pericarditis and pleuritis were observed and the stomach contained blood from multiple small ulcerations in the lower part of the oesophagus.

**Case 2.** Male, aged 27 years, with four months history of increasing cough. Biopsy of an enlarged lymph node in the left supraclavicular fossa revealed Hodgkin's disease, type lymphocytic depletion (reticular form) and roentgenography (Fig 4) disclosed a diffusely outlined tumour, 10 cm in diameter, in the left of the superior mediastinum. Small parenchymatous changes with atelectasis were present in the adjacent parts of the left upper lobe. The trachea was displaced somewhat to the right. No other abnormality was noted in the lung. Besides the lymphomas in the left supraclavicular fossa, similar masses lay at the right side of the neck. The bone marrow of the manubrium sterni was normal. Scintigraphy of the liver demonstrated slight enlargement of the liver, which extended 6 cm caudally to the costal margin in the mid clavicular line; the hepatic uptake was uneven. Scintigraphy of the spleen indicated nothing abnormal and roentgenography of the skeleton, lymphography and inferior cavography revealed no changes. The disease (Fig 1) was thus confined to lymph nodes on both sides of the neck and the mediastinum and perhaps also to the



Fig 4 Case 2 Roentgenography at beginning of mantle treatment. Mass in left of superior mediastinum causing slight displacement of the trachea to the right. Parenchymatous changes with small atelectases in the tumour adjacent lung mainly in the upper lobe of left lung. The remaining lung and pleura are normal.

liver parenchyma clinically however the hepatic involvement was uncertain and was therefore not considered to contraindicate mantle treatment.

This treatment was given for two months with  $^{60}\text{Co}$  in two series. Two thirds of the total absorbed dose was delivered in the first series and the interval between the two series was 33 days. Both fields were irradiated at each fraction, a beam flattening filter and an individual contour compensating filter of copper was used. The total absorbed dose in the target was 3900 to 4300 rad given in 22 to 24 fractions over 61 to 63 days. The absorbed dose in the spinal cord was 3900 to 4300 rad and the shielded lung tissue received 400 to 700 rad.

Roentgen examination a few weeks later disclosed irradiation effects medially in both upper lobes (Fig 5). The patient gradually felt better but two months later developed pruritus and fever. Roentgenography now revealed pleural effusion on the left side (Fig 6). There were still signs of radiation reactions paramediastinally on the two sides, only parts of the left lung were aerated. Further scintigraphy of the liver indicated definite and more marked changes than before the beginning of treatment. Apart from a low hemoglobin value the blood values were normal. The pleural effusion was treated by pleuracentesis and treatment with Vmblastine was started after a few weeks. Because of supervening leucopenia the chemotherapy had to be modified and sometimes interrupted. The patient felt better for a while but six months later had many superficial lymphomas. He then developed purulent bronchitis with the left side of the thorax almost totally filled with fluid and practically no air in the left lung. A small pleural effusion was present on the right side and the right dome of the diaphragm was elevated by the enlarged liver. The patient was admitted to hospital in poor condition and died 14 months after the beginning of the mantle treatment.



Fig. 5. Case 2. Three weeks after conclusion of treatment. Patient symptom free. Regression of the tumour in the superior mediastinum. New parenchymatous changes at apex of left lung. Both sides display further small apical pleural reactions. Some contrast medium in the tracheal lymph nodes after lymphangiography performed 3 months previously.



Fig. 6. Case 2. Seven months after beginning of mantle treatment. The disease was clinically general. Examination revealed a left pleural effusion and atelectasis at base of left lung. Regression of paramediastinal parenchymatous changes but persistent changes suggesting pulmonary fibrosis. Further regression of tumour in superior mediastinum.

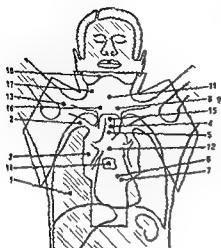


Fig 7 Anatomic sites from which autopsy specimens were obtained 1—lung tissue from base of right lower lobe 2—lung tissue from apex of right upper lobe 3—lung tissue from right hilar region 4—trachea 5—oesophagus 6—myocardium 7—ventral part of pericardium 8—thyroid 9—parathyroid (only Case 2) 10—cerebellum 11—spinal cord (region C6) 12—spinal cord (region Th7) 13—right plexus cervico-brachialis 14—bone marrow from vertebra Th7 15—bone marrow from manubrium sterni 16—skin and subcutaneous tissue from suprasternal region 17—musculus sternocleidomastoideus

Autopsy confirmed Hodgkin's disease in among other tissues the mediastinum pericardium myocardium both lung and the left pleura as well as in the diaphragm the left lobe of the liver the kidneys and the lymph nodes of several regions Apart from stasis the spleen appeared normal

### Autopsy findings

Specimens were obtained for microscopic examination from seventeen different sites within the irradiated volume that had not been clinically involved by Hodgkin's disease at the time of the mantle treatment (Fig 7)

Microscopy revealed extensive growth of malignant tissue in the visceral and parietal linings of the pleural cavity mainly on the left side and in lymph nodes in the mediastinum and hilar regions as well as in the axillae and supraclavicular regions in both cases and in Case 2 in the pericardium as well Several areas of tumour tissue necrosis and large tumour cells of the kind noted after irradiation therapy were present in most sites however vital tumour tissue that might have invaded the area after conclusion of the radiation treatment could be demonstrated

The histology at the different sites indicated in Fig 7 are summarized in the Table

Obvious changes attributed mainly to radiation therapy were present at the apex of the right upper lobe hilar region and in the lymph nodes around the right cervico brachial plexus (2 3 and 13 Fig 7) Marked fibrosis and teleangiectatic capillary vessels occasionally with minor thrombosis and proliferation

**Table**  
*Survey of histologic findings in autopsy specimens*

Histologic changes	Site No (Fig. 7)	Tissue	Absorbed dose (rad) / number of fractions / number of days
Marked and mainly attributable to radia- tion	9	Lung from apex of upper lobe	4000-4400/22-25/61-68
	3	Lung from hilar region	
	13	Tissue around cervico brachial plexus	
Obvious but mainly attributable to factors other than radiation	7	Pericardium	3700-4400/23-32/34-77
	10	Cerebellum	
	11	Cervical spinal cord	
	12	Thoracic spinal cord	
	17	Sternocleidomastoid muscle	
Slight and mainly attributable to radiation	14	Bone marrow from Th 7	4000-4300/24-25/63-68
	15	Bone marrow from sternum	
No changes attri- butable to radiation	4	Trachea	3700-4300/23-28/37-77
	5	Oesophagus	
	6	Myocardium	
	8	Thyroid	
	9	Parathyroid	
	16	Skin and subcutaneous tissue from suprasternal region	
	1	Lung from base of lower lobe	

of the endothelial cells lining the vessels were evident at these sites. Much necrosis was noted as well as scarring, which occasionally resembled the nodular sclerosis type of Hodgkin's disease in areas with tumour growth. The absorbed dose in these regions had been 4 100 to 4 400 rad in 25 fractions over 68 days in Case 1 and 4 000 to 4 300 rad in 22 to 24 fractions over 61 to 63 days in Case 2.

The morphologic examination revealed changes in the pericardium, cerebellum, spinal cord and musculus sternocleidomastoideus (7, 10, 11, 12 and 17, Fig. 7) that must be ascribed mainly to direct effect of the malignant tissue growth or secondary effects such as interference with the vascular supply or drainage from a particular area. Thus mild general oedema of the nervous tissue of the spinal cord may most likely be explained by the extensive malignant growth in the thoracic cavity on the left side in both cases, while a slight reduction in the number of the Purkinje cells in the cerebellum was probably due to termi-

nal anoxic changes. The absorbed dose in these five areas had been 3 700 to 4 400 rad in 23 to 32 fractions over 34 to 77 days in Case 1 and 4 000 to 4 200 rad in 24 fractions over 63 days in Case 2.

The bone marrow (14 and 15 Fig 7) from the manubrium sterni, but not from the 7th thoracic vertebra, showed decreased cellularity in Case 2, although the ratios between the different cell series seemed to be preserved. No significant depression was observed in Case 1. The absorbed dose in areas 14 and 15 (Fig 7) was 4 000 to 4 300 rad in 25 fractions over 68 days in Case 1 and 4 200 to 4 300 rad in 24 fractions over 63 days in Case 2.

No abnormal findings attributable to the irradiation were noted in the trachea, oesophagus, myocardium, thyroid, parathyroid or the skin with the subcutaneous tissue (4, 5, 6, 8, 9 and 16 Fig 7). It is remarkable that the ciliated cells of the trachea seemed to be well preserved in both cases. The absorbed dose in these areas was 3 700 to 4 300 rad in 23 to 28 fractions over 32 to 71 days in Case 1 and 4 000 to 4 300 rad in 24 fractions over 63 days in Case 2. The dose reported here for the trachea was read from the dose plan and thus does not include a slight correction for gas volume in the trachea.

The basal parts of the right lower lobe (1 Fig 7) appeared normal. This area had received an absorbed dose of about 400 rad in 28 fractions over 71 days in Case 1 and about 400 rad in 24 fractions over 63 days in Case 2.

The radiation effects on clinically unaffected tissues were thus microscopically most obvious in the lung tissue at the hilar region, the apex of the upper lobe and the supraclavicular region. Some tissues presented changes that might have been due at least partly, to radiation effects, whereas no signs of such effects could be demonstrated microscopically in other tissues. Death was due clinically and pathologically to advanced Hodgkin's disease in both cases and not to radiation.

### Discussion

Both patients had received chemotherapy, and the disease was far advanced at the time of death. These two factors might have contributed to some of the microscopy findings reported.

In the radiation therapy of Hodgkin's disease many radiation therapy centres give an absorbed dose of 4 000 rad to the target over 4 weeks with five fractions a week. KAPLAN (1966) reported that at this dose level the frequency of local recurrence per field treated was about 5 per cent.

According to JLLIS (1969) the normal connective tissue tolerance to irradiation (the Nominal Standard Dose) may be calculated for different fractionation schedules from the equation

- $NSD = D \times N^{-0.4} \times t^{0.11}$   
 $NSD$  = Nominal Standard Dose (ret)  
 $D$  = Total absorbed dose (rad)  
 $N$  = Number of fractions  
 $t$  = Elapsed time (days)

WINSTON et coll (1971) stated that at Oxford the NSD for connective tissue is 1 800 ret for cobalt 60. The authors further considered this figure to be valid for connective tissue apart from that of bone and brain throughout the body.

It was planned in the present material to deliver 4 000 rad to the target in 24 fractions over 60 days with split course treatment with 5 fractions a week and two thirds of the total absorbed dose in the first series. The NSD would then have been about 1 200 ret.

The most serious side effects so far encountered in mantle treatment are probably those arising from irradiation of the lungs, the heart and pericardium, the nervous system and the bone marrow. A short review is given below of the literature on the radiation sensitivity of those tissues in the dose ranges concerned. Most of the information emanates from the investigation of cases that had received radiation therapy for conditions other than lymphoma e.g. carcinoma of the breast, bronchus and hypopharynx. The follow up that is reported is usually only of some years duration and little has been published on effects that may not become evident before long after the irradiation.

**Lung tissue.** The acute radiation reaction is usually evident within six months (SMITH 1963, EGER & GREGL 1965, TEATES & COOPER 1966) and gradually merges into the late reaction (radiation lung fibrosis). It is difficult to say exactly where radiation pneumonitis ends and fibrosis begins. The latter may also develop even if no radiation pneumonitis has been observed (DEELEY 1960).

Besides the size of the absorbed dose to the lung tissue (HELLMAN et coll 1964, EGER & GREGL 1965) several factors have been considered to be of importance in the causation of radiation pulmonary reaction, e.g. the size of the irradiated lung volume (KUTZ 1958, BENNETT et coll 1969), hypersensitivity (WIERNICK 1965) and infection (BENNETT et coll). The length of the treatment period also seems to be important. GISH et coll (1959) pooled their data with those from the literature and constructed a dose time line for radiation lung reactions separating those that were temporary and those that were permanent. The line passed 4 000 rad in approximately 29 days. GISH et coll found the slope of the curve (about 0.35) to be slightly greater than that for the tolerance of any other tissue. This indicated that if the irradiation to a given absorbed dose level be protracted over a long period the reaction may be less marked. A similar observation was made by HOLSTI (1967) who observed a somewhat better

tolerance of the lung tissue when the treatment was given in split course in two series than when it was continuous and even when the patients in the former groups received larger absorbed doses

An absorbed dose of the order of 4 000 rad over 4 weeks is probably sooner or later always followed by radiation fibrosis (DEFLEY 1960, HELLMAN et coll 1964) of varying degree. If only part of the lung tissue has been irradiated the signs of radiation fibrosis may be absent or negligible, and ventilatory function tests indicate only little reduction which usually occurs within the first year (TEATES & COOPER). However irradiation of very large volumes of lung tissue e.g. mantle treatment may often cause permanent impairment of ventilation

*Heart and pericardium* It is conceivable that cardiac and pericardial reactions after radiation therapy are more frequent than widely supposed

Electrocardiographic changes are common after an absorbed dose of 2 200 to 3 300 rad given over 3 weeks. These changes are limited to the T wave and are usually only temporary (CATTERALL 1960). Serious damage to the myocardium and the coronary arteries may, however, occur and fatal cardiac infarction due to severe atheromatous changes in the coronary arteries in a 15 year-old boy 16 months after mantle treatment for Hodgkin's disease has been described by COHN et coll (1967). They also reported myocardial fibrosis of varying severity after mantle treatment in 5 other cases

Radiation therapy is probably more often followed by pericardial than by myocardial reactions. The complication usually appears as acute pericardial effusion (COHN et coll 1967, FAJARDO et coll 1968) which may be self limiting but sometimes progresses to chronic pericardial contraction and may require pericardiectomy. The degree of pericardial reaction to irradiation seems to be dose dependent and STEWART & FAJARDO (1971) gave the pericardial tolerance as 1 500 ret to large volume treatments and 1 850 ret to small volume treatments

It has been postulated that patients are more susceptible to pericardial reactions after radiation therapy if the adjacent node bearing regions be clinically involved than if no mediastinal disease has been demonstrated (mediastino-pericardial reactions. JONES & WEDGWOOD 1960, PIERCE et coll 1969)

An absorbed dose of the order of 4 000 rad over 4 weeks is thus probably only exceptionally followed by severe radiation reactions of the myocardium. Pericardial effusion usually self limiting but sometimes progressing to chronic pericardial disease may occur

*Nervous system* Opinions differ regarding the radiation sensitivity of the nervous system. Not only dosage but factors such as the relative size of the



irradiated volume (BODEN 1950, BERG & LINDGREN 1963) and the condition of the vascular supply (ASSCHER & ANSON 1962) are also of importance.

Investigations into the radiation reactions in the cerebellum of the rabbit (BERG & LINDGREN 1958) indicate that the smallest absorbed dose that carries a risk of necrosis is probably larger than 4 000 rad over 4 weeks and DAVIDOFF et coll. (1938) also found experimentally that the cerebellum is relatively insensitive to radiation.

The peripheral nerves also seem to be relatively resistant to radiation, the motor nerves more so than the sensory nerves (HAYMAKER & LINDGREN 1970). Brachial neuropathy of varying degree was reported by STOLL & ANDREWS (1966) in 10 to 20 per cent of cases that had received 4 100 to 5 100 rad over 3 to 4 weeks postoperatively for carcinoma of the breast. However, in the development of nerve injury postoperative effects and oedema causing fibrosis and pressure might have been of greater causal importance than direct effect on the nerves from the irradiation.

The spinal cord is probably the most susceptible part of the nervous system to injury by mantle treatment though signs of radiation myelitis may be transient and are then attributed to oedema (JONES 1964). Radiation myelitis has been observed at varying intervals after irradiation, but usually within one year (BODEN 1950, PALLIS et coll. 1961, PHILLIPS & BUSCHKE 1969). Most of the reports on the radiation sensitivity of the spinal cord indicate a threshold value for symptomatic radiation myelitis in the order of 3 900 rad over 4 weeks (BODEN, PALLIS et coll., PHILLIPS & BUSCHKE) but smaller absorbed doses have also been recommended for large fields e.g. 3 000 to 4 000 rad over 28 days (PALLIS et coll.). The radiation sensitivity of the spinal cord seems to be time dependent and in a diagram with logarithmic scales the slope of the time-dose line has been found to be 0.26 (LINDGREN 1958) or 0.21 (PALLIS et coll.). Relatively larger absorbed doses may then be tolerated if the treatment be extended over a long period provided that the absorbed dose at each fraction be not too large (ATKINS & TRETTER 1966, PHILLIPS & BUSCHKE 1969).

**Bone marrow.** It may be calculated from the figures given by ELLIS (1961) on the distribution of active bone marrow in the adult that the mantle field includes about 30 per cent of the red bone marrow. Even after small absorbed doses of the order of 100 rad or less changes though transient may occur in the red marrow. The larger the absorbed dose the greater the depletion of the marrow and the slower the recovery if any (DENSTAD 1943).

Compensation may occur in two different ways in radiation induced depletion of the bone marrow. First previously inactive marrow outside the irradiated volume may become active, as judged from an increased uptake of colloidal  $^{199}\text{Au}$  (KJELLGREN & JONSSON 1969). Secondly the irradiated marrow may be

repopulated by circulating cells (ŠCERBOVA et coll 1968 KABAKOV et coll 1968) Irradiated marrow will not always regenerate The dose permitting recovery of the sternal bone marrow was considered by SYKES et coll (1960) to be at the most 4 000 to 4 500 rad over 3.5 weeks and by SYKES et coll (1964) to be 2 500 to 3 500 rad over 2 to 4 weeks At such levels the marrow became permanently acellular in about half the cases

The chemotherapy induced bone marrow depression may reverse within 1 to 2 weeks after Vinblastine treatment (SELLEI et coll 1970) and within 1 to 3 weeks after Procarbazine treatment (D'ALESSANDRI et coll 1963 MATHE et coll 1963) The two patients in the present series received no chemotherapy during the last 3 weeks of their illness

### SUMMARY

Clinical observations and post mortem findings in various tissues irradiated during mantle treatment with the split course technique in two cases of Hodgkin's disease are reported The radiation sensitivity of the lungs heart and pericardium nervous system and bone marrow is discussed It is suggested that the irradiation may with advantage be extended over a relatively large number of fractions and a long period of time in order to minimize the risk of radiation reactions of healthy tissue

### ZUSAMMENFASSUNG

Es wird über klinische Beobachtungen und post mortem Befunde von verschiedenen bestrahlten Geweben bei der Mantelbehandlung mit der Split-course Technik bei zwei Fällen von Hodgkin'scher Erkrankung berichtet Es wird die Strahlenempfindlichkeit der Lungen, des Herzens und Perikards des Nervensystems und des Knochenmarks diskutiert Es wird darauf hingewiesen dass die Bestrahlung mit Vorteil über eine relativ große Anzahl von Fraktionen und eine lange Zeitperiode ausgedehnt werden kann, um die Gefahr von Strahlenreaktionen des normalen Gewebes auf ein Minimum zu vermindern

### RÉSUMÉ

Les auteurs présentent leurs observations cliniques et les constatations postmortem dans différents tissus irradiés au cours d'un traitement par champs en mantelet avec la technique split-course dans 2 cas de maladie de Hodgkin Ils examinent la radio-sensibilité des poumons du cœur et du péricarde du système nerveux et de la moelle osseuse Les auteurs pensent que l'irradiation pourrait avec avantage être étalée sur un nombre relativement grand de fractions et sur une longue période de temps de façon à minimiser le risque des réactions aux radiations des tissus sains

### REFERENCES

- D'ALESSANDRI A KEEL H J BOLLAG W und MARTZ G Erste klinische Erfahrungen mit einem neuen Cytostaticum Schweiz med Wschr 93 (1963) 1018  
ASCHER A W and ANSON S G Arterial hypertension and irradiation damage to the nervous system Lancet 1962 II p 1343

- ATKINS H. L. and TRETTER I. Time dose considerations in radiation myelopathy. *Acta radiol Ther Phys Biol* 5 (1966) 79
- BENNETT M. E. MILLION R. R. and ACKERMAN L. V. Bilateral radiation pneumonitis. A complication of the radiotherapy of bronchogenic carcinoma. *Cancer* 23 (1969) 1001
- BERG N. O. and LINDGREN M. Time-dose relationship and morphology of delayed radiation lesions of the brain in rabbits. *Acta radiol* (1958) Suppl No 167
- — Relation between field size and tolerance of rabbit's brain to roentgen irradiation (200 kV) via a slit shaped field. *Acta radiol Ther Phys Biol* 1 (1963) 147
- BODEN G. Radiation myelitis of the brain stem. *J Fac Radiol (Lond)* 2 (1950) 79
- CATTERALL M. The effect of radiation upon the heart. *Brit J Radiol* 33 (1960) 159
- COHN K. E. STEWART J. R. FAJARDO L. F. and HANCOCK E. W. Heart disease following radiation. *Medicine* 46 (1967) 281
- DAVIDOFF L. M. DYKE C. G. ELSBERG C. A. and TARLOV I. M. The effect of radiation applied directly to the brain and spinal cord. *Radiology* 31 (1938) 451
- DEELEY T. J. The effects of radiation on the lungs in the treatment of carcinoma of the bronchus. *Clin Radiol* 11 (1960) 33
- DENSTAD F. The radiosensitivity of the bone marrow. *Acta radiol* (1913) Suppl No 52
- EOER W. and GREGL A. *Die Strahlenpneumonitis*. Hippokrates Verlag Stuttgart 1965
- ELLIS F. Dose time and fractionation: a clinical hypothesis. *Clin Radiol* 20 (1969) 1
- ELLIS R. E. The distribution of active bone marrow in the adult. *Phys in Med Biol* 5 (1961) 255
- FAJARDO L. I. STEWART J. R. and COHN K. E. Morphology of radiation induced heart disease. *Arch Path* 86 (1968) 512
- GISH J. R. COATES E. O. DUSALT L. A. and DOUB H. P. Pulmonary radiation reaction: a vital capacity and time dose study. *Radiology* 73 (1959) 679
- HAYMAKER W. and LINDGREN M. Nerve disturbances following exposure to ionizing radiation. In: *Handbook of clinical neurology* Vol 7 p 388 North Holland Publ Company Amsterdam 1970
- HELLMAN S. KLIGERMAN M. M. VON ESSEN C. F. and SCHIFFTA M. I. Sequelae of radical radiotherapy of carcinoma of the lung. *Radiology* 82 (1964) 1055
- HOLSTI L. Radiation reactions in the lung after continuous and split course megavoltage radiotherapy of bronchial carcinoma. *Brit J Radiol* 40 (1967) 280
- JONES A. Transient radiation myelopathy. *Brit J Radiol* 37 (1964) 727
- and WEDGWOOD J. Effects of radiation on the heart. *Brit J Radiol* 33 (1960) 138
- KABAKOV E. N. FOPANOVA K. A. and PERESTORONINA N. N. Die Regeneration des Knochenmarkes bei der Kombination von lokaler Bestrahlung und Ganzkörperbestrahlung. Die Rolle der klonbildenden Zellen und der Lymphozyten. *Radiobiol Radiother* 9 (1968) 533
- KAPLAN H. S. Evidence for a tumoricidal dose level in the radiotherapy of Hodgkin's disease. *Cancer Res* 26 (1966) 1221
- KJELLGREN O. and JONSSON L. Bone marrow depression in the pelvis after megavoltage irradiation for ovarian cancer. *Amer J Obstet Gynec* 105 (1969) 819
- KUTZ F. R. Intensive cobalt 60 teletherapy of lung cancer. *Radiology* 71 (1958) 327
- LANDBERG T. SAHN TAPPER G. and WINTZELL K. Mantle treatment of Hodgkin's disease. Preliminary report of side effects and early results. *Acta radiol Ther Phys Biol* 10 (1971) 174
- LINDGREN M. On tolerance of brain tissue and sensitivity of brain tumours to irradiation. *Acta radiol* (1958) Suppl No 170

- MATHÉ G, SCHWEISGUTH O, SCHNEIDER M, AMIEL J L, BERLMAN L, BRULE G, CATTAN A and SCHWARZENBERG L. Methyl hydrazine in treatment of Hodgkin's disease. *Lancet* 1963 II p 1077
- PALLIS C A, LOUIS S and MORGAN R L. Radiation myelopathy. *Brain* 84 (1961) 460
- PHILLIPS T L and BUSCHKE F. Radiation tolerance of the thoracic spinal cord. *Amer J Roentgenol* 103 (1969) 659
- PIERCE R H, HAERDMANN M D and KAGAN A R. Changes in the transverse cardiac diameter following mediastinal irradiation for Hodgkin's disease. *Radiology* 93 (1969) 619
- ŠCERBOVA E N, GRUŠEV G P and BELOUSOVA O J. Zu Fragen des Mechanismus der Wiederherstellung des Knochenmarkes bei lokaler Bestrahlung. *Radiobiol Radiother* 9 (1968) 517
- SELLEI C, FCKHARDT S and NEMETH L. Chemotherapy of neoplastic diseases. Hungarian Academy of Sciences Budapest 1970
- SMITH J C. Radiation pneumonitis. *Amer Rev resp Dis* 87 (1963) 647
- STEWART R J and FAJARDO L F. Dose response in human and experimental radiation induced heart disease. *Radiology* 99 (1971) 403
- STOLL B A and ANDREWS J T. Radiation induced peripheral neuropathy. *Brit med J* 1966 I p 834
- STAHN TAPPER G and LANDBERG T. Mantle treatment of Hodgkin's disease with cobalt 60. Technique and dosimetry. *Acta radiol Ther Phys Biol* 10 (1971) 33
- SIXES M P, CHU F C H and WILKERSON W G. Local bone marrow changes secondary to therapeutic irradiation. *Radiology* 75 (1960) 919
- —, SÁVEL H, BONADONNA G and MATHIS H. The effects of varying dosages of irradiation upon sternal marrow regeneration. *Radiology* 83 (1964) 1084
- TEATES D and COOPER G JR. Some consequences of pulmonary irradiation. *Amer J Roentgenol* 96 (1966) 612
- WIERNICK G. Radiation pneumonitis following a low dose of cobalt teletherapy. *Brit J Radiol* 38 (1965) 312
- WINSTON B M, ELLIS F and HALL E J. The Oxford NSD calculator for clinical use. *Clin Radiol* 20 (1969) 8

## THYMIC SHIELDING IN IRRADIATED MICE

by

B JARPLID

Protection from external irradiation has been a valuable technique in investigating haematopoietic tissues in mice in reference to function, interrelationships and roles in radiation leukaemogenesis. Bone marrow and spleen have been thoroughly investigated in these respects. Although the greatest interest during recent years has been focused on the thymus, radiation protective investigations on this organ have not been reported in mice. This is probably because of the inaccessibility of the thymus within the thoracic cavity. In some experiments in rats (STAPLES *et coll.* 1966) and rabbits (VELDMAN 1970, NIEUWENHUIS 1971) the thymus has been shielded together with the sternal and vertebral bone marrow with a lead shield outside the thorax. In the present experiments efforts have been made to protect the thymus in mice without protection of any other tissue including bone marrow of the thoracic vertebrae.

The *equipment* (Figs 1-2) consists of three main parts: an operating board (ABC), two thymic shields (D) and an angled stand (E). The plastic operating board consists of a base plate (A) with a groove (B) for the mouse and an arrangement (C) for stretching the mouse and fixing the shield (D). The base plate is sized 2 mm  $\times$  105 mm  $\times$  150 mm. The groove has a semicircular cross

Submitted for publication 15 June 1979

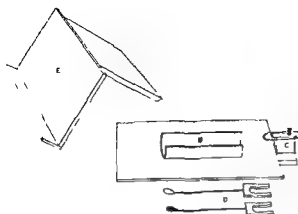


Fig 1 Equipment for thymic shielding A — Base plate B — Groove for the mouse C — Arrangement for stretching and fixing the mouse D — A proper shield of platina (black) and a sham shield of silver-coated plastic E — Stand for the base plate forming an angle of 50° with the horizontal plane

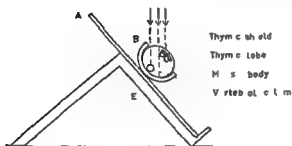


Fig 2 The equipment for thymic shielding with a mouse in position for irradiation

ection with an inner diameter of 24 mm and wall thickness of 2 mm. The horizontal surface at the top of B is sized 12 mm  $\times$  22 mm and is located 21 mm above the base plate. At this surface the shield (D) is fixed with a screw, a spring and a piece of metal. The shield (D) is composed of a hollowed plastic plate sized 15 mm  $\times$  12 mm  $\times$  22 mm, a 0.8 mm thick bar of steel and the thymic shield proper of either a plastic (sham shield) or a platina material. The thymic shield is crescent shaped in cross section and is sized 5 mm  $\times$  9 mm. The thickness of the shield is 2.3 mm. To avoid static electricity the plastic shield is covered with a thin layer of silver. The platina shield is estimated to afford protection corresponding to about 43 mm lead. The protective effect of the plastic shield is negligible. The plastic stand (E) for the base plate forms an angle of 50 degrees with the horizontal plane (Fig 2).

**Technique** For the experiment the mouse was anaesthetized with an intraperitoneal injection of pentobarbital sodium (Mebumal) and placed in a dorsal position in the groove (Fig 3). A rubber band was affixed to the teeth and the



Fig 3

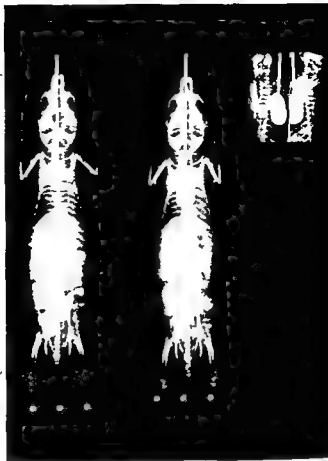


Fig 4

Fig 3 Anesthetized mouse fixed and equipped with the thymic shield for irradiation

Fig 4 Left and middle Dorsoventral films of mice with a thymic shield of plastic (sham shielding; left) and platinum (middle), respectively. Right Shielded area of thymic-shielded mouse in left and right position as for irradiation. No protection of the vertebral column.

animal was stretched backwards to get the vertebral column as straight as possible and fixed with tapes over the hindlegs and tail. The thymus was exposed by the method of Sjöström et coll (1963). The bisected sternum was opened with a forceps and the shield was inserted along the ventral surface of the thymus so as to cover part of both lobes leaving the shield bar passing through the sternal slit. The skin wound was closed around the bar and the fore legs were fixed along the edges of the plastic tube. The base plate with the mouse was then placed on the plastic stand for irradiation from an angle of 40 degrees with the transversal plane through the animal (Fig 2). The animal was irradiated in two

Table

Total weight of thymus ( $m_0$ ) 1 to 6 days after irradiation with 600 R n for each sample = 5 Mean  $\pm$  standard error

Days after irradiation	Thymus shielded	Thymus sham shielded	Controls untreated
—	—	—	70.54 $\pm$ 2.19
1	33.24 $\pm$ 1.79	33.64 $\pm$ 1.34	—
2	25.10 $\pm$ 2.14	19.04 $\pm$ 1.18	—
4	20.70 $\pm$ 1.26	12.14 $\pm$ 0.83	—
6	25.30 $\pm$ 1.63	13.07 $\pm$ 0.59	—

phases one on each side, with a short interruption for turning the base plate with mouse. After irradiation the animal was examined roentgenologically for checking the position of the shield. A dorsoventral film showed the position of the shield in the median plane (Fig. 4). To ensure that the vertebral column had not been protected films were also exposed of the shielding area with the animal in position as for irradiation above (Fig. 4). For that purpose small films (about 1 cm  $\times$  3 cm) were placed just beneath the thorax of the animal in the groove. The films were developed and animals with the shield not in proper position were excluded.

After roentgenography the sternum was opened again, the shield was removed and the cutaneous wound was finally closed with clips.

*Preliminary experiments.* In preliminary experiments irradiations were performed with a roentgen apparatus Muller MG 300 operating at 260 kV and 12 mA. The radiation was filtered by 0.5 mm Cu and 0.5 mm Al. The focal distance was 25 cm and the dose rate 250 R/min. One hundred and ten two-month old C<sub>7</sub>Bl female mice were divided into two equal groups and irradiated with 2  $\times$  300 R. During the irradiation the thymus was shielded in one group with platinum and in the other with plastic (sham shielding). The day for irradiation was called day 0. Twenty mice served as untreated controls. The animals were subjected to blood examination and killed in groups of five at 1, 2, 4, 6, 10, 12, 16, 20, 24 and 30 days after the irradiation. The thymus, spleen and brachial, inguinal and mesenteric lymph nodes were weighed and fixed in Stueve's fluid (Romeis 1948) together with sternum for histologic investigation. The number of mononuclear cells in the peripheral blood was counted in a Burkner chamber.



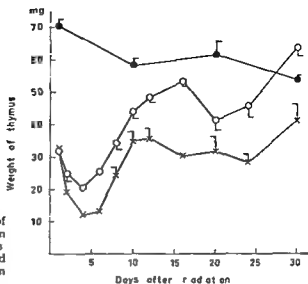


Fig. 5 Total weight of thymus of female C57Bl mice after irradiation with 600 R. ● untreated controls ○ shielded thymus × sham shielded thymus n for each sample = 5 Mean  $\pm$  SE

## Results

**Thymus** The size of the shielded part of the thymus was difficult to state exactly. It may be estimated, however, to have been about 20 to 30 per cent judging from the difference in weight decrease of the thymus between shielded and sham shielded animals and from the extension of the histologically preserved areas of the thymus in the shielded animals. The histologic observations and the mean weight of the thymus with its standard error 2, 4 and 6 days after irradiation (Table) indicate that this shielded part of the thymus was of similar order of magnitude between different individuals in the same group.

During the first phase of lymphocyte depletion, days 1 to 4 (JARPLID 1968) the weight of the thymus in the sham shielded animals decreased to almost 60 per cent of that of the shielded animals by day 4 (Fig. 5, Table). Shielded thymus had then a faster and greater increase of weight and also more evident second phases of depletion and regeneration (JARPLID 1968) than the sham shielded thymus.

Histologically the well known initial phases of destruction and depletion of lymphocytes (MURRAY 1948) were seen in all unshielded and sham shielded parts of the thymic cortex. The shielded areas seemed to be well preserved and were in general rather sharply delimited from the unshielded areas (Fig. 6). On the 4th day a regeneration started in these irradiated areas in four out of five animals with a platinum shield and in one out of five animals with a plastic shield. Two days later the regeneration in these areas was of similar appearance in both

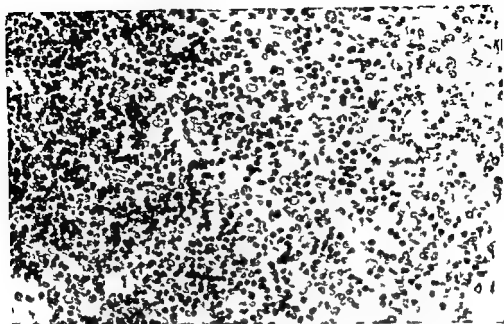


Fig. 6 Thymus one day after irradiation with 600 R. Left: Rather well preserved part of cortex shield with platinum. Right: Sham shielded part of cortex with destruction and depletion of lymphocytes. Haematoxylin and eosin.  $\times 250$ .

groups. On day 11 the whole of the thymus appeared normal again. A slight degree of cortical thinning was seen during the period 16 to 24 days in the sham shielded animals and during the period 20 to 24 days in animals with a thymic shield. After 30 days the histologic appearance of the entire thymus was normal again.

**Spleen.** The changes in weight of the spleen predominantly reflected the development in the red pulp (Fig. 7). The initial destruction and depletion of cells was of similar order of magnitude in the two groups. In two animals with a shielded thymus the extramedullary haematopoiesis started on day 6 and in all other animals on day 8. The extent of this extramedullary haematopoiesis was somewhat greater in the shielded than in the unshielded animals. There was no difference in cellularity of the white pulp with the possible exception of day 6. On this day the centrollicular parts seemed to be somewhat more depleted in the unshielded than in the shielded group. The entire spleen had a normal histologic appearance again on days 20 to 24.

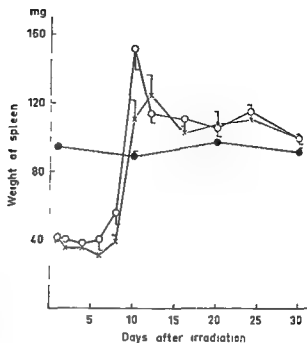


Fig 7 Weight of spleen after irradiation with 600 R ● untreated controls ○ shielded thymus × sham shielded thymus  $n$  for each sample = 5 Mean  $\pm$  SE

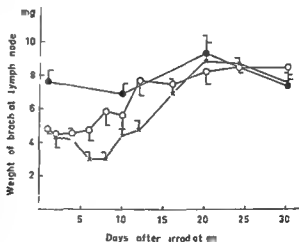


Fig 8 Weight of brachial lymph node after irradiation with 600 R ● untreated controls ○ shielded thymus × sham shielded thymus  $n$  for each sample = 5 Mean  $\pm$  SE

**Lymph nodes** After the initial decrease in weight the increase in weight of the lymph nodes was faster in the group with a thymic shield than in the unshielded group (Fig 8). Histologically no notable differences between the two groups could be detected. However, as the paracortical zone (a thymus-dependent area, PARROT et coll 1966) is a dominating part of the lymph node in the mouse, the

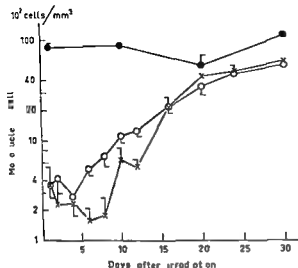


Fig. 9 Number of mononuclear cells in the peripheral blood after irradiation with 600 R ● untreated controls ○ shielded thymus × sham-shielded thymus  $n$  for each sample = 5 Mean  $\pm$  SE

difference in weight probably reflects differences in the cellularity mainly of this part

**Bone marrow** During the different phases of destruction depletion and regeneration both groups had a similar histologic appearance

**Peripheral blood** Protection of the thymus seemed to lead to a higher number of mononuclear cells (mainly lymphoid cells) in the peripheral blood 6 to 12 days after irradiation (Fig. 9)

### Comments

The most important differences between shielded and sham shielded animals appeared in the weight and histology of the thymus. The findings in extrathymic tissues indicate that partial shielding of the thymus during irradiation promotes the regeneration of other lymphoid organs including the so called thymus-dependent areas, and increases the number of lymphoid cells in the peripheral blood. These results confirm the central role of the thymus for the lymphoid tissues and for the circulating pool of lymphocytes.

The size of the shielded part of the thymus could only be grossly estimated from the degree of weight decrease and from the extension of the histologically observed damage. The experiments indicate however, that the method of shielding of the thymus, when further developed may be a valuable new technique for experimental investigations of the thymus and its relation to other haematopoietic tissues.

## Acknowledgement

The excellent technical assistance of R. von Knorring and H. M. Stedenstal is gratefully acknowledged.

## SUMMARY

A method for shielding of the thymus in mice during external irradiation is described. The results of the experiments indicate that thymic shielding during roentgen irradiation promotes the regeneration of extrathymic lymphoid tissues and the recovery of the number of lymphoid cells in the peripheral blood.

## ZUSAMMENFASSUNG

Es wird eine Methode beschrieben um den Thymus von Mäusen während externer Bestrahlung zu schützen. Die Ergebnisse der Untersuchungen deuten darauf hin, dass ein Schutz des Thymus während der Röntgenbestrahlung die Regeneration der ausserhalb des Thymus gelegenen lymphoiden Gewebe und die Erholung der lymphoiden Zellanzahl im peripheren Blut beschleunigt.

## RÉSUMÉ

L'auteur décrit une méthode de protection du thymus des souris au cours de l'irradiation externe. Les résultats d'expérience montrent que la protection du thymus au cours de l'irradiation roentgen favorise la régénération des tissus lymphoïdes extrathymiques et la restauration du nombre des cellules lymphoïdes dans le sang périphérique.

## REFERENCES

- JARPLID B. Radiation induced asymmetry and lymphoma of thymus in mice. *Acta radiol.* (1968) Suppl. No. 279.
- MURRAY R. G. The thymus. In: *Histopathology of irradiation from external and internal sources*. Chapter 7, p. 243. Edited by W. Bloom. McGraw-Hill Book Company, New York, 1948.
- NIEUWENHUIS P. On the origin and fate of immunologically competent cells. Wolters Noordhoff Publishing, Groningen, 1971.
- PARROTT D. M. V., DE SOUSA M. A. B. and EAST J. Thymus dependent areas in the lymphoid organs of neonatally thymectomized mice. *J. exp. Med.* 123 (1965) 191.
- ROWEIS H. *Mikroskopische Technik*. Leibniz Verlag, München, 1948.
- SJÖDIN K., DALMASSO A. P., SMITH J. M. and MARTINEZ C. Thymectomy in newborn and adult mice. *Transplantation* 1 (1963) 521.
- STAPLES P. J., GERY I. and WAXSMAN B. H. Role of the thymus in tolerance. III. Tolerance to bovine gamma globulin after direct injection of antigen into the shielded thymus of irradiated rats. *J. exp. Med.* 124 (1966) 127.
- VELDMAN J. E. *Histophysiology and electron microscopy of the immune response*. Boekdrukkerij Dijkstra-Niemeyer, Groningen, 1970.

FROM THE DEPARTMENTS OF NEUROSURGERY (DIRECTOR PROF L LEASELL),  
RADIATION THERAPY (DIRECTOR PROF J EINHORN) KAROLINSKA SJUKHUSET  
CLINICAL RADIATION PHYSICS (DIRECTOR PROF R WALSTAM) NATIONAL INSTITUTE OF RADIATION PROTECTION, STOCKHOLM AND NEUROLOGY (DIRECTOR DOG O BERG) REGION SJUKHUSET OREBRO SWEDEN

---

## CLOSED STEREOTAXIC HYPOPHYSECTOMY BY MEANS OF $^{60}\text{CO}$ GAMMA RADIATION

by

E O BACKLUND T RAHN M SARBY A DE SCHRYVER and J WENNERSTRAND

LEIF et coll introduced hypophysectomy in 1952 as a therapeutic procedure in patients with advanced mammary carcinoma. The importance of this contribution to endocrine surgery has been manifested in a great variety of ablation techniques and a large number of patients. Apart from conventional surgical procedures hypophysectomy has included physical agents such as cold heat and ultrasound (RAND 1964 ZERVAS 1965 ARSLAN 1969). Nevertheless all experience to date indicates that it is still difficult in spite of sophisticated techniques to perform really radical ablation free from the risks of complications and untoward side effects on the structures in the vicinity of the pituitary gland. Various irradiation techniques have been used mainly as open stereotaxic procedures for the introduction of radioactive sources into the pituitary gland (FORREST et coll 1959 TALAIRACH et coll 1962 NOTTER 1969). The rate of complications after this type of treatment must however be taken into con-

Submitted for publication 8 April 1972

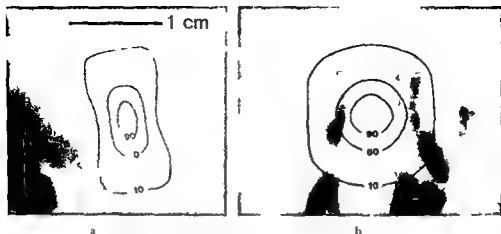


Fig. 1. Sella turcica with the position of the sagittal (a) and frontal (b) sections of the total dose distribution when a single target is irradiated with a 3 mm  $\times$  5 mm beam. The curves indicate 90, 50 and 10 isodoses in relation to the dose at the target point.

sideration (PIOTROWSKI & PENZHOLZ 1971). Closed radiosurgical procedures with beams of heavy charged particles through the intact skull have been developed and are employed in certain cyclotron laboratories (TOBIAS et coll. 1952; LARSSON et coll. 1963; LAWRENCE et coll. 1963; KJELLBERG 1968). These techniques appear to date to have indicated the best means of performing radical pituitary ablations.

A preliminary report of another kind of radiosurgical technique for hypophysectomy in which the anterior lobe is treated selectively with  $^{60}\text{Co}$  gamma radiation is now presented. The technique has also been applied by the authors to pituitary tumours, the preliminary experiences of which have been published (BACKLUND 1969). It also enables the radiation sensitivity of the normal anterior lobe to be investigated under virgin conditions when its viability has not been compromised by surgical trauma and when the radiation dose to the hypothalamus, the infundibulum and the posterior lobe as well as to the arteries supplying the pituitary is kept to a minimum.

**Irradiation technique.** The gamma unit described by LEKSELL (1968, 1971) was used for the irradiation. This unit was designed within the field of functional stereotaxic neurosurgery for the purpose of producing minute disc shaped radiation lesions deep down in the brain (LARSSON et coll. 1970). The lesion is induced by collimated beams from  $^{60}\text{Co}$  sources distributed within a spherical sector with a latitude angle of  $70^\circ$  and a longitude angle of  $160^\circ$ . The beams are radially directed towards the centre of the sector of the unit at which the

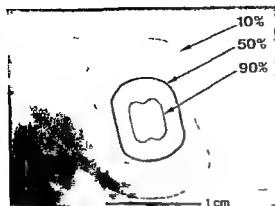


Fig 2 Dose distribution (sagittal) when two target points are irradiated each with a relative dose of 100 and with a mutual distance anteroposteriorly of 3.6 mm. Beam size 3 mm  $\times$  5 mm

target point in the gland has to be positioned (Fig 3). The inner collimator helmet containing the diaphragms that define the geometric cross section of the beams is exchangeable: two different helmets alter the cross section of the beams at the centre to either 3 mm  $\times$  5 mm or 3 mm  $\times$  7 mm. Total dose distributions based upon photographic measurements in one single beam have been calculated (SARBY & LARSSON 1965; DAHLIN *et al.* 1970). Two or three target points in a spatial pattern may be used to adapt the irradiated volume to the shape of the individual pituitary: total dose distributions with configurations as in figures 2 and 7 can be obtained. The dose values mentioned below indicate the dose administered to the target points.

The stereotaxic localization of the pituitary, the determination of the coordinates of the target points and the positioning of the patient in the irradiation unit were the same as in an open stereotaxic technique (LEKSELL 1957). The radiation treatment was given at one session and comprised irradiation of one or more target points with only minor interruptions for change in the position of the patient. The treatment time for 20 krad to one target point is at present about two hours.

**Material.** The patients were selected by the Department of Radiation Therapy and so far 8 have been treated. All had advanced carcinoma of the breast with bone metastases. No patient had undergone oophorectomy or adrenalectomy. Most had had a long free interval between the primary treatment of the condition and the appearance of the first metastatic lesion: all were in the postmenopausal period, aged between 50 and 76 years.

The anterior two-thirds of the pituitary, as judged from the contours of the sella turcica, were given a dose of 20 or 25 krad to each target point. The 50



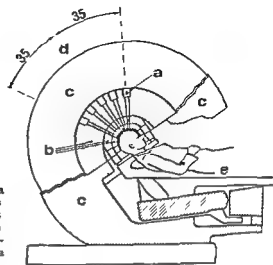


Fig. 3 Section through the  $^{60}\text{Co}$  gamma unit showing five of the beam channels  
 a —  $^{60}\text{Co}$  source b — Collimator helmets  
 c — Shielding material d — Central beam  
 e — Movable operating table (The apparatus was manufactured by AB Motala Verkstad Motala Sweden)

per cent isodose was directed entirely within the boundaries of the sella the intention was to keep the optic nerves below the 10 per cent isodose limit. With one target point the lesion was somewhat too thin in its anteroposterior direction (Fig. 1) and because of this two targets behind one another during the same procedure were also employed (Fig. 2).

### Results

Three of the 8 patients treated died one, three and eight months respectively after the irradiation; another died following haemorrhage from intestinal ulceration three weeks after the treatment, the observation times for the 4 survivors were four to nine months. Although no far reaching conclusions can be drawn from this small material a certain varying influence upon the postoperative hormonal state was demonstrated (Fig. 4). An interesting observation was the frequent occurrence of diabetes insipidus, which according to REED & PIZEY (1967) indicates good therapeutic response. The treatment obviously yielded relief of pain and an increased sense of well being in the 4 survivors. In the main the rate of clinical response did not differ significantly from that in other series published.

The non surviving group consisted of 3 patients who had received a dose of 25 krad to one target point and one patient with 20 krad to each of two target points. The latter was the woman who died 3 weeks after the treatment from intestinal haemorrhage.

Case	LH /serum	FSH /serum	Total gonadotrophins /urine	Urine osmolarity	PBI	T <sub>3</sub>
1	—	Response	—	Response	Response	—
2	Response	Response	—	Response	Response	—
3	Response	—	—	—	Response	—
4	Response	Response	Response	Response	—	—
5	—	—	Response	Response	—	—
6	Response	—	Response	Response	Response	Response
7	Response	—	Response	Response	Response	—
8	Response	—	Response	Response	Response	Response

Response   
 No response   
 Not conclusive / Not adequate   
 No response   
 Not conclusive / Not adequate

Fig 4 Alterations in the hormonal state of the 8 patients as indicated by laboratory findings. Decrease in the values lasting during the whole observation time = Response. Temporary decrease in the values within the 2nd or 3rd week after the irradiation = Transient response. Values unaltered as compared with those before treatment = No response.

The macroscopic appearances of the lesion at autopsy were similar in the 3 patients who received a dose of 25 krad to one target point. All died more than a month after the irradiation. The area of the necrosis was sharply demarcated and the border zone in the section examined was confined within the 70 and 80 per cent isodose curves, i.e. within  $18.5 \pm 1.5$  krad (Fig 5). The reconstruction in figure 5b is based on the assumption of the shrinkage of the section being insignificant (RASMUSSEN 1924). The woman who was given 20 krad to each of two target points and died three weeks after the treatment had no macroscopic lesion but, on the other hand, pyknosis and other nuclear changes were scattered throughout the anterior lobe, indicating that its almost complete destruction might have been expected if the patient had survived the intercurrent disease.

A thorough systematic histologic examination was performed only in one patient (the same as in Fig 5). No microscopic changes were observed in the vicinity of the hypophysis and the bone of the sella, the hypothalamus and the optic nerve pathways appeared completely normal. The general histologic appearance of the lesion was essentially the same as in similar lesions produced by implanted radioisotopes (KELLY et coll 1958, FORREST et coll 1959, NOTTER 1959, BORNER et coll 1960, BERINGER et coll 1965) although the lesion was more regular in shape and well defined (Fig 5). This corresponds with the experiences with the same technique when used in brain tissue (WENNERSTRAND & UNGERSTEDT 1970). The fibrillar stroma within the lesion proved to be intact which corresponds with the findings of BORNER et coll and BERINGER

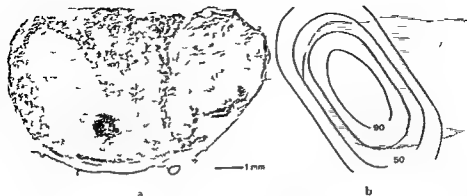


Fig. 5. a) Radiation lesion in the anterior lobe four weeks after the delivery of 25 krad to one target. The necrosis is well demarcated. b) Reconstruction of the same section in relation to the dose distribution. Beam size 3 mm  $\times$  7 mm. Dotted area: posterior lobe.

et coll. and coincides with the observations of BAILEY (1962) that fibrous structures are relatively resistant to radiation. Congested vessels were evident at the edge of the necrosis, a border zone that has been described as haemorrhagic by NOTTER and BERINGER et coll. With the exception of one macroscopic haemorrhage within the necrotic area, no evidence of bleeding was observed in the patient examined. A rim of normal glandular parenchyma was present immediately outside the necrosis (Fig. 6), a few cells of which however were degenerated with pyknotic nuclei, while again outside this zone the tissue was fibrous and the parenchyma reduced; the latter might have been a direct consequence of the irradiation (NOTTER 1959) or an indication of ageing.

BLICHER 1965): Slight inflammatory reaction in the surviving glandular tissue but no signs to suggest regeneration of the parenchyma were present. Differences in radiation sensitivity between the various cell types were not observed.

### Discussion

The intention of this tentative investigation was to develop a method for pituitary ablation as far as possible free from risks. It was possible to perform the procedures smoothly. No general anaesthesia was required and the patients were cared for in a nonsurgical ward. The radiation treatment was based on a dose distribution for the 179 contributing beams calculated from measurements on one single collimated beam. The multiple target technique was based on superimposed dose distributions. The physicist took no part in the clinical planning and the performance of the treatments. No undesirable side effects due to

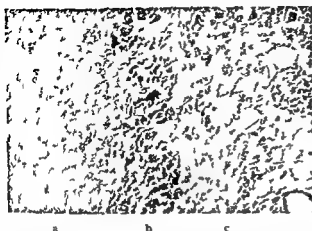


FIG. 6 The border zone of the lesion. Immediately outside the necrotic area (a) a narrow zone of glandular parenchyma (b) is evident in its turn surrounded by fibrotic tissue (c) containing an increased number of vessels and reduced parenchyma.

the irradiation were encountered. However simplicity and safety of a method for hypophysectomy should not be a substitute for its effectiveness. Even if a satisfactory clinical response after subtotal destruction of the pituitary is sometimes achieved — as in the present series — really complete destruction of the gland should be the intention (LUFT 1969).

When the first patient was treated by means of one target point it was fairly obvious that the radiation lesion expected would not cover the whole anterior lobe. The treatment was therefore planned as a two-stage procedure, the intention being to complete the irradiation with destruction of the surviving parenchyma at a second session. Surprisingly enough this patient responded well both as regards her general condition and the laboratory findings. As the biologic response of the pituitary after this type of irradiation could not be entirely predicted it was surmised that the lesion had become more extensive than was expected. Because of this the second irradiation was postponed for the future. Similar experiences were also gained in some of the other patients.

The conditions for performing total hypophysectomy by means of external irradiations have been thoroughly investigated at the cyclotron departments of the Donner Laboratory, Berkeley (TORIAS *et coll.* 1952, 1964, LAWRENCE *et coll.* 1958) and Harvard University (KJELLBERG *et coll.* 1964, KJELLBERG 1968). Favourable results have been attained in a great number of patients treated with multiple beams of heavy charged particles. The intention of applying the  $^{60}\text{Co}$  gamma unit for hypophysectomy should be to produce dose distributions that approximate to the physical properties of those obtained with the methods mentioned. At Berkeley most of the patients with metastatic mammary carcinoma received doses to the centre of the pituitary ranging from 13 krad in 6 weeks to 31 krad in 12 days, the latter doses and and fractionations proving the most

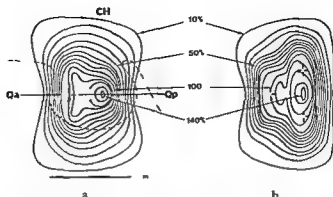


Fig 7 The total dose distribution when three target points are used each with a relative dose of 100 % a) Sagittal and b) horizontal (Qa—Qp) section. The positions of the target points are indicated by crosses. Superimposed upon the isodose curves (10 % separation) the grey templates indicate a normal sized pituitary gland that fits an average sella (according to Di CUIRO & NELSON 1962). The optic chiasm (CH) will be situated outside the 20 % isodose. The cross sections of the beams for the anterior target are 3 mm × 7 mm and for the two posterior targets 3 mm × 5 mm.

effective (TOBIAS et coll 1964). The energy of the radiation (340 MeV protons or 980 MeV alpha particles) were high enough for the beams to penetrate the head. At Harvard the patients received doses of 17 krad to the gland with protons of an initial energy of 160 MeV. The range of the protons was moderated by plexiglass absorbers in order to position the Bragg peak within the gland and the treatments were performed at one sitting. The biologic effect of  $^{60}\text{Co}$  gamma radiation for necrotising hypophyseal tissue may, compared with the particle radiation according to the Berkeley technique, be expected to be about the same (McCOMBS 1957) but in relation to the Harvard technique somewhat lower (KJELLBERG et coll 1964).

Because of this and since it was desirable for practical reasons to give the treatments at one sitting with the  $^{60}\text{Co}$  gamma unit it was decided to apply doses of 20 to 25 krad to each target point in the first series of patients. With the single target technique (Fig 1) only partial destruction of the anterior lobe was obtained even a modification with two target points (Fig 2) usually does not produce complete destruction of the most lateral extensions of the gland. The correlation between the dose distributions and the post mortem findings (Fig 5) however indicates the possibility of obtaining complete destruction of the anterior lobe with three target points. One example is given in figure 7. This modification which will be used in the next series is a compromise between the intention of attaining a steep dose gradient at the surface of the pituitary, a homogenous dose within the gland, tolerable doses to adjacent nervous tissue as well as to vessels and the practical problems connected with too many super

imposed irradiations. With this technique overdosage in the zona intermedia will be unavoidable although it is expected to be insignificant. In comparison with the dose distributions used for hypophysectomy with heavy, charged particles (McCOMBS 1957, TOBIAS et coll. 1964, KJELLBERG et coll. 1964) this distribution for  $^{60}\text{Co}$  gamma radiation will produce about the same dose gradients at the borders of the gland as well as comparable doses to adjacent nerves and vessels if the dose to each target point is 25 krad.

The main advantages in using the gamma unit for hypophysectomy apart from its simplicity and easiness for the patient are the high accuracy and satisfactory reproducibility of applying a predetermined individualized dose distribution to the pituitary. This is due to the precision of the stereotaxic system including the coordinate determination and the fixation of the patient (maximum error = 0.7, LEXSELL 1957) as well as to the mechanical alignment of the beams in the gamma unit (the maximum deviation of the beam axes relative to the centre of the unit is 0.1 mm).

### Dedication

This is one of a number of papers dedicated to Professor Herbert Olivecrona by friends and pupils on the occasion of his eightieth birthday 11 July 1971.

### SUMMARY

A preliminary report upon a new technique of closed stereotaxic hypophysectomy in which the anterior lobe of the pituitary gland is treated selectively with  $^{60}\text{Co}$  gamma radiation is presented. The material consisted of 8 patients with carcinoma of the breast with bone metastases. The small size of the series prevented any far reaching conclusions being drawn although the 4 surviving patients obtained considerable relief.

### ZUSAMMENFASSUNG

Es wird ein vorläufiger Bericht über eine neue Technik der geschlossenen stereotaktischen Hypophysektomie bei der der Vorderlappen der Hypophyse selektiv durch  $^{60}\text{Co}$  Gamma-Bestrahlung behandelt wird gegeben. Das Material bestand aus 8 Patienten mit einem Brustkrebs mit Knochenmetastasen. Der geringe Umfang der Serie macht es unmöglich irgendwelche weiterreichenden Schlüsselsätze zu ziehen, obwohl die 4 überlebenden Patienten beträchtliche Erleichterung hatten.

### RÉSUMÉ

Les auteurs présentent une note préliminaire sur une nouvelle technique d'hypophysectomie stéréotaxique à crâne fermé dans laquelle le lobe antérieur de l'hypophyse est traité sélectivement par la radiation gamma du  $^{60}\text{Co}$ . Ils ont traité 8 malades atteintes de cancer du sein avec métastases osseuses. Le petit nombre de malades empêche de tirer des conclusions à longue portée bien que les 4 malades survivantes aient bénéficié d'un soulagement considérable.

## REFERENCES

- ARSLAN M. Ultrasonic selective hypophysectomy for advanced prostate and breast cancer and for pituitary diseases. In Nobel Symposium 10 Disorders of the skull base region, p 223. Edited by C. H. Hamberger and J. Wersall. Almqvist & Wiksell, Stockholm 1969.
- BACKLUND E. O. Stereotactic treatment of craniopharyngiomas. In Nobel Symposium 10 Disorders of the skull base region, p 237. Edited by C. A. Hamberger and J. Wersall. Almqvist & Wiksell, Stockholm 1969.
- BAILEY O. T. Basic problems in the histopathology of radiation of the central nervous system. In Response of the nervous system to ionizing radiation, p 165. Edited by T. J. Haley and R. S. Snider. Academic Press, New York 1962.
- BERINGER A., BURIAN K., ELLEGAST H., FREY R. G., FRISCHALF H. und ZEITLHOFFER J. Die strahlentherapeutische Ausschaltung der Hypophyse. Fortschr. Hals- u. Ohrenheilk. 12 (1963) 47.
- BORNER P., SCHLUMPFEDER N., WINKLER C. und MENTZEL G. Morphologie und Funktion der Hypophyse nach Implantation von Radiogold. Virchows Arch. path. Anat. 333 (1960) 219.
- BUECHER O. Histologie und mikroskopische Anatomie des Menschen. Hans Huber, Bern, Stuttgart 1963.
- DAHLIN H., ROSANDER K. and SVEDBERG J. On the selection of dose distributions in clinical cerebral radiosurgery. Paper read at the Ninth Symposium Neuroradiologicum, Gothenburg 1970.
- DI CHIRO G. and NELSON K. B. The volume of the sella turcica. Amer. J. Roentgenol. 87 (1962) 989.
- FORREST A. P. M., BLAIR D. W., PEEBLES BROWN D. A., STEWART H. J., SANDISON A. T., HARRINGTON R. W., VALENTINE J. M. and CARTER P. T. Radio active implantation of the pituitary. Brit. J. Surg. 47 (1959) 61.
- KELLY W. A., EVANS J. P., HARPER P. V. and HUMPHREYS E. M. The effect upon the hypophysis of radioactive strontium. Surg. Gynec. Obstet. 106 (1958) 600.
- KJELLBERG R. N. Proton beam irradiation of the pituitary. In Clinical endocrinology, Vol. 2, p 103. Edited by E. B. Asinwood and C. E. Cassidy. Grune & Stratton, New York 1968.
- , KOEHLER A. M., PRESTON W. M. and SWEET W. H. Intracranial lesions made by Braeg peak of proton beam. In Response of the nervous system to ionizing radiation, p 35. Edited by T. J. Haley and R. S. Snider. Little Brown & Co., Boston 1964.
- LARSSON B., LEKSELL L. and REYED B. The use of high energy protons for cerebral surgery in man. Acta chir. scand. 125 (1963) 1.
- , LIDEN K. and SARBY B. Techniques for irradiation of small intracranial structures through the intact skull. Paper read at the Ninth Symposium Neuroradiologicum, Gothenburg 1970.
- LAWRENCE J. H., TOBIAS C. A. and BORN J. L. Hypophysectomy for advanced breast cancer using high energy particle beams — Proton and alpha particles. In Radioactive Isotope in Klinik und Forschung, Vol. III, p 245. Strahlentherapie (1958) Sonderband 38.
- , —, —, GOTTSCHALK A., LINFORTH J. A. and KELSO R. P. Alpha particle and proton beams in therapy. J. Amer. med. Ass. 186 (1963) 236.
- LEKSELL L. Gezielte Hirnoperationen. In Handbuch der Neurochirurgie, Vol. VI, p 168. Herausgegeben von H. Olivecrona und W. Tonnies. Springer, Berlin 1957.
- Cerebral radiosurgery. I. Gamma thalamotomy in two cases of intractable pain. Acta chir. scand. scand. 134 (1968) 585.

- Stereotaxis and radio surgery Charles C Thomas Springfield 1971
- LEFF R Pre operative evaluation of pituitary function *In* Nobel Symposium 10 Disorders of the skull base region p 177 Edited by C A Hamberger and J Wersall Almqvist & Wiksell Stockholm 1969
- OLIVECRONA H och SJÖGREN H Hypofysektomi på manniska (In Swedish) Nord Med 47 (1952) 351
- MCCOMBS R K Proton irradiation of the pituitary and its metabolic effects Radiology 68 (1957) 797
- MOTTER G A technique for destruction of the hypophysis using  $Y^{90}$  spheres Acta radiol (1959) Suppl No 184
- Interstitial irradiation of the hypophysis *In* Nobel Symposium 10 Disorders of the skull base region p 245 Edited by C A Hamberger and J Wersall Almqvist & Wiksell Stockholm 1969
- PIOTROWSKI W und PENZHOLZ H Komplikationsmöglichkeiten bei perkutaner paranasaler transphenoidaler Radiogoldimplantation in Hypophysentumoren Neuro-chirurgie 14 (1971) 150
- RAND R W Stereotaxic transphenoidal hypophysectomy Bull Los Angeles neurol Soc 29 (1964) 40
- RASCHKEV A T A quantitative study of the human hypophysis cerebri or pituitary body Endocrinology 8 (1924) 509
- REED P I and PIZEY N C D Trans sphenoidal hypophysectomy in the treatment of advanced breast cancer Brit J Surg 54 (1967) 369
- SARBY B och LARSSON H Fysikaliska experiment rörande förutsättningar för användning av smala gammastrålar vid cerebral strålkirurgi (In Swedish) Report from the Gustaf Werner Institute Uppsala 1965
- TALAIRACH G SZIKLA G TOURNOUX P BOVIS P et BANCAUD J La chirurgie stéréotaxique hypophysaire Confin neurol 22 (1962) 204
- TOBIAS C A ANGER H O and LAWRENCE J H Radiological use of high energy deuterons and alpha particles Amer J Roentgenol 67 (1952) 4
- LAWRENCE J H LYMAN J BORN J L GOTTSCHALK A LINTFOOT J and McDONALD J Progress report of pituitary irradiation *In* Response of the nervous system to ionizing radiation p 19 Edited by T J Haley and R S Snider Little Brown & Co Boston 1964
- VENNERSTRAND J and UNGERSTEDT L Cerebral radiosurgery II An anatomical study of gamma radiolesions Acta chir scand 136 (1970) 133
- ZERVAS N T Technique of radiofrequency hypophysectomy Confin neurol 26 (1965) 157



EFFECTS OF  $^{60}\text{Co}$  GAMMA RADIATION ON  
THE DISTRIBUTION, CATABOLISM AND  
INCORPORATION OF  $^{125}\text{I}$ -5 IODO 2'-DEOXYURIDINE  
INTO INTSTINAL AND SPLENIC  
DEOXYRIBONUCLEIC ACID IN MICE

by

K. J. JOHANSSON

180 MeV protons and  $^{60}\text{Co}$  gamma radiation produce similar effects on the incorporation of the thymidine analogue  $^1\text{I}$  5 Iodo 2' deoxyuridine ( $^1\text{IUdR}$ ) into DNA of the small intestine and the spleen in mice (JOHANSSON & IARSSON 1972). Two hours after  $^{60}\text{Co}$  gamma irradiation at 400 rad, for example, the incorporation of  $^1\text{IUdR}$  into DNA was 13 per cent of the controls.

GITLIN *et coll.* (1962) using  $^{125}\text{I}$ UdR and whole body counting in a large crystal reported that 2 hours after irradiation of mice at 416 R 250 kV roentgen radiation the retention of  $^{125}\text{I}$  was 12 per cent of the normal value. The result was confirmed and extended by JOHANSSON (1972) and reflects a more marked depression of the DNA synthesis than has been demonstrated with  $^3\text{H}$  thymidine or other DNA precursors used (cf MITCHELL 1966). The marked effect on the

---

This work was supported by the Swedish Atomic Research Council. Submitted for publication 13 January 1972.

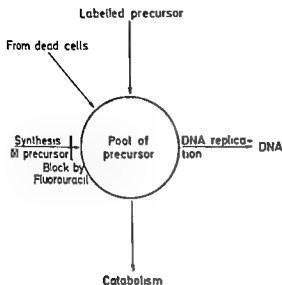


Fig 1 Modified four factor model (five factor model) for the metabolic pathways of thymidine (QLASTLER 1963) The new factor included is thymidine from dead cells

incorporation of  $^1\text{IUdR}$  after irradiation may depend upon several factors. The following effects have been investigated: (a) disturbance of precursor distribution, (b) disturbance of precursor catabolism, and (c) increase in the thymidine pool due to the break down of DNA from dead cells.

An experiment was designed in which the kinetics of the distribution of  $^1\text{IUdR}$  in the blood stream, the small intestine and the spleen was examined. (a) The appearances of the catabolic products in the blood were examined. (b) It is known that  $\text{IUdR}$  is mainly broken down to iodouracil (IU) and further to iodide (PRUSOFF et coll 1960, HAMPTON & EDINOFF 1961). Fluorouracil was used in an experiment to increase the incorporation of  $^1\text{IUdR}$  into DNA. (c) Fluorouracil blocks the synthesis of thymidine de novo (HEIDELBERGER et coll 1957, DANNEBERG et coll 1958) and in this way decreases the thymidine pool. A mouse given fluorouracil is probably a more sensitive indicator than the normal mouse for changes in the thymidine pool (Fig 1) which is smaller than in the untreated animal.

### Material and Methods

**Animals.** Male NMRI mice weighing 26 to 28 g were given water ad libitum but had no access to food from 20 hours before irradiation.

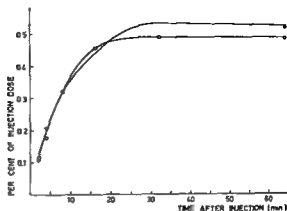


Fig. 2 The total activity of  $^{125}\text{I}$  in 100  $\mu\text{l}$  blood after intraperitoneal injection of  $10 \mu\text{Ci } ^{125}\text{I IUdR}$  — control ○ irradiated ●

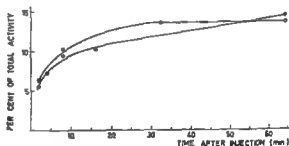


Fig. 3 Percentage of the total activity of  $^{125}\text{I}$  in blood insoluble in cold 0.2% perchloric acid — control ○ irradiated ●

**Gamma irradiation** Irradiation was applied with a  $^{60}\text{Co}$  source as previously described (JOHANSON & LARSSON 1972) at a dose rate of 56 rad per minute. The control mice were sham irradiated.

**Administration of  $^{125}\text{I IUdR}$  and fluorouracil** Ten  $\mu\text{Ci } ^{125}\text{I IUdR}$  (Radiochemical Centre, Amersham) and 0.1  $\mu\text{mole}$  carrier IUdR (Sigma Chem. Co.) in 1 ml 0.9% NaCl were injected intraperitoneally two hours after irradiation or sham irradiation. The mice in one experiment were given an intraperitoneal injection of  $5 \times 10^{-3}$  mole fluorouracil (Schuchardt, Munchen) in isotonic saline 10 min before the injection of  $^{125}\text{I IUdR}$ .

**Preparations of organs** Groups of 3 control and 3 irradiated mice were killed by decapitation 2, 4, 8, 16, 32 or 64 min after injection of  $^{125}\text{I IUdR}$ . Of the blood collected, 100  $\mu\text{l}$  were transferred with a heparinized pipette to a plastic tube with 2 ml water for measurement of the total activity of  $^{125}\text{I}$ . The radioactivity of the precipitate was determined after deproteinization with perchloric acid (PCA) and centrifugation. Another sample of blood was transferred to a test tube with 500  $\mu\text{l}$  water and the sample was stored at  $-20^\circ\text{C}$  until analyzed by thin layer chromatography after deproteinization with PCA. The spleen and

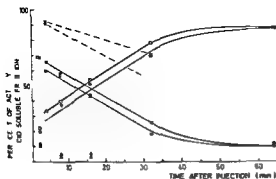


Fig. 4. Percentage of  $^1\text{I}$  activity in the acid-soluble fraction of blood and of peritoneal fluid as  $^1\text{IUdR}$   $^1\text{IU}$  and  $^1\text{I}$  Blood  $\circ$  0 rad  $\bullet$  200 rad  $\triangle$  0 rad  $\blacktriangle$  200 rad  $\square$  200 rad  $\nabla$  200 rad  $^1\text{IU}$  Intrapertoneal fluid  $\circ$  0 rad  $\bullet$  200 rad  $\triangle$  0 rad  $\blacktriangle$  200 rad

10 cm of the jejunum were also removed as quickly as possible and the content of the intestine was flushed out with ice-cold isotonic saline. Both organs were frozen on solid  $\text{CO}_2$  and kept at  $-20^\circ\text{C}$  until analyzed. A sample of the peritoneal fluid was stored at  $-20^\circ\text{C}$  until analyzed by thin layer chromatography after deproteinization with PCA. The mice in the fluorouracil experiment were killed by cervical dislocation 90 min after injection of  $^1\text{IUdR}$  and the spleen and 10 cm of the jejunum were prepared as described above.

**Extraction and estimation of nucleic acids.** Low molecular weight compounds were extracted with ice-cold 0.2 N PCA, the acid-soluble fraction and the nucleic acids with 0.5 N PCA at  $90^\circ\text{C}$  for 60 min, the nucleic acid fraction. The extraction procedure has been described in more detail elsewhere (JOHANSSON & LARSSON). The DNA was estimated by the diphenylamine method modified by BURTON (1956) with calf thymus DNA (Sigma Chem. Co.) as a standard. The absorbency was measured at 600 nm in a Zeiss PMQ II spectrophotometer.

**Radiometry.** The activity of  $^1\text{I}$  was measured in a well-type  $\text{NaI}(\text{Tl})$  crystal with  $0.2\ \mu\text{Ci}$   $^1\text{IUdR}$  in 1 ml solution as a standard. A quantity called specific activity was calculated from

$$\frac{\text{radioactivity recorded (c.p.m.)}}{\text{absorbency at 600 nm}}$$

**Thin layer chromatography.** The distribution of radioactive components in the deproteinized blood and peritoneal fluid was analyzed by thin layer chromatography with Merck TLC-plates silica gel F 254 and isopropanol-chloroform (20:80 v/v) as the solvent (FOX & PRUSOFF 1966). Non-radioactive samples were run with IU and IUdR (Sigma Chem. Co.) in parallel to the radioactive

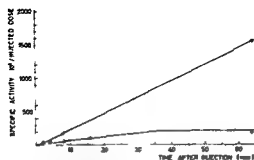


Fig 5 Relative activity of  $^{125}\text{I}$  in the nucleic acid fraction of the small intestine after injection of  $^{125}\text{I}$  Udr.  $\circ$  control  $\bullet$  irradiated

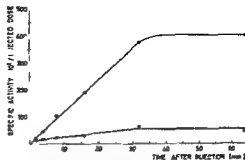


Fig 6 Relative activity of  $^{125}\text{I}$  in the nucleic acid fraction of the spleen after injection of  $^{125}\text{I}$  Udr.  $\circ$  control  $\bullet$  irradiated

sample. The position of the spots were located under UV light. The chromatography of the catabolic products of  $^{125}\text{I}$  Udr on thin layer plates with the solvent system employed permitted excellent separation of the iodide, iodouracil and iododeoxyuridine. A suitable area was scraped off and its activity of  $^{125}\text{I}$  determined.

## Results

*The appearance of  $^{125}\text{I}$  in the blood.* The total radioactivity in 100  $\mu\text{l}$  blood at various times after injection appears in Fig 2. The activity increased up to 32 min and then reached a plateau at about 5 per mille of the injected  $^{125}\text{I}$  activity in 100  $\mu\text{l}$  of blood. Assuming that the blood volume of a 27 g mouse be 1.5 ml (BERNSTEIN 1966) the corresponding total activity of  $^{125}\text{I}$  in the blood was about 7.5 per cent of the injected dose, about 10 to 15 per cent of this activity was insoluble in 0.2 N PCA (Fig 3).

*The catabolism of  $^{125}\text{I}$  Udr.* The activity of  $^{125}\text{I}$  in the acid soluble fraction of blood is mainly in the chemical form of Udr, IU and I (PERLOFF et coll 1960; HAMPTON & EIDENOFF 1961). A linear decrease in the activity of the Udr occurred from 4 to 32 min after injection, 60 per cent remaining unchanged at 4 min and about 20 per cent at 32 min (Fig 4). The IU concentration was always low and the I concentration increased inversely compared with that of the Udr, indicating a rapid breakdown of IU to I in accordance with previous observations (HUGHES et coll 1964). About 5 per cent higher radioactivity was evident in the Udr fraction of the irradiated mice than in the control mice. The  $^{125}\text{I}$  activity remaining as  $^{125}\text{I}$  Udr was higher in the peritoneal

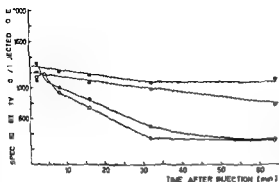


Fig 7 Relative activity of  $^{125}\text{I}$  in the acid soluble fraction from the small intestine and the spleen after injection of  $^1\text{I}$  UdR. Spleen  $\circ$  control  $\bullet$  irradiated Small intestine  $\square$  control  $\blacksquare$  irradiated

fluid than in the blood. Four minutes after injection over 90 per cent of the radioactivity was still in the form of IUdR in the peritoneal fluid (60 to 70 per cent in the blood). At 32 min about 70 per cent of the radioactivity in the irradiated mice and 55 per cent in the control mice remained as IUdR (20 per cent in the blood).

*Incorporation of  $^1\text{I}$  IUdR into jejunal and splenic DNA* The incorporation of  $^1\text{I}$  IUdR into DNA is presented in Figs 5 and 6. The incorporation in the spleen was almost completed 32 min after injection both in the irradiated and control groups. The rate of incorporation was constant during the first 32 min. The incorporation rate of  $^1\text{I}$  IUdR in the small intestine was also constant in the irradiated group for 32 min and in the control group for at least 64 min. Only small changes in the relative activity in the acid soluble fraction of the small intestine were present from 2 to 64 min after injection. A 75 per cent decrease in the relative activity in the spleen was recorded during the same period (Fig 7).

*Effects of fluorouracil on the incorporation of  $^1\text{I}$  IUdR into DNA* Fluorouracil increased the incorporation of  $^1\text{I}$  IUdR into DNA in the control group with 54 per cent in the small intestine and 17 per cent in the spleen (see Table) and 2 hours after irradiation with 200 rad with 95 per cent in the small intestine and 42 per cent in the spleen. The results indicate an enhancing effect of fluorouracil on the incorporation of  $^1\text{I}$  IUdR into DNA after irradiation.

### Discussion

The route of injection of IUdR influences the period during which the precursor is available for the synthesis of DNA. After an intraperitoneal injection of  $^1\text{I}$  IUdR the maximum concentration of  $^{125}\text{I}$  activity in the blood appeared

Table

*Incorporation of  $^{125}\text{IUdR}$  into DNA during a 90 minute period in the small intestine and the spleen of mice 2 hours after 200 rad with and without fluorouracil (FU) treatment Mean of 6 mice and standard error (SE) of mean*

	Dose (rad)	Acid soluble fraction		Nucleic acid fraction	
		Relative activity	SE	Relative activity	SE
Small intestine					
FU treated	0	795	60	1859	321
FL treated	200	862	148	326	64
No FL	0	878	100	1211	315
No FL	200	168	95	167	24
Spleen					
FL treated	0	362	30	230	48
FL treated	200	433	74	34	4
No FL	0	329	34	197	115
No FL	200	286	52	24	5

at 32 min (Fig 2) A uniform distribution of injected  $^1\text{I}$  ( $12.8 \times 10^6$  c p m) in the whole mouse would give 47 000 c p m or 0.36 per cent of injected activity in a 100  $\mu\text{l}$  blood sample The value obtained 64 min after injection was 63 000 c p m (0.49 per cent) in the control and 67 000 c p m (0.52 per cent) in the irradiated mice There was no significant difference in the  $^1\text{I}$  activity in the blood of control and irradiated mice (Fig 2) a t test on the 32 and 64 min groups pooled together giving  $0.2 > p > 0.1$  A difference of at least 2 000 c p m/100  $\mu\text{l}$  blood could be explained by the higher incorporation of  $^1\text{IUdR}$  into DNA in the control group The  $^1\text{I}$  activity in the blood that was not soluble in the cold PCA (Fig 3) was probably associated with the plasma proteins and cell fragments Small amounts of  $^1\text{IUdR}$  may have been incorporated into DNA of cells which had then entered the blood stream

Once in the blood stream, IUdR is rapidly catabolized, particularly in the liver The first step is the cleavage of the nucleoside to iodouracil and deoxyribose (PRUSOFF et coll 1960) This appears to be a rate limiting enzymatic reaction (HUGHES et coll 1964) an assumption corroborated by the present observation that there was only a small amount of iodouracil in the blood (Fig 4) The next step is the deiodination of iodouracil which begins with reduction to give 5,6-dihydro-iodouracil resulting in spontaneous loss of iodide (BARRETT & WEST 1956 GRISOLIA & CARDOSO 1957, NEWMARK et coll 1962)

The half life of  $^1\text{IUdR}$  in the blood appears to be about 3 min (HUGHES et coll 1964)

The incorporation of  $\text{IUdR}$  into intestinal DNA after intravenous injection is thought to be completed within 20 min (HUGHES et coll) The present results indicate that after an intraperitoneal injection a pool of  $^1\text{IUdR}$  is produced in the peritoneal fluid and is available for transport via the blood stream This would increase the period of  $^1\text{IUdR}$  incorporation into DNA to about 30 min in the spleen and about an hour in the small intestine It is possible that the periods are still longer after subcutaneous injection since a higher retention of  $^{131}\text{IUdR}$  in mice has been reported after subcutaneous than after intraperitoneal injection (ROTENBERG et coll 1962)

Only small differences appear to exist in the kinetics of the  $^1\text{IUdR}$  distribution in the blood the small intestine and the spleen as well as in the catabolism of  $^1\text{IUdR}$  in the control and irradiated mice The differences observed might be explained by the decreased incorporation of  $^1\text{IUdR}$  into DNA in the irradiated mice

The results of the fluorouracil experiments (Table) indicate that an increase in the thymidine pool due to breakdown of DNA from dead cells in the small intestine and in the spleen 2 hours after 200 rad  $^{60}\text{Co}$  gamma radiation are of minor importance It is known that fluorouracil blocks the synthesis of thymidine de novo (the conversion of the methyl group in the formation of thymidine) to produce a decrease in the thymidine pool (HEIDELBERGER et coll 1957 DANNEBERG et coll 1958) It seems reasonable that the incorporation of  $^1\text{IUdR}$  into DNA would be less in fluorouracil treated mice than in control mice if there were a flow of thymidine from dead cells into the DNA synthesizing cells

An overproduction of precursor for DNA may of course occur in each cell due to a disturbed balance between synthesis of the precursor and its incorporation into DNA

## SUMMARY

The effect of 200 rad  $^{60}\text{Co}$  gamma radiation on the kinetics of the distribution and catabolism of  $^1\text{IUdR}$  was investigated in mice No significant changes were observed Fluorouracil injected before  $^1\text{IUdR}$  increased its incorporation into DNA This increase was more marked two hours after irradiation indicating that changes in the thymidine pool due to flooding of thymidine from dead cells are of minor importance

## ZUSAMMENFASSUNG

Die Wirkung von 200 rad  $^{60}\text{Co}$  Gamma Strahlung auf die Kinetik der Verteilung und des Katabolismus von  $^1\text{IUdR}$  wurde bei Mäusen untersucht Es wurden keine signifikanten Veränderungen beobachtet Fluorouracil das vor  $^1\text{IUdR}$  injiziert wurde steigerte dessen



Einbau in die DNS Dieser gesteigerte Einbau war zwei Stunden nach Bestrahlung starker ausgeprägt was darauf hinweist dass Änderungen im Thymidin Pool durch Einstrom von Thymidin von getöteten Zellen von untergeordneter Bedeutung ist

## RÉSUMÉ

L'auteur a étudié l'effet de 200 rad de radiation gamma du  $^{60}\text{Co}$  sur la cinétique de la distribution et sur le catabolisme de  $^3\text{H}$  IUDR sur des souris Il n'a pas observé de modification significative Le fluorouracile injecté avant la  $^3\text{H}$  IUDR augmente son incorporation dans l'ADN Cette augmentation est moins marquée deux heures après l'irradiation indiquant que les modifications du pool de thymidine dues à l'inondation par la thymidine provenant des cellules mortes sont d'importance mineure

## REFERENCES

- BARRETT H W and WEST R A Dehalogenation of substituted pyrimidines in vivo *J Amer chem Soc* 78 1956, 1612
- BERNSTEIN S E Physiological characteristics *In Biology of the laboratory mouse* p 337 Edited by E L Green McGraw Hill Book Co New York 1966
- BURTON K A study on the conditions and mechanism of the diphenylamine reaction for the colorimetric estimation of deoxyribonucleic acid *Biochem J* 62 (1956) 315
- DANNEBERG P B MONTAG B J and HEIDELBERGER C Studies on fluorinated pyrimidines IV Effects on nucleic acid metabolism in vivo *Cancer Res* 18 (1958) 329
- FOX B W and PRUSOFF W H Effect of thymine ribonucleoside on the metabolism of  $^{125}\text{I}$  deoxyuridine *Biochem Pharmacol* 15 (1966) 1317
- GITLIN D COMMERFORD S L AMSTERDAM E and HUGHES W A rays affect the incorporation of 5 iododeoxyuridine into deoxyribonucleic acid *Science* 133 (1962) 1074
- GRISOLIA S and CARDOSO S S The purification and properties of hydropyrimidine dehydrogenase *Biochim biophys Acta (Amst)* 25 (1957) 430
- HAMPTON E G and EIDINOFF M Administration of 5 iododeoxyuridine I 131 in the mouse and rat *Cancer Res* 21 (1961) 345
- HEIDELBERGER C CHANDHURI K DANNEBERG P MOOREN D GRIESBACH L DUSCHINSKY H SCHWITZER R J PLEVEN E and SCHEINER J Fluorinated pyrimidines a new class of tumor inhibitory compounds *Nature* 179 (1957) 663
- HUGHES W L COMMERFORD S L GITLIN D KRELGER R C SCHULTZ B SHAIH V and REILLY P Deoxyribonucleic acid metabolism in vivo I Cell proliferation and cell death as measured by incorporation and elimination of iododeoxyuridine *Fed Proc* 23 (1964) 640
- JOHANSON K J Retention of  $^{125}\text{I}$  given as  $^{125}\text{I}$  5-iodo-2 deoxyuridine in mice after 180 MeV proton or  $^{60}\text{Co}$  gamma irradiation *Acta radiol Ther Phys Biol* 11 (1972) 463
- and LARSSON H Effect of 180 MeV protons or  $^{60}\text{Co}$  gamma radiation on the incorporation of  $^3\text{H}$  5-iodo-2-deoxyuridine into intestinal and splenic deoxyribonucleic acid of mice *Acta radiol Ther Phys Biol* 11 (1972) 452
- MITCHELL J S Some aspects of the effects of radiations on the metabolism of tissues and tumours *In Encyclopaedia of medical radiology* Volume II part I p 353 Edited by A Zuppinger Springer Verlag Berlin Heidelberg 1966

- NEWMARK P., STEPHENS J. D. and BARRETT H. W. Substrate specificity of the dihydrouracil dehydrogenase and uridine phosphorylase of the rat liver. *Biochim. biophys. Acta (Amst.)* 67 (1962) 414.
- PRUSOFF W. H., JAFFE J. J. and GUNTHER H. Studies in the mouse of the pharmacology of 5 iododeoxyuridine: an analog of thymidine. *Biochem. Pharmacol.* 3 (1960) 110.
- QLASTLER H. Effects of irradiation on synthesis and loss of DNA. In: *Actions chimiques et biologiques des radiations*. Edited by M. Haissinsky. Masson et Cie, Paris, 1963.
- ROTTENBERG A. D., BRUCE W. R. and BAKER R. G. Incorporation of 5 iododeoxyuridine <sup>131</sup>I in spontaneous C<sub>3</sub>H mouse mammary tumours. *Brit. J. Radiol.* 35 (1962) 337.

## COMPARISON OF TUMOR UPTAKE AND KINETICS OF DIFFERENT RADIOPHARMACEUTICALS UNDER EXPERIMENTAL CONDITIONS

by

D. EMRICH, A. VON ZUR MÜHLEN, F. WILLGEROTH and A. LAMMICH

Radiopharmaceuticals for the delineation of tumors have been mainly selected empirically and by the physical properties of the radionuclide. Little data is available for comparison of physiologic behaviour of such radiopharmaceuticals although the extent of radiation activity in the tumor, the ratio of tumor to background radiation activity and their changes in relation to time may heavily influence the usefulness of a substance for tumor detection. We have investigated these parameters for eight radiopharmaceuticals utilizing a transplantable rat sarcoma.

### Materials and Methods

The Yoshida sarcoma (YOSHIDA 1949) was used in male Wistar rats (A/F Hann. Gesellschaft für Versuchstierzucht, Hannover, Germany) weighing 200–300 g. Since preliminary experiments had shown that the tumor uptake of  $^3\text{H}\text{gCl}$  decreased after several passages, each group of definite experiments

Table 1  
*Radiopharmaceuticals and doses*

Rad opharmaceut cal	Range of specific activity (mCi/mg)	Doses administered ( $\mu$ Ci)
Ga-citrate	Carrier free	50
<sup>99m</sup> Tc <sup>m</sup> pertechnetate	Carrier free	300-745
Se selenite	7.6-24.5 $\times 10^3$ /SeO <sub>3</sub>	11-20
<sup>203</sup> HgCl <sub>2</sub>	6.0-10.8 $\times 10^3$ /HgCl <sub>2</sub>	10
Hg H albumin	10.5-17.5 $\times 10^3$ /H albumin	20-35*
Hg BMHP	6.4-50.0 $\times 10^3$ /BMHP	20-40
<sup>203</sup> Hg-chlormerodrin	5.4-9.5 $\times 10^3$ /chlormerodrin	20
I H albumin	5.3-12.6 $\times 10^3$ /H albumin	30-50*

\* = 0.289 mg H albumin

was started by a frozen preparation of the tumor (GERICKE & ENGELBART 1962) delivered by the Cancer Research Laboratory of Hoechst AG, Frankfurt Germany. In order to grow sufficient tumor tissue to implant 20 to 30 rats 0.5 to 1.0 ml of the thawed tumor suspension was injected per animal in 2 to 4 rats over the scapula. After 7 to 10 days the tumors were excised under general anaesthesia (Nembutal 5 mg/100 g body weight). Slices of 0.5 to 1.0 mm thickness were transferred into 0.9% saline at 4° C. Here they were cut in pieces of approximately 1 mm  $\times$  2 mm. Three to four pieces per animal were transplanted over the scapula of the animal using a cannula of Krebs. Pieces containing macroscopically necrotic areas were carefully excluded. Seven days after the transplantation the radiopharmaceuticals were injected. At that time the tumors measured 0.5-1.0 cm by 1.0-2.0 cm.

The radiopharmaceuticals used are presented in Table 1. All were commercially available preparations except <sup>197</sup>Hg H albumin which was specially prepared by Hoechst AG, Frankfurt, Germany. Preliminary experiments had shown that the subsequent blood concentrations of only <sup>131</sup>I H albumin and <sup>199</sup>Hg H albumin differed after intravenous and intraperitoneal injection. Therefore these substances were injected intravenously and the other radiopharmaceuticals were administered intraperitoneally.

Samples were taken for investigation at 6, 24 and 48 hours. For <sup>99m</sup>Tc<sup>m</sup> pertechnetate samples were also taken at 15, 30 and 120 hours and for Se selenite at 72 hours. The tumors were dissected and macroscopically nonnecrotic slices were cut. Muscle tissue was obtained from the erector trunci. The tissue samples were weighed wet and were then dissolved in 5.0 ml concentrated nitric

Table 2

Effect of time after intraperitoneal (i.p.) and intravenous (i.v.) administration on the concentration of radiation activity in tumor, blood and muscle. Mean values  $\pm$  SE. Number of animals in parenthesis.

Hour after administration	Tumor ( /g)						Blood ( /ml)			
	15	3	11	12	24	48	72	15	3	0
<sup>203</sup> Hg-chloromerodrin (i.p.)			(10) 0.20 $\pm 0.07$		(9) 0.17 $\pm 0.004$	(11) 0.10 $\pm 0.007$				0.109 $\pm 0.004$
<sup>203</sup> HgCl (i.p.)			(10) 0.50 $\pm 0.02$		(13) 0.52 $\pm 0.03$	(10) 0.36 $\pm 0.02$				0.41 $\pm 0.03$
Hg BMHP (i.p.)			(9) 0.58 $\pm 0.04$		(9) 0.63 $\pm 0.03$	(10) 0.56 $\pm 0.02$				0.98 $\pm 0.06$
Hg H albumin (i.v.)			(10) 1.07 $\pm 0.09$		(10) 0.81 $\pm 0.07$	(8) 0.75 $\pm 0.07$				0.64 $\pm 0.06$
I albumin (i.v.)			(17) 1.22 $\pm 0.07$		(8) 0.34 $\pm 0.02$	(12) 0.13 $\pm 0.01$				3.50 $\pm 0.19$
Se selenite (i.p.)			(5) 0.58 $\pm 0.05$		(5) 0.62 $\pm 0.05$	(5) 0.60 $\pm 0.07$	(5) 0.62 $\pm 0.02$			1.29 $\pm 0.10$
Ga-citrate (i.p.)			(5) 0.91 $\pm 0.07$		(6) 1.53 $\pm 0.13$	(6) 1.88 $\pm 0.09$				1.29 $\pm 0.06$
Tc <sup>99m</sup> per technetate (i.p.)	(6) 0.46 $\pm 0.03$	(6) 0.19 $\pm 0.03$	(6) 0.15 $\pm 0.006$	(6) 0.12 $\pm 0.01$	(5) 0.009 $\pm 0.001$			0.91 $\pm 0.02$	0.41 $\pm 0.05$	0.26 $\pm 0.007$

acid. Blood was withdrawn by puncture of the heart and samples of 1.0 ml were hemolyzed in 4.0 ml of distilled water. The samples of radiation activity were measured in an automatic well scintillation counter with spectrometer using the photopeak of the radionuclide. Aliquots of the injected doses were measured at the same time in the case of <sup>99m</sup>Tc after every fifth sample. Counting statistics were kept below 2 per cent. The concentration of the radiation activity was calculated as a percentage of the given dose per g wet tissue or per ml blood.

### Results

The concentrations of the radiation activity in tumor, blood and muscle at various times are presented in Table 2. Three patterns of tumor uptake emerged

Table 2 (cont.)

Muscle ( %/g)										
12	24	48	72	15	3	6	12	24	48	72
	0.034 ±0.003	0.026 ±0.001				0.012 ±0.002		0.010 ±0.002	0.003 ±0.001	
	0.26 ±0.01	0.14 ±0.01				0.078 ±0.003		0.014 ±0.008	0.009 ±0.0001	
	0.36 ±0.02	0.22 ±0.02				0.096 ±0.003		0.087 ±0.003	0.077 ±0.001	
	0.34 ±0.02	0.25 ±0.03				0.08 ±0.01		0.06 ±0.01	0.03 ±0.01	
	0.89 ±0.06	0.31 ±0.03				0.07 ±0.003		0.04 ±0.003	0.03 ±0.003	
	0.38 ±0.03	0.49 ±0.04	0.50 ±0.02			0.10 ±0.01		0.16 ±0.02	0.15 ±0.02	0.12 ±0.10
	0.30 ±0.02	0.09 ±0.01				0.14 ±0.01		0.10 ±0.03	0.12 ±0.03	
0.16 ±0.009	0.08 ±0.004			0.087 ±0.003	0.028 ±0.005	0.031 ±0.002	0.017 ±0.001	—		

(1)  $> 1$  %/g  $^6\text{Ga}$  citrate,  $^{125}\text{I}$  H albumin, and  $^{199}\text{Au}$  H albumin (2) 0.5—1.0 %/g  $^{199}\text{Au}$  BMHP,  $^{75}\text{Se}$  selenite,  $^{203}\text{HgCl}_2$  (3)  $< 0.5$  %/g  $^{99\text{m}}\text{Tc}$  per technetate and  $^{203}\text{Hg}$  chlormerodrin

The tumor uptake of  $^6\text{Ga}$  citrate increased until 48 hours after administration. The radiation activity concentrations of  $^{75}\text{Se}$  selenite in the tumor remained about the same. The radiation activity concentrations of the other substances in the tumor decreased after the 6 hour measurements. This decrease was rather rapid for  $^{125}\text{I}$  H albumin and  $^{99\text{m}}\text{Tc}$  pertechnetate.

The decrease of the radiation activity in the blood varied considerably (Table 2). We determined the half life of the activity in the blood between 6 and 48 hours for the different radiopharmaceuticals by the graphic method using the

Table 3

*Half lifes in the blood between 6 and 48 hours after injection*

Radiopharmaceutical	Hours
Tc <sup>m</sup> pertechnetate	8.5
Ga-citrate	14.0
I H albumin	16.5
<sup>203</sup> Hg-chlormerodrin	20.5
<sup>203</sup> HgCl <sub>2</sub>	27.0
Hg BMHP	34.0
Hg H albumin	41.5
<sup>75</sup> Se selenite	72.0

mean of the concentration values for the different time intervals. The data which are presented in Table 3 may be an approximate parameter for the biologic half lives of the substances in the blood after their distribution had taken place.

The values for the tumor blood ratios of radiation activities at various times are presented in Table 4 together with values and times of maximum tumor uptake. The blood concentrations for <sup>131</sup>I H albumin and of <sup>99</sup>Tc<sup>m</sup> pertechnetate were always higher than their concentrations in the tumor. Except for <sup>67</sup>Ga citrate, which ranged as high as 22.3, the maximum tumor blood ratios ranged from 0.4—1.2. The concentration of <sup>99</sup>Tc<sup>m</sup> pertechnetate in tumors reached its peak measurement at 12 hours; the others were highest at 48 hours. The time of maximum tumor uptake coincided with the highest blood tumor ratio only in the case of <sup>75</sup>Se selenite and <sup>67</sup>Ga-citrate.

The uptake of muscle was investigated since it is an ubiquitous tissue. It was below the tumor uptake for all radiopharmaceuticals investigated, but there were differences between them which lead to the following classification (Table 2): (1) Muscle uptake < 10% of the tumor uptake: <sup>203</sup>HgCl<sub>2</sub>, <sup>203</sup>Hg chlormerodrin, <sup>199</sup>Hg H albumin, and <sup>131</sup>I H albumin. (2) Muscle uptake 10 to 20% of the tumor uptake: <sup>199</sup>Hg BMHP, <sup>99</sup>Tc<sup>m</sup> pertechnetate and <sup>67</sup>Ga citrate (only after 6 hours). (3) Muscle uptake 20 to 30% of tumor uptake: <sup>75</sup>Se selenite.

### Discussion

The three biologic factors mainly determining the value of a tumor delineating radiopharmaceutical are: (1) The degree of tumor specificity, (2) the concentration of radiation activity in the tumor and (3) the ratio between the radiation activity in the tumor and the blood and the surrounding tissue.

Table 4

Maximum tumor uptake and effect of time after administration on tumor blood ratio Mean values  $\pm$  SE

Radiopharmaceutical	Maximum tumor uptake (%/g)	At h	Tumor uptake/blood concentration (at h)					
			15	3	6	12	24	48
Ga citrate	1.88	48			0.72		5.05	22.31
	$\pm 0.09$				$\pm 0.08$		$\pm 0.24$	$\pm 1.53$
<sup>203</sup> Hg-chlormerodrin	0.20	6			1.86		3.24	4.24
	$\pm 0.07$				$\pm 0.24$		$\pm 0.25$	$\pm 0.25$
<sup>51</sup> Cr H albumin	1.07	6			1.45		2.39	3.87
	$\pm 0.09$				$\pm 0.12$		$\pm 0.14$	$\pm 0.35$
<sup>203</sup> HgCl	0.52	24			1.20		1.93	2.60
	$\pm 0.03$				$\pm 0.08$		$\pm 0.13$	$\pm 0.17$
<sup>131</sup> I Hg BMHP	0.63	24			0.59		1.78	2.58
	$\pm 0.03$				$\pm 0.05$		$\pm 0.08$	$\pm 0.17$
Se selenite	0.62	24-72			0.46		1.07	1.22
	$\pm 0.05$				$\pm 0.05$		$\pm 0.06$	$\pm 0.07$
<sup>125</sup> I H albumin	1.22	6			0.37		0.39	0.43
	$\pm 0.07$				$\pm 0.02$		$\pm 0.07$	$\pm 0.03$
Tc <sup>m</sup> pertechnetate	0.46	15	0.50	0.47	0.59	0.77	0.68	—
	$\pm 0.03$		$\pm 0.02$	$\pm 0.03$	$\pm 0.03$	$\pm 0.10$	$\pm 0.09$	

We have investigated the last two factors as a function of time after the administration of the radiopharmaceuticals. In agreement with MATHEWS & MOLINARO (1963), LONG et coll (1963) and TATOR (1969) we found a higher maximum tumor uptake of <sup>131</sup>I H albumin than of <sup>203</sup>Hg chlormerodrin although they used different tumors in rats and mice. The maximum uptake of <sup>99</sup>Tc<sup>m</sup>-pertechnetate was over twice as high as that of <sup>203</sup>Hg chlormerodrin. A similar ratio was observed by McAFFEE et coll (1964) when they compared the uptake of these radiopharmaceuticals by a transplantable ependymoma in mice. <sup>67</sup>Ga citrate exhibited the highest tumor uptake of all substances which we tested. The same conclusion was drawn by HAYES (1971) and FLANIGAN et coll (1971) after comparing tumor delineating radiopharmaceuticals in experimental tumors but details of their investigations are not yet available.

When we considered the influence of time on the extent of the activity concentration in the tumor two patterns became apparent in the substances tested. <sup>75</sup>Se selenite and <sup>67</sup>Ga citrate remained in the tumor or increased with time while the other substances all decreased with time, some of them rather rapidly like <sup>125</sup>I H albumin and <sup>99</sup>Tc<sup>m</sup> pertechnetate. MATHEWS & MOLINARO (1963) also



Table 5

*Tumor index in relation to time after administration. Maximum values in italics*

Radiopharmaceutical	Time after administration (h)					
	1.5	3	6	12	24	48
Ga citrate			0.65		7.73	<i>41.90</i>
<sup>125</sup> I Hg H albumin			1.55		1.94	<i>2.90</i>
<sup>125</sup> I Hg BNHP			0.34		1.12	<i>1.45</i>
HgCl			0.60		1.00	<i>0.91</i>
Se-selenite			0.27		0.66	<i>0.73</i>
<sup>201</sup> Tl Hg chlormerodrin			0.37		0.55	<i>0.42</i>
<sup>125</sup> I H albumin			<i>0.45</i>		0.13	<i>0.06</i>
<sup>99m</sup> Tc pertechnetate	0.23	0.09	0.09		0.06	—

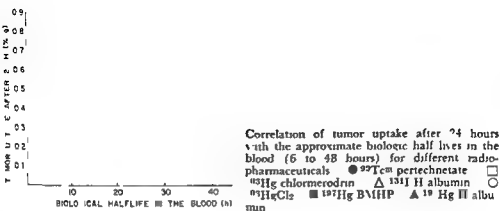
reported a decrease in the tumor concentration of <sup>131</sup>I H albumin. LONO et coll (1963) observed a constant concentration and TAYOR (1969) demonstrated even an increase during 48 hours after administration. This difference may reflect differences in the preparations of radioiodine labeled H albumin and in the animals used.

The background in tumor delineation consists of radiation activity in the blood and in surrounding tissues. Among the substances tested <sup>67</sup>Ga citrate had the most favorable tumor blood ratio and <sup>131</sup>I H albumin and <sup>99m</sup>Tc<sup>m</sup> pertechnetate the most unfavorable. Tumor muscle ratios were considerably higher for all substances tested and showed only small differences except in the case of Se-selenite. The ratio tumor blood and tumor muscle, however, did not remain constant indicating a different change of the radiation activity concentration in the tumor blood and muscle compartment. That means that the demonstration of a tumor may be improved by considering the optimum tumor background ratio in relation to time.

In most substances tested the maximum tumor radiation activity did not coincide with the optimum tumor blood ratio. In order to compare simultaneously tumor radiation activity and tumor blood ratio for the different radiopharmaceuticals we calculated a

$$\text{tumor index} = \text{tumor uptake} \times \frac{\text{tumor uptake}}{\text{blood concentration}}$$

postulating that both factors are of equal significance for the delineation of a tumor (Table 5). These indices predict different relative usefulness for the radiopharmaceuticals when compared to their relative usefulness as predicted



by either their maximum tumor uptake or their optimum blood tumor ratio. Furthermore the indices predict what time may be most favorable for the delineation of the tumor. The predicted optimum time also differed considerably for some of the substances judged only by their maximum tumor uptake or by their optimum tumor blood ratio. The tumor index may be extended by multiplication with the decay factor of the labeling isotope in relation to the time after the administration of the radiopharmaceutical. This takes into consideration the effective half life of the radiopharmaceutical. The ratio to surrounding tissues can also be included in such an index. In practice the significance of these parameters may be different depending on the type of tumor and the types of surrounding tissues. But from a comparative point of view the index is useful since it combines different parameters which do not always run parallel.

The mechanisms of tumor uptake by radiopharmaceuticals are not known. They may depend on the agents used and on the tumors. The different aspects have been discussed previously in relation to brain tumors (BAKAY 1967, 1969). None of the substances which have been used clinically to date are specific for malignant tumors. The extent of their tumor uptake does not exceed their extent of uptake by other organs (MATHEWS & MOLINARO 1963, LONG et coll 1963, TAYLOR 1969). Therefore the question arises if there are also general factors which influence the tumor uptake. When we compared the extent of tumor uptake after 24 hours with the approximate biologic half life in the blood between 6 and 48 hours for the substances tested we observed except for  $^{67}\text{Ga}$  citrate and  $^{75}\text{Se}$  selenite that the longer they remained in the blood the higher was their uptake by the tumor (Figure). MATHEWS & MOLINARO (1963) reported some correlation between the radiation activity concentration in the blood and in the tumor for several of the agents they tested. They postulated that

this would indicate a predominantly extracellular deposition in the tumor, whereas a tumor concentration independent of the blood level would suggest a mainly intracellular deposition. There is evidence from biochemical and autoradiographic investigations that  $^{75}\text{Se}$  selenite and  $^{67}\text{Ga}$  citrate are deposited intracellularly (CAVALERI et coll 1966, WENZEL et coll 1971, HAYES et coll 1971, SWARTZENDRUBER et coll 1971) and that radioiodine labeled H albumin like some other agents is localized extracellularly (MUNDINGER & GERHARD 1963, TATOR et coll 1965, GERHARD et coll 1965). However, a mainly extracellular deposition would not exclude intracellular deposition to some extent. For example, it has been shown that tumor cells can incorporate serum albumin (GHOSE et coll 1962, MEGO & MCQUEEN 1965, TATOR & OLSZEWSKI 1966). Although our data are consistent with the hypothesis of MATHEWS & MOLINARO (1963), other explanations cannot be excluded. Further intensive investigations are necessary to clarify the localization of radiation active agents in malignant tumors and the mechanisms of their uptake. Such data may lead to a more systematic selection and evaluation of potential tumor delineating substances.

An important question is whether experimental results of tumor delineating radiopharmaceuticals can be applied to the situation in the human. This is uncertain to date. But comparative investigations in brain tumors by LORSLAY et coll (1974) showed some predictive value of animal experiments. The predictive value of our animal model is supported by the experimental findings which led to the time at which tumor scanning is normally performed in the human, i.e. after 48 hours or later for  $^{67}\text{Ga}$  citrate, after 24 hours for  $^{113}\text{In}$  chloride, after 48 hours or later for  $^{75}\text{Se}$  selenite, after 24 hours for  $^{201}\text{Tl}$  chlormerodrin, and after 15 hours of  $^{99\text{m}}\text{Tc}$  pertechnetate.

### Acknowledgement

The authors wish to thank Privatdozent D. Gericke, Laboratory for Cancer Research, Farbwerke Hoechst AG, Frankfurt, Germany, for his support and advice in tumor transplantation.

### SUMMARY

Using the transplantable Yoshida sarcoma in the rat, radiation activity concentrations were determined in tumor, blood and muscle at various times for  $^{67}\text{Ga}$  citrate,  $^{99\text{m}}\text{Tc}$  pertechnetate,  $^{75}\text{Se}$ -selenite,  $^{201}\text{Tl}$  chloride,  $^{113}\text{In}$  H albumin,  $^{203}\text{Hg}$  BMHP,  $^{201}\text{Tl}$  chlormerodrin and  $^{125}\text{I}$  H albumin.  $^{67}\text{Ga}$  exhibited the highest tumor uptake and the most favorable tumor/blood ratio. For some radiopharmaceuticals the extent of tumor uptake correlated with their biologic half life in the blood. There is some evidence that the model might be comparable with the human.

## ZUSAMMENFASSUNG

Am transplantablen Yoshida Sarkom der Ratte wurden Tumoraufnahme Blut und Muskelkonzentration sowie einige kinetische Parameter für  $^6\text{Ga}$  Zitat  $^{99}\text{Tc}^m$  Pertechnetat Se Selenit  $^{203}\text{HgCl}$   $^{199}\text{Hg}$  H Albumin  $^{197}\text{Hg}$  BMPH  $^{203}\text{Hg}$  Chlormerodrin und  $^{131}\text{I}$  Albumin untersucht und miteinander verglichen  $^6\text{Ga}$  Zitat zeigte die höchste Tumoraufnahme und das günstigste Tumor/Blut Verhältnis Für einige der geprüften Substanzen bestand eine Korrelation zwischen dem Ausmaß ihrer Tumoranreicherung und ihrer biologischen Halbwertszeit im Blut Es ergaben sich ferner Hinweise daß das Modell vom kinetischen Standpunkt aus mit den Verhältnissen beim Menschen vergleichbar ist

## RÉSUMÉ

En utilisant le sarcome d'Yoshida transplantable sur le rat les auteurs ont déterminé les concentrations de radioactivité dans la tumeur le sang et le muscle à différentes dates pour le citrate de  $^6\text{Ga}$  le pertechnetate de  $^{99}\text{Tc}^m$  le selenite de Se  $^{203}\text{HgCl}$   $^{199}\text{Hg}$  H albumine  $^{197}\text{Hg}$  BMPH  $^{203}\text{Hg}$  chlormerodrine et  $^{131}\text{I}$  H albumine C'est le  $^6\text{Ga}$  qui a présenté la plus forte fixation tumorale et le rapport tumeur/sang le plus favorable Pour certains agents radiopharmaceutiques l'importance de la fixation tumorale était en rapport avec leur demi vie biologique dans le sang Il y a des preuves que ce modèle peut être comparable avec l'homme

## REFERENCES

- BAKAY L. Basic aspects of brain tumor localization by radioactive substances J Neurosurg 27 (1967) 239  
 — Brain tumor scanning with radioisotopes Charles C Thomas Springfield Ill 1969  
 CAVALIERI R C SCOTT K G and SAJENJI E Selenite ( $^{76}\text{Se}$ ) as a tumor localizing agent J nucl Med 7 (1966) 197  
 FLANNAGAN C V HOLSCHER M A DYER N C BROWN L and BRILL A H Experimental model for evaluation of tumor localizing radiopharmaceuticals J nucl Med 12 (1971) 335  
 GERHARD H MÜNDINGER F GABRIEL E und WALDBAUR H Neuere Untersuchungen über die Tumoranreicherung radioaktiver Schwermetallisotope ( $^{203}\text{Hg}$   $^{204}\text{Bi}$  und  $^{64}\text{Cu}$ ) Nucl Med (Stuttg) (1965) Suppl No 3 S 229  
 GERICKE D und ENGELBART K Über die Konservierung von Tumorgewebe bei  $-70^\circ\text{C}$  Krebsforsch 65 (1962) 147  
 GHOTE T NAIK R C and FOTHERGILL J E Uptake of proteins by malignant cells Nature 196 (1967) 1108  
 HAYES R L Personal communication (1971)  
 — NELSON B SWARTZENDRUBER H C BROWN D H CARLTON J E and BYRD B L Factors affecting the localization of  $^{67}\text{Ga}$  in animal tumors J nucl Med 12 (1971) 364  
 LOKLEY H H SWEET W H POWSNTER H J and DOW E Suitability of tumor bearing mice for predicting relative usefulness of isotopes in brain tumors Arch Neurol Psychiat 71 (1954) 684  
 LONG R G McAFFEE J G and WINKELMAN J Evaluation of radioactive compounds for the external detection of cerebral tumors Cancer Res 23 (1963) 98

- MATHEWS C. M. E. and MOLINARO G.: A study of the relative value of radioactive substances used for brain tumour localization and of the mechanism of tumour brain concentration uptake in transplantable fibrosarcoma brain and other organs in the rat. *Brit. J. exp. Path.* 44 (1963) 260.
- McAFFEE J. G., FLEGER C. F., STERN H. S., WAGNER H. N. JR and MIGHTA T.:  $^{99m}\text{Tc}$  per technetate for brain scanning. *J. nucl. Med.* 5 (1964) 811.
- MEOG J. L., McQUEEN J. D.: The uptake of labeled proteins by particulate fractions of tumor and normal tissues after injection into mice. *Cancer Res.* 25 (1965) 865.
- MÜNDINGER F. and GERHARD H.: Untersuchungen über die Verteilung der zur Hirntumor diagnostik verwendeten Radioisotope in der Blutbahn in experimentellen Tumoren und menschlichen Hirngeschwulsten. *Acta neurochir.* 11 (1963) 398.
- SWARTZENDRUBER D. C., NELSON B. and HAYES R. L.: Gallium 67 localization in lysosomal like granules of leukemic and nonleukemic murine tissues. *J. nat. Cancer Inst.* 46 (1971) 941.
- TATOR C. H.: Factors involved in the uptake and distribution of radioactive tracers in brain tumors and brain. *In*: Brain tumor scanning with radioisotopes, p. 21. Edited by L. Bakay, Charles C. Thomas, Springfield, Ill. 1969.
- MORLEY T. P. and OLSZEWSKI J.: A study of factors responsible for the accumulation of radioactive iodinated human serum albumin (RIHSA) by intracranial tumours and other lesions. *J. Neurosurg.* 22 (1965) 60.
- OLSZEWSKI J.: Factors responsible for the distribution of radioactivity in a mouse glioma and brain after injection of radioiodinated human serum albumin (RIHSA). *Cancer Res.* 26 (1966) 1569.
- WENZEL M., OTTO R. and RIZHILE I.: Der Einbau von  $^{76}\text{Se}$  nach Applikation von radioaktivem Natrium Selenit in Normalgewebe und in Tumoren *in vitro* und *in vivo*. *Int. J. appl. Radiat.* 22 (1971) 361.
- YOSHIDA T.: The Yoshida sarcoma: an ascites tumor. *Gann* 40 (1949) 1.

## LATE EFFECTS OF IRRADIATION ON THE THYROID GLAND IN MICE

### II Irradiation of mouse foetuses

by

G WALINDER and ANNE MARIE SJÖDEN

The neoplastic changes occurring in the thyroids of CBA mice exposed during maturity to ionizing radiation either by roentgen irradiation localized to the gland or by injection of  $^{131}\text{I}$  have been reported in the first part of this investigation (WALINDER 1972 b). In the present part, the thyroids of mouse foetuses were irradiated on the 18th day of gestation (usually 2 days before birth) either by intravenous injection of  $^{131}\text{I}$  to the mothers, by whole body exposure of the mothers to roentgen radiation or with a combination of both types of radiation. The object of these investigations was among other things to compare the radiation sensitivity of the growing thyroid in mouse foetuses with that of mature mice as reflected in the occurrence of radiation induced neoplasms. Such a comparison could not be made however as it was found that the thyroids of the 2 year-old control mice used in the present experiments weighed twice as much as those in the earlier experiments (Fig. 1).

Submitted for publication 24 February 1972

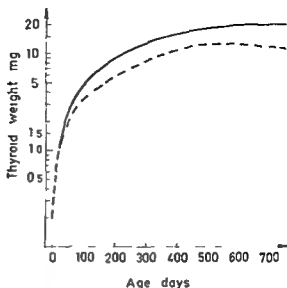


Fig. 1. Thyroid weights in relation to age in male CBA mice. The lower (broken) curve was obtained from mice in the earlier experiments and the upper (solid) curve from mice in the present ones.

The results obtained in the mice irradiated in the foetal stage will, however, be described here as they throw light when compared with the earlier experiments using adult mice on the part played by the growth factors in the development of radiation damage into tumours in the thyroid of the CBA mouse.

### Material and Methods

The housing and management of the mice were the same as in the experiments on adult animals. The methods for the  $^{131}\text{I}$  injections and the determination of the  $^{131}\text{I}$  doses in the thyroids have been described in more detail by WALINDER (1971) and WALINDER & SJÖDEN (1971).

The irradiation of the pregnant mothers with roentgen rays was carried out with the animals placed in a slowly rotating plexiglass wheel at a distance of 45 cm from the anode of the roentgen tube. Radiation data: 260 kV, 10 mA, filter 5 mm Al + 0.85 mm Cu and HVL 2 mm Cu. The dose rate was 72 R per min to the central parts of the animal (calculated on the basis of measurements with LUI LP's LiF dosimeters in mouse phantoms). All mice given roentgen irradiation were exposed for 2.63 min and it was calculated that the mean dose to the foetuses was approx. 190 R = 180 rad (ICRU Handbook 85, 1964).

The techniques used for sectioning, fixation and staining of the thyroid and pituitary tissues for examinations with the light microscope have been described earlier (WALINDER 1972b).

Males and females of the CBA mouse strain were used. The thyroid weights were measured in 550 males and 584 females when the mice had reached an age of between 680 and 750 days. Some moribund animals had to be killed before that age, however, the number was especially large in the groups that received roentgen irradiation. The histologic analysis covered 1 511 mice (815 males and 696 females). The distribution of the mice over the different radiation groups is indicated in the following tabulation (M = males, F = females)

Roentgen dose rad	I doses to lobe centres rad	No. of thyroids weighed		No. of thyroids examined histologically	
		M	F	M	F
—	—	207	215	263	225
—	1 900—2 100	138	141	172	160
—	3 800	37	23	89	58
—	4 700—4 900	12	18	16	20
—	6 800—7 300	69	60	102	83
180	—	27	39	48	47
180	1 500—1 800	43	55	79	73
180	2 600—3 000	17	33	46	30

The pituitary glands from most of the mice that had been selected for determination of the thyroid weight were also removed for weighing. Some pituitaries from the controls as well as all those that weighed more than 6 mg. were examined histologically.

## Results

### *Thyroid and hypophysis weights*

The thyroids in the 2 year old mice weighed as mentioned before much more than those in the earlier experiments (WALINDER et coll 1971; WALINDER 1972 b). The immediate explanation of this increase seems to be that besides the colloid goitre which was the main reason for the previously observed enlargement in the aging CBA mouse (WALINDER et coll.) there was in the present investigation also a considerable increase in number and size of hyperplastic areas and nodules (Fig. 2) as well as a relatively high frequency of thyroidal neoplasms (Table 2). The basic cause of this adenomatous development is not clear however. The weight of the pituitary glands in the control mice was also higher than in the earlier experiments (Table 1).

In contrast with what was observed in the earlier experiments with mice irradiated during maturity no correlation between thyroid dose and pituitary weight was found. On the other hand, there was a positive correlation between



Table 1

*Thyroid and pituitary weights of mice exposed to  $^{131}\text{I}$  roentgen rays or a combination of the two types of radiation*

I dose to central thyroid lobe rad	Roent- gen dose rad	Sex	Thyroid weight mg ( $\pm$ SE)	$\Pi$	Pituitary weight mg ( $\pm$ SE)	Thyroid weight Pituitary weight ( $\pm$ SE)	p
—	—	M	20.8 $\pm$ 0.3		2.02 $\pm$ 0.13	10.6 $\pm$ 0.3	
—	—	F	15.1 $\pm$ 0.3		2.36 $\pm$ 0.07	6.7 $\pm$ 0.1	
1 900—2 100	—	M	20.3 $\pm$ 0.4	—	2.05 $\pm$ 0.14	10.1 $\pm$ 0.3	—
1 900—2 100	—	F	14.9 $\pm$ 0.3	—	2.20 $\pm$ 0.15	6.8 $\pm$ 0.2	—
3 800	—	M	19.3 $\pm$ 0.7	<0.05	2.22 $\pm$ 0.26	8.8 $\pm$ 0.3	<0.001
3 800	—	F	13.2 $\pm$ 0.7	<0.01	2.25 $\pm$ 0.11	5.8 $\pm$ 0.2	<0.001
4 700—4 900	—	M	16.5 $\pm$ 0.8	<0.001	2.33 $\pm$ 0.11	6.8 $\pm$ 0.3	<0.001
4 00—4 900	—	F	11.9 $\pm$ 0.4	<0.001	2.17 $\pm$ 0.16	5.2 $\pm$ 0.2	<0.001
6 800—300	—	M	15.5 $\pm$ 0.5	<0.001	2.17 $\pm$ 0.15	6.6 $\pm$ 0.2	<0.001
6 800—300	—	F	10.8 $\pm$ 0.5	<0.001	2.25 $\pm$ 0.08	4.8 $\pm$ 0.2	<0.001
—	180	M	20.1 $\pm$ 0.6	—	2.13 $\pm$ 0.15	10.8 $\pm$ 0.3	—
—	180	F	14.9 $\pm$ 0.4	—	2.18 $\pm$ 0.16	7.0 $\pm$ 0.2	—
1 500—1 800	180	M	19.4 $\pm$ 0.5	<0.05	2.22 $\pm$ 0.10	8.8 $\pm$ 0.2	<0.001
1 500—1 800	180	F	13.2 $\pm$ 0.4	<0.001	2.16 $\pm$ 0.08	5.6 $\pm$ 0.1	<0.001
2 600—3 000	180	M	17.2 $\pm$ 1.0	<0.001	2.39 $\pm$ 0.22	7.0 $\pm$ 0.3	<0.001
2 600—3 000	180	F	12.1 $\pm$ 0.5	<0.001	2.24 $\pm$ 0.26	5.0 $\pm$ 0.2	<0.001

thyroid and pituitary weights within the different experimental groups. Because of this correlation the quotient between these gland weights displayed a much smaller degree of scattering around the mean values than was the case with the thyroid weights. The significance of the changes in the weight relations between the two glands was in consequence more evident in the lower dose range than were the corresponding significance figures for the thyroid weights (Table 1). It was found also that the ratio between the mean weight of the thyroids in the mice given 4 700 to 4 900 rad to the centre of the lobes and that in the controls was the same as had been observed when the mice were 1 to 11 months old (WALINDER & SJÖDEN 1971).

Table 2

Number and frequency of thyroid neoplasms. The figures within brackets refer to surviving mice (killed at 680 to 750 days of age) in groups that included moribund animals which had to be killed prematurely

I dose to central thyroid lobe rad	Roent- gen dose rad	No of mice examined	Sex	No of adeno- mas	No of carcinomas				Percentage of mice with neoplasms
					Foll	Pap	Anapl	Total	
—	—	263	M	9	1	0	1	2	4.2 (4.2)
—	—	275	F	4	0	0	0	0	1.2 (1.2)
1 900—2 100	—	172 (140)	M	15 (14)	2	0	1	3	10 (12)
1 900—2 100	—	160 (135)	F	5	0	0	0	0	3.1 (3.7)
3 800	—	89 (57)	M	10	0	1	2	3	15 (23)
3 800	—	58 (48)	F	2	0	0	0	0	3.5 (4.9)
4 000—4 900	—	16 (11)	M	4	1	0	0	1 (0)	31 (36)
4 000—4 900	—	20 (16)	F	4 (3)	1	0	0	1	25 (25)
6 800—7 300	—	102 (90)	M	29	4	1	1	6	34 (39)
6 800—7 300	—	83 (73)	F	12 (10)	1	0	2	3	18 (18)
—	180	48 (27)	M	2	0	0	0	0	4.2 (7.4)
—	180	47 (39)	F	0	0	0	0	0	0 (0)
1 500—1 800	180	79 (41)	M	4	0	0	1	1 (0)	6.3 (10)
1 500—1 800	180	73 (53)	F	5	0	0	0	0	6.9 (9)
2 600—3 000	180	46 (26)	M	8	0	0	1	1 (0)	20 (31)
2 600—3 000	180	30 (25)	F	6	0	0	0	0	20 (24)

WALINDER 1972 a) In the higher dose range the corresponding quotient had decreased slightly

An addition of 180 rad of roentgen radiation increased the inhibitory effect of the radioiodine on the thyroid weight. A ten times higher extra dose of  $^{131}\text{I}$  to the centre of the lobes was required to produce the same increased inhibition as was obtained with the roentgen dose (Table 1). As the  $^{131}\text{I}$  dose decreases towards the periphery of the lobes and amounts in that area to 50 per cent of the dose in the central parts of the gland (WALINDER 1971) the effectiveness of the roentgen irradiation in inhibiting age dependent thyroidal enlargement may be said to be between 5 and 10 times greater than that of  $^{131}\text{I}$  irradiation.

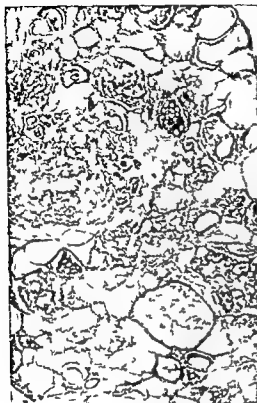


Fig. 2



Fig. 3

Fig. 2. Thyroid tissue in an unirradiated 2-year-old mouse. The follicles are irregular with vesicular or granular colloid. The hyperplastic foci and nodules contain degenerated cells (H & E  $\times 300$ ).

Fig. 3. Histiocytic tumour containing highly pleomorphic cells with bizarre nuclei. Nuclear inclusion and vesicular nuclei are common (Tripas  $\times 300$ ).

### *Histologic observations*

*Frequency of thyroid tumours.* The classification of benign and malignant tumours in the CBA mouse thyroids followed the same definitions as those used for the adult mice.

The total number of mice and tumours and the tumour frequency, are given in Table 2. Most of the mice were killed when they were between 680 and 750 days old. Some moribund animals had to be killed before the age of 680 days. The values in Table 2 have therefore been supplemented with the number of mice and tumours and the tumour frequency in surviving animals (within brackets), i.e. mice killed after the age of 680 days. None of the tumours observed



Fig 4



Fig 5

Fig 4 Follicular carcinoma Follicular elements can be seen in the capsular blood vessel (H & E  $\times 300$ )

Fig 5 Papillary carcinoma The cells are irregularly arranged and the nuclei are vesicular. These cellular characteristics are in marked contrast to the more uniform cells and usually hyperchromatic nuclei in the papilliferous structures of hyperplastic nodules (van Gieson  $\times 300$ )

in moribund mice were present in animals under 558 days of age. The thyroid weights in the controls were roughly the same at that age as they were when the mice were 750 days old (Fig. 1).

The number of thyroid tumours was in these experiments much higher than in the earlier experiments. In the lower dose range the number of neoplasms increased more or less linearly with the dose, while in the range between 3 800 and 4 000 rad there was an abrupt increase in tumour frequency which ceased when the dose was further raised to 6 800 to 7 300 rad.

Table 2 does not give such a clear picture regarding the relation between the effectiveness of roentgen irradiation and that of  $^{131}\text{I}$  irradiation. Additional roentgen radiation did not appear to raise the tumour frequency in the lower

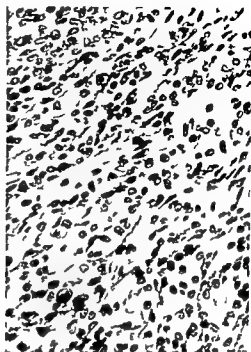


Fig 6 Anaplastic transition of a follicular carcinoma. Some follicular remains can be seen in the lower right corner (H & E  $\times 300$ )

dose range but the sharp increase in frequency which in mice treated with  $^{131}\text{I}$  alone took place in the dose range between 3 800 and 4 900 rad was obtained already with  $^{131}\text{I}$  doses of less than 3 000 rad if this radiation was combined with a roentgen dose of 180 rad

A striking difference noted between the effects of irradiation with  $^{131}\text{I}$  alone and those obtained with combined irradiation was that the former gave a much higher tumour rate in males than in females while this effect was not observed when the two forms of radiation were combined

*Morphology of the pituitary tumours* The hypophyseal tissues had the same hyperplastic characteristics as those observed in the mice irradiated at a mature age. In contrast with the findings in the earlier experiments, however, such tissue changes were now often seen in the glands of the controls as well. Especially in the mice that had been exposed to both  $^{131}\text{I}$  and roentgen irradiation there were often very large pituitary glands weighing as much as 85 mg. The largest pituitary observed in the mice irradiated with  $^{131}\text{I}$  alone weighed 11 mg. The largest pituitary tumours were composed of very large chromophobe cells with nuclear inclusions and a high mitotic frequency (Fig 3)

*Morphology of the thyroid tumours* A much larger number of different tumour forms was found in the present experiments than in the preceding ones. Both

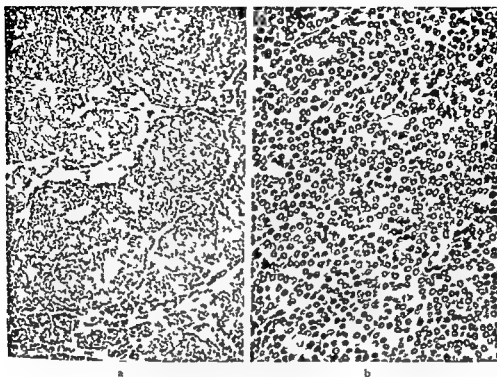


Fig 7 Small cell carcinoma a) Lobulated part of the tumour (H & E  $\times 125$ ) b) Magnified view of the same section showing a diffusely growing part of the tumour ( $\times 300$ )

benign and malignant tumours were observed even in the controls a finding that was not obtained in earlier investigations on the thyroids of old mice (WALINDER et al. WALINDER 1972 b). A relatively large number of anaplastic thyroid carcinomas of small cell giant cell and solid pleomorphic type were encountered such forms were not observed in any of the previous experiments (Figs 4–8). However in spite of this finding and despite the occurrence of numerous vascular invasions no metastases were seen either in cervical lymph nodes lungs or skeleton.

### Discussion

*Thyroid and hypophysis weights* As a result of the afore mentioned adenomatous goitre in the controls the thyroid weights were nearly twice as high as in the earlier experiments. This development obviously was a consequence of a more marked thyroidal hypofunction than had been present in the previous experi-

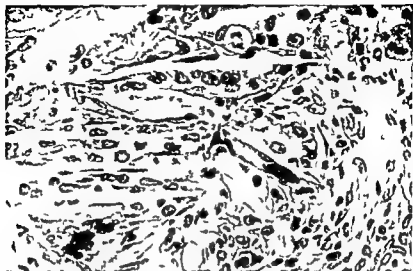


Fig 8 Giant cell carcinoma. The cells are often multinucleated. The mitotic frequency is high (H & E  $\times 500$ )

ments a condition which manifested itself in pituitary glands that were larger than had previously been observable in unirradiated non gonadotropin stimulated mice and in a distinctly positive correlation between pituitary and thyroid weights.

Irradiation of the thyroid in mouse foetuses led, as has been demonstrated earlier (WALINDER 1972 a), to suppression of cell division, and cell death during the first week after exposure. After a  $^{131}\text{I}$  dose (to the lobe centre) of 4 600 rad, however, cell division was resumed to the same extent as in the thyroids of the controls from the second week and onwards after the injection of the radioiodine. The mitoses were often atypical, however, and did not result in daughter cells. In consequence there also occurred a certain amount of cell death after the first week of life. Notwithstanding this, the thyroid weights increased at the same rate as in the control mice, a process that was, however, due rather to increasing hyperaemia than to compensatory processes such as increased cell size or increased colloid formation. The irradiated thyroid glands never reached the same weights as those of the controls. The probable explanation of this is that the radiation damage to surviving cells as well had been so extensive that compensatory effects such as have been observed for instance in mice partially thyroidectomized by surgery (WALINDER et coll.) had been unable to normalize the partial thyroidectomy produced by the irradiation. This inability was also reflected in a smaller thyroid weight/pituitary weight quotient in the irradiated mice as

compared with the unirradiated animals (Table 1). It may however be mentioned in this connection that  $^{131}\text{I}$  doses (to the centres of the lobes) of 5 000 to 6 000 rad to mature CBA mice led to greater differences between the weights of irradiated and unirradiated thyroids when the mice had reached the age of 2 years than was the case when the mouse foetuses in the present experiments were irradiated with the same doses (cf. WALINDER 1972 b). The reason for this may once again however lie in the more powerful TSH pressure on the thyroid glands and the nodule formation resulting from it in the mice irradiated in the foetal stage in the present experiments as compared with the earlier ones in which adult mice were irradiated.

*Radiation induced thyroid tumours.* In view of the extreme thyroid growth in the aging CBA mouse — extreme in comparison with earlier observations — the high tumour frequency and the tendency toward more anaplastic tumour forms noted in the present experiments cannot be attributed solely to the early growth in the immature mouse or to the late very rapid growth in the old gland. Experiments have been started however with the object of combining the investigations presented in this report and those described earlier (WALINDER 1972 b). The experiments have been carried out with mice born at the same time. In some groups the pregnant mothers were injected with  $^{131}\text{I}$  or irradiated with roentgen rays alone or in combination with  $^{131}\text{I}$  on the 18th day of gestation and in other groups the corresponding irradiations were not given until the mice had reached the age of 3 months. It should then be possible by investigating the development of thyroid tumours in all the offspring until they reach the age of 2 years to detect any differences between the tumour inducing effect of the irradiation in the thyroids of the foetuses and of the mature mice irrespective of how the gland subsequently develops in the old mouse. These experiments are not yet ready for histologic analysis.

The present experiments have however demonstrated in general the significance of the growth factors in the radiation induced tumour genesis. Increased thyroidal growth may in itself serve as a tumour provoking factor and it potentiates the tumour inducing effect. The process apparently takes place in the following way. The irradiation first inhibits the epithelial proliferation. This process probably counteracts the development of radiation damage into macroscopic tumours. In the CBA mouse however the colloidal goitre increasing with the age of the animal as well as the radiation induced inhibition of the epithelial proliferation leads to increased TSH pressure on the glands which by degrees gives rise to hyperplastic centres and nodules from which tumours may develop if the radiation dose has not been too high. Many of the nodules observed in the thyroid glands which had received the highest doses of  $^{131}\text{I}$  (6 800 to 7 300 rad to the lobe centres) were composed of strikingly degenerated tissue displaying



marked cell damage (karyorrhexis, pyknosis) this may explain why tumour frequency was not higher than in glands that had been exposed to 4 700 to 4 900 rad (Table 2). In the earlier experiments in which the thyroidal growth had been more moderate the optimal tumour dose was higher.

## SUMMARY

The thyroid gland of mouse foetuses was irradiated by exposing the mothers on the 18th day of gestation to intravenous injections of  $^{131}\text{I}$  whole body roentgen irradiation or a combination of the two forms of radiation. The occurrence of thyroid tumours was investigated when the offspring had reached the age of about 2 years. The frequency of both benign and malignant thyroid tumours was high. As the aging thyroids of the unirradiated mice revealed adenomatous changes to an extent that had not been seen in earlier investigations the high frequency of tumours in the irradiated thyroids could not be attributed unequivocally to any special radiation sensitivity in the foetal glands. The significance of the growth factors in the development of radiation induced thyroid neoplasms is discussed.

## ZUSAMMENFASSUNG

Die Thyreoidea der foetalen Maus wurde durch Exposition der Muttertiere am 18. Graviditätstag durch intravenöse Injektion von  $^{131}\text{I}$  Gesamtkörperbestrahlung mit Röntgen oder einer Kombination dieser beiden Bestrahlungsformen bestrahlt. Das Vorkommen von Tumoren der Thyreoidea bei diesen Foeten wurde untersucht, wenn diese ein Alter von etwa 2 Jahren erreicht hatten. Die Frequenz von sowohl benignen als auch malignen Tumoren war hoch. Da die alternde Thyreoidea von nicht bestrahlten Mäusen adenomatöse Veränderungen in einem Umfang aufwies wie sie nicht in früheren Untersuchungen gefunden worden war, kann die hohe Frequenz von Tumoren in der bestrahlten Thyreoidea nicht ohne weiteres auf eine besondere Strahlenempfindlichkeit der foetalen Drüsen zurückgeführt werden. Die Bedeutung von Wachstumsfaktoren an der Entwicklung von Strahlen hervorgerufenen Neoplasmen der Thyreoidea wird besprochen.

## RÉSUMÉ

La glande thyroïde de foetus de souris a été irradiée en exposant les mères au 18ème jour de la gestation à l'injection intra-veineuse de  $^{131}\text{I}$  à l'irradiation par les rayons de Roentgen de tout le corps ou à une association de ces deux formes de radiation. Les auteurs ont étudié l'apparition de tumeurs thyroïdiennes quand les souris irradiées in utero ont atteint environ l'âge de deux ans. La fréquence des tumeurs thyroïdiennes bénignes et malignes était élevée. Étant donné que les thyroïdes des souris non irradiées ont présenté avec l'âge des lésions adénomateuses dans une mesure qui n'avaient pas été observée au cours des recherches précédentes, la grande fréquence des tumeurs dans les thyroïdes irradiées n'a pu être attribuée de façon certaine à une sensibilité spéciale aux radiations des thyroïdes foetales. Les auteurs examinent l'importance des facteurs de croissance dans le développement de néoplasmes thyroïdiennes dues aux radiations.

## REFERENCES

- ICRU Report No 10a Physical aspects of irradiation NBS Handbook 85 National Bureau of Standards Washington D C 1964
- WALINDER G Determination of the  $^{131}\text{I}$  dose to the mouse thyroid Acta radiol Ther Phys Biol 10 (1971) 558
- (a) Quantitative effects of  $^{131}\text{I}$  on different tissue components in foetal and goitrogen-challenged mouse thyroids Acta radiol Ther Phys Biol 11 (1972) 1
  - (b) Late effects of irradiation on the thyroid gland in mice I Irradiation of adult mice To be published in Acta radiol Ther Phys Biol 11 (1972)
  - and SJÖDEN A M Effect of irradiation on thyroid growth in mouse foetuses and goitrogen-challenged adult mice Acta radiol Ther Phys Biol 10 (1971) 579
  - and JOHANSSON C J Aging processes in the thyroid gland of the CBA mouse FOA Reports Vol 5 No 7 (1971)

## MODIFICATION OF ISODOSE CURVES BY MEANS OF COMPENSATING FILTERS

by

N E SORENSSEN

Two parallel opposing fields may be the best means of irradiating carcinoma of the thyroid or other cervical neoplasms although masking of the lower part of the area by the shoulders has to be overcome. The fields may be angled  $10^\circ$  to  $25^\circ$  if only a small area is cut off depending on the size of the region to be covered (Fig. 1). The isodose curve, which touches the longitudinal axis of the patient will follow curve C if a plane field be compensated for missing tissue. Added to the corresponding curve from the opposing field it produces an inhomogeneous absorbed dose distribution with a hot spot in the upper part of the affected area. A change from C to an isodose curve such as C', is needed for homogeneous distribution over the central part of the area.

DUTREIX & DUTREIX (1962) and later JOHNS & CUNNINGHAM (1969) described an empirical method of parallel shifting of the isodose curves to correct for an airgap  $h$  the displacement for  $^{60}\text{Co}$  irradiation is  $2/3 h$ . This method reversed makes it possible to determine the contour of the patient which alters the isodose curve from C to C'.

A series of lines is drawn parallel to the central axis (e.g. at 1 cm intervals). The distance  $d$  from C to C' along the lines is measured and  $3/2 d$  marked out

Submitted for publication 12 July 1971

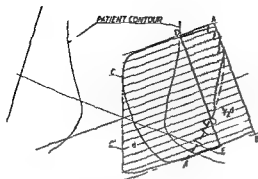


Fig 1

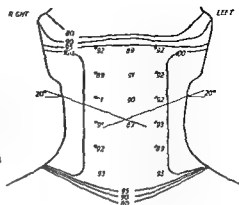


Fig 2

Fig 1 The principle of the method

Fig 2 A comparison between calculated and measured absorbed dose distribution in an Alderson phantom. The calculations are represented by the curves and the measuring points by \*. Figures indicate percentages of doses given.

from the line AB, which indicates the reference plane of the isodose curve. Contour AOA' (the broken curve in Fig 1) which must be produced by means of the compensating filter is thus obtained. The filter is designed from aluminum columns (ELLIS et coll 1959, HALL et coll 1961) of square cross section. The length of the columns corresponds (to the nearest cm) to the amount of missing tissue and the square is equivalent to 1 cm in the treatment distance. The contour AOA is then approached with the saw tooth curve, i.e. the sum of the compensating filter and the true contour of the patient.

A normal filter that compensates up to the plane DE is first designed. The filter is then increased with block DOA and decreased with block EOA (hatched areas) so that both a correction for missing tissue and adjustment of the isodose curves are obtained in the same filter.

Calculated and measured absorbed dose distribution with opposing fields (size 15 cm  $\times$  10 cm) angled at 20° for an Alderson phantom are compared in Fig 2. No corrections were made for body inhomogeneities. The measurements were obtained by means of thermoluminescence with LiF powder; the standard deviation was  $\pm 3.5$  per cent.

## SUMMARY

A method of modifying isodose curves by means of compensating filters in the treatment of malignant disease of the neck is described. This is required when the shoulders interfere with parallel opposing fields in radiation therapy.

## ZUSAMMENFASSUNG

Die Anwendung von Ausgleichsfiltern bei der Strahlenbehandlung von malignen Erkrankungen des Halses wird erörtert. Diese Filter dienen zum Dosisausgleich entgegengesetzter Felder, wenn die Schultern im Wege sind.

## RÉSUMÉ

L'auteur décrit une méthode de modification des courbes isodoses par des filtres compensateurs dans le traitement des affections malignes du cou. Ceci est nécessaire quand les épaules s'interposent dans la radiothérapie par des champs parallèles opposés.

## REFERENCES

- DUTREIX A. et DUTREIX J. Construction des isodoses pour les surfaces obliques et irrégulières. *J. Radiol. Électrol.* 43 (1962) 671.
- ELLIS F., HALL E. J. and OLIVER R. A compensator for variations in tissue thickness for high energy beams. *Brit. J. Radiol.* 32 (1959) 421.
- HALL E. J. and OLIVER R. The use of standard isodose distributions with high energy radiation beams. The accuracy of a compensator technique in correcting for body contours. *Brit. J. Radiol.* 34 (1961) 43.
- JOHN H. E. and CUNNINGHAM J. R. *The physics of radiology*. Third edition, p. 355. Charles C. Thomas, Springfield, Illinois, 1969.

## ANGULAR DISTRIBUTION OF RADIATION SCATTERED FROM A PHANTOM EXPOSED TO 10 TO 50 kVp ROENTGEN RAYS

by

D M J BENSTOCK and T E BURLIN

Several investigations of the radiation scattered from anthropomorphic phantoms exposed to radiation from therapy installations are extant (GLASSER et coll 1961 LORENTZON 1954 WALSTAM 1954 LINDELL 1954 FRANTZ & WYCKOFF 1959 SANDERS et coll 1960 HETTINGER 1960 MARTIN & MULLER 1961). In reviewing the data provided by these investigations, BOMFORD & BURLIN (1963) noted a lack of information concerning scattered radiation at angles other than  $90^\circ$  and  $180^\circ$  and carried out measurements to provide the required data for irradiation of 100 to 300 kVp. McEWAN (1966) made a very similar series of measurements to those of BOMFORD & BURLIN but extended them down to an energy of 50 kVp. In the treatment of dermatologic conditions by ionising radiation roentgen rays of energy 10 to 50 kVp are frequently employed. There appears to be a complete lack of information concerning the scattered radiation in this energy range even though the dose rates from the beryllium window tubes used are very much greater than those from conventional therapy machines and

Submitted for publication 12 January 1972

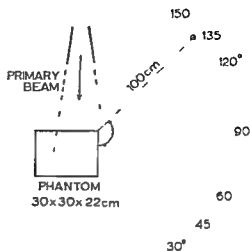


Fig 1 Experimental set up

in addition the operator is permitted to remain in the treatment room (Code of practice 1964). This paper presents measurements of the angular distribution of the scattered radiation in this energy range

### Experiment

As the purpose of this investigation was to provide data relevant to protection in a radiation therapy department the atomic number of the scatterer was not varied. The measurements were confined to a tissue equivalent phantom of cross-section 30 cm  $\times$  30 cm and depth 22 cm. This latter dimension simulates the antero-posterior thickness of a large patient. The roentgen ray beam was directed horizontally at the phantom as shown in Fig 1. Two fields 21 cm  $\times$  21 cm and 9 cm diameter circle at 30 cm focal skin distance were used and both fields lightly overlapped the edge of the phantom to ensure that the maximum scattered radiation was measured particularly in the forward direction. The details of the position of the fields with respect to the phantom are shown in Fig 2. The surface areas of the phantom irradiated by the field were 54 cm<sup>2</sup> and 431 cm<sup>2</sup>. Measurements were made at five different tube potentials the filtration and half value thickness being shown in Table 1.

The exposure rate at the incident surface was measured and the scattered radiation was measured at 1 metre from the corner of the phantom at 30° 45° 60° 90° 120° 135° 150° degrees to the central axis of the beam. A 350 cm<sup>3</sup> ionization chamber was used in conjunction with a portable electrometer (F 1 L 37C dosimeter) to measure the scattered radiation in these positions. The ionization

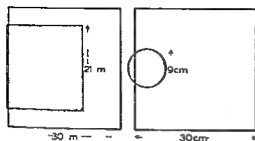


Fig. 2 The shaded area represents the irradiated field and shows its position with respect to the phantom.

chamber was enclosed in a 11 mm thick lead shield, which had a window wide enough for the whole of the chamber to just see the whole of the phantom. This chamber was thus shielded from the leakage radiation from the tube housing and the extraneous scattered radiation from the walls, floor, etc., and it recorded only the radiation scattered from the phantom.

The ionization chamber required calibration in the scattered photon spectrum to which it was exposed at the different angles. This is facilitated by the fact that the photon energy spectrum changes very little during scattering in this energy region. This may be seen by firstly considering the change in the photon energy in a single Compton scattering event. Table 2 illustrates how small the maximum and mean photon energy changes are in fact. Secondly, it should also be noted that below 20 kVp (9 keV effective) Rayleigh scattering, where no energy change occurs, is the dominant scattering process. Experimental confirmation of the assertion that the photon energy spectrum is almost unchanged on scattering

Table 1

*Half value thickness and effective photon energy of the primary beams*

Tube potential (keV)	Added filtration (mm)	Half value thickness		Effective roentgen energy $E_{eff}$ (keV)
		mm Al	mm Cu	
10	—	0.017		5.4
20	0.17 Al	0.078		9.4
30	0.40 Al	0.28		14
40	1.67 Al	0.53		18
50	1.1 Al	0.72		20
100	—	1.7		28
140	3 Cu + 1.0 Al		0.4	56
200	3 Cu + 1.0 Al		1.9	105
250	3 Cu + 1.0 Al		1.85	104
300	1 Sn + 0.5 Cu		3.2	142



Table 2

*Maximum and mean change in the photon energy occurring in a single Compton scattering of the maximum and the effective photon energies in the roentgen spectra (keV)*

Tube potential	Maximum energy $E_{\max}$	Maximum change in $E_{\max}$	Mean change in $E_{\max}$	Effective energy $E_{\text{eff}}$	Maximum change in $E_{\text{eff}}$	Mean change in $E_{\text{eff}}$
50	50	8.1	4.0	20	1.4	0.60
40	40	5.4	2.5	18	1.2	0.50
30	30	3.1	1.5	14	0.8	0.3
20	20	1.5	0.6	9.4	0.3	0.1
10	10	0.4	0.1	5.4	0.1	0.04

is provided by the work of McEwan (1966). He found, to within the limits of his experimental accuracy, the half value thickness of the scattered radiation for 50 kVp roentgen rays was identical with that of the primary radiation at all scattering angles. Nevertheless roentgen ray spectra generated at 10 to 50 kVp change significantly with distance from the target due to filtration by the intervening air. The total path length of the photons from the target to the phantom and thence to the ionization chamber is about 130 cm. It then follows that as the spectrum is unchanged by scattering, the scattered photon spectrum, to which the ionization chamber was exposed, will be virtually the same as the primary photon spectrum at 130 cm from the target. The ionization chamber was therefore calibrated against a Victoreen Grenz ray chamber, which had been standardized at the National Physical Laboratory, at 130 cm from the target in the primary beam. The half value thickness of the primary photon beam at 130 cm was measured in order to determine the appropriate NPL quality correction factor to use with the Victoreen Grenz ray chamber.

## Results

*Magnitude of the scattered radiation.* The results of the measurements are presented in Figs 3 and 4. The scattered radiation, expressed as a percentage of the surface dose, is presented in a polar form. Fig. 3 refers to the scattered radiation from the 54 cm<sup>2</sup> and 431 cm<sup>2</sup> areas respectively. Fig. 4 refers to the radiation scattered from both areas at 10 kV.

The range of values obtained for the radiation scattered at 100 cm from the surface of the phantom with a 431 cm<sup>2</sup> field was  $2 \times 10^{-6}$  to  $8 \times 10^{-6}$  of the surface dose for all the angles examined. At 90° the magnitude of the scatter

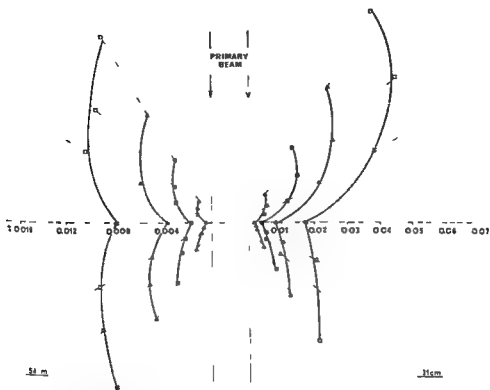


Fig 3 Polar distribution of scattered radiation at 100 cm from the phantom surface expressed as a percentage of the surface dose 54 cm (left) and 431 cm (right) irradiated area ▲ 30 kV ● 40 kV and □ 50 kV

from the 431 cm area was between  $2 \times 10^{-6}$  and  $2 \times 10^{-4}$  of the surface dose. These values for 10 to 50 kVp roentgen rays are mostly lower than those reported by BOMFORD & BURLIN for 100 to 300 kVp and by McEWAN for 50 to 250 kVp and indicate that the trend to lower values of the percentage scattered radiation with decreasing roentgen ray energy observed at the higher energies continues below 50 kVp.

*Variations of scattering with primary roentgen ray energy* The scattered radiation in all directions increases with the energy of the primary beam between 10 kVp and 50 kVp. The tube potential, added filter and half value thickness used by BOMFORD & BURLIN as well as those used in the present measurements are listed in Table 1. The effective photon energy was determined from the half

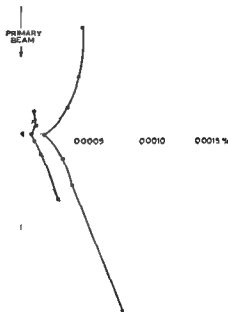


Fig 4 The same as Fig 3 but at 10 kV □ 54 cm  
and ■ 131 cm irradiated area

value thickness using mass attenuation coefficients (BIERMANN 1936 GROSS KURTZ 1934 GRODSTEIN 1957)

In Fig 5 the percentage scattered radiation intensity for 400 cm field is plotted against photon energy for both sets of measurements. It should be noted that BOYFORD & BURLIN's experimental set up was slightly different in that the radiation beam did not overlap the phantom. This results in a slight discontinuity between 50 kVp and 100 kVp for radiation scattered in the forward direction. The scattered radiation intensity tends to reach a plateau value at 150 keV effective photon energy but the maxima reported by other workers were not observed in these measurements.

*Variation of scattering with angle to the primary beam* Fig 6 shows the radiation scattered at different angles. In all cases the minimum value occurs at  $90^\circ$ . In the backwards direction the scatter increases quite rapidly from  $90^\circ$  to  $150^\circ$  at all energies. Above 20 kVp the magnitude of the back scatter exceeds that of the forward scatter but at 10 kVp the forward scatter is the greater. Although the exposure rate from back scattered radiation is often taken as about three times the exposure rate from side scatter radiation (Code of practice 1957), these measurements show that in the energy range 10 to 50 kVp the back scattered radiation is always considerably greater than this.

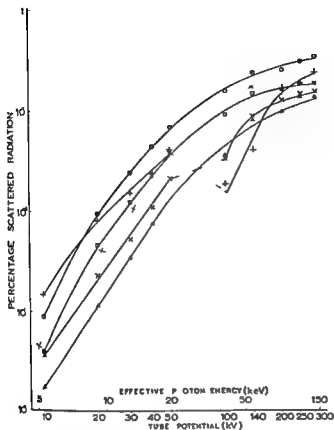
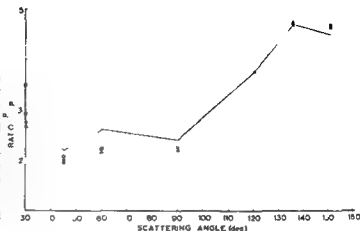


Fig 5 The variation of scattered radiation at 100 cm from the phantom surface from an irradiated area of 400 cm<sup>2</sup> expressed as a percentage of the surface dose with the photon energy  
 ○ 130° □ 120° △ 90°  
 × 60° and + 30°

*Variation of scattering with area* Only two areas 54 cm<sup>2</sup> and 431 cm<sup>2</sup> were investigated in these experiments. The ratio P431/P54 of the percentage scattered radiation from the 431 cm<sup>2</sup> area to the percentage scattered radiation from the 54 cm<sup>2</sup> area was determined for each angle at every potential (Fig 6). The line joins the mean value of P431/P54 at each angle. It was found that at each angle the ratio was nearly independent of the energy i.e. the values of the ratio lay within (P431/P54) mean  $\pm$  0.5.

The ratio of scattered radiation is considerably below the ratio of the irradiated areas (viz 8.0). Thus the radiation scattered from a phantom is not strictly proportional to the irradiated area. This finding is consistent with most of the results at higher energies the one exception being the results of MARTIN & MULLER (1961). This difference probably arises from the different experimental arrangements. (MARTIN & MULLER used a roentgen ray beam at 45° to the incident face of the scatterer.)

Fig 6 The variation in the ratio of the percentage scattered radiation for a 431 cm irradiated area to the percentage scattered radiation for a 54 cm irradiated area with the scattering angle. The line connects the mean values of the ratio at each angle  
 × 50 kV Δ 40 kV  
 ○ 30 kV □ 20 kV and  
 + 10 kV



### Conclusion

The scattered radiation expressed as a percentage of the surface exposure rate is smaller for 10 to 50 kV p energies used most frequently in radiation therapy. Nevertheless it must be remembered that the exposure rate from the beryllium window tubes employed in dermatologic treatments can be an order of magnitude greater than those used in conventional radiation therapy (i.e., in excess of 2 000 R/min). The absolute magnitude of the scattered radiation may therefore be greater in dermatologic treatments than in conventional radiation therapy. This emphasises the caution needed in interpreting the permissive regulations allowing persons in the treatment room during irradiation with roentgen below 100 kV and dispensing with structural shielding when energies below 50 kV are used (ICRP 1960). Certainly the adequacy of local shielding or protective clothing must be scrupulously checked, whenever a person is allowed in the treatment room during irradiation.

The results also stress the need for caution in applying approximations which may be valid for high energy roentgen rays for estimating the magnitude of the scattered radiation at 10 to 50 kVp. One example is the method suggested for estimating the scattered radiation in directions other than 90° to the primary beam.

To equate scattered radiation in all directions to that at 90° (ICRP 1960) or to evaluate the back scattered radiation as three times that at 90° (code of practice 1957) can be a large underestimate. Another example of a source of misestimation is in the assumption that the scattered radiation is proportional to the area.

## Acknowledgements

We wish to thank Sister P. Simpson for the valuable assistance in making the measurements recorded here and Dr L. Szur and Mr J. Yarwood for their encouragement. This work forms part of a third year project in medical physics submitted by one of us (D.M.J.B.) in partial fulfilment of the requirements for the B.Sc. degree of the Polytechnic. Professor J. E. Roberts kindly lent some tissue equivalent material for these measurements.

## SUMMARY

The radiation scattered from an anthropomorphic phantom irradiated by roentgen ray beams of energy 10 to 50 kVp has been measured. The variation of the scattered radiation with scattering angle, photon energy and field size are discussed. Caution is needed in interpreting permissible regulations relating to low energy rays contained in Codes of Practice. The approximations used to estimate the magnitude of scattered radiation for radiation of high energy are not always valid for radiation of low energy.

## ZUSAMMENFASSUNG

Es wurde die Streustrahlung von einem antropomorphen mit Röntgenstrahlen von einer Energie zwischen 10 und 50 kVp bestrahlten Phantom gemessen. Die Veränderungen der Streustrahlung mit dem Streuwinkel, der Photonenenergie und der Feldgrösse werden diskutiert. Bei der Interpretation zulässiger Grenzen für Röntgenstrahlen von niedriger Energie wie sie in Codes of Practice enthalten sind, ist Vorsicht notwendig. Die verwendeten Approximationen um die Grösse der Streustrahlung für Röntgenstrahlen von hoher Energie abzuschätzen, sind nicht immer für Röntgenstrahlung von niedriger Energie gültig.

## RÉSUMÉ

Le rayonnement diffusé par un fantôme anthropomorphe irradié par un faisceau de rayons Roentgen d'une énergie comprise entre 10 et 50 kVp a été mesuré. Les auteurs étudient la variation du rayonnement diffusé en fonction de l'angle de diffusion, de l'énergie des photons et des dimensions du champ. Il est nécessaire d'être prudent dans l'interprétation des réglementations concernant les rayonnements de faible énergie qui sont contenues dans les Codes of Practice. Les approximations utilisées pour estimer l'importance du rayonnement diffusé pour les rayons de haute énergie ne sont pas toujours valables pour les rayonnements de faible énergie.

## REFERENCES

- BIERMANN H. H. Die Massenschwächungskoeffizienten monochromatischer Röntgenstrahlen für Cellophan Al, Se, Ag, Ca, Sn, Sb und Te bis 100 ÅE. *Ann. Physik* 26 (1936) 740.  
 BONFORD C. H. and BURLIN T. E. The angular distribution of radiation scattered from a phantom exposed to 100–300 kVp X-rays. *Brit. J. Radiol.* 36 (1963) 436.  
 CODE OF PRACTICE FOR THE PROTECTION OF PERSONS EXPOSED TO IONISING RADIATION. H.M.S.O. London 1957.  
 CODE OF PRACTICE FOR THE PROTECTION OF PERSONS AGAINST IONISING RADIATION ARISING FROM MEDICAL AND DENTAL USE. H.M.S.O. London 1964.

- FRANTZ F S and WYCKOFF H O Attenuation of scattered cesium 137 gamma rays Radiology 73 (1959) 263
- GLASSER O QUIMBY E H TAYLOR L S and WEATHERWAX J L Physical foundations of radiology Cassel London 1961
- GRODSTEIN G W X ray attenuation coefficients from 10 keV to 100 MeV National Bureau of Standards Circular 583 (1957)
- GROSSKURTH K Neubestimmung der Massenschwachungskoeffizienten monochromatischer Rontgenstrahlen für 16 Elemente und Paraffin zwischen 0.128 und 2.5 Å E. Ann. Physik 20 (1934) 197
- HETTINGER G Angular and spectral distribution of back-scatter radiation from slabs of water brass and lead irradiated by photons between 50 and 250 keV Acta radiol 54 (1960) 129
- LINDELL H Secondary roentgen radiation Acta radiol 41 (1954) 353
- LORENTZON L Secondary roentgen radiation from wax Al Fe and Pb at tube voltages between 40 and 70 kV Acta radiol 41 (1954) 201
- MARTIN J H and MÜLLER G M Quantity and quality of scattered X rays Brit J Radiol 34 (1961) 227
- McEWAN A C Scattered radiation from a cuboid phantom Phys in Med Biol 11 (1966), 393
- PROTECTION AGAINST X RAYS UP TO ENERGIES OF 3 MeV AND BETA AND GAMMA RAYS FROM SEALED SOURCES ICRP Publication 3 (1960)
- SANDERS A P CHIN C W SHARPE K W REEVES R J and BAYLIN G J Right angle scatter for X ray beams for 0.14 to mm 2.5 mm copper HVL Radiology 75 (1960) 595
- WALSTAM R Dose measurements on secondary roentgen radiation Acta radiol 41 (1954) 348

# PROCEDURES IN RADIATION THERAPY DOSIMETRY WITH 5 TO 50 MeV ELECTRONS AND ROENTGEN AND GAMMA RAYS WITH MAXIMUM PHOTON ENERGIES BETWEEN 1 AND 50 MeV

Recommendations by the Nordic Association of Clinical Physics

The International Commission on Radiation Units and Measurements (ICRU) has published general recommendations on dosimetry procedures for photons (ICRU 1969) and others are in preparation for electrons (ICRU 1971). These may be supplemented to advantage by national or regional suggestions covering practical details of routine dosimetry procedures and taking into account the particular requirements and provisions of the country and region. Local data have been prepared for the United Kingdom (HPA 1969-1971) and the USA (SCRAD 1966-1971) and more are under way in West Germany (German Standards Association 1971). This paper deals with the establishment of recommendations that are pertinent to the situation in Denmark, Finland, Iceland, Norway and Sweden.

**Objective.** The aim is to give the hospital physicist a code of practice to be followed at all radiation therapy centres in the Nordic countries so as to secure uniformity of dosimetry. This is intended to cover both the initial measurements when dosimetry is first performed with a new therapy apparatus and the continuous supervision necessary to ensure that the basic dosimetry is properly employed to facilitate adequate and consistent radiation therapy. In weighing high accuracy and theoretic strictness against practical usefulness, the latter has been given much emphasis so that the procedures may easily be followed at all therapy centres.

The implementation of these recommendations will probably have to be carried out in steps. The various centres following the suggestions are encouraged to adopt the procedures for the determination of the absorbed dose as soon as possible. On the other hand, the work aimed at improving beam uniformity will for instance often necessitate gradual improvements and additional equipment, such as well designed sealed monitor chambers, balancing chambers, scattering foils and flattening filters and high quality equipment enabling good definition of the irradiation geometry. Above all, it is highly desirable that in considering the purchase of new accelerators much weight is given to the availability of equipment that facilitates correct dosimetry. Finally, each centre will have to base its control procedures on its own experiences. It is implied that dosimetry connected with modern megavoltage therapy requires a qualified hospital physicist to accept responsibility for the complex physical measurements needed.



The recommendations are to a large extent based on work with accelerators at present in use in the Nordic countries: that is betatrons below 50 MeV and linear accelerators below 10 MeV: the latter only with photon beams.

*Principal features* For the purposes of radiation therapy dosimetry the absorbed dose in water should be specified at a reference point in a water phantom (ICRU 1969, 1971): more research is needed on the absorbed dose in other materials. At the high energies with which this report deals, however, the absorbed dose in a small specimen of muscle, fat or bone at the reference point will rarely differ from that in water by more than ten per cent.

No standards of absorbed dose are at present available at any national laboratory. The question of transfer of absorbed dose calibration from the national laboratory to the user of the calibration is still a matter of research: an international situation reflected in the recommendations. Widespread calibration of the absorbed dose will presently have to be based on  $^{60}\text{Co}$  exposure calibration and in view of their simplicity and precision ionization methods are recommended for the transfer of absorbed dose calibration to the user.

When an ionization chamber is used for the assessment of absorbed dose, a factor is necessary to convert its reading to the absorbed dose in water. Such conversion has been done with a conversion factor  $C_1$  (ICRU 1969) for photon radiation while a factor  $C_E$  has been suggested (ICRU 1971) for electron radiation. The present recommendations retain factors  $C_A$  and  $C_E$  but extend the applicability of the  $C_A$  concept to other measurement depths by means of the experimental results of SVENSSON (1971) based on the use of an effective measuring point (DUTREIX & DUTREIX 1966; HETTINGER et al. 1967; HARDER 1968).

With regard to the standardized depth of absorbed dose measurements, one depth (5 cm) is recommended over the whole range of photon energies considered. This eliminates the risk of mistakes in measurement depth at centres having several types of radiation equipment and the construction of measurement phantoms is simplified. Contrasting these advantages, a risk of error in the conversion factor ( $C_A$ ) exists due to the possibility of electron contamination at high photon energies. A considerable degree of contamination will be clearly distinguished from examination of the shape of the depth dose curve. A twenty per cent contamination by electrons may occur without being easily discernible: in the worst case (at high energies) this would introduce an error of less than two per cent in the absorbed dose determination. This should be acceptable in view of the unambiguity and simplicity in using a single depth of measurement.

An accurate specification of the size and alignment of the radiation beam is essential in radiation therapy. Unfortunately, there is no generally accepted specification available and further consideration is needed. One reason for the difficulties stems from the differences between the beams defined from theoretic geometric considerations and those of the actual radiation. The cross section area of the beam is now defined from purely geometric considerations whereas the alignment is made with due attention to the actual radiation beam.

Recent investigations (SVENSSON & HETTINGER 1971) have indicated that the flattening of the radiation beam of some betatrons leaves much to be desired. It is imperative that the beam flatness be investigated and adjusted to make the rest of the dosimetry meaningful. A uniformity index has been used to describe the flattening. This concept has been preferred because it includes the possibility of having irregularly shaped isodoses — with the present techniques such should still be common — at least with some types of accelerators.

The recommendations listed contain only the procedures without extensive comments on their background or alternative methods. The reader is referred to previously published papers for more details (HPA 1969, 1971; SCRAD 1966, 1971; ICRU 1969).

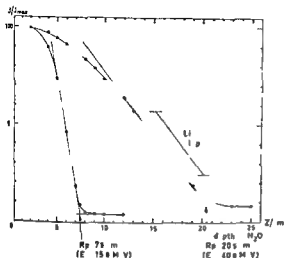


Fig. 1 Determination of energy at the surface by range analysis SSD 100 cm Field size 12 cm / 12 cm

$$E = \frac{R_p + 0.3}{0.52}$$

The recommendations concerning procedures with electron beams have been worked out after consultations with the ICRU task group on electron dosimetry but may need modification when the final ICRU report becomes available. The recommendations for photon beams (ICRU 1969) have been followed with two exceptions (extension of the  $C_1$  concept and the use of a single depth of measurement) which have been discussed above.

### Energy determination at accelerators

A knowledge of some measure of radiation quality is necessary both because the absorbed dose conversion factors  $C_1$  and  $C_2$  are energy dependent and because standardized depth dose tables may be used by laboratories having accelerators similar in construction provided that the energy is determined in a uniform manner (SVEINSSON & HETTINGER 1971, SVEINSSON 1971a). Different methods dependent on the particular aspect in which interest lies are recommended (that is conversion factor determination or depth dose table selection).

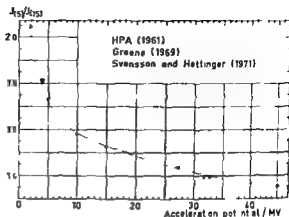
**Electrons** The electron energy should be evaluated by means of a range analysis. The depth ionization curve in water is measured at a beam size of 12 cm  $\times$  12 cm (above 30 MeV 16 cm  $\times$  16 cm) or larger by means of the concept of an effective measuring point (p 611). The point where the extrapolation of the linear fall-off at the inflexion point of this curve meets the roentgen ray background is called the practical range  $R_p$  (Fig. 1). The energy at the surface  $E_0$  of the electrons is derived (MARKUS 1964, SCRAD 1966, SVEINSSON & HETTINGER 1971) from the relationship

$$R_p = C_1 E_0 - C_2 \quad (1)$$

where  $C_1 = 0.02 \text{ cm (MeV)}^{-1}$  and  $C_2 = 0.3 \text{ cm}$  (The electron energy determined from eq. (1) is close to the most probable energy at the surface of the phantom.) The average energy  $\bar{E}$  of the electrons at depth  $z$  in the phantom is estimated (HAPPER 1965 b) with

$$\bar{E} = E_0 (1 - z/R_p) \quad (2)$$

Fig 2 The ratio of the 5 cm and 15 cm depth ionizations  $J(5)$  and  $J(15)$  (SSD 100 cm 10 cm 10 cm) as a function of the acceleration potential (maximum photon energy). The full line gives the recommended values.



**Photons** When photon and electron beams are available with the same betatron the photon energy may (within a few MeV) be obtained from the electron energy at the same energy setting by calculation of the energy of the electrons before they leave the acceleration tube. This calculation means that electron energy losses in all scattering materials in the radiation beam must be added to the electron energy measured. The sum will give an estimate of the photon energy sufficiently accurate for determination of the absorbed dose conversion factor  $C_A$ .

When it is not possible to use this simplified procedure for energy determination and the maximum photon energy is less than 10 MeV a depth ionization method should be used for evaluation of the maximum photon energy in the spectrum used both for conversion factor determination and for selection of depth dose tables. A calculation is made of the ratio of the ionization measured with the effective measuring point (p 611) of the chamber at 5 cm and at 15 cm depth in a water phantom. The maximum photon energy is then taken from the full line of Fig 2. The spread of the experimental results in Fig 2 gives an idea of the accuracy of the method.

When the maximum photon energy is higher than 10 MeV the ionization ratio method indicated above is sufficiently accurate for an evaluation of the absorbed dose conversion factor. The published depth dose data (Table 7) however should only be used if the maximum photon energy of the spectrum has been determined by methods based on  $(\gamma, n)$  or  $(2n)$  threshold energies. The four recommended reactions and their threshold energies (ICRL 1969) are listed in Table 1 along with a short commentary on measuring procedures.

Determination of the thresholds at the  $(\gamma, n)$  processes may be made with a pulse counting radiation detector measuring annihilation quanta or beta radiation. Considerable interference from the  $(\gamma, n)$  process occurs at the detection of the  $(\gamma, 2n)$  process in oxygen; the activity produced being several decades higher. Measurement of the 2.3 MeV  $\gamma$  ray from the former reaction is therefore necessary by means of pulse height analysis. A pile up of pulses from competing annihilation photons may be considerably reduced by filtering with several centimeters of lead. The settings of energy at the threshold values are determined by extrapolation to the energy axis in a diagram of the square root of the measured net counting rate against instrument setting (SCRAD 1966 Fig 3).

Table 1

*Recommended threshold reactions The irradiated specimens should always be measured without the irradiation container or cover*

Reaction	Threshold energy/MeV	Irradiation procedure
$\text{Cu}(n, \gamma)\text{Cu}$	10.8	Pure copper plate irradiated in 0.5 mm cadmium cover
$\text{O}(n, \gamma)\text{O}$	15.7	Distilled water in plastic container
$\text{C}(n, \gamma)^{12}\text{C}$	18.7	n heptane in a plastic container
$\text{O}(2n, \gamma)^{16}\text{O}$	28.9	Distilled water in plastic container

### Geometric considerations

The definition of the point from which the radiation emerges is not critical for the beam size determination nor for the beam alignment. The essential factors in the specification of beam size are the source surface distance and the beam defining diaphragm and in the alignment the properties of the radiation beam at the point of irradiation are the most significant. The term source centre which is primarily defined with the source surface distance in mind will therefore also be used in discussing alignment although it is realized that strictly speaking the term is ambiguous.

The use of a nominal specification in terms of geometric beam size is only justified if there is a close correspondence between the geometric and the useful radiation beams. Requirements concerning alignment and beam size are given below to ensure such a correspondence. The discussions concern unmodified beams only, that is open beams without wedges or blocks.

**Geometric beam** Source centre refers to a point that is defined in a  $^{60}\text{Co}$  source as the centre of the front surface of that source, in accelerators producing photon beams as the centre of the front surface of the target and in accelerators emitting electron beams as the point determined by the cross wire method (POHLIT 1963). The first grid  $G_1$  in this method (Fig. 4) is made up of four wires (1 to 3 mm) and the second grid  $G_2$  of two wires (under 1 mm); a photographic film is irradiated behind  $G_2$ . The transmission chamber may be removed from the beam and an external monitor behind  $G_1$  may be used instead to decrease electron scattering and thus improve the film image. The position of the source centre is determined from the relation given in the figure. (The misalignment indicated results in a non uniform beam.)

The nominal specification of the radiation beam should be by means of the geometric beam. This beam is defined by the straight lines drawn from the source centre through the distal end of the beam defining diaphragm.

The geometric beam axis at symmetric diaphragms is defined as the straight line passing through the source centre and the centre of symmetry of the plane figure formed by the edge of the beam defining diaphragm system.

**Beam alignment** A parallelpipedic phantom is often used in measurements relating to dosimetry. The phantom surface is positioned normally to the geometric beam axis. The reference plane is defined as the plane at a given depth beneath and parallel to the phantom surface. The selection

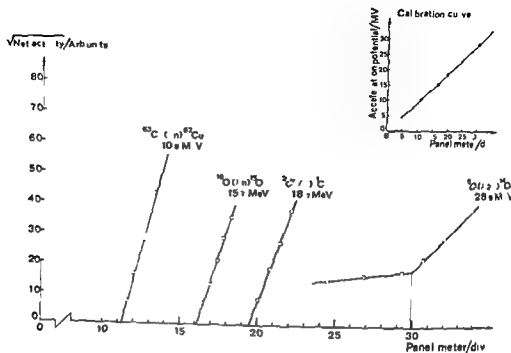


Fig 3 Evaluation of the maximum photon energy by the threshold method

of the depth  $z$  was previously discussed (p 604) and the recommended values are given in Table 2

A reference point lies in the reference plane of symmetric diaphragms and is the intersection point of the geometric beam axis and the reference plane (Fig 5). The commonly used light beam should be adjusted so that the light source is at the same distance from the irradiated surface as the radiation source centre. The symmetry axis of the light beam should intersect the reference plane at the reference point.

The centre point of the radiation beam in the reference plane may be defined as the centre of gravity of the area within which the absorbed dose exceeds 50 per cent of the maximum absorbed dose in the same plane. This point should be found and should be less than 4 mm from the reference point. The centre point will be closely the same if the 50 per cent area of net film blackening, or ionization is employed as discussed below (p 610).

The light beam should be used to indicate the treatment area on the patient. In the absence of a light beam in electron therapy the treatment area will in practice be defined by the inner contour of the collimator.

Practical alignment procedures have been detailed in the case of photon beams (III A 19.0). The cross-wire method should be used with electron beams (Fig 4). It is strongly recommended that the alignment is checked on the installation of a new accelerator. The accelerator manufacturer should be held responsible for any adjustments required before the accelerator is handed over for routine treatments.

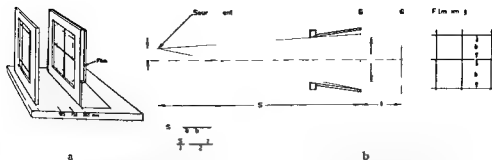


Fig 4 Determination of the source centre of electron beams with the cross wire method. The source centre does not necessarily coincide with the position of the scattering foil. a) Set up for the determination. b) Evaluation of source centre and the source-surface distance from the measurement.

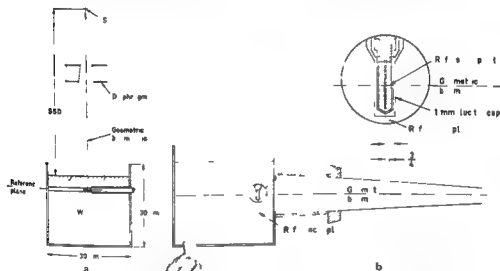


Fig 5 Examples of measurement geometries. a) Determination of absorbed dose in the reference point. The symmetry axis of the beam is positioned in the reference plane. b) Determination of absorbed dose at point along the beam axis. An effective measuring point enables simple determination of the depth absorbed dose curve from the depth ionization curve. In the example the ionization measured is assigned to the reference point.

**Uniformity of the radiation beam in a given plane.** A useful measure of beam uniformity is the uniformity index. This is defined in the reference plane for a specified quantity (e.g. absorbed dose or net film blackening) as the ratio of the area containing points where the value of this quantity exceeds 90 per cent of its value at the reference point and the geometric beam cross section area of the phantom surface. The uniformity index of absorbed dose should exceed 0.80 with both photon and electron beams. In addition the beam uniformity with electron beams should be such that the absorbed dose at an arbitrary point in the reference plane should be less than 105 per cent of that at the reference point. The corresponding figure with photon beams should be 100 per cent.

Table 2  
*Depth of reference plane*

Type of radiation	Depth cm
Photons maximum energy 1—30 MeV	11
Electrons energy at the surface 3—10 MeV	1
10—20 MeV	2
20—50 MeV	3

Some accelerators are overflattened in order to produce uniformity at a specified depth differing from that of the reference plane. The uniformity figures given should then apply at the particular specified depth.

Beam uniformity may be measured in different ways. Photographic film in a polystyrene phantom offers the advantages of high spatial resolution, simplicity of handling, short irradiation times and above all the fact that it will lead to simultaneous recording of the entire radiation field. With some care, as discussed below, the figures given above for absorbed dose uniformity may be substituted by the same figures for net film blackening uniformity. A drawback of the film method is, however, that it can hardly be employed without an automatic or semi-automatic density plotter.

Alternatively, an ionization chamber traversing the beam in the reference plane in a water tank for gantry angles at 90° from the vertical could be used. This method will produce higher precision than the film method provided that the readings are related to a highly reproducible monitor chamber preferably covering the central part of the beam. If the ionization method is used, the uniformity at other gantry angles could be investigated by means of a polystyrene block with holes drilled in the side to take the ionization chamber (NAYLOR & CHIVALLS 1970). The absorbed dose uniformity figures may then be substituted by the same ionization uniformity figures provided that the chamber meets the specifications given later (p. 611).

With the film method the beam uniformity should be investigated by means of photographic film in a light tight cover of regular thickness but not of a radiation fluorescent material. Industrially pre-wrapped film may be used. The film should be irradiated in a polystyrene slab phantom and the absorbed dose should exceed 50 rad so as to minimize the influence of initial perturbations in accelerator beams and of shutter movement in <sup>60</sup>Co beams. Before irradiation, accelerators should have been run under operating conditions for a sufficient period of time to effect a proper warm up. The relation between film blackening and the absorbed dose depends critically on the development procedure used; parameters of importance are type of film and developer, development time and temperature. All these should be combined to produce a linear relationship between blackening and absorbed dose over a large range of the former. The aperture diameter of the density readers should be selected to exert negligible influence on the spatial pattern recorded. The variation in film density on a homogeneously irradiated film should be less than  $\pm 2$  per cent; only a few types of film seem to meet these requirements (RASSOW *et al.* 1969).

The film blackening should be checked regularly for slope and linearity against the absorbed dose curve; at least every time the film emulsion number or developer is changed.

### Determination of absorbed dose at the reference point

The absorbed dose determination should be made by ionization methods. This determination must also be thoroughly controlled when new conditions of irradiation are employed for instance when an accelerator comes into action for the first time. The checking should preferably be done with an independent dosimetric method for instance based on calorimetry or ferrous sulphate dosimetry. Even less accurate methods for instance those based on solid state dosimetry may be worth while. If no alternative dosimetry method is available all steps involved in the absorbed dose determination should be checked by somebody other than the one responsible for the determination.

It is frequently useful in measurements with a cylindric ionization chamber to assign the measured ionization to a point displaced three-quarters of the radius of the chamber cavity (irrespective of the diameter of the central electrode cf ionization chamber requirements below) from the centre of the sensitive volume of the chamber towards the radiation source parallel to the beam axis. This is called the *effective measuring point*.

**Ionization chamber and electrometer** The ionization chamber for the assessment of absorbed dose must fulfil certain requirements. It should have an inner diameter of less than 11 mm and a length of less than 20 mm and the central electrode must not be too massive. The spectral sensitivity should vary by less than 5 per cent in the range from moderately filtered 100 kV x-ray (filter 2 mm Al HVL 2 mm Al) to  $^{60}\text{Co}$  radiation. It should not have a metal stem that causes marked influence on the ionization current. The current produced when only the chamber stem is irradiated must be negligible. If the losses due to ion recombination at the absorbed dose rates used are less than 1 per cent recombination correction will not always be necessary. It is obvious that instruments giving this low recombination should preferably be employed. A low recombination may be difficult to realize however in the case of pulsed radiation (ELLIS & READ 1969) the loss is for instance 2 per cent with the Siemens Sondenfingerhutkammer (collection voltage 300 V) and 3.5 per cent with the Farmer 116 cm<sup>3</sup> chamber and the Farmer dosimeter (185 V) at a dose rate of 0.15 rad/pulse. (The recombination loss is a function of the charge liberated per pulse in the chamber. The ratio of the absorbed dose and the ionization and therefore the recombination losses as well vary by less than 20 per cent for the radiations with which this report is concerned. The figures above are calculated with  $\bar{E} = 20 \text{ MeV}$  at the measurement point.) Correction must then be made for recombination losses either by calculation (BOAG 1956 ICRU 1964) or by measurements (LOEVINGER 1961) the current in the latter instance is plotted against the inverse of the applied voltage (in the region of recombination losses below 5 per cent) and the corrected current is determined by extrapolation to infinite applied voltage.

Suitable ionization chambers are marketed by Nuclear Enterprises (Farmer), Victoreen, Siemens and Physikalisch Technische Werkstätten (Pychau) among others. Almost any commercially available high quality low current measuring instrument may be used in connection with an ionization chamber. The current measurement system should preferably be based on either an integrating Townsend balance system or on one with an electrometer amplifier with loop-gain exceeding  $10^3$  in order to reduce variations of the collecting electrode voltage. The Farmer Secondary Standard Dosimeter is a Townsend balance electrometer. Several makes of vibrating reed electrometers such as those manufactured for instance by Cary and Keithley may be obtained. Special attention should be drawn to the possibility of using electrometer operational amplifiers. A solid state electrometer amplifier may be built by any laboratory with Field Effect Transistors (FET) (MALDERIA & BRUNO 1969). An alternative to FET input amplifiers offered by varactor bridge input amplifiers (JOHANSSON et coll. 1970)



Both types may be obtained for instance through Analog Devices Betatron Burr Brown or Keithley.

The radio frequency fields that exist about microwave linear accelerators may affect the responses of electrometers coupled with ionization chambers. Special attention is needed to ensure that this does not occur.

Each radiation therapy centre should have a local ionization chamber together with an electrometer selected as a reference (secondary standard) instrument preferably for the purpose of calibration of other dosimeters only. The reference instrument should be recalibrated at a standardizing laboratory particularly for  $^{60}\text{Co}$  gamma rays at least once every two years. Its sensitivity should be checked at least quarterly against a suitable radioactive source in the interval between these calibrations. When a  $^{60}\text{Co}$  teletherapy source is used for these controls occasional constancy controls against a second teletherapy source is advisable. A  $^{60}\text{Co}$  half life of 5.27 a ( $\pm 0.01$  a, Rytz 1970) is recommended for such controls. Any change in sensitivity of more than 3 per cent revealed by the constancy control should lead to a thorough investigation of the instrument and subsequent recalibration at the standardizing laboratory.

Ionization chambers of dosimeters for routine clinical measurements should be calibrated against the local secondary standard and be subjected to constancy controls. The frequencies of these must depend on local conditions.

*Exposure calibration.* Reference (secondary standard) instruments should be exposure calibrated through the entire energy range over which they are employed at least once every second year. The exposure calibration for  $^{60}\text{Co}$  should be made in free air against a teletherapy  $^{60}\text{Co}$  unit at a field size of 10 cm  $\times$  10 cm and a distance of 100 cm between the front of the source and the centre of the chamber. The latter should then have an additional polymethyl methacrylate (trade names Perspex, Lucite, Plexiglass) cap with a total wall thickness of about 0.5 g cm $^{-2}$ .

The energy spectra of photons from  $^{60}\text{Co}$  teletherapy units have a continuous distribution from low energies up to the two primary gamma ray energies. Along the beam axis the contribution to the total exposure from secondary photons amounts to 10 to 15 per cent (ICRU 1970, Lofroth 1970). Energy spectrum differences between different teletherapy units are not likely to be of any significance in the exposure calibration except with very accurate measurements.

The exposure calibration factor  $R/\text{division}$  of the secondary standard chamber used as national Swedish standard at the National Institute of Radiation Protection Stockholm has recently been reassessed. As from 1 January 1972 the new calibration factor (which is 1.03 times the old one) will be applied by the Stockholm laboratory when calibrating instruments from other Swedish institutions.)

*Measurement procedure.* The absorbed dose should be determined with a water filled polymethylmethacrylate or polystyrene phantom with outer dimensions of 30 cm  $\times$  30 cm  $\times$  30 cm, the water filling being at least 25 cm (Fig. 5). At large field sizes a larger phantom with a water filling exceeding 25 cm should be used in such a way that a minimum distance of 5 cm between the edge of the beam and the phantom wall exists at the entrance surface. The thickness of phantom walls oriented towards the radiation source should be 0.5 cm or less. The ionization chamber should be protected during the measurement by a tube with a wall thickness of 1 mm, manufactured from polymethylmethacrylate. This tube is attached to a holder that can be adjusted for measurements at various depths. The symmetry axis of the chamber must be positioned in the reference plane.

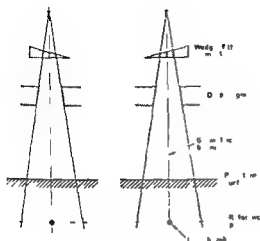


Fig 6 Determination of absorbed dose of photon beams with a wedge. The absorbed dose at the reference point should be taken as the average of the results from the two measurements indicated. The difference between the two cases arises from 180° rotation of diaphragm and wedge.

Measurements should be made for all combinations of irradiation conditions. A horizontal or vertical beam direction may be employed. Whether this influences the dose determination has to be controlled. With wedge fields, the edge of the wedge should be placed parallel to the symmetry axis of the ionization chamber. The measurement should be made at the two possible 180° different orientations of the wedge (Fig 6) and the average result should represent the absorbed dose with the wedge.

**Calculation of absorbed dose.** The assessment of absorbed dose is based on the use of an exposure calibration factor  $N$  (R/division) for  $^{60}\text{Co}$  (p 612) and a conversion factor  $C_A$  or  $C_E$  (p 604). The absorbed dose  $D_w$  (rad) in water at the reference point is calculated from the exposure meter reading  $M$  (divisions, corrected for temperature, pressure, stem effects and the like) with eq (3a) for photon and eq (3b) for electron radiation:

$$D_w = C_A \cdot M \quad (3a)$$

$$D_w = C_E \cdot M \quad (3b)$$

Eq (3a) thus defines the conversion factor  $C_A$  in the same way as it was indicated by the ICRU (1969) although the definition is extended to other measurement depths. The recommended numerical values of  $C_A$  in Table 3 have been adjusted above 10 MeV to allow for the changed depths by means of the experimental data of SVENSSON (1971a). At these energies the  $C_A$  value at 5 cm is typically 1 per cent higher than that at 7 cm or 10 cm.

The energy dependence of  $C_E$  for electron beams may be assessed to a sufficient degree of accuracy with the average electron energy  $\bar{E}$  calculated from eq (2) (HARDER 1965, SVENSSON & PETERSSON 1967, RASOW 1970). The values of  $C_E$  presented in Table 3 have been evaluated with  $\bar{E}$  but for convenience are listed for different energies at the phantom surface  $E_0$  and are given for the reference depth. The values recommended are within about  $\pm 1$  per cent consistent with data calculated from theoretic consideration and are also in close agreement with the mean values of experimental results from different investigators (RASOW 1970).

The following relationship was used in the theoretic derivation of  $C_E$  values:

Table 3

*Recommended values of the conversion factors  $C_A$  and  $C_E$  at the reference point in a water phantom*

Electron radiation				Photon radiation	
Energy at surface	Reference depth	Average energy at reference depth	Conversion factor	Radiation quality	Conversion factor
$E_0/\text{MeV}$	$z, \text{cm}$	$\bar{E}/\text{MeV}$	$\frac{C_E}{\text{rad/R}}$		$\frac{C_A}{\text{rad/R}}$
6	1	3.9	0.90	$^{60}\text{Co } \gamma$	0.93
8		5.9	0.89	4 MV	0.94
10		8.0	0.87	6	0.94
12	2	8.0	0.87	8	0.93
14		10.0	0.86	10	0.93
16		12.0	0.85	15	0.92
18		14.0	0.85	20	0.91
20		16.0	0.84	25	0.91
25	3	19.1	0.83	30	0.90
30		24.1	0.82	35	0.90
35		29.1	0.81	40	0.89
40		34.1	0.80	45	0.89
45		39.2	0.79		

$$C_E = S_{\text{air}} \text{ at } \frac{W}{e} p_{\text{air}} A$$

where

$S_{\text{air}}$  = mean mass stopping power ratio water to air calculated for different energies  $E$  and depths (KESSARS 1970)

$$\frac{W}{e} = 33.7 \text{ J/C} = 0.869 \text{ rad/R} \quad (W = 33.7 \text{ eV/ion } p_{\text{air}})$$

The factor  $p_{\text{air}}$  corrects for the absence of electron scattering in the air volume of the ionization chamber and its numerical values have been chosen for a cylindrical 8 mm diameter chamber (HARDER 1968). The largest deviation of  $p_{\text{air}}$  from unity is for low energies ( $p_{\text{air}} = 0.978$  at  $E = 3 \text{ MeV}$ ). Within one half per cent the same values will apply for chamber diameters between 3 mm and 8 mm. Attention is paid to the attenuation in the build up cap of  $^{60}\text{Co}$  exposure calibration by the use of the correction factor  $A = 0.983$  which applies for the 0.5 g cm $^{-2}$  cap recommended.

Table 3 gives the conversion factors  $C_A$  and  $C_E$  in units of rad in water per roentgen (rad/R). The  $C_E$  values are calculated for use when the absorbed dose is assigned to the effective measuring point. The same values may also be employed, however, at the reference point when the absorbed dose is assigned to the centre of the chamber with an error that rarely exceeds 0.5 per cent; this is because of the slow variation in the depth ionization curve near the reference depth.

Table 4

Main sources of inconsistency between different centres in the determination of absorbed dose in water at the reference point from exposure calibration of  $^{60}\text{Co}$  gamma rays. About 95% confidence limits of random errors attainable under well controlled laboratory conditions are listed.

Source of inconsistency (eqs (3a) and (3b))	Uncertainty (per cent)	
	Electrons	Photons
1 Transfer of exposure calibration factor $\chi$	0.5	0.5
2 Exposure meter reading including corrections $W$	0.5	0.5
3 Differences in stem scattering and leakage conditions between calibration and absorbed dose determination	0.2	0.2
4 Differences in the conversion factor $C_A$ or $C_E$ due to minor differences in photon or electron spectrum	1.5	0.5
5 Differences in the conversion factor $C_A$ or $C_E$ due to chamber construction e.g. caused by scattering in the air cavity	1.0	1.0
Overall rms uncertainty	1.9	1.3

The  $C_E$  values may also be conveniently described by the relationship

$$C_E = C_3 - C_4 \log_{10} (\bar{E} C_5 + 1) \quad (\text{HARDER 1965a})$$

where

$C_3 = 0.987 \text{ rad/R}$ ,  $C_4 = 0.120 \text{ rad/R}$  and  $C_5 = 1 \text{ MeV}^{-1}$  with a thimble ionization chamber of 5 mm diameter.

(This relation is also valid for calculations of  $C_E$  for depths other than that of the reference point as described below (p. 618). It could be employed in the energy range  $3 < \bar{E} < 40 \text{ MeV}$ .)

**Consistency and accuracy** The main sources of inconsistency between different centres in the absorbed dose determination under well controlled laboratory conditions appear in Table 4. The overall uncertainty amounts to less than  $\pm 2$  per cent which should be a lower limit to the kind of consistency that might be attained. It should be possible for the various centres following these recommendations to have a consistency within  $\pm 3$  per cent in statements concerning the absorbed dose in water at the reference point. Should any evidence suggest a greater difference a reassessment must be made.

It should be noted that in addition to being subject to the sources of error given in Table 4 the absorbed dose may be incorrect due to uncertainties in the reference value of exposure of  $^{60}\text{Co}$  and in the  $C_A$  and  $C_E$  values. The latter two uncertainties however do not influence the consistency between various centres firstly because a coordination of the Nordic national reference values of exposure with  $^{60}\text{Co}$  is being planned and secondly because the same values of  $C_A$  and  $C_E$  will be used by all centres.

Table 5

Depth dose data for electron radiation with BBC betatrons. Depth (cm) at which a certain percentage depth dose is obtained. Data at 6–30 MeV derived with 8 different BBC 35 MeV betatrons and those at 35 and 40 MeV with one 45 MeV betatron. The energy at the surface was determined by range analysis. SSD = 110 cm according to the manufacturer. The data refer to circular beams except for the square 10 cm  $\times$  10 cm beams.

Energy at phantom surface $E_0$ MeV	Beam size Diameter cm	Percentage depth dose									
		95	90	80	70	60	50	40	30	20	10
6	10 10	17	18	19	21	22	23	24	25	26	30
10	5	22	25	30	33	36	38	41	43	45	50
	10 10	26	28	32	34	36	39	41	43	45	49
15	4	25	29	36	42	46	51	56	61	66	73
	6	33	38	45	49	53	57	60	64	67	73
	8	35	40	47	52	56	59	62	66	69	75
	10 10	38	43	50	54	57	60	63	66	70	74
20	4	28	34	43	50	57	63	70	77	85	96
	6	42	49	59	65	70	77	81	86	91	98
	8	43	51	62	69	74	80	85	90	95	103
	10 10	47	56	66	73	78	82	86	90	95	101
25	4	31	38	50	59	67	75	83	93	103	119
	6	47	57	69	78	85	92	99	106	114	124
	8	49	61	74	83	91	98	104	111	117	128
	10 10	53	65	79	88	95	102	107	113	119	127
	12	54	66	80	89	97	103	108	113	119	127
30	4	35	45	58	68	78	87	96	108	121	140
	6	43	59	76	87	97	105	114	123	132	142
	8	54	68	85	96	106	114	123	131	139	151
	10 10	55	72	91	103	112	120	128	134	143	151
	12	56	73	92	105	114	122	129	135	143	151
35	4	37	48	63	75	86	98	109	122	138	165
	8	46	61	82	98	111	124	136	149	162	180
	15	57	73	95	111	125	138	148	158	170	199
40	4	38	50	67	81	93	105	119	134	158	194
	8	48	65	87	106	122	136	150	165	184	214
	15	62	77	98	118	135	151	164	179	195	230

Table 6

Depth dose data for electron radiation with Siemens 42 MeV betatron. Depth (cm) at which a certain percentage depth dose is obtained. Data measured for two different betatrons with agreement within  $\pm 2$  cm SSD = 103 cm by the cross wire method (the manufacturer's value is SSD = 100 cm). The energy at the surface was determined by range analysis.

Energy in MeV according to MeV meter	Energy at phantom surface $E_0$ /MeV	Scattering foil Lead thickness /mm	Field size Diameter/cm	Percentage depth dose									
				95	90	80	70	60	50	40	30	20	10
6	6.0	0	> 12	16	17	19	20	21	22	23	25	26	27
10	10.0	0.1	> 12	29	32	35	37	39	41	43	45	47	49
15	15.0	0.25	> 12	39	46	53	58	61	64	67	70	73	76
15	14.8	0.1	8	43	45	50	54	57	59	63	66	68	72
15	14.8	0.1	6	39	44	49	53	56	59	62	65	67	72
20	20.0	0.25	> 12	45	55	65	73	78	82	87	91	96	101
20	19.8	0.1	8	44	53	63	70	75	80	85	89	93	98
20	19.8	0.1	6	43	51	59	66	71	76	82	86	92	97
25	25.0	0.5	> 12	46	57	72	84	93	100	106	113	120	127
25	24.6	0.25	8	45	58	72	82	90	96	102	109	115	122
25	24.6	0.25	6	45	55	68	77	84	91	98	105	112	120
30	30.0	0.5	> 12	46	58	78	94	106	117	125	134	143	154
30	29.6	0.25	8	48	63	80	93	103	112	120	129	137	148
30	29.6	0.25	6	47	58	74	86	95	104	114	123	133	145
35	35.0	1.0	> 12	47	60	83	102	116	130	143	155	167	185
35	34.2	0.5	8	51	66	86	101	113	124	135	146	158	175
35	34.2	0.5	6	49	61	79	93	105	115	127	138	151	167

It is supposed that the MeV meter has been calibrated for large field sizes and thus with a thicker scattering foil in the beam than when smaller field sizes are used.

#### Determination of absorbed dose at any point in a phantom

*Points along the beam axis.* The absorbed dose at the reference point is essential for the determination of the absorbed dose at other points in a phantom for all radiations. The absorbed dose at points of interest along the beam axis may usually be obtained from published beam axis depth dose tables. The absorbed dose at the reference point is then multiplied by the ratio of the depth doses at the point of interest as well as at the reference point.

The tables published by IAEA (1961, 1968) should be used with  $^{60}\text{Co}$  radiation both with open and wedge fields. The depth dose curves both of photon and electron beams with different accelerators of similar design tend to nearly equal. Tables 5, 6 and 7 should be used when

Table 7

*Depth dose data for photon radiations. The energy was determined by the 5 cm—15 cm ionization ratio method at 6 MV and threshold methods at the higher energies*

Type of accelerator	Varian 6 MV linear accelerator					BBC 35 MeV betatron			Siemens 42 MeV betatron	BBC 45 MeV betatron
Accelerator voltage, MV	6					37			43	45
SSD cm	100					100			100	110
Field size cm cm	6	6	10	10	20	20	$4 \times 4(\lambda_1)^*$	$>10 \times 10$ $(\lambda_1)^*$	$8 \times 8(\lambda_1)^*$	$>10 \times 10$ $(\lambda_1)^*$
Depth cm:										
1 3	100 0		100 0		100 0					
2	99 7		99 0		98 7	88 7	92 6	86 0	97 8	97 5
3	94 9		95 0		95 1	96 6	98 2	95 0	98 4	98 0
4	90 2		90 7		91 2	99 7	100 0	98 8	100 0	99 8
5	85 7		86 4		87 5	100 0	99 4	100 0	99 3	100 0
6	81 2		87 4		83 8	98 6	97 3	99 3	97 7	99 2
7	76 9		78 5		80 3	96 1	94 5	97 6	95 5	97 2
8	72 7		74 6		76 8	93 1	91 4	95 2	93 1	94 3
9	68 7		71 0		73 6	89 7	88 3	92 2	90 3	91 5
10	64 8		67 4		70 3	86 4	85 1	89 1	87 4	88 7
12	57 8		60 7		64 2	79 9	79 2	87 7	81 4	87 5
14	51 6		54 5		58 3	73 8	73 6	76 7	76 0	76 5
16	46 0		48 9		53 2	68 1	68 5	71 0	70 7	71 0
18	41 1		43 9		48 3	62 9	63 9	65 8	65 7	66 4
20	36 7		39 5		43 9	58 2	59 4	61 1	61 0	62 0
22	32 8		35 5		40 0	53 9	55 3	56 6	56 7	57 8
24	29 3		31 8		36 3	49 9	51 6	52 5	52 8	54 0

\*  $\lambda_1$  and  $\lambda_2$  designate different beam flatteners

appropriate (HORSLEY et al. 1968, SVENSSON 1971). The shape of these curves should then be subject to a rough control at one or two points outside the reference point and if these are more than 4 mm off the published curve the latter should be avoided. In other cases the beam axis depth dose curve of photon beams should be assumed to equal the beam axis depth ionization curve as measured with effective measuring points (SVENSSON 1971). An additional adjustment of the depth ionization curve must be made with electron beams by means of eqs (2) and (3) and Table 3.

*Points outside the beam axis.* The absorbed dose of electron beams at points outside the beam axis may be assessed by means of photographic film placed parallel to the beam axis in polystyrene phantoms. A significant difference between the relative depth dose curve and the

relative depth blackening curve exists at depths under 2 cm (LOEVINGER et coll 1961 HERTINGER & SVENSSON 1967). The beam axis depth dose curve is first obtained as already described (p 617) and is used to assign a depth dose value to all points along the beam axis in the film. Isodensity curves joining points in the film with the same net blackening are assigned to the depth dose at the point where they pass the beam axis. It is frequently sufficient to construct the isodensity curves with gross blackening.

The same method for photon beams as for electron beams may be employed although the accuracy of this method in the penumbra region is less satisfactory. An approach involving little experimental work consists in transversal measurements at four depths with an ionization chamber (decrement line method (ORCHARD 1964 ORR et coll 1964)) followed by computer calculation of the isodose curves (HALLAES & MUNK 1971). Alternatively complete ionization curves also present the isodose pattern directly.

### Control systems relating to the basic dosimetry

The following paragraphs deal only with control systems relating to the basic dosimetry. All technical checking procedures prescribed by the apparatus manufacturer should also be followed. In deciding upon the frequency of the various procedures the attainability of a high degree of safety for the patient must be weighed against the high cost of frequent controls. The number will also to some extent depend on the behaviour of the particular machine and its intended use: if previous examinations indicate few or slow changes some decrease in their frequency may be satisfactory. A good evaluation of the results should make use of all possibilities of cross controls that will be available — usually one particular test directly or indirectly involves several items of interest. The controls listed below are as a rule part of a suggestion of how a system could be designed in this case the word *could* has been used. Where the word *should* has been used only strong counter arguments might justify a different control system or lower control frequency.

The control system for the ionization chambers and associated instruments has been discussed earlier (p 612).

*Beam monitoring of accelerators* The radiation quality, absorbed dose rate, position of the source centre and similar parameters are with  $^6\text{Co}$  units likely to remain constant for a given set of irradiation conditions. With accelerators however variations do occur and it is essential that these are kept under control. Some general principles concerning this control are given below and a number of recommended applications of these principles appear later (p 619).

It is fundamentally important that the total absorbed dose at the reference point delivered during a given period of irradiation should be known. To that end the accelerator should be provided with an integrating absorbed dose monitor: this should be well calibrated, that is the relationship between its response and the absorbed dose at the reference point should be accurately known when a given field size and energy setting are used. The calibration should as far as possible be insensitive to changes in the settings of the accelerator panel (e.g.  $\text{MeV}$ , meter and extraction) the field size, absorbed dose rate, temperature of the accelerator magnets, accelerator beam direction, the scattering foil or flattening filters etc. The response of hermetically sealed monitor chambers should be examined as regards their independence upon air pressure and temperature.

The nominal absorbed dose monitor calibration factor refers to a given set of values of some of the parameters mentioned (for instance dose rate or extraction). These parameter values will in the normal course of accelerator operation fluctuate. Permissible ranges should be



stated for all the values involved in order to ensure that the use of the nominal calibration factor leads to acceptably small errors in absorbed dose determination at the reference point. The ranges should be selected in such a way that at any setting of parameters within the given ranges the absorbed dose monitor calibration factor differs by less than  $\pm 2$  per cent from the nominal factor.

The absorbed dose at any point within the irradiated volume bears a certain relationship to the absorbed dose at the reference point. It is essential that this relationship is not significantly changed during normal accelerator operation. The isodose pattern and the beam uniformity should thus be investigated similarly to the absorbed dose at the reference point as regards the influence of beam parameter variation.

*Geometric controls.* The purpose of these should be to ensure that the pointers, the geometric beam and the light beam are all centred at the reference point, further the relationship between the sizes and centre points of the radiation field (e.g. the 50% isodose line) and the light field must not change. Rotational therapy units or units with isocentric set up of patient also have to be examined regularly for consistency between the radiation beam axis and the centre of rotation. Deviations of the order of a few millimeters contribute significantly to the overall errors. These controls should be made in several beam directions at least  $-90^\circ$ ,  $0^\circ$  and  $+90^\circ$  and in the  $180^\circ$  direction if this is used for treatments. It will often be convenient to combine the control of consistency between light field and radiation beam with the examination of field homogeneity. Detailed information on suitable procedures has been given by the HPA (1970a).

*Beam uniformity controls of accelerators.* The uniformity may be examined with photographic film in the reference plane by the methods outlined earlier (p. 610). Each control should determine the position of the maximum blackening point of the film, the blackening at this point relative to the reference point and the blackening along two axes through the reference point perpendicular to each other. Naturally a full evaluation of the film blackening is of greater value as the uniformity index may then be calculated. Other control systems should present information corresponding to that obtained from the film measurements as given above. Parameters to be included in the control system of the uniformity are the following: accelerator beam direction (for instance  $-90^\circ$ ,  $0^\circ$ ,  $+90^\circ$ ), all foils, flattening filters and energies used. The controls could be made weekly with cyclical permutation of some parameters so that each combination is controlled at least once every month. A special balancing system is required with some betatrons (PETERSSON & HETTINGER 1965, VOX ARX 1965, ROBINSON & McDONNELL 1967). When applicable this system should also be subjected to a control program.

*Energy controls of accelerators.* Some accelerators designed for one fixed energy may not need a separate control of the beam energy. Control of the energy setting for electron beams only is however sufficient when photon and electron beams are available with the same betatron. The measurement should be based on depth ionization and the control system calibrated in connection with the energy determination (p. 605). An energy below 20 MeV is necessary. The measurement could be performed with an ionization chamber inserted in the polymethylmethacrylate or polystyrene block forming part of the phantom employed for control of the absorbed dose. The response of this chamber could be compared with that of the same chamber placed approximately at the reference point, the reading at the former depth should be 40 to 50 per cent of that at the latter (LOUNAST 1969). The energy could be controlled once a week.

When only photon beams are available the energy control could be made with the ratio of ionization measurements at 5 and 15 cm depth in water or polystyrene. Alternatively above

10. *One of the reactions in Table 1 could be selected and a certain amount of material irradiated. The control should then aim at proving that the activation measured at fixed irradiation and measurement conditions is constant.*

*Absorbed dose controls.* The constancy of the absorbed dose in the reference point should be examined by ionization measurements in a special control phantom designed for ease of handling. Parameters to include in the system are the same as above (p. 620) and the same frequency of the controls could be applied.

### Control of the absorbed dose given to the patient

It is essential that the absorbed dose given to each patient in each treatment is under proper control (ICRP 1970). Pertinent radiation protection aspects are being dealt with by a Nordic working party that will soon produce detailed recommendations for the Nordic countries (Lindell 1971). The comments given below have been discussed with this committee but carry no official cognizance.

To protect the patient from overdose or from incorrect treatment conditions dual monitoring systems are recommended. Apart from mistakes made by the operator, incorrect functioning of the dosimetry system will significantly add to other sources of error connected with radiation therapy (Lindkvist et al. 1972, Ayling & Henderson 1972, RASMP 1969). The measurements and control systems indicated below should be used at each treatment. In addition, wherever there are dual monitoring systems these should be controlled against one another each morning before patient treatments start. Monitoring ionization chambers should be hermetically sealed, particularly if they are located in the close proximity of magnetic coils that can become heated.

All  $^{60}\text{Co}$  units should be provided with a timer that will automatically return the beam control mechanism to the off position after the pre-set time has elapsed. In addition, a checking chamber could be positioned on the patient side of the shutter to be employed as an integrating meter capable of preserving its accumulated response in the event of any failure or interruption in the operation of the equipment during treatment. Alternatively, an independent timer system triggered by the shutter could be used. The absorbed dose derived from the monitor or control timer reading should for each patient be compared with that derived from the timer setting.

All accelerators should be provided with dual integrating monitoring systems. Both of these should be capable of terminating the exposure after a pre-set value has been reached. One of these values should correspond to the absorbed dose intended for the patient, the other to a higher value, for instance a fixed high value (several times hundred rad) or a certain increment (several times ten rad) above the desired value. At least one system should have its sensitive volume on the patient side of any scattering foils or flattening filter. At least one of these systems should preserve its accumulated signal in the event of any failure or interruption in the operation of the equipment during treatment. At least one of the systems should start at zero setting at the beginning of the patient treatment. Both monitor readings should be compared for each patient treatment.

### Acknowledgements

These recommendations have been produced by the Swedish Association of Radiation Physics and the Nordic Association of Clinical Physics aided by a large number of their members and coordinated by Gunnar Bengtsson, Bengt Lindkvist and Hans Svensson. Representatives of various bodies (such as the ICRU and the HPV) have offered invaluable criticism and the

aid of the following is gratefully acknowledged: Dietrich Harder, George Innes, Alan Jennings, John Laughlin and Wolfgang Pohlitz. The meetings of the working party were supported by the Swedish Cancer Society.

Reprints may be obtained from G Bengtsson, Statens Strålskyddsinstitut, Fack S 104 01, Stockholm 60, Sweden.

## SUMMARY

Recommendations for dosimetry procedures of  $^{60}\text{Co}$  radiation therapy apparatus and accelerators in the Nordic countries are presented. These deal both with initial measurements of the apparatus and continuous controls of items important for the dosimetry. They include methods for energy determination, considerations regarding beam definition and means of calculating the absorbed dose at any point in a phantom.

## REFERENCES

- VOX ARX A. Continuous or periodical control of field homogeneity. In: Symposium on high energy electrons, p. 85. Edited by A. Zuppinger and G. Poretti. Springer Verlag, Berlin, 1965.
- AYLING R. R. and HENDERSON C. I. Safety aspects of modern medical linear accelerators. In: Proceedings of the sixth conference of the Nordic Association for Clinical Physics, p. 36. Acta radiol. (1972) Suppl. No. 313.
- BOAG J. W. Ionization chambers. In: Radiation dosimetry, p. 153. Edited by G. J. Hine and G. L. Brownell. Academic Press Inc., New York, 1956.
- DUTREIX J. et DUTREIX A. Etude comparée d'une série de chambres d'ionisation dans les faisceaux de 20 et 10 MeV. Biophysik 3 (1966) 249.
- ELLIS R. E. and READ L. R. Recombination in ionization chambers irradiated with pulsed electron beams. II. The effect in the Farmer thimble chambers. Phys. in Med. Biol. 14 (1969) 411.
- GERMAN STANDARD ASSOCIATION DIN 6809 Clinical dosimetry (in press) and DIN 6800 Dosimetry procedures (in preparation); private communication by D. Harder, 1971.
- GREENE D. The HPA and AAPM survey of depth-dose data for teleisotope  $\gamma$  rays and megavoltage X rays. In: High-energy radiation therapy dosimetry. Edited by J. S. Laughlin. Ann. N.Y. Acad. Sci. 161 (1969) 168.
- HARDER D. a. Berechnung der Energiedosis aus Ionisationsmessungen bei sekundärelektronen Gleichgewicht. In: Symposium on high-energy electrons, p. 40. Edited by A. Zuppinger and G. Poretti. Springer Verlag, Berlin, 1965.
- b. Energiespektren schneller Elektronen in verschiedenen Tiefen. In: Symposium on high-energy electrons, p. 26. Edited by A. Zuppinger and G. Poretti. Springer Verlag, Berlin, 1965.
- Einfluss der Vielfachstreuung von Elektronen auf die Ionization in gasgefüllten Hohlräumen. Biophysik 5 (1968) 157.
- HETTINGER G. and SVENSSON H. Photographic film for determination of isodose curves from betatron electron radiation. Acta radiol. Ther. Phys. Biol. 6 (1967) 74.
- PETTERSON C. and SVENSSON H. Displacement effect of thimble chambers exposed to a photon or electron beam from a betatron. Acta radiol. Ther. Phys. Biol. 6 (1967) 61.
- HORSLEY R. J., PRICE R. H., SAUNDERS J. E. and DRINGWALL P. W. Performance of a 6 MeV Varian linear accelerator. Brit. J. Radiol. 41 (1968) 312.

- HOSPITAL PHYSICISTS ASSOCIATION (HPA) Depth dose tables for use in radiotherapy Brit J Radiol (1961) Suppl No 10
- A review of Suppl 10 Depth dose tables for use in radiotherapy Brit J Radiol 41 (1968) 939
- A code of practice for the dosimetry of 2 to 35 MV X ray and Caesium 137 and Cobalt 60 gamma ray beams Phys in Med Biol 13 (1969) 1
- A suggested procedure for the mechanical alignment of telegamma and megavoltage X ray beam units HPA Report Series No 3 1970
- A practical guide to electron dosimetry (5–35 MeV) HPA Report Series No 4 1971
- INTERNATIONAL COMMISSION ON RADIOLOGICAL PROTECTION (ICRP) Publication 15 Protection against ionizing radiation from external sources Pergamon Press Oxford 1970
- INTERNATIONAL COMMISSION ON RADIATION UNITS AND MEASUREMENTS (ICRU) Report No 10 b Physical aspects of irradiation NBS Handbook 83 Washington D C 1964
- Report No 14 Radiation dosimetry X rays and gamma rays with maximum photon energies between 0.6 and 50 MeV Washington D C 1969
- Report No 18 Specification of high activity gamma ray sources Washington D C 1970
- Private communication from the task group on electron dosimetry 1971
- JOHANSSON K, A. BENGTSSON B. E. and LINDSKOG B. A digital electrometer In Proceedings of the sixth conference of the Nordic Association for Clinical Physics p 76 Acta radiol (1972) Suppl No 313
- KALNAES O. and MUNK J. Automatic production of isodose curves Acta radiol Ther Phys Biol 11 (1972) 90
- KESSARIIS N. D. Absorbed dose and cavity ionization for high-energy electron beams Radiat Res 43 (1970) 288
- LINDELL B. Personal communication 1971
- LINDSKOG B. BENGTSSON G. and SVENSSON H. The importance of two independent integrating monitoring systems in medical accelerators In Proceedings of the sixth conference of the Nordic Association for Clinical Physics p 90 Acta radiol (1972) Suppl No 313
- LOEVINGER R. Ionization chamber recombination loss in high intensity radiation fields In Selected topics in radiation dosimetry p 173 IAEA Vienna 1961
- KARZMARK C. J. and WEISSBLUTH M. Radiation therapy with high energy electrons Part I Physical considerations 10 to 60 MeV Radiology 77 (1961) 906
- LOFROTH P. O. Fotonstrålning från en kilocurie  $^{60}\text{Co}$  strålkälla (In Swedish) Umeå universitet Umeå 1970
- MARKUS B. Beiträge zur Entwicklung der Dosimetrie schneller Elektronen Teil III Strahlen therapie 124 (1964) 33
- MALDERLY W. and BRUNO F. P. Solid state electrometer amplifier Phys in Med Biol 11 (1966) 543
- NAYLOR G. P. and CHIVERALLS K. The stability of the X ray beam from an 8 MV linear accelerator designed for radiotherapy Brit J Radiol 43 (1970) 414
- ORCHARD P. G. Decrement lines A new presentation of data in Cobalt-60 beam dosimetry Brit J Radiol 37 (1964) 756
- ORR J. S. LAURIE J. and WAKERLEY S. A study of 4 MeV transverse data and associated methods of constructing isodose curves Phys in Med Biol 9 (1964) 505
- PETTERSSON C. and HETTINGER G. A balancing chamber for stabilizing the homogeneity of the electron field between 10 and 35 MeV In Symposium on high energy electrons p 89 Edited by A. Zuppinger and G. Poretta Springer Verlag Berlin 1965

- POHLIT W Dosimetrie zur Betatrontherapie Georg Thieme Verlag Stuttgart 1970
- Energy calibration of betatron X rays and electrons up to 40 MeV In High energy radiation therapy dosimetry Edited by J S Laughlin Ann N Y Acad Sci 161 (1969) 119
- RASMP/68/2 Requirements for dose control of high energy X rays and electron United Kingdom Department of Health and Social Security March 1969
- RASSOW J Grundlagen und Planung der Elektronentiefentherapie mittels Pendelbestrahlung Habilitationsschrift Strahlenklinik des Klinikum Essen der Ruhr Universität Essen 1970
- IRDMANN U und STRUTER H D Beitrag zur Filmdosimetrie energiereicher Strahlung Strahlentherapie 138 (1969) 149
- ROBINSON J E and Mc DOUGALL R S Electron beam instability and isodose asymmetry associated with a 35 MeV medical betatron Phys in Med Biol 12 (1967) 315
- RYTZ Personal communication 1970
- SUB-COMMITTEE ON RADIATION DOSIMETRY OF THE AMERICAN ASSOCIATION OF PHYSICISTS IN MEDICINE (SCRAD) Protocol for the dosimetry of high energy electrons Phys in Med Biol 11 (1966) 505
- Protocol for the dosimetry of X and gamma ray beams with maximum energies between 0.6 and 50 MeV Phys in Med Biol 16 (1971) 379
- SVENSSON H (a) Dosimetric measurements at the Nordic medical accelerators II Absorbed dose measurements Acta radiol Ther Phys Biol 10 (1971) 631
- (b) Personal communication 1971
- and HETTINGER G Dosimetric measurements at the Nordic medical accelerators I Characteristics of the radiation beam Acta radiol Ther Phys Biol 10 (1971) 369
- and PETTERSSON C Absorbed dose calibration of thimble chambers with high energy electrons at different phantom depths Arkiv för Fysik 34 (1967) 377

